

**OXA- AND AZARHODACYCLOBUTANES
AS POTENTIAL INTERMEDIATES IN NOVEL CATALYTIC TRANSFORMATIONS**

by

Alexander Dauth

Mag.rer.nat (Diploma), University of Vienna, 2006

A THESIS SUBMITTED IN PARTIAL FULFILLMENT OF
THE REQUIREMENTS FOR THE DEGREE OF

DOCTOR OF PHILOSOPHY

in

THE FACULTY OF GRADUATE AND POSTDOCTORAL STUDIES
(Chemistry)

THE UNIVERSITY OF BRITISH COLUMBIA
(Vancouver)

August 2013

© Alexander Dauth, 2013

Abstract

Oxa- and azametallacyclobutanes are commonly invoked as reactive intermediates in transition-metal catalyzed reactions. However, experimental and theoretical support for their involvement in certain transformations is often scarce. In recent years, our group has been investigating the chemistry of oxa- and azarhodacyclobutanes to gain a deeper understanding of their formation and reactivity.

The reactivity of oxarhodacyclobutanes (rhodaoxetanes) with organometallic reagents was investigated. Successful transmetalation with a variety of organoboron nucleophiles was achieved in good yields. This constitutes the first step in a proposed carbohydroxylation protocol. Studies towards reductive elimination have been performed but have to date remained unsuccessful. Rhodaoxetanes were also found to undergo migratory insertion with electron deficient alkynes. The resulting six-membered oxarhodametallacycles were fully characterized.

Substituted rhodaoxetanes were prepared from the corresponding rhodium-olefin complexes. Exclusive selectivity for incorporation of the oxygen atom on the more substituted olefin carbon was achieved.

Oxidation of rhodium ethylene complexes with a selection of nitrene precursors led to formation of azarhodacyclobutanes as two isomers. Appropriate choice of solvent and oxidant allowed for the selective preparation of either isomer. Preliminary reactivity studies revealed the high thermal and chemical stability of the product complexes.

Similar to rhodaoxetanes, substituted azarhodacyclobutanes were formed by oxidation of rhodium complexes bearing substituted olefins. In this case, one isomer was formed as the major or sole product with good-to-excellent selectivity for incorporation of the nitrogen atom on the less substituted olefin carbon.

Preliminary mechanistic considerations suggest that two independent mechanisms are operative including oxidation of a coordinated olefin and cycloaddition with a free olefin in solution.

Preface

Chapter 1 incorporates elements of two review articles, published in Chemical Reviews and Dalton Transactions. Portions of the introductory text are used with permission from the American Chemical Society (2011) and the Royal Chemical Society (2012). All schemes and figures have been modified compared to the published version. I assembled the Chemical Reviews manuscript and the majority of the Dalton Transactions manuscript and Prof. Jennifer Love edited prior to submission. Dauth, A.; Love, J. A. *Chem. Rev.* **2011**, *111*, 2010; Dauth, A.; Love, J. A. *Dalton Trans.* **2012**, *41*, 7782.

Parts of the work presented in Chapter 2 have been published as a communication in Angewandte Chemie International Edition (Dauth, A.; Love, J. A. *Angew. Chem., Int. Ed.* **2010**, *49*, 9219.) Portions of the text are used with permission from Wiley-VCH (2010). All schemes and figures have been modified compared to the published version. I assembled the manuscript and Prof. Jennifer Love edited prior to submission. The results disclosed in the chapter are extended in scope and discussion compared to the published data. Two ligands discussed in the chapter were synthesized by Nadine Kuhl, an exchange student in the Glorius group from the University of Münster, as indicated in the text. Preliminary coordination and oxidation experiments have also been performed by Nadine Kuhl.

The work presented in Chapters 3 and 5 was partly assisted by Jennifer Tsoung and Carla Rigling. I was the lead investigator, responsible for all major areas of concept formation, synthesis, data collection and analysis, as well as manuscript composition. Jennifer Tsoung performed preliminary olefin-exchange studies and first attempts to oxidize and isolate product complexes. Her work is summarized in her Chem448 Thesis at The University of British Columbia (2009). Carla Rigling reproduced and optimized the olefin exchange reactions and performed PhINTs-based oxidations described in Chapter 5. Her work resulted in the preparation of a Master thesis at the Eidgenössische Technische Hochschule (ETH) Zürich (2012). Parts of this work have furthermore been submitted as a full article. The results disclosed here are extended in scope and discussion compared to the submitted data.

Parts of the work presented in Chapter 4 have been published as a communication in *Angewandte Chemie International Edition*. Dauth, A.; Love, J. A. *Angew. Chem., Int. Ed.* **2012**, *51*, 3634). Portions of the text are used with permission from Wiley-VCH (2012). All schemes and figures have been modified compared to the published version. I assembled the manuscript and Prof. Jennifer Love edited prior to submission. The results reported here are extended in scope and discussion compared to the published data. The work presented in subsequent sections of Chapter 4 was partly assisted by Taraneh Hajiashrafi and Alireza Azhdari Teherani, exchange students from the University of Teheran. They performed optimization studies of the oxidation of TPA and MeTPA Rh-ethylene complexes with PhINTs, PhINNs, N₃Ts and TrocNHOTs. I was the lead investigator, responsible for all major areas of concept formation, synthesis, data collection and analysis.

Table of Contents

Abstract	ii
Preface	iii
Table of Contents.....	v
List of Tables	ix
List of Figures	x
List of Schemes	xii
List of Abbreviations	xvi
Acknowledgements	xix
Dedication.....	xxi
1 Oxa- and Azametallacyclobutanes As Reactive Intermediates	1
1.1 Introduction.....	1
1.2 Oxametallacyclobutanes/Metallaoxetanes	2
1.2.1 Transient Intermediates.....	4
1.2.2 Isolated Cases	17
1.3 Azametallacyclobutanes	31
1.3.1 [2+2] Addition.....	31
1.3.2 One Atom Insertions Into Aziridines.....	40
1.3.3 Other Methods to Generate Azametallacyclobutanes.....	46
1.4 Summary.....	46

2	Reactivity of Rhodaoxetanes.....	48
2.1	Transmetalation as Part of a Carbohydroxylation Protocol	48
2.1.1	Transmetalation with Organoboron Nucleophiles	53
2.1.2	Proposed Mechanism	65
2.2	Attempts to Induce Reductive Elimination	66
2.2.1	Thermal Approaches	67
2.2.2	Additives.....	68
2.2.3	Ligand Modifications	69
2.3	Insertion of Electron-Poor Alkynes.....	78
2.3.1	Insertion of Acetylenedicarboxylates.....	78
2.3.2	Structural Elucidation	79
2.4	Experimental.....	82
2.4.1	General Information.....	82
2.4.2	Experimental Procedures and Characterization Data	82
3	Formation of Substituted Rhodaoxetanes.....	97
3.1	Formation of TPA-Rhodium Complexes with Substituted Olefins.....	97
3.2	Oxidation with H ₂ O ₂	107
3.3	Discussion.....	112
3.4	Experimental.....	116
3.4.1	Experimental Procedures and Characterization Data	118
4	Formation of Unsubstituted Azarhodacyclobutanes.....	143
4.1	Oxidation by PhINTs.....	143
4.1.1	Formation of Two Isomers.....	144
4.1.2	Influence of Experimental Conditions	152

4.2	Oxidation with Alternative Nitrene Precursors.....	156
4.2.1	<i>N</i> -Tosyl Substituted Nitrene Precursors.....	157
4.2.2	Nitrene Precursors with Different <i>N</i> -Substitution.....	158
4.3	Reactivity of Azarhodacyclobutanes.....	167
4.4	Experimental.....	171
4.4.1	General Information.....	171
4.4.2	Experimental Procedures	172
4.4.3	Identification of By-Products	180
5	Formation of Substituted Azarhodacyclobutanes	182
5.1	Preparation of MeTPA-Rhodium Complexes with Substituted Olefins.....	182
5.2	Oxidation with PhINTs	185
5.2.1	Oxidation of TPA-Rh-Olefin Complexes with PhINTs	185
5.2.2	Oxidation of a TPA-Rh Complex with a Symmetrically Substituted Olefin.....	191
5.2.3	Oxidation of MeTPA-Rh-Olefin Complexes with PhINTs.....	192
5.3	Preliminary Reactivity Studies.....	194
5.4	Experimental.....	195
5.4.1	General Information.....	195
5.4.2	Experimental Procedures	197
6	Preliminary Mechanistic Studies.....	231
6.1	Three Possible Mechanisms	231
6.2	Compilation of Relevant Experimental Data.....	233
6.2.1	Solvent Effect on Selectivity.....	233
6.2.2	Effect of Oxidants on Selectivity.....	233
6.2.3	Attempts to Effect Insertion into Aziridines.....	235

6.2.4	Observations in the Oxidation of Substituted Olefin Complexes.....	237
6.2.5	Analysis of By-Products.....	240
6.2.6	Oxidation of a Symmetrically Substituted TPA-Rh Olefin Complex.....	241
6.3	Reconciliation of Experimental Data and Proposed Mechanisms.....	244
7	Conclusions and Future Work	247
7.1	Summary and Conclusions.....	247
7.2	Future Work.....	250
	References	252
	Appendix	274
A.1	NMR Spectra.....	274
A.2	HPLC-MS chromatograms.....	318
A.3	Sample plot for ^1H -NMR monitoring of transmetalation	327

List of Tables

Table 2.1 Scope of transmetalation with organoboronic nucleophiles	61
Table 2.2 Thermal reductive elimination attempts	68
Table 3.1 Olefin exchange in TPA complex 152.	100
Table 3.2 Formation of substituted oxarhodacyclobutanes and key ¹ H NMR chemical shift data.	109
Table 4.1 Tabulated ¹ H NMR data comparison for 190, 191 and 153 (600MHz, CD ₂ Cl ₂ , 298K)	147
Table 4.2 NOESY contacts in 190 and 191.	149
Table 4.3 ¹³ C and ¹⁵ N shifts in 190 and 191 acquired by direct and indirect detection NMR methods.	151
Table 4.4 Parameters which did not affect the ratio of 190:191. Best conditions underscored (least side products).	154
Table 4.5 Influence of methanol content on isomer ratio 190:191.	156
Table 5.1 Olefin exchange with MeTPA complex 210.	183
Table 5.2 Oxidation of TPA-Rh complexes with PhINTs	187
Table 5.3 Oxidation of MeTPA-Rh complexes with PhINTs	193

List of Figures

Figure 1.1.1 Generic structure of oxametallacyclobutanes/metallaoxetanes.....	2
Figure 1.1.2 Pioneering Mn-salen catalyst systems used in olefin epoxidation.....	7
Figure 1.1.3 Lone pair orientation allows strong M-O interactions.....	18
Figure 2.1 Proposed product from reaction of 153 with PhMgBr	54
Figure 2.2 ¹ H NMR spectrum comparing 153 (top) to 155a (bottom) (400MHz, <i>d</i> ₆ -acetone, 298K).	55
Figure 2.3 Reaction product with (<i>E</i>)-styrylboronic acid.....	56
Figure 2.4 Possible alternative structures.	57
Figure 2.5 HSQC of (<i>E</i>)-styrylboronic acid.	58
Figure 2.6 HSQC of 155b.	59
Figure 2.7 NOE correlatios in the product complexes.....	60
Figure 2.8 Tridentate TPA-modifications reported by de Bruin.	69
Figure 2.9 Sterically and electronically modified tripodal ligands.....	73
Figure 2.10 Possible isomers of 165 with trigonal bipyramidal geometry.....	75
Figure 2.11 Alternative ligands	77
Figure 2.12 Possible isomers after insertion of alkynes.....	80
Figure 2.13 Crude ¹ H NMR of alkyne insertion product 174, (<i>d</i> ₆ -acetone, 298K, 400MHz). 81	
Figure 3.1 ¹ H NMR spectra of TPA-Rh-ethylene (152, top) and TPA-Rh-vinylpyridine (179e, bottom), CD ₂ Cl ₂	103
Figure 3.2 Diagnostic ¹ H NMR signals for isomers 179a and 180a (400 MHz, CD ₂ Cl ₂ , 298K)	104
Figure 3.3 Interconversion of 179 and 180.....	106
Figure 3.4 Possible isomers in the formation of substituted rhodaoxetanes.....	107
Figure 3.5 HPLC-MS shows formation of only one isomer	108
Figure 3.6. ¹ H NMR (400MHz, MeOD) and ¹³ C NMR (100MHz, MeOD) spectra of 181e.	111
Figure 3.7 ¹ H NMR (400MHz, MeOD) and ¹³ C NMR (100MHz, MeOD) spectra of the oxidation product of 179f.	113
Figure 3.8 Possible structures for the product of oxidation of 179f.	115

Figure 4.1 Comparison of the ^1H NMR spectra of azarhodacyclobuanes 190 and 191 with rhodaoxetane 153 (600 MHz, CD_2Cl_2 , 298K).....	146
Figure 4.2 Possible reason for the anion effect in ^1H NMR data – through space shielding or de-shielding.....	150
Figure 4.3 Long-range $^1\text{H}/^{15}\text{N}$ correlated HMQC (left) and HSQC (right) establish Rh-C, Rh-N and C-N connectivity.....	152
Figure 4.4 By-products identified in the PhINTs based oxidation of 152.....	153
Figure 4.5 Dependence of 190:191 on solvent (ϵ = dielectric constant).....	155
Figure 4.6 Alternative nitrene precursors.	157
Figure 4.7 Formation of two isomers after oxidation with 197.....	159
Figure 4.8 ^1H NMR comparison of 190 and 200 (400MHz, CD_2Cl_2 , 298K).....	160
Figure 4.9 Comparison of ^1H NMR spectra of Ts-protected azarhodacyclobutanes 190, 191 and a mixture of Troc-protected azarhodacyclobutanes 202/203 (600 MHz, CD_2Cl_2 , 298K).	163
Figure 4.10 Syn- and anti-rotamers of azarhodacyclobutane 203.	164
Figure 4.11 A selection of organic azides to test as nitrene precursors.....	166
Figure 4.12 Thermal stability of 190 and 191	167
Figure 5.1 Crude ^1H NMR spectrum of 211g (300 MHz, 298K, CD_2Cl_2).....	184
Figure 5.2 Four possible isomers in the formation of substituted azarhodacyclobutanes.....	186
Figure 5.3 ^1H NMR spectrum of 215e (400MHz, 298K, MeOD)	189
Figure 5.4 Indicative correlations in NOESY spectrum of 215e (400MHz, 298K, MeOD) ...	190
Figure 5.5 ^1H NMR spectrum of 216l (400MHz, 298K, d_6 -acetone)	191
Figure 5.6 Possible stereoisomers with disubstituted olefins	191
Figure 5.7 HPLC-MS of a crude reaction mixture of 220i and 221i.....	192
Figure 6.1 Curtin Hammett conditions could explain formation of 191, even though 152 cannot be detected in the starting mixture.....	240

List of Schemes

Scheme 1.1 The first reported metallaoxetane.	3
Scheme 1.2 Chromyl chloride catalyzed epoxidation of olefins.	5
Scheme 1.3 [2+2] vs. [3+2] addition.....	6
Scheme 1.4 Proposed mechanisms for the Mn-salen catalyzed epoxidation of olefins.....	8
Scheme 1.5 Heptacoordinate Mn-species as metallaoxetane intermediates.....	8
Scheme 1.6 De-oxygenation of epoxides with Fe(CO) ₅	9
Scheme 1.7 Oxygen transfer from epoxides to PPh ₃ or olefins.	10
Scheme 1.8 [2+2] and [3+2] addition pathways in olefin dihydroxylation.....	11
Scheme 1.9 [3+2] addition after reversible olefin precoordination.	11
Scheme 1.10 Dihydroxylation and di-dehydroxylation with rhenium oxides.	13
Scheme 1.11 Nickelaoxetane intermediates in the CO ₂ fixation with epoxides.	14
Scheme 1.12 Proposed nickelaoxetane intermediate in reductive coupling of alkynes and epoxides.....	15
Scheme 1.13 Gas-phase formation of a nickel alkylidene species from a nickelaoxetane. ...	15
Scheme 1.14 ROMP via a ruthenaoxetane.	16
Scheme 1.15 The Tebbe olefination.....	17
Scheme 1.16 Preparation of a titanaoxetane via two different pathways.	17
Scheme 1.17 Titanaoxetanes with two exocyclic double bonds.....	18
Scheme 1.18 Titanaoxetane via [2+2] addition of a metal oxide and an olefin.	19
Scheme 1.19 Tantalaoxetane is not involved in epoxide de-oxygenation.	20
Scheme 1.20 Isolated molybdaoxtanes and tungstenoxtanes.....	20
Scheme 1.21 Formation of a ruthenaoxetane from a Ru-benzyne complex.	21
Scheme 1.22 A crystalline ruthenaoxetane.....	22
Scheme 1.23 Formation of a substituted rhodaoxetane through oxidative addition to an epoxide.....	23
Scheme 1.24 The first isolable unsubstituted metallaoxetane.....	24
Scheme 1.25 Mechanism of rhodaoxetane formation.	24
Scheme 1.26 Reactivity of rhodaoxetane 71.	25

Scheme 1.27 Tridentate ligands increase reactivity of rhodaoxetane.	26
Scheme 1.28 Rhodaoxetane from an internal alkene.	26
Scheme 1.29 Oxidation of olefins to ketones via a rhodaoxetane.	27
Scheme 1.30 A nickelaoxetane from a formal [2+2] cycloaddition.	28
Scheme 1.31 An isolable platinaoxetane from norbornene.	29
Scheme 1.32 Olefin epoxidation via a platinaoxetane.	30
Scheme 1.33 Formation and reactivity of the first stable auroxetane.	30
Scheme 1.34 Proposed mechanisms for β -lactam formation.	32
Scheme 1.35 Proposed mechanism for imine coupling.	33
Scheme 1.36 Formation of azatitanacyclobutanes.	33
Scheme 1.37 Formation and reactivity of the first isolable azametallacyclobutane.	34
Scheme 1.38 Azazirconacyclobutane and -butene formation via [2+2] cycloaddition.	35
Scheme 1.39 Formation of azazirconacyclobutanes from [2+2] cycloaddition with allenes.	36
Scheme 1.40 Formation of azatitanacyclobutanes and azatitanacyclobutenes.	36
Scheme 1.41 Formation of azatitanacyclobutane via alkyne isomerization to allene-intermediates.	37
Scheme 1.42 Proposed intermediacy of an azaferrocyclobutane in aziridination of olefins.	39
Scheme 1.43 Transient formation of an azanickelacyclobutane.	40
Scheme 1.44 Proposed azarhodacyclobutane intermediate in β -lactam formation.	41
Scheme 1.45 Formation of an azanickelacyclobutane by Ni-oxidative addition to aziridines.	41
Scheme 1.46 Azapalladacyclobutanes as proposed intermediates in aziridine isomerization.	42
Scheme 1.47 Formation and reactivity of azapalladacyclobutanes.	42
Scheme 1.48 Catalytic alkylation of styrenyl aziridines.	43
Scheme 1.49 Proposed intermediacy of an azatantalacyclobutane.	44

Scheme 1.50 Formation of an azatantalacyclobutane through double insertion of isocyanides.....	44
Scheme 1.51 Formation of azazircona- and azahafnacyclobutanes.....	45
Scheme 1.52 Double insertion of isocyanides to afford azatitanacyclobutanes.....	45
Scheme 1.53 Formation and reactivity of an azairidacyclobutane.....	46
Scheme 2.1 Generic example for carbohydroxylation.....	48
Scheme 2.2 Examples for multi-step carbohydroxylation protocols.....	49
Scheme 2.3 Examples for one-pot carbohydroxylation protocols.....	50
Scheme 2.4 Au-catalyzed three-component oxyarylation	51
Scheme 2.5 Proposed catalytic cycle for carbohydroxylation of olefins	52
Scheme 2.6 Reported synthesis of 2-rhodaioxetane 153.	52
Scheme 2.7 Rh catalyzed 1,4-conjugate addition.	53
Scheme 2.8 Transmetalation with organoboronic nucleophiles.....	61
Scheme 2.9 Oxidation of arylboronic acids to phenol derivatives.....	65
Scheme 2.10 Proposed mechanism for transmetalation.....	66
Scheme 2.11 Attempts to effect reductive elimination with maleic anhydride.....	69
Scheme 2.12 Opening of a coordination site on rhodaioxetanes.....	70
Scheme 2.13 Transmetalation on complexes with tridentate ligands.	71
Scheme 2.14 Efforts towards reductive elimination.....	72
Scheme 2.15 Failed transmetalation attempt with a sterically modified ligand.....	73
Scheme 2.16 Attempt to form a rhodaioxetane with modified ligand 161.....	74
Scheme 2.17 Efforts towards reductive elimination employing ligand 162.....	76
Scheme 2.18 Envisaged Rh-O insertion of alkynes and subsequent reactivity	78
Scheme 3.1 Preparation of substituted TPA-Rh-olefin complexes.....	98
Scheme 3.2 Ethylene substitution with higher olefins	99
Scheme 3.3 Mechanism of the formation of unsubstituted rhodaioxetane 153	112
Scheme 3.4 Formation of substituted oxarhodacyclobutanes	112
Scheme 3.5 Proton – deuterium exchange in 181.....	116
Scheme 4.1 Proposed formation of azarhodacyclobutane 189.	144

Scheme 4.2 Complementary selectivity of nitrene precursors.	158
Scheme 4.3 Preparation of nosyl nitrene precursor, 197	159
Scheme 4.4 Synthesis and reactivity of Troc nitrene precursor 198.....	161
Scheme 4.5 Formation of two isomeric Troc-protected azarhodacyclobutanes.....	162
Scheme 4.6 Organic azides could act as versatile oxidants for <i>N</i> -substituted azarhodacyclobutanes.	165
Scheme 4.7 Proposed formation of by-product 207.	166
Scheme 4.8 Azarhodacyclobutane 190 is unreactive towards boronic acids.....	168
Scheme 4.9 No reductive elimination of aziridines from 190 was observed.	169
Scheme 4.10 Lack of reactivity of 190 towards reducing agents.	169
Scheme 4.11 No transmetalation with organozinc halides.	170
Scheme 4.12 Acidic ring opening of 191.	171
Scheme 5.1 Solvent dependent formation of unsubstituted azarhodacyclobutanes.	185
Scheme 5.2 Acid mediated ring opening of azarhodacyclobutanes bearing a MeTPA ligand.	195
Scheme 6.1 Proposed mechanisms for formation of azarhodacyclobutanes.	232
Scheme 6.2 Different selectivity depending on oxidant.....	234
Scheme 6.3 Two different mechanisms are responsible for formation of the different isomers.....	235
Scheme 6.4 Attempt to effect Rh insertion into aziridines	235
Scheme 6.5 Experiment to test whether aziridine insertion is occurring.	237
Scheme 6.6 Selectivity in the oxidation of substituted olefin complexes 179 and 180.	238
Scheme 6.7 Formation of unsubstituted azarhodacyclobutane 191 if ethylene is not completely removed prior to oxidation.	239
Scheme 6.8 Possible formation of different by-products.	241
Scheme 6.9 Stereochemical implications of the reaction mechanism.....	243
Scheme 6.10 Possible effect of steric parameters on the reaction pathway with substituted olefins.	246

List of Abbreviations

α	alpha
AcOH	acetic acid
Ar	aryl substituent
β	beta
Bn	benzyl substituent
BnBPA	<i>N</i> -benzyl- <i>N,N</i> -di(2-pyridylmethyl)amine
BPh ₄	Tetraphenylborate
Bu	butyl substituent
BuBPA	<i>N</i> -butyl- <i>N,N</i> -di(2-pyridylmethyl)amine
br	broad
calc	calculated
COSY	correlation spectroscopy
Cp	cyclopentadienyl
Cp*	pentamethylcyclopentadienyl
δ	chemical shift [ppm]
d	doublet
d[AB]	doublet in an AB spin-system (second order doublet)
dba	dibenzylideneacetone
dt	doublet of triplets
DFT	density functional theory
ebthi	bis(tetrahydroindenyl)ethane
eq.	Equivalent
ESI	electrospray ionization
<i>et al.</i>	and others/co-workers
EtOH	ethanol
glyme	dimethoxyethane
HMBC	heteronuclear multiple bond correlation
HMQC	heteronuclear multiple-quantum correlation

HPLC	high performance liquid chromatography
HRMS	high resolution mass spectrometry
HSQC	heteronuclear single-quantum correlation
<i>i</i> -Pr	iso-propyl substituent
<i>i</i> -PrOH	isopropanol
<i>J</i>	coupling constant [Hz]
L	neutral ligand
lr	long range
LRMS	low resolution mass spectrometry
m	multiplet
M	metal
Me	methyl substituent
MeBPA	<i>N</i> -methyl- <i>N,N</i> -di(2-pyridylmethyl)amine
MeOH	methanol
MeTPA	<i>N</i> -[(6-methyl-2-pyridyl)methyl]- <i>N,N</i> -di(2-pyridylmethyl)amine
MS	mass spectrometry
MTO	methyltrioxyrhenium
m/z	mass to charge ratio
nb	norbornene
n.d.	not determined
NMR	nuclear magnetic resonance
NOE	nuclear overhauser effect
NOESY	nuclear overhauser effect spectroscopy
π	pi
PF ₆	hexafluorophosphate
PG	protecting group
Ph	phenyl
PhINTs	[<i>N</i> -(toluenesulfonyl)imino]phenyliodinane
PhINNs	[<i>N</i> -(4-nitrophenylsulfonyl)imino]phenyliodinane

ppm	parts per million
Py	pyridyl substituent
q	quartett
R	organic substituent
ROMP	ring-opening metathesis polymerization
r.t.	room temperature
s	singlet
salen	class of chelating ligands, contraction for salicylaldehyde and ethylenediamine
t	triplet
<i>t</i> -Bu	Tert-butyl substituent
TEMPO	(2,2,6,6-Tetramethylpiperidin-1-yl)oxyl
THF	tetrahydrofuran
TMU	tetramethylurea
TPA	<i>N,N,N</i> -trispyridylmethyl amine
Troc	2,2,2-Trichloroethylformyl substituent
TrocNHOTs	2,2,2-trichloroethyl- <i>N</i> -tosyloxycarbamate
Ts	Toluenesulfonyl (tosyl)
TsN ₃	toluenesulfonyl azide

Acknowledgements

Preamble. The completion of a dissertation always happens in a broader context than just the academic level. A full list of names of the people who have directly and indirectly supported me in these last years through my PhD work would go beyond the scope allotted for the acknowledgment section. Thus, I have the challenging task to limit the expression of my gratitude to two pages. At this point I want to acknowledge all those whose names have not made it in here but whose friendship, advice, mentorship and help was still a vital asset to my work. *Thank you!*

First, I would like to thank my supervisor, Dr. Jennifer A. Love for her guidance, support, trust and encouragement. The freedom I was granted in pursuing own ideas in my research, the opportunities given to acquire new skills and the responsibility entrusted in training and teaching junior students made the last years an exciting – yes – enjoyable period of my life and inspired me to continue on the academic path. I would also like to acknowledge the past and present members of the Love group for discussions and the exchange of ideas: Dr. Tongen Wang, Dr. Shiva Shoai, Dr. Alex Sun, Sara Van Rooy, Lauren Fraser, Jun Yang, Anthony Sabarre, Heather Buckley, Erica Kiemele, Lauren Keyes, Tin Nguyen and Nicole Laberge. Special thanks go to Dr. Paul Bichler for hosting me and for good chats, good laughs, and good music as well as to Matthew Wathier for proofreading and helping with the printing and binding of the thesis and the delivery of the paper copies to FoGS. Phil Provencher, Addison Desnoyer and Marcus Drover are acknowledged for proofreading chapters of my thesis. The latter two I wish all the best in carrying on the oxa- and azarhodacyclobutane baton – a beautifully challenging project.

Further thanks go to the talented undergraduate and exchange students who helped with parts of the project: Jennifer Tsoung, Nadine Kuhl, Kanghee Park, Kevin Shih, Taraneh Hajiashrafi, Alireza Azhdari Tehrani and Carla Rigling.

I also want to express my gratitude to my committee members: Dr. Glenn Sammis for helping edit my thesis as well as Dr. Gregory Dake and Dr. Elliott Burnell. Furthermore, I want to acknowledge Dr. Laurel Schafer for good project ideas as well as helpful discussions about future career steps.

I am also indebted to the support and administrative staff in the UBC chemistry department: Dr. Paul Xia, Dr. Maria Ezhova, Dr. Jason Traer, Zorana Danilovic (all NMR), Dr. Yun Ling, Marshall Lapawa, Derek Smith (all MS), Dr. Brian Patrick (X-ray crystallography), Dr. Emily Seo (Shared Instrument Facility), David Tonkin (electrical engineering), Ken Love (mechanical engineering), Brian Ditchburn (glassblowing), Judy Wrinskelle and Sheri Harbour (both admin).

I was also fortunate to have people who facilitated and fostered my interest in teaching: Dr. Sophia Nussbaum and Anka Lekhi (UBC Chemistry) as well as Dr. Joseph Topornycky and Roselynn Verwoord (Centre for Teaching, Learning and Technology), to whom I wish to extend my gratitude.

I wish to express my appreciation to the various sources funding my graduate studies: UBC (Partial Graduate Fellowship, Graduate 4-Year Fellowship, Gladys Estella Laird Fellowship, Killiam Teaching Assistant Award, Edward Piers Memorial Award) and Mountain Equipment Coop (Graduate Research Fellowship in Sustainability).

My gratitude goes to friends and mentors at University Chapel: Nathan and Karen Daniels, Dan Ray and Christina Lui, Rob and Margaret Cottle, Clement Tsui and Ginimi Chan, Joe Surachett and Pei-Ling Lin, Hank Shih, Chris McDonell, Robin Frohnmayer, John and Myra Butler and Bev Hicks among many others.

Further, I would like to thank friends and neighbours in Acadia Park and beyond: Craig and Racheal Bateman, Usman and Zaineab Waheed, Donnard and Niki MacKenzie, Chris and Yoshika Campbell, Abdul and Zubaida Razique, Dafna Zur and Mansop Kim, Scott and Lindsay Wells, Sally Shi and Ran Gu, Chris and Liv Rensch and Rachael Louton among many others.

Special thanks are owed to my Mamsch and my parents in law for their endless encouragement, support and prayers.

Finally, to the love of my life – my lovely wife Tabea – for living with me this great adventure. And to the most wonderful children on earth and my greatest achievements: Paulina, Anna-Olivia, Niklas Leander and Johanna – I love you more than I can say.

To Tabea
And to Paulina, Anna-Olivia, Niklas Leander and Johanna

"A man who doesn't spend time with his family can never be a real man."
Don Vito Corleone, The Godfather I

"God is like the sun; you cannot look at it, but without it, you cannot look at anything else."
G.K. Chesterton

1 Oxa- and Azametallacyclobutanes As Reactive Intermediates

1.1 Introduction

Transition metal catalyzed reactions play a pivotal role in chemical synthesis both in the academic and industrial realm.^{1,2} In recent years, not only have the selectivity and efficiency of such reactions been at the center of attention, but their ecological and economic impact has become a key focus. Thus, many existing transition metal catalyzed protocols are being modified to align with green chemistry principles. Efforts in this regard include the use of less toxic catalysts, decreased waste production and increased energy efficiency through ambient reaction conditions.³

The development of new, efficient chemical transformations by rational design is another elegant approach to the task of increasing sustainability. Such a design process can be started with a reactive intermediate which is known or at least postulated to participate in a number of transformations. The study of these reactive intermediates and the controlled preparation and functionalization thereof can open doors to yet unknown reaction protocols.

In the Love group we have chosen heteroatom-metallacyclobutanes to pursue studies towards new reactivity. In the work presented in this thesis, I will elaborate specifically on the formation and reactivity of oxa- and azarhodacyclobutanes as potential structures for novel catalytic transformations.

This first chapter shall serve to give an overview of the proposed and actual involvement of oxa- and azametallacyclobutanes in chemical transformations over the last decades. It incorporates elements of two review articles published in Chemical Reviews⁴ and Dalton Transactions.⁵

The second and third chapters cover the research done on oxarhodacyclobutanes (rhodaoxetanes). In chapter two, the reactivity of unsubstituted rhodaoxetanes will be highlighted with an emphasis on a proposed olefin carbohydroxylation protocol employing these structures as key intermediates. The successful transmetalation with boronic acids and studies towards reductive elimination will be discussed. Furthermore, the insertion of

alkynes into rhodaoxetanes to form six-membered oxarhodacycles will be presented. Chapter three will then showcase the formation of substituted rhodaoxetanes starting from substituted olefins.

The following three chapters will focus on research done on azarhodacyclobutanes. Chapters four and five will introduce the successful formation of unsubstituted and substituted azametallacyclobutanes, respectively, while in chapter six mechanistic considerations on the formation of these metallacyclic structures will be discussed.

Chapter seven will give a conclusion and outline potential future work in the different projects.

1.2 Oxametallacyclobutanes/Metallaoxetanes

Oxa-2-metallacyclobutanes are four-membered rings containing an oxygen atom and an adjacent metal atom (Figure 1.1). Due to this four-membered, oxygen containing ring-structure they are commonly referred to as 2-metallaoxetanes in the literature. This convention will be followed in this chapter. To limit the scope of the introduction the focus will be on compounds that contain metals from the d-block of the periodic table (i. e., transition metals) and in which the ring oxygen is formally anionic (X-type donor ligand). Structures with a neutral ring oxygen (L-type donor ligand) are left out of the discussion as these species show substantially different chemical behaviour than the complexes with X-type oxygen ligands.

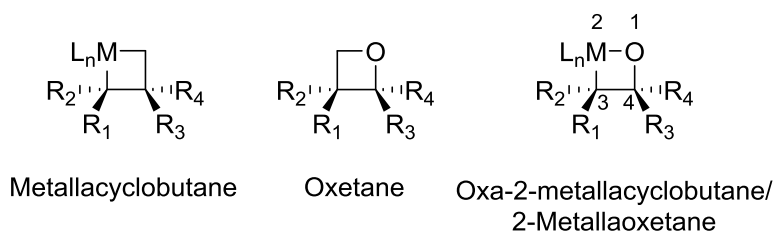


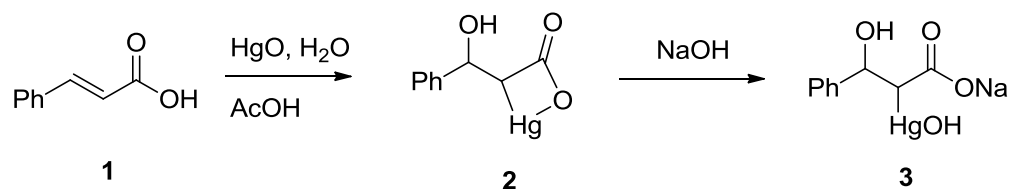
Figure 1.1.1 Generic structure of oxametallacyclobutanes/metallaoxetanes.

2-Metallaoxetanes have been postulated as intermediates in numerous reactions and have been the subject of many experimental and computational studies.^{4,6,7} In several cases, subsequent mechanistic investigations could not support the intermediacy of 2-metallaoxetanes. Nevertheless, there are many reactions where 2-metallaoxetanes have

been established as intermediates in the lowest energy pathway. As a result, the reactivity of 2-metallaoxetanes has received increased attention in recent years and these complexes have enormous potential for development of novel catalytic reactions.

After the establishment of a rough historical context, an account will be given of the proposed involvement of 2-metallaoxetanes as transient intermediates in metal mediated and catalyzed reactions. The structure will be based on the reaction type in which the metallaoxetane intermediate is proposed. This discussion will be followed by a description of cases where 2-metallaoxetanes have been isolated and will be structured according to the position of the parent metal in the d-block. In the course of this discussion, the properties of 2-metallaoxetanes will be described, as well as general methods for their preparation and their reactivity.

The first time the structural motif of a 2-metallaoxetane (metallaoxetane from here) was reported in a publication was in 1900.⁸ During studies of oxymercuration of olefins, Biilmann found that α,β -unsaturated carboxylic acids such as cinnamic acid **1**, converted into a compound described as an inner salt of a 3-phenyl-3-hydroxy-2-mercuripropionic acid **2** (Scheme 1.1).



Scheme 1.1 The first reported metallaoxetane.

Treatment with aqueous sodium hydroxide led to cleavage of the Hg-O bond and yielded the ring-opened product (**3**). This structure was proposed again in related reports by Biilmann^{9,10} as well as Schrauth et al.¹¹ and later by Park and Wright.¹²

Over 70 years after these initial reports, De Pasquale invoked the intermediacy of a nickelaoxetane in the Ni-catalyzed formation of cyclic carbonates from epoxides and CO₂.¹³ Shortly after that, Sharpless proposed a metallaoxetane intermediate in the chromyl chloride mediated epoxidation of alkenes.¹⁴ This report can possibly be regarded as the hour of birth

for many mechanistic speculations about an involvement of metallaoxetanes in transition metal catalyzed reactions.

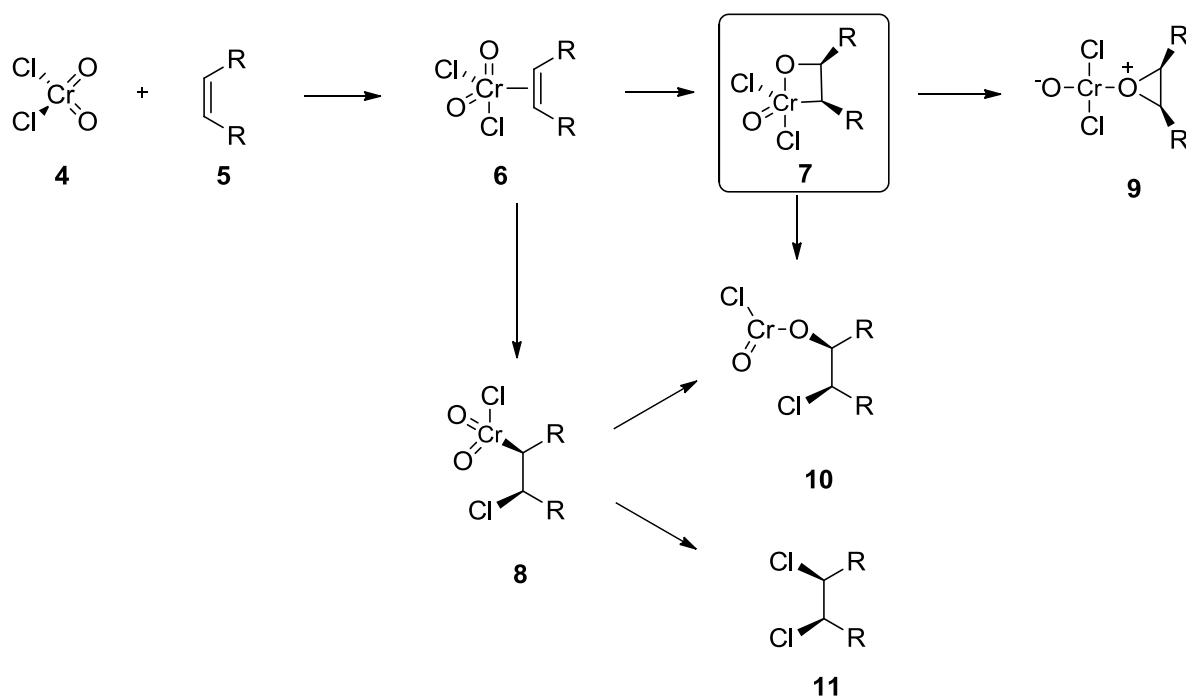
1.2.1 Transient Intermediates

1.2.1.1 Oxygen Transfer Reactions

1.2.1.1.1 Epoxidation and De-oxygenation of Epoxides

The oxidation of olefinic substrates under incorporation of one or more oxygen atoms is the most common transformation in which the intermediacy of metallaoxetanes has been proposed. One example is the epoxidation of olefins, where metallaoxetane intermediates have been invoked in multiple cases.^{6,15} In fact, the postulate of such an intermediate in the chromyl chloride catalyzed epoxidation of alkenes reported by Sharpless et al. in 1977 had significant impact.¹⁴ As mentioned earlier, this report marked the onset of many mechanistic speculations regarding the potential intermediacy of metallaoxetanes in transition metal-catalyzed or -mediated oxygen-transfer reactions. However, the mechanism of this classic reaction is still under debate/investigation.

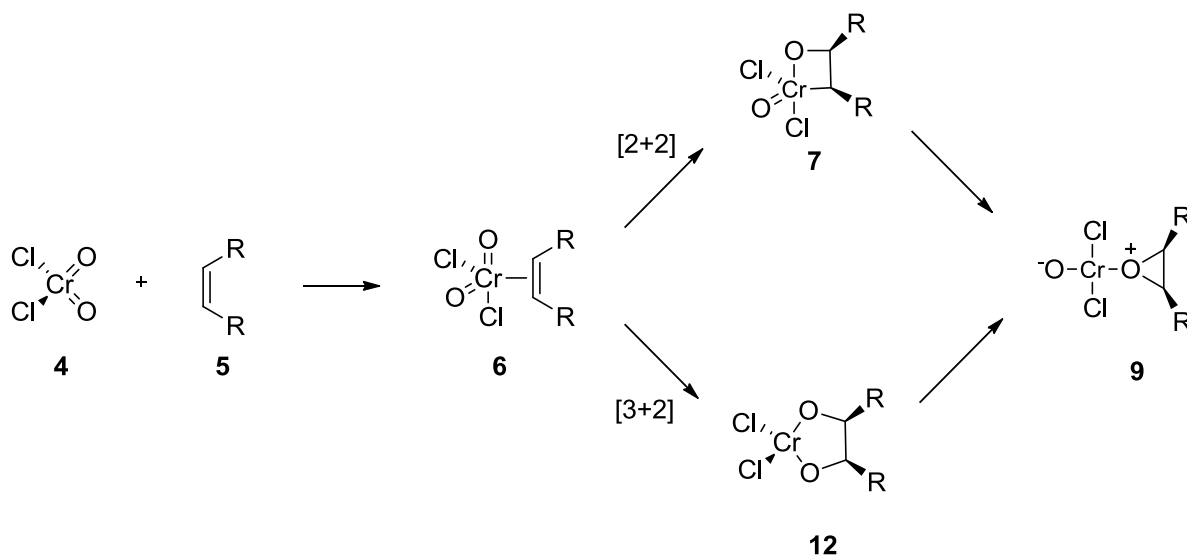
In their initial report, Sharpless and co-workers stated that chromaoxetane intermediate **7** – formed after olefin-metal pre-coordination (**6**) and subsequent [2+2] addition with an oxo ligand – would best explain the product distribution in the reaction of chromyl chloride **4** with olefins.¹⁴ The main products observed were the epoxide (**9**), a chlorohydrin (**10**) and a vicinal dichloride (**11**) (Scheme 1.2). Several theoretical studies were conducted to further elucidate this reaction mechanism.



Scheme 1.2 Chromyl chloride catalyzed epoxidation of olefins.

The first computational studies of this reaction mechanism were *ab initio* calculations performed by Goddard and Rappé,¹⁶⁻¹⁹ which supported the formation of a chromaoxetane intermediate. Further gas-phase studies by Bierbaum²⁰ and Beauchamp²¹ also corroborated this reaction pathway. The same intermediate was proposed in olefin oxidations performed with other oxochromium compounds, albeit without direct experimental evidence.²²⁻²⁴ Arguments against an oxametallacyclic intermediate in this reaction were voiced by Barrett based on product distribution analysis but without further spectroscopic or theoretical support.²⁵

Further scepticism arose with the onset of the animated debate about the reaction mechanism of transition metal catalyzed olefin dihydroxylation (Section 1.2.1.1.2). Detailed DFT calculations by Ziegler *et al.* contradicted the original hypothesis of Sharpless. In contrast to Goddard's earlier work¹⁶⁻¹⁹, Ziegler reported that a [3+2] addition of ethylene to chromyl chloride via chromadioxolane **12** was kinetically and thermodynamically favoured over the [2+2] addition (Scheme 1.3).^{26,27}



Scheme 1.3 [2+2] vs. [3+2] addition.

More recently, Tia *et al.* used hybrid DFT to carry out a theoretical study of this reaction.²⁸ Their work differed from Ziegler's calculations effectively in that a spin cross-over (from the singlet to the triplet state) was not found necessary. This in turn made the [2+2] pathway via a chromaoxetane more favourable again. However, DFT is known to have some severe deficiencies in calculating relative energies of different spin surfaces and cross-over between these is often undetectable with traditional methods and algorithms.²⁹

Another important class of olefin epoxidation where metallaoxetanes have been invoked include transition metal salen complexes. The asymmetric catalytic epoxidation of alkenes first reported by the groups of Jacobsen³⁰ and Katsuki³¹ is perhaps the most prominent olefin oxidation employing these complexes. Even earlier, Kochi *et al.* had reported non stereoselective catalytic epoxidation of unactivated alkenes employing a chromium-salen system with iodosobenzene as stoichiometric oxidant (Figure 1.2).^{32,33} A subsequent report described a manganese-salen system that displayed increased reaction rates and a broader substrate scope.³⁴ These and related Mn- and Cr-salen systems gained considerable interest with respect to their utility, as well as for purposes of elucidating the active mechanism.^{15,35,36}

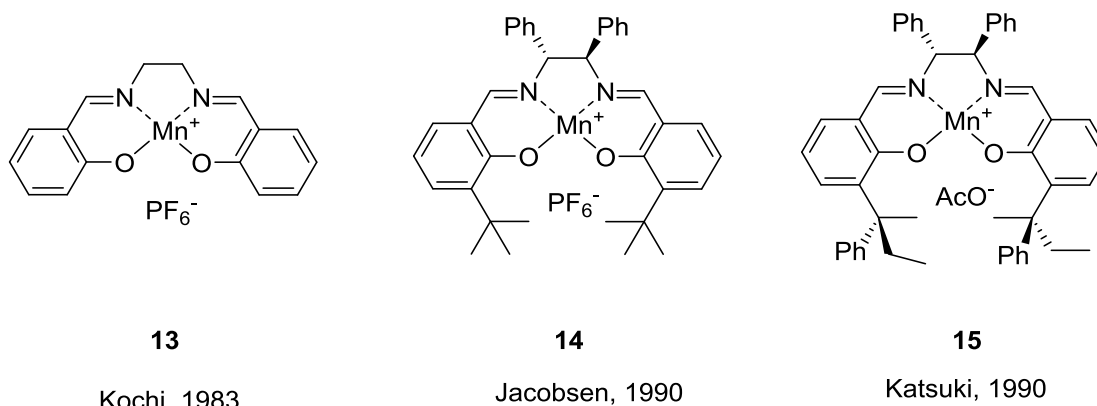
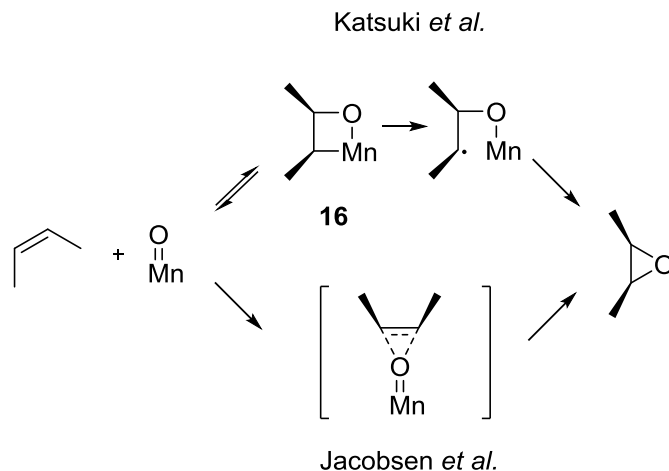


Figure 1.1.2 Pioneering Mn-salen catalyst systems used in olefin epoxidation.

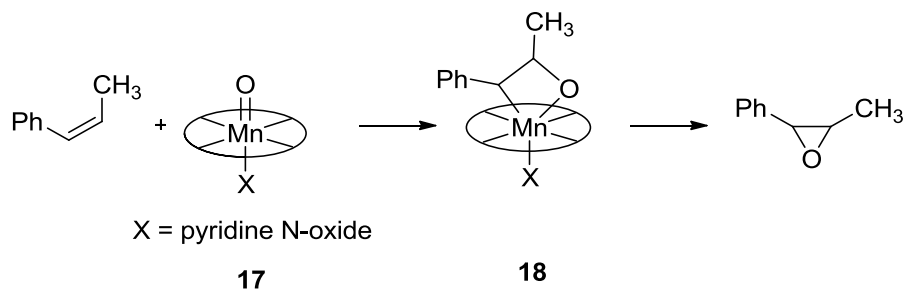
Kochi proposed a radical intermediate for the Mn-salen system,³⁴ and tentatively offered two possible intermediates for the Cr system, one of which was a chromaoxetane.³³

After the discovery of the asymmetric versions of this reaction by Jacobsen and Katsuki, more and more mechanistic studies were reported. Through this, the discussion about putative mechanisms intensified. Nevertheless, no definitive answer to the mechanistic question has been found to date. Indeed, most probably several mechanisms are operational and competing with each other in the individual cases.³⁶ Jacobsen suggested the direct transfer of the oxo ligand to the alkene in his original report.³⁰ Katsuki and co-workers initially rationalized the stereochemical results with a radical intermediate but later reviewed their mechanistic proposal to invoke a metallaoxetane intermediate (Scheme 1.4).³⁷ In this proposal, the reversible formation of manganaoxetane **16** was followed by irreversible formation of a radical intermediate and fast epoxide closure.



Scheme 1.4 Proposed mechanisms for the Mn-salen catalyzed epoxidation of olefins.

The most noteworthy opposition against metallaoxetane intermediates in these reactions came from the Jacobsen group when it was found that pyridine *N*-oxide additives enhanced yield and selectivity of the reaction.^{38,39} The main argument presented was that in the case of a metallaoxetane intermediate (**18**), the Mn center in this species would have to be heptacoordinate Mn, which is unusual.³⁹ This is the case when pyridine *N*-oxide additives are present in the reaction mixture, taking up the sixth coordination site on **17** (Scheme 1.5). These additives led to increased yield and stereoselectivity of the reaction, which implies that they are in some interaction with the metal.⁴⁰ Heptacoordinate Mn complexes have been reported, but only for Mn(II) complexes.^{41,42}



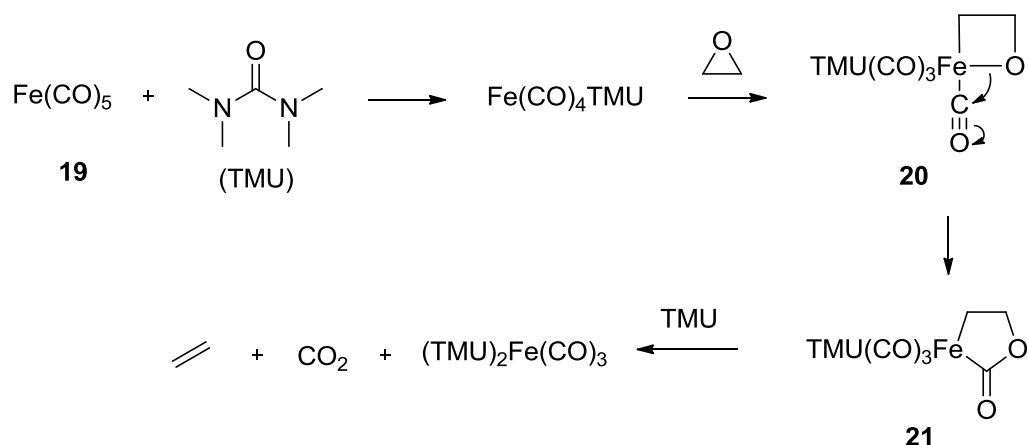
Scheme 1.5 Heptacoordinate Mn-species as metallaoxetane intermediates.

Katsuki also proposed a metallaoxetane intermediate for the Cr-salen systems, although the same considerations as with the Mn catalyst arose regarding the necessity of a heptacoordinate chromium species to accommodate the metallaoxetane.⁴³ Unambiguous

proof for the involvement of metallaoxetane species in this transformation has, to date, not been found.

Among other work, the involvement of metallaoxetanes has also been discussed in heterogeneous epoxidation,^{44,45} epoxidations catalyzed by metal-porphyrin based systems⁴⁶⁻⁴⁹ and in the asymmetric epoxidation of olefins by a Ru catalyst employing a sugar-based ligand.⁵⁰⁻⁵² Reductive elimination of an epoxide from an isolated auraoxetane⁵³ as well as platinaoxetanes^{54,55} was later verified experimentally (Section 1.2.2.3).

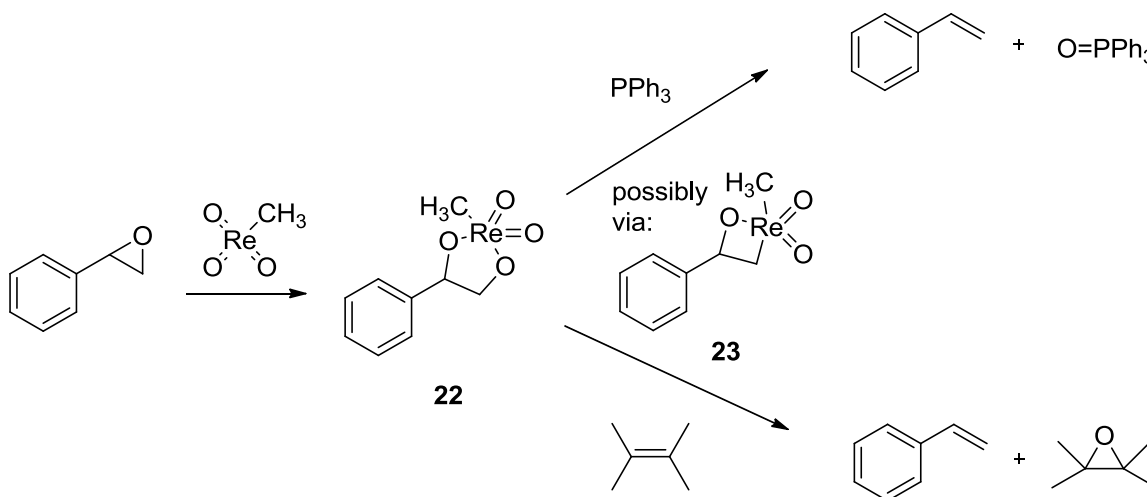
The de-oxygenation of epoxides with transition metal complexes is formally the reverse reaction of olefin epoxidation with transition metal oxo complexes. Thus, it is of little surprise that metallaoxetane intermediates have been postulated for this transformation as well. In the same year as Sharpless' proposal of metallaoxetane intermediates, Alper suggested a ferraioxetane as a possible intermediate in the deoxygenation of epoxides with a stoichiometric amount of iron pentacarbonyl (**19**). After oxidative addition to the C-O bond the metallaoxetane **20** could rearrange to the five-membered metallalactone **21** from which CO₂ and ethylene could be eliminated (Scheme 1.6).⁵⁶



Scheme 1.6 De-oxygenation of epoxides with Fe(CO)₅.

Rhenium oxides such as methyltrioxyrhenium (MTO), CH₃ReO₃, besides their employment in olefin epoxidation⁵⁷⁻⁵⁹ and dihydroxylation^{57,59-61} could also be used for epoxide deoxygenation.⁶²⁻⁶⁷ Espenson and co-workers described the transfer of an oxygen atom from epoxides to triphenylphosphine,⁶³ as well as to other olefins under MTO catalysis.⁶⁴ They found that rhenadioxolane **22** was formed in this process from which the

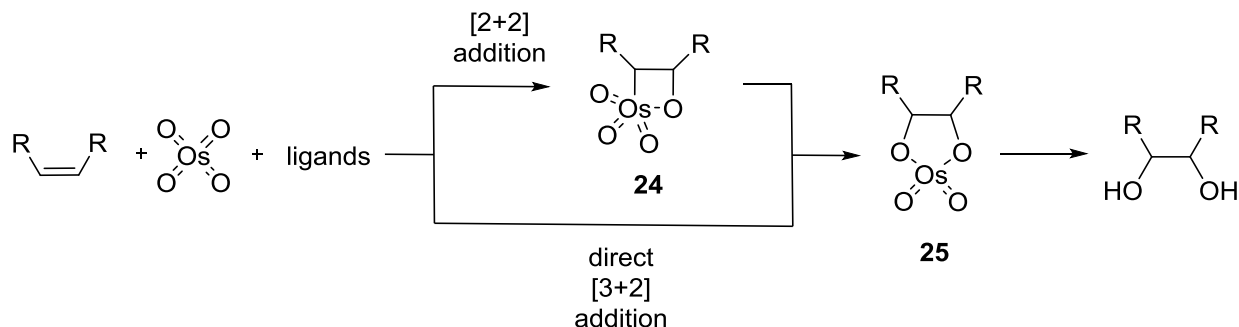
alkene is expelled. It was hypothesized that the decomposition of **22** could lead via rhenaoxetane **23** (Scheme 1.7). Alkene extrusion from rhenadioxolanes has been studied by Gable and co-workers^{62,68} as well as Chen and co-workers⁶⁹⁻⁷² and the intermediacy of metallaoxetanes has been corroborated through these experimental and computational investigations (Section 1.2.1.1.2).



Scheme 1.7 Oxygen transfer from epoxides to PPh₃ or olefins.

1.2.1.1.2 Dihydroxylation and Di-dehydroxylation

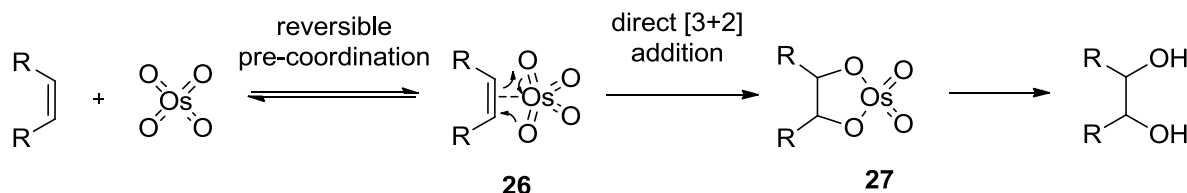
When Sharpless proposed a metallaoxetane intermediate in his report on the chromyl-chloride epoxidation of alkenes,¹⁴ the involvement of this structure in other metal mediated oxidation reactions of olefins, such as the dihydroxylation of alkenes by osmium tetroxide, was also considered. [2+2] Addition of Os=O to a C=C double bond would form osmaoxetane **24**, which could then rearrange to 2,5 osmadioxolane **25**. Up to that point, a direct [3+2] addition mechanism was generally considered for this transformation (Scheme 1.8).⁷³⁻⁷⁶



Scheme 1.8 [2+2] and [3+2] addition pathways in olefin dihydroxylation.

The challenge to this mechanistic proposal^{14,77-85} triggered extensive experimental and theoretical studies along with controversial reports thereof over the following two decades.^{7,86} Initial support for a stepwise mechanism including formation of an osmaoxetane came from the observed non-linearity of Eyring plots of temperature vs. stereoselectivity, which indicated a change in mechanisms throughout the reaction.⁷⁹ A direct [3+2] mechanism was considered unlikely based on the observed electronic effects of bases and substrates employed in the reaction.^{82,85,87} Similar proposals were made by Tomioka⁸⁸⁻⁹⁰ and others.⁹¹⁻⁹³ Early theoretical studies supported the possibility of initial formation of the oxetane and subsequent rearrangement to the dioxolane but transition state energies were not calculated.^{83,94,95}

Corey *et al.* rejected a stepwise [2+2] mechanism, arguing instead for a direct [3+2] addition.⁹⁶⁻¹¹⁰ The observed Michaelis-Menten kinetics were attributed to a fast, reversible coordination of the olefin to the metal center as in structure **26**, which then underwent direct [3+2] addition to yield the metalladioxolane **27** (Scheme 1.9).¹⁰⁶ The non-linearity in Eyring plots reported earlier by Göbel *et al.* was thus ascribed to this pre-equilibrium.⁷⁹



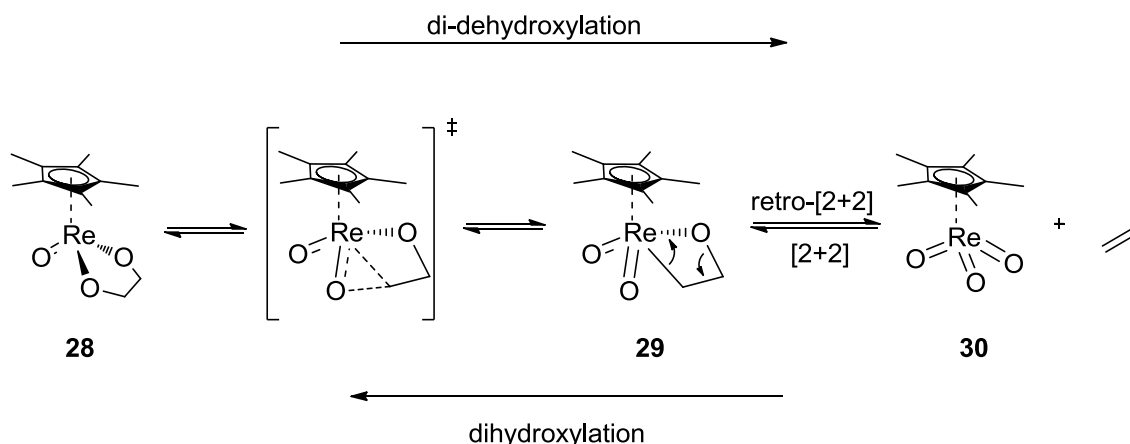
Scheme 1.9 [3+2] addition after reversible olefin precoordination.

Theoretical orbital symmetry studies by Jørgensen and Hoffman^{111,112} were likewise in support of a [3+2] addition. In 1996 and 1997, three groups independently reported DFT

studies comparing the [2+2] and [3+2] pathways.¹¹³⁻¹¹⁵ These calculations unequivocally disfavoured the [2+2] mechanism involving the metallaoxetane formation, based on prohibitively high activation barriers for oxetane formation as well as rearrangement to the dioxolane. In the same time period, the Corey and Sharpless groups published results on kinetic isotope effect measurements which revealed a highly symmetric transition state.^{107,116} These theoretical and experimental findings along with some later reports on OsO₄¹¹⁷⁻¹²¹ and similar systems^{86,122,123} established that the osmium tetroxide mediated olefin dihydroxylation and its asymmetric analogue⁷⁸ do not proceed through an osmaoxetane intermediate.

Other longstanding dihydroxylation protocols employ permanganate salts or ruthenium tetroxide. Similar to the case of OsO₄, the mechanism was considered to follow a direct [3+2] addition pathway⁷³ even though some reports at least did not rule out the possibility of a manganaoxetane intermediate.¹²⁴⁻¹²⁶ The concerted mechanism was corroborated by several theoretical and experimental studies^{96,127-135} and the metallaoxetane intermediate was dismissed in the light of the collected data.

Various rhenium oxides have also been shown to dihydroxylate olefins.¹³⁶⁻¹³⁹ For the di-dehydroxylation of diols the intermediacy of a rhenaoxetane has been proposed by Gable and co-workers.^{68,140-143} Rhenadioxolane **28** decomposed to rhenium oxide **30** and olefins, which was suggested to occur through a retro [2+2] addition of an intermediate rhenaoxetane **29** (Scheme 1.10). It was postulated that dihydroxylation (the microscopic reverse of the studied reaction) would follow through the same pathway in the opposite direction.



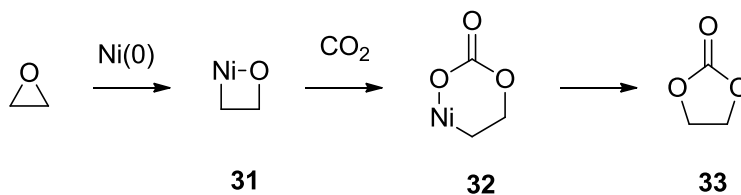
Scheme 1.10 Dihydroxylation and di-dehydroxylation with rhenium oxides.

Experimental support for such a decomposition pathway of rhenium dioxolanes was given by kinetic investigations^{68,140-143}, frontier orbital calculations.^{62,71,72} as well as mass spectrometric studies⁶⁹⁻⁷¹ by the groups of Gable and Chen.

The reactions of several other group 6, 7 and 9 transition metal oxides with alkenes have been studied using computational methods by Frenking and others.^{128,144-147} In general, [2+2] addition of olefins and mid- to late transition metal-oxo bond are energetically disfavoured by most modern theoretical methods.⁷ Among the few exceptions are selected rhenium oxide systems.^{57,148-151}

1.2.1.1.3 Other Oxygen-Transfer Reactions

In 1973, a metallaoxetane intermediate had been suggested by De Pasquale for the fixation of CO₂ with epoxides to give cyclic carbonates under Ni catalysis.¹³ In this reaction, the first step was proposed to be oxidative addition of the Ni(0) catalyst to one of the C-O bonds of the epoxide which yields the intermediate nickelaoxetane **31** (Scheme 1.11). Subsequent CO₂ insertion afforded metallacycle **32** from which Ni was reductively eliminated with concomitant formation of carbonate **33**.



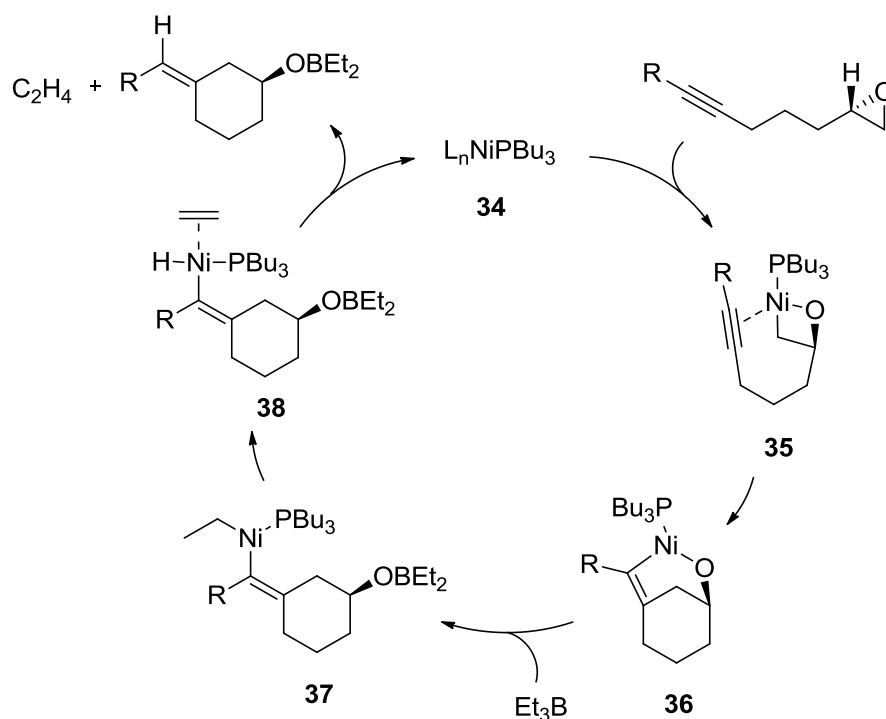
Scheme 1.11 Nickelaoxetane intermediates in the CO₂ fixation with epoxides.

A similar reaction pathway has been suggested by Jiang *et al.* in a later adaption of this reaction employing a Re catalyst. In analogy to De Pasquale's proposal they invoked oxidative addition of a Re(CO)₅Br catalyst to the less hindered C-O bond of the epoxide followed by CO₂ insertion into the Re-O bond and reductive elimination of the metal to give the cyclic carbonate.^{152,153}

Recent DFT studies by Guo *et al.* of the transformation catalyzed by Jiang's Re(CO)₅Br system gave theoretical support for the intermediacy of a rhenaioxetane by comparison with the energetic profiles of possible alternative pathways.¹⁵⁴

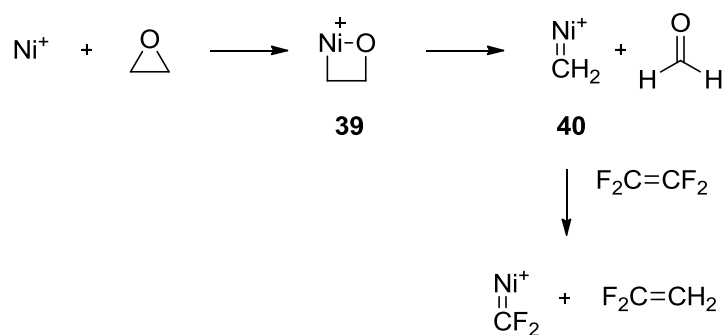
1.2.1.2 C-C Bond Forming Reactions

Jamison and co-workers reported the Ni-catalyzed reductive coupling of alkynes and epoxides. In the proposed reaction mechanism, nickelaoxetane **35** appears after oxidative addition of the Ni(0) catalyst (**34**) to the epoxide.¹⁵⁵ Similar insertions have been reported for Ni and other group 10 metals before.^{13,156-160} The tethered alkyne then undergoes migratory insertion into the Ni-C bond to yield the six-membered oxametallacycle **36** containing a bridgehead olefin. Jamison reasoned that the comparably long Ni-O and Ni-C bonds should release ring strain to an extent that the "anti-Bredt" double bond can be accommodated. Upon reaction with triethylborane the Ni-O bond is cleaved (**37**) and Ni is eliminated through β-H elimination and subsequent reductive elimination (**38**) (Scheme 1.12).



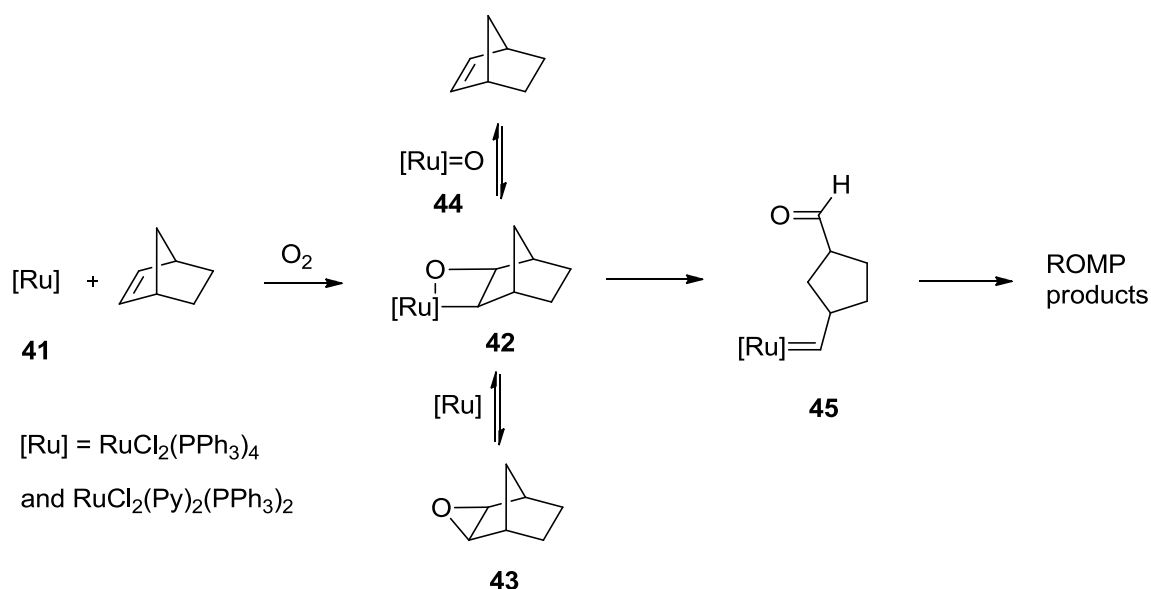
Scheme 1.12 Proposed nickelaoxetane intermediate
in reductive coupling of alkynes and epoxides.

Furthermore, metallaoxetanes have been proposed as intermediates in olefin metathesis reactions as precursors of the propagating metalla alkylidene species.¹⁶¹ Beauchamp and co-workers hypothesized the formation of nickelaoxetane **39** in the reaction of gaseous Ni^+ with ethylene oxide in an ion beam apparatus.¹⁶² A [2+2] cycloreversion yielded nickel alkylidene **40** and formaldehyde. The alkylidene was then able to undergo cross metathesis with perfluoroethylene $\text{CF}_2=\text{CF}_2$ (Scheme 1.13).



Scheme 1.13 Gas-phase formation of a nickel alkylidene species from a nickelaoxetane.

Rooney and co-workers observed a significant increase of reaction rates in the ring-opening metathesis polymerization (ROMP) of norbornene with various ruthenium complexes (**41**) in the presence of molecular oxygen.¹⁶³ At the same time epoxidation products **43** were found. When the ruthenium complex was oxidized in a preceding step (**44**) and then used in the reaction under exclusion of air, the same rate acceleration was noted as was when the epoxide was used as substrate. These observations led the authors to propose that after oxidation of the Ru complex the formation of the transient ruthenaoxetane **42** took place which underwent ring opening to give the metal alkylidene species **45** that promoted ROMP (Scheme 1.14).



Scheme 1.14 ROMP via a ruthenaoxetane.

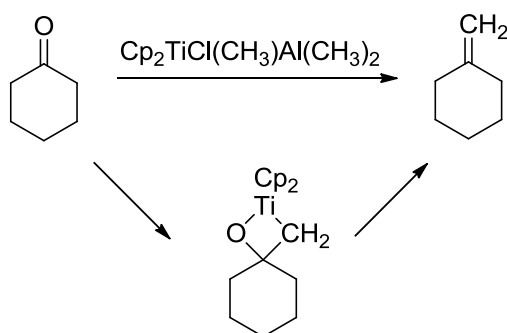
Ab-initio calculations by Rappé and Goddard supported such a proposal.¹⁶⁻¹⁹ Several years later, Rooney and Gilheany reported that OsO₄ catalyzed ROMP of norbornene when heated to 60 °C for three days in a sealed tube.¹⁶⁴ When a stoichiometric mixture of norbornene and OsO₄ were reacted at room temperature, the expected osmiumdioxolane was formed along with a small amount of polymerization product. This reactivity requires the formation of metal alkylidenes at some place in the reaction mechanism and the authors concluded that these would be formed directly from an intermediate osmaoxetane.

Interestingly, these results were never considered in the discussion of the mechanism of OsO_4 catalyzed dihydroxylation of olefins (Section 1.2.1.1.2).

1.2.2 Isolated Cases

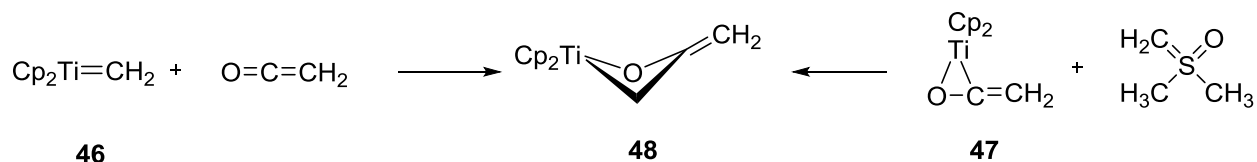
1.2.2.1 Early Transition Metallaoxetanes

The Tebbe olefination of carbonyl groups is a classic example for an organometallic transformation¹⁶⁵ for which the intermediacy of a metallaoxetane was postulated (Scheme 1.15).



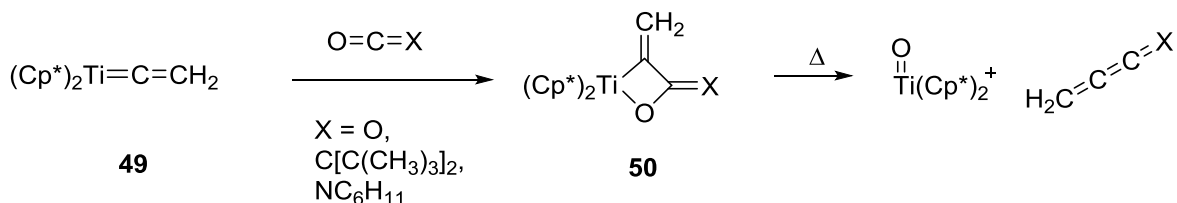
Scheme 1.15 The Tebbe olefination.

Stimulated by the studies towards a better understanding of the Tebbe reaction mechanism, several groups set out to prepare and analyze titanaoxetanes, which were the proposed intermediates.¹⁶⁵⁻¹⁶⁹ Grubbs and co-workers were the first to report the preparation of such a species (**48**) from the reaction of a titanium alkylidene complex **46** with ketene as well as from a titanium ketene complex **47** with dimethylsulfonium methylide (Scheme 1.16). They based the structural assignment on NMR spectroscopic studies and concluded the symmetry of the complex was disturbed due to puckering of the titanaoxetane ring.¹⁷⁰



Scheme 1.16 Preparation of a titanaoxetane via two different pathways.

In 1993, Beckhaus et al. succeeded in isolating titanaoxetanes **50** with two exocyclic double bonds formed from the reaction of Cp^{*}Ti vinylidene **49** with CO₂, ketenes and isocyanates (Scheme 1.17).¹⁷¹ The crystal structure of the isocyanate product revealed a twisted conformation of the oxametallacycle while the *t*-butylketene product was essentially planar.



Scheme 1.17 Titanaoxetanes with two exocyclic double bonds.

The resulting complex was thermally stable up to 150 °C, but underwent [2+2] metathesis in the mass spectrometer in a “classical” Tebbe-like fashion to yield a metal oxide and an alkene.¹⁷²

Böhme and Beckhaus undertook theoretical studies confirming that planarity of the titanaoxetanes is the energetically preferred conformation and that exo-double bonds in the 4 position stabilize the ring towards cycloreversion and metathesis. They also provided a theoretical explanation for the classical metathesis of titanaoxetanes to give a titanium oxide and an alkene or allene. Due to the two energetically low lone pairs on oxygen in and perpendicular to the ring plane, strong interactions between the oxygen and the metal center are present (Figure 1.3). This leads to metathesis rather than cycloreversion or electrocyclic ring-opening.¹⁷³

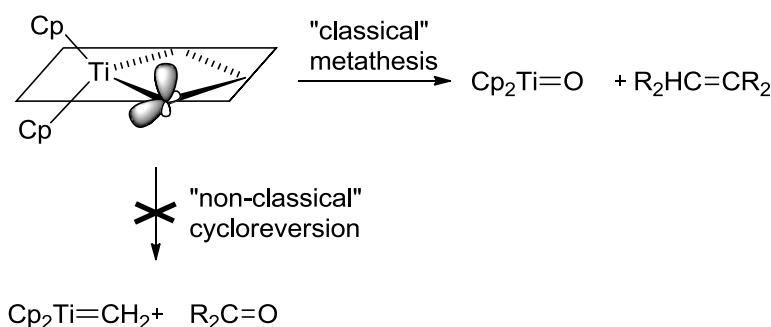
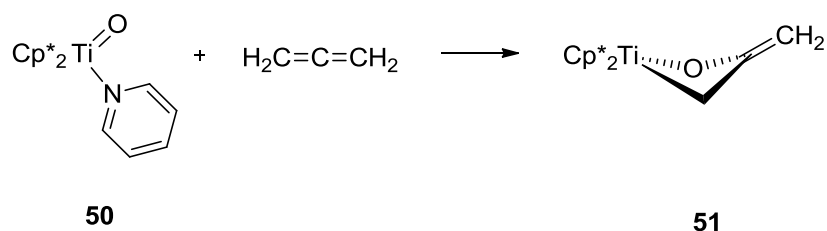


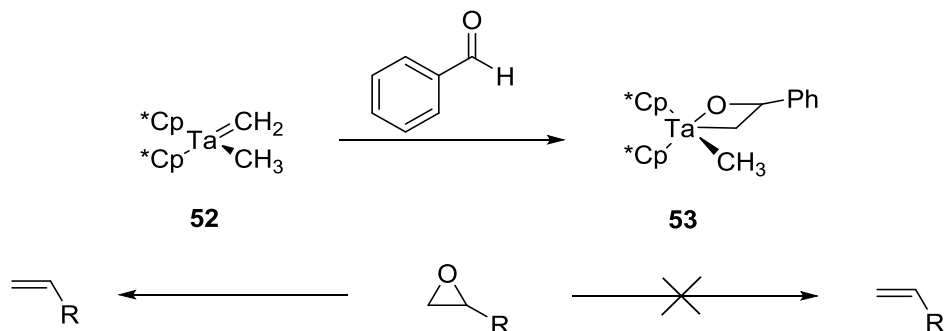
Figure 1.1.3 Lone pair orientation allows strong M-O interactions.

Another notable way for the preparation of titanaoxetanes was reported by Andersen and co-workers.¹⁷⁴ They described the formation of titanaoxetane **52** from $\text{Cp}^*_2\text{Ti}(\text{O})\text{py}$ (**51**) and allene, the first synthesis of such a structure from a metal oxide and an olefin. In the extensive discussion of [3+2] vs [2+2] addition mechanism of metal oxo compounds with alkenes in regards to olefin epoxidation and dihydroxylation such a pathway had been widely considered as energetically too demanding (Sections 1.2.1.1.1 and 1.2.1.1.2). The authors described the titanaoxetane as puckered based on the crystal structure when compared to the complexes isolated by Beckhaus.¹⁷¹ An increased Ti-O bond length was observed which is in accordance with calculations of a weakening of that bond in the case of ring puckering (Scheme 1.18).¹⁶⁶



Scheme 1.18 Titanaoxetane via [2+2] addition of a metal oxide and an olefin.

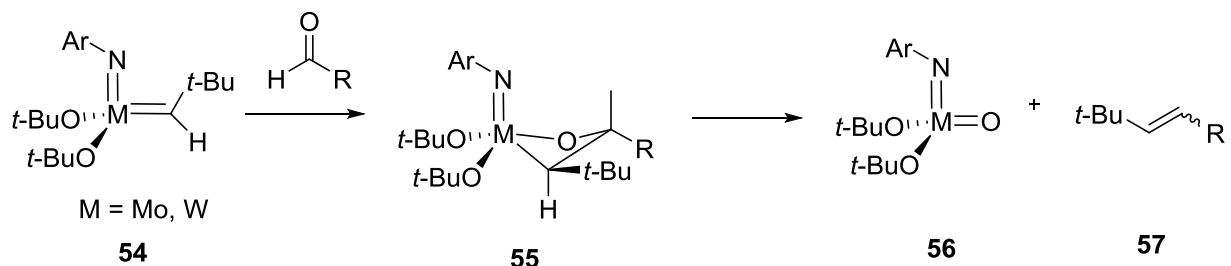
In an effort to elucidate whether the mechanism of transition metal catalyzed deoxygenation of epoxides (Section 1.2.1.1.1) involved metallaoxetane intermediates, Bercaw and co-workers prepared moderately stable tantalaoxetanes by [2+2] cycloaddition of tantalum alkylidenes and aldehydes.¹⁷⁵ The crystal structure of the product from the reaction of $\text{Cp}^*_2\text{Ta}(=\text{CH}_2)\text{CH}_3$ with benzaldehyde showed a slightly puckered ring. However, while the parent alkylidene **52** was able to catalyze the deoxygenation of epoxides successfully, the derived tantalaoxetanes **53** failed to promote this reaction (Scheme 1.19). During monitoring of the reaction progress no intermediates could be detected. The authors concluded thus that this deoxygenation does not proceed via a stepwise metallaoxetane mechanism.



Scheme 1.19 Tantalaoxetane is not involved in epoxide de-oxygenation.

1.2.2.2 Mid Transition Metallaoxetanes

As mentioned earlier, metallaoxetanes were also postulated to be intermediates in the formation of metathesis-active alkylidene species (Section 1.2.1.2). Schrock and co-workers prepared tungsten- and molybdaoxetanes **55** through [2+2] cycloadditions of aldehydes with the appropriate metal-alkylidenes **54**.¹⁷⁶ These underwent metathetical ring opening and formed a metal-oxo species **56** and coupled products **57** (Scheme 1.20). A molybdaoxetane could be isolated and revealed a slightly puckered ring. Therefore, Schrock and co-workers concluded that the metallaoxetanes are structurally and possibly mechanistically closely related to their all-carbon metallacyclobutane counterparts.

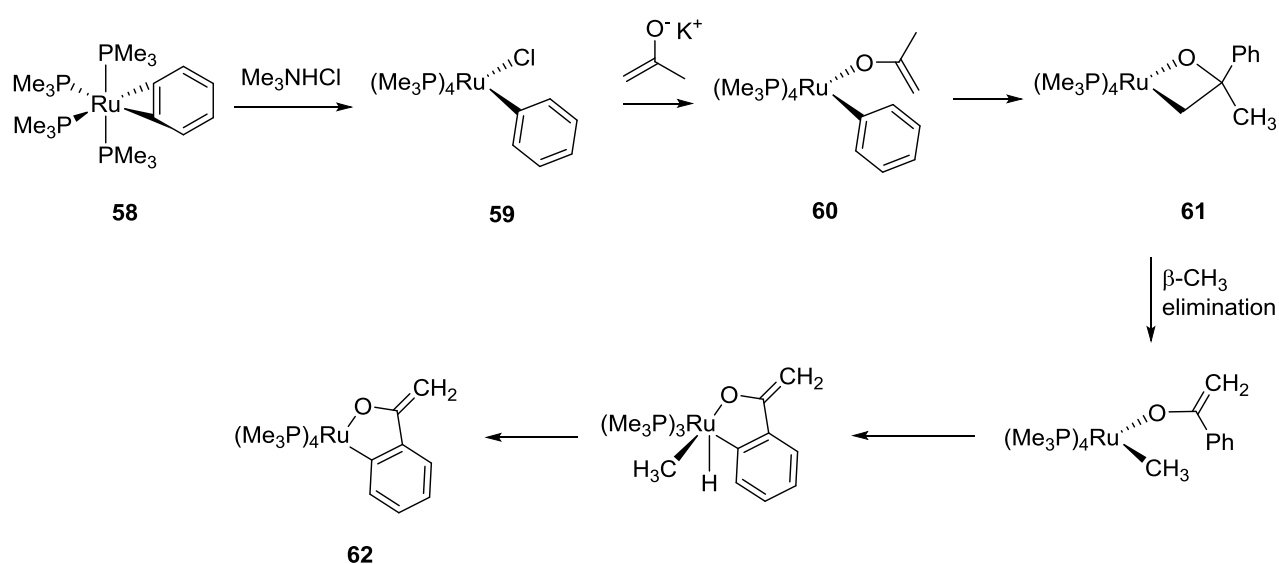


Scheme 1.20 Isolated molybdaoxetanes and tungstenaioxetanes.

Another class of metallaoxetanes was detected by Bergman and co-workers upon closer investigation of the highly reactive Ru-benzyne complex **58**.^{177,178} Treatment of **58** with Me_3NHCl generated phenylchlororuthenium complex **59**. Upon exposure of **59** to the potassium enolate of acetone, ruthenaioxetane **61** was formed via the O-bound metallaoxetane (**60**) as a transient intermediate. The mechanistically unusual formation of the

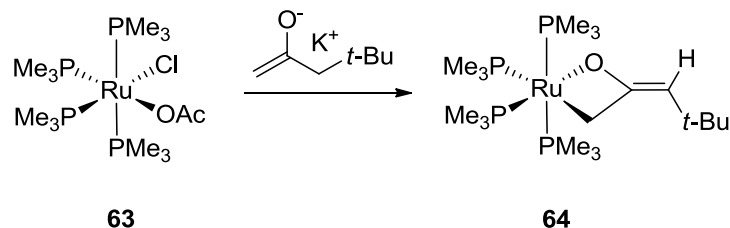
metallaoxetane formally happens through migration of the Ru bound phenyl group to the central carbon of the enolate and subsequent ring closure.¹⁷⁹

The reactivity of these metallaoxetanes is diverse and mechanistically unique.¹⁸⁰ For example, β -CH₃ elimination occurs upon gentle heating and leads to cleavage of the Ru-C bond. Subsequent ortho-metalation of the migrated Ph group and C-H reductive elimination led to the extrusion of methane and formation of the five membered oxametallacycle **62** (Scheme 1.21). In the course of this reaction, one new C-C bond was formed and one was cleaved.



Scheme 1.21 Formation of a ruthenaoxetane from a Ru-benzyne complex.

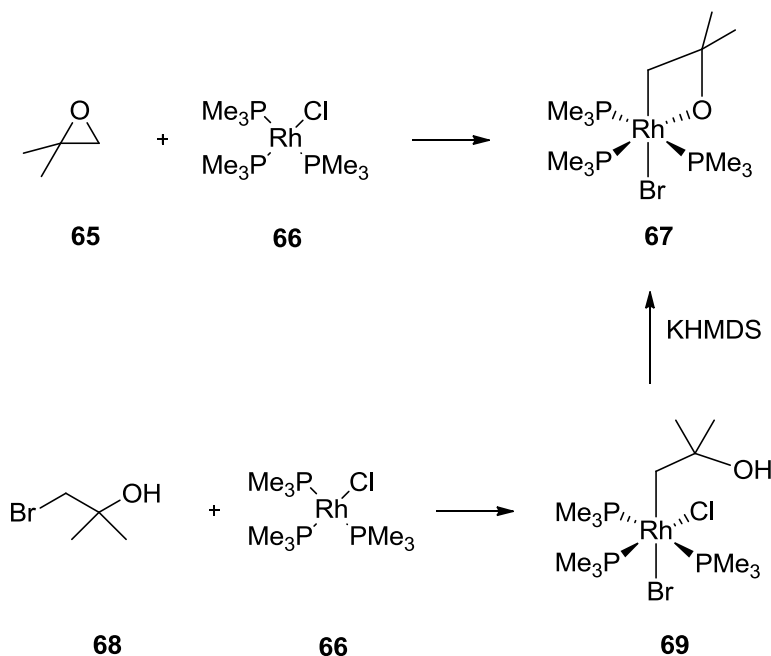
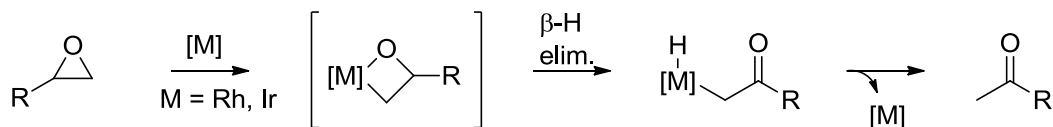
Reaction of the ruthenium acetate chloride complex $[(\text{PMe}_3)_4\text{Ru}(\text{OAc})\text{Cl}]$, **63** with the potassium enolate of 4,4-dimethyl-2-pentanone yielded the related ruthenaoxetane **64** (Scheme 1.22).¹⁷⁹ Unlike the all sp^3 -hybridized ruthenaoxetanes above, this structure could be crystallized and subjected to X-ray crystallography showing that the metallacycle portion is essentially planar, which was ascribed to presence of the exocyclic double bond.¹⁸⁰



Scheme 1.22 A crystalline ruthenaoxetane.

1.2.2.3 Late Transition Metallaoxetanes

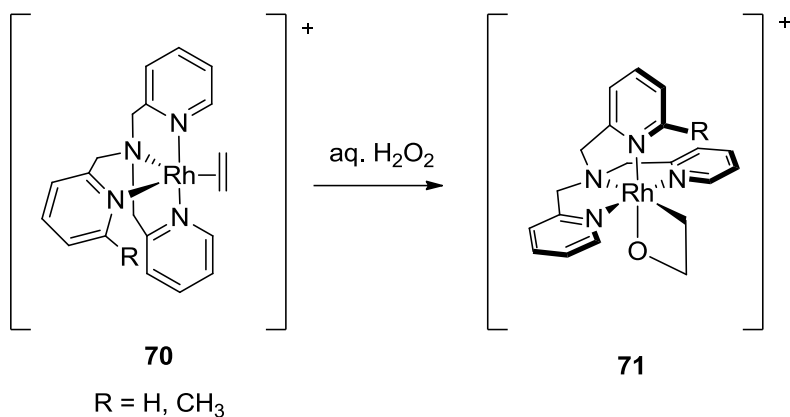
The exposure of simple epoxides to low-valent Ir and Rh complexes as Ir(COE)(PMe₃)₃Cl or Rh(PMe₃)₃Cl leads to rearrangement of the epoxides to ketones.^{181,182} In their initial reports of this transformation, Milstein *et al.* proposed sequential C-O oxidative addition, formation of a metallaoxetane, β-H elimination and reductive elimination, although they could not isolate any intermediates. In a subsequent publication, Milstein reported the generation of rhodaoxetane **67** from the reaction of isobutylene oxide (**65**) and Rh(PMe₃)₃Br (**66**), which proved the feasibility of their proposal as well as the general possibility of oxidative addition of low valent late metal complexes to simple non-activated epoxides.¹⁸³ Rhodaoxetane **67** could also be prepared by C-Br oxidative addition of Rh-complex **66** to a halohydrin and subsequent treatment with base (Scheme 1.23). X-ray analysis revealed the four membered ring to be effectively planar,¹⁸⁴ which was also supported by a theoretical study of the bonding interactions.¹⁸³



Scheme 1.23 Formation of a substituted rhodaoxetane through oxidative addition to an epoxide.

As the oxidative addition to an epoxide had been observed, a theoretical study of reductive elimination – the microscopic reverse – was performed to see whether formation of an epoxide from a metallaoxetane was feasible. However, the calculations led to the conclusion that the stability of the metallaoxetane was significantly higher than epoxide plus metal fragment. This explained the observed direction of the reaction towards metallaoxetane formation.¹⁸³

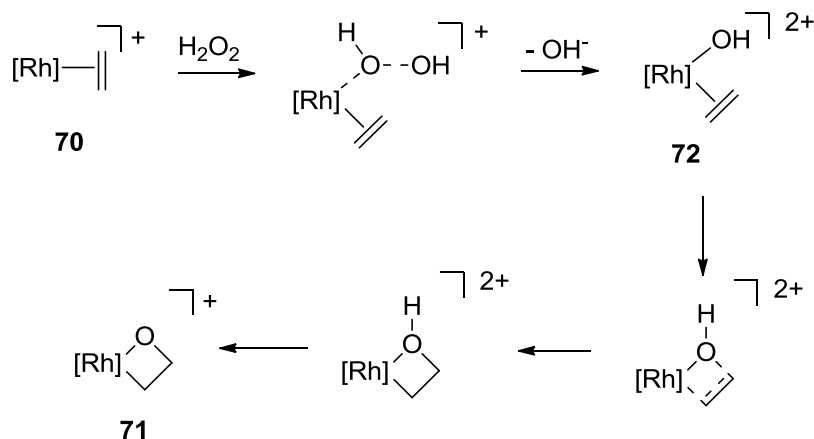
In 1997 De Bruin *et al.* reported the oxidation of Rh-ethylene and Rh-COD complexes with aqueous H₂O₂ to give the corresponding rhodaoxetanes.¹⁸⁵ Rhodaoxetane **71**, derived from ethylene, was the first stable unsubstituted 2-metallaoxetane reported (Scheme 1.24). As this system is the foundation of our work with oxametallacyclobutanes, it will be discussed in greater detail in the following.



Scheme 1.24 The first isolable unsubstituted metallaoxetane.

Iridium analogues of the described rhodaoxetanes have been prepared by O₂ oxidation of the respective ethylene complexes.¹⁸⁵

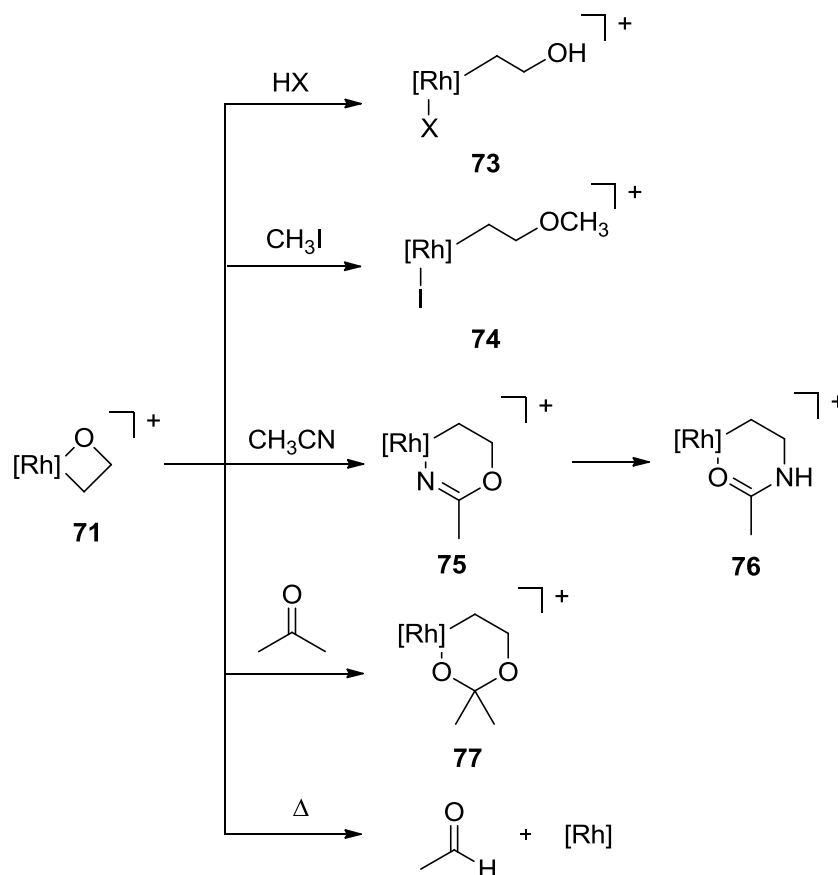
The mechanism of this metallaoxetane formation with hydrogen peroxide was investigated by DFT-calculations by Budzelaar *et al.*¹⁸⁶ After initial homolytic H₂O₂ cleavage, a Rh(III)-hydroxo species (**72**) is formed oxidatively. Subsequent cyclization and deprotonation yields Rh(III)-oxetane **71** (Scheme 1.25).



Scheme 1.25 Mechanism of rhodaoxetane formation.

Investigation of the reactivity of the unsubstituted rhodaoxetane revealed significant nucleophilicity of the oxetane oxygen. Thus, the reactivity of **71** towards many electrophiles was examined (Scheme 1.26).¹⁸⁷ Under Brønsted acidic conditions, the proton activated the oxetane, promoting ring opening. Depending on the choice of anion, a stable Rh(III) complex

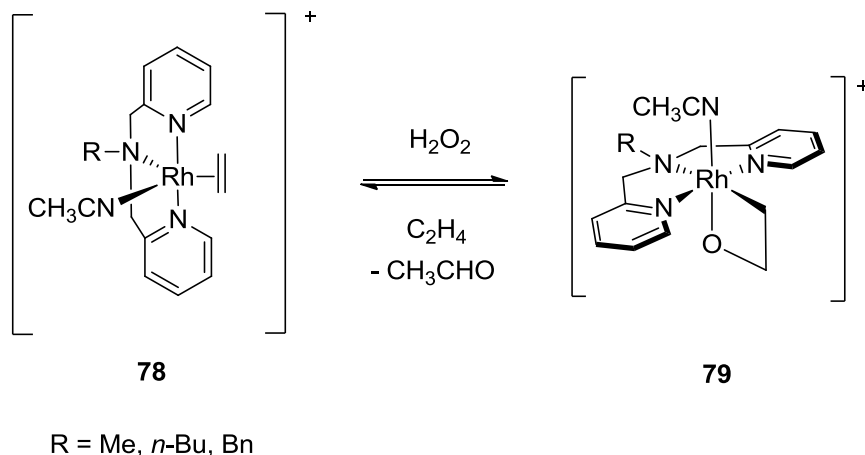
with coordinated anion could be formed (**73**). Similar reactivity was observed with methyl iodide (**74**). Acetonitrile was incorporated into rhodaoxetane **71** by attack of the oxetane oxygen on the electrophilic nitrile carbon. The extended 6-membered metallacycle **75** was formed which underwent rearrangement at elevated temperatures to perform a net amination of the coordinated olefin (**76**).¹⁸⁸ A very slow incorporation of acetone was also observed. In this case the six membered 4-metalla-1,3-dioxane **77** was the reaction product. Upon heating rhodaoxetane **71** in DMSO, β -H elimination occurred and the generation of acetaldehyde was observed.¹⁸⁷



Scheme 1.26 Reactivity of rhodaoxetane **71**.

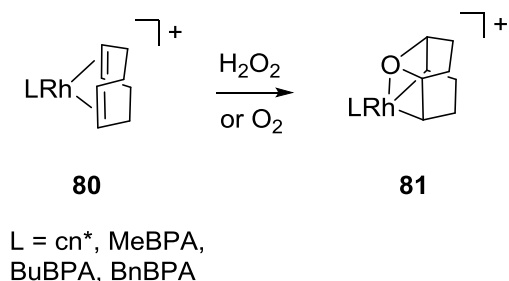
Substitution of the tetradentate TPA ligand to tridentate derivatives and the employment of a labile acetonitrile ligand further increased the reactivity of the rhodaoxetane **79**.¹⁸⁹ Acetaldehyde formation occurred through dissociation of the acetonitrile ligand and opening of a coordination site, which allowed for ligand

rearrangement and β -H elimination at room temperature in CD_2Cl_2 for all three TPA analogues (Me, Bu and Bn-BPA). In the presence of ethylene, the BnBPA-Rh(I)-ethylene complex was reformed (Scheme 1.27). However, catalytic turnover could not be achieved, presumably because of decomposition or poisoning of the catalyst through competing reactions with H_2O_2 .



Scheme 1.27 Tridentate ligands increase reactivity of rhodaoxetane.

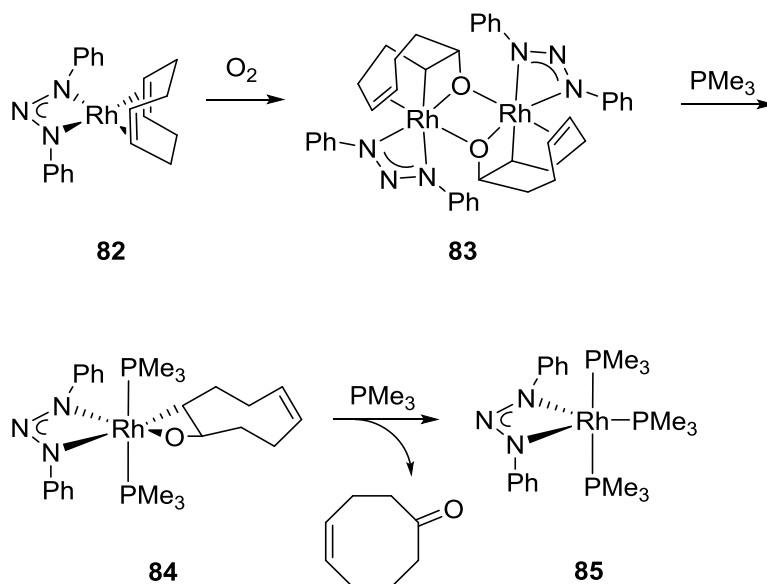
The Rh-COD complexes **80** were oxidized by H_2O_2 in a similar way to give substituted rhodaoxetanes **81**. Both internal olefins were oxygenated by the same oxygen resulting in a transannular ether formation.^{185,190} Ether formation was proposed to occur through rhodaoxetane formation on one olefin and subsequent migratory insertion of the second double bond into the Rh-O bond (Scheme 1.28).



Scheme 1.28 Rhodaoxetane from an internal alkene.

Tejel and co-workers reported the aerobic oxidation of a diphenyltriazenide-Rh-COD complex **82** to a dimeric Rh-oxetane **83** under 100% O_2 incorporation.¹⁹¹ When this dimeric metallaoxetane was treated with trimethylphosphane in benzene at 35 °C, transformation

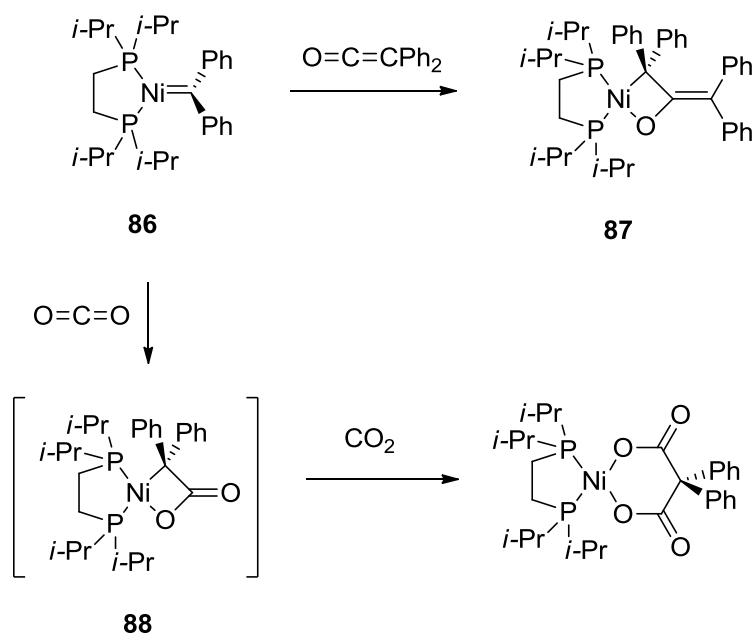
into the monomeric rhodaoxetane **84** and consequent quantitative formation of 4-cyclooctenone **85** was observed yielding the oxidation of an internal alkene to a ketone as net-reaction (Scheme 1.29).¹⁹²



Scheme 1.29 Oxidation of olefins to ketones via a rhodaoxetane.

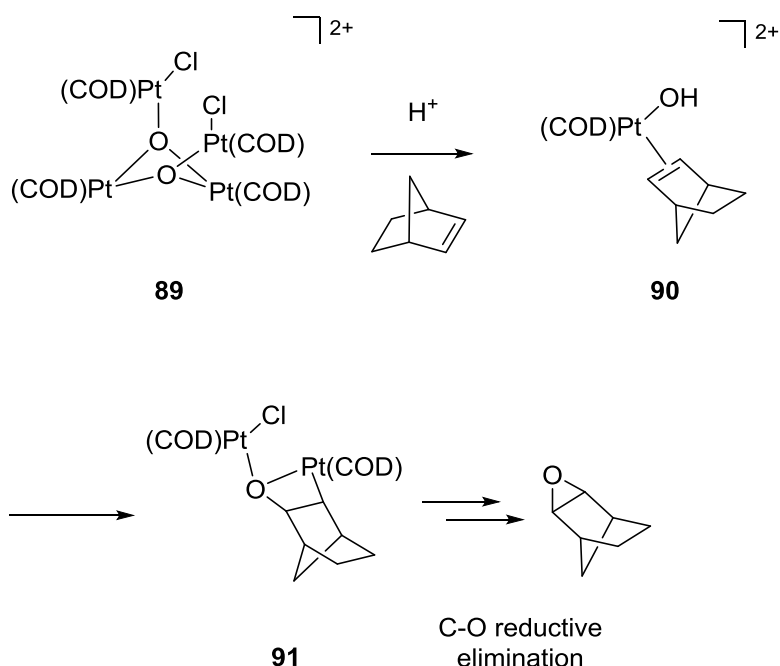
Several of the preceding Rh and Ir systems and their involvement in the oxidation of organic substrates have been reviewed in even greater detail.¹⁹³

A stable and isolable nickelaoxetane (**87**) was prepared by Hillhouse and co-workers by a formal [2+2] cycloaddition of nickel alkylidene **86** and diphenylketene. In the same report the authors proposed that the transient nickelaoxetane **88** might be formed as a first step during the incorporation of 2 equivalents of CO₂ followed by an insertion of the second equivalent into the Ni-C bond (Scheme 1.30).¹⁹⁴



Scheme 1.30 A nickelaoxetane from a formal [2+2] cycloaddition.

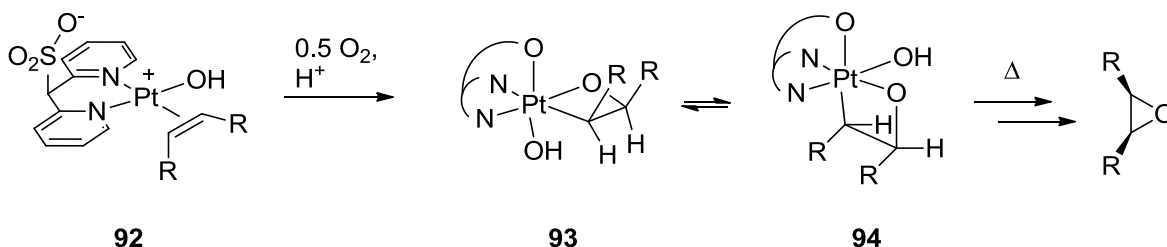
In 2003 Sharp and co-workers reported the oxidation of ethylene to acetaldehyde and reductive coupling of ethylene through a $\text{Pt}(\text{COD})\text{oxo}$ complex **89** and the formation of a platinaoxetane **91** by that same complex and norbornene (Scheme 1.31).¹⁹⁵ The platinaoxetane **91** could be isolated and subjected to X-ray crystallography. The mechanism of the formation was proposed to involve the proton catalyzed formation of a $\text{Pt}(\text{II})$ hydroxo complex **90** that then undergoes coupling with the alkene.¹⁹⁶ Based on the observation that a metallaoxetane was formed with norbornene as substrate the authors suggested the intermediacy of a platinaoxetane in the ethylene oxidation, as well.



Scheme 1.31 An isolable platinaoxetane from norbornene.

Further work in the same group gave access to a whole range of stable norbornene-Pt-oxetanes.¹⁹⁷ At the same time, reactivity studies revealed a diverse reactivity of these compounds including reversible alkene extrusion, ring-opening, insertions and most interestingly epoxide formation through C-O reductive elimination.^{55,196,198,199} These findings constitute an epoxidation mechanism with the proven intermediacy of a metallaoxetane (Section 1.2.1.1.1).

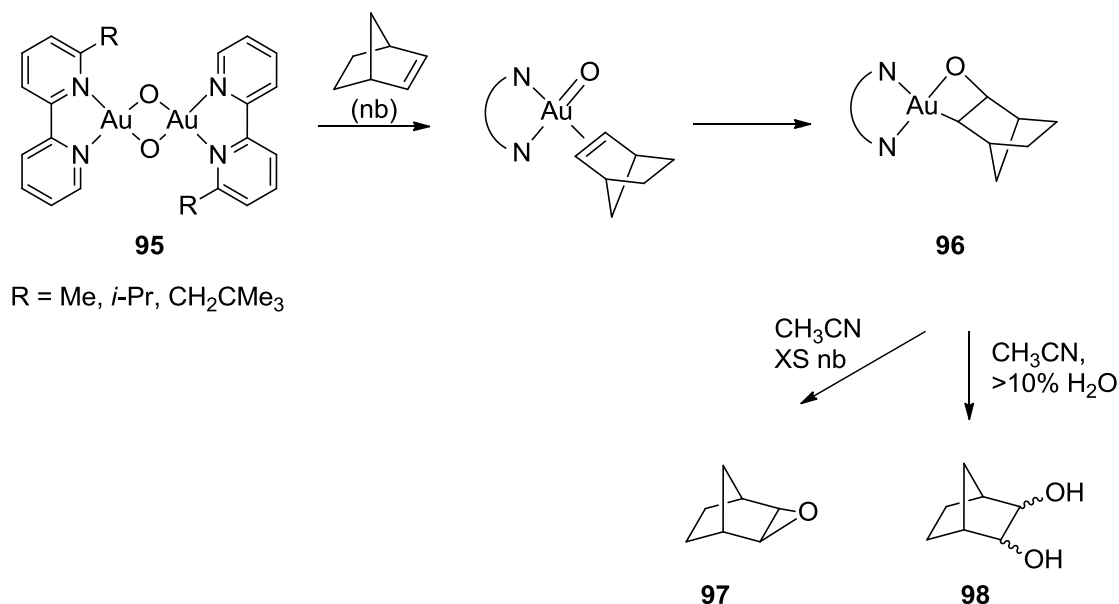
Vedernikov and co-workers reported the preparation and isolation of platinaoxetane isomers **93** and **94** with an anionic sulfonate ligand through aerobic oxidation of a Pt(II)-olefin-hydroxo (olefin = cis-cyclooctene, norbornene) complex (**92**) in water.⁵⁴ The X-ray structure revealed the strained character of the metallaoxetane. Indeed, upon heating in various solvents (H₂O, DMSO, MeOH, CD₂Cl₂) and even under solvent-free conditions, formation of the epoxide occurred via direct reductive elimination (Scheme 1.32). As of yet, the reported epoxidation oxidation is stoichiometric and all attempts at rendering the reaction catalytic led to decomposition of the metal complex.



Scheme 1.32 Olefin epoxidation via a platinaoxetane.

The preparation and isolation of an auraoxetane from a dinuclear μ -oxo-Au complex **95** and norbornene was reported by Cinellu *et al.* in 2005.⁵³ The proposed mechanism for the formation of the auraoxetane consists of a formal [2+2] cyclization with the coordinated olefin to yield the metallaoxetane **96**.

Interestingly, with large excess of norbornene (nb) in CH_3CN , the formation of the corresponding epoxide **97** could be observed. Furthermore, in the presence of >10% H_2O in the solvent, cis and trans diols **98** were also formed (Scheme 1.33). No further mechanistic investigations about the formation of the metallaoxetane itself or the epoxide and diol products have been reported. Thus, further exploration of olefin dihydroxylation and epoxidation via auraoxetanes intermediates is necessary to gain insight in the underlying mechanism.



Scheme 1.33 Formation and reactivity of the first stable auraoxetane.

1.3 Azametallacyclobutanes

In the following, an overview of 2-azametallacyclobutanes will be given. As with the metallaoxetanes described previously, the focus will lie on complexes of transition metals in which the ring nitrogen is anionic (amido). The term “metallaazetidine” is sometimes found in the literature and is synonymous with “azametallacyclobutane”.²⁰⁰⁻²⁰² Although both are acceptable, I opted to use the more widely employed denotation of azametallacyclobutane.

In contrast to the great variety in the formation of the oxygen analogues discussed above, the formation of azametallacyclobutanes is proposed to follow one of two general pathways – either [2+2] addition of appropriate partners or a one-atom-insertion into aziridines. Thus, the following discussion is structured not strictly chronologically but according to the presumed mechanism of azametallacyclobutane formation. Undoubtedly, as more evidence emerges, a number of the proposed mechanisms will be revised.

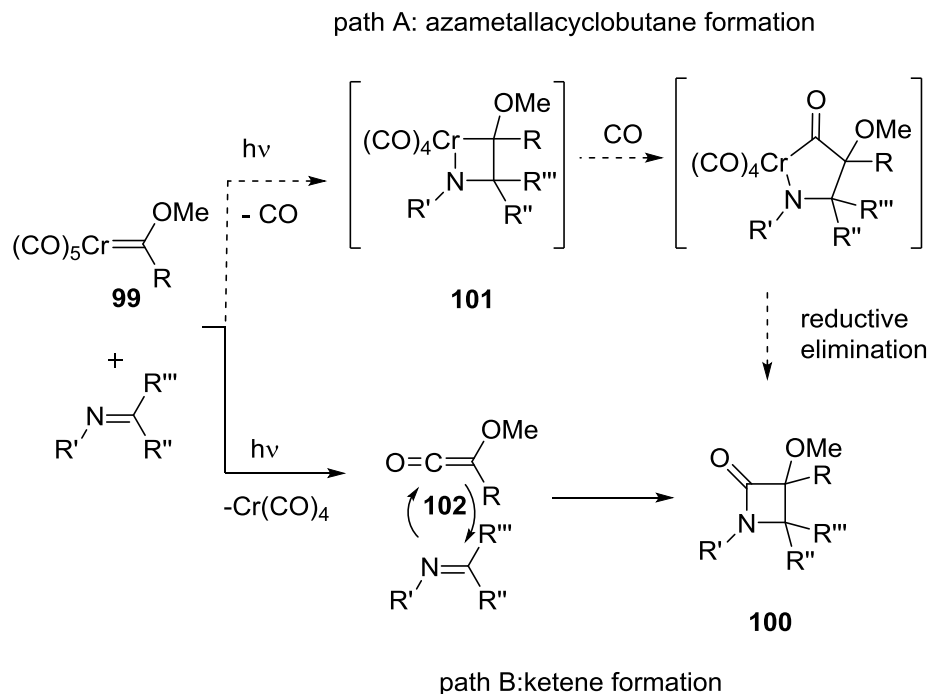
Azametallacyclobutanes were first postulated as catalytic intermediates in the early 1980s first for the [2+2] cycloaddition of imines and metal alkylidenes²⁰³⁻²⁰⁵ and later by metal insertion into aziridines.^{206,207} After these pioneering studies, a number of azametallacyclobutanes were identified spectroscopically and/or were isolated.

1.3.1 [2+2] Addition

1.3.1.1 [2+2] Additions of Metal Alkylidenes and C-N Multiple Bonds

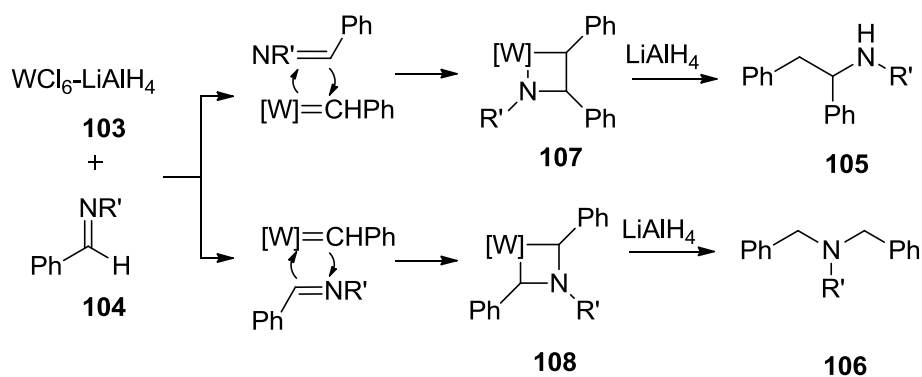
The first time an azametallacyclobutane was invoked as a potential reaction intermediate was in 1982 by Hegedus and co-workers.^{203,204} In a study of the reactivity of chromium alkylidene complexes, the authors irradiated mixtures of pentacarbonyl(methoxyalkylidene) chromium compounds (**99**) and various imines with sunlight at ambient temperature. After 1-3 hours, the respective β -lactams (**100**) could be isolated from the reaction mixture (Scheme 1.34). Although detailed mechanistic studies were not described in the initial reports, one of the proposed mechanisms involved an initial [2+2] cycloaddition of the alkylidene and the imine substrate to form azachromacyclobutane **101** (path A in Scheme 1.34). Subsequent insertion of a CO ligand into the Cr-C bond and reductive elimination would yield the product lactam. In later mechanistic investigations, the

authors found evidence for ketene intermediates (path B in Scheme 1.34) and moved away from the original proposal of an azachromacyclobutane intermediate.²⁰⁸⁻²¹⁰



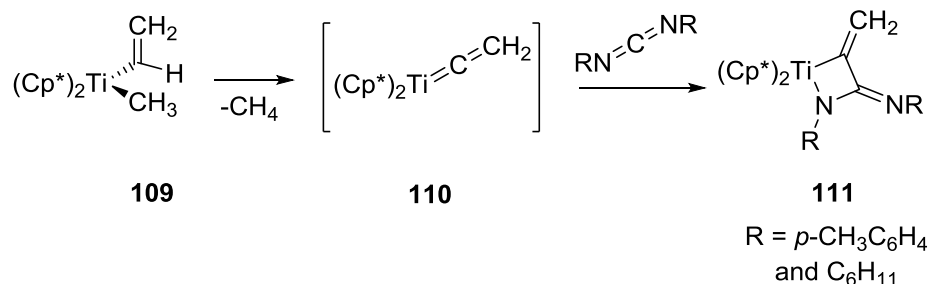
Scheme 1.34 Proposed mechanisms for β -lactam formation.

Only a few years after Hegedus' proposal, Ikariya *et al.* reported the $\text{WCl}_6 / \text{LiAlH}_4$ (**103**) promoted transformation of imines (**104**) into secondary (**105**) and tertiary amines (**106**).²⁰⁵ To account for the observed solvent-dependent selectivity, the authors suggested the formation of an intermediary (albeit not directly detectable) tungsten alkylidene complex derived from the reaction between WCl_6 and imine. This species could then undergo a [2+2] cycloaddition with another equivalent of imine. Depending on the orientation of the imine in relation to the tungsten alkylidene, a 2-aza (**107**) or 3-azatungstenacyclobutane (**108**) would result, which in turn would liberate the tertiary and secondary amines, respectively, after reaction with LiAlH_4 (Scheme 1.35).



Scheme 1.35 Proposed mechanism for imine coupling.

Several years later, Beckhaus et al. were able to prepare, isolate and characterize a variety of azatitanacyclobutanes.²¹¹ Starting from methyl-vinyl titanocene complex **109**, titana-vinylidene **110** was formed in situ by methane elimination. This compound could be trapped at room temperature with carbodiimides to give azatitanacyclobutanes **111**, which contain exocyclic C=C and C=N double bonds (Scheme 1.36). Some of the products exhibited remarkable thermal and chemical stability. Computational studies in collaboration with Böhme ascribed this stability in part to the exocyclic C=C double bond which stems from the Ti-vinylidene intermediate.¹⁷³

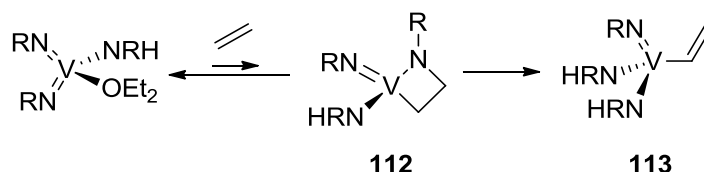


Scheme 1.36 Formation of azatitanacyclobutanes.

1.3.1.2 [2+2] Additions of Metal Imido Complexes and C-C Multiple Bonds

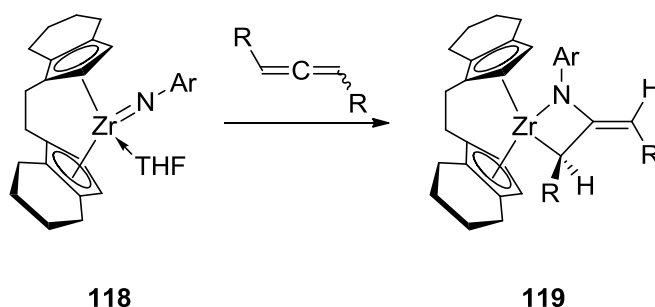
While the intermediacy of azametallacyclobutanes was postulated as early as 1982, the first concrete experimental evidence for their existence was only provided over a decade later. Horton and co-workers reported the formation of azavanadacyclobutane **112** from the [2+2] cycloaddition of a transient vanadium bis(imido) complex and ethylene.²¹² An excess of the olefin and cooling to $-70\text{ }^\circ\text{C}$ was necessary to obtain an isolable product on which

structural elucidation was performed employing a variety of NMR techniques including ^1H , ^{13}C and ^{51}V NMR spectroscopy. The authors also found that the complex was fluxional at room temperature, indicating fast break-up and re-formation of the azametallacycle during which rotation of the ethylene fragment could occur. The unsubstituted azavanadacyclobutane reacted slowly as a solid to form vinyl vanadium amido complex **113** by C-H activation of the ethylene fragment (Scheme 1.37).



Scheme 1.37 Formation and reactivity of the first isolable azametallacyclobutane.

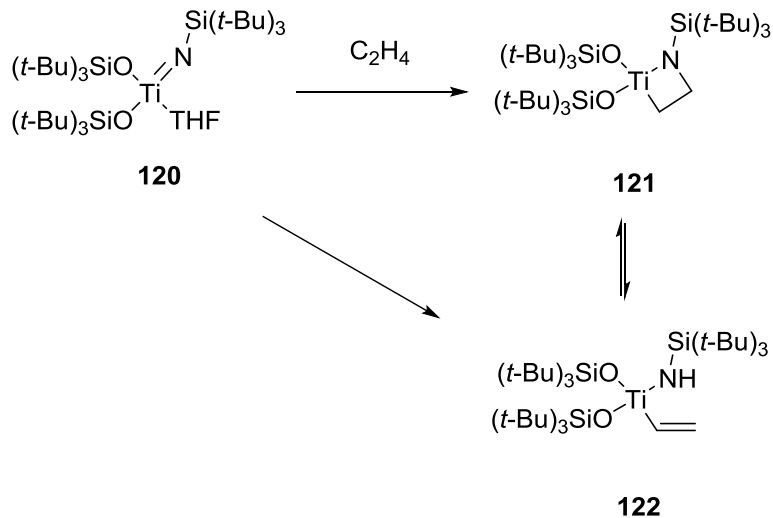
Bergman and co-workers discovered that zirconocene methyl amido complexes form imido zirconocene species; upon heating, these complexes could be trapped as the THF adducts (**114**).²¹³ Shortly after Horton's report on azavanadacyclobutane **113**, reactivity studies in the Bergman group revealed that the imido zirconocene complexes **114** can undergo [2+2] additions with other π -systems. While alkynes underwent facile cycloaddition at room temperature to give isolable azazirconacyclobutenes **115** (Scheme 1.38, a), the equilibrium of the [2+2] cycloaddition with simple alkenes was found to lie to the side of the starting materials.²¹⁴ Only with a 30-fold excess of norbornene could the respective azazirconacyclobutane **116** be obtained (Scheme 1.38, b). In the reaction with ethylene, formation of the unsubstituted cycloaddition product **117** was invoked based on similarities in the NMR spectral data at low temperature, but isolation of the complex was elusive (Scheme 1.38, c).



Scheme 1.39 Formation of azazirconacyclobutanes from [2+2] cycloaddition with allenes.

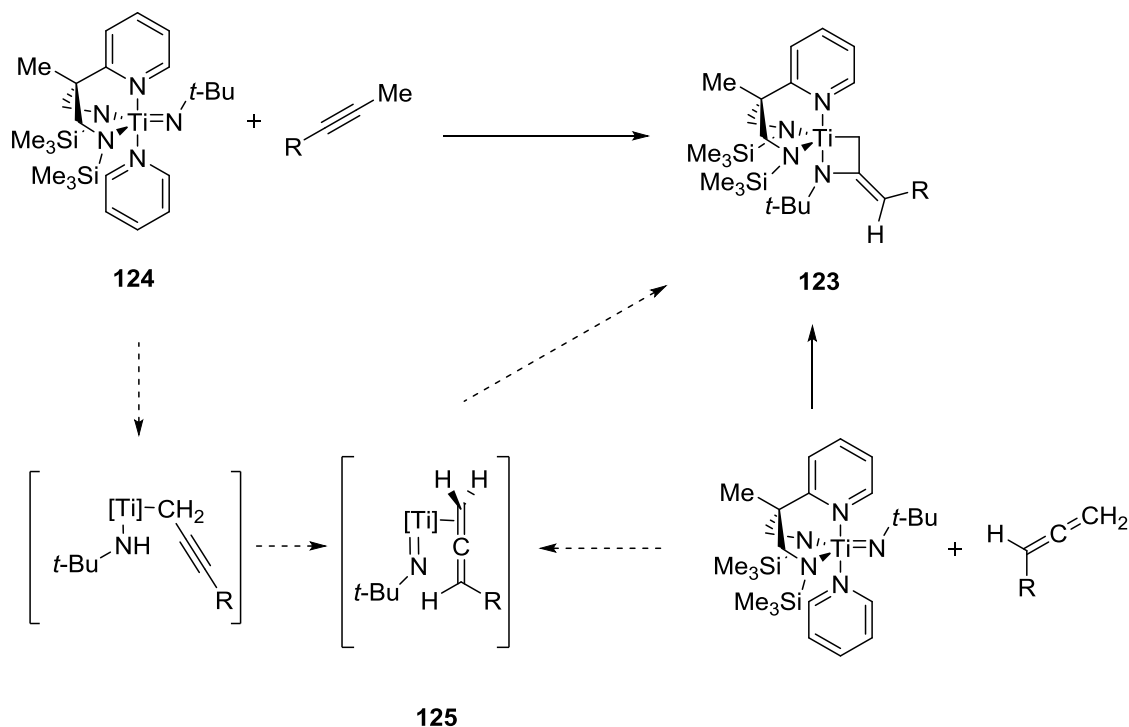
Hydroamination was also performed with Ti-based catalyst systems by various groups.²²²⁻²³¹ In all of these reports azametallacyclobutanes were invoked as part of the catalytic cycle. While computational work by Bergman²³² and Tobisch²²⁰ supports this proposal, unambiguous experimental evidence is still outstanding.

Wolczanski and co-workers prepared transient Ti-imido complexes that could be trapped as their THF adducts (**120**), not unlike Bergman's imido-zirconocenes discussed earlier.²³³ These compounds could perform C-H activation as well as cycloadditions to unsaturated C-C bonds.²³⁴ The use of 2 equivalents of ethylene yielded the azatitanacyclobutane **121** as well as the C-H activated Ti-vinyl amido complex **122** (Scheme 1.40). At room temperature the ratio of [2+2] addition to C-H activation products was 87:13 in favour of the azametallacycle. The structural elucidation was based on NMR spectroscopic studies and comparison with previously reported related structures.



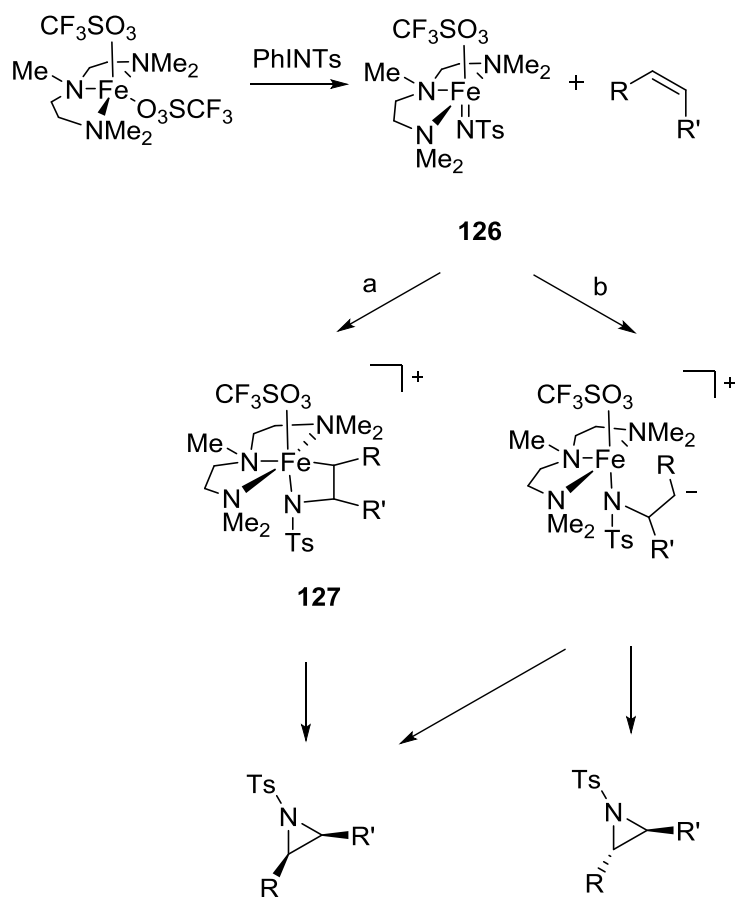
Scheme 1.40 Formation of azatitanacyclobutanes and azatitanacyclobutenes.

The formation and isolation of azatitanacyclobutane **123** was reported by Gade and Mountford.^{235,236} Interestingly, a [2+2] cycloaddition of the titanium imido complex **124** with methylacetylenes by heating to 80 °C for 10-14 days afforded the azatitanacyclobutane **123** with an exocyclic *E*-double bond (Scheme 1.41). The reaction was also not reversible, even at elevated temperature, in good agreement with previous reports by Beckhaus and Böhme regarding the increased stability of azametallacyclobutanes with exocyclic double bonds (vide supra).¹⁷³ The same products could be obtained by exposure of the Ti-imido species to the respective allenes which suggests that the two reactions follow a pathway with identical intermediates. As a potential mechanism, the authors proposed an isomerization of the methylacetylene by stepwise C-H activation and subsequent proton transfer to form the titanium allene-intermediate **125** (Scheme 1.41).^{235,236} The reactivity of these azatitanacyclobutanes was not further studied. Of note, the authors later reported the generation of related azatitanacyclobutanes by isocyanide insertion into a titanaaziridine derived from imido complex **124** (vide infra).



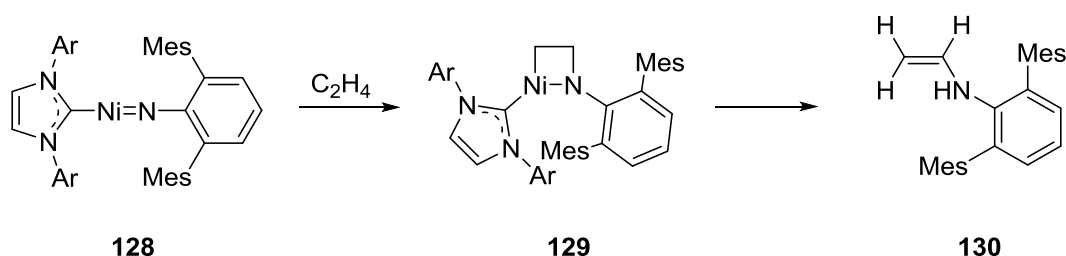
Scheme 1.41 Formation of azatitanacyclobutane via alkyne isomerization to allene-intermediates.

In 2007, Halfen and co-workers reported the discovery of a set of non-heme iron(II) complexes that could mediate olefin aziridination.²³⁷ Further experimental and computational studies helped elucidate the mechanism of this transformation.²³⁸ When Z-olefins were exposed to the reaction conditions, a mixture of *cis*- and *trans*-aziridines was afforded. Two different concurrent mechanistic pathways involving the formation of the common Fe-imido intermediate **126** were, thus, proposed. For one mechanistic option, this complex could undergo a concerted [2+2] cycloaddition with an olefin and form azaferrocyclobutane **127**. Subsequent C-N reductive elimination would then yield the product which retained the *cis*-orientation of the substrate (Scheme 1.42, a). Alternatively, a stepwise mechanism with attack of the imido nitrogen on the olefin and free rotation around the former C=C bond before ring-closure would lead to mixtures of *cis* and *trans*-aziridines depending on the rotational barrier (Scheme 1.42, b). No spectroscopic evidence for the intermediacy of the azametallacycle was reported, but DFT calculations for a model system with ethylene showed the formation of this intermediate to be thermodynamically feasible. However, the DFT studies were not expanded to investigate the energetics of a C-N reductive elimination from this complex.



Scheme 1.42 Proposed intermediacy of an azaferrocyclobutane in aziridination of olefins.

Recently, the [2+2] addition of the isolated two-coordinate nickel-imido complex **128** and ethylene was described by Hillhouse and co-workers.²³⁹ An organometallic intermediate was observed at low temperature that had spectroscopic features consistent with azanickelacyclobutane **129**. The same group had prepared and isolated such a compound before by oxidative addition of a Ni-complex to an aziridine (vide infra).²⁴⁰ When warmed, the vinyl amine **130** was eliminated from the metallacycle, potentially proceeding through β -H elimination and subsequent N-H reductive elimination. Amine **130** formally constitutes the product of C-H insertion of the imido moiety into the olefin (Scheme 1.43). Furthermore, calculations by Cundari showed that a [2+2] cycloaddition of a $\text{Ni}=\text{NR}$ species with olefins is thermodynamically and kinetically feasible.²⁴¹



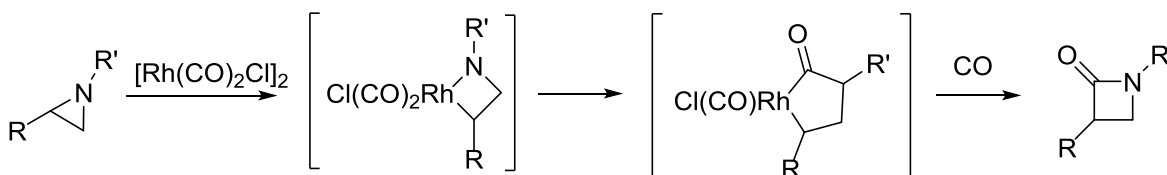
Scheme 1.43 Transient formation of an azanickelacyclobutane.

Further computational studies of [2+2] additions of metal-imido species with ethylene were performed among others in the Ziegler and Frenking labs. For molybdenum¹⁴⁷ and tungsten¹⁴⁶ complexes, the cycloadditions were essentially thermoneutral with fairly significant kinetic barriers. In the osmium systems, the [2+2] addition was kinetically and thermodynamically unfavourable by calculation.²⁴²

1.3.2 One Atom Insertions Into Aziridines

1.3.2.1 Metal Insertion into Aziridines

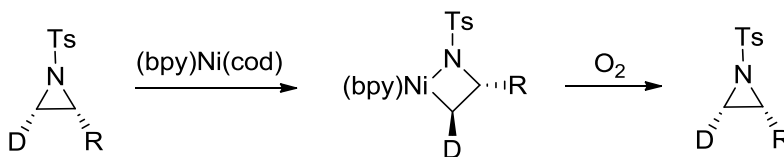
Only one year after Hegedus had invoked the intermediate formation of an azachromacyclobutane in the preparation of β -lactams from chromium alkylidenes and amines,²⁰³ a similar proposal was put forward by Alper and co-workers. They reported the formation of β -lactams by Rh-catalyzed insertion of CO into aziridines (Scheme 1.44).^{206,207} In the course of this transformation, azarhodacyclobutane **131** was proposed to be formed through oxidative addition to the more substituted C-N bond of the aziridine. This was suggested to be followed by CO insertion into the Rh-C bond and subsequent reductive elimination to yield the lactam products. Nevertheless, no concrete experimental evidence for the existence of an azarhodacyclobutane was produced before our lab succeeded in preparing and isolating such a structure almost 3 decades after this proposal (Chapters 4-5).



131

Scheme 1.44 Proposed azarhodacyclobutane intermediate in β -lactam formation.

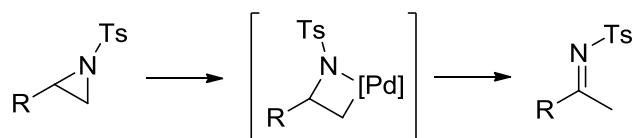
The first time definitive evidence for oxidative addition of a transition metal to an aziridine was reported was in 2002 by the group of Hillhouse. It was found that a variety of tosyl aziridines reacted with a Ni-COD to form the corresponding azanickelacyclobutanes **132** (Scheme 1.45).²⁴⁰ Deuterium labelling studies revealed an S_N2 -type mechanism in which the metal center attacks the less hindered carbon on the aziridine. This mechanism accounted for the observed selectivity of insertion into the less substituted C-N bond, which was opposite to that reported by Alper. The azanickelacyclobutanes could expel the parent aziridines if they were exposed to air. This oxidatively induced reductive elimination resulted in inversion of stereochemistry which excluded a concerted mechanism or one in which Ni-C homolysis occurred. Instead, it is consistent with either Ni-N homolysis or heterolysis



132

Scheme 1.45 Formation of an azanickelacyclobutane by Ni-oxidative addition to aziridines.

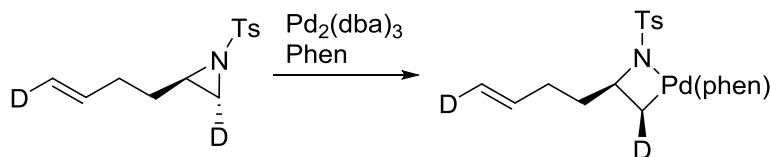
Wolfe and co-workers proposed that azapalladacyclobutane **133** was the intermediate in the Pd-catalyzed isomerization of *N*-tosylaziridines to *N*-tosylimines (Scheme 1.46).²⁴³



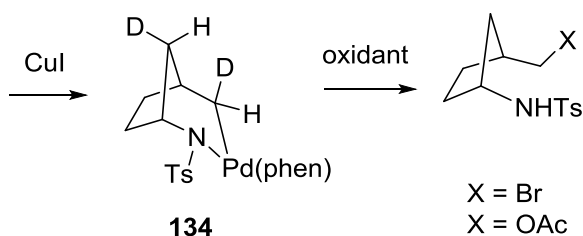
133

Scheme 1.46 Azapalladacyclobutanes as proposed intermediates in aziridine isomerization.

In their later work, they could indeed prepare and characterize various azapalladacyclobutanes.²⁴⁴ Similar to Hillhouse's Ni system, deuterium labelling experiments confirmed that the formation of azapalladacyclobutanes resulted in inversion of the stereochemistry, indicating an S_N2 -type mechanism (Scheme 1.47). The reactivity of the azapalladacyclobutanes was also investigated. Migratory insertion of tethered alkenes into the Pd-C bond could be observed which led to the extended azapalladacycles **134** in the presence of a catalytic amount of CuI as oxidant. Deuterium labelling showed that this carbopalladation proceeded in a *syn*-fashion. Oxidative treatment of **134** with CuBr₂ and PhI(OAc)₂ allowed for functionalization of the Pd-C bond. However, C-N reductive elimination could not be observed, even at elevated temperatures.



133



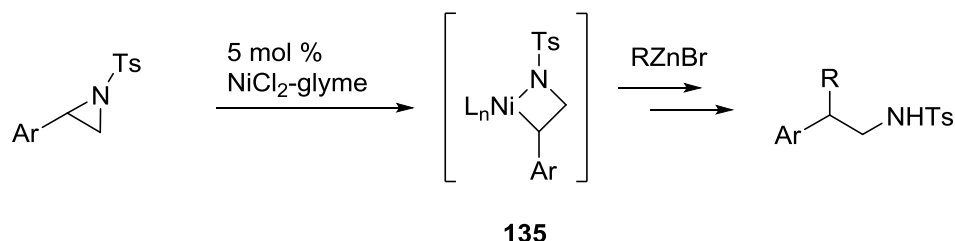
134

X = Br
X = OAc

Scheme 1.47 Formation and reactivity of azapalladacyclobutanes.

Another recent example for the involvement of an azanickelacyclobutane was presented by Huang and Doyle. They reported the coupling of N-tosyl styrenyl aziridines with organozinc reagents under Ni catalysis (Scheme 1.48) and proposed the intermediacy

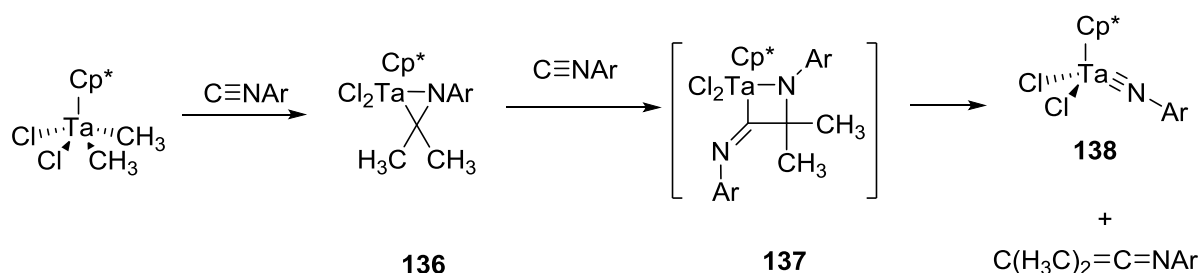
of azanickelacyclobutane **135**.²⁴⁵ To test this hypothesis, the azanickelacyclobutane was synthesized independently and treated with alkylzinc halides to yield the corresponding amine products. Interestingly, the reaction does not follow the selectivity of other group 10 metals into aziridines for the least substituted C-N bond (*vide supra*). Instead, cleavage of the most substituted C-N bond was observed, consistent with Alper's report of β -lactam synthesis using Rh catalysts.^{206,207} This was ascribed to the weaker benzylic C(sp³)-N bond and the greater stability of the presumed azanickelacyclobutane intermediate, relative to cleavage of the less substituted bond.



Scheme 1.48 Catalytic alkylation of styrenyl aziridines.

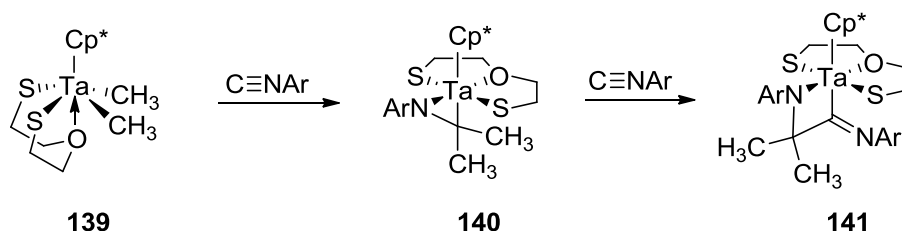
1.3.2.2 Carbon Insertion into Metallaaziridines

In addition to the insertion of a metal atom into an organic aziridine, azametallacyclobutanes can also be accessed through insertion of one-carbon units like isocyanides into the M-C bonds of preformed metallaziridines. This approach has been proven for several early transition metals to be a reliable method for generating azametallacyclobutanes, as both transient and isolable species. For example, in the conversion of tantalazaaziridine **136** (derived from Cp^{*}Ta(CH₃)₂Cl₂) into tantalum nitride species **138**, azatantalacyclobutane **137** was proposed as an intermediate (Scheme 1.49). As no 3-azatantalacyclobutanes were formed, the insertion of isocyanide has to occur exclusively at the Ta-C bond of **136**.²⁴⁶



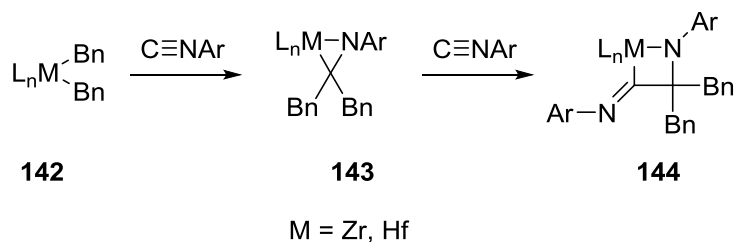
Scheme 1.49 Proposed intermediacy of an azatantalacyclobutane.

Similarly, Fandos, Otero and co-workers reported that Ta-Cp* complex **139** can incorporate two equivalents of isocyanide. In the first step, tantalaaaziridine **140** was generated (Scheme 1.50). Insertion of a second equivalent provided azatantalacyclobutane **141**, which was characterized spectroscopically, as well as by X-ray analysis.^{247,248}



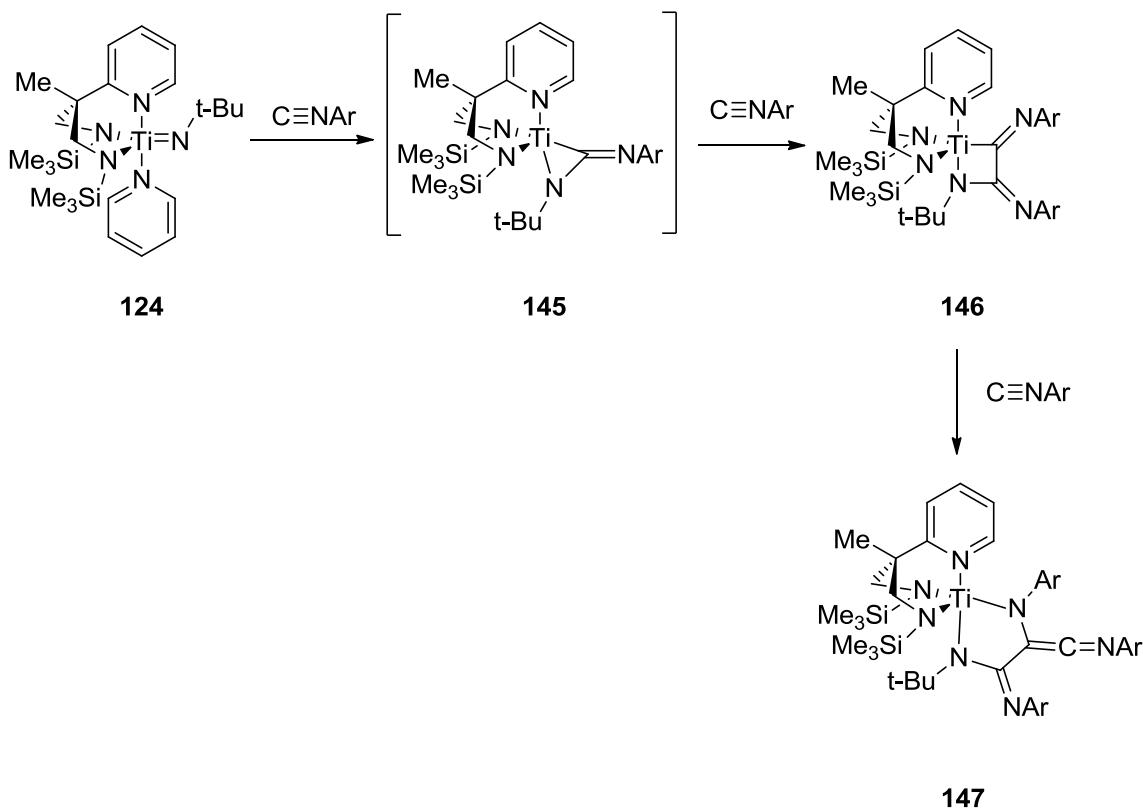
Scheme 1.50 Formation of an azatantalacyclobutane through double insertion of isocyanides.

Scott and Lippard succeeded to prepare and isolate group 4 azametallacyclobutanes in an analogous fashion. Again, incorporation of two equivalents of the isocyanide into Zr and Hf di-benzyl complexes (**142**) led first to the formation of the metallaaaziridene species **143**. Subsequent 1,1-insertion of a second equivalent of isocyanide into the M-C bond afforded the corresponding azametallacyclobutanes **144** (Scheme 1.51). Both the zirconium and hafnium azametallacycles were characterized spectroscopically and crystallographically.²⁴⁹



Scheme 1.51 Formation of azazircona- and azahafnacyclobutanes.

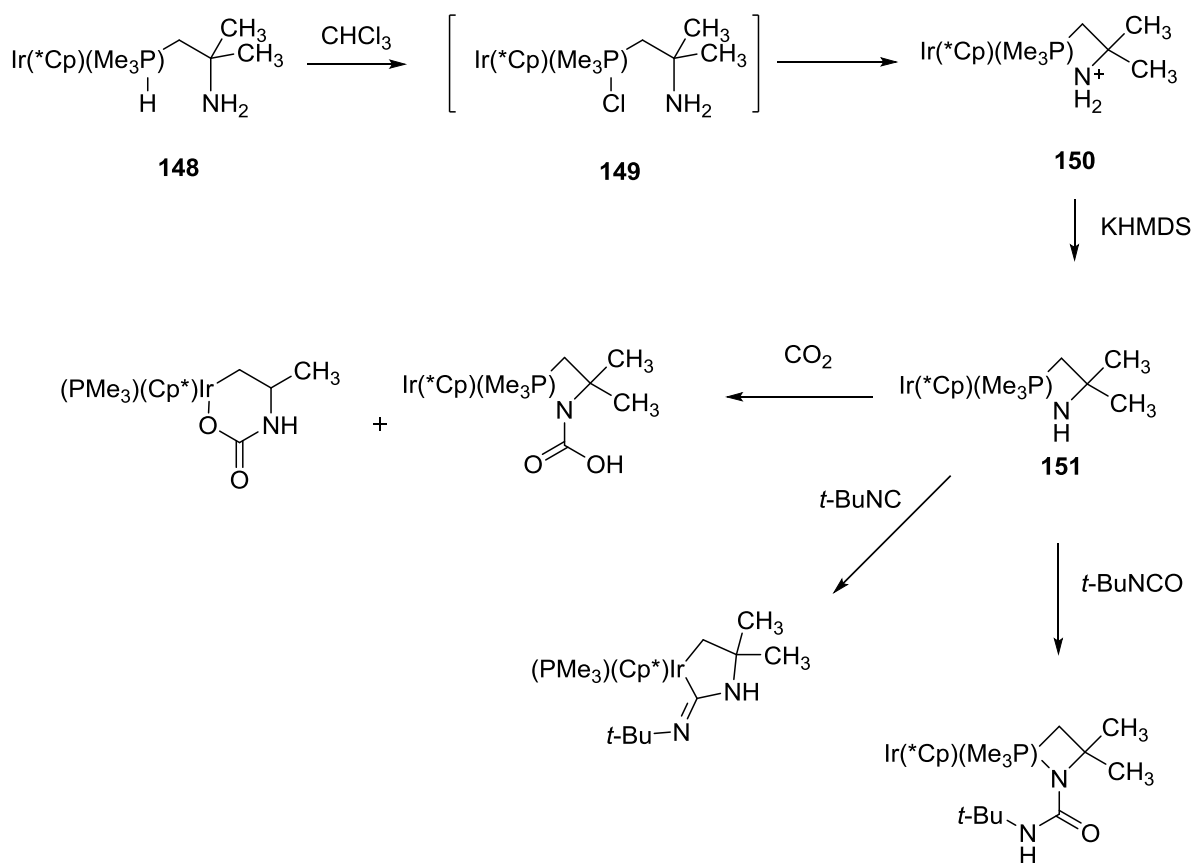
Gade and Mountford reported the formation of azatitanacyclobutanes by [2+2] cycloaddition of methylacetylenes with Ti imido complex **124** (see 1.3.1.2).^{235,236} In addition to cycloadditions, complex **124** could also undergo isocyanide double insertion of an isocyanide into the Ti imido bond. This produced the corresponding azatitanacyclobutane **146**, possibly via a transient titanaaziridene species **145**. Azatitanacyclobutane **146** was isolated and could be spectroscopically and crystallographically characterized. In the presence of excess isocyanide, a third equivalent was inserted, again into the M-C bond to furnish imido-yl iminoketene complexes **147** (Scheme 1.52).²⁵⁰



Scheme 1.52 Double insertion of isocyanides to afford azatitanacyclobutanes.

1.3.3 Other Methods to Generate Azametallacyclobutanes

Bergman and co-workers reported the formation of metallacycle **150** by treatment of iridium hydride **148** with chloroform, which presumably forms chloride **149**. Salt **151** is air-stable and isolable, albeit hygroscopic. Treatment of **150** with a hindered base at low temperature produced **151**, which could be isolated as an air-sensitive solid. Complex **151** was characterized by ^1H and ^{13}C NMR spectroscopy, IR and HRMS. It reacted with a number of electrophiles, including CO_2 , *tert*-butyl isocyanide and *tert*-butyl isocyanate (Scheme 1.53).²⁵¹



Scheme 1.53 Formation and reactivity of an azairidacyclobutane.

1.4 Summary

The interest in metallaoxetanes as possible reaction intermediates has increased considerably over the last 30 years. Their involvement in catalytic transformations was proposed on many occasions but experimental evidence was often scarce. The growing

number of isolated metallaoxetanes again showed various reliable ways to access them synthetically and allowed for in-depth studies of their reactivity. With thorough product analysis studies and especially the evolvement of ever more powerful computational methods, the intermediacy of these structures was corroborated for some reactions, but disputed for others.

As the above discussion illustrates, it is not always possible to make generalized predictions as to how metallaoxetanes can be formed or how they react. For example, addition to epoxides as well as the microscopic reverse can be found with early, mid and late transition metals. However, [2+2] additions and retro-additions are more frequently found with early-to-mid transition metals whereas β -X elimination is almost exclusively happening from low-valent late transition metals.

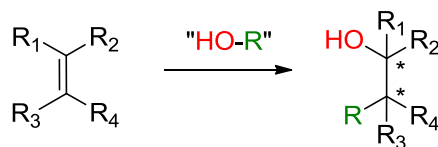
Likewise, azametallacyclobutanes have been proposed as reaction intermediates since their first occurrence in the literature more than thirty years ago. Since then a significant number of these compounds have been specifically prepared and studied. Notably, more early than mid or late transition metal azametallacyclobutanes have been reported to date. Their formation seems to follow only a limited number of different pathways. By far the majority of them are formed by [2+2] cycloadditions, especially of discrete or transient metal imido species and unsaturated C-C bonds. While the one-carbon insertion into metallaziridines has so far only been observed with early transition metals, the insertion of a metal into aziridines seems to be feasible mostly for transition metals of groups 9 or higher. The microscopic reverse of this reaction – reductive elimination of aziridines from azametallacyclobutanes – has to date not yet been unambiguously proven without having to oxidize the metal center. Among the more frequently observed reactivity one can find β -H elimination and small molecule insertion especially involving unsaturated C-C, C-O and C-N bonds.

2 Reactivity of Rhodaoxetanes

As introduced in Chapter 1, the intermediacy of metallaoxetanes has been verified in a variety of catalytic transformations and, therefore, these structures provide a formidable starting point for the rational design of new chemical reactions. We sought to explore rhodaoxetanes as potential reactive intermediates in such newly designed reactions. In this chapter, first, an approach to a novel carbohydroxylation protocol based on a rhodaoxetane intermediate will be presented. Parts of this work have been published as a communication in *Angewandte Chemie International Edition*.²⁵² The results disclosed here are extended in scope and discussion compared to the published data. Furthermore, as of yet, unpublished studies on the reactivity of rhodaoxetanes towards electron deficient alkynes will be presented.

2.1 Transmetalation as Part of a Carbohydroxylation Protocol

The vicinal difunctionalization of olefins is a synthetically highly desirable transformation. At the expense of a π -bond, two new substituents are introduced into the molecule which provides a means to convert readily available petrochemical feedstocks into valuable synthetic building blocks. Of particular merit is the selective introduction of two different substituents in a single step. 1,2-Carbohydroxylation, for example, involves the addition of a hydroxyl group (OH) and an organic moiety (R = alkyl or aryl) across an alkene double bond to generate functionalized alcohols (Scheme 2.1).



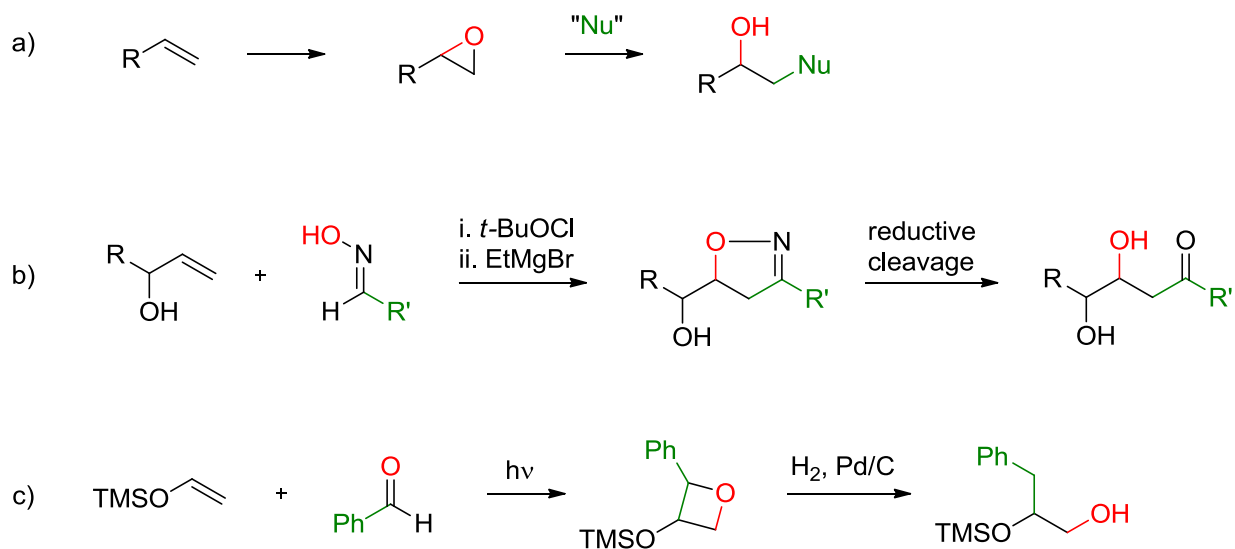
Scheme 2.1 Generic example for carbohydroxylation

A conventional method for the stepwise addition of an OH and R group across olefins involves sequential olefin epoxidation and nucleophilic ring-opening (Scheme 2.2a). Generally though, this strategy is often limited by the requirement of harsh reaction conditions. Specifically, when the formation of enantiopure products is desired, the need for strong nucleophiles for the ring opening step can pose a severe drawback when other leaving

groups are present in the substrate molecule. Moreover, conversion of terminal aliphatic olefins into chiral products remains problematic, owing to the low enantioselectivity of terminal aliphatic olefin epoxidation, despite recent progress.²⁵³ Indeed, the typical strategy to obtain chiral, aliphatic epoxides derived from terminal olefins is by resolution of the enantiomeric mixture, which by definition results in loss of half of the material.

Another approach to carbohydroxylation involves the dipolar cycloaddition of oximes with appropriate dipolarophiles. Subsequent reductive N-O bond cleavage yields the desired products (Scheme 2.2b).^{254,255}

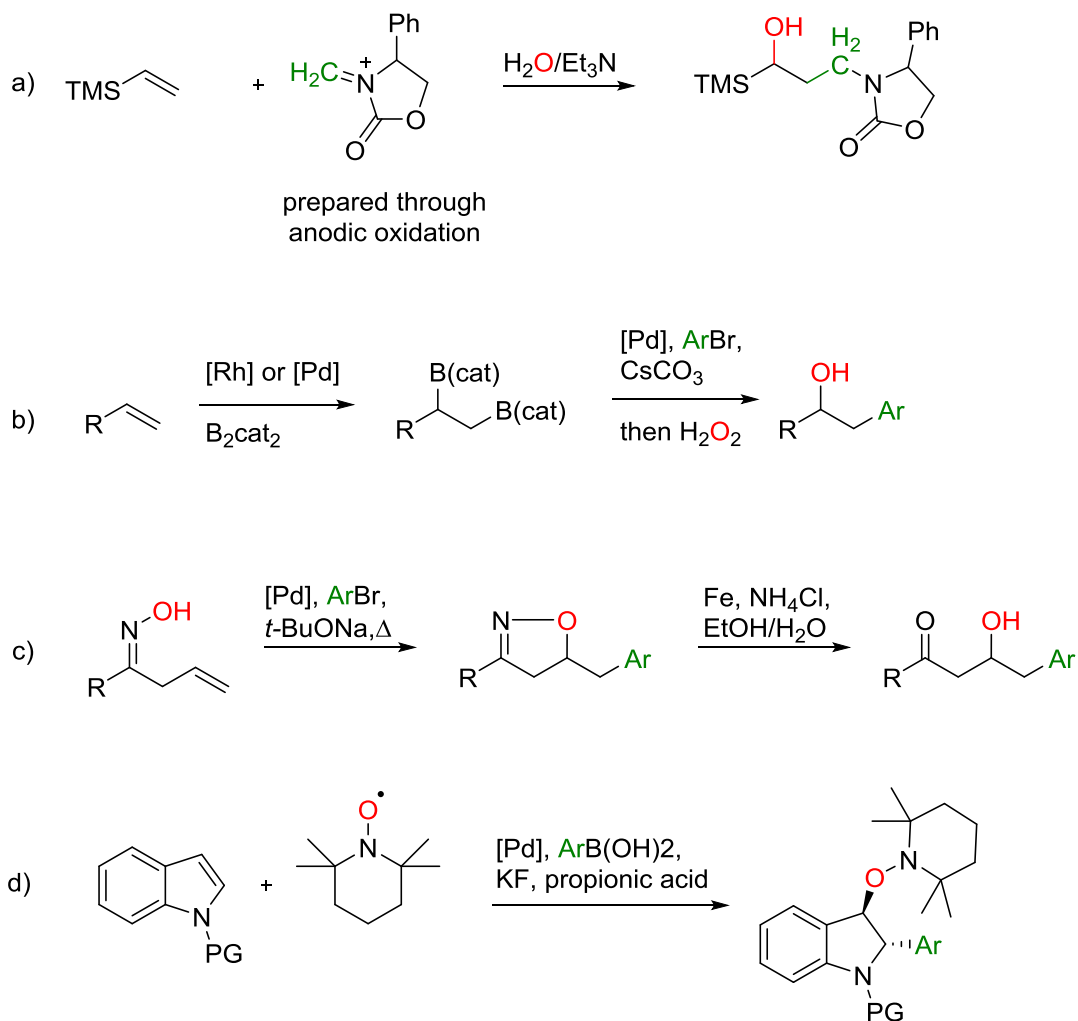
Alternatively, Bach and co-workers reported the formation of oxetanes from enol ethers under Paterno-Büchi conditions. This was followed by hydrogenation and provided the corresponding carboxydroxylated products (Scheme 2.2c). All of the above procedures involve more than one step and/or have significant substrate limitations.



Scheme 2.2 Examples for multi-step carbohydroxylation protocols

In comparison, a one-step carbohydroxylation reaction would be more efficient. Nevertheless, only a few one-step protocols have been disclosed, which also suffer from inefficiency or limited scope. For example, Suga and Yoshida described cationic carbohydroxylation, but this process is only applicable to substrates that can generate *N*-acyliminium ions through anodic oxidation (Scheme 2.3a).²⁵⁶ Morken, and later Fernandez, reported that catalytic diboration, cross-coupling and boronate oxidation in a tandem one-

pot set-up is an effective strategy for carbohydroxylation.²⁵⁷ However, the substrate scope remains limited and the process is not atom-economical, requiring one equivalent of a diboronate reagent (Scheme 2.3b).

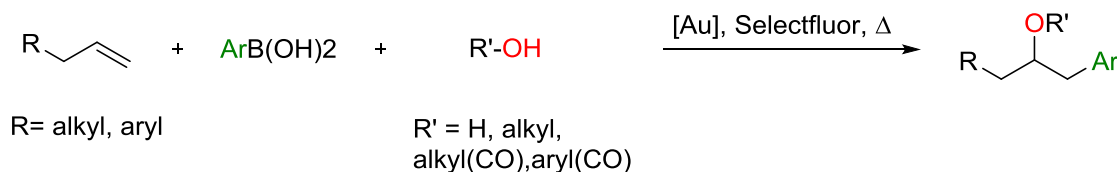


Scheme 2.3 Examples for one-pot carbohydroxylation protocols

An intramolecular Pd-catalyzed carbohydroxylation protocol has been developed by Chen but only allows β,γ -unsaturated oximes as substrates (Scheme 2.3c).²⁵⁸ Finally, Studer reported stereoselective palladium-catalyzed carboaminoxylation, but the procedure requires stoichiometric TEMPO and is restricted to indoles (Scheme 2.3d).²⁵⁹

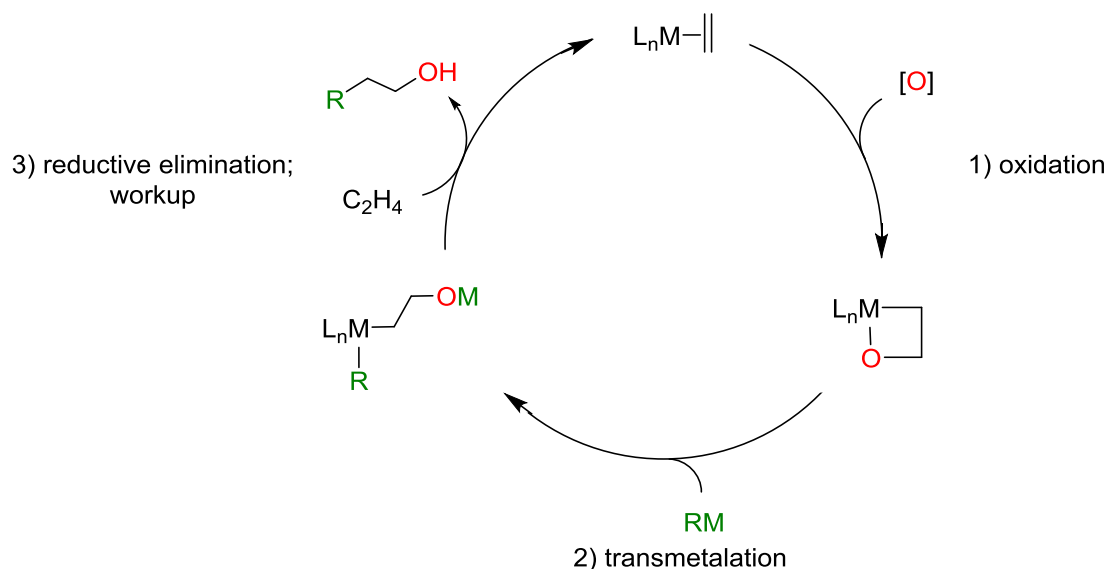
Simultaneously with our first contribution to this field,²⁵² Toste and co-workers published an elegant gold catalyzed three-component oxyarylation.²⁶⁰ While the carbon moiety was transferred from boronic acids, the oxygen moiety could originate from alcohols,

carboxylic acids or water and gave rise to the respective ethers, esters or alcohols (Scheme 2.4). However, two equivalents of Selectfluor[®] reagent were necessary as terminal oxidant which increases waste production and lowers atom-economy. Furthermore, the substrate scope was limited to olefins with aliphatic substituents.



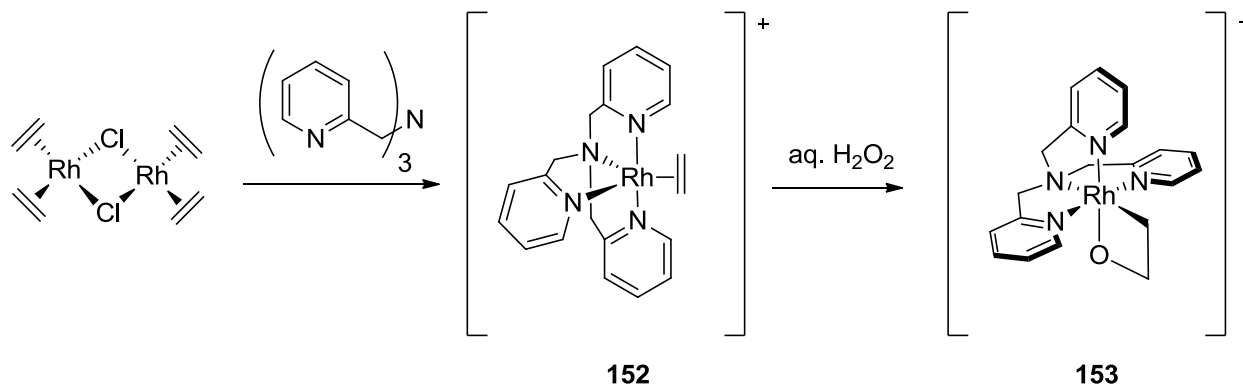
Scheme 2.4 Au-catalyzed three-component oxyarylation

We envisioned a carbohydroxylation approach based on a metallaoxetane intermediate could involve the following steps: (1) oxidation of an olefin-coordinated metal complex to the 2-metallaoxetane; (2) transmetalation, resulting in ring-opening of the metallaoxetane; (3) reductive elimination and subsequent olefin coordination to regenerate the catalyst (Scheme 2.5). Upon workup, a functionalized alcohol product would be produced. The proposed carbohydroxylation would constitute a mild, one-step equivalent to olefin epoxidation/nucleophilic ring-opening, with different stereochemical implications. With substituted olefins, this method would provide complementary stereochemistry to simple epoxidation/ring-opening if reductive elimination proceeds with retention of configuration. The proposed catalytic process can also be considered the equivalent of olefin insertion into C-O bonds.



Scheme 2.5 Proposed catalytic cycle for carbohydroxylation of olefins

Of particular interest was the report by de Bruin et al., demonstrating the conversion of a TPA-Rh(I)-ethylene complex **152** (TPA = trispyridylmethylamine) to the corresponding rhodaoxetane **153** by aqueous hydrogen peroxide solution (Scheme 2.6, discussed in detail in section 1.2.2.3).^{185,187} This would constitute the first step in a potential catalytic oxidative olefin functionalization reaction (Scheme 2.5).



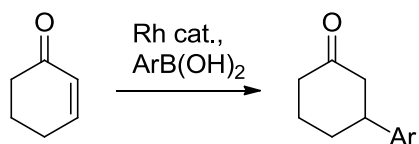
Scheme 2.6 Reported synthesis of 2-rhodaoxetane **153**.

Inspired by the elegant simplicity of de Bruin's work we decided to use rhodaoxetane **153** for preliminary stoichiometric investigations. The preparation of the model system was carried out according to a modified literature procedure under air- and moisture-free

conditions.^{185,187} We were able to obtain X-ray quality crystals of the complex with a hexafluorophosphate counterion which had not been previously published (the rhodaoxetane had been crystallized with a modified ancillary MeTPA ligand and a tetraphenylborate counterion). It is worthwhile to note that the preparation could also be performed under bench-top conditions with minimal effect on the yield and purity of the product and that the compound is stable at room temperature under air for about 2 weeks and at -20 °C for more than 6 weeks. De Bruin had reported reactivity of the rhodaoxetane species with electrophiles, but nucleophiles were found to be ineffective.^{185,187} Nevertheless, we anticipated that transmetalation could be achieved under suitable conditions. Thus, our first objective was to explore the reactivity of rhodaoxetane **153** with various organometallic reagents.

2.1.1 Transmetalation with Organoboron Nucleophiles

Rh(I)-O bonds are well known to undergo transmetalation with organometallic reagents.²⁶¹⁻²⁶³ A common example for the reactivity of rhodium(I) alkoxide and hydroxide bonds towards organometallic reagents is the Rh catalyzed 1,4-conjugate addition of arylboronic acids to activated alkenes (Scheme 2.7). During this reaction the Rh-O bond in the active catalyst is broken and the organic moiety is transferred onto the Rh while the oxygen is transferred to boron.^{264,265}

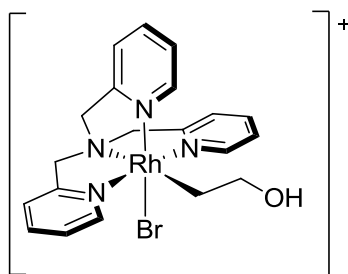


Scheme 2.7 Rh catalyzed 1,4-conjugate addition.

However, there are no literature reports of transmetalation with Rh(III)-O bonds. Wilkinson et al. reported transmetalation of aryl groups onto Rh(III) -halide and -aryl centers by using hard nucleophiles, such as organolithium or Grignard reagents.²⁶⁶

The preliminary reactions of **153** with organometallic reagents were performed on small scale (NMR tube) and repeated at up to 1 mmol scale in cases where notable reactivity was observed.

Our first attempts to perform transmetalation focussed on organolithium, organozinc or Grignard reagents but proved unsuccessful and in most cases only decomposition to unidentified products was observed. When phenylmagnesium bromide was employed, one major product was formed which was tentatively assigned structure **154** based on NMR spectroscopy and MS data (Figure 2.1).



154

Figure 2.1 Proposed product from reaction of **153** with PhMgBr

We then turned to organoboronic acids as nucleophiles and were delighted to observe the clean formation of a new product. For example, when rhodaoxetane **153**.PF₆ is treated with 1 equivalent of *p*-BrC₆H₄B(OH)₂ in methanol at room temperature over 8 hours, one new product (**155a**.PF₆) is formed as indicated by ¹H NMR spectroscopy (Figure 2.2). Based on comparison to 1,3,5-trimethoxybenzene (TMB) as an internal standard, **155a**.PF₆ is produced in 71% yield. Upon isolation, a 42% yield of **155a**.PF₆ is obtained.

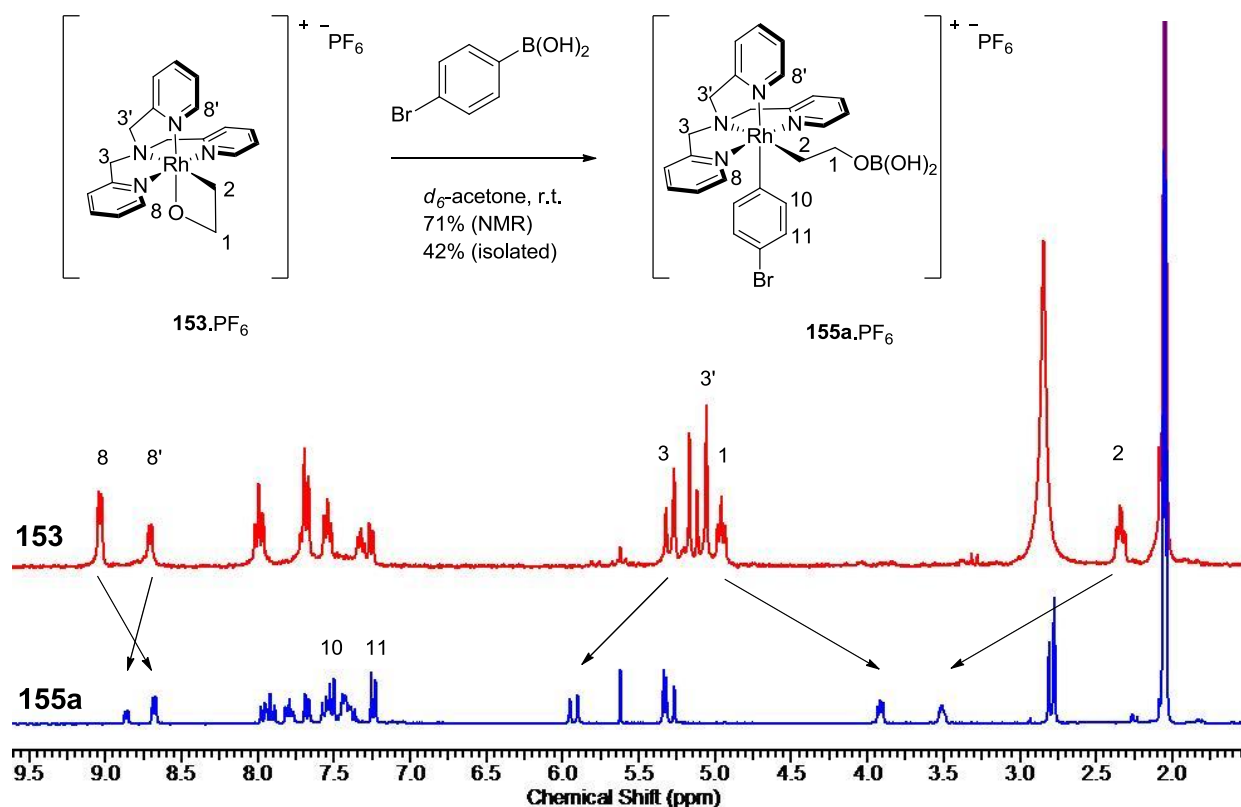


Figure 2.2 ¹H NMR spectrum comparing **153** (top) to **155a** (bottom)
(400MHz, *d*₆-acetone, 298K).

Characterization of the product was conducted as follows. The rhodaoxetane moiety of **153** has two signals (4.99 ppm, t, ³*J* = 7.5 Hz, H1, and 2.40 ppm, dt, ³*J* = 7.6 Hz, ²*J*_(Rh-H) = 2.5 Hz, H2) that disappear during the course of the reaction while the product shows two new signals (H1 = 3.92 ppm, dd, ³*J* = 5.5 Hz, 5.3 Hz and H2 = 3.55-3.47 ppm, m). Likewise, the signals for the protons in the methylene bridges of the TPA ligand, H3, are shifted to lower field (5.37 ppm, d[AB], ²*J* = 15.3 Hz, H3 in **153**; 5.91 ppm, d[AB], ²*J* = 15.1 Hz, H3 in **154a**). Finally, H8 and H8', the signals ascribed to the protons ortho to the pyridine N also shift. Rhodaoxetane **153** has signals at 9.04 ppm (d, ³*J* = 5.3 Hz, H8) and 8.71 ppm (d, ³*J* = 6.1 Hz, H8') whereas **155a** has signals at 8.67 (d, ³*J* = 5.5 Hz, H8) and 8.85 ppm (d, ³*J* = 5.9 Hz, H8'). Two additional new signals can be observed in the aromatic region of the ¹H-NMR spectrum: Two [AB] type doublets arise at 7.52 ppm and 7.25 ppm both integrating to 2 H. Their correlation is affirmed through the clear roofing effect as well as cross-peaks observed in the

COSY spectrum of the compound. Similar results were obtained with (*E*)-styrylboronic acid as a substrate which gave rise to compound **155b** (Figure 2.3).

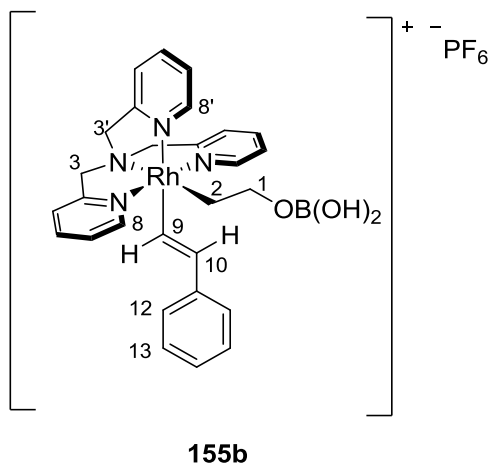


Figure 2.3 Reaction product with (*E*)-styrylboronic acid.

The chemical shifts are consistent with the observations of de Bruin, et al. regarding acid-mediated rhodaoxetane ring-opening. The smaller ^3J coupling constants for the signal at 3.92 ppm (H1) of 5.5 Hz and 5.3 Hz could also indicate a ring-expansion via transesterification of the organoboronic acid to a six-membered oxametallacycle rather than ring-opening¹⁸⁷ to give a compound of the general structure of **156** (Figure 2.4). Low resolution ESI mass spectra of the reaction products show a single signal at M^+ reduced by 18 mass units. This can be best explained by dehydration of the boronic acid moiety of the transmetalated products in the ion source of the spectrometer. It should be noted that the MS results are also consistent with transesterification of the boronic acid. High resolution mass spectra confirm the empirical formula.

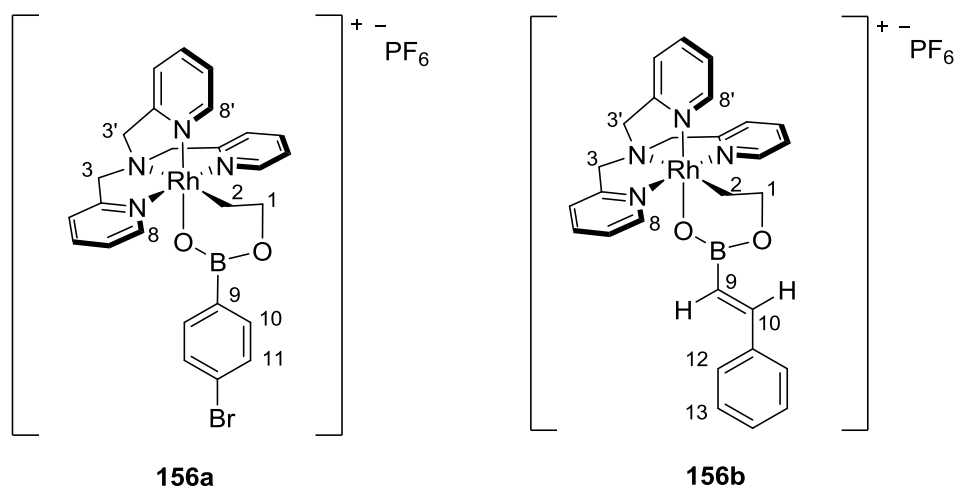


Figure 2.4 Possible alternative structures.

In the absence of X-ray quality crystals, we performed further spectroscopic investigations to differentiate between these options (formation of **155** or **156**-type products). The multiplicity of the ^{13}C NMR signal of C9 should elucidate this issue. A doublet would appear in the case of coupling to Rh ($I = \frac{1}{2}$) while a quartet should indicate connectivity to boron ($I = \frac{3}{2}$). Unfortunately, ^{13}C NMR data of the isolated product complexes was inconclusive as the quarternary signal of interest (C9) could not be detected directly. Cases where carbon atoms directly bound to boron or rhodium(III) centers cannot be observed in ^{13}C NMR spectra are known in the literature. This effect is usually ascribed to either very fast or very slow relaxation for example through the influence of the neighbouring atom.²⁶⁷⁻²⁶⁹

In an attempt to observe potentially fast-relaxing spins (e.g. through quadrupolar relaxation with the boron nucleus) we modified the acquisition parameters to have a very short P1 pulse (4 μsec), D1 delay (1 μsec), pre-scan delay (DE = 5 μsec) and acquisition time (AQ = 400 msec) in a standard, proton-decoupled ^{13}C NMR without spin-echo. (100MHz, d_6 -acetone, 298K). Still, no signal could be observed for C9 in the ^{13}C NMR spectrum of the product complex.

Quarternary carbons (e.g. C9 in **155a**) tend to relax slower than primary, secondary or tertiary carbons so we increased the acquisition time to AQ = 60s (150MHz, cryoprobe,

*d*₆-acetone, 298K) but still no signal accounting for C9 could be detected. Furthermore, heating of the sample to 50 °C²⁶⁸ in MeOD did not give rise to any newly observable signals.

In **155a** indirect detection of the quarternary carbon C9 was possible at 137.2 ppm (*d*₆-acetone, 298K) via HMBC contacts to H10 and H11. In compound **155b** an HSQC experiment allowed for indirect detection of C9 at 124.2 ppm (MeOD, 298K).

We, therefore, concentrated on the shape of the HSQC signal. In the HSQC spectrum of the parent (*E*)-styrylboronic acid the two signals arising from the doublet in the ¹H (F2) dimension (400MHz, 298K, 6.33 ppm, ³*J*_{trans} = 18.1 Hz) were aligned perfectly to correlate with an unobservable signal at 117.2 ppm in the ¹³C (F1) dimension (Figure2.5).

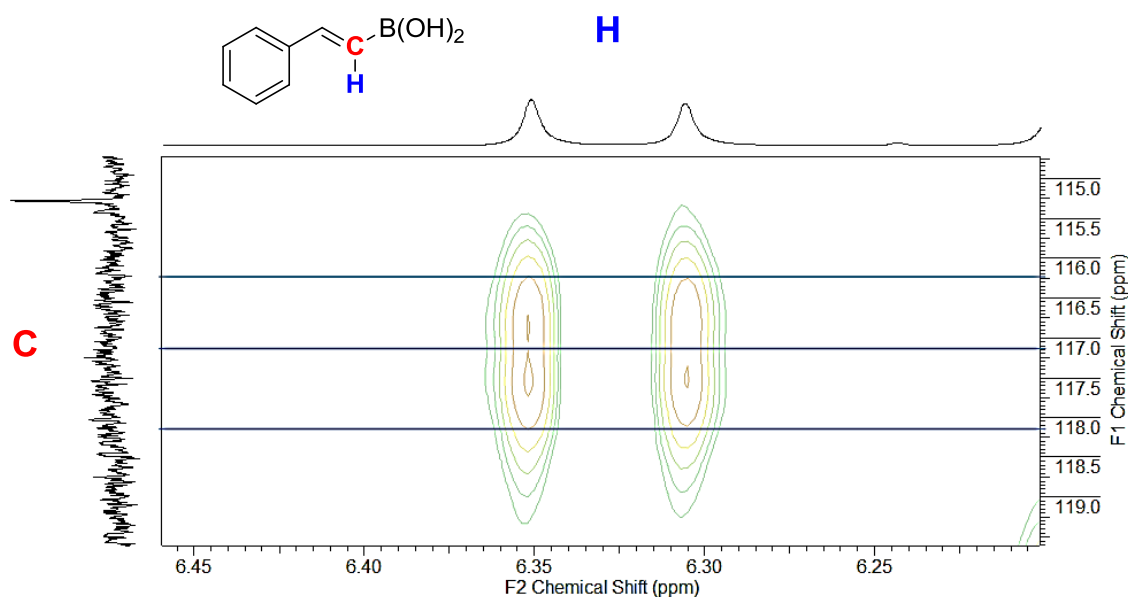


Figure 2.5 HSQC of (*E*)-styrylboronic acid.

The HSQC of the product complex was optimized for olefinic C-H couplings (J1, CNST2 = 165 Hz), the P1 pulse calibrated, the spectral window narrowed to 4 ppm in the F2 dimension (offset, O1P = 6.5 ppm) and 50 ppm in the F1 dimension (offset O2P = 120 ppm) and the time domain increased to TD = 2048 in F2 and TD = 512 in F1. The data was acquired at 600/150 MHz employing a cryoprobe for increased S/N ratio and sensitivity. The shape of the HSQC signal indicates the multiplicity of a doublet for the carbon signal with a coupling constant ²*J* of ca. 6 Hz (Figure 2.6). Although the digital resolution of the experiment (7.4 Hz after linear prediction) is on the same scale as the observed coupling constant, the offset of

the HSQC signal was reproducible and it was not detected in any of the other signals in the spectrum which suggests that the observation is valid.

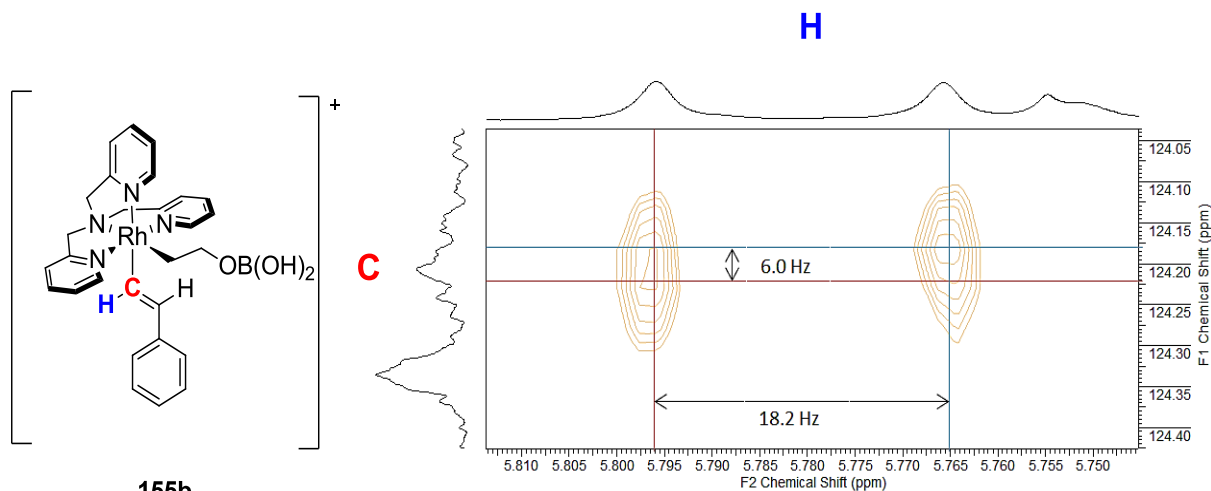


Figure 2.6 HSQC of **155b**.

In addition, the 2D NOESY spectrum of **155a** showed a clear NOE contact between the axial TPA-methylene bridge proton signal at 5.91 ppm (H3) and the H10 signal at 7.52 ppm. (Figure 2.7) In the (*E*)-styrylboronic acid product **155b** a similar contact is observed between H10 and H3 (axial). There are also contacts between H9 and H3 (axial) as well as H10 and H1. It is questionable whether these correlations would be possible in the six-membered ring structures **156a** or **156b**.

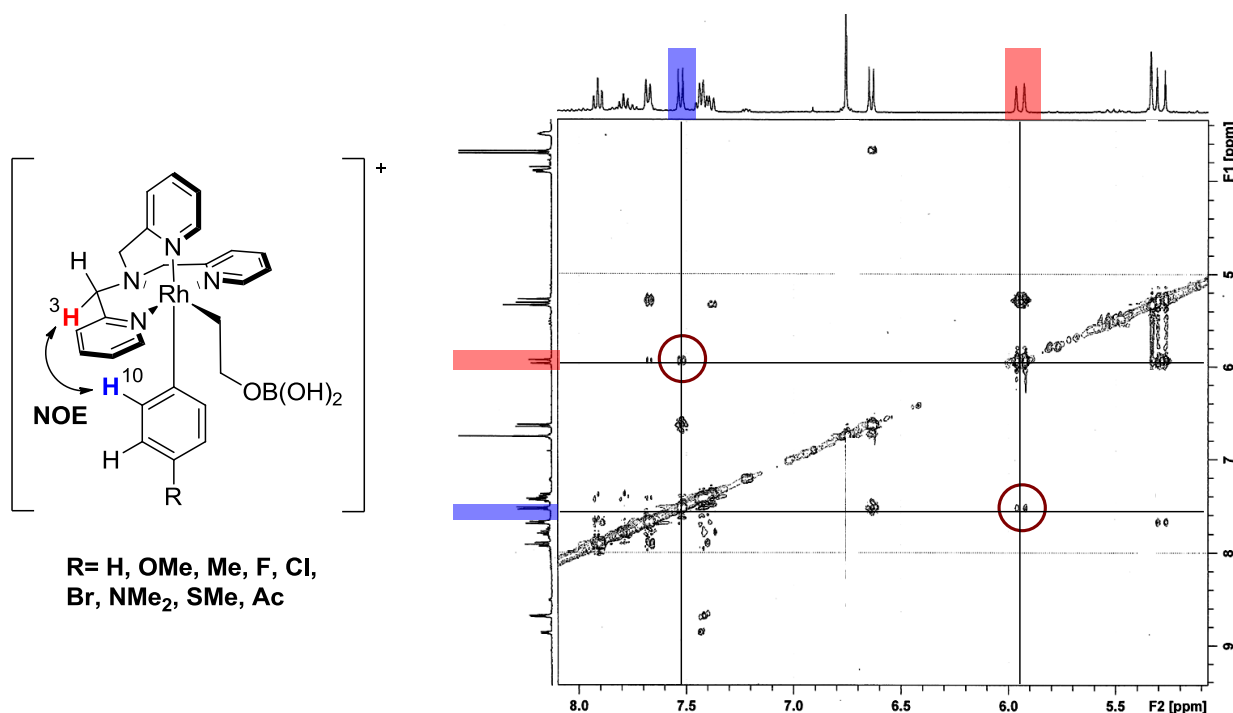
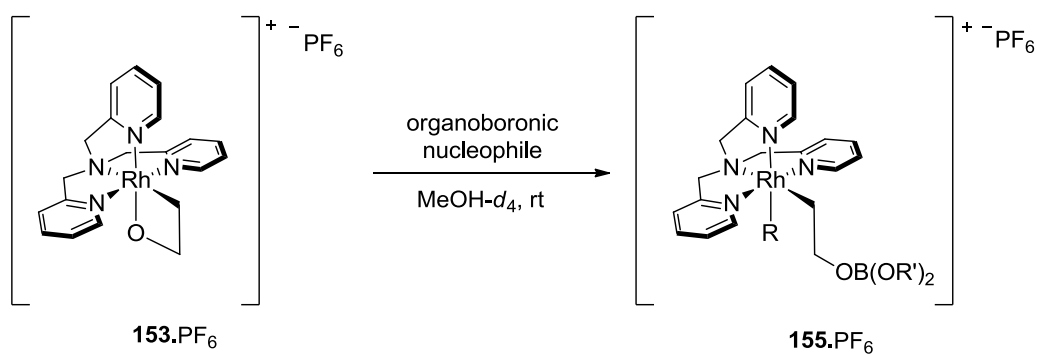


Figure 2.7 NOE correlations in the product complexes

When rhodaoxetane **153** was exposed to alkylboronic acids under standard conditions no conversion of starting material could be detected over the course of 2 weeks at room temperature (Table 2.1, entries 21-23). This can be interpreted as a lower aptitude of sp^3 hybridized carbon centers to perform transmetalation which is commonly observed. In comparison, we would expect that alkylboronic acids should undergo the ring-expansion (transesterification) in the same manner as their aryl and alkenyl counterparts. Overall, the accumulated data is more supportive of transmetalation of 4-bromophenylboronic acid than transesterification/ring expansion.

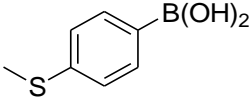
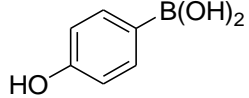
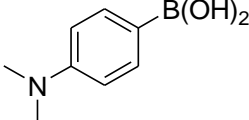
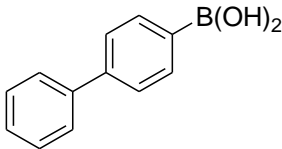
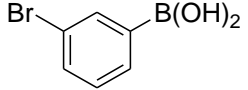
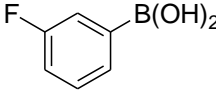
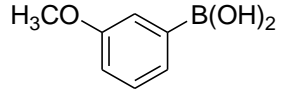
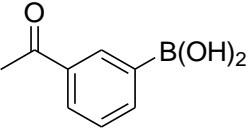
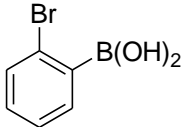
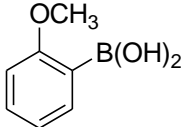
Having established that transmetalation was feasible, we sought to explore the reactivity of a series of organoboronic nucleophiles (Scheme 2.8, Table 2.1). The yields reported are based on ^1H NMR spectroscopy, using 1,3,5-trimethoxybenzene as an internal standard and ranged from 31-94%. In some cases, the product was isolated and the isolated yields are given in parentheses. ^1H NMR spectra, as well as HRMS, have been obtained for all products; ^{13}C NMR spectra were acquired for the isolated products.

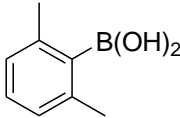
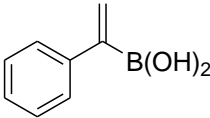
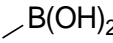
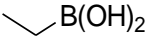
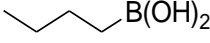
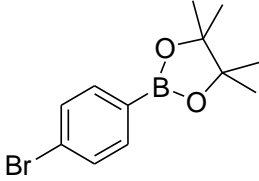
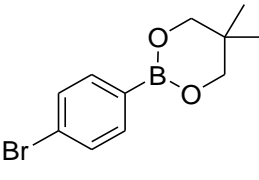
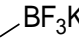
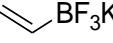
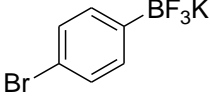


Scheme 2.8 Transmetalation with organoboronic nucleophiles

Table 2.1 Scope of transmetalation with organoboronic nucleophiles

Entry	Organoboronic reagent	Product ^a	Reaction time ^b	Relative rate	Yield ^c
1		155a	280 min	2.0	71% (42%)
2		155b	420 min	1.3	63% (56%)
3		155c	200 min	2.8	92%
4		155d	250 min	2.2	71%
5		155e	560 min	1.0	94% (75%)
6		155f	490 min	1.1	69%
7		155g	600 min	0.9	87% (48%)
8		155h	180 min	3.1	77%

Entry	Organoboronic reagent	Product ^a	Reaction time ^b	Relative rate	Yield ^c
9		155i	400 min	1.4	53%
10		no product	n/a		n/a
11		155j	380 min	1.5	73%
12		155k	270 min	2.1	42%
13		155l	300 min	1.9	71%
14		155m	210 min	2.7	86%
15		155n	240 min	2.3	84%
16		155o	240 min	2.3	84%
17		155p	270 min	2.1	75%
18		155q	450 min	1.2	86%

Entry	Organoboronic reagent	Product ^a	Reaction time ^b	Relative rate	Yield ^c
19		155r	14 days	0.03	31%
20		155s	280 min	2.0	57%
21		no product	n/a		n/a
22		no product	n/a		n/a
23		no product	n/a		n/a
24		155t	440 min	1.3	62%
25		155u	350 min	1.6	68%
26		no product	n/a		n/a
27		no product	n/a		n/a
28		no product	n/a		n/a

^a reaction conditions: 5mg **2** (0.1mL of a 0.086M standard solution), 10eq boronic acid, 0.5mL MeOD, r.t. ^b Reaction times were determined by monitoring the reaction by ¹H NMR spectroscopy in 5 – 30 minute intervals. When no further progress was detected, reaction time and yield were recorded. ^c NMR-yield referenced to an internal standard of 1,3,5-trimethoxybenzene; isolated yield after purification in brackets

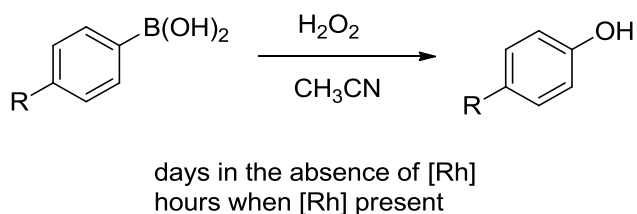
The transmetalation reaction could also be carried out successfully in acetonitrile, acetone or dichloromethane although limited solubility of the boronic acids in the latter required slightly longer reaction times.

The reaction shows a broad applicability to numerous organoboronic nucleophiles. Arylboronic acids with electron-withdrawing substituents work equally well as those with electron-neutral and electron-donating substituents mostly independent from their substitution pattern. Only ortho-disubstitution led to a significant decrease in reaction rate (entry 19). While an unprotected alcohol functionality was not tolerated by the protocol (entry 9), ethers (entries 6, 14, 17), thioethers (entry 8), alkylamines (entry 10) and ketone (entries 7, 15) functionalities were fully compatible with the applied conditions and gave products in moderate to excellent yields. Other sp^2 -hybridized organoboronic acids such as (*E*)-styrylboronic acid (entry 2) and 1-phenylvinylboronic acid (entry 20) also underwent successful transmetalation while sp^3 -hybridized boronic acids were unreactive as mentioned earlier. Organoboronic acid esters reacted successfully (entries 24-25) and the expected products were formed in comparable yields yet notably longer reaction times when compared to their parent boronic acid (entry 1). The use of trifluoroborates did not lead to any conversion of the starting material (entries 26-28).

One equivalent of boronic acid was sufficient to completely consume the starting rhodaoxetane. As expected, reaction rates increased with an increase of concentration of the organoboron nucleophiles. It is noteworthy that the reaction rate still was dependent on the concentration of the boronic acid even up to 150 equivalents and that saturation was not reached. While the reaction of **153** with 1 equivalent of 4-bromophenylboronic acid takes just over 7 hours to come to completion at room temperature, the employment of 10 equivalents reduces the reaction time to 280 minutes and upon use of 100 equivalents the reaction is completed after 90 minutes (reaction times monitored by ^1H -NMR in 5-10 minute intervals).

It is noteworthy that the rhodaoxetane formation and subsequent transmetalation could be performed in a one-pot setup. The desired transmetalation product and the phenolic by-product from H_2O_2 oxidation of the arylboronic acid were formed in nearly equal

amounts. This suggests that the rate of the two reactions is on the same order of magnitude. Furthermore, in a control experiment the oxidation of $p\text{-BrC}_6\text{H}_4\text{B(OH)}_2$ by H_2O_2 proceeded very slowly if performed in acetonitrile in the absence of a rhodium species. Only when either chlorobis(ethylene)rhodium (I) dimer or complexes **152** or **153** were added to the reaction mixture, the reaction rate of the phenol formation increased dramatically (Scheme 2.9). Phenol formation was even observed when a solution of $p\text{-BrC}_6\text{H}_4\text{B(OH)}_2$ and chlorobis(ethylene)rhodium (I) dimer was let to stand under air without addition of hydrogen peroxide. These findings show that the rhodium species plays an active role in the oxidation. In the prospect of eventual one-pot/catalytic feasibility of the protocol other oxidants than H_2O_2 should be assessed to get maximum compatibility with the boron nucleophiles employed.



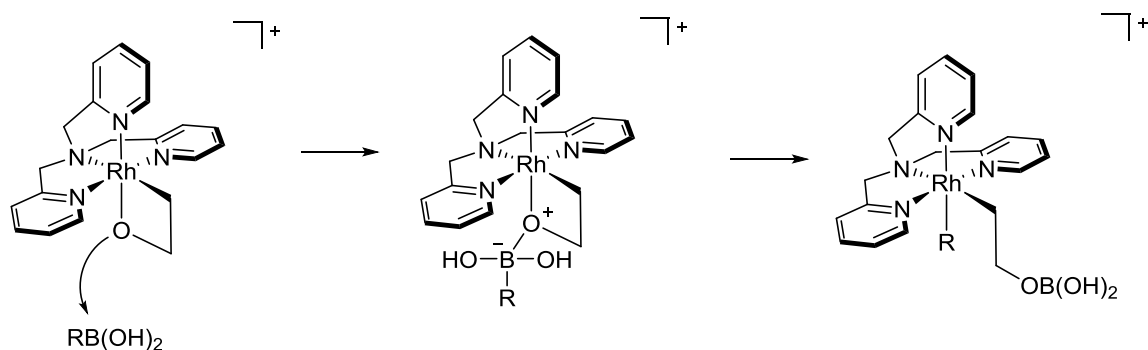
Scheme 2.9 Oxidation of arylboronic acids to phenol derivatives

Although Kuwano and co-workers proposed transmetalation of organoboron nucleophiles to a Rh(III) center as a possible catalytic pathway,²⁷⁰ to the best of our knowledge, our work presents the first experimental evidence for transmetalation involving a Rh(III)-O bond.

2.1.2 Proposed Mechanism

De Bruin et al., suggested a mechanism for acid-mediated ring-opening of rhodaoxetane **153**; protonation of the rhodaoxetane oxygen activates the structure which then opens under Rh-O bond cleavage in the presence of a coordinating ligand.¹⁸⁷ In transmetalation, coordination of the rhodaoxetane oxygen to the boron center would generate an -ate complex. In the present studies, no intermediates were observed spectroscopically (d_4 -methanol, rt). The data in Table 2.1 show that arylboronic acids bearing electron-withdrawing groups reacted the fastest, although there is no apparent

linear correlation. Typically, formation of borate complexes via transmetalation is rate limiting and sensitive to electronics,²⁷¹ which is consistent with both of our observations. Accordingly, we propose the following mechanism for transmetalation: In a first step the rhodaoxetane oxygen coordinates to the boron center to give the -ate complex. This activates both, the oxetane and the boronic acid for the next step, the actual transmetalation from boron to rhodium (Scheme 2.10).



Scheme 2.10 Proposed mechanism for transmetalation.

In light of this mechanistic hypothesis, we examined the collected data from the transmetalation experiments (Table 2.1). Increased steric bulk around the boron center (as with ortho substitution or boronic esters) should impede coordination of the oxetane and thus slow the reaction. In addition, if an -ate complex is indeed formed, trifluoroborates – in which the boron center is already tetravalent – should react slowly, if at all. If no pre-coordination of the oxetane is necessary, trifluoroborates should be reactive.

As evident in Table 2.1, ortho or meta mono-substitution did not affect the reaction rate or the yield significantly (Table 2, entries 13-18). In the case of two ortho substituents (Table 2, entry 19) though, both, reaction rate and yield are decreased substantially. The reactivity of aryl boronic esters and lack of reactivity of aryl trifluoroborates supports the postulated mechanism of involving pre-coordination of boron to the rhodaoxetane oxygen, although other possibilities cannot be rigorously excluded at present.

2.2 Attempts to Induce Reductive Elimination

The successful transmetalation described above is a key step towards our proposed carbohydroxylation protocol via a metallaoxetane intermediate. The last step necessary to

close the catalytic cycle proposed in Scheme 2.5 is reductive elimination. We explored multiple conditions to effect this transformation, which are discussed below.

2.2.1 Thermal Approaches

The first approach to facilitate reductive elimination was conventional heating in various solvents. Boiling under reflux was unsuccessful in solvents as methanol, ethanol isopropanol or dichloroethane. The reaction mixture remained unchanged for approximately two hours and then started to slowly decompose into a mixture of mostly unidentified products (Table 2.2). In some cases, evidence for expulsion of acetaldehyde through β -H elimination was observed by ^1H NMR spectroscopy. The same decomposition pathway was reported by de Bruin for rhodaoxetane **153** at higher temperatures and in the presence of acid with a non-coordinating counterion. Formation of the desired functionalized alcohols resulting from reductive elimination could not be observed. The reaction mixture tolerated microwave heating in methanol at 100 °C and up to 180 °C in dichloroethane for 15 minutes. Repeated microwave exposure led to decomposition, again, without evidence for reductive elimination. Conventional heating and microwave heating of the reaction mixture in DMSO only afforded decomposition products after 30 minutes and 5 minutes respectively.

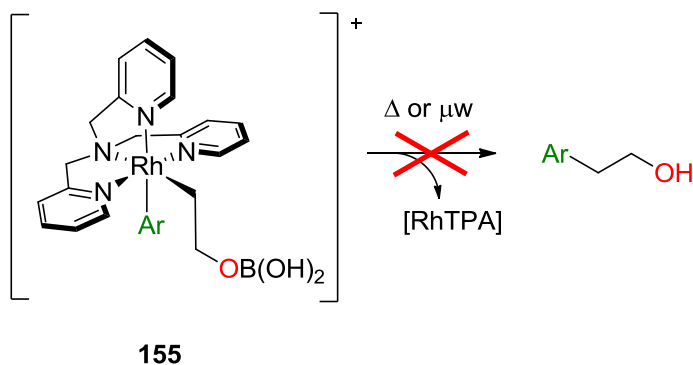
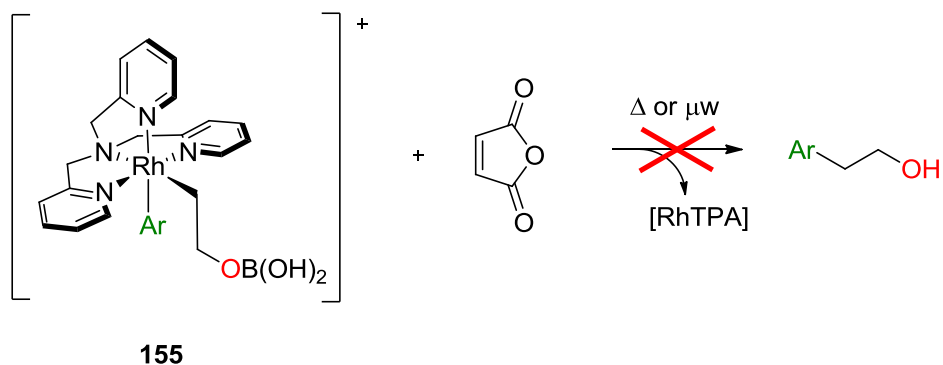


Table 2.2 Thermal reductive elimination attempts

	ROH R = Me, Et, <i>i</i> -Pr	DCE	DMSO
Reflux (2 h)	No reaction	No reaction	Decomposition
Reflux (24 h)	Decomposition	Decomposition	
μwave Reactor	No reaction (15 min), Decomposition when repeated	No reaction (15 min), Decomposition when repeated	Decomposition (5min)

2.2.2 Additives

Since thermal treatment of the transmetalated complex **155** did not prove fruitful, we introduced additives into the reaction mixture to facilitate reductive elimination. Due to the strongly electron donating nature of the four *N*-donor atoms of the TPA ligand, we aimed to reduce the electron density on the metal. Electron deficient olefins for example are known to facilitate reductive elimination processes.^{272,273} Thus, we added 2-5 equivalents of maleic anhydride to a solution of **155** in different solvents (MeOH, CH₃CN, DCM, DCE). In all cases standing at room temperature for 7 days left the transmetalated complex unchanged (Scheme 2.11). When heat was applied in addition to the maleic anhydride additive similar results were obtained as in the absence of the additive (compare Table 2.2).



Scheme 2.11 Attempts to effect reductive elimination with maleic anhydride.

2.2.3 Ligand Modifications

As the attempts to effect reductive elimination on the model system containing the TPA ligand (**155**) were unsuccessful we focussed on a re-design of the ancillary ligand with respect to the mode of coordination, as well as the steric and the electronic properties.

2.2.3.1 Tridentate Ligands

It has been shown that coordinatively saturated octahedral complexes have significantly higher barriers to reductive elimination than their unsaturated counterparts.²⁷⁴⁻²⁷⁶ Thus, our initial goal was to free up a coordination site on the complex by reducing the denticity of the ancillary ligand.

De Bruin had employed tridentate ligands that were modifications of the TPA ligand (Section 1.2.2.3, Figure 2.8).¹⁸⁹ One of the methylpyridyl arms of TPA was substituted with a non-coordinating aliphatic (MeBPA or BuBPA) or benzylic (BnBPA) arm.

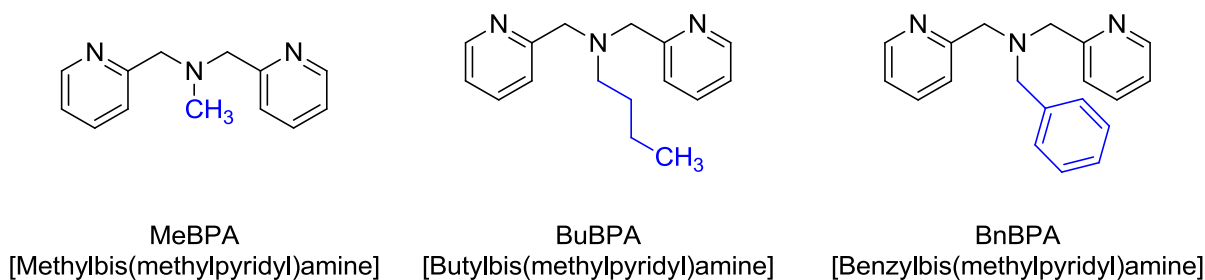
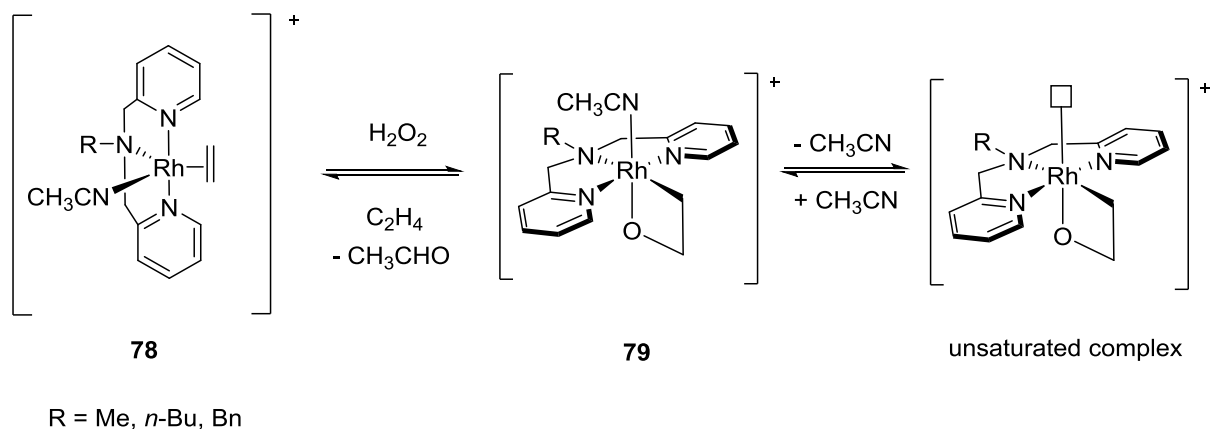


Figure 2.8 Tridentate TPA-modifications reported by de Bruin.

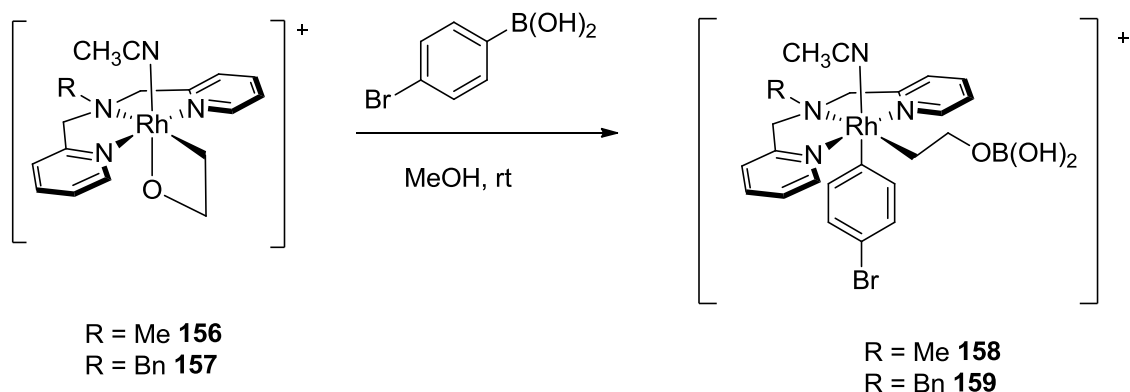
It was possible to prepare the ethylene complexes (**78**) analogous to **152** and oxidize them to the corresponding oxetanes (**79**). The free coordination site was occupied by an acetonitrile solvent molecule that could easily dissociate and lead to the unsaturated compound (Scheme 2.12). Indeed, de Bruin and co-workers observed increased reactivity of the resulting complexes including β -H elimination and acetaldehyde expulsion at room temperature.¹⁸⁹



Scheme 2.12 Opening of a coordination site on rhodaoxetanes.

We therefore reproduced complexes bearing the MeBPA (**156**) and BnBPA (**157**) ligands to explore their aptitude to transmetalation and subsequent reductive elimination.

In our hands, the formation and isolation of clean **156** was possible, while **157** could never be obtained in greater than 50% purity because of rapid decomposition of the complex. Due to their increased reactivity, **156** and **157** were generally prepared in situ and treated with the transmetalating agent immediately. Gratifyingly, transmetalation employing 4-bromobenzeneboronic acid was feasible with both complexes as judged by MS analysis (Scheme 2.13). The expected product signals ($M^+ - 18$) were observed for **158** and **159**, as well as daughter ions that indicated the loss of the labile acetonitrile ligand (41 *m/z*). Crude ¹H NMR spectra also indicated the successful transmetalation and formation of complex **158**. Compared to the clean transmetalation achieved with the analogous TPA-rhodaoxetane **153** the product spectra were convoluted through the formation of a series of unidentified by-products.

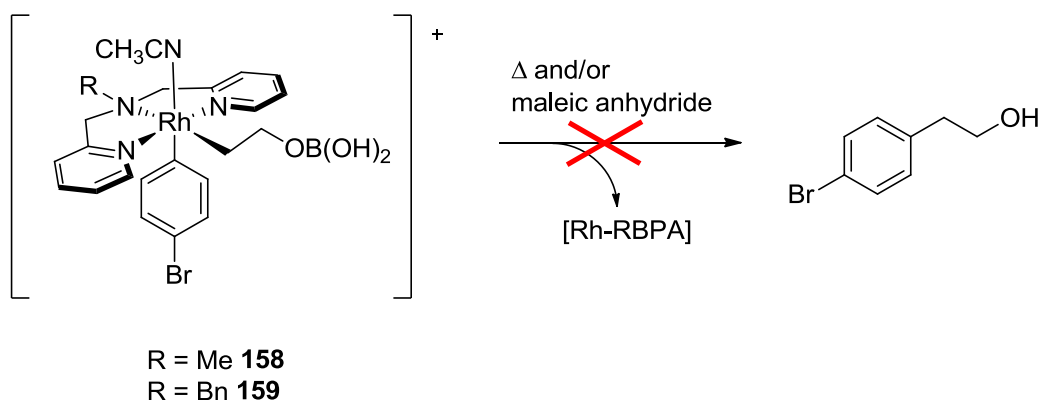


Scheme 2.13 Transmetalation on complexes with tridentate ligands.

To promote reductive elimination, **158** and **159** were left stirring in acetonitrile or dichloromethane at room temperature for extended periods of time. The Bn-BPA complex **159** underwent complete decomposition to acetaldehyde and other unidentified products within 6 hours without formation of the reductive elimination products. In contrast, Me-BPA complex **158** remained unchanged over a period of 5 days.

As a result, complex **158** was heated in methanol to 35 °C for 2 hours and to reflux in methanol, acetonitrile and dichloroethane for 30 minutes. In all cases, decomposition products were formed along with the β -H elimination product acetaldehyde; the desired carbohydroxylated product was not observed.

Exposing a solution of **158** in methanol, dichloromethane or acetonitrile to 2 equivalents of maleic anhydride, to further remove electron density from the metal center also only led to decomposition of the transmetalated complex to a mixture of unidentified products. This process was expedited at elevated temperatures (Scheme 2.14).



Scheme 2.14 Efforts towards reductive elimination.

2.2.3.2 Steric and Electronic Modifications

Hitherto, our investigations towards promoting reductive elimination through ligand modifications amounted to the observation that the tetradentate TPA complex (**155**) was too stable to reductively eliminate, while the tridentate MeBPA and BnBPA complexes (**158**, **159**) were too reactive and gave rise to β -H elimination rather than the desired C-C reductive elimination. We, therefore, turned to modifying the electronic and/or steric properties of the ligands. Starting from the tripodal, tetradentate TPA scaffold we envisaged the following ligand modifications.

Increasing the steric congestion around the metal center reportedly facilitates reductive elimination by forcing the ligands of interest into closer proximity of each other as well as through the release of steric strain on the complex after elimination.^{277,278} On the other hand, removing electron density from the metal center either through decreased σ -donation or increased π -backbonding can also promote reductive elimination.^{277,279}

Under these considerations we envisaged the use of ligands **160-162** which incorporate one or both of the criteria mentioned above. Ligand **160** has an additional methyl substituent in the ortho position to the pyridine nitrogen on one methylpyridyl arm which presumably forces the oxyethyl ligand closer to the transmetalated aryl moiety. This ligand was already employed by de Bruin and is known to be compatible with rhodaoxetane formation.¹⁸⁷ Ligand **161** combines both aspects, being sterically more demanding through the bulky triphenylphosphine group and having increased π -backbonding capability due to

the phosphorus atom. Finally, ligand **162** is electronically modified. The chloride substituent in para position to the pyridine nitrogen of one pyridylmethyl arm should effectively decrease the σ -donation capability of this arm (Figure 2.9). Potentially, this can also allow for a switch from a κ^4 to a κ^3 binding mode which would temporarily open a coordination site.

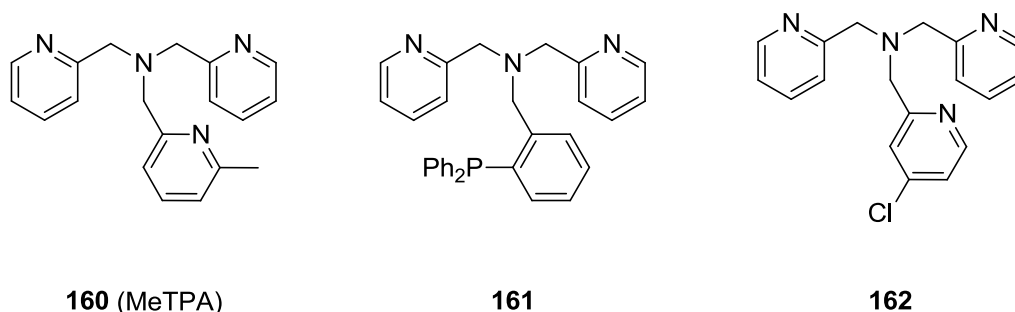
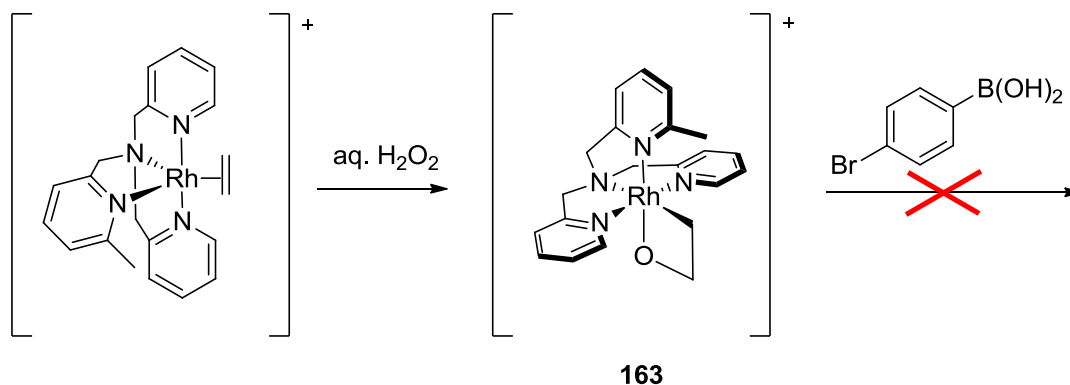


Figure 2.9 Sterically and electronically modified tripodal ligands

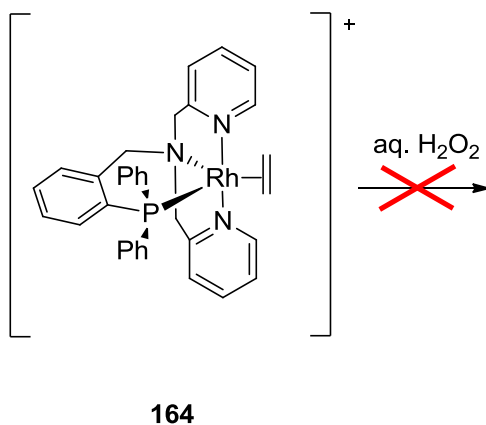
We were able to reproduce de Bruin's synthesis of rhodaoxetane **163** bearing ligand **160** according to literature procedures.¹⁸⁷ However, **163** did not undergo transmetalation when treated with 4-bromobenzenboronic acid under standard conditions (Scheme 2.15). Notably, **163** did not undergo acid promoted ring opening in a previous report, either.¹⁸⁷ Most likely, the steric hindrance by the methyl substituent on **160** is too great and renders it impossible for the rhodaoxetane to open. In this case the steric modification was too stark and impeded formation of the transmetalated complex.



Scheme 2.15 Failed transmetalation attempt with a sterically modified ligand.

Ligands **161** and **162** were synthesized by Nadine Kuhl, an exchange student in the group from the University of Münster according to modified literature procedures²⁸⁰⁻²⁸². She also successfully performed the coordination of the ligands to the dichlorobis(ethylene)rhodium(I) dimer giving rise to the respective Rh-ethylene complexes **164** and **165**.

Ethylene complex **164** proved to be fluxional and only at $-60\text{ }^{\circ}\text{C}$ sharp signals could be obtained in the ^1H NMR spectrum. The spectrum gave evidence for loss of symmetry compared to the TPA-ethylene complex **152**, judged by the inequivalence of the ancillary ligand protons and olefin protons. It was tentatively assigned a trigonal bipyramidal structure which is distorted through the steric demand of the triphenylphosphine arm. One concern with the use of this ligand was its potential propensity to oxidation under the standard conditions required for formation of the corresponding rhodaoxetane. To our surprise, when **164** was treated with 2 equivalents of H_2O_2 no reaction occurred over the period of 6 hours. In comparison, the oxidation of TPA-ethylene complex **152** was complete within minutes of the addition of H_2O_2 at $-10\text{ }^{\circ}\text{C}$. After addition of another 2 equivalents of the oxidant or mild heating to $40\text{ }^{\circ}\text{C}$ **164** was consumed and transformed into a variety of unidentified products, none of which were the desired rhodaoxetane (Scheme 2.16).



Scheme 2.16 Attempt to form a rhodaoxetane with modified ligand **161**.

Lastly, ligand **162** was employed and formation of ethylene complex **165** could be achieved under standard conditions as a mixture of isomers. While the exact structure of the different isomers was not further elucidated (proposed structures in Figure 2.10), this

isomerism suggests de-coordination and re-coordination of a ligand arm which could be ascribed to the reduced σ -bonding capability of the unique methyl(4-chloropyridyl) moiety and potentially flexible κ^4/κ^3 denticity of the ancillary ligand.

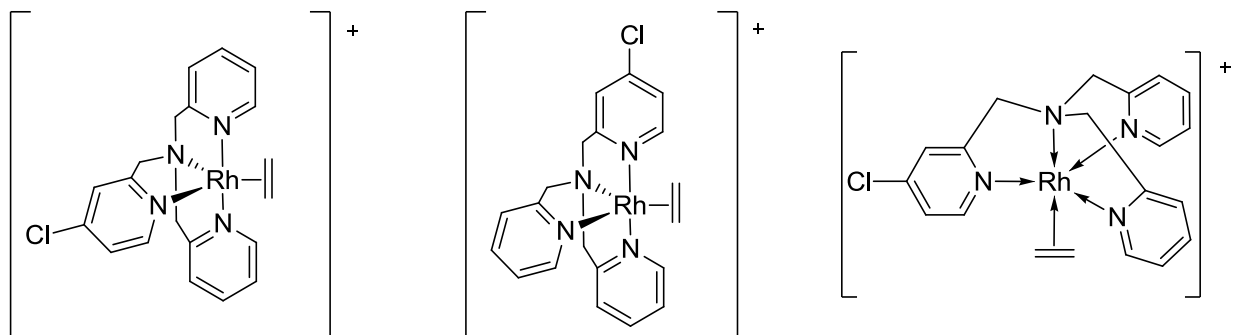
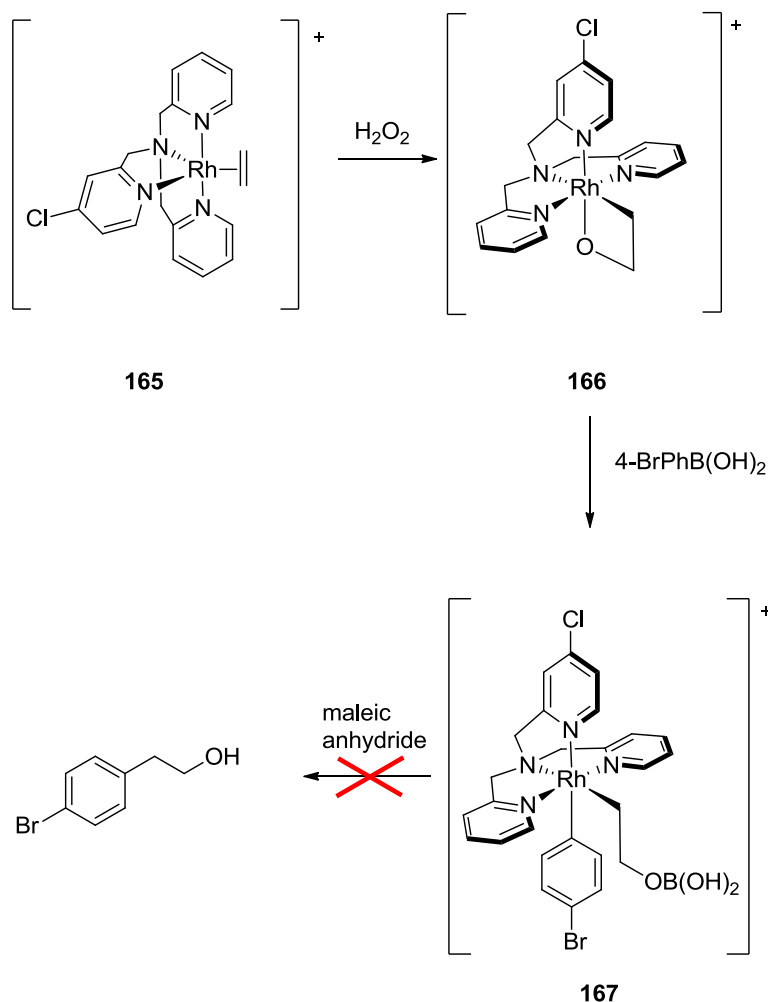


Figure 2.10 Possible isomers of **165** with trigonal bipyramidal geometry.

Upon oxidation with H_2O_2 the corresponding rhodaoxetane **166** was formed as a single isomer. Transmetalation with 4-bromobenzeneboronic acid was carried out successfully under the formation of complex **167** as a single isomer. The product was allowed to stir at room temperature for four days but no sign of reductive elimination was observed. When a solution of **167** in d_4 -methanol was treated with 2 equivalents of maleic anhydride at room temperature, slow decomposition to a mixture of unidentified products was recorded. To our disappointment, no formation of the reductive elimination product could be verified by NMR spectroscopy or MS (Scheme 2.17).



Scheme 2.17 Efforts towards reductive elimination employing ligand **162**.

To date, all efforts towards reductive elimination from the transmetalated complexes have been unsuccessful. Thermal approaches as well as the introduction of electron-withdrawing additives did not have the desired effect. Similarly, modifications of the ancillary ligand in terms of coordination mode, sterics and electronics did not lead to satisfying results. Future efforts should be directed towards further modification of the ancillary ligand, thereby potentially moving away from the TPA scaffold. A number of other ligands have been prepared in our lab but not yet tested on this system. Figure 2.11 shows a selection of these ligands.

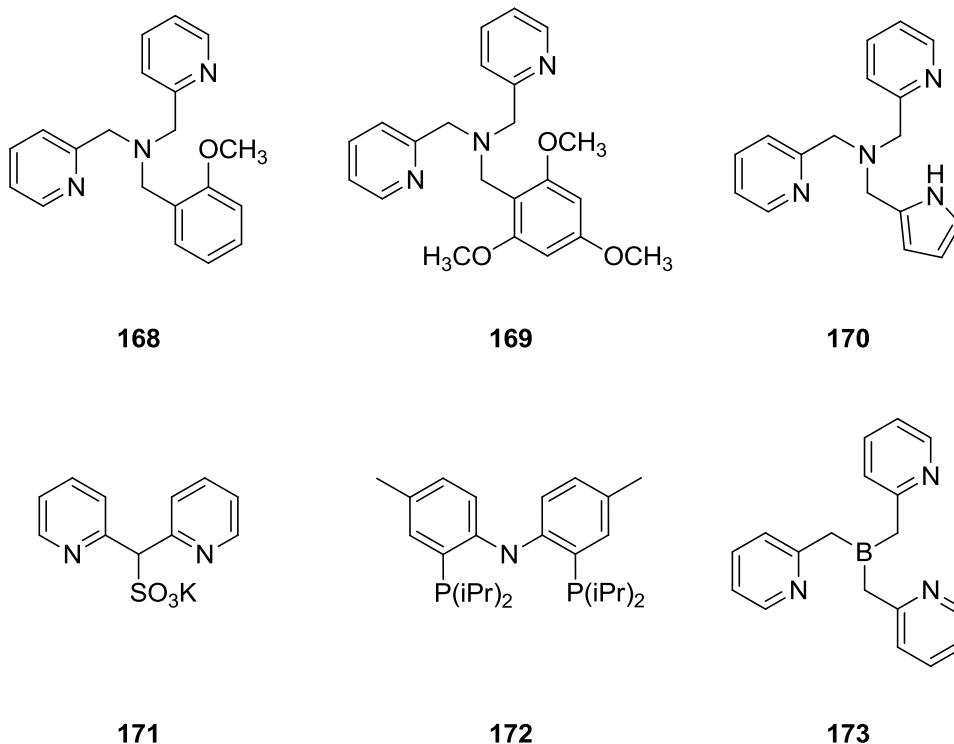
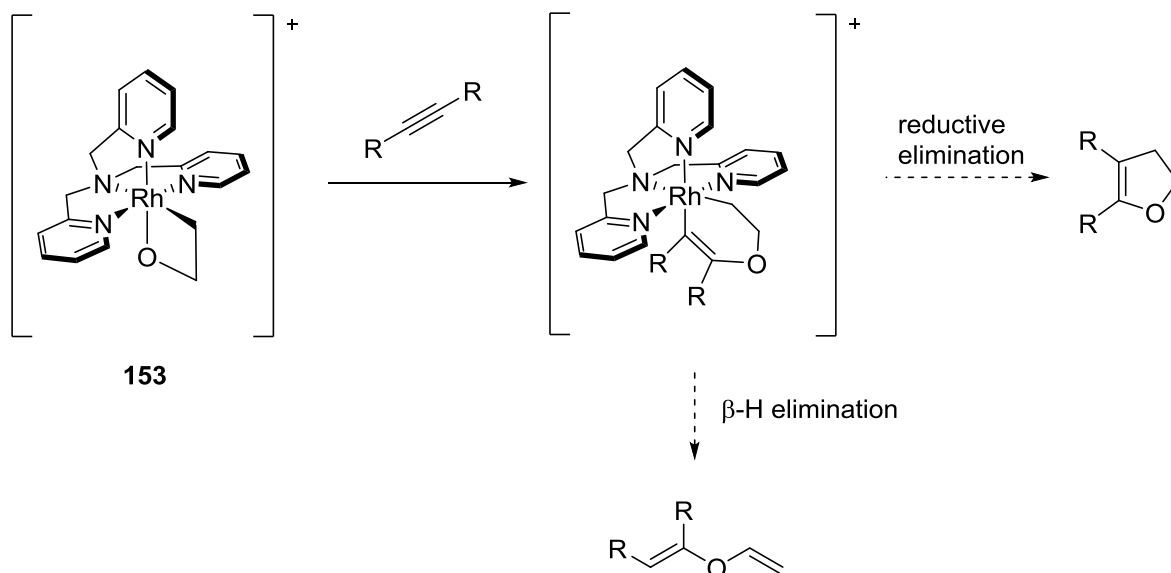


Figure 2.11 Alternative ligands

Ligands **168** and **169** are bearing one arm with oxygen instead of nitrogen donor atoms and were prepared by Alireza Azdari Tehrani according to a modified literature procedure.²⁸³ Ligand **170** bearing a methylpyrrole sidearm was synthesized by Yumin Shih following the same general procedure. The sulfonate-bearing ligand **171** had previously been employed by Vedernikov in the preparation of platinaoxetanes⁵⁴ (Section 1.2.2.3) while the PNP-pincer ligand **172** was prepared by Ozerov and shown to promote $\text{C}(\text{sp}^2)\text{--C}(\text{sp}^3)$ reductive elimination from a $\text{Rh}(\text{III})$ center at room temperature.²⁸⁴ Both compounds were synthesized by Kanghee Park. Finally, ligand **173** has to date not been reported in the literature. It is a modified version of TPA with the central atom being boron instead of nitrogen. The underlying rationale for this ligand design is a potential σ -back-donation from the Rh center to the ligand which would remove electron density from the metal thus possibly facilitating reductive elimination.²⁸⁵ So far, attempts to synthesize the ligand have not been successful.

2.3 Insertion of Electron-Poor Alkynes

In addition to our pursuit of developing a carbohydroxylation procedure based on transmetalation from boronic acids onto rhodaoxetanes and subsequent reductive elimination, we also sought to explore further unusual reactivity of these intriguing compounds. For example, rhodaoxetane **153** had been reported to be unreactive towards alkynes.¹⁸⁷ However, findings by Yamamoto *et al.* regarding the formation of oxametallacycles through insertion of electron deficient alkynes into a Rh(III)-O bond led us to test the reactivity of **153** towards electron deficient alkynes.²⁸⁶ Presumably, the insertion of substituted alkynes yields extended oxametallacycles which in turn could follow various reaction pathways. Reductive elimination would afford substituted dihydrofurans while β -H elimination would give rise to acyclic vinyl ethers (Scheme 2.18).



Scheme 2.18 Envisaged Rh-O insertion of alkynes and subsequent reactivity

2.3.1 Insertion of Acetylenedicarboxylates

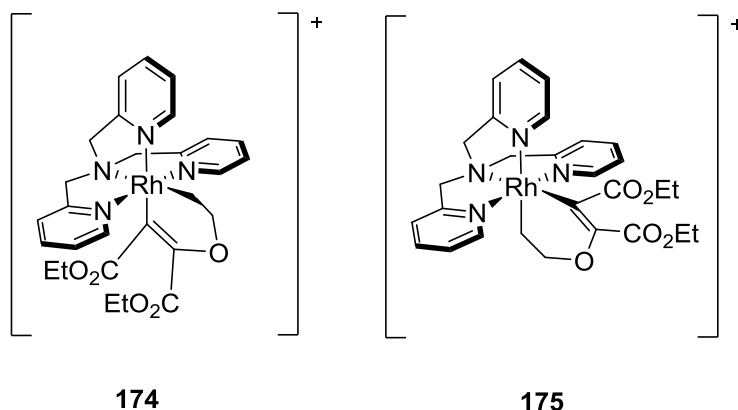
We therefore treated a solution of **153**.PF₆ in *d*₆-acetone with 5 equivalents of diethylacetylenedicarboxylate at room temperature. After 4 hours the starting material was completely consumed and one new product had been formed cleanly according to ¹H NMR spectroscopic data. ESI-MS analysis of the crude product mixture showed a single signal with the *m/z* of the envisaged product complex. The same could be observed when

dimethylacetylenedicarboxylate (DMAD) was used as substrate. When the reaction was carried out in *d*₄-methanol a mixture of unidentified products was formed with no indication of formation of the insertion product by MS or ¹H NMR spectroscopy.

2.3.2 Structural Elucidation

Based on Yamamoto's report, we expected the alkyne to insert into the Rh-O bond but insertion into the Rh-C bond could not be categorically excluded. (For an example of M-C insertion of alkynes into late transition metallaoxetanes see ¹⁵⁵) Additionally, the insertion can proceed in a concerted or stepwise fashion. In the latter case, two isomeric metallacycles can be formed. Therefore, the reaction can yield a total of four possible isomers, as shown in Figure 2.12.

Rh-O insertion:



Rh-C insertion:

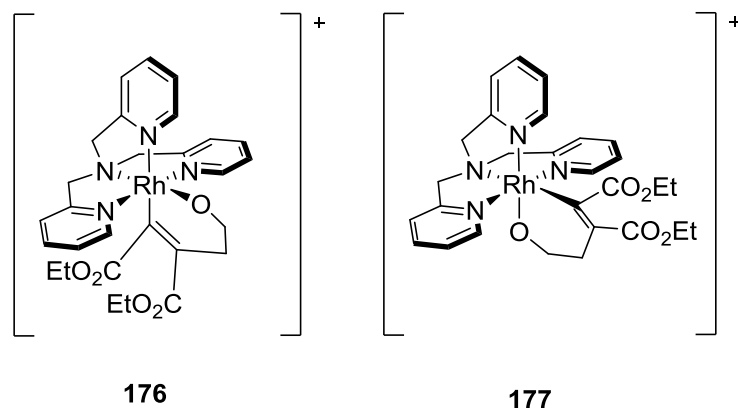


Figure 2.12 Possible isomers after insertion of alkynes

To differentiate between these options we utilized NMR spectroscopy. The ¹H NMR spectrum of the product complex revealed that the mirror symmetry of the starting material was retained, judged by the equivalence of proton signals of two methylpyridyl arms and the extended metallacycle. In case of insertion into the Rh-O bond, the ring protons should still show coupling to Rh, as observed in **153**, whereas with insertion into Rh-C bond, no Rh coupling should be observable. A clear doublet of triplets at 3.23 ppm (³J = 7.3 Hz, ²J_(Rh,H) = 3.1 Hz, H1) displayed that Rh-H coupling was still intact thus the alkyne had indeed inserted into the Rh-O bond as anticipated. The same signal also exhibited a strong NOE correlation to H8' on the unique methylpyridyl arm (8.96 ppm, d, 1H, ³J = 5.5 Hz) which indicated that the isomer formed was **174** (Figure 2.13). As there was no indication of a second isomer by

^1H NMR it is safe to assume that insertion proceeded in a concerted fashion therefore not allowing for rearrangement of the oxyethyl fragment.

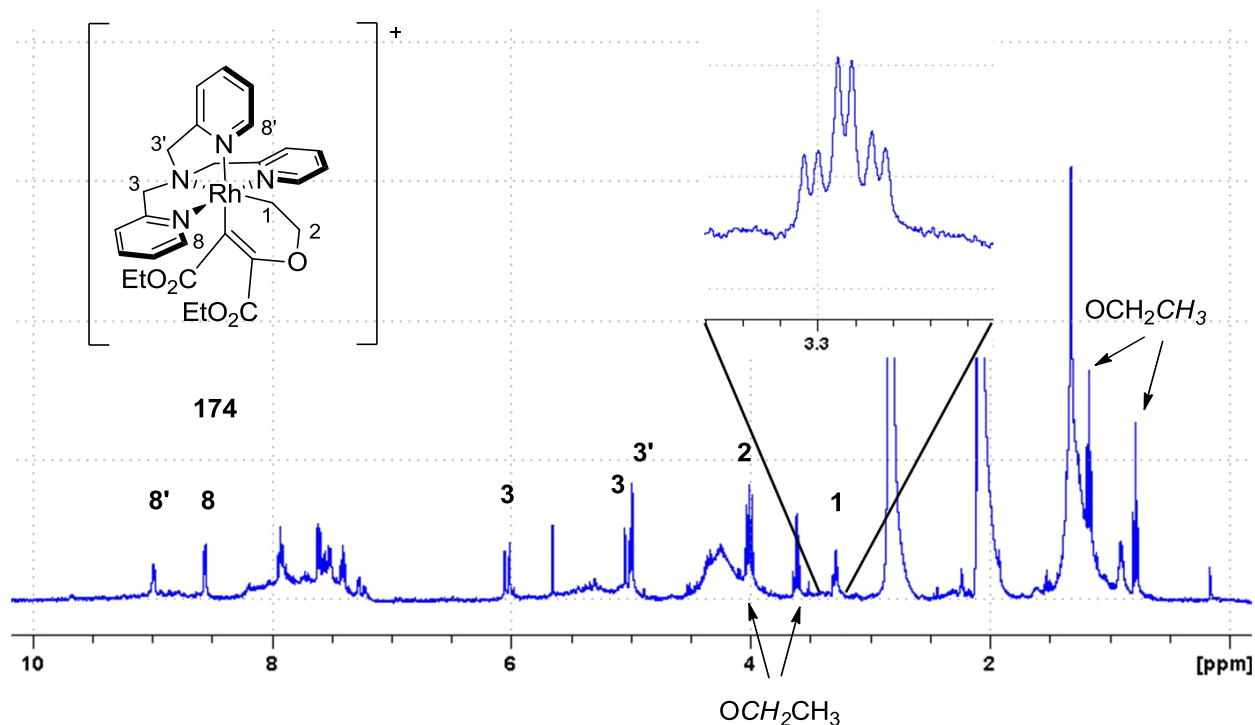


Figure 2.13 Crude ^1H NMR of alkyne insertion product **174**, (d_6 -acetone, 298K, 400MHz).

Full assignment of all proton signals was possible by the aid of COSY, NOESY and HSQC spectroscopy.

To this point we have demonstrated that insertion of the symmetrically disubstituted electron deficient alkynes diethylacetylenedicarboxylate and dimethylacetylenedicarboxylate into the Rh-O bond of rhodaoxetane **153** is possible. A full substrate scope study as well as reactivity studies will be performed by Addison Desnoyer, a new PhD student in our group.

2.4 Experimental

2.4.1 General Information

All experiments were carried out under standard Schlenk techniques under an atmosphere of dry nitrogen employing degassed solvents unless stated otherwise. All reagents were used as received without any further purification. Room temperature corresponds to ~20 °C. NMR spectra were recorded on Bruker Avance 300, 400 and 600 MHz spectrometers. ¹H NMR spectra are reported in parts per million and were referenced to residual solvent (2.05 ppm for d₆-acetone, 3.31 ppm for d₄-MeOH, 5.32 ppm for CD₂Cl₂). The multiplicities are abbreviated as follows: s = singlet, d = doublet, d[AB] = doublet in an AB system, t = triplet, q = quartet, dt = doublet of triplets, m = multiplet) MS-data was obtained on a Waters LC/MS for low resolution and Waters/Micromass LCT for high resolution spectra.

NMR yields were obtained by referencing 2 or 3 well isolated signals of the desired product to the aryl-proton signals of 1,3,5-trimethoxybenzene (TMB, 99+% purity, Sigma Aldrich). TMB was added as 1/3 equivalent of starting material (standard solution: 100mg/mL; δ = 6.08 ppm in d₆-acetone, 6.10 ppm in MeOD). Quantitative ¹H-NMR was performed with a calibrated 30 degree P1 pulse and delay + acquisition time being a minimum of 5 * T₁

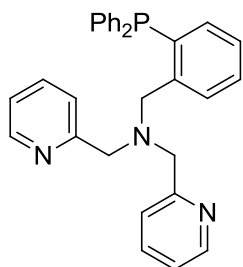
NMR yields are averaged over a minimum of two experiments. Isolated yields were obtained after multiple liquid-liquid extractions.

2.4.2 Experimental Procedures and Characterization Data

2.4.2.1 Preparation of Ligands

The previously reported ligands TPA²⁸⁷, MeTPA (**160**)²⁸⁷, MeBPA²⁸⁸ and BnBPA¹⁹⁰ were prepared by reductive amination according to a modified literature procedure.²⁸³ The characterization data matched the literature reports.

Ligands **161** and **162** were prepared and characterized by Nadine Kuhl according to the following procedures.

***N*-[2-(Diphenylphosphino)benzyl]-*N,N*-bis(2-pyridylmethyl)amine, 161:**

2-Diphenylphosphinobenzaldehyde (300 mg, 1.0 mmol, 1.0 eq.) and dipicolylamine (0.18 mL, 1.0 mmol, 1.0 eq.) were dissolved in degassed 1,2-dichloroethane (10 mL). The mixture was stirred for one hour at room temperature before $\text{NaBH}(\text{OAc})_3$ (340 mg, 1.6 mmol, 1.6 eq.) was added. After stirring at room temperature for 18 h the reaction mixture was neutralized with saturated NaHCO_3 solution (5 mL). The phases were separated and the aqueous phase was extracted with dichloromethane (3 x 5 mL). The combined organic layers were washed with brine and dried over MgSO_4 . The solvent was removed under vacuum and the crude product was purified by column chromatography on neutral alumina with DCM/methanol 99:1. Repeated purification by silica column chromatography with DCM/Methanol/ Et_3N 93/5/2 gave the pure product as a yellow oil in 75% yield (357 mg, 0.753 mmol)

R_f (DCM/Methanol 99:1) = 0.5; R_f (DCM/Methanol/ Et_3N 93 :5 :2) = 0.64

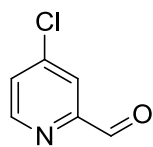
^1H NMR (300 MHz, CD_2Cl_2 , T = 298 K): δ / ppm: 8.45 (d, 3J = 4.7 Hz, 2H); 7.79 (dd, $^4J_{\text{P,H}}$ = 4.3 Hz, 3J = 7.2 Hz, 1H); 7.57 (td, 3J = 7.7 Hz, 4J = 1.7 Hz, 2H); 7.08-7.37 (m, 16H); 6.89 (ddd, 4J = 1.0 Hz, $^4J_{\text{P,H}}$ = 4.3 Hz, 3J = 7.5 Hz, 1H); 3.91 (d, $^4J_{\text{P,H}}$ = 2.4 Hz, 2H); 3.70 (s, 4H).

^{13}C NMR (100 MHz, CD_2Cl_2 , T = 298 K): δ / ppm: 160.2, 149.4, 144.5 (d, $J_{\text{P,C}}$ = 23.8 Hz), 137.7 (d, $J_{\text{P,C}}$ = 11.5 Hz), 137.0 (d, $J_{\text{P,C}}$ = 14.6 Hz), 136.6, 134.4 (d, $J_{\text{P,C}}$ = 19.9 Hz), 134.1, 129.7 (d, $J_{\text{P,C}}$ = 5.4 Hz), 129.4, 129.1 (t, $J_{\text{P,C}}$ = 6.9 Hz), 127.6, 123.4, 122.3, 60.3, 57.2 (d, $^3J_{\text{P,C}}$ = 23 Hz).

^{31}P NMR (121.49 MHz, CD_2Cl_2 , T = 298 K): δ / ppm: -15.8 (s).

HRMS: Calc: 474.2099, $[\text{C}_{31}\text{H}_{29}\text{N}_3\text{P}]^+$ Found: 474.2096.

Elemental Analysis: Calc.: C: 78.63%, H: 5.96%, N: 8.87%; Found: C: 75.76%, H: 5.86%, N: 8.52%.

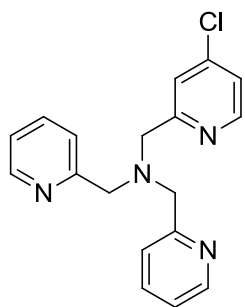
***N*-(4-chloro-2-pyridylmethyl)-*N,N*-bis(2-pyridylmethyl)amine, 162:**

Anhydrous DMSO (0.79 mL, 11 mmol, 6.1 eq.) was added to a solution of oxalyl chloride (0.53 mL, 5.6 mmol, 3.1 eq.) in dry dichloromethane (15 mL) at -78 °C. After stirring for 15 min. a solution of 3-chlorobenzylalcohol (400 mg,

2.79 mmol, 1.5 eq.) in dry dichloromethane (7 mL) was slowly added to the reaction mixture over a period 5 min. and the resulting mixture was stirred for 25 min. Anhydrous triethylamine (3.1 mL, 22 mmol, 12 eq.) was added over 5 min. and the mixture was allowed to warm to room temperature for 2 h. Water (30 mL) was poured onto the brown mixture and the phases were separated. The aqueous phase was extracted with dichloromethane (3 x 20 mL). The organic layers were combined, washed with brine and dried over MgSO₄. The solvent was evaporated carefully while cooling the flask containing the product with ice to minimize product loss through evaporation. The residue was used in the next step without further purification. For characterization of the aldehyde the crude product was purified by sublimation at room temperature at 200 mTorr.

¹H NMR (300 MHz, CDCl₃, T = 298 K): δ / ppm: 10.05 (s, 1H), 8.69 (d, ³J = 5.2 Hz, 1H), 7.95 (d, ⁴J = 2.1 Hz, 1H), 7.53 (dd, ⁴J = 2.1 Hz, ³J = 5.2 Hz, 1H).

LRMS (APCI): 142.1 [C₅H₅ClNO]⁺



The obtained yellow solid was dissolved in degassed 1,2-dichloroethane (10 mL). Dipicolylamine (0.33 mL, 1.8 mmol, 1.0 eq.) was added and the solution was stirred for 30 min. under N₂ at room temperature. After adding NaBH(OAc)₃ (617 mg, 2.91 mmol, 1.6 eq.) the reaction mixture was stirred again for 18 h at room temperature. The deep orange solution was neutralized with saturated NaHCO₃ solution (10 mL). The two phases were separated and the aqueous phase was extracted with dichloromethane (3 x 10 mL). The combined organic layers were washed with brine and dried over MgSO₄. The solvent was removed under vacuum. The brown crude product was purified by column chromatography over neutral alumina with EtOAc to obtain the pure product as a yellow-brown oil in 65% yield over two steps (384 mg, 1.18 mmol).

R_f (EtOAc) = 0.48.

¹H NMR (400 MHz, CD₂Cl₂, T = 298 K): δ / ppm: 8.51 (d, ³J = 4.8 Hz, 2H); 8.39 (d, ³J = 5.3 Hz, 1H); 7.67 (td, ³J = 7.7 Hz, ⁴J = 1.7 Hz, 2H); 7.64 (d, ⁴J = 1.9 Hz, 1H); 7.54 (d, ³J = 7.9 Hz, 2H); 7.14-7.17 (m, 3H); 3.85 (s, 6H).

^{13}C NMR (100 MHz, CD_2Cl_2 , $T = 298\text{ K}$): δ / ppm: 162.3, 159.8, 150.5, 149.6, 144.8, 136.8, 123.6, 123.5, 122.8, 122.5, 60.8, 60.3.

HRMS: Calc: 347.1039 [$\text{C}_{18}\text{H}_{17}\text{ClN}_4\text{Na}$] $^+$, Found: 347.1045.

Elemental Analysis; Calc: C: 66.56%, H: 5.28%, N: 17.25%; Found: C: 66.34%, H: 5.57%, N: 17.06%.

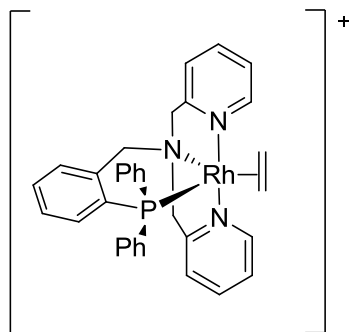
2.4.2.2 Preparation of Rh-ethylene Complexes

Rh-ethylene complexes bearing ligands TPA, MeBPA, BnBPA and MeTPA were prepared according to literature procedures^{187,189,190} and generally oxidized in situ without isolation.

Complexes **164** and **165** were prepared and characterized by Nadine Kuhl according to the following procedures.

General Procedure

$[\text{RhCl}(\text{C}_2\text{H}_4)_2]_2$ (5 mg, 0.01 mmol, 0.5 eq.) was weighed into a screw-cap NMR-tube and dissolved in degassed CD_2Cl_2 . A solution of the corresponding ligand (0.02 mmol, 1 eq) in degassed CD_2Cl_2 was prepared in a vial which was sealed with a septum. The solution of the ligand was added to $[\text{RhCl}(\text{C}_2\text{H}_4)_2]_2$ at $-78\text{ }^\circ\text{C}$ via syringe. After one hour the reaction mixture was warmed to room temperature to characterize the obtained compound by NMR spectroscopy and mass spectrometry.



164

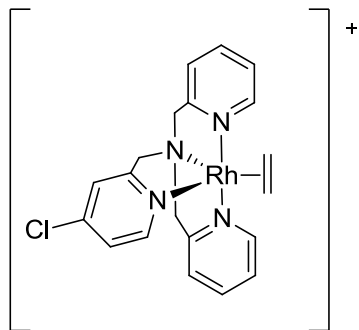
After the coordination reaction a yellow-brown solution was obtained.

^1H NMR (400 MHz, CD_2Cl_2 , $T = 213\text{ K}$): δ / ppm: 8.99 (d , $^3J = 5.0\text{ Hz}$, 1H); 8.28 (s , 1H); 7.23-7.80 (m , 17H); 6.97-7.04 (m , 3H); 6.93 (t , $^3J = 6.2\text{ Hz}$, 1H); 6.62-6.66 (m , 2H); 5.12 (d , $^2J = 14.3\text{ Hz}$,

1H); 5.11 (*d*, $^2J = 11.5$ Hz, 1H); 4.89 (*d*, $^2J = 14.3$ Hz, 1H); 4.75 (*d*, $^2J = 11.5$ Hz, 1H); 4.25 (*d*, $^2J = 17.2$ Hz, 1H); 3.73 (*d*, $^2J = 17.2$ Hz, 1H); 3.62-3.65 (*m*, 2H); 2.19-2.22 (*m*, 2H); 2.09 (*t*, $^3J = 9.2$ Hz, 1H); 1.88 (*br s*, 1H); 1.49 (*br s*, 1H); 1.20 (*t*, $^3J = 9.0$ Hz, 1H).

^{31}P NMR (121.49 MHz, CD_2Cl_2 , T = 298 K): δ / ppm: 51.3 (*d*, $^1J_{\text{Rh,P}} = 153.0$ Hz).

HRMS: Calc: 604.1389 [$\text{C}_{33}\text{H}_{32}\text{N}_3\text{PRh}$] $^+$, Found: 604.1401.



165

After the coordination reaction the solution had a green colour.

^1H NMR (300 MHz, CD_2Cl_2 , T = 298 K): δ / ppm: 9.29 (*d*, $^3J = 4.8$ Hz, 0.5H); 9.19 (*d*, $^3J = 5.6$ Hz, 0.5H); 7.93 (*d*, $^3J = 5.4$ Hz, 1H); 7.84 (*d*, $^3J = 5.9$ Hz, 1H); 7.50-7.60 (*m*, 3H); 7.41 (*d*, $^3J = 7.0$ Hz, 1H); 7.37 (*d*, $^3J = 6.5$ Hz, 1H); 7.28 (*d*, $^3J = 7.8$ Hz, 1H); 7.15-7.19 (*m*, 1H); 7.00-7.03 (*m*, 2H); 5.34-5.50 (*m*, 4H); 4.78-4.95 (*m*, 2H); 2.01 (*br s*, 4H).

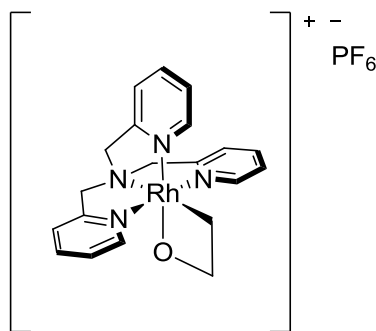
^1H NMR (300 MHz, CD_3CN , T = 298 K): δ / ppm: 9.32 (*d*, $^3J = 4.9$ Hz, 0.5H); 9.24 (*d*, $^3J = 5.7$ Hz, 0.5H); 8.00 (*d*, $^3J = 5.5$ Hz, 1H); 7.94 (*d*, $^3J = 5.8$ Hz, 1H); 7.58-7.65 (*m*, 2H); 7.03-7.38 (*m*, 6H); 5.48 (*d*, $^2J = 15.8$ Hz, 1H); 5.47 (*d*, $^2J = 15.5$ Hz, 1H); 4.84 (*d*, $^2J = 15.3$ Hz, 2H); 4.53 (*s*, 1H); 4.51 (*s*, 1H); 2.02 (*br s*, 4H).

LRMS (ESI): 455.2. [$\text{C}_{20}\text{H}_{21}\text{ClN}_4\text{Rh}$] $^+$

2.4.2.3 Preparation of Rhodaoxetanes

Rhodaoxetane complexes bearing ligands MeBPA (**156**), BnBPA (**157**) and MeTPA (**163**) were prepared according to literature procedures^{187,189,190} and characterized by ^1H NMR spectroscopy and MS. The characterization data matched the reported data, albeit for **157** a purity greater than 50% could not be achieved upon multiple repetition.

Rhodoxetane **153**.PF₆ was prepared according to a modified literature procedure¹⁸⁷:

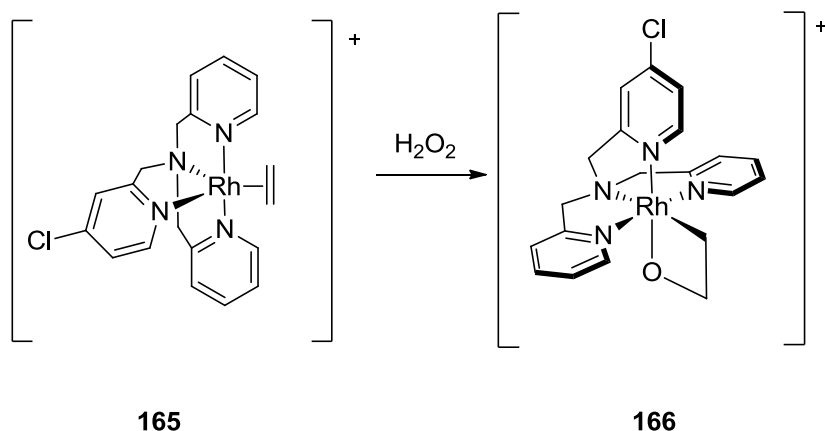


153.PF₆

[RhCl(C₂H₄)₂]₂ (100 mg, 0.257 mmol, Alfa Aesar) was weighed into a 100 mL Schlenk flask equipped with a stirbar. The flask was fitted with a teflon septum and put under an N₂ atmosphere. Dry, degassed methanol (15 mL) was added via syringe and the resulting solution was cooled to -78 °C. While the solution was cooling, TPA (150 mg, 0.516 mmol) was weighed into a 20 mL scintillation vial in a N₂ filled drybox. The vial was sealed with a septum and brought out of the drybox. Dry, degassed methanol (10 mL) was used to transfer the TPA solution into the cooled Rh-dimer solution by dropwise addition with a syringe. The resulting mixture was left stirring at -78 °C for one hour. A 30% aqueous H₂O₂ solution (120 µL, 1.029 mmol, Fisher) was added to the reaction mixture using a microsyringe which caused the solution to lighten in colour. The flask was taken out of the dry ice/acetone bath and slowly let warm to room temperature while stirring for another hour. At this point the solution appeared dirty yellow, and contained some black particles. KPF₆ (104 mg, 0.565 mmol, 99.9% purity, Sigma Aldrich) was added through a powder funnel under a N₂ counterflow. After stirring for an additional 10 min, Et₂O (40 mL) was added to the mixture. The flask was placed into the refrigerator (~ 7 °C) for 1 h; a beige-orange precipitate formed. The solution was filtered via cannula into a 250 mL Schlenk tube. An additional 80 mL of Et₂O was added to the filtrate while the filter residue was discarded. The filtrate was placed in the -20 °C freezer. After 3 days, slow crystallization yielded small yellow crystals that were suitable for X-ray diffraction (unprecedented for the TPA-complex and the PF₆ anion in the existing literature). Yield: 208 mg (69 %); analytical data (NMR, MS) was consistent with literature reports.

NOTE: the preparation could also be performed under “bench top conditions” with minimal effect on the yield and purity of the product.

Complex **166** was prepared and characterized by Nadine Kuhl according to the following procedure.



A solution of freshly prepared **165** (0.02mmol) in a screw-cap NMR tube was cooled to -78°C . An aqueous solution of H_2O_2 (30%) (5.4 μL , 0.05 mmol, 2.5 eq.) was added under N_2 atmosphere and the tube was inverted several times to mix the contents before leaving the mixture at -78°C . After 15 min. the mixture was allowed to warm to room temperature and let stand for another 45 min. During this time a colour change from green to deep yellow could be observed. The solvent was evaporated under vacuum and the residue was dissolved in degassed CD_2Cl_2 . The obtained reaction mixture was characterized by ^1H NMR and mass spectroscopy.

^1H NMR (300 MHz, CD_2Cl_2 , $T = 298\text{ K}$): δ / ppm: 8.78 (*d*, $^3J = 5.5\text{ Hz}$, 2H); 8.68 (*d*, $^3J = 6.4\text{ Hz}$, 1H); 8.45 (*d*, $^3J = 6.6\text{ Hz}$, 1H); 8.36 (*d*, $^3J = 5.8\text{ Hz}$, 1H); 7.11-7.86 (*m*, 22H); 5.49-5.69 (*m*, 4H); 5.40 (*s*, 2H); 5.11 (*dd*, $J = 5.1\text{ Hz}$, $J = 15.4\text{ Hz}$, 2H); 4.97 ppm (*dt*, $^3J = 7.4\text{ Hz}$, $^3J_{\text{H,Rh}} = 2.9\text{ Hz}$, 2H); 2.19 ppm (*dt*, $^3J = 7.6\text{ Hz}$, $^2J_{\text{H,Rh}} = 2.1\text{ Hz}$, 2H).

LRMS (ESI): 471.2 [$\text{C}_{20}\text{H}_{21}\text{ClN}_4\text{ORh}$] $^+$

2.4.2.4 General Procedure for Transmetalation (Isolable Scale)

In the glovebox, a 5 mL vial equipped with a stirbar was charged with **2** (50mg, 0.086 mmol) and 1 equivalent of boronic acid (0.086 mmol). The vial was fitted with a screwcap with a PTFE septum and brought out of the glovebox. Dry, degassed methanol (4mL) was added via syringe and the mixture was stirred at room temperature for 16 h. The volatiles were removed *in vacuo* and the residue taken up in 2 ml dichloromethane. All further work-up was performed open to atmosphere. The solution was extracted with water (3 x 2 mL) then with brine (1 x 2 mL). After re-extraction of the combined aqueous phases with dichloromethane (5 mL) the combined organic phases were dried over Na₂SO₄, filtered and the volatiles removed *in vacuo* to give the desired products.

NOTE: On some occasions a part of the boronic acid was oxidized to the corresponding phenol derivative. This byproduct could be eliminated by heating the product mixture with a heatgun under oilpump vacuum (~ 30 mTorr).

(κ^1 -C-2-ethyldihydrogenboratyl)-(4-bromophenyl)-(κ^4 -N,N,N-tri(2-pyridylmethyl)amine)-rhodium(III) hexafluorophosphate **155a:**

¹H NMR (*d*₆-acetone, 400MHz, 298K): δ 8.86 (d, 1H, *J* = 5.4 Hz), 8.67 (d, 2H, *J* = 5.6 Hz), 7.91 (dt, 2H, ³*J* = 7.8 Hz, ⁴*J* = 1.4Hz), 7.79 (dt, 1H, ³*J* = 7.8 Hz, ⁴*J* = 1.4 Hz), 7.67 (d, 2H, *J* = 7.6 Hz), 7.51 (d[AB], 2H, *J* = 8.3 Hz), 7.46-7.33 (m, 4H), 7.25 (d[AB], 2H, *J* = 8.3 Hz), 5.91 (d[AB], 2H, *J* = 15.1 Hz), 5.33 (s, 2H), 5.29 (d[AB], *J* = 15.2 Hz), 3.92 (dd, 2H, ³*J*(H,H) = 5.5 Hz, 5.3 Hz), 3.54-3.46 (m, 2H).

(*d*₄-methanol, 300MHz, 298K): δ 8.74 (d, 1H, *J* = 5.7 Hz), 8.61 (d, 2H, *J* = 5.5 Hz), 7.82 (t, 2H, *J* = 7.7 Hz), 7.77-7.53 (m, strong, from boronic acid reagent), 7.46-7.26 (m), 6.10 (s, from internal standard), 5.75 (d[AB], 2H, *J* = 15.4 Hz), 5.12 (d[AB], 2H, *J* = 15.3 Hz), 5.11 (s, overlap with d[AB] at 5.12ppm), 4.04-3.96 (m, 2H), 3.56-3.50 (m, 2H).

¹³C NMR (*d*₆-acetone, 100 MHz, 298 K): δ 165.3, 164.3, 150.5, 150.1, 139.4, 138.6, 136.6, 135.9, 130.6, 129.8, 125.3, 125.0, 124.2, 122.2, 112.2, 66.2, 64.7, 63.5, 34.5 (d, *J*_{Rh,C} = 27.6 Hz)
HRMS: Calcd: 619.0387 (C₂₆H₂₆BN₄O₂BrRh⁺, M⁺ - H₂O). Found: 619.0370

(κ^1 -C-2-ethyldihydrogenboratyl)-((*E*)styryl)-(κ^4 -N,N,N-tri(2-pyridylmethyl)amine)-rhodium(III) hexafluorophosphate 155b:

^1H NMR (d_6 -acetone, 600MHz, 298K): δ 8.84 (d, 1H, J = 5.6 Hz), 8.67 (d, 2H, J = 5.6 Hz), 7.93 (dt, 2H, J = 7.8 Hz, 1.5 Hz), 7.78 (dt, 1H, J = 7.8 Hz, 1.4 Hz), 7.68 (d, 2H, J = 7.9 Hz), 7.46-7.35 (m, 4H), 7.31-7.28 (m, 2H), 7.22 (t, 2H, J = 7.6 Hz), 7.15 (t, 1H, J = 7.3 Hz), 6.92 (d[AB], 1H, J = 18.2 Hz), 5.93 (d[AB], 1H, J = 18.2 Hz), 5.89 (d[AB], 2H, J = 15.1 Hz), 5.32 (s, 2H), 5.26 (d[AB²], 2H, J = 15.1 Hz), 3.82 (t, 2H, J = 5.3 Hz), 3.49-3.42 (m, 2H).

^{13}C { ^1H } NMR (d_6 -acetone, 150 MHz, 298 K): δ 166.6, 151.7, 151.4, 144.0, 140.5, 139.7, 129.6, 128.6, 127.6, 126.5, 126.2, 125.3, 123.4, 67.4, 65.9, 64.2, 63.5, 36.2 (d, $J_{\text{Rh,C}}$ = 27.5 Hz)

LRMS: 567.1 ($\text{C}_{28}\text{H}_{29}\text{BN}_4\text{O}_2\text{Rh}^+$, M^+ - H_2O)

(κ^1 -C-2-ethyldihydrogenboratyl)-(phenyl)-(κ^4 -N,N,N-tri(2-pyridylmethyl)amine)-rhodium(III) hexafluorophosphate 155e:

^1H NMR (d_6 -acetone, 400MHz, 298K): δ 8.86 (d, 1H, J = 5.6 Hz), 8.68 (d, 2H, J = 5.4 Hz), 7.90 (dt, 2H, 3J = 7.6 Hz, 4J = 1.4 Hz), 7.79 (t, 1H, 3J = 7.8 Hz, 4J = 1.4 Hz), 7.67 (d, 2H, J = 7.6 Hz), 7.59 (dd, 2H, 3J = 7.8 Hz, 4J = 1.4 Hz), 7.47-7.34 (m, 4H), 7.13-7.03 (m, 3H), 5.94 (d[AB], 2H, J = 15.0 Hz), 5.32 (s, 2H), 5.29 (d[AB], J = 15.1 Hz), 3.95-3.89 (m, 2H), 3.54-3.48 (m, 2H).

^{13}C { ^1H } NMR (d_6 -acetone, 75 MHz, 298 K): δ 165.3, 164.3, 150.5, 150.1, 139.3, 138.5, 133.9, 128.3, 126.7, 125.3, 125.0, 124.1, 122.2, 66.2, 64.6, 63.4, 34.6 (d, $J_{\text{Rh,C}}$ = 27.6 Hz)

HRMS: Calc: 541.1271 ($\text{C}_{26}\text{H}_{27}\text{BN}_4\text{O}_2\text{Rh}^+$, M^+ - H_2O). Found: 541.1282

(κ^1 -C-2-ethyldihydrogenboratyl)-(4-methoxyphenyl)-(κ^4 -N,N,N-tri(2-pyridylmethyl)amine)-rhodium(III) hexafluorophosphate 155h:

^1H NMR (d_6 -acetone, 400MHz, 298K): δ 8.85 (d, 1H, J = 6.2 Hz), 8.67 (d, 2H, J = 5.6 Hz), 7.90 (dt, 2H, 3J = 7.8 Hz, 4J = 1.4Hz), 7.78 (t, 1H, 3J = 7.8 Hz, 4J = 1.4Hz), 7.67 (d, 2H, J = 7.8Hz), 7.53 (d[AB], 2H, J = 8.6 Hz), 7.47-7.33 (m, 4H), 6.63 (d[AB], J = 8.6 Hz), 5.94 (d[AB²], 2H, J = 15.1 Hz), 5.32 (s, 2H), 5.28 (d[AB²], J = 15.1 Hz), 3.94-3.84 (m, 2H), 3.67 (s, 3H), 3.54-3.45 (m, 2H).

^{13}C { ^1H } NMR (d_6 -acetone, 100 MHz, 298 K): δ 165.3, 164.3, 160.4, 150.5, 150.1, 139.3, 138.5, 135.3, 125.3, 124.9, 124.1, 122.2, 112.2, 66.2, 64.7, 63.2, 54.3, 34.7 (d, $J_{\text{Rh,C}}$ = 27.5 Hz)

HRMS: Calcd: 571.1388 ($\text{C}_{27}\text{H}_{29}\text{BN}_4\text{O}_3\text{Rh}^+$, M^+ - H_2O). Found: 571.1377

2.4.2.5 General Procedure for Transmetalation (NMR Scale):

In the glovebox, an NMR tube was charged with 10 equivalents (0.0859 mmol) of boronic acid. The tube was fitted with a screwcap with a PTFE septum and brought out of the glovebox. Dry, degassed d_4 -methanol (500 μ L) was added. With a microsyringe **2** (100 μ L of a 50mg/mL standard solution, 0.00859 mmol) and 2,4,6-trimethoxybenzene as internal standard (4.8 μ L of a 100mg/mL standard solution, 0.00286 mmol) were added, the tube was inverted and the reaction monitored by ^1H -NMR for 24 h. The contents of the tube were emptied into a 5 mL vial, the volatiles removed *in vacuo* and the residue taken up in d_6 -acetone.

The following spectral data is from crude reaction mixtures so some of the data is incomplete. As an excess of boronic acid was used, the signals of the remaining reagent are dominant and partly obscure product signals, especially in the aromatic region of the ^1H -NMR spectrum

(κ^1 -C-2-ethyldihydrogenboratyl)-(4-chlorophenyl)-(κ^4 -N,N,N-tri(2-pyridylmethyl)amine)-rhodium(III) hexafluorophosphate 155d:

^1H NMR (d_6 -acetone, 300MHz, 298K): δ 8.85 (d, 1H, J = 5.8 Hz), 8.67 (d, 2H, J = 5.6 Hz), 7.91 (dt, 2H, 3J = 7.8 Hz, 4J = 1.5 Hz), 7.85 (d, strong, from boronic acid reagent) 7.78 (dt, 2H, 3J = 7.8 Hz, 4J = 1.5 Hz), 7.67 (d, 2H, J = 7.9 Hz), 7.58 (d[AB], 2H, J = 8.3 Hz), 7.46-7.20 (m, strong, from boronic acid reagent), 7.09 (d[AB], 2H, J = 8.3 Hz), 6.09 (s, from internal standard), 5.92 (d[AB], 2H, J = 15.2 Hz), 5.32 (s, 2H), 5.28 (d[AB], 2H, J = 15.2 Hz), 3.95-3.88 (m, 2H), 3.54-3.46 (m, 2H).

HRMS: Calcd: 575.0892 ($\text{C}_{26}\text{H}_{26}\text{BN}_4\text{O}_2\text{ClRh}^+$, $\text{M}^+ - \text{H}_2\text{O}$). Found: 575.0885

(κ^1 -C-2-ethyldihydrogenboratyl)-(4-fluorophenyl)-(κ^4 -N,N,N-tri(2-pyridylmethyl)amine)-rhodium(III) hexafluorophosphate 155c:

^1H NMR (d_6 -acetone, 300MHz, 298K): δ 8.85 (d, 1H, J = 5.8 Hz), 8.67 (d, 2H, J = 5.6 Hz), 7.97-7.87 (m, strong, from boronic acid reagent) 7.78 (dt, 2H, 3J = 7.8 Hz, 4J = 1.5 Hz), 7.67 (d, 2H, J = 7.6 Hz), 7.65-7.58 (m), 7.21-7.04 (m, strong, from boronic acid reagent), 6.85-6.76 (m, probably oxidized boronic acid byproduct), 6.09 (s, from internal standard), 5.92 (d[AB], 2H, J = 15.2 Hz), 5.32 (s, 2H), 5.29 (d[AB], 2H, J = 15.2 Hz), 3.95-3.87 (m, 2H), 3.55-3.46 (m, 2H).

HRMS: Calcd: 559.1188 (C₂₆H₂₆BN₄O₂FRh⁺, M⁺ - H₂O). Found: 559.1196

(κ¹-C-2-ethyldihydrogenboratyl)-(4-methylphenyl)-(κ⁴-N,N,N-tri(2-pyridylmethyl)amine)-rhodium(III) hexafluorophosphate 155f:

¹H NMR (*d*₆-acetone, 300MHz, 298K): δ 8.84 (d, 1H, *J* = 5.7 Hz), 8.65 (d, 2H, *J* = 5.5 Hz), 7.89 (dt, 2H, ³*J* = 7.7 Hz, ⁴*J* = 1.4 Hz), 7.76 (d, strong, from boronic acid reagent), 7.64 (d, 2H, *J* = 7.9 Hz), 7.47 (d[AB], 2H, *J* = 7.9 Hz), 7.32-6.95 (m, strong, from boronic acid reagent), 6.89 (d[AB], 2H, *J* = 7.4 Hz), 6.09 (s, from internal standard), 5.89 (d[AB], 2H, *J* = 15.1 Hz), 5.28 (s, 2H), 5.24 (d[AB²], 2H, *J* = 15.2 Hz), 3.93-3.86 (m, 2H), 3.52-3.44 (m, 2H).

HRMS: Calcd: 555.1439 (C₂₇H₂₉BN₄O₂Rh⁺, M⁺ - H₂O). Found: 555.1423

(κ¹-C-2-ethyldihydrogenboratyl)-(biphenyl)-(κ⁴-N,N,N-tri(2-pyridylmethyl)amine)-rhodium(III) hexafluorophosphate 155k:

¹H NMR (*d*₆-acetone, 300MHz, 298K): δ 8.83 (d, 1H, *J* = 5.5 Hz), 8.66 (d, 2H, *J* = 5.4 Hz), 8.19 (d, *J* = 7.8 Hz), 7.97 (d, strong, from boronic acid reagent) 7.87 (t, *J* = 8.2 Hz) 7.80-7.25 (m, strong, from boronic acid reagent), 7.19 (s, 5.93 strong, from boronic acid reagent), 5.93 (d[AB], 2H, *J* = 15.2 Hz), 5.30 (s, 2H), 5.25 (d[AB], 2H, *J* = 15.1 Hz), 3.97-3.90 (m, 2H), 3.54-3.46 (m, 2H).

HRMS: Calcd: 617.1586 (C₃₂H₃₁BN₄O₂Rh⁺, M⁺ - H₂O). Found: 617.1595

(κ¹-C-2-ethyldihydrogenboratyl)-(4-*N,N*-dimethylaminophenyl)-(κ⁴-N,N,N-tri(2-pyridylmethyl)amine)-rhodium(III) hexafluorophosphate 155j:

¹H NMR (MeOD, 400MHz, 298K): δ 8.72 (d, 1H, *J* = 5.4 Hz), 8.58 (d, 2H, *J* = 5.7 Hz), 7.80 (dt, 2H, ³*J* = 7.8 Hz, ⁴*J* = 1.4 Hz), 7.70 (dt, 1H, ³*J* = 7.6 Hz, ⁴*J* = 1.3 Hz) 7.66-7.50 (m, strong, from boronic acid reagent), 7.43-7.24 (m, 8H), 7.24-6.65 (m, strong, from boronic acid reagent), 6.52 (d[AB], 2H, *J* = 8.7 Hz), 5.73 (d[AB²], 2H, *J* = 15.3 Hz), 5.10 (d[AB], 2H, *J* = 15.2 Hz), 5.07 (s, 2H), 4.02-3.96 (m, 2H), 3.54-3.47 (m, 2H), 2.84 (s, 6H).

HRMS: Calcd: 584.1716 (C₂₈H₃₂BN₅O₂Rh⁺, M⁺ - H₂O). Found: 584.1704

(κ^1 -C-2-ethyldihydrogenboratyl)-(4-acetylphenyl)-(κ^4 -N,N,N-tri(2-pyridylmethyl)amine)-rhodium(III) hexafluorophosphate 155h:

^1H NMR (d_6 -acetone, 300MHz, 298K): δ 8.86 (d, 1H, J = 5.4 Hz), 8.68 (d, 2H, J = 5.6 Hz), 8.25-7.92 (m, strong, from boronic acid reagent), 7.90 (dt, 2H, 3J = 7.9 Hz, 4J = 1.4 Hz), 7.84-7.20 (m), 6.09 (s, from internal standard), 5.93 (d[AB], 2H, J = 15.4 Hz), 5.33 (s, 2H), 5.31 (d[AB], 2H, J = 15.2 Hz), 3.97-3.91 (m, 2H), 3.57-3.48 (m, 2H).

HRMS: Calcd: 583.1388 ($\text{C}_{28}\text{H}_{29}\text{BN}_4\text{O}_3\text{Rh}^+$, $\text{M}^+ - \text{H}_2\text{O}$). Found: 583.1400

(κ^1 -C-2-ethyldihydrogenboratyl)-(4-methylthiophenyl)-(κ^4 -N,N,N-tri(2-pyridylmethyl)amine)-rhodium(III) hexafluorophosphate 155i:

^1H NMR (d_6 -acetone, 300MHz, 298K): δ 8.84 (d, 1H, J = 5.6 Hz), 8.66 (d, 2H, J = 5.5 Hz), 7.96-7.83 (m, 3H), 7.76 (d, strong, from boronic acid reagent), 7.65 (d, 2H, J = 7.8 Hz), 7.47 (d[AB], 2H, J = 7.8 Hz), 7.43-7.31 (m, 4H), 7.21-6.94 (m, strong, from boronic acid reagent), 6.89 (d[AB], 2H, J = 7.5 Hz), 6.09 (s, from internal standard), 5.91 (d[AB], 2H, J = 15.1 Hz), 5.31 (s, 2H), 5.26 (d[AB], 2H, J = 15.1 Hz), 3.93-3.86 (m, 2H), 3.52-3.43 (m, 2H).

HRMS: Calcd: 587.1152 ($\text{C}_{27}\text{H}_{29}\text{BN}_4\text{O}_2\text{SRh}^+$, $\text{M}^+ - \text{H}_2\text{O}$). Found: 587.1159

(κ^1 -C-2-ethyldihydrogenboratyl)-(2-bromophenyl)-(κ^4 -N,N,N-tri(2-pyridylmethyl)amine)-rhodium(III) hexafluorophosphate 155p:

^1H NMR (d_4 -methanol, 300 MHz, 298 K): δ 8.75 (d, 1H, J = 5.7 Hz), 8.64 (d, 2H, J = 5.5 Hz), 7.87 (t, 2H, J = 7.5 Hz), 7.71 (t, 1H, J = 7.3 Hz), 7.52 (d, strong, from boronic acid reagent), 7.45-7.18 (m, strong, from boronic acid reagent), 7.06-6.95 (m, 2H), 6.92-6.83 (m, 1H), 6.10 (s, from internal standard), 5.71 (d[AB], 2H, J = 15.1 Hz), 5.04 (s, 2H), 4.99 (d[AB], 2H, J = 15.1 Hz), 4.05-3.94 (m, 2H), 3.57-3.47 (m, 2H).

HRMS: Calcd: 619.0387 ($\text{C}_{26}\text{H}_{26}\text{BN}_4\text{O}_2\text{BrRh}^+$, $\text{M}^+ - \text{H}_2\text{O}$). Found: 619.0381

(κ^1 -C-2-ethyldihydrogenboratyl)-(3-bromophenyl)-(κ^4 -N,N,N-tri(2-pyridylmethyl)amine)-rhodium(III) hexafluorophosphate 155l:

^1H NMR (d_4 -methanol, 300MHz, 298K): δ 8.75 (d, 1H, J = 5.7 Hz), 8.64 (d, 2H, J = 5.5 Hz), 7.87 (t, 2H, J = 7.5 Hz), 7.71 (t, 1H, J = 7.3 Hz), 7.52 (d, strong, from boronic acid reagent), 7.45-7.18 (m, strong, from boronic acid reagent), 7.06-6.95 (m, 2H), 6.92-6.83 (m, 1H), 6.10 (s, from

internal standard), 5.71 (d[AB], 2H, $J = 15.1$ Hz), 5.04 (s, 2H), 4.99 (d[AB], 2H, $J = 15.1$ Hz), 4.05-3.94 (m, 2H), 3.57-3.47 (m, 2H).

HRMS: Calcd: 619.0387 ($C_{26}H_{26}BN_4O_2BrRh^+$, $M^+ - H_2O$). Found: 619.0373

(κ^1 -C-2-ethyldihydrogenboratyl)-(2,6-dimethylphenyl)-(κ^4 -N,N,N-tri(2-pyridylmethyl)amine)-rhodium(III) hexafluorophosphate 155r:

Due to the low yield (31%), small amount of material and the long reaction time (14 days) this spectrum was especially difficult to assign, the most indicative signals for ring-opening (at δ 5.63, 4.01-3.93 and 3.57-3.48) could still be clearly identified. The good match for HRMS corroborates successful transmetalation.

1H NMR (d_4 -methanol, 300 MHz, 298 K): δ 9.07-8.57 (m), 8.17-7.17 (m), 7.16-6.83 (m, strong from boronic acid reagent), 6.74-6.60 (m), 6.10 (s, from internal standard), 5.63 (d[AB], 2H, $J = 15.4$ Hz), 5.09 (s, 2H), 4.96 (d[AB], 2H, $J = 15.3$ Hz), 4.01-3.93 (m, 2H), 3.57-3.48 (m, 2H).

HRMS: Calcd: 569.1595 ($C_{28}H_{31}BN_4O_2Rh^+$, $M^+ - H_2O$). Found: 569.1580

(κ^1 -C-2-ethyl-4,4,5,5-tetramethyl-1,3,2-dioxaborolanyl)-(4-bromophenyl)-(κ^4 -N,N,N-tri(2-pyridylmethyl)amine)-rhodium(III) hexafluorophosphate 155t:

1H NMR (d_4 -methanol, 300 MHz, 298 K): δ 8.76 (d, 1H, $J = 5.4$ Hz), 8.62 (d, 2H, $J = 5.5$ Hz), 7.85 (t, 2H, $J = 7.8$ Hz), 7.71 (t, 1H, $J = 7.9$ Hz), 7.63 (d, strong, from boronic acid reagent), 7.52 (d, strong, from boronic acid reagent), 7.40-7.19 (m), 6.10 (s, from internal standard), 5.74 (d[AB], 2H, $J = 15.3$ Hz), 5.14 (d[AB], 2H, $J = 15.3$ Hz), 5.11 (s, 2H), 4.03-3.95 (m, 2H), 3.59-3.52 (m, 2H), 0.89 (s, partly overlapping with boronic ester signal)

LRMS: 619.1 ($C_{26}H_{26}BN_4O_2BrRh^+$, $M^+ - C_7H_{14}O \rightarrow$ pinacol ester).

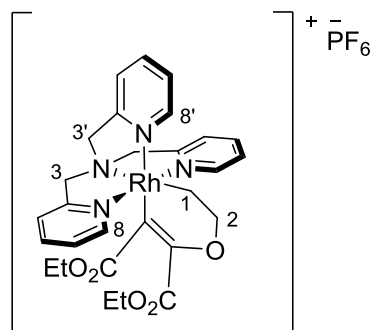
(κ^1 -C-2-ethyl-5,5-dimethyl-1,3,2-dioxaborinanyl)-(4-bromophenyl)-(κ^4 -N,N,N-tri(2-pyridylmethyl)amine)-rhodium(III) hexafluorophosphate, 155u:

1H NMR (d_4 -methanol, 300 MHz, 298 K): δ 8.76 (d, 1H, $J = 5.9$ Hz), 8.62 (d, 2H, $J = 5.6$ Hz), 7.84 (t, 2H, $J = 7.8$ Hz), 7.74 (t, 1H, $J = 7.8$ Hz), 7.66 (d, strong, from boronic acid reagent), 7.49 (d, strong, from boronic acid reagent), 7.43-7.22 (m), 6.10 (s, from internal standard), 5.75 (d[AB], 2H, $J = 15.4$ Hz), 5.14 (d[AB], 2H, $J = 15.4$ Hz), 5.11 (s, 2H), 4.07-3.96 (m, 2H), 3.58-3.51 (m, 2H), 1.22 (s, partly overlapping with boronic ester signal)

LRMS: 619.1 ($C_{26}H_{26}BN_4O_2BrRh^+$, $M^+ - C_5H_{10}O \rightarrow$ neopentyl glycol ester).

2.4.2.6 General Procedure for Alkyne Insertion

An NMR tube was charged with a solution of rhodaoxetane **153**.PF₆ (10mg, 0.017mmol) in *d*₆-acetone (500 μL). 5 equivalents (0.086 mmol) of alkyne were added, the tube was sealed and inverted several times to mix the contents. After 4 hours the reaction mixture was investigated with ¹H NMR spectroscopy.

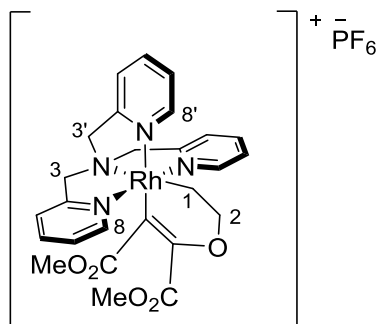


174.PF₆

¹H NMR (*d*₆-acetone, 400 MHz, 298 K): δ 8.96 (d, 1H, *J* = 5.5 Hz, H8'), 8.52 (d, 2H, *J* = 5.6 Hz, H8), 7.93-7.83 (m, 3H), 7.60-7.45 (m, 4H), 7.37 (t, 2H, *J* = 6.7 Hz), 6.00 (d[AB], 2H, *J* = 16.2 Hz, H3), 5.00 (d[AB], 2H, *J* = 16.3 Hz, H3), 4.96 (s, 2H, H3'), 3.99 (t, 2H, *J* = 7.3 Hz, H2), 3.96 (q, 2H, *J* = 7.1 Hz), 3.58 (q, 2H, *J* = 7.3 Hz), 3.26 (dt, 2H, *J* = 7.3 Hz, ²*J*_{Rh,H} = 3.1 Hz, H1), 1.14 (t, 3H, 7.1 Hz), 0.75 (t, 3H, 7.2 Hz).

¹³C NMR (*d*₆-acetone, 100 MHz, 298 K): 151.1 (C8), 147.2 (C8'), 138.9, 138.6, 124.8, 124.6, 124.4, 123.4, 71.8 (C2), 68.3, 65.4, 59.8 (2C), 28.3 (C1), 13.6 (2C).

LRMS: 607.4 (C₂₉H₃₆N₄O₅Rh⁺, M⁺).



^1H NMR (d_6 -acetone, 300 MHz, 298 K): δ 8.94 (d, 1H, $J = 5.5$ Hz, H8'), 8.51 (d, 2H, $J = 5.7$ Hz, H8), 7.92-7.81 (m, 3H), 7.59-7.44 (m, 4H), 7.35 (t, 2H, $J = 6.6$ Hz), 5.91 (d[AB], 2H, $J = 16.5$ Hz, H3), 5.01 (d[AB], 2H, $J = 16.5$ Hz, H3), 4.93 (s, 2H, H3'), 3.99 (t, 2H, $J = 7.3$ Hz, H2), 3.49 (s, 3H), 3.26 (dt, 2H, $J = 7.3$ Hz, $^2J_{\text{Rh,H}} = 3.0$ Hz, H1), 3.12 (s, 3H).

LRMS: 595.3 ($\text{C}_{27}\text{H}_{32}\text{N}_4\text{O}_5\text{Rh}^+$, M^+).

3 Formation of Substituted Rhodaoxetanes

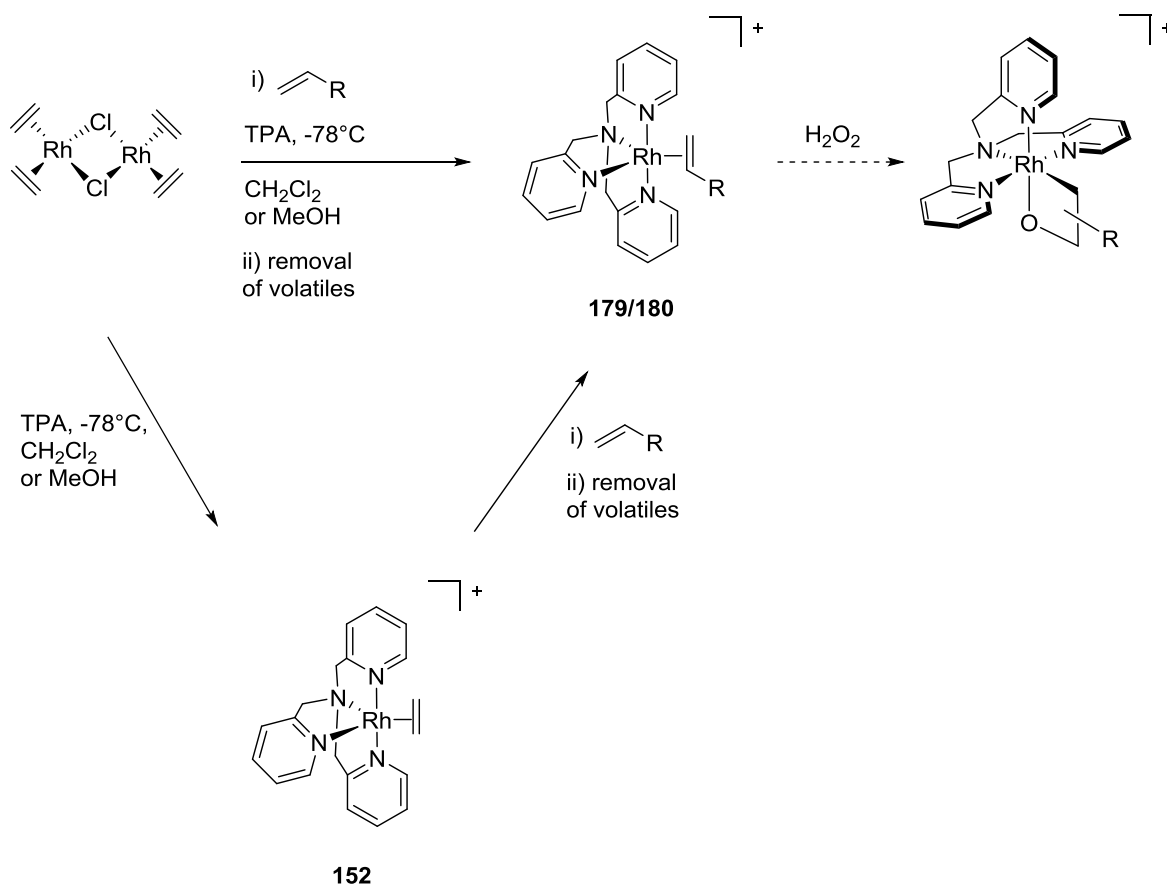
Encouraged by the preliminary findings with regards to the reactivity of unsubstituted rhodaoxetane **153** described in Chapter 2, we were interested whether substituted rhodaoxetanes could be formed by exchange of the ethylene ligand in **152** for substituted olefins and subsequent oxidation by H₂O₂ (Scheme 3.1). Of particular interest was the stereochemical outcome, as multiple isomers could in principle be formed. This knowledge is crucial to the eventual development of efficient catalytic olefin functionalization protocols via rhodaoxetane intermediates as proposed in Chapter 2 (Scheme 2.5). The results of these studies are presented in this chapter. First, the formation of the substituted TPA-rhodium olefin complexes will be reported, followed by a description of the results obtained after oxidation. A discussion of the observed reactivity and selectivity of formation will conclude the chapter.

Two undergraduate students in our lab have helped with parts of this project. Jennifer Tsoung performed preliminary olefin-exchange studies and first attempts to oxidize and isolate product complexes. Her work is summarized in her Chem448 Thesis at The University of British Columbia (2009). Carla Rigling reproduced and optimized the olefin exchange reactions and performed PhINTs-based oxidations which will be described in greater detail in Chapter 5. Her work resulted in the preparation of a Master thesis at the Eidgenössische Technische Hochschule (ETH) Zürich (2012). Parts of this work have furthermore been submitted as a full article. The results disclosed here are extended in scope and discussion compared to the submitted data.

3.1 Formation of TPA-Rhodium Complexes with Substituted Olefins

Our first goal was to prepare TPA-Rh(I) complexes derived from a series of substituted olefins. We anticipated that the ethylene ligand of **152** would readily exchange with an excess of different substituted olefins. TPA-Rh-ethylene complex **152** was readily synthesized by adding *N,N,N*-tris(pyridylmethyl)amine (TPA) to a stirred solution of the Rh-dimer [RhCl(C₂H₄)₂]₂ in CH₂Cl₂ or MeOH at -78 °C according to de Bruin's reported procedure.^{185,187} A wide variety of unsymmetrically substituted olefins (**178a-l**, **178p-v**) and

five symmetrical di-substituted olefins (**178m-o, w, x**) were explored. As shown in Table 3.1, addition of olefin with subsequent removal of free ethylene by evaporation of the volatiles and addition of fresh solvent cleanly generated the desired products in complete conversion in many cases. Alternatively, addition of the substituted olefin during formation of **152** and subsequent removal of free ethylene by evaporation of the volatiles and addition of fresh solvent also successfully yielded the product complexes (Scheme 3.1).

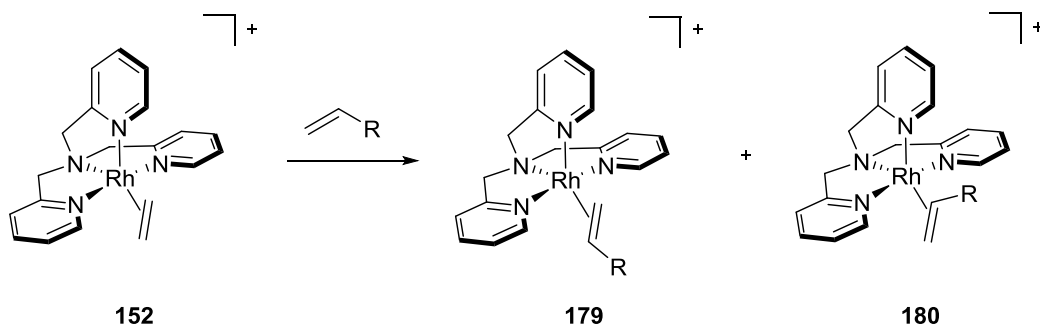


Scheme 3.1 Preparation of substituted TPA-Rh-olefin complexes

Removal of ethylene was necessary, both to push the reaction to completion and to prevent the concomitant formation of unsubstituted rhodaoxetane **153** upon addition of H_2O_2 (see section 3.2). The product complexes lacked sufficient stability for separation and isolation but were characterized in situ by ^1H NMR spectroscopy, NOESY and ESI mass spectrometry.

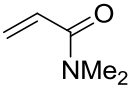
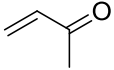
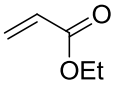
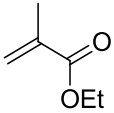
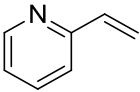
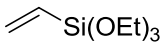
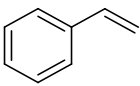
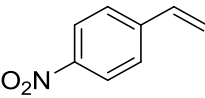
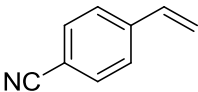
Electron-deficient olefins underwent efficient exchange for ethylene (Table 3.1, entries 1-4, 13). This follows the expected trend of increased coordination strength through a higher π -backbonding potential.^{289,290} Substitution also proceeded readily with 2-vinylpyridine and triethoxyvinylsilane (entries 5 and 6, respectively). Vinylsilanes are reported to be better π -acceptors than their carbon analogues and coordinate more readily to Rh(I) centers.^{291,292} Likewise, a selection of styrene derivatives could also be successfully exchanged with the ethylene ligand (entries 7-12). Olefins with low π -backbonding capability or increased steric bulk did not coordinate to an appreciable extent (entries 14-24). The fact that cyclohexenone (entry 20) could not successfully substitute the ethylene ligand is surprising, given the electron-poor nature of the alkene. At this point we have no satisfactory explanation for this observation.

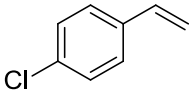
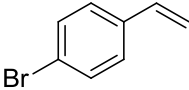
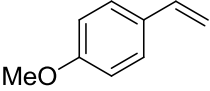
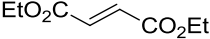
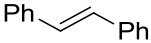
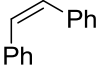


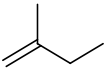
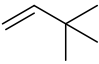
While exchange with the symmetrical olefin **178m** gives rise to only one product (complex **179m**), coordination of unsymmetrical olefins **178a-l** led to two different isomeric complexes; one where the olefin substituent points away from the central TPA pyridyl arm (**179**) and another where the substituent points towards it (**180**) (Scheme 3.2). In all cases, one product isomer clearly predominated and the major-to-minor product ratio ranged from exclusive formation of one isomer to 2:1 in favour of complex **179** (Table 3.1).

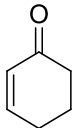
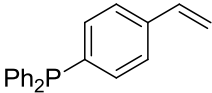

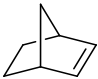
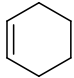


Scheme 3.2 Ethylene substitution with higher olefins

Table 3.1 Olefin exchange in TPA complex **152**.

Entry ^a	Olefin	TPA-Complex ratio	Selected ¹ H NMR shifts of major isomer ^b		
			δ H1	δ H2a	δ H2b
1	178a	 2:1 179a:180a	3.17	2.79	2.18
2	178b	 3:1 179b:180b	3.41	2.61	2.23
3	178c	 14:1 179c:180c	2.99	2.56	2.21
4	178d	 >95:5 179d:180d	n/a	2.79	2.07
5	178e	 11:1 179e:180e	3.91	2.82	2.27
6	178f	 >95:5 179f:180f	3.53	2.51	2.25
7	178g	 4:1 179g:180g	3.85	2.65	2.25
8	178h	 5:1 179h:180h	3.94	2.70	2.42
9	178i	 6:1 179i:180i	3.87	2.64	2.34

Entry ^a	Olefin	TPA-Complex ratio	Selected ¹ H NMR shifts of major isomer ^b		
			δ H1	δ H2a	δ H2b
10	178j	 4:1 179j:180j	3.78	2.59	2.26
11	178k	 6:1 179k:180k	3.79	2.58	2.26
12	178l	 7:1 179l:180l	3.76	2.58	2.22
13	178m	 179m	3.65	n/a	n/a
14	178n	 traces			
15	178o	 traces			
16	178p	 traces			
17	178q	 traces			
18	178r	 no reaction			
19	178s	 no reaction			

Entry ^a	Olefin	TPA-Complex ratio	Selected ¹ H NMR shifts of major isomer ^b		
			δ H1	δ H2a	δ H2b
20	178t		no reaction		
21	178u		no reaction		
22	178v		no reaction		
23	178w		no reaction		
24	178x		no reaction		

^a Conditions: 0.5 eq. [RhCl(C₂H₄)₂]₂, 1 eq. TPA, CH₂Cl₂, -78 °C, 1h; then 1.5 eq. olefin, warm to r.t., 30 min; removal of volatiles. ^b 300 MHz or 400MHz, 298K, CD₂Cl₂

Characterization of the major isomer is illustrated for complex **179e** (Figure 3.1). Upon exchange of ethylene with substituted olefins, the complex loses its σ_v -plane. Thus, the chemically equivalent protons in the TPA ligand of complex **152** become diastereotopic in **179** and each of the protons in the TPA and the olefin ligand gives rise to a separate signal.

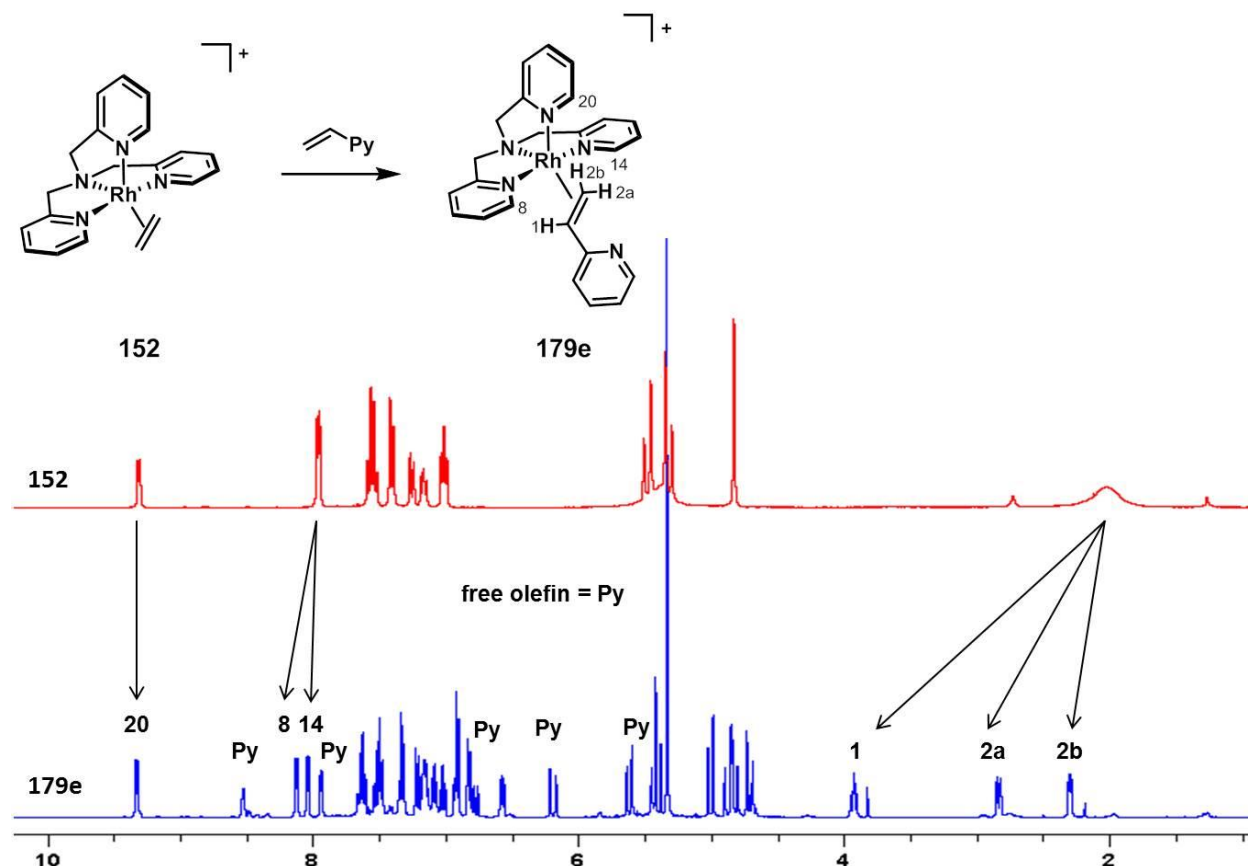


Figure 3.1 ¹H NMR spectra of TPA-Rh-ethylene (**152**, top) and TPA-Rh-vinylpyridine (**179e**, bottom), CD₂Cl₂

The loss of symmetry of the TPA-Rh-olefin complex is confirmed by the appearance of three new doublets in the low-field region of the ¹H NMR spectrum. These signals are ascribed to the ortho pyridine protons (H₈, H₁₄, and H₂₀) of the TPA ligand, with each integrating to one proton. NOESY data and comparison with the ¹H NMR spectrum of TPA-Rh-ethylene complex **152** suggest that the signal at 9.33 ppm corresponds to H₂₀, whereas the two signals at 8.11 ppm and 8.03 ppm stem from the formally equivalent H₈ and H₁₄, respectively. This assignment is also consistent with the magnetic anisotropy effect of double bonds, which results in de-shielding of protons near the C=C axis.

The proton signals of the bound olefin were detected at significantly higher field compared to the corresponding free alkene in solution. While H₁, H_{2a} and H_{2b} of the unbound vinylpyridine gave rise to doublets of doublets at 6.79 ppm ($J_{\text{trans}} = 17.6$ Hz, $J_{\text{cis}} = 10.9$ Hz), 6.19 ppm ($J_{\text{trans}} = 17.6$ Hz, $J_{\text{gem}} = 1.2$ Hz) and 5.43 ppm ($J_{\text{cis}} = 10.9$ Hz, $J_{\text{gem}} = 1.2$ Hz)

respectively, the signal for the bound H1 appeared as a doublet of doublets of doublets at 3.91 ppm ($J_{\text{trans}} = 10.4$ Hz, $J_{\text{cis}} = 8.0$ Hz, $J_{\text{Rh,H}} = 2.8$ Hz), H2a at 2.82 ppm (ddd, $J_{\text{trans}} = 10.4$ Hz, $J_{\text{Rh,H}} = 2.8$ Hz, $J_{\text{gem}} = 1.9$ Hz) and H2b at 2.27 ppm (ddd, $J_{\text{cis}} = 8.0$ Hz, $J_{\text{Rh,H}} = 2.8$ Hz, $J_{\text{gem}} = 1.9$ Hz). The relative configuration was established by NOESY experiments. NOE correlations of H2a and H2b with H20 also unambiguously confirmed the orientation of the olefin substituent away from the central TPA pyridyl arm. A vicinal Rh-H coupling of 2.8 Hz could be observed for all olefinic protons and gave evidence for η^2 -bonding of the double bond. The observed chemical shifts and coupling constants are in good agreement with other pentacoordinate Rh-olefin complexes.^{187,293,294}

Diagnostic ^1H NMR signals for the minor isomer **180** could also be identified and were used to determine the ratio of **179**:**180**. For example, H2b in **179a** appeared as a doublet of triplets at 2.18 ppm in CD_2Cl_2 while the same proton gave rise to an identical pattern only at higher field (1.95 ppm) in **180a** (Figure 3.2 a). Similarly, the signal for H20 in **180a** was high-field shifted compared to its counterpart in **179a** (Figure 3.2 b).

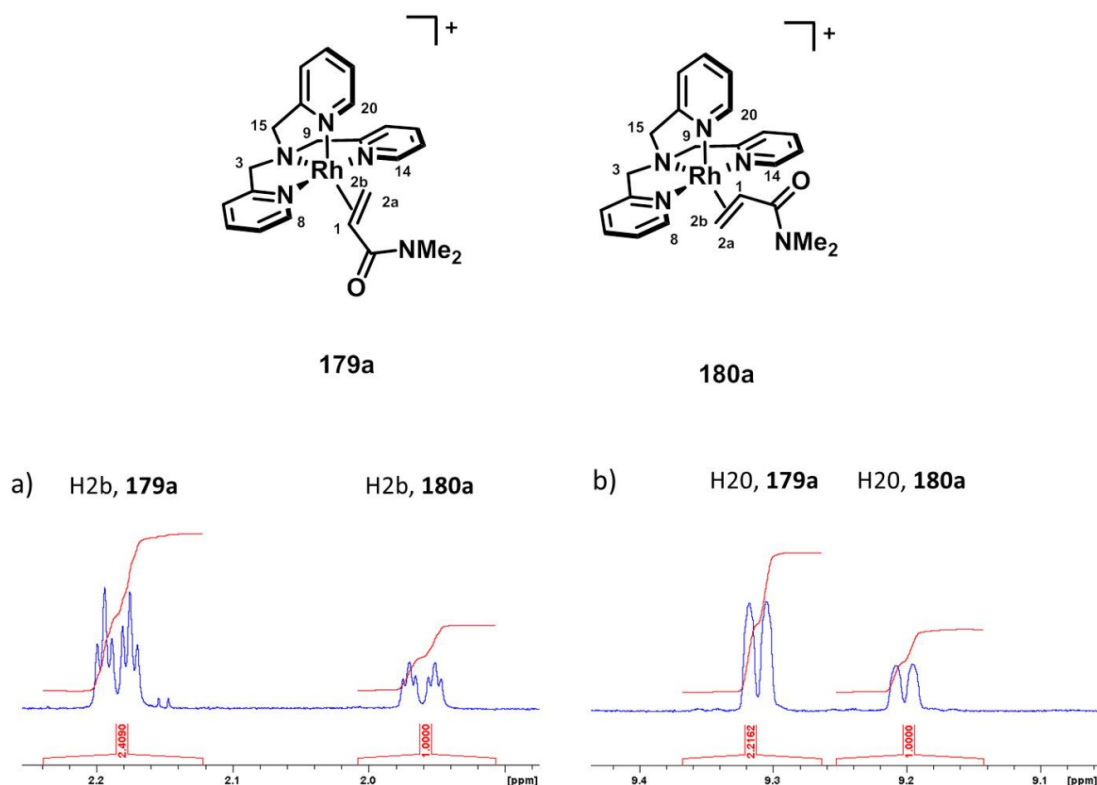


Figure 3.2 Diagnostic ^1H NMR signals for isomers **179a** and **180a** (400 MHz, CD_2Cl_2 , 298K)

As previously mentioned, the major-to-minor product ratio (**179**:**180**) ranged from exclusive formation of one isomer to 2:1 in favour of complex **179**. There is no obvious electronic correlation with product ratio, as a series of *para*-substituted styrenes did not show a linear correlation based on Hammett constants. Notably, temperature had no clear effect on the product ratio, within the margin of error of integration: VT-NMR experiments showed that in complex **179/180a** the isomer ratio changes only slightly from 1.9:1 to 2.2:1 in a temperature range from -60 °C to +35 °C. The ethylene fragment in TPA-Rh-ethylene complex **152** gives rise to a single broad resonance at room temperature due to fast rotation of the bound olefin. Upon cooling, the rotation slows, giving rise to two individual signals for the two sets of equivalent protons.¹⁸⁷ We would expect a similar effect on complexes **179** and **180**. If interconversion between the two isomers was happening by rotation about the Rh-olefin bond, the rate of rotation should be affected by variation of the temperature, which should have a more pronounced impact on the isomer ratio. For example, higher temperature should lead to an equilibration of the isomer ratio or coalescence of the signals, which was not observed. Thus, interconversion of **179** and **180** by rotation about the Rh-olefin bond does not appear to be occurring.

Nonetheless, strong anti-phase off-diagonal cross peaks in the 2D NOESY spectrum between the free and the bound olefin in both isomers are evidence for rapid coordination/de-coordination of the olefin at room temperature. No such exchange signals could be detected between the bound olefin signals of the two isomers. These data substantiate that the interconversion of **179** and **180** proceeds through a fast de-coordination/re-coordination event rather than rotation of the bound olefin (Figure 3.3).

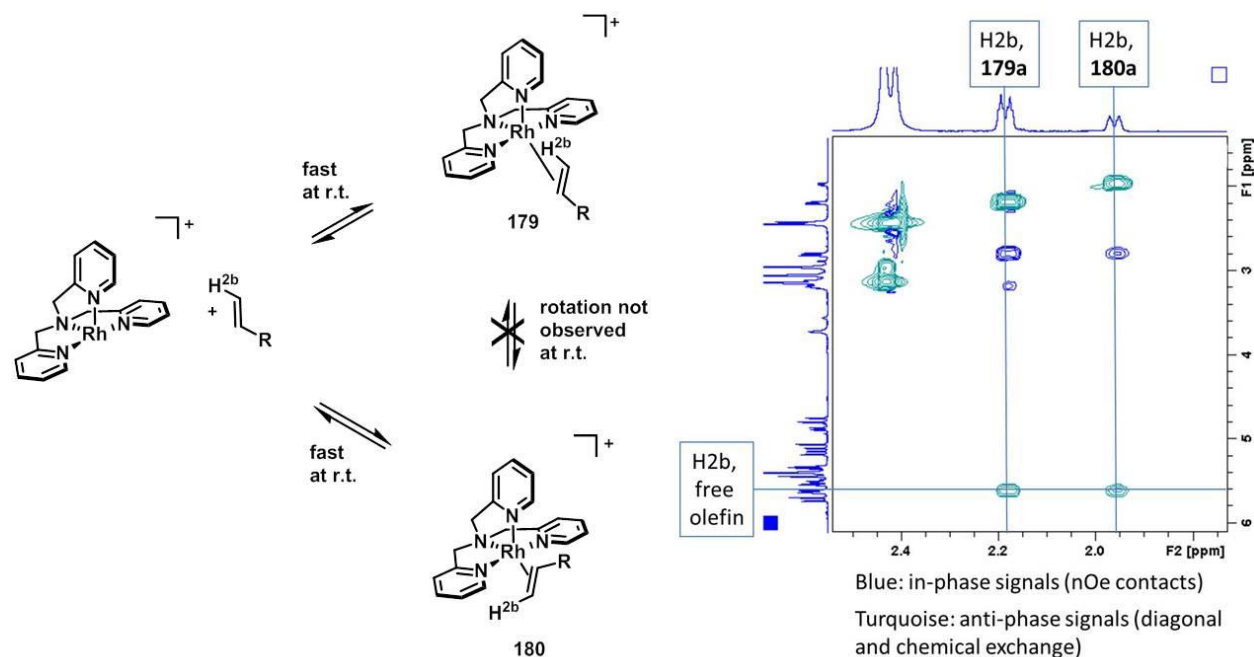


Figure 3.3 Interconversion of **179** and **180**.

Cramer reported that olefin exchange in rhodium(I) complexes can be a faster process than rotation of the ligand.²⁹⁵ In addition, Rossi and Hoffmann predicted an increase in the rotational barrier in pentacoordinate d^8 complexes with increasing π -acceptor capability of the olefin.²⁹⁶ Likewise, Harman and co-workers demonstrated on selected rhenium olefin complexes that the barrier of alkene rotation is strongly dependent on the electronics of the ancillary ligands.²⁹⁷ They found that the barrier of rotation increases as the π -acidity of the ligand decreases. This could be an explanation – besides steric reasons – for the apparent rigidity of complexes **179** and **180** with π -accepting olefins and the fairly π -basic TPA ancillary ligand. Fast exchange of an olefin ligand has been ascribed to an associative mechanism, whereas dissociative mechanisms were usually considered more sluggish.^{289,290,298,299} As **179** and **180** have 18 electron configurations, it would be more intuitive to assume a dissociative mechanism, though. Further studies must be performed to fully elucidate the interconversion of the major and minor isomer.

3.2 Oxidation with H₂O₂

The TPA-Rh-olefin complexes were then subject to oxidation by H₂O₂ to generate the corresponding substituted oxarhodacyclobutanes. In contrast to H₂O₂ oxidation of complex **152**, the transformation was unsuccessful when carried out in CD₂Cl₂, leading instead to a complex mixture of unidentified products. However, a number of Rh olefin complexes (Table 3.2, entries 1, 6-12) successfully underwent oxidation using MeOD as the solvent. Due to the limited stability of the Rh olefin complexes **179** and **180**, oxidation was performed immediately after their formation. Aqueous H₂O₂ was added to a solution of the olefin complex in MeOD at -10 °C and the reaction mixture was allowed to slowly warm to room temperature over a period of 2 h. The reaction progress was monitored using ¹H NMR spectroscopy and mass spectrometry.

It is noteworthy, that even after complete exchange of ethylene with styrene derivatives, as judged by ¹H NMR, the presence of free ethylene dissolved in solution and in the headspace of the NMR tube led to the formation of **153** as the major product. This further confirms a rapid exchange of free and bound olefin in solution even at low temperatures, as discussed earlier.

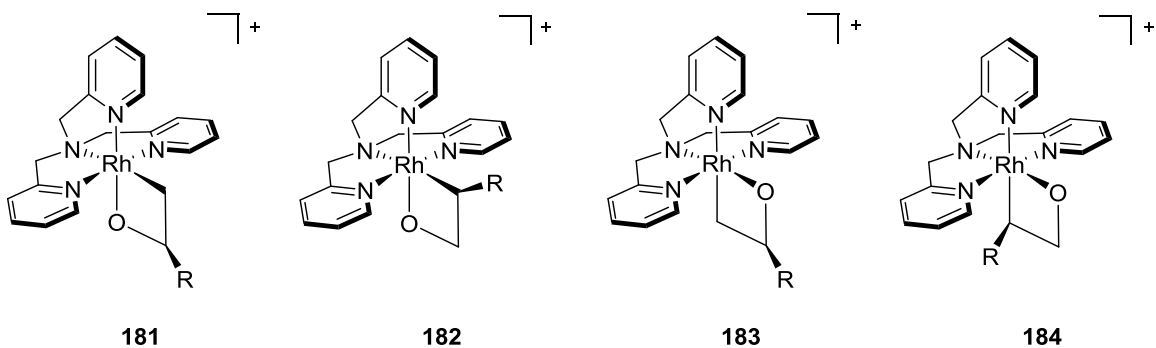


Figure 3.4 Possible isomers in the formation of substituted rhodaoxetanes.

In this transformation up to four possible isomers can be formed differing by the position of the ring oxygen atom relative to the central nitrogen atom of the TPA ligand, as well as the substituent relative to the ring oxygen atom (Figure 3.4). In isomers **181** and **182** the ring oxygen has the same orientation as in the unsubstituted rhodaoxetane **153**, which is cis with respect to the central nitrogen atom of the TPA ligand. Isomer **181** would arise from C-O bond formation at the more substituted carbon of the olefin, whereas **182** would

arise from C-O bond formation at the least substituted carbon. On the other hand, the ring oxygen and central TPA amine in isomers **183** and **184** have a trans relationship and again differ in the position of the olefin substituent. Due to the exclusive formation of only one isomer in the preparation of unsubstituted **153**, we anticipated preference for the formation of isomers **181** and **182**. We were interested whether a similar trend in the formation of the substituted metallacycles could be observed, considering our findings for the preferred formation of **179** over **180**.

Notably, based on NMR spectroscopy and HPLC-MS data, isomer **181** was formed exclusively in all cases (Figure 3.5, Table 3.2). More specifically, Rh-olefin complexes of dimethylacrylamide (entry 1), vinylpyridine (entry 5) and styrene derivatives (entries 7-12) underwent successful oxidation to the corresponding substituted oxarhodacyclobutanes **181**.

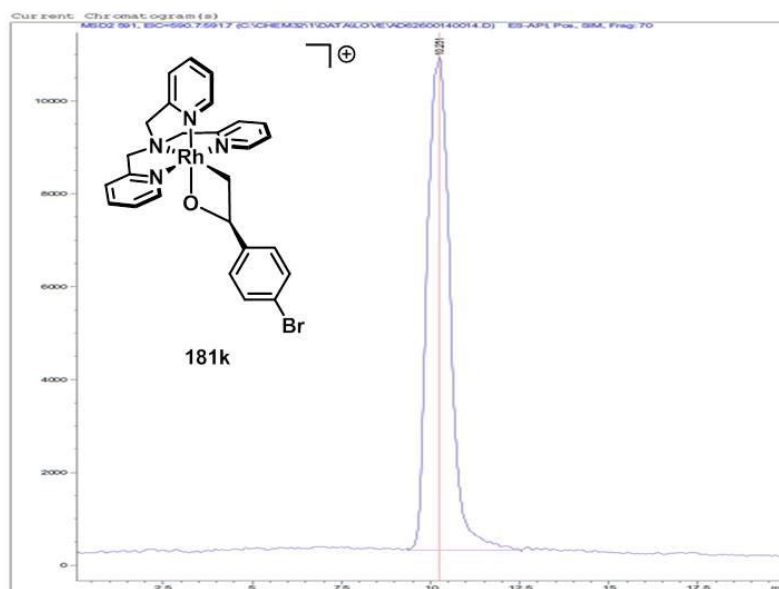
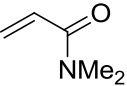
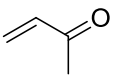
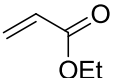
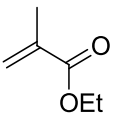
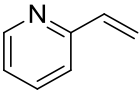
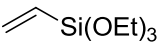
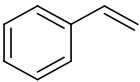


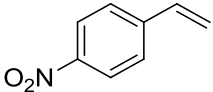
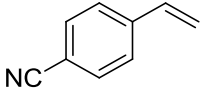
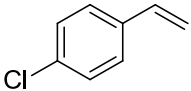
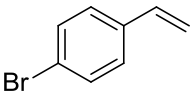
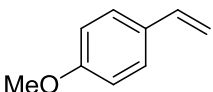
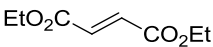
Figure 3.5 HPLC-MS shows formation of only one isomer

Yields were determined by ^1H NMR spectroscopy using tetramethylsilane as internal standard and ranged from 26% – 80%. In general, the crude spectra were of sufficient quality to identify the products. Complexes **181a**, **181e**, **181g** and **181i** were furthermore isolated via semi-preparative HPLC with a purity of >80% in sufficient quantities for full NMR analysis. Due to the instability of the complexes especially in the presence of acidic media, we were unable to obtain a higher degree of purity, even when employing an aqueous 0.3%

ammonium hydroxide buffer (pH = 8) as eluent in HPLC. Key ^1H NMR characterization data for the new oxarhodacyclobutanes are summarized in Table 3.2.

Table 3.2 Formation of substituted oxarhodacyclobutanes and key ^1H NMR chemical shift data.

Entry ^a	Olefin	Complex	NMR yield ^b	Selected ^1H NMR shifts ^c		
				δH1	δH2a	δH2b
1	178a 	181a	71% (10%)	5.64	2.43	2.77
2	178b 		No reaction			
3	178c 		No reaction			
4	178d 		No reaction			
5	178e 	181f	80% (7%)	5.99	2.30	3.05
6	178f 		Formation of unidentified product			
7	178g 	181g	36% (3%)	5.85	2.41	3.02

Entry ^a	Olefin	Complex	NMR yield ^b	Selected ¹ H NMR shifts ^c		
				δ H1	δ H2a	δ H2b
8	178h 	181h	26%	obscured	2.24	3.09
9	178i 	181i	27% (14%)	obscured	2.27	3.11
10	178j 	181j	36%	5.88	2.34	3.04
11	178k 	181k	44%	5.86	2.33	3.04
12	178l 	181l	36%	5.78	2.48	3.01
13	178m 		No reaction			

^a Conditions: 0.5 eq. [RhCl(C₂H₄)₂]₂, 1 eq. TPA, CH₂Cl₂, -78 °C, 1h; then 1.5 eq. olefin, warm to r.t., 30 min; removal of volatiles; then MeOH (or MeOD for NMR scale), 2 eq. H₂O₂ (30% aq.), -10 °C, 2h. ^b NMR yields based on tetramethylsilane as internal standard (isolated yields in parentheses). ^c 300 MHz or 400 MHz, 298K, MeOD.

Representative NMR spectra are shown for complex **181e** in Figure 3.6. In the ¹H NMR spectrum, two new signals with a Rh coupling of 2.3 Hz appear at 2.30 ppm and 3.05 ppm and were ascribed to H2a (apparent dt, J_{gem}, J_{trans} ~ 7.0 Hz, J_{Rh,H} = 2.3 Hz) and H2b (ddd, J_{cis} = 8.4 Hz, J_{gem} = 6.7 Hz, J_{Rh,H} = 2.3 Hz), respectively. An apparent triplet with COSY contacts to these signals was observed at 5.99 ppm (J_{cis}, J_{trans} ~ 7.6 Hz) corresponding to H1. The Rh coupling can also be observed in the ¹³C NMR spectrum in which C2 can be found at 10.5 ppm

(d, $^2J_{Rh,C} = 18.6$ Hz) and C1 at 90.4 ppm (d, $^3J_{Rh,C} = 4.0$ Hz) with the expected downfield shift of C1 due to de-shielding through the neighbouring ring oxygen and a smaller Rh-C coupling constant. In the 1H NMR spectrum, the diagnostic low-field ortho pyridine proton signals of the TPA ligand H8, H14, and H20 arose at 8.47 ppm (d, $J = 5.5$ Hz), 9.07 ppm (d, $J = 5.6$ Hz) and 8.40 ppm (d, $J = 5.6$ Hz), respectively. The relative configurations could be clearly determined by NOESY experiments showing strong correlations between H1 and H2b, H2b and H14 as well as H2a and H8; H20 showed equally strong correlations to H2a and H2b. These NOE contacts also confirm the formation of isomer **181** in which the C-O bond was formed on the more substituted carbon of the olefin. The other new complexes (**181a**, **181g-l**) exhibited similar spectra (see section 3.4 for details).

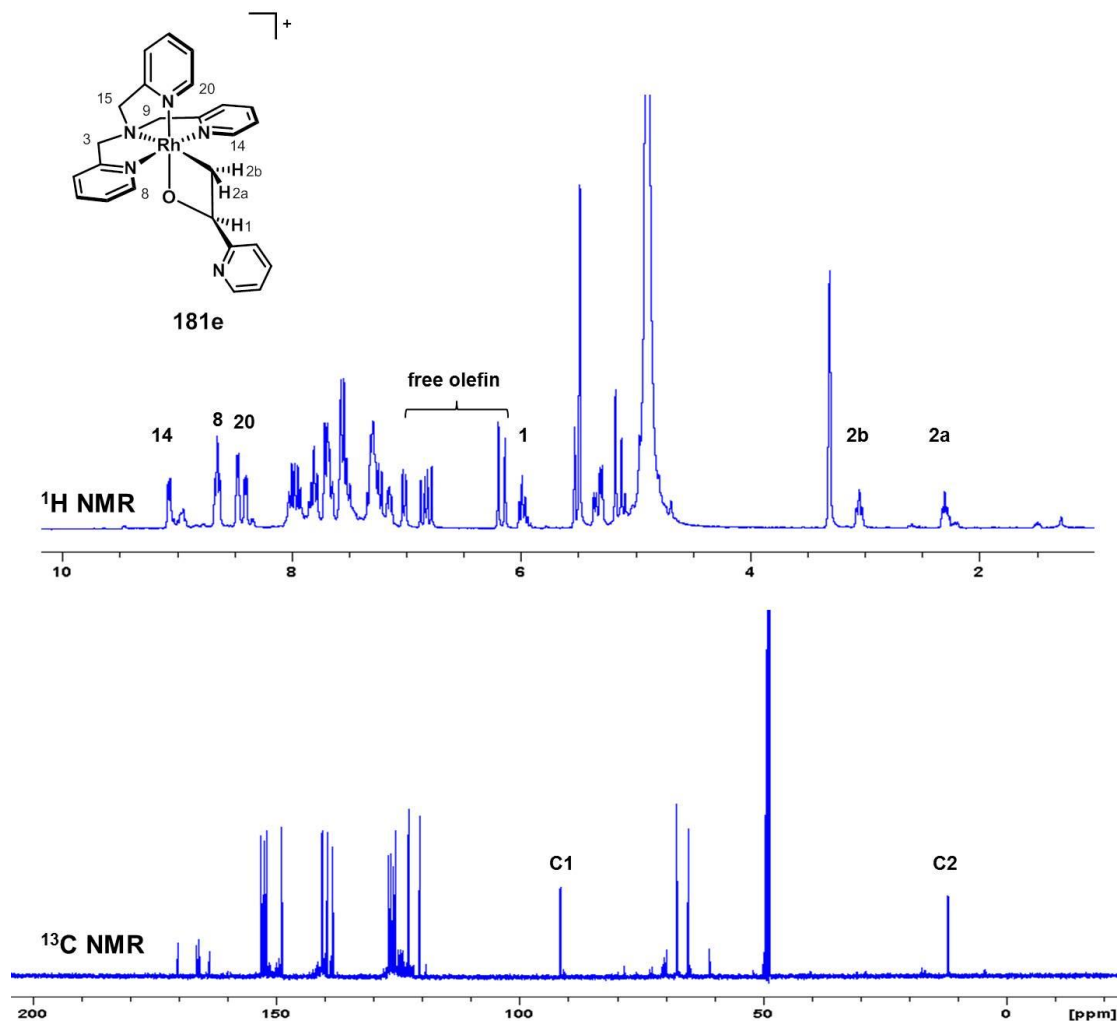
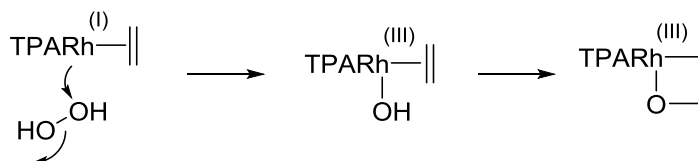


Figure 3.6. 1H NMR (400MHz, MeOD) and ^{13}C NMR (100MHz, MeOD) spectra of **181e**.

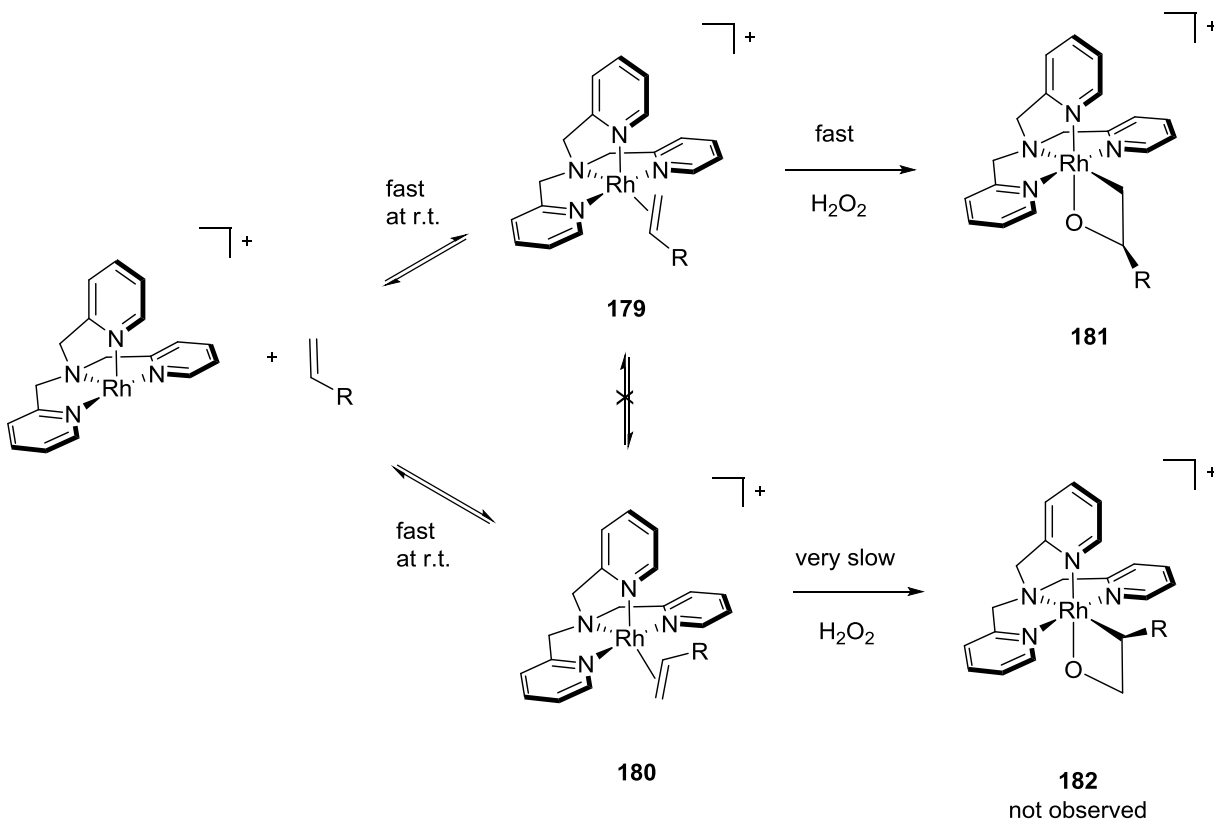
3.3 Discussion

The mechanism of formation of the unsubstituted oxarhodacyclobutane **153** is postulated to involve the formation of a Rh(III)-hydroxo species with the olefin still coordinated, which then ring-closes in a concerted fashion (Scheme 3.3).¹⁸⁶



Scheme 3.3 Mechanism of the formation of unsubstituted rhodaoxetane **153**

Assuming the same mechanism is operative in this case, **181** would directly result from olefin complex **179** and **182** would be the oxidation product of complex **180** (Scheme 3.4).



Scheme 3.4 Formation of substituted oxarhodacyclobutanes

The fact that formation **182** is not observed in the reaction of crude mixtures of **179** and **180**, despite rapid interconversion between these isomers (see section 3.1), indicates

that the transition state for the transformation of **179** to **181** is significantly lower in energy than that of conversion of **180** to **182**.

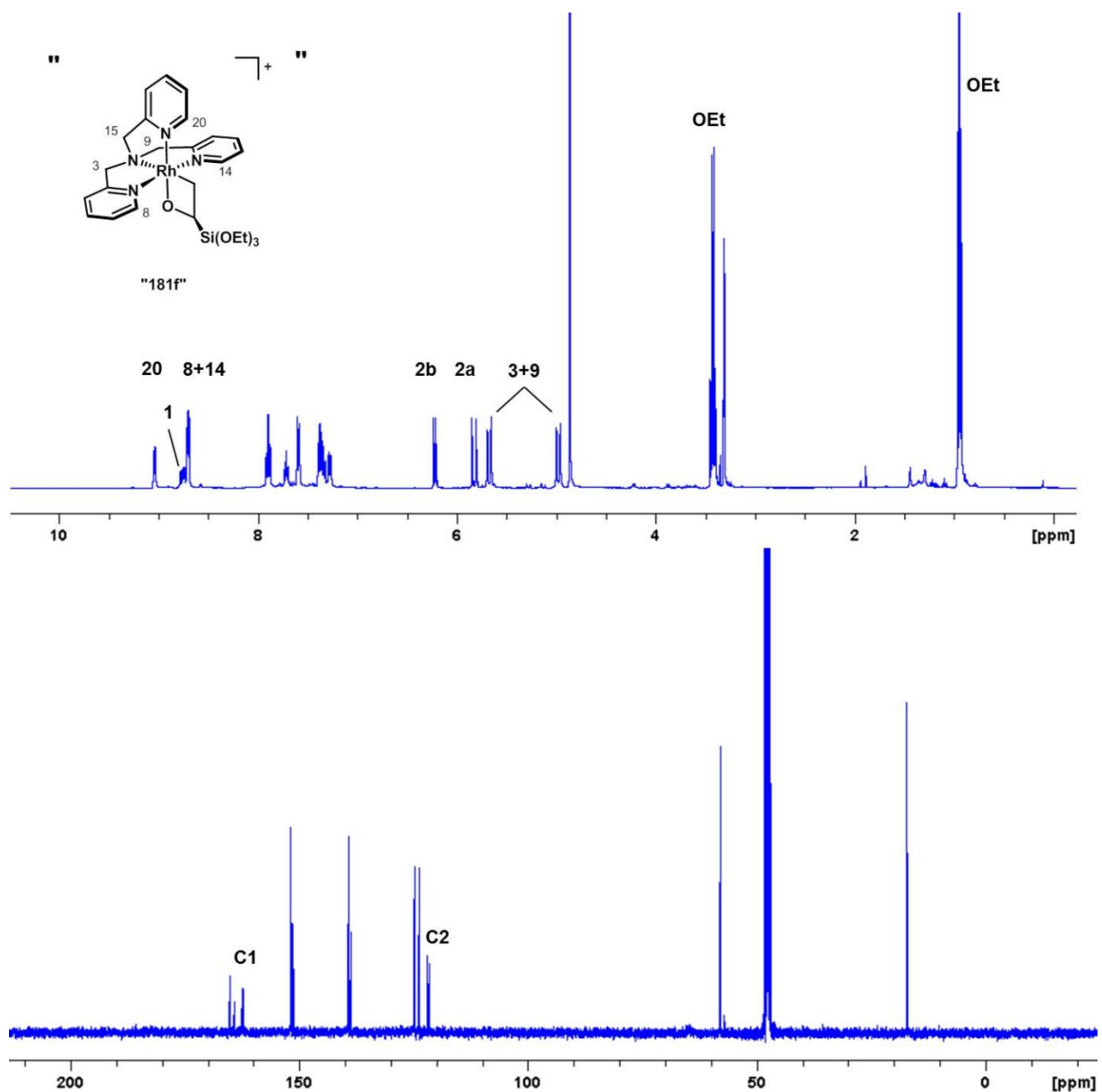


Figure 3.7 ^1H NMR (400MHz, MeOD) and ^{13}C NMR (100MHz, MeOD) spectra of the oxidation product of **179f**.

Complexes with strongly electron deficient olefins (Table 3, entries 2-4, 13) were resistant to oxidation by H_2O_2 even after prolonged reaction times. The olefin complexes were recovered after 24 hours with some decomposition to unidentified TPA-Rh complexes, but without formation of the corresponding oxarhodacyclobutanes. This can be explained by

the decreased electron density on the rhodium center, making it less prone to oxidation by H₂O₂.

In addition, complex **179f** did undergo clean oxidation to a new product, which was not the expected oxarhodacyclobutane. While the mass spectrum of the product complex showed the incorporation of oxygen it became evident from NMR investigations that the double bond of the coordinated vinylsilane was still intact (Figure 3.7). This was indicated by the chemical shifts of the olefinic proton and carbon signals which were at significantly lower field than in the oxarhodacyclobutanes discussed earlier. Even in direct comparison with the starting olefin complex **179f**, the chemical shifts and coupling patterns resembled more a free olefin than one bound to the metal center. At the same time, the ¹³C NMR spectrum showed equally strong Rh-C couplings of ca. 30 Hz for both olefin carbon signals C1 (162.3 ppm) and C2 (121.8 ppm) indicating the persistence of η² hapticity. The ¹H NMR spectrum resembled that of a complex in which the symmetry had been restored. Only one signal was found for the formerly inequivalent H8 and H14 protons, and H3 and H9 afforded two sets of [AB] doublets analogous to complex **152**. The three ethoxy groups appeared to be equivalent as they gave rise to only two signals integrating to 6 and 9 protons respectively. The signal for H15 could not be found but is likely a singlet overlapped by the water signal at 4.86 ppm. Some possible structures are shown in Figure 3.8.

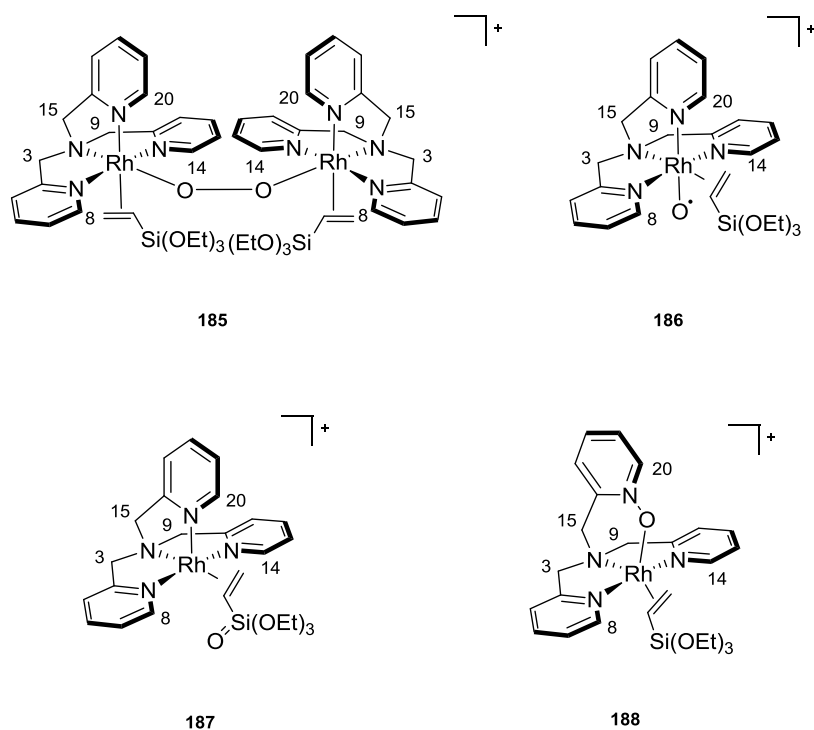
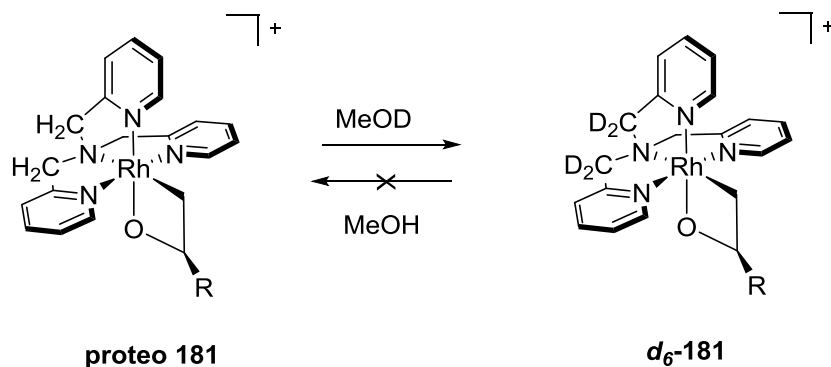


Figure 3.8 Possible structures for the product of oxidation of **179f**.

Instead of metallaoxetane formation, a peroxo-bridged dimer (**185**) could have been formed. As ESI-MS does not give any indication of a dimeric structure, one could imagine a homolytic cleavage of **185** in the gas phase before reaching the detector as the monomer **186**. Another possibility is that oxidation has occurred on the silicon atom to form a structure like **187**. However, there are no descriptions of such a compound in the literature. Silanones, which are related compounds containing silicon-oxygen double bonds are usually only four-coordinate and highly reactive.^{300,301} In contrast, the oxidation product of **179f** clearly contains three ethoxy groups, based on ^1H NMR spectroscopy. Finally, oxidation could have occurred on the TPA ligand leading to a pyridyl *N*-oxide sidearm as in **188**. However, this has not been observed in any other case here. Further structural elucidation of this compound is necessary.

Another observation was that upon standing in deuterated methanol, a successive proton-deuterium exchange took place in the substituted rhodaoxetanes. This process could be monitored via an increase of the m/z in MS data of up to +6. Furthermore, in the ^1H NMR spectrum of the product complexes the intensity of the TPA-methylene signals, H3, H9 and

H15 decreased over time (Scheme 3.5). Interestingly, we were not able to reverse the exchange to attain the re-protonated complexes, even after prolonged stirring in methanol or repeated evaporation and dissolution in the proteo-solvent.



Scheme 3.5 Proton – deuterium exchange in **181**.

3.4 Experimental

All experiments were carried out under air free conditions employing standard Schlenk techniques but with regular wet solvents which were freeze-pump-thawed during the reaction set-up. Note that all oxidation experiments could also be performed under bench top conditions open to air without significant impact on the reaction outcome. All reagents were used as received without further purification. Room temperature corresponds to ~20 °C.

NMR spectra were recorded on Bruker Avance 300, 400 and 600 MHz spectrometers. ¹H and ¹³C NMR spectra are reported in parts per million and were referenced to residual solvent (CD₂Cl₂: δH = 5.32 ppm δC = 53.84 ppm; acetone-d₆: δH = 2.05 ppm, δC = 206.26 ppm, MeOD: δH = 3.31 ppm, δC = 49.00 ppm). The multiplicities are abbreviated as follows: s = singlet, d = doublet, t = triplet, q = quartet, m = multiplet, br = broad signal, ob = obscured signal, d[AB] = second order doublet. All spectra were obtained at 25 °C. TopSpin 3.0 was used for data processing. Unless otherwise denoted coupling constants correspond to ¹H/¹H couplings.

MS-data were obtained on a Waters LC/MS instrument for low resolution and Waters/Micromass LCT for high resolution spectra.

Semi preparative HPLC was performed on a Varian ProStar system with a Varian ProStar 325 UV detector operating at 254 nm and a Varian 1200L triple quadrupole mass spectrometer with Electrospray Ionization. For semi-preparative mode a TMS-end-capped Phenomenex Luma C18(2) column (250x10 mm, 5 μ m, 100 Å) was employed and a 99/1 post column splitter was installed for UV/MS parallel detection. Gradients of H₂O/acetonitrile were used at 5mL flow. Due to the limited stability of the oxametallacyclobutane complexes **181** on the HPLC column an aqueous 0.3% ammonium hydroxide buffer (pH = 8) was used as aqueous component of the eluent for semi-preparative separation. Repeated injection of 200 μ L of the crude product in 70/30 H₂O/acetonitrile allowed purification as collected from the UV detector.

Analytical HPLC was performed on the above system and an Agilent 1260 system with a 6120 single quadrupole LC/MS system using a TMS-end-capped Phenomenex Luma C18(2) column (150x4.6 mm, 5 μ m, 100 Å). The MS was set to SIM (single ion monitoring) mode for m/z = mass of the corresponding positively charged complex. 2 μ L of a solution of approximately 0.5 mg of the crude reaction mixture in 10 mL 70/30 H₂O/acetonitrile was injected. For successful separation solvent gradients of H₂O/acetonitrile were used at a flow rate of 0.4 mL/min. All retention times given refer to the apex of the peak. Retention times and isomer ratios are averaged over two injections.

NMR yields were obtained by referencing 2 or 3 well-resolved signals in the starting material and product spectra to the tetramethylsilane protons (TMS, 99.9% purity, Alfa Aesar). ¹H NMR was performed with a calibrated 30 or 45 degree P1 pulse and delay + acquisition time being 5 x T1. Assignments of the signals in the ¹H and ¹³C NMR spectra were made as far as possible with the aid of 2D spectroscopy (COSY, NOESY, HSQC, HMBC). ¹H NMR assignment of the signals in the crude reaction mixture are partly incomplete and over-integrate due to overlapping signals with the other isomer, excess starting material (olefin) and by-products.

3.4.1 Experimental Procedures and Characterization Data

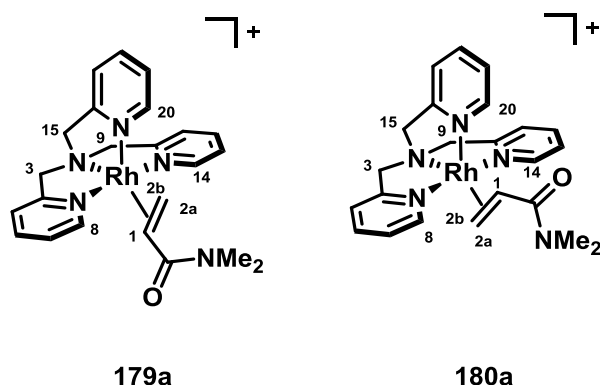
TPA (*N,N,N*-trispyridylmethyl amine) and MeTPA (*N*-[(6-methyl-2-pyridyl)methyl]-*N,N*-di(2-pyridylmethyl)amine) were prepared according to literature procedures and purified by recrystallization from boiling petrol ether (40 – 60 °C).²⁸³

3.4.1.1 Preparation of TPA-Rh-Olefin Complexes 179 and 180 (NMR Scale) in Dichloromethane

3.4.1.1.1 General Procedure

[RhCl(C₂H₄)₂]₂ (50 mg, 0.13 mmol, 0.5 equiv., Alfa Aesar) was weighed into a 5 mL reaction vial. The vial was equipped with a magnetic stir bar and sealed with a screw cap fitted with a PTFE coated rubber septum. CH₂Cl₂ (1mL) was added, the resulting solution was frozen in a liquid nitrogen bath and the vial evacuated for 5 minutes on a Schlenk manifold. Dry N₂ was then used to back-fill the vial. TPA (75 mg, 0.26 mmol, 1 equiv.) was weighed into a small vial and dissolved in CH₂Cl₂ (1mL). The resulting solution was transferred with a syringe on top of the frozen Rh-dimer suspension and allowed to freeze. Two more freeze-pump-thaw cycles were performed and subsequently the vial was kept at -78 °C with stirring. After 1 h the solution was transferred in 0.4 mL portions into five NMR tubes sealed under N₂ with a screw cap fitted with a PTFE coated rubber septum. The alkene of interest (1.5 equiv.) was added to the solution, the NMR tube was inverted several times and the solution was allowed to warm to room temperature. After 30 minutes the volatiles were removed on high vacuum and CD₂Cl₂ was added for NMR analysis.

[TPA-Rh-*N,N*-Dimethylacrylamide]Cl, 179a/180a



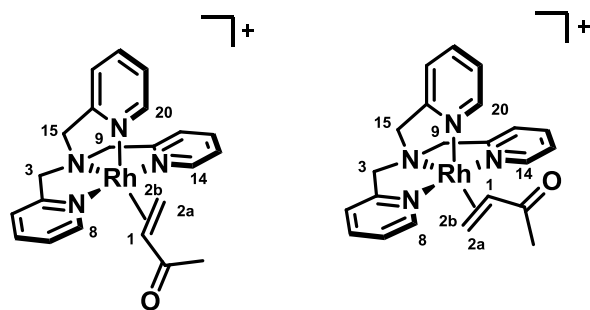
The title compound was synthesized from *N,N*-dimethylacrylamide (8.3 μ L, 0.08 mmol, 1.5 equiv.) according to the general procedure. The reaction produced 179a:180a in a 2:1 ratio.

179a (major) ^1H NMR (400 MHz; CD_2Cl_2): δ 9.31 (d, $^3J = 4.9$ Hz, 1H, H₂₀), 8.10 (d, $^3J = 5.6$ Hz, 1H, H_{8/14}), 7.93 (d, $^3J = 5.6$ Hz, 1H, H_{8/14}), 7.68-6.88 (m, 9H, H_{py}), 5.71 (d[AB], $^2J = 16.0$ Hz, 1H, H_{3/9/15}), 5.55-5.35 (m, 2H, H_{3/9/15}), 5.15 (d[AB], $^2J = 14.7$ Hz, 1H, H_{3/9/15}), 5.07 (d[AB], $^2J = 18.5$ Hz, 1H, H_{3/9/15}), 4.76 (d[AB], $^2J = 18.5$ Hz, 1H, H_{3/9/15}), 3.20-3.14 (m, 1H, H₁), 3.13 (s, 3H, NMe), 2.79 (apparent dt, $^3J_{\text{trans}} = 9.3$ Hz, $^2J = ^2J_{\text{Rh,H}} \sim 2.0$ Hz, 1H, H_{2a}), 2.43 (s, 3H, NMe), 2.18 (apparent dt, $^3J_{\text{cis}} = 7.5$ Hz, $^2J = ^2J_{\text{Rh,H}} \sim 2.2$ Hz, 1H, H_{2b}).

180a (minor) ^1H NMR (400 MHz; CD_2Cl_2): δ 9.20 (d, $^3J = 4.8$ Hz, 1H, H₂₀), 8.06 (d, $^3J = 5.8$ Hz, 1H, H_{8/14}), 3.71 (s, 3H, NMe), 3.10 (s, 3H, NMe), 1.95 (apparent dt, $^3J_{\text{cis}} = 7.5$ Hz, $^2J_{\text{Rh,H}} = 1.8$ Hz, 1H, H_{2b}).

LRMS (ESI, product mixture): $[\text{C}_{23}\text{H}_{27}\text{N}_5\text{ORh}]^+$: m/z 492.3 (M^+).

[TPA-Rh-Methylvinylketone]Cl, 179b/7b



179b

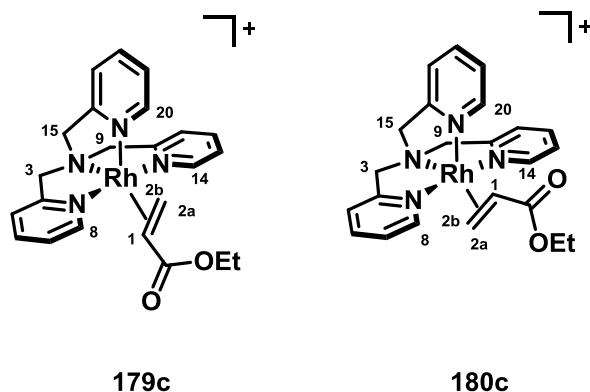
180b

The title compound was synthesized from methylvinylketone (6.8 μ L, 0.08 mmol, 1.5 equiv.) according to the general procedure. The reaction produced 179b:7b in a 3:1 ratio. *179b (major)* ^1H NMR (300 MHz; CD_2Cl_2): δ 9.28 (d, $^3J = 5.0$ Hz, 1H, H₂₀), 8.00 (d, $^3J = 5.4$ Hz, 1H, H_{8/14}), 7.94 (d, $^3J = 5.5$ Hz, 1H, H_{8/14}), 7.84-6.95 (m, H_{py}), 5.71 (d[AB], $^2J = 15.3$ Hz, 1H, H_{3/9/15}), 5.52-5.43 (m, 2H, H_{3/9/15}, H_{3/9/15}), 5.24 (d[AB], $^2J = 15.4$ Hz, 1H, H_{3/9/15}), 4.98 (apparent s, 2H, H_{3/9/15}), 3.41 (ddd, $^3J_{\text{trans}} = 9.7$ Hz, $^3J_{\text{cis}} = 7.2$ Hz, $^2J_{\text{Rh,H}} = 2.4$ Hz, 1H, H₁), 2.65-2.58 (m, 1H, H_{2a}), 2.23 (apparent dt, $J = 4.7$ Hz, $^2J_{\text{Rh,H}} = 2.3$ Hz, 1H, H_{2b}), 1.85 (s, 3H, (CO)CH₃).

180b (minor) ^1H NMR (300 MHz; CD_2Cl_2): δ 9.21 (d, $^3J = 4.7$ Hz, 1H, H₂₀), 8.18 (d, $^3J = 5.2$ Hz, 1H, H_{8/14}), 3.66 (ddd, $^3J_{\text{trans}} = 9.6$ Hz, $^3J_{\text{cis}} = 7.3$ Hz, $^2J_{\text{Rh,H}} = 1.9$ Hz, 1H, H₁), 2.47 (s, 3H, (CO)CH₃).

LRMS (ESI, product mixture): $[\text{C}_{22}\text{H}_{24}\text{N}_4\text{ORh}]^+$: m/z 463.1 (M^+).

[TPA-Rh-Ethylacrylate]Cl, 179c/7c



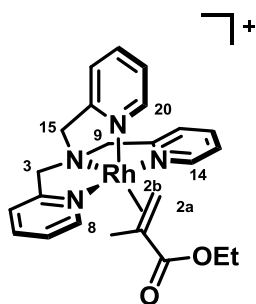
The title compound was synthesized from ethylacrylate (8.5 μ L, 0.08 mmol, 1.5 equiv.) according to the general procedure. The reaction produced 179c:180c in a 14:1 ratio.

179c (major) ^1H NMR (300 MHz; CD_2Cl_2): δ 9.30 (d, $^3J = 4.9$ Hz, 1H, H20), 8.09 (d, $^3J = 5.5$ Hz, 1H, H8/14), 7.94 (d, $^3J = 5.5$ Hz, 1H, H8/14), 7.68-7.02 (m, 9H, H_{py}), 5.58 (d[AB], $^2J = 15.3$ Hz, 1H, H3/9/15), 5.50 (d[AB], $^2J = 15.3$ Hz, 1H, H3/9/15), 5.43 (d[AB], $^2J = 15.0$ Hz, 1H, H3/9/15), 5.25 (d[AB], $^2J = 14.9$ Hz, 1H, H3/9/15), 5.01 (apparent s, 2H, H3/9/15), 3.58 (dq, $^2J = 10.9$ Hz, $^3J = 7.1$ Hz, 1H, OCH_2CH_3), 3.39 (dq, $^2J = 10.8$ Hz, $^3J = 7.1$ Hz, 1H, OCH_2CH_3), 2.99 (ddd, $^3J_{\text{trans}} = 9.7$ Hz, $^3J_{\text{cis}} = 7.4$ Hz, $^2J_{\text{Rh,H}} = 2.5$ Hz, 1H, H1), 2.56 (ddd, $^3J_{\text{trans}} = 9.7$ Hz, $^2J = 2.9$ Hz, $^2J_{\text{Rh,H}} = 2.1$ Hz, 1H, H2a), 2.21 (ddd, $^3J_{\text{cis}} = 7.4$ Hz, $^2J = 2.9$ Hz, $^2J_{\text{Rh,H}} = 2.3$ Hz, 1H, H2b), 0.92 (t, $^3J = 7.1$ Hz, 3H, OCH_2CH_3).

180c (minor) ^1H NMR (300 MHz; CD_2Cl_2): δ 9.28 (partly overlapped by 179c, H20), 8.15 (d, $^3J = 5.2$ Hz, 1H, H8/14), 3.18-3.11 (m, 1H, H1), 2.08-2.05 (m, 1H, H2b), 1.39 (t, $^3J = 7.1$ Hz, 3H, OCH_2CH_3).

LRMS (ESI, product mixture): $[\text{C}_{23}\text{H}_{26}\text{N}_4\text{O}_2\text{Rh}]^+$: m/z 493.1 (M^+).

[TPA-Rh-Methethylacrylate]Cl, 179d

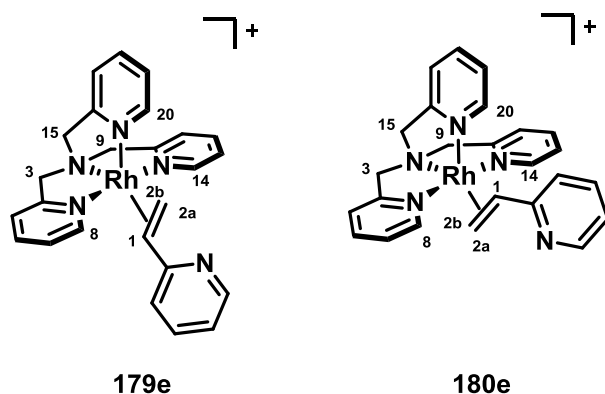


179d

The title compound was synthesized from ethylmethacrylate (10.5 μ L, 0.08 mmol, 1.5 equiv.) according to the general procedure. The reaction produced 179d as single isomer. ^1H NMR (300 MHz; CD_2Cl_2): δ 9.28 (d, $^3J = 4.9$ Hz, 1H, H20), 8.12 (d, $^3J = 5.7$ Hz, 1H, H8/14), 8.00 (d, $^3J = 5.6$ Hz, 1H, H8/14), 7.69-6.99 (m, 9H, H_{py}), 5.78-5.44 (m, 1H, H3/9/15), 5.40 (d[AB], $^2J = 14.9$ Hz, 1H, H3/9/15) 5.35 (d[AB], $^2J = 14.4$ Hz, 1H, H3/9/15), 5.29 (d[AB], $^2J = 14.8$ Hz, 1H, H3/9/15), 4.92 (d[AB], $^2J = 18.2$ Hz, 1H, H3/9/15), 4.86 (d[AB], $^2J = 18.6$ Hz, 1H, H3/9/15), 3.39 (dq, $^2J = 10.8$ Hz, $^3J = 7.1$ Hz, 1H, OCH_2CH_3), 3.06 (dq, $^2J = 10.8$ Hz, $^3J = 7.1$ Hz, 1H, OCH_2CH_3), 2.79 (apparent t, $^2J = 2.6$ Hz, 1H, H2), 2.07 (apparent t, $^2J = 2.4$ Hz, 1H, H2), 0.91 (t, $^3J = 7.1$ Hz, 3H, OCH_2CH_3), 0.82 (d, $^4J = 1.4$ Hz, 3H, CCH_3).

LRMS (ESI): $[\text{C}_{24}\text{H}_{28}\text{N}_4\text{O}_2\text{Rh}]^+$: m/z 507.3 (M^+).

[TPA-Rh-vinylpyridine]Cl, 179e/180e



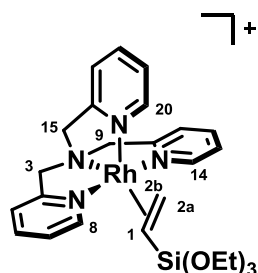
The title compound was synthesized from 2-vinylpyridine (8,6 μL , 0.08 mmol, 1.5 equiv.) according to the general procedure. The reaction produced 179e:180f in a 11:1 ratio.

179e (major) ^1H NMR (400 MHz; CD_2Cl_2): δ 9.33 (d, $^3J = 5,1$ Hz, 1H, H20), 8.04 (d, $^3J = 5,4$ Hz, 1H, H8), 7.93 (d, $^3J = 5,4$ Hz, 1H, H14), 7.68-6.56 (m, 12H, H_{py}), 5.61 (d[AB], $^2J = 15.4$ Hz, 1H, H3/9/15), 5.48-5.32 (m, 1H, H3/9/15), 5.00 (d[AB], $^2J = 14.9$ Hz, 1H, H3/9/15), 4.90-4.79 (m, 2H, H3/9/15), 4.71 (d, $^2J = 18.3$ Hz, 1H, H3/9/15), 3.92 (ddd, $^3J_{\text{trans}} = 10.4$ Hz, $^3J_{\text{cis}} = 7.8$ Hz, $^2J_{\text{Rh,H}} = 2,6$ Hz, 1H, H1), 2.83 (dt, $^3J_{\text{trans}} = 10.3$ Hz, $^2J_{\text{Rh,H}}$, $^2J_{\text{H,H}} \sim 2,4$ Hz, 1H, H2a), 2.29 (dt, $^3J_{\text{cis}} = 7,7$ Hz, $^2J_{\text{Rh,H}}$, $^2J_{\text{H,H}} \sim 2,6$ Hz, 1H, H2b).

180f (minor) ^1H NMR (400 MHz; CD_2Cl_2): δ 4.28 (apparent t, $J = 8,1$ Hz, 1H, H1), 2.94 (apparent d, $J = 10.0$ Hz, 1H, H2a), 1.96 (apparent d, $J = 7,2$ Hz, 1H, H2b).

LRMS (ESI, product mixture): $[\text{C}_{25}\text{H}_{25}\text{N}_5\text{Rh}]^+$: m/z 498.2 (M^+).

[TPA-Rh-triethoxyvinylsilane]Cl, 179f

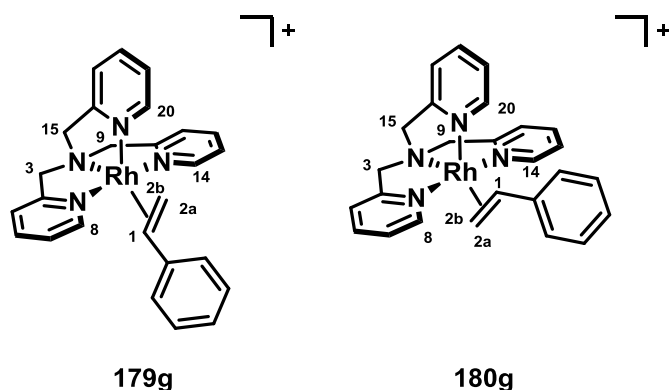


179f

The title compound was synthesized from triethoxyvinylsilane (18.8 μ L, 0.08 mmol, 1.5 equiv.) according to the general procedure. The reaction produced 179f as single isomer. ^1H NMR (400 MHz; CD_2Cl_2): δ 9.30 (d, $^3J = 4.9$ Hz, 1H, H₂₀), 8.00 (d, $^3J = 5.0$ Hz, 1H, H_{8/14}), 7.89 (d, $^3J = 5.2$ Hz, 1H, H_{8/14}), 7.61-7.44 (m, 4H, H_{py}), 7.24 (t, $^3J = 7.1$ Hz, 2H, H_{py}), 7.14 (t, $^3J = 6.2$ Hz, 1H, H_{py}), 7.03 (t, $^3J = 6.3$ Hz, 1H, H_{py}), 6.88 (t, $^3J = 6.3$ Hz, 1H, H_{py}), 5.52 (d[AB], $^2J = 14.8$ Hz, 1H, H_{3/9/15}), 5.37-5.25 (m, 2H, H_{3/9/15}, H_{3/9/15}), 5.07 (d[AB], $^2J = 14.4$ Hz, 1H, H_{3/9/15}), 4.87 (d, [AB] $^2J = 18.4$ Hz, 1H, H_{3/9/15}), 4.78 (d[AB], $^2J = 18.5$ Hz, 1H, H_{3/9/15}), 3.58-3.50 (m, 6H, OCH_2CH_3), 2.51 (dt, $^3J_{\text{cis}} = 10.4$ Hz, $^2J_{\text{Rh,H}}$, $^2J_{\text{H,H}} \sim 1.5$ Hz, 1H, H_{2b}), 2.25 (dt, $J = 11.9$ Hz, $^2J_{\text{Rh,H}}$, $^2J_{\text{H,H}} \sim 1.4$ Hz, 1H, H_{2a}), 1.20 (t, $^3J = 6.9$ Hz, 9H, OCH_2CH_3), 1.01 (partly overlapped by free olefin, H₁).

LRMS (ESI): $[\text{C}_{26}\text{H}_{36}\text{N}_4\text{O}_3\text{RhSi}]^+$: m/z 583.3 (M^+).

[TPA-Rh-Styrene]Cl, 179g/180g



The title compound was synthesized from 4-styrene (8.3 μ L, 0.08 mmol, 1.5 equiv.) according to the general procedure. The reaction produced 179g:180g in a 4:1 ratio.

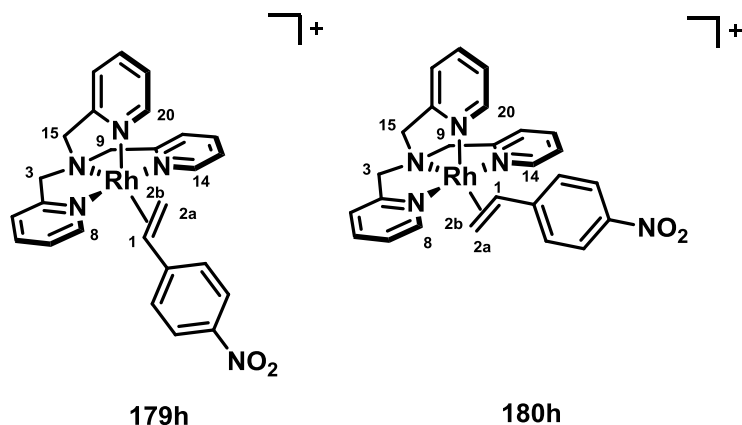
179g (major) ^1H NMR (400 MHz; MeOD): δ 9.40 (d, $^3J = 5.1$ Hz, 1H, H20), 8.26 (d, $^3J = 5.4$ Hz, 1H, H8/14), 8.15 (d, $^3J = 5.5$ Hz, 1H, H8/14), 7.76-6.87 (m, 23H, H_{Ar} + free olefin), 5.61 (d[AB], $^2J = 15.5$ Hz, 1H, H3/9/15), 4.90 (d[AB], $^2J = 15.5$ Hz, 1H, H3/9/15), 4.78 (d[AB], $^2J = 14.7$ Hz, 1H, H3/9/15), 4.57 (d[AB], $^2J = 18.1$ Hz, 1H, H3/9/15), 4.55 (d[AB], $^2J = 14.7$ Hz, 1H, H3/9/15), 4.44 (d[AB], $^2J = 18.1$ Hz, 1H, H3/9/15), 3.85 (ddd, $^3J_{\text{trans}} = 10.4$ Hz, $^3J_{\text{cis}} = 8.1$ Hz, $^2J_{\text{Rh, H}} = 2.4$ Hz, 1H, H1), 2.79 (ddd, $^3J_{\text{trans}} = 10.5$ Hz, $^2J = 2.9$ Hz, $^2J_{\text{Rh, H}} = 1.8$ Hz, 1H, H2a), 2.25 (ddd, $^3J = 7.8$ Hz, $^2J = 3.0$ Hz, $^2J_{\text{Rh, H}} = 2.4$ Hz, 1H, H2b).

(300 MHz; CD_2Cl_2): δ 9.31 (d, $^3J = 5.0$ Hz, 1H, H20), 8.11 (d, $^3J = 5.4$ Hz, 1H, H8/14), 8.01 (d, $^3J = 5.2$ Hz, 1H, H8/14), 7.69-6.76 (m, 14H, H_{py}), 5.51-5.38 (m, 2H, H3/9/15), 4.98 (d[AB], $^2J = 15.0$ Hz, 1H, H3/9/15), 4.91 (d[AB], $^2J = 18.1$ Hz, 1H, H3/9/15), 4.71 (d[AB], $^2J = 15.5$ Hz, 1H, H3/9/15), 4.64 (d[AB], $^2J = 18.6$ Hz, 1H, H3/9/15), 3.85 (ddd, $^3J_{\text{trans}} = 10.5$ Hz, $^3J_{\text{cis}} = 8.0$ Hz, $^2J_{\text{Rh, H}} = 2.7$ Hz, 1H, H1), 2.65 (ddd, $^3J_{\text{trans}} = 10.5$ Hz, $^2J = 3.4$ Hz, $^2J_{\text{Rh, H}} = 2.1$ Hz, 2H, H2a), 2.25 (ddd, $^3J = 7.9$ Hz, $^2J = 3.2$ Hz, $^2J_{\text{Rh, H}} = 2.5$ Hz, 1H, H2b).

180g (minor) ^1H NMR (300 MHz; CD_2Cl_2): δ 9.18 (d, $^3J = 4.3$ Hz, 1H, H20), 8.30 (d, $^3J = 4.6$ Hz, 1H, H8/14), 4.27-4.20 (m, 1H, H1), 1.89-1.85 (m, 1H, H2b).

LRMS (ESI, product mixture): $[\text{C}_{26}\text{H}_{26}\text{N}_4\text{Rh}]^+$: m/z 497.2 (M^+).

[TPA-Rh-4-nitrosytrene]Cl, 179h/180h



The title compound was synthesized from 4-nitrosytrene (10.2 μL , 0.08 mmol, 1.5 equiv.) according to the general procedure. The reaction produced 179h:180h in a 5:1 ratio.

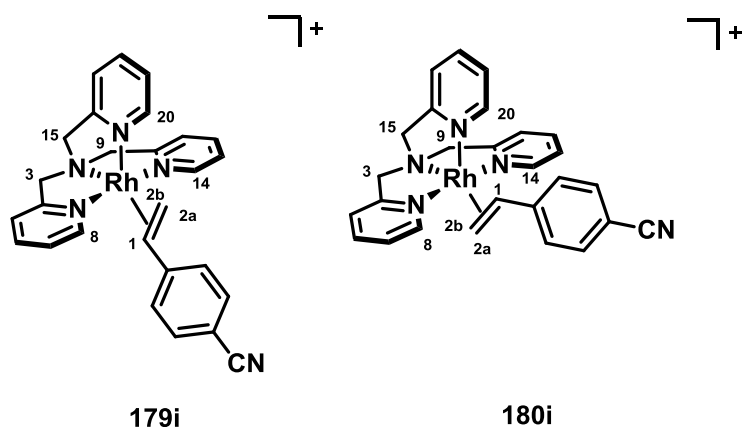
179h (major) ^1H NMR (400 MHz; MeOD): δ 9.42 (d, $^3J = 5.0$ Hz, 1H, H20), 8.33 (d, $^3J = 5.5$ Hz, 1H, H8/14), 8.20 (d, $^3J = 5.6$ Hz, 1H, H8/14), 7.79-6.97 (m, 18H, H_{Ar} + free olefin), 5.63 (d[AB], $^2J = 15.3$ Hz, 1H, H3/9/15), 4.96 (d[AB], $^2J = 15.3$ Hz, 1H, H3/9/15), 4.73 (d[AB], $^2J = 15.0$ Hz, 1H, H3/9/15), 4.66 (d[AB], $^2J = 15.0$ Hz, 1H, H3/9/15), 4.64 (d[AB], $^2J = 18.5$ Hz, 1H, H3/9/15), 4.51 (d[AB], $^2J = 18.5$ Hz, 1H, H3/9/15), 4.00 (ddd, $^3J_{\text{trans}} = 10.3$ Hz, $^3J_{\text{cis}} = 7.7$ Hz, $^2J_{\text{Rh,H}} = 2.6$ Hz, 1H, H1), 2.90 (ddd, $^3J_{\text{trans}} = 10.4$ Hz, $^2J = 3.8$ Hz, $^2J_{\text{Rh,H}} = 1.8$ Hz, 1H, H2a), 2.25 (ddd, $^3J = 7.5$ Hz, $^2J = 3.8$ Hz, $^2J_{\text{Rh,H}} = 2.1$ Hz, 1H, H2b).

(300 MHz; CD_2Cl_2): δ 9.31 (d, $^3J = 4.8$ Hz, 1H, H20), 8.18-8.09 (m, 1H, H8/14), 8.03 (d, $^3J = 5.4$ Hz, 1H, H8/14), 7.88-6.99 (m, 13H, H_{py}), 5.74 (d[AB], $^2J = 14.7$ Hz, 1H, H3/9/15), 5.61-5.43 (m, 1H, H3/9/15), 5.11 (d[AB], $^2J = 15.0$ Hz, 1H, H3/9/15), 4.99 (d[AB], $^2J = 18.4$ Hz, 1H, H3/9/15), 4.69 (d[AB], $^2J = 18.4$ Hz, 1H, H3/9/15), 4.65 (d[AB], $^2J = 15.1$ Hz, 1H, H3/9/15), 3.94 (ddd, $^3J_{\text{trans}} = 10.2$ Hz, $^3J_{\text{cis}} = 7.8$ Hz, $^2J_{\text{Rh,H}} = 2.5$ Hz, 1H, H1), 2.70 (ddd, $^3J_{\text{trans}} = 10.4$ Hz, $^2J = 3.8$ Hz, $^2J_{\text{Rh,H}} = 1.8$ Hz, 1H, H2a), 2.42 (ddd, $^3J_{\text{cis}} = 7.6$ Hz, $^2J = 3.9$ Hz, $^2J_{\text{Rh,H}} = 2.2$ Hz, 1H, H2b).

180h (minor) ^1H NMR (300 MHz; CD_2Cl_2): δ 9.09 (d, $^3J = 4.4$ Hz, 1H, H20), 8.34 (d, $^3J = 5.7$ Hz, 1H, H8/14), 4.36 (apparent t, $J = 8.2$ Hz, 1H, H1), 2.77 (apparent dt, $^3J_{\text{trans}} = 10.3$ Hz, $^2J = 2.4$ Hz, 1H, H2a), 2.06 (apparent dt, $^3J_{\text{cis}} = 7.5$ Hz, $^2J = 2.7$ Hz, 1H, H2b).

LRMS (ESI, product mixture): $[\text{C}_{26}\text{H}_{25}\text{N}_5\text{O}_2\text{Rh}]^+$: m/z 542.2 (M^+).

[TPA-Rh-4-cyanostyrene]Cl, 179i/180i



The title compound was synthesized from 4-cyanostyrene (10.3 μ L, 0.08 mmol, 1.5 equiv.), according to the general procedure. The reaction produced 179i:180i in a 6:1 ratio.

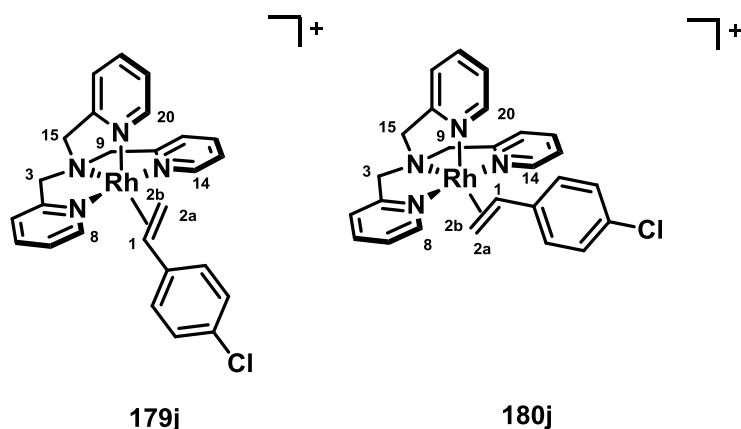
179i (major) ^1H NMR (400 MHz; MeOD): δ 9.41 (d, $^3J = 5.2$ Hz, 1H, H20), 8.29 (d, $^3J = 5.7$ Hz, 1H, H8/14), 8.18 (d, $^3J = 5.4$ Hz, 1H, H8/14), 7.77-6.98 (m, 22H, H_{Ar} + free olefin), 5.61 (d[AB], $^2J = 15.4$ Hz, 1H, H3/9/15), 4.94 (d[AB], $^2J = 15.4$ Hz, 1H, H3/9/15), 4.73 (d[AB], $^2J = 14.9$ Hz, 1H, H3/9/15), 4.65 (d[AB], $^2J = 14.9$ Hz, 1H, H3/9/15), 4.63 (d[AB], $^2J = 18.4$ Hz, 1H, H3/9/15), 4.50 (d[AB], $^2J = 18.4$ Hz, 1H, H3/9/15), 3.92 (ddd, $^3J_{\text{trans}} = 10.4$ Hz, $^3J_{\text{cis}} = 7.8$ Hz, $^2J_{\text{Rh, H}} = 2.8$ Hz, 1H, H1), 2.84 (ddd, $^3J_{\text{trans}} = 10.3$ Hz, $^2J = 3.9$ Hz, $^2J_{\text{Rh, H}} = 1.9$ Hz, 1H, H2a), 2.46 (ddd, $^3J = 7.7$ Hz, $^2J = 3.8$ Hz, $^2J_{\text{Rh, H}} = 2.2$ Hz, 1H, H2b).

^1H NMR (400 MHz; CD_2Cl_2): δ 9.30 (d, $^3J = 4.8$ Hz, 1H, H20), 8.10 (d, $^3J = 4.8$ Hz, 1H, H8/14), 8.01 (d, $^3J = 5.2$ Hz, 1H, H8/14), 7.68-6.99 (m, 13H, H_{py}), 5.63 (d[AB], $^2J = 15.5$ Hz, 1H, H3/9/15), 5.49-5.26 (m, 1H, H3/9/15), 5.14 (d[AB], $^2J = 15.1$ Hz, 1H, H3/9/15), 5.02 (d[AB], $^2J = 18.5$ Hz, 1H, H3/9/15), 4.69 (d[AB], $^2J = 19.2$ Hz, 1H, H3/9/15), 4.64 (d[AB], $^2J = 15.4$ Hz, 1H, H3/9/15), 3.87 (ddd, $^3J_{\text{trans}} = 10.1$ Hz, $^3J_{\text{cis}} = 7.8$, $^2J_{\text{Rh, H}} = 2.6$ Hz, 1H, H1), 2.64 (ddd, $^3J_{\text{trans}} = 10.4$ Hz, $^2J = 3.8$ Hz, $^2J_{\text{Rh, H}} = 1.8$ Hz, 1H, H2a), 2.34 (ddd, $^3J_{\text{cis}} = 7.8$ Hz, $^2J = 3.8$ Hz, $^2J_{\text{Rh, H}} = 2.3$ Hz, 1H, H2b).

180i (minor) ^1H NMR (400 MHz; CD_2Cl_2): δ 9.08 (d, $^3J = 4.6$ Hz, 1H, H20), 8.30 (d, $^3J = 5.0$ Hz, 1H, H8/14), 4.29-4.24 (m, 1H, H1), 2.72 (apparent d, $^3J_{\text{trans}} = 10.1$ Hz, 1H, H2a).

LRMS (ESI, product mixture): $[\text{C}_{27}\text{H}_{25}\text{N}_5\text{Rh}]^+$: m/z 522.2 (M^+).

[TPA-Rh-4-chlorostyrene]Cl, 179j/180j



The title compound was synthesized from 4-chlorostyrene (9.6 μ L, 0.08 mmol, 1.5 equiv.) according to the general procedure. The reaction produced 179j:180j in a 4:1 ratio.

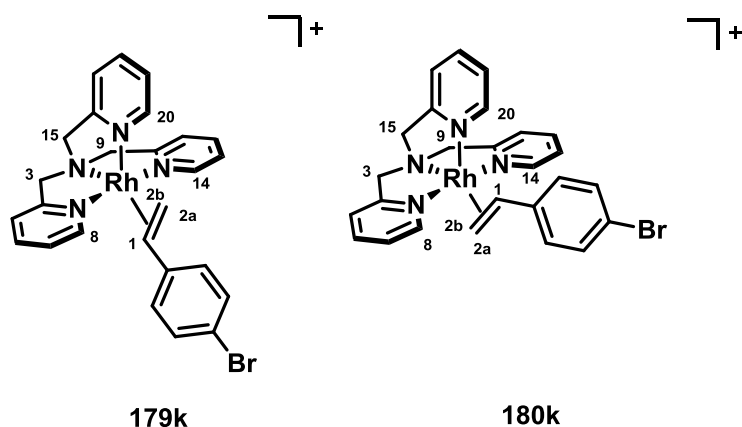
179j (major) ^1H NMR (400 MHz; MeOD): δ 9.39 (d, $^3J = 5.1$ Hz, 1H, H20), 8.26 (d, $^3J = 5.3$ Hz, 1H, H8/14), 8.15 (d, $^3J = 5.5$ Hz, 1H, H8/14), 7.75-6.73 (m, 24H, H_{Ar} + free olefin), 5.61 (d[AB], $^2J = 15.0$ Hz, 1H, H3/9/15), 4.91 (d[AB], $^2J = 15.2$ Hz, 1H, H3/9/15), 4.80 (d[AB], $^2J = 14.9$ Hz, 1H, H3/9/15), 4.62 (d[AB], $^2J = 14.9$ Hz, 1H, H3/9/15), 4.59 (d[AB], $^2J = 18.7$ Hz, 1H, H3/9/15), 4.47 (d[AB], $^2J = 18.7$ Hz, 1H, H3/9/15), 3.82 (ddd, $^3J_{\text{trans}} = 10.5$ Hz, $^3J_{\text{cis}} = 8.0$ Hz, $^2J_{\text{Rh}, \text{H}} = 2.7$ Hz, 1H, H1), 2.76 (ddd, $^3J_{\text{trans}} = 10.3$ Hz, $^2J = 3.2$ Hz, $^2J_{\text{Rh}, \text{H}} = 1.8$ Hz, 1H, H2a), 2.36 (ddd, $^3J = 7.8$ Hz, $^2J = 3.5$ Hz, $^2J_{\text{Rh}, \text{H}} = 2.6$ Hz, 1H, H2b).

^1H NMR (300 MHz; CD_2Cl_2): δ 9.30 (d, $^3J = 4.9$ Hz, 1H, H20), 8.10 (d, $^3J = 5.3$ Hz, 1H, H8/14), 7.99 (d, $^3J = 5.3$ Hz, 1H, H8/14), 7.69-6.92 (m, 13H, H_{py}), 5.53 (d[AB], $^2J = 15.4$ Hz, 1H, H3/9/15), 5.43 (d[AB], $^2J = 14.9$ Hz, 1H, H3/9/15), 5.06 (d[AB], $^2J = 15.0$ Hz, 1H, H3/9/15), 4.94 (d[AB], $^2J = 18.2$ Hz, 1H, H3/9/15), 4.71 (d[AB], $^2J = 15.2$ Hz, 1H, H3/9/15), 4.66 (d[AB], $^2J = 18.4$ Hz, 1H, H3/9/15), 3.78 (ddd, $^3J_{\text{trans}} = 10.4$ Hz, $^3J_{\text{cis}} = 7.8$ Hz, $^2J_{\text{Rh}, \text{H}} = 2.7$ Hz, 1H, H1), 2.59 (ddd, $^3J_{\text{trans}} = 10.5$ Hz, $^2J = 3.5$ Hz, $^2J_{\text{Rh}, \text{H}} = 1.9$ Hz, 1H, H2a), 2.26 (ddd, $^3J_{\text{cis}} = 7.9$ Hz, $^2J = 3.6$ Hz, $^2J_{\text{Rh}, \text{H}} = 2.3$ Hz, 1H, H2b).

180j (minor) ^1H NMR (300 MHz; CD_2Cl_2): δ 9.13 (d, $^3J = 5.4$ Hz, 1H, H20), 8.28 (d, $^3J = 5.1$ Hz, 1H, H8/14), 4.19-4.13 (m, 1H, H1), 1.91-1.87 (m, 1H, H2b).

LRMS (ESI, product mixture): $[\text{C}_{26}\text{H}_{25}\text{ClN}_4\text{Rh}]^+$: m/z 531.2 (M^+).

[TPA-Rh-4-bromostyrene]Cl, 179k/180k



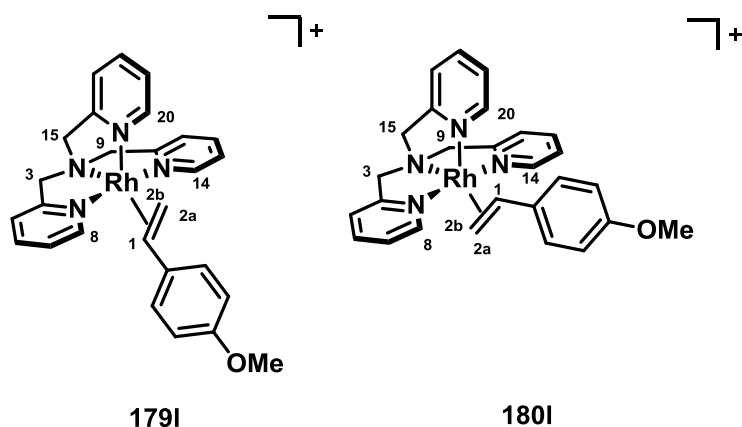
The title compound was synthesized from 4-bromostyrene (10.5 μ L, 0.08 mmol, 1.5 equiv.) according to the general procedure. The reaction produced 179k:180k in a 6:1 ratio.

179k (major) ^1H NMR (400 MHz; MeOD): δ 9.39 (d, $^3J = 5.3$ Hz, 1H, H20), 8.26 (d, $^3J = 5.5$ Hz, 1H, H8/14), 8.15 (d, $^3J = 5.3$ Hz, 1H, H8/14), 7.75-6.73 (m, 23H, H_{Ar} + free olefin), 5.61 (d[AB], $^2J = 15.3$ Hz, 1H, H3/9/15), 4.91 (d[AB], $^2J = 15.4$ Hz, 1H, H3/9/15), 4.79 (d[AB], $^2J = 14.9$ Hz, 1H, H3/9/15), 4.62 (d[AB], $^2J = 14.9$ Hz, 1H, H3/9/15), 4.59 (d[AB], $^2J = 18.3$ Hz, 1H, H3/9/15), 4.47 (d[AB], $^2J = 18.0$ Hz, 1H, H3/9/15), 3.80 (ddd, $^3J_{\text{trans}} = 10.6$ Hz, $^3J_{\text{cis}} = 8.2$ Hz, $^2J_{\text{Rh, H}} = 2.8$ Hz, 1H, H1), 2.76 (ddd, $^3J_{\text{trans}} = 10.5$ Hz, $^2J = 3.4$ Hz, $^2J_{\text{Rh, H}} = 1.8$ Hz, 1H, H2a), 2.36 (ddd, $^3J = 7.6$ Hz, $^2J = 3.4$ Hz, $^2J_{\text{Rh, H}} = 2.3$ Hz, 1H, H2b).

^1H NMR (300 MHz; CD_2Cl_2): δ 9.30 (d, $^3J = 4.7$ Hz, 1H, H20), 8.09 (d, $^3J = 4.7$ Hz, 1H, H8/14), 7.99 (d, $^3J = 5.0$ Hz, 1H, H8/14), 7.89-6.88 (m, 13H, H_{py}), 5.94-5.23 (m, 2H, H3/9/15), 5.06 (d[AB], $^2J = 15.1$ Hz, 1H, H3/9/15), 4.95 (d[AB], $^2J = 18.7$ Hz, 1H, H3/9/15), 4.71 (d[AB], $^2J = 15.5$ Hz, 1H, H3/9/15), 4.66 (d[AB], $^2J = 18.3$ Hz, 1H, H3/9/15), 3.84-3.74 (m, 1H, H1), 2.60-2.56 (m, 1H, H2a), 2.26 (ddd, $^3J_{\text{cis}} = 8.2$, $^2J = 3.9$ Hz, $^2J_{\text{Rh, H}} = 2.3$ Hz, 1H, H2b).

180k (minor) ^1H NMR (300 MHz; CD_2Cl_2): δ 2.68-2.62 (m, 1H, H2a), 1.93-1.87 (m, 1H, H2b).
LRMS (ESI, product mixture): $[\text{C}_{26}\text{H}_{25}\text{BrN}_4\text{Rh}]^+$: m/z 575.1/577.1 (M^+).

[TPA-Rh-4-Methoxystyrene]Cl, 179I/180I



The title compound was synthesized from 4-methoxystyrene (10.4 μ L, 0.08 mmol, 1.5 equiv.) according to the general procedure. The reaction produced 179I:180I in a 7:1 ratio.

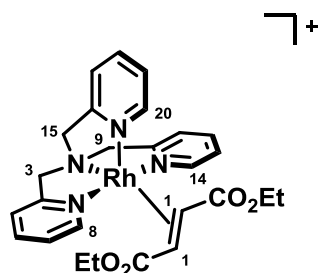
179I (major) ^1H NMR (400 MHz; MeOD): δ 9.38 (d, $^3J = 4.8$ Hz, 1H, H20), 8.25 (d, $^3J = 5.2$ Hz, 1H, H8/14), 8.13 (d, $^3J = 4.8$ Hz, 1H, H8/14), 7.73-6.31 (m, 27H, H_{Ar} + free olefin), 5.62-5.58 (m, 1H, H3/9/15), 4.91-4.81 (m, 2H, H3/9/15), 4.62-4.51 (m, 2H, H3/9/15), 4.34 (d[AB], $^2J = 17.3$ Hz, 1H, H3/9/15), 3.86-3.76 (m, 1H, H1, overlapped), 3.54 (s, 3H, OCH_3), 2.77-2.69 (m, 1H, H2a), 2.35-2.27 (m, 1H, H2b).

^1H NMR (300 MHz; CD_2Cl_2): δ 9.30 (d, $^3J = 4.5$ Hz, 1H, H20), 8.11 (d, $^3J = 4.6$ Hz, 1H, H8/14), 7.99 (d, $^3J = 5.1$ Hz, 1H, H8/14), 7.88-6.84 (m, 13H, H_{py}), 5.90-5.21 (m, 2H, H3/9/15), 4.99 (d[AB], $^2J = 15.1$ Hz, 1H, H3/9/15), 4.87 (d[AB], $^2J = 18.5$ Hz, 1H, H3/9/15), 4.74 (d[AB], $^2J = 14.8$ Hz, 1H, H3/9/15), 4.62 (d[AB], $^2J = 18.5$ Hz, 1H, H3/9/15), 3.76 (partly overlapped, H1), 3.56 (s, 3H, OCH_3), 2.58 (apparent d, $^3J_{\text{trans}} = 10.9$ Hz, 1H, H2a), 2.22 (d, $^3J_{\text{cis}} = 7.4$ Hz, 1H, H2a).

180I (minor) ^1H NMR (300 MHz; CD_2Cl_2): δ 8.30-8.27 (m, 1H, H8/14), 4.25-4.13 (m, 1H, H1), 1.90-1.82 (m, 1H, H2b).

LRMS (ESI, product mixture): $[\text{C}_{27}\text{H}_{28}\text{N}_4\text{ORh}]^+$: m/z 527.3 (M^+).

[TPA-Rh-diethylfumarate]Cl, 179m



The title compound was synthesized from diethylfumarate (13.1 μ L, 0.08 mmol, 1.5 equiv.) according to the general procedure. The reaction produced 179m as single isomer.

^1H NMR (600 MHz; CD_2Cl_2): δ 9.23 (d, $^3J = 5.4$ Hz, 1H, H20), 8.49 (d, $^3J = 4.6$ Hz, 1H, H8/14), 8.26 (d, $^3J = 5.6$ Hz, 1H, H8/14), 7.69-7.55 (m, 7H, H_{py}), 7.47 (d, $^3J = 7.6$ Hz, 1H, H_{py}), 7.33 (d, $^3J = 8.0$ Hz, 1H, H_{py}), 7.23 (t, $^3J = 6.1$ Hz, 1H, H_{py}), 7.16-7.10 (m, 2H, H_{py}), 7.05 (d, $^3J = 6.7$ Hz, 1H, H_{py}), 5.62 (d[AB], $^2J = 15.3$ Hz, 1H, H3/9/15), 5.61 (d[AB], $^2J = 14.6$ Hz, 1H, H3/9/15), 5.53 (d[AB], $^2J = 14.8$ Hz, 1H, H3/9/15), 5.20 (d[AB], $^2J = 18.9$ Hz, 1H, H3/9/15), 5.15 (d[AB], $^2J = 15.3$ Hz, 1H, H3/9/15), 4.92 (d[AB], $^2J = 18.9$ Hz, 1H, H3/9/15), 4.35 (dq, $^2J = 10.6$ Hz, $^3J = 7.2$ Hz, OCH_2CH_3 , 1H), 4.28 (dq, $^2J = 10.6$ Hz, $^3J = 7.2$ Hz, OCH_2CH_3 , 1H), 3.69 (dq, $^2J = 10.8$ Hz, $^3J = 7.2$ Hz, OCH_2CH_3 , 1H), 3.65 (dd, $^3J_{\text{trans}} = 9.4$ Hz, $^2J_{\text{Rh,H}} = 2.3$ Hz, 1H, H1), 3.63 (dd, $^3J_{\text{trans}} = 9.4$ Hz, $^2J_{\text{Rh,H}} = 2.3$ Hz, 1H, H1), 3.48 (dq, $^2J = 10.8$ Hz, $^3J = 7.2$ Hz, OCH_2CH_3 , 1H), 1.43 (t, $^3J = 7.4$, 3H, OCH_2CH_3), 0.97 (t, $^3J = 7.4$, 3H, OCH_2CH_3).

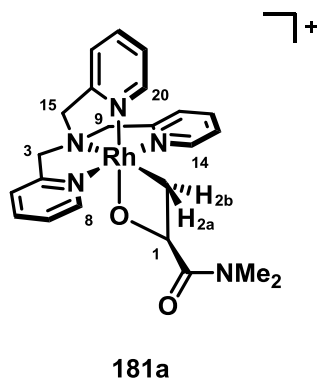
3.4.1.2 Preparation of Substituted TPA-Oxarhodacyclobutane Complexes 181 in Methanol

3.4.1.2.1 Isolable Scale - General Procedure

$[\text{RhCl}(\text{C}_2\text{H}_4)_2]_2$ (0.5 equiv., Alfa Aesar) was weighed into a 10 mL reaction vial. The vial was equipped with a magnetic stir bar and sealed with a screw cap fitted with a PTFE coated rubber septum. CH_2Cl_2 (10 mL/mmol) was added, the resulting solution was frozen in a liquid nitrogen bath and the vial evacuated for 5 minutes on a Schlenk manifold. Dry N_2 was then used to back-fill the vial. TPA (1 equiv.) was weighed into a small vial and dissolved

in CH₂Cl₂ (5 mL/mmol). The resulting solution was transferred with a syringe on top of the frozen Rh-dimer suspension and allowed to freeze. The olefin substrate (1.5 equiv.) was added by microsyringe. Two more freeze-pump-thaw cycles were performed and subsequently the vial was kept at -78 °C with stirring. After 2 h the volatiles were removed on high vacuum and the residue was dissolved in degassed MeOH (20 mL/mmol TPA). The solution was cooled to -10 °C and H₂O₂ (30% aq, 2 equiv.) was added via microsyringe. The reaction mixture was allowed to slowly warm to room temperature under stirring over a period of 2h during which it lightened to a light yellow/brown solution. The volatiles were removed on a rotary evaporator and the crude was subject to purification on semi-preparative HPLC.

[TPA-*N*, *N*-Dimethylacrylamide-oxarhodacyclobutane]Cl, 181a



The title compound was synthesized from [RhCl(C₂H₄)₂]₂ (60 mg, 0.15 mmol), TPA (90 mg, 0.30 mmol), dimethylacrylamide (49 μL, 0.45 mmol) and H₂O₂ (67 μL, 0.60 mmol), according to the general procedure. Semi-preparative HPLC separation was performed with a H₂O (0.3% ammonium hydroxide)/acetonitrile gradient starting at 5% ACN and increasing to 15% over 20 minutes with a 5mL/min flow rate. The product was collected from 8 – 18 minutes along with some unidentified decomposition products.

Yield after purification: 15 mg (10%)

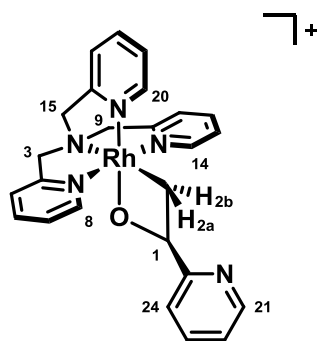
¹H NMR (600 MHz; MeOD): δ 8.98 (d, ³J = 5.6 Hz, 1H, H14), 8.85 (d, ³J = 5.6 Hz, 1H, H8), 8.64 (d, ³J = 5.6 Hz, 1H, H20), 7.98 (t, ³J = 7.7 Hz, 1H, H12), 7.91 (dt, ³J = 7.6 Hz, ⁴J = 1.3 Hz, 1H, H6), 7.70-7.65 (m, 2H, H11 + H18), 7.60 (d, ³J = 7.7 Hz, 1H, H5), 7.52 (t, ³J = 6.5 Hz, 1H, H13), 7.39 (t, ³J = 6.9 Hz, 1H, H7), 7.29 (t, ³J = 7.1 Hz, 1H, H19), 7.20 (d, ³J = 7.9 Hz, 1H, H17), 5.64 (t, ³J

= 8.0 Hz, 1H, H1), 5.37 (d[AB], $^2J = 15.3$ Hz, 1H, H3), 5.24-5.15 (m, 3H, H9 + H15), 5.09 (d[AB], $^2J = 15.3$ Hz, 1H, H9), 5.02 (d[AB], $^2J = 15.3$ Hz, 1H, H3), 3.10 (s, 3H, NMe), 2.86 (s, 3H, NMe), 2.75 (ddd, $^3J_{cis} = 8.7$ Hz, $^2J = 6.6$ Hz, $^2J_{Rh,H} = 2.4$ Hz, 1H, H2b), 2.42 (apparent dt, $^2J = ^3J_{trans} \sim 7.3$ Hz, $^2J = ^2J_{Rh,H} = 2.5$ Hz, 1H, H2a).

^{13}C -NMR (151 MHz; MeOD): δ 177.9 (C(O)Me₂), 166.2 (C10), 165.9 (C4), 163.7 (C16), 153.2 (C8), 152.5 (C14), 151.7 (C20), 140.8 (C12), 140.3 (C6), 139.6 (C18), 127.1 (C13), 126.5 (C7), 126.1 (C19), 125.7 (C11), 125.2 (C5), 123.0 (C17), 86.8 (d, $^2J_{Rh,C} = 3.4$ Hz, C1), 67.7 (C3) 67.6 (C9 + C15), 32.1 (C(O)NMe₂), 31.9 (C(O)NMe₂), 6.3 (d, $^2J_{Rh,C} = 18.5$ Hz, C2)

HRMS (ESI): calc. [C₂₃H₂₇N₅O₂Rh]⁺: 508.1220; found: 508.1213

[TPA-vinylpyridine-oxarhodacyclobutane]Cl, **181e**



181e

The title compound was synthesized from [RhCl(C₂H₄)₂]₂ (60 mg, 0.15 mmol), TPA (90 mg, 0.30 mmol), vinylpyridine (50 μL , 0.45 mmol) and H₂O₂ (67 μL , 0.60 mmol) according to the general procedure. Semi-preparative HPLC separation was performed with a H₂O (0.3% ammonium hydroxide)/acetonitrile gradient starting at 10% ACN and increasing to 50% over 26 minutes, then isocratic flow at 90% until 37 minutes, with a 5mL/min flow rate. The product was collected from 16.5 – 29 minutes along with some unidentified decomposition products.

Yield after purification: 10 mg (7 %)

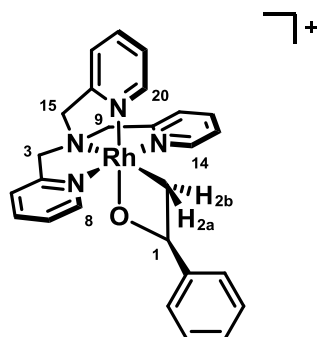
^1H NMR (600 MHz; MeOD): δ 9.07 (d, $^3J = 5.5$ Hz, 1H, H14), 8.67 (d, $^3J = 6.1$ Hz, 1H, H20), 8.65 (d, $^3J = 5.6$ Hz, 1H, H8), 8.41 (d, $^3J = 4.6$ Hz, 1H, H21), 8.00 (t, $^3J = 7.5$ Hz, 1H, H12), 7.95 (t, $^3J = 7.8$ Hz, 1H, H6), 7.71-7.65 (m, 3H, H5 + H11 + H18), 7.57 (t, $^3J = 6.4$ Hz, 1H, H13), 7.52 (dt, $^3J = 7.8$ Hz, $^4J = 1.5$ Hz, 1H, H23), 7.32 (t, $^3J = 6.6$ Hz, 1H, H7), 7.28 (t, $^3J = 6.1$ Hz, 1H, H19), 7.22

(d, $^3J = 7.9$ Hz, 1H, H17), 7.15 (t, $^3J = 6.0$ Hz, 1H, H22), 7.22 (d, $^3J = 7.9$ Hz, 1H, H24), 5.99 (t, $^3J = 8.0$ Hz, 1H, H1), 5.33 (d[AB], $^2J = 14.9$ Hz, 1H, H3/9/15), 5.30 (d[AB], $^2J = 14.3$ Hz, 1H, H3/9/15), 5.14 (d[AB], $^2J = 15.2$ Hz, 2H, H3/9/15), 3.05 (ddd, $^3J_{cis} = 8.5$ Hz, $^2J = 6.6$ Hz, $^2J_{Rh,H} = 2.1$ Hz, 1H, H2b), 2.30 (apparent dt, $^2J = ^3J_{trans} \sim 7.1$ Hz, $^2J = ^2J_{Rh,H} = 2.4$ Hz, 1H, H2a).
Note: Two signals for H3/9/15 seem to be missing which is ascribed to either fast relaxation, H/D exchange with the solvent (which is sometimes observed but usually only after longer periods of standing in MeOD) or potentially overlapping with the nearby H₂O signal (4.88 ppm)

¹³C-NMR (151 MHz; MeOD): δ 170.3 (C25), 166.4 (C10), 165.9 (C4), 163.7 (C16), 153.1 (C8), 152.6 (C14), 151.9 (C20), 148.9 (C21), 140.7 (C12), 140.6 (C6), 139.5 (C18), 138.4 (C23), 127.0 (C13), 126.5 (C7), 126.1 (C19), 125.6 (C5/11), 125.5 (C5/11), 123.0 (C17), 122.7 (C22), 120.6 (C24), 91.7 (d, $^2J_{Rh,C} = 3.3$ Hz, C1), 67.74 (C3/9/15), 67.72 (C3/9/15), 67.64 (C3/9/15), 32.1 (C(O)Me₂), 31.9 (C(O)Me₂), 12.0 (d, $^2J_{Rh,C} = 19.4$ Hz, C2)

HRMS (ESI): calc. [C₂₅H₂₅N₅ORh]⁺: 514.1114; found: 514.1110

[TPA-styrene-oxarhodacyclobutane]Cl, **181g**



181g

The title compound was synthesized from [RhCl(C₂H₄)₂]₂ (100 mg, 0.26 mmol), TPA (150 mg, 0.52 mmol), styrene (71 μ L, 0.62 mmol, 1.2 equiv.) and H₂O₂ (120 μ L, 1.0 mmol), in a slight modification to the general procedure (1.2 equiv. olefin instead of 1.5 equiv.). Semi-preparative HPLC separation was performed with a H₂O (0.3% ammonium hydroxide)/acetonitrile gradient starting at 5% ACN and increasing to 15% over 15 minutes, isocratic flow at 15% until 23 minutes, gradient to 20% until 33 minutes and finally a

gradient to 55% until 37 minutes with a 5mL/min flow rate. The product was collected from 18 – 21.5 minutes along with some unidentified decomposition products.

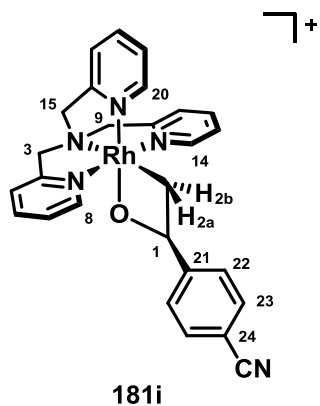
Yield after purification: 8 mg (3 %)

^1H NMR (600 MHz; MeOD): δ 9.02 (d, 3J = 5.3 Hz, 1H, H14), 8.86 (d, 3J = 5.4 Hz, 1H, H8), 8.70 (d, 3J = 5.5 Hz, 1H, H20), 7.99 (t, 3J = 7.8 Hz, 1H, H12), 7.96 (t, 3J = 7.8 Hz, 1H, H6), 7.70-7.63 (m, 3H, H5 + H11 + H18), 7.55 (t, 3J = 6.8 Hz, 1H, H13), 7.42 (t, 3J = 6.4 Hz, 1H, H_{Styr}), 7.33 (t, 3J = 6.4 Hz, 1H, H7), 7.28 (t, 3J = 7.3 Hz, 1H, H19), 7.21 (d, 3J = 7.8 Hz, 1H, H17), 7.17-7.10 (m, 4H, H_{Styr}), 5.85 (t, 3J = 7.8 Hz, 1H, H1), 5.30 (d[AB], 2J = 15.6 Hz, 1H, H3/9/15), 5.26 (d[AB], 2J = 15.3 Hz, 1H, H3/9/15), 5.13-5.05 (m, 3H, H3/9/15), 3.02 (ddd, $^3J_{\text{cis}}$ = 8.2 Hz, 2J = 6.5 Hz, $^2J_{\text{Rh,H}}$ = 2.1 Hz, 1H, H2b), 2.41 (ddd, $^3J_{\text{trans}}$ = 8.1 Hz, 2J = 6.4 Hz, $^2J_{\text{Rh,H}}$ = 2.3 Hz, 1H, H2a).

^{13}C -NMR (151 MHz; MeOD): δ 166.4 (C10), 166.0 (C4), 163.7 (C16), 153.8 (C_{Styr}), 153.1 (C8), 152.6 (C14), 152.0 (C20), 140.7 (C12), 140.6 (C6), 139.5 (C18), 129.5 (2C, C_{Styr}), 127.5 (C_{Styr}), 126.9 (C13), 126.7 (C7), 126.0 (C19), 125.9 (2C, C_{Styr}), 125.6 (C5/11), 125.5 (C5/11), 123.0 (C17), 91.3 (d, $^2J_{\text{Rh,C}}$ = 3.4 Hz, C1), 67.8 (C3/9/15), 67.7 (C3/9/15), 67.6 (C3/9/15), 14.2 (d, $^2J_{\text{Rh,C}}$ = 18.7 Hz, C2)

HRMS (ESI): calc. $[\text{C}_{26}\text{H}_{26}\text{N}_4\text{ORh}]^+$: 513.1162; found: 513.1163

[TPA-4-cyanostyrene-oxarhodacyclobutane]Cl, 181i



The title compound was synthesized from $[\text{RhCl}(\text{C}_2\text{H}_4)_2]_2$ (55 mg, 0.14 mmol), TPA (83 mg, 0.28 mmol), 4-cyanostyrene (58 μL , 0.42 mmol, 1.5 equiv.) and H_2O_2 (62 μL , 0.56 mmol) according to the general procedure. Semi-preparative HPLC separation was performed with a H_2O (0.3% ammonium hydroxide)/acetonitrile gradient starting at 5% ACN and increasing to 15% over 15 minutes, isocratic flow at 15% until 23 minutes, gradient

to 20% until 33 minutes and finally a gradient to 55% until 37 minutes with a 5mL/min flow rate. The product was collected from 17.5 – 33 minutes.

Yield after purification: 20 mg (14 %)

^1H NMR (400 MHz; MeOD): δ 9.05 (d, $^3J = 5.7$ Hz, 1H, H14), 8.67 (d, $^3J = 5.4$ Hz, 1H, H8), 8.66 (d, $^3J = 5.4$ Hz, 1H, H20), 8.00 (t, $^3J = 7.5$ Hz, 1H, H12), 7.96 (t, $^3J = 7.5$ Hz, 1H, H6), 7.70-7.63 (m, 3H, H5 + H11 + H18), 7.55 (t, $^3J = 6.9$ Hz, 1H, H13), 7.50 (d[AB], $^3J = 8.4$ Hz, 2H, H23), 7.35 (t, $^3J = 6.6$ Hz, 1H, H7), 7.28 (t, $^3J = 6.3$ Hz, 1H, H19), 7.25 (d[AB], $^3J = 8.4$ Hz, 2H, H22) 7.21 (d, $^3J = 7.8$ Hz, 1H, H17), 5.98 (t, $^3J = 7.8$ Hz, 1H, H1), 5.32 (d[AB], $^2J = 15.1$ Hz, 1H, H3/9/15), 5.28 (d[AB], $^2J = 14.6$ Hz, 1H, H3/9/15), 5.12 (d, $^3J = 15.5$ Hz, 2H, H3/9/15), 4.76 (d, $^3J = 18.0$ Hz, 1H, H3/9/15), 3.06 (ddd, $^3J_{\text{cis}} = 8.5$ Hz, $^2J = 6.5$ Hz, $^2J_{\text{Rh,H}} = 2.2$ Hz, 1H, H2b), 2.24 (apparent dt, $^2J = ^3J_{\text{trans}} \sim 7.1$ Hz, $^2J = ^2J_{\text{Rh,H}} = 2.4$ Hz, 1H, H2a).

^{13}C -NMR (151 MHz; MeOD): δ 166.3 (C10), 165.9 (C4), 163.7 (C16), 157.8 (C24), 153.0 (C8), 152.6 (C14), 151.9 (C20), 140.7 (C12), 140.6 (C6), 139.5 (C18), 133.0 (2C, C23, 2C), 127.0 (C13), 126.6 (C7), 126.2 (2C, C22) 126.1 (C19), 125.6 (C5/11), 125.5 (C5/11), 122.9 (C17), 120.4 (-CN), 110.5 (C21), 90.4 (d, $^2J_{\text{Rh,C}} = 3.4$ Hz, C1), 67.8 (C3/9/15) 67.73 (C3/9/15), 67.69 (C3/9/15), 13.2 (d, $^2J_{\text{Rh,C}} = 18.9$ Hz, C2)

HRMS (ESI): calc. $[\text{C}_{27}\text{H}_{25}\text{N}_5\text{ORh}]^+$: 538.1114; found: 538.1119

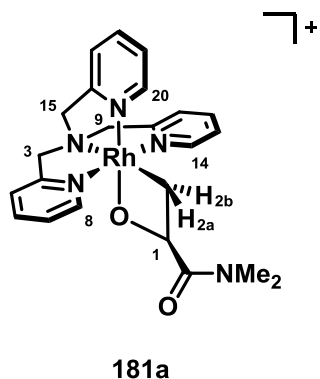
3.4.1.2.2 NMR Scale - General Procedure

$[\text{RhCl}(\text{C}_2\text{H}_4)_2]_2$ (50 mg, 0.13 mmol, 0.5 equiv., Alfa Aesar) was weighed into a 5 mL reaction vial. The vial was equipped with a magnetic stir bar and sealed with a screw cap fitted with a PTFE coated rubber septum. CH_2Cl_2 (1mL) was added, the resulting solution was frozen in a liquid nitrogen bath and the vial evacuated for 5 minutes on a Schlenk manifold. Dry N_2 was then used to back-fill the vial. TPA (75 mg, 0.26 mmol, 1 equiv.) was weighed into a small vial and dissolved in CH_2Cl_2 (1mL). The resulting solution was transferred with a syringe on top of the frozen Rh-dimer suspension and allowed to freeze. Two more freeze-pump-thaw cycles were performed and subsequently the vial was kept at -78°C with stirring. After 1 h the solution was transferred in 0.4 mL portions into five NMR tubes sealed under N_2 with a screw cap fitted with a PTFE coated rubber septum. The alkene of interest (1.5 equiv.) was added to the solution, the NMR tube was inverted several times

and the solution was allowed to warm to room temperature. After 30 minutes the volatiles were removed on high vacuum and the residue was taken up in MeOD (0.4mL). TMS was added as internal standard, a reference spectrum was recorded and the tube was cooled to -10 °C. Subsequently, H₂O₂ (30% aq, 13 µL, 0.10 mmol, 2 equiv.) was added via microsyringe, the tube was inverted several times and allowed to warm to room temperature. A product spectrum was recorded after 2 hours.

After removal of the volatiles 0.5 mg of the crude residue was dissolved in a H₂O/acetonitrile = 3/1 mixture (10 mL) and subject to HPLC-MS analysis on an Agilent 1260 system with a 6120 single quadrupole LC/MS system using a TMS-end-capped Phenomenex Luma C18(2) column (150x4.6 mm, 5 µm, 100 Å). The MS was set to SIM (single ion monitoring) mode for m/z = mass of the corresponding positively charged complex. 2 µL of the product solution were injected and a H₂O/acetonitrile gradient was employed starting at 30% acetonitrile increasing to 90% over 20 minutes with a 0.4mL flow rate.

[TPA-*N,N*-Dimethylacrylamide-oxarhodacyclobutane]Cl, 181a

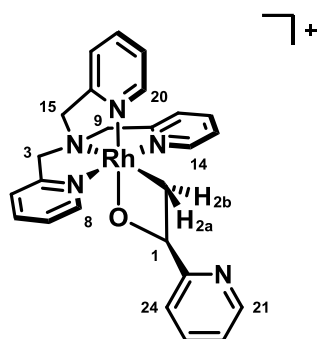


The title compound was synthesized from *N,N*-dimethylacrylamide (8.3 µL, 0.08 mmol, 1.5 equiv.) according to the general procedure.

NMR yield: 71%

Characterization data reported above.

[TPA-vinylpyridine-oxarhodacyclobutane]Cl, 181e



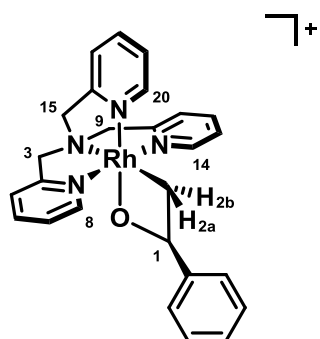
181e

The title compound was synthesized from 2-vinylpyridine (8,6 μ L, 0.08 mmol, 1.5 equiv.) according to the general procedure.

NMR yield: 80%

Characterization data reported above.

[TPA-styrene-oxarhodacyclobutane]Cl, 181g



181g

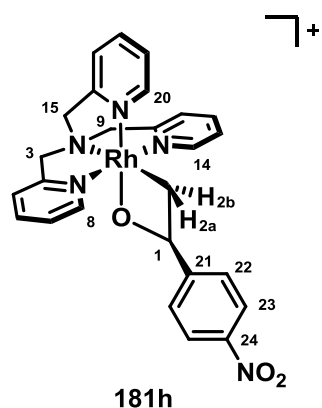
The title compound was synthesized from 4-styrene (8.3 μ L, 0.08 mmol, 1.5 equiv.) according to the general procedure.

NMR yield: 36%

Retention time: 5.6 minutes

Characterization data reported above.

[TPA-4-nitrostyrene-oxarhodacyclobutane]Cl, 181h



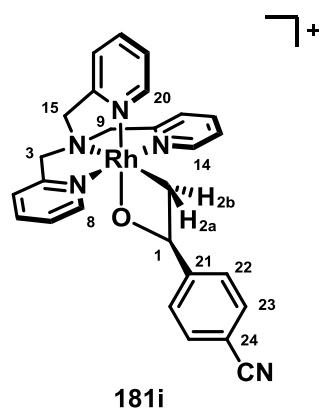
The title compound was synthesized from 4-nitrostyrene (10.2 μ L, 0.08 mmol, 1.5 equiv.) according to the general procedure.

NMR yield: 26%

^1H NMR (400 MHz; MeOD): δ 9.04 (d, $^3J = 5.6$ Hz, 1H, H14), 8.83 (d, $^3J = 5.2$ Hz, 1H, H8), 8.67 (d, $^3J = 5.6$ Hz, 1H, H20), 8.06-7.21 (m, $\text{H}_{\text{py}} + \text{H}_{\text{styr}}$), 3.14-3.05 (m, 1H, H2b), 2.30-2.20 (m, 1H, H2a).

HRMS (ESI): calc. $[\text{C}_{26}\text{H}_{25}\text{N}_5\text{O}_3\text{Rh}]^+$: 558.1012; found: 558.1017

[TPA-4-cyanostyrene-oxarhodacyclobutane]Cl, 181i



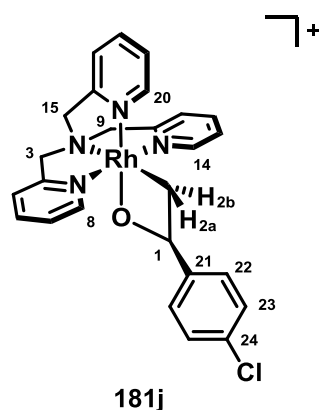
The title compound was synthesized from 4-cyanostyrene (10.3 μ L, 0.08 mmol, 1.5 equiv.), according to the general procedure.

NMR yield: 27%

Retention time: 10.4 minutes

Characterization data reported above.

[TPA-4-chlorostyrene-oxarhodacyclobutane]Cl, 181j



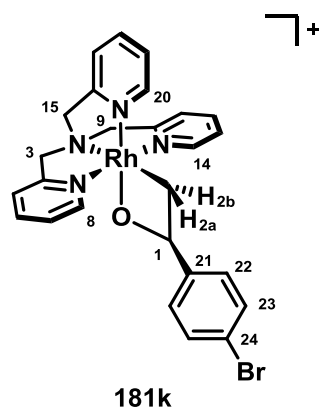
The title compound was synthesized from 4-chlorostyrene (9.6 μ L, 0.08 mmol, 1.5 equiv.) according to the general procedure.

NMR yield: 36%

^1H NMR (400 MHz; MeOD): δ 9.03 (d, $^3J = 5.6$ Hz, 1H, H14), 8.80 (d, $^3J = 5.1$ Hz, 1H, H8), 8.70 (d, $^3J = 5.6$ Hz, 1H, H20), 8.08-7.07 (m, $\text{H}_{\text{py}} + \text{H}_{\text{styr}}$), 5.88 (t, $^3J = 7.9$ Hz, 1H, H1), 3.04 (apparent dt, $^2J = ^3J_{\text{cis}} \sim 7.6$ Hz, $^2J_{\text{Rh,H}} = 2.2$ Hz, 1H, H2b), 2.34 (apparent dt, $^2J = ^3J_{\text{trans}} \sim 7.2$ Hz, $^2J_{\text{Rh,H}} = 2.3$ Hz, 1H, H2a).

HRMS (ESI): calc. $[\text{C}_{26}\text{H}_{25}\text{N}_4\text{OClRh}]^+$: 547.0772; found: 547.0771

[TPA-4-bromostyrene-oxarhodacyclobutane]Cl, 181k



The title compound was synthesized from 4-bromostyrene (10.5 μ L, 0.08 mmol, 1.5 equiv.) according to the general procedure.

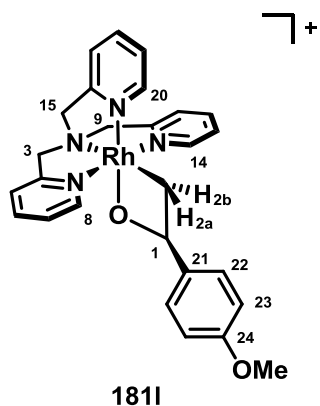
NMR yield: 44%

Retention time: 10.3 minutes

^1H NMR (400 MHz; MeOD): δ 9.03 (d, $^3J = 5.5$ Hz, 1H, H14), 8.79 (d, $^3J = 6.3$ Hz, 1H, H8), 8.69 (d, $^3J = 5.5$ Hz, 1H, H20), 8.10-7.00 (m, $\text{H}_{\text{py}} + \text{H}_{\text{styr}}$), 5.86 (t, $^3J = 7.5$ Hz, 1H, H1), 3.04 (apparent dt, $^2J = ^3J_{\text{cis}} \sim 7.5$ Hz, $^2J = ^2J_{\text{Rh,H}} = 2.4$ Hz, 1H, H2b), 2.33 (apparent dt, $^2J = ^3J_{\text{trans}} \sim 7.5$ Hz, $^2J = ^2J_{\text{Rh,H}} = 2.4$ Hz, 1H, H2a).

HRMS (ESI): calc. $[\text{C}_{26}\text{H}_{25}\text{N}_4\text{OBrRh}]^+$: 591.0267; found: 591.0256

[TPA-4-methoxystyrene-oxarhodacyclobutane]Cl, 181I



The title compound was synthesized from 4-methoxystyrene (10.4 μL , 0.08 mmol, 1.5 equiv.) according to the general procedure.

NMR yield: 36%

Retention time: 7.2 minutes

^1H NMR (400 MHz; MeOD): δ 9.05 (d, $^3J = 5.6$ Hz, 1H, H14), 8.91 (d, $^3J = 5.9$ Hz, 1H, H8), 8.73 (d, $^3J = 5.6$ Hz, 1H, H20), 8.09-6.73 (m, $\text{H}_{\text{py}} + \text{H}_{\text{styr}}$), 5.78 (t, $^3J = 8.0$ Hz, 1H, H1), 3.04 (apparent dt, $^2J = ^3J_{\text{cis}} \sim 7.3$ Hz, $^2J = ^2J_{\text{Rh,H}} = 2.4$ Hz, 1H, H2b), 2.48 (ddd, $^3J_{\text{trans}} = 8.4$ Hz, $^2J = 6.1$ Hz, $^2J_{\text{Rh,H}} = 2.4$ Hz, 1H, H2a).

HRMS (ESI): calc. $[\text{C}_{27}\text{H}_{28}\text{N}_4\text{O}_2\text{Rh}]^+$: 543.1267; found: 543.1261

Oxidation Product of [TPA-Rh-triethoxyvinylsilane]Cl

The title compound was synthesized from triethoxyvinylsilane (18.8 μL , 0.08 mmol, 1.5 equiv.) according to the general procedure.

^1H NMR (400 MHz; MeOD): δ 9.04 (d, $^3J = 5.9$ Hz, 1H), 8.75 (ddd, $^3J_{\text{trans}} = 16.3$ Hz, $^3J_{\text{cis}} = 8.8$ Hz, $^2J = 4.0$ Hz, 1H), 8.70 (d, $^3J = 5.7$ Hz, 2H), 7.89 (t, $^3J = 7.8$ Hz, 2H), 7.71 (t, $^3J = 7.8$ Hz, 1H), 7.59 (t, $^3J = 7.8$ Hz, 2H), 7.41-7.24 (m, 4H), 6.22 (d, $^3J_{\text{cis}} = 8.6$ Hz, 1H), 5.82 (d, $^3J_{\text{trans}} = 16.6$ Hz,

1), 5.67 (d[AB], $^3J = 15.2$ Hz, 2H), 4.98 (d[AB], $^3J = 15.1$ Hz, 2H), 3.42 (q, $^3J = 7.1$ Hz, 6H), 0.94 (q, $^3J = 7.1$ Hz, 9H).

^{13}C NMR (100 MHz; MeOD): 165.1 (2C), 164.1 (1C), 162.4 (d, $^2J_{Rh,C} = 30.3$ Hz, 1C), 151.8 (2C), 151.3 (1C), 139.3 (2C), 138.7 (1C), 124.8 (2C), 123.8 (2C), 121.8 (d, $^2J_{Rh,C} = 30.3$ Hz, 1C), 58.0 (3C), 17.2 (3C).

Two C signals seem to be missing. Through the H/D exchange the signal could have broadened into the baseline.

LRMS (ESI): $[\text{C}_{27}\text{H}_{28}\text{N}_4\text{O}_2\text{Rh}]^+$: m/z 599.1 (M^+)

4 Formation of Unsubstituted Azarhodacyclobutanes

The last two chapters have focused on the formation and reactivity of unsubstituted and substituted rhodaoxetanes (oxarhodacyclobutanes) as accessed by H_2O_2 oxidation of Rh-olefin complexes. In the following three chapters the nitrogen analogues, azarhodacyclobutanes, will be discussed. The present chapter will highlight the oxidation of Rh-ethylene complexes by nitrogen-based oxidants to yield unsubstituted azarhodacyclobutanes. First, the oxidation by [*N*-(toluenesulfonyl)imino]phenyliodinane (PhINTs) will be presented and the influence of the solvent and other experimental parameters will be discussed. This will be followed by an overview of the oxidation using alternative nitrene precursors and finally an insight into preliminary reactivity studies will be given.

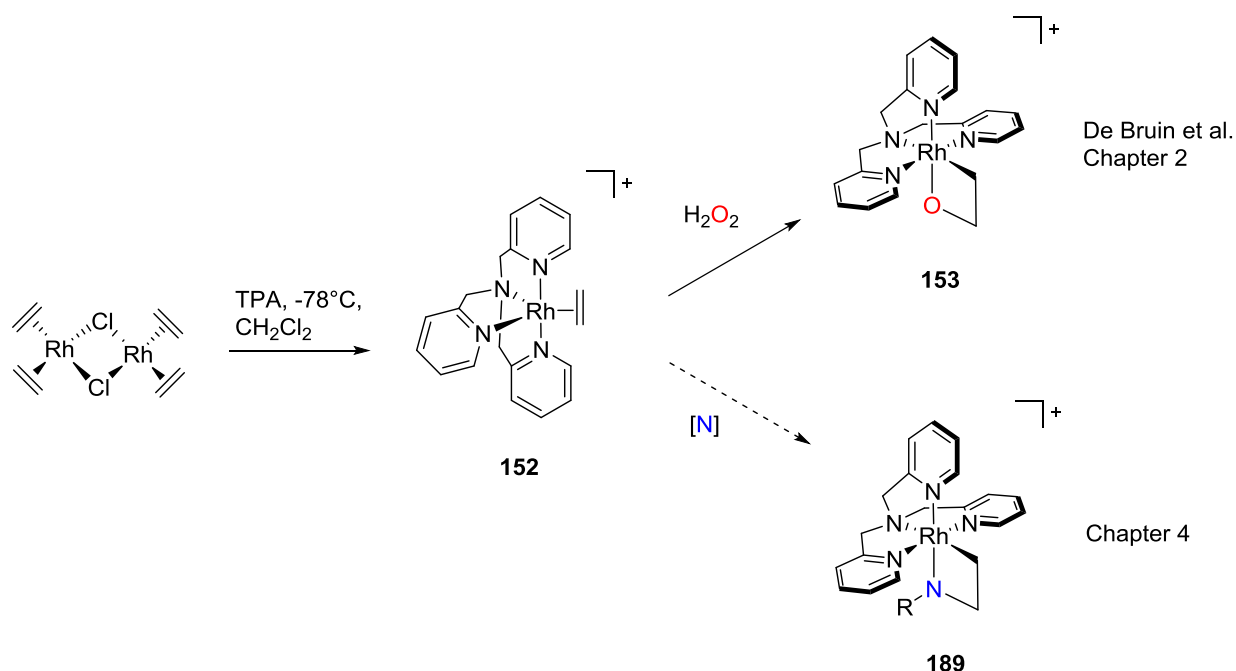
Two visiting students from the University of Teheran have helped with parts of this project. Taraneh Hajiashrafi and Alireza Azhdari Teherani performed optimization studies of the oxidation of TPA and MeTPA Rh-ethylene complexes with PhINTs, PhINNs, N_3Ts and TrocNHOTs (Chapter 4.2).

Parts of the work presented in this chapter have been published as a communication in *Angewandte Chemie International Edition*.³⁰² The results reported here are extended in scope and discussion compared to the published data. Specifically, the investigations employing alternative nitrene precursors to PhINTs as well as the reactivity studies presented here have not otherwise been published.

4.1 Oxidation by PhINTs

At the time when the work on this project started, no azarhodacyclobutane had been isolated and characterized. As mentioned in Chapter 1, an azarhodacyclobutane had been proposed by Alper to be the intermediate in the Rh-catalyzed carbonylation of aziridines to form β -lactams.²⁰⁶ The ability to directly access such structures would allow further investigation of their involvement in this and similar reactions. At the same time, the design of new transformations with an azarhodacyclobutane intermediate – in analogy to the carbohydroxylation protocol proposed in Chapter 2 – would be facilitated.

Following our work on the reactivity of rhodaoxetanes²⁵² we were curious whether the TPA-Rh ethylene complex **152** could react with nitrogen-based oxidants. We hypothesized that by choosing an appropriate *N*-based oxidant 2-azarhodacyclobutanes (**189**) could be synthesized from the same Rh(I)-ethylene complex (Scheme 4.1). *N*-[(4-toluenesulfonyl)imino]phenyliodinane (PhINTs) was selected for initial study, given the utility of this reagent in olefin aziridination.^{237,303,304}



Scheme 4.1 Proposed formation of azarhodacyclobutane **189**.

4.1.1 Formation of Two Isomers

Upon exposure of complex **152** to 1 equivalent of PhINTs in CH_2Cl_2 at room temperature, the reaction mixture almost instantaneously darkened from a light olive-green to a deep rust-coloured, almost black solution. The ESI mass spectrum of the crude product mixture showed a dominant signal at 590 m/z , which corresponded to the expected mass of azarhodacyclobutane **190** and indicated the effective incorporation of the *N*-tosyl fragment. High-resolution mass spectrometry further confirmed the corresponding molecular formula.

The crude ^1H NMR spectrum was considerably more complicated than anticipated from studies of rhodaoxetane **153**. Nonetheless, we were able to identify features in the ^1H

NMR spectrum of the crude reaction mixture that closely resembled signals found in the ^1H NMR spectrum of **153**. Specifically, we observed a doublet of triplets at ~ 2 ppm with $^2J_{\text{Rh-H}}$ coupling of about 2 Hz. Rhodaoxetane **153** exhibits one doublet of triplets with a similar chemical shift and coupling constants. Likewise, we observed a triplet at ~ 4 ppm. Rhodaoxetane **153** displays one triplet, again with a similar shift and coupling constant. The signals in complex **153** correspond to H1 and H2, respectively, in the rhodaoxetane (Figure 1). Based on this information we believed that we had prepared the desired azarhodacyclobutane next to a number of partly unidentified by-products. Attempts to purify the crude material by crystallization (for complexes with Cl^- , BPh_4^- and PF_6^- counterions), liquid extraction or silica gel column chromatography were unsuccessful. Gratifyingly, separation on a C18 reverse phase column via HPLC was effective. Two isomeric compounds with the expected m/z of 590 could be isolated in sufficient quantities for further analysis. We tentatively assigned them as isomers **190** and **191**. Isomer **190** has an identical configuration with rhodaoxetane **153** in which the tosyl nitrogen (contained within the azametallacycle) is cis to the central amine of the TPA ligand. In **191**, the tosyl nitrogen (contained within the azametallacycle) is trans to the central amine of the TPA ligand. Although the pure substances were resistant to crystallization, NMR spectroscopy proved expedient for structural assignments.

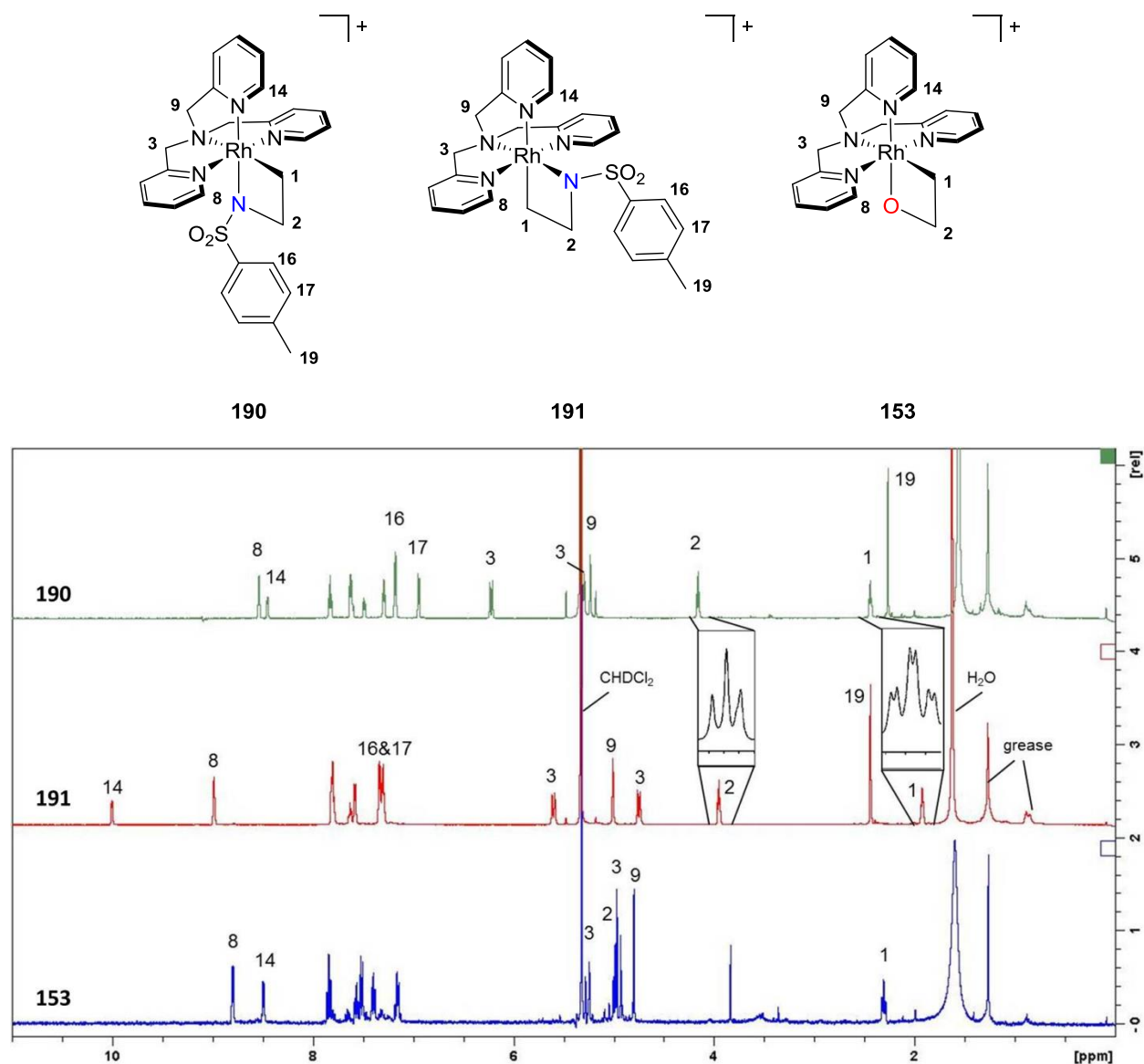


Figure 4.1 Comparison of the ^1H NMR spectra of azarhodacyclobuanes **190** and **191** with rhodaoxetane **153** (600 MHz, CD_2Cl_2 , 298K).

Consistent with our expectations, the ^1H NMR spectra of pure **190** and **191** were indeed similar to that of rhodaoxetane **153**.¹⁸⁷ The rhodaoxetane has octahedral configuration with a plane of symmetry which renders two of the methylpyridyl arms of the TPA ligand equivalent. The methylene protons in the central, unique methylpyridyl arm as well as the protons in the oxametallacycle are thus also equivalent. As in that spectrum, the protons in the azametallacyclobutane ring (H1 and H2) and in the methylene linker of the

unique methylpyridine arm of the ligand (H9) were equivalent. The protons of the two remaining methylpyridyl arms (H3-H8) gave only one set of signals which integrated to double intensity. This showed that the complexes at hand also contained the same plane of symmetry which further indicated that the inversion of the stereogenic nitrogen center was fast on the NMR time-scale.

The following discussion is based on the ^1H NMR data for isomer **190** with a chloride anion. For ^1H NMR data of isomer **191** see Table 4.1. In close analogy to the rhodaoxetane spectrum we could observe a doublet of triplets with distinctive Rh coupling (2.44 ppm, dt, 2H, $^3J_{\text{H,H}} = 7.8$ Hz, $^2J_{\text{Rh-H}} = 2.0$ Hz, H1) and a triplet (4.16 ppm, 2H, $^3J_{\text{H,H}} = 7.8$ Hz, H2) for the protons in the azametallacyclobutane ring. The methylene protons of the equivalent methylpyridyl arms (H3) were diastereotopic and appeared as second order [AB] type doublets at 6.22 ppm and 5.30 ppm (2H, $^2J_{\text{H-H}} = 15.3$ Hz) while the methylene protons in the unique TPA arm (H9) gave a singlet at 5.23 ppm (s, 2H). Further characteristic signals were found at 8.54 ppm (d, 2H, $^3J_{\text{H,H}} = 5.4$ Hz, H8) and 8.45 ppm (d, 1H, $^3J_{\text{H,H}} = 7.7$ Hz, H14) for protons H8 and H14 on the pyridine rings. The aromatic protons of the tosyl moiety, H16 and H17 could be observed at 7.20-7.15 ppm (m, 3H, includes H13) and 6.95 ppm (d, 2H, $^3J_{\text{H,H}} = 7.7$ Hz) respectively while the methyl group, H19 appeared as a singlet at 2.27 ppm (s, 3H). **Table 4.1** Tabulated ^1H NMR data comparison for **190**, **191** and **153** (600MHz, CD_2Cl_2 , 298K)

H	190	191	153^a
1	2.44 (dt, 2H, $^3J_{\text{H,H}} = 7.8$ Hz, $^2J_{\text{Rh-H}} = 2.0$ Hz)	1.92 (dt, 2H, $^3J_{\text{H,H}} = 6.9$ Hz, $^2J_{\text{Rh-H}} = 1.7$ Hz)	2.30 (dt, 2H, $^3J_{\text{H,H}} = 7.5$ Hz, $^2J_{\text{Rh-H}} = 2.4$ Hz)
2	4.16 (t, 2H, $^3J_{\text{H,H}} = 7.8$ Hz)	3.95 (t, 2H, $^3J_{\text{H,H}} = 6.9$ Hz)	4.99 (t, 2H, $^3J_{\text{H,H}} = 7.5$ Hz)
3	6.22 (ax) and 5.30 (eq) ([AB]d, 2H, $^2J_{\text{H-H}} = 15.3$ Hz)	5.60 (eq) and 4.75 (ax) ([AB]d, 2H, $^2J_{\text{H-H}} = 15.5$ Hz)	5.26 (ax) and 4.96 (eq) (d, 2H, $^2J_{\text{H-H}} = 15.2$ Hz)
5	7.65-7.58 (m, 3H, includes H12)	7.58 (d, 2H, $^3J_{\text{H,H}} = 7.5$ Hz)	7.65-7.58 (m, 3H, includes H12)

H	190	191	153 ^a
6	7.83 (apparent t, 2H, $^3J_{H,H}$ = 7.7 Hz, 6.3 Hz)	7.32-7.26 (m, 2H)	
7	7.29 (apparent t, 2H, $^3J_{H,H}$ = 6.3 Hz, 5.7 Hz)	7.85-7.76 (m, 4H, includes H11 and H12)	
8	8.54 (d, 2H, $^3J_{H,H}$ = 5.4 Hz)	8.99 (d, 2H, $^3J_{H,H}$ = 5.1 Hz)	8.80 (d, 2H, $^3J_{H,H}$ = 5.4 Hz)
9	5.23 (s, 2H)	5.01 (s, 2H)	4.80 (s, 2H)
11	7.49 (d, 1H, $^3J_{H,H}$ = 7.7 Hz)	7.85-7.76 (m, 4H, includes H7 and H12)	
12	7.65-7.58 (m, 3H, includes H5)	7.85-7.76 (m, 4H, includes H7 and H11)	7.65-7.58 (m, 3H, includes H5)
13	7.20-7.15 (m, 3H, includes H16)	7.63 (apparent t, 1H, $^3J_{H,H}$ = 7.6 Hz, 5.5 Hz)	
14	8.45 (d, 1H, $^3J_{H,H}$ = 7.7 Hz)	10.01 (d, 1H, $^3J_{H,H}$ = 5.3 Hz)	8.49 (d, 1H, $^3J_{H,H}$ = 5.0 Hz)
16	7.20-7.15 (m, 3H, includes H13)	7.37-7.32 (m, 4H)	
17	6.95 (d, 2H, $^3J_{H,H}$ = 7.7 Hz)	7.37-7.32 (m, 4H)	
19	2.27 (s, 3H)	2.44 (s, 3H)	

^a NMR data for this complex has previously been reported in *d*₆-acetone.¹⁸⁷ For direct comparison with this work, we re-acquired the spectrum in CD₂Cl₂.

Our initial proposal that **190** was the isomer with the nitrogen in the cis position was supported judging from the overall pattern of the ¹H-NMR spectra and the apparent similarity – especially of **190** – in direct comparison with the ¹H-NMR spectrum of rhodaoxetane **153**. To further verify this assumption, 2D NOESY spectra were acquired and showed the following spatial correlations (Table 4.2). In **190**, the ring proton adjacent to the Rh center (H1) showed cross peaks with H8 and H14 on the equivalent and unique pyridine

rings respectively. This indicated that this proton must be trans to the central TPA amine. Furthermore, H16 on the tosyl group showed correlations with H3, the axial methylene protons in the equivalent methylpyridyl arms, which was consistent with the *N*-Ts group being cis to the TPA amine. In **191** on the other hand H1 showed through-space correlation with H3, the axial methylene protons in the equivalent methylpyridyl arms and with the protons in the ortho-position of the equivalent pyridine rings H8, but not with H14. The latter displayed a cross peak with H16, the protons on the *N*-Ts group. These correlations unambiguously established the configuration of **190** and **191** to be consistent with our hypothesis.

Table 4.2 NOESY contacts in **190** and **191**.

H	190	191
1	H8, H14	H3, H8 (weak)
2	H8, H14 (weak), H16	H8, H7
3	H5, H16	H1
5	H3	
7		H2
8	H1, H2	H2
14	H1, H2	H16, H17
16	H2, H3, H8 (weak)	H14
17	H19	H14
19	H17	

While most of the ^1H NMR signals of **191** are comparable with **190**, proton H14 experiences a ~ 1.5 ppm downfield shift while the signal of the axial H3 proton is shifted upfield by approximately the same amount compared to **190**. A de-shielding effect through space by the ring-current of the tosyl moiety is the likely reason for this observation.

The ^1H NMR spectra of the hexafluorophosphate salts are largely identical apart from a slight upfield shift of H3(eq) and H9. The reason for this difference is not fully understood. One hypothesis is to assume a close ion pair with the anion being located at the “back” side of the TPA ligand, i.e. distant from the azarhodacyclobutane ring (Figure 4.2). Depending on the anion, through space shielding (PF_6^-) or de-shielding (Cl^-) of the relevant ligand protons could then occur. A possible experiment for further verification of this hypothesis would be a heteronuclear $^1\text{H}/^{19}\text{F}$ NOESY experiment, which was, unfortunately, not available in our NMR facilities.

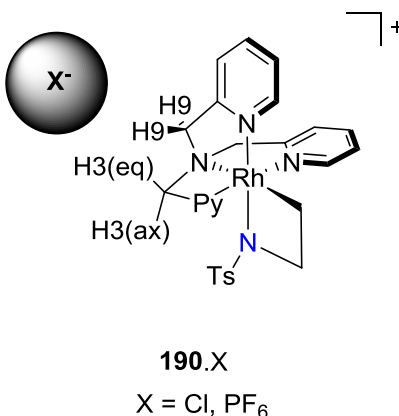


Figure 4.2 Possible reason for the anion effect in ^1H NMR data – through space shielding or de-shielding.

Further structural evidence for the formation of an azarhodacyclobutane was obtained from the $^{13}\text{C}\{\text{H}\}$ NMR spectrum of **190**. A resonance at 8.1 ppm was attributed to C1, which is one of the metallacycle carbons and appeared as a doublet with a $^2J_{\text{Rh-C}}$ coupling constant of 18.4 Hz. Through the neighbouring *N*-Ts moiety, C2 is de-shielded and appeared at 57.9 ppm (Table 4.3). These data are in good analogy to related azametallacyclobutanes.^{239,240}

Table 4.3 ^{13}C and ^{15}N shifts in **190** and **191** acquired by direct and indirect detection NMR methods.

	190	191
	^{13}C NMR; $^1\text{H}/^{15}\text{N}$ HMQC	^{13}C NMR $^1\text{H}/^{15}\text{N}$ HMQC
C1	8.1 (d, $^2J_{(\text{Rh}-\text{C})} = 18.4$ Hz)	1.6 (d, $^2J_{(\text{Rh}-\text{C})} = 16.1$ Hz)
C2	57.9	57.7
N(Py)	-155, -156	-145, -114
N(amine)	-338	-350
N(cycle)	-379 (d, $^2J_{\text{Rh}-\text{N}} = 14$ Hz)	-370

The Rh-coupling observed in both the ^1H and ^{13}C NMR spectra clearly demonstrated the Rh-CH₂ connectivity. A long range $^1\text{H}/^{15}\text{N}$ -correlated HMQC spectrum highlighted the scalar coupling of H1 and H2 and the azarhodacyclobutane nitrogen, for which we could thus elicit a ^{15}N chemical shift of -379 ppm (referenced to CH₃NO₂) through indirect detection (Figure 4.3, Table 4.3). Moreover, in a $^1\text{H}/^{15}\text{N}$ -correlated HSQC spectrum modified for long range resonance a coupling of this nitrogen to the Rh center could be observed with a coupling constant of $^2J_{(\text{Rh}-\text{N})} = 14$ Hz. The magnitude of the coupling compares well with previously reported five-membered cyclic Rh- toluenesulfonyl-1,2-diphenylethanediamine (TsDPEN) structures.³⁰⁵ The chemical shift is approximately 100 ppm lower field compared to those compounds which can be ascribed to the increased ring strain in the four-membered ring of the present structure.

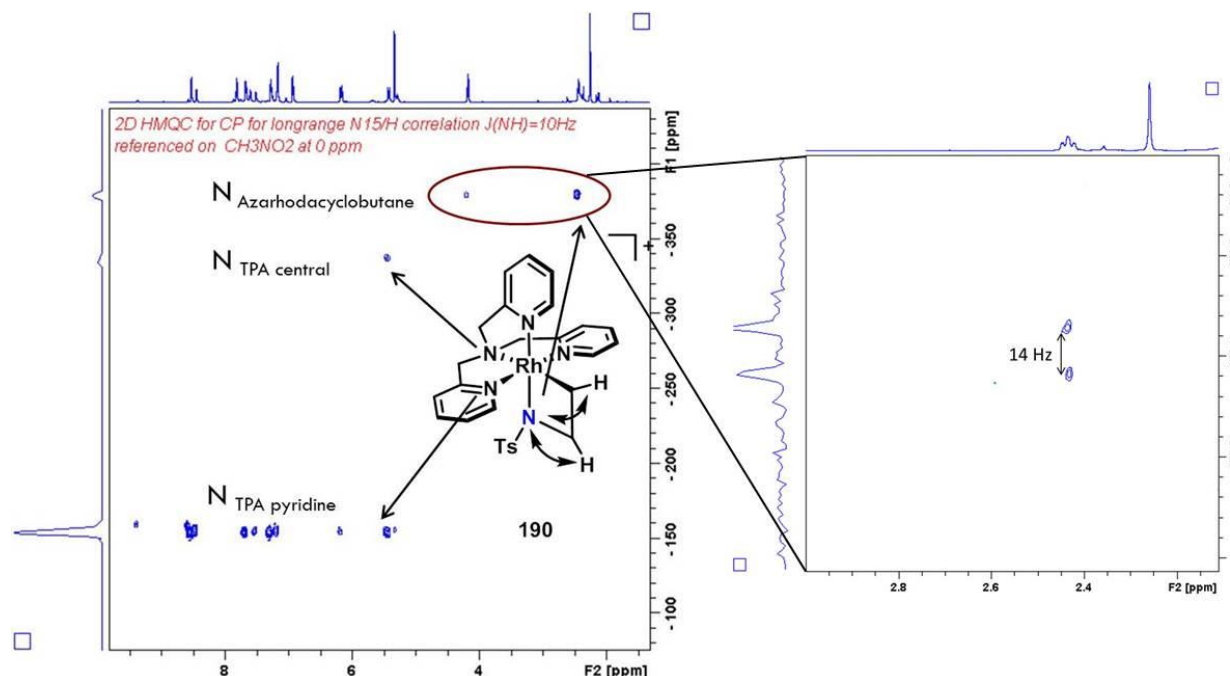


Figure 4.3 Long-range $^1\text{H}/^{15}\text{N}$ correlated HMQC (left) and HSQC (right) establish Rh-C, Rh-N and C-N connectivity.

The combined mass spectrometric and NMR spectral data presented above unambiguously proved the formation of the first isolated azarhodacyclobutanes, **190** and **191** and their respective assignments.

It is noteworthy that in the H_2O_2 oxidation of **152**, only one isomer of rhodaoxetane **153** (with a configuration like azarhodacyclobutane **190**) was formed when the reaction was performed at -10°C . A rhodaoxetane with a configuration like **191** was not observed. In computational studies Budzelaar *et al.* only found a very small energy difference for the formation of the two possible rhodaoxetane isomers which could not fully account for this experimental observation.¹⁸⁶ When the oxidation was performed at room temperature the formation of a geometrical isomer was postulated but no further characterization was presented.¹⁸⁵

4.1.2 Influence of Experimental Conditions

NMR yields for **190** and **191** were determined based on 1,3,5-trimethoxybenzene and tetramethylsilane as internal standards. In CD_2Cl_2 , olefin complex **152** was converted to a

1:1.7 mixture of **190** and **191** in combined 61% yield. The minor isomer, **190**, was formed in 22% yield, whereas **191** was formed in 39%. A similar ratio of **190:191** (1:1.5) was determined by HPLC-MS. The product ratio was independent of the reaction temperature (–78 °C, 25 °C, 70 °C in a sealed tube) and the concentration of the nitrene precursor (1, 2, 5 equivalents). It was found that fewer by-products were produced when only one equivalent of PhINTs was employed and the reaction was run at room temperature. Increasing the dilution also yielded cleaner crude mixtures but did not affect the ratio of **190:191**. Likewise, the change of the counterion had no effect on the isomer ratio. However, slightly decreased by-product formation was noted with the PF₆ anion, although it proved impossible to remove all fortuitous chloride. Some side products that could be identified are shown in Figure 4.4. Complex **192** has already been reported by De Bruin and results from protonation of **152** in the presence of chloride.¹⁸⁷ The formation of **193** is hypothesized to occur through protonation of an intermediate Rh-imido species (for greater detail see Chapter 6). Compound **194** can be formed from **193** through ligand exchange. Finally, when MeTPA was used instead of TPA as the ancillary ligand, the ratio also remained constant.

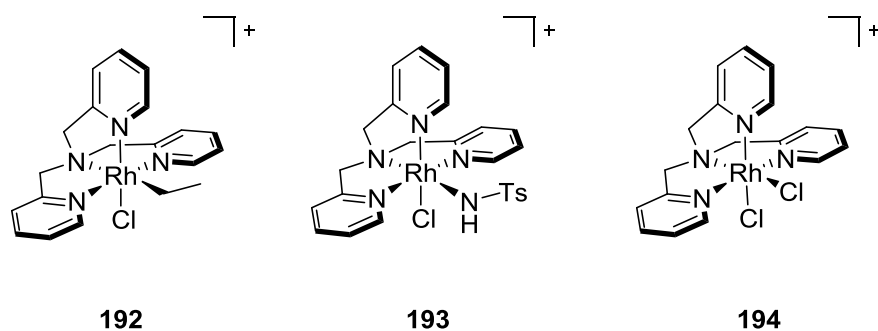


Figure 4.4 By-products identified in the PhINTs based oxidation of **152**.

Table 4.4 Parameters which did not affect the ratio of **190:191**. Best conditions underscored (least side products).

<i>Parameter</i>	<i>Increments</i>
Temperature	-78 °C, <u>25 °C</u> , 70 °C
Equivalents PhINTs	<u>1</u> , 2, 5
Concentration	0.086M, <u>0.043M</u> , 0.017M, 0.0086M, 0.0043M
Counter ion	Cl ⁻ , <u>PF₆⁻</u> , BPh ₄ ⁻
Ancillary ligand	TPA, MeTPA

Importantly, **190** and **191** did not interconvert even at high temperature or prolonged reaction time (3 days at room temperature). In addition, a mixture of **190** and **191** was recovered unchanged after heating for 30 minutes in either refluxing acetonitrile or water.

We then went on to explore how the formation of the azarhodacyclobutanes was affected when the reaction was carried out in different solvents. While we still observed mixtures when employing acetone, acetonitrile or chloroform, the ratios of **190** and **191**, as determined by HPLC-MS, only varied slightly (Figure 4.5).

On the other hand, when the reaction was performed in a 1:1 mixture of dichloromethane and methanol, azarhodacyclobutane **190** was formed exclusively. Likewise, in pure methanol or water, **190** was found as only product with the appropriate m/z (Figure 4.5). The presence of protic solvents must either greatly favor the formation of **190** or inhibit the formation of **191**. In the former case, increased yields of **190** would be expected when employing MeOH while an overall decrease of yield would imply inhibitory action of the solvent. Notably, the NMR yield was reduced from 22% formation of **190** in CD₂Cl₂ (in a mixture with 39% of **191**) to 14% of **190** in MeOH. This suggests that the presence of the protic solvent inhibits the formation of **191** rather than advancing the formation of **190**. The dielectric constants of the various solvents do not appear to play a key role, as mixtures were also obtained in polar, aprotic solvents like acetonitrile.

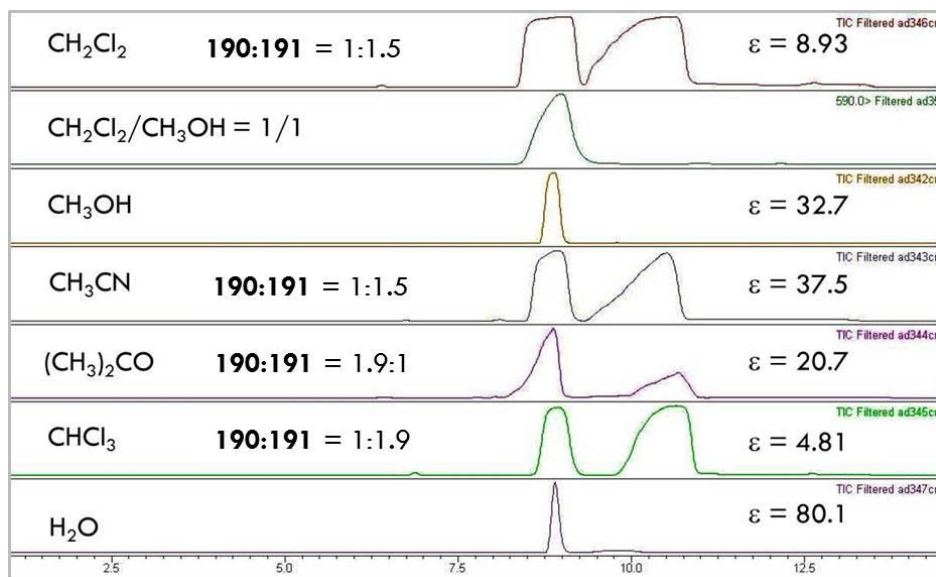


Figure 4.5 Dependence of **190:191** on solvent (ϵ = dielectric constant).

As can be seen in Figure 4.5, a 1:1 mixture of dichloromethane and methanol led to exclusive formation of **190**. We were interested how the ratio of **190:191** was affected by incremental increase of the methanol content in a dichloromethane/methanol mixture. Therefore, we performed the reaction in solvent mixtures ranging from 5% - 50% MeOH.

By ¹H NMR spectroscopy, the presence of B in the crude reaction mixture could only be observed up to a MeOD content of 10%. By using HPLC-MS it could be shown that the ratio of **190:191** was already reversed to 2.9:1 at only 5% MeOH content. At 15% MeOH content the ratio was found to be 6.7:1 (Table 4.5).

Table 4.5 Influence of methanol content on isomer ratio **190:191**.

<i>% MeOH</i> <i>in CH₂Cl₂</i>	190:191
0	1:1.5
5	2.9:1
7	4.4:1
12	4.9:1
15	6.7:1
50	1:0

These data show that only a minimal amount of protic solvent is sufficient to shift the isomer ratio towards formation of **190** until exclusive formation of this isomer is reached.

4.2 Oxidation with Alternative Nitrene Precursors

The successful preparation and full characterization of the first azarhodacyclobutanes reported above allowed selective access to isomer **190** and, after HPLC separation, to isomer **191**. We were interested whether similar azarhodacyclobutanes could be formed by using nitrene precursors alternative to *N*-(*p*-toluenesulfonyl)iminophenyliodinane (PhINTs). Specifically, the selective preparation of **191** would be desirable. Furthermore, protecting groups different from the toluenesulfonyl group (Ts, “tosyl”) in **190** and **191** would be an asset. This would obviate the harsh deprotection conditions of the tosylamide necessary to access the free amine.³⁰⁶

We, therefore, envisaged the use of *N*-chloro-4-toluenesulfonamide sodium salt trihydrate (Chloramine-T trihydrate), **195**, and 4-toluenesulfonyl azide, **196**, as oxidants to assess their selectivity in the formation of **190** and **191**. In addition, [*N*-(4-nitrophenylsulfonyl)imino]phenyliodinane, **197**, 2,2,2-trichloroethyl-*N*-tosyloxycarbamate, **198** and various alkyl, aryl and acylazides, **199**, were chosen as candidates for the preparation of azarhodacyclobutanes with varying *N*-substitution (Figure 4.6).

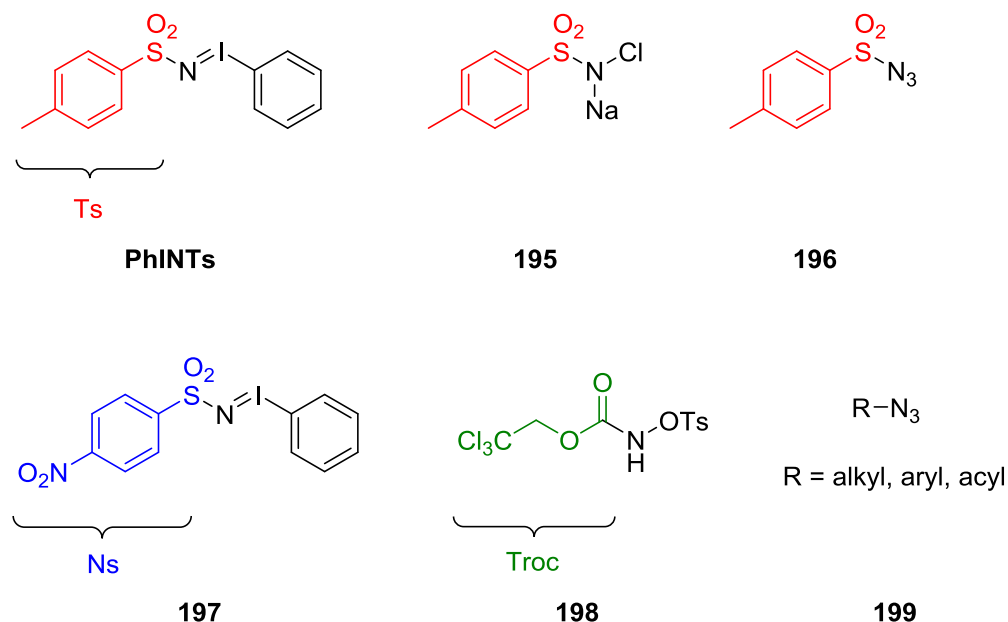


Figure 4.6 Alternative nitrene precursors.

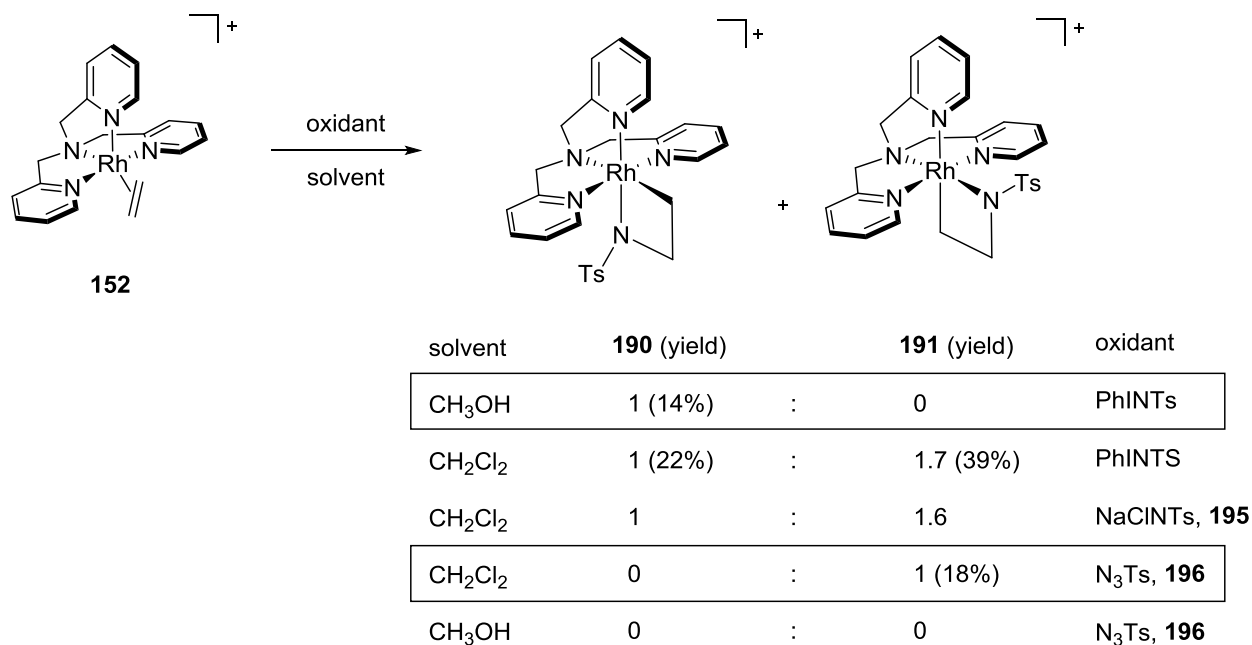
4.2.1 *N*-Tosyl Substituted Nitrene Precursors

Chloramine-T trihydrate (**195**) is a relatively cheap, commercially available oxidant and offers a convenient alternative to PhINTs, which has to be synthesized from toluenesulfonylamide and (diacetoxyiodo)benzene.³⁰³ A CD_2Cl_2 solution of TPA-Rh-ethylene complex **152** was exposed to one equivalent of chloramine-T under conditions identical to the employment of PhINTs. Mass spectrometric and ^1H NMR spectroscopic analysis of the crude reaction mixture confirmed the formation of a mixture of **190** and **191**. The isomer ratio was determined by ^1H NMR to be 1:1.6, which was almost identical to the oxidation with PhINTs (Scheme 4.2). However, the crude reaction mixture showed a significant increase in by-product formation as qualitatively judged by mass spectrometry and ^1H NMR spectroscopy. Thus, the use of chloramine-T trihydrate as oxidant was not further pursued.

Tosyl azide, **196**, can be readily prepared from toluenesulfonyl chloride and sodium azide according to literature procedures.³⁰⁷ A solution of **152** in CD_2Cl_2 was then treated with one equivalent of **196** under standard conditions. To our gratification, **191** was formed as single isomer in course of the reaction, based on the ^1H NMR spectrum of the crude reaction mixture. Since organic azides can be sensitive to UV light exposure, the reaction was repeated

under exclusion of ambient light with identical results. The NMR yield was determined to be 18% which is considerably lower than in the case of PhINTs based oxidation. Nevertheless, the ability to selectively access isomer **191** complements the exclusive formation of **190** by oxidation with PhINTs in protic solvents (Scheme 4.2).

Interestingly, when the reaction was carried out in methanol under otherwise identical conditions, only decomposition products were found without formation of either isomer **190** or **191**. The mechanistic implications of these observations will be discussed in greater detail in Chapter 6.

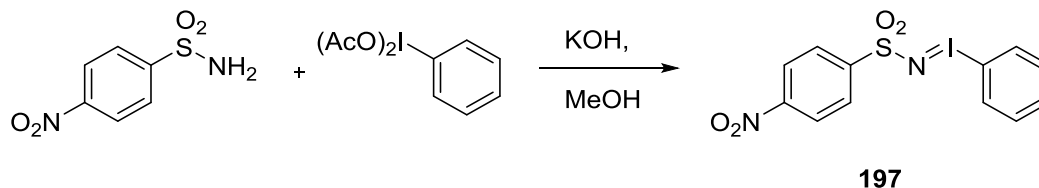


Scheme 4.2 Complementary selectivity of nitrene precursors.

4.2.2 Nitrene Precursors with Different *N*-Substitution

Deprotection of a toluenesulfonyl protected amine requires strongly basic conditions using sodium naphthalenide.³⁰⁶ In order to be able to afford azarhodacyclobutanes with an unprotected nitrogen atom under less harsh conditions, we aimed to replace the tosyl group with more easily removable protecting groups. The 4-nitrophenylsulfonyl (Ns, “nosyl”) group is closely related to the tosyl moiety but can be de-protected under milder conditions.³⁰⁸ The corresponding nitrene precursor, [*N*-(4-

nitrophenylsulfonyl]imino]phenyliodinane (**197**) could be synthesized from 4-nitrophenylsulfonylamide and (diacetoxyiodo)benzene in a fashion analogous to the synthesis of the PhINTs precursor (Scheme 4.3).³⁰⁹



Scheme 4.3 Preparation of nosyl nitrene precursor, **197**

A CD₂Cl₂ solution of TPA-Rh-ethylene complex **152** was then treated with **197** under the same conditions as applied in the oxidation with PhINTs. Examination of the crude reaction mixture by MS and ¹H NMR spectroscopy revealed that again, a mixture of two isomers (**200** and **201**) had been formed (Figure 4.7). The ratio was determined by ¹H NMR spectroscopy to be 1:1.3. This is comparable to the ratio of **190:191**.

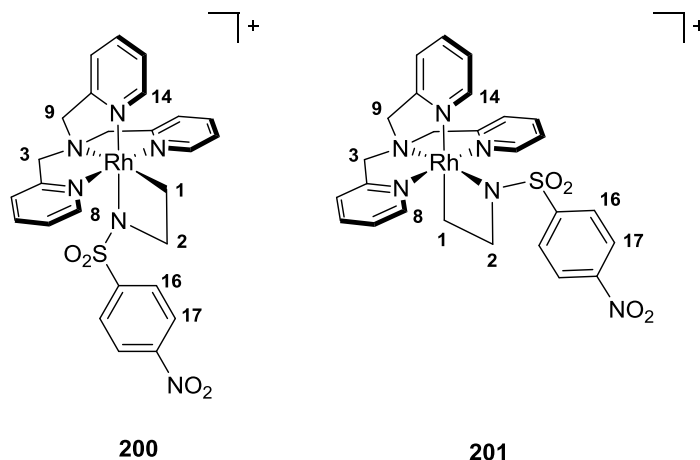


Figure 4.7 Formation of two isomers after oxidation with **197**.

It was possible to isolate sufficient amounts of the minor isomer, **200**, by semi-preparative HPLC for further analysis. As evident in Figure 4.8, the ¹H NMR spectra of **190** and **200** are almost identical, differing only in the absence of a signal for H19 (the tosyl methyl group) and minimal differences in chemical shifts in the aromatic region.

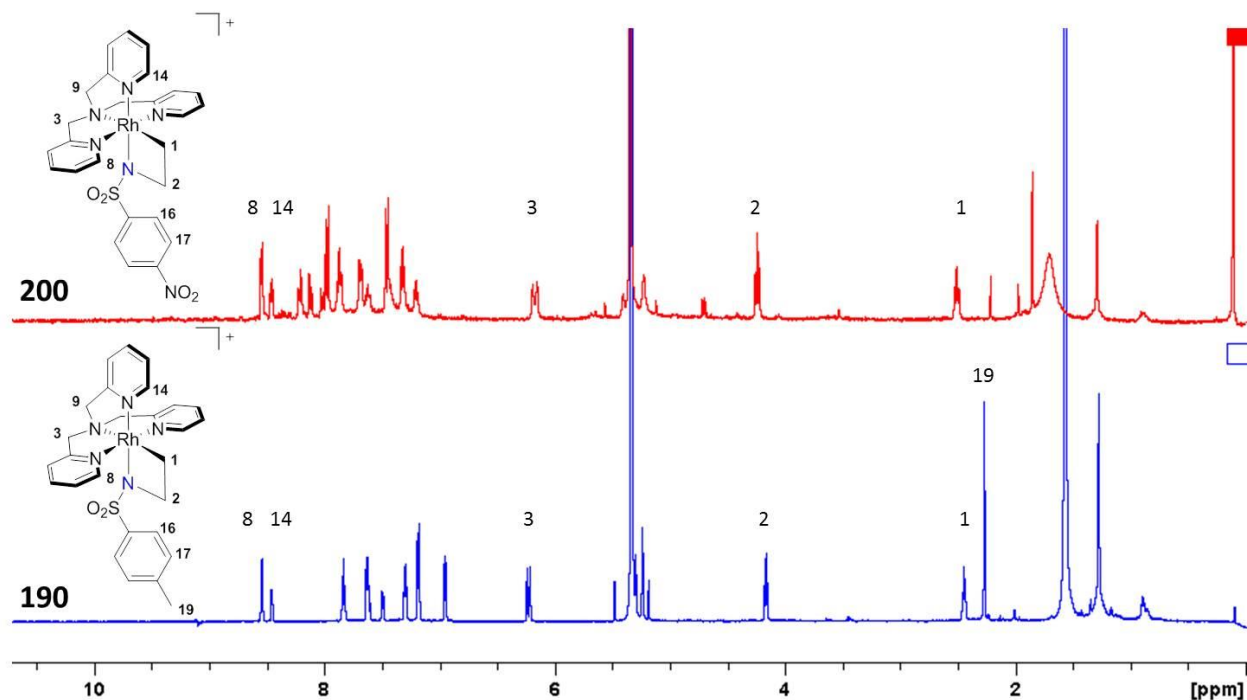
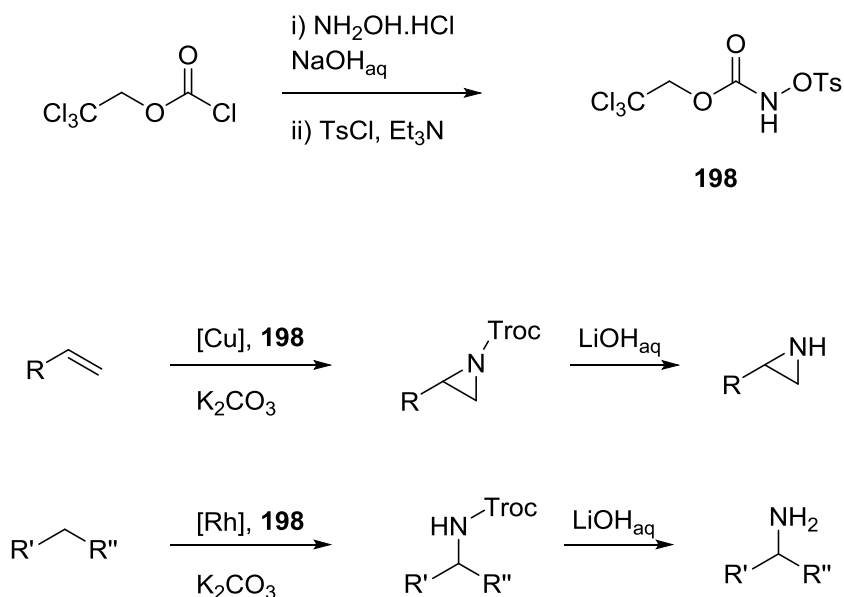


Figure 4.8 ^1H NMR comparison of **190** and **200** (400MHz, CD_2Cl_2 , 298K).

Finally, two-dimensional NMR methods (COSY, NOESY, HSQC) confirmed the configuration of **200** to be identical to the conformation of **190**.

Another nitrene precursor, that had been employed recently by Lebel *et al.* in aziridination and C-H amination reactions is 2,2,2-trichloroethyl-*N*-tosyloxycarbamate, **198** (Scheme 4.4).³¹⁰⁻³¹² According to the literature, the carbamate moiety (Troc) can be easily hydrolyzed under mild basic conditions yielding the corresponding free amines. We, therefore, synthesized **198** to investigate its suitability to form azarhodacyclobutanes.

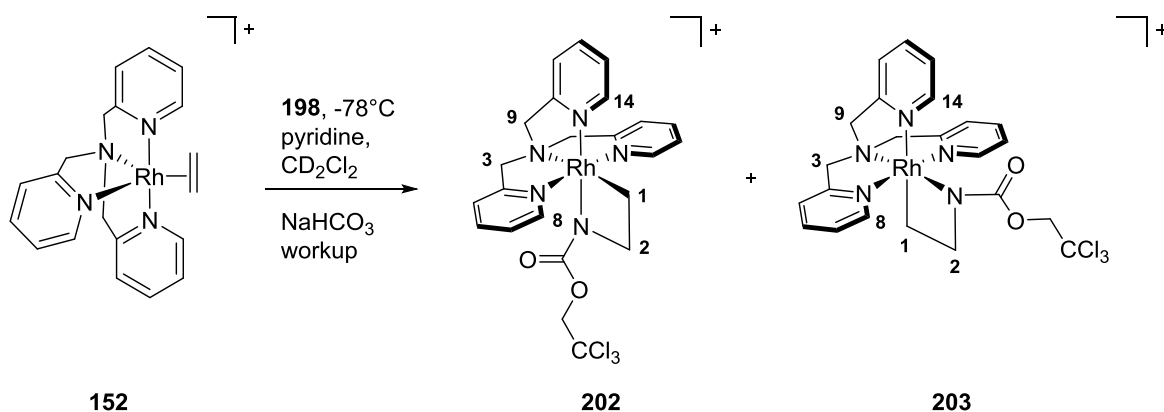


Scheme 4.4 Synthesis and reactivity of Troc nitrene precursor **198**.

In the course of the oxidation with **198**, one equivalent of toluenesulfonic acid is formed per equivalent of nitrene precursor. One consideration in using this precursor in the oxidation of TPA-Rh ethylene complex **152** was the propensity of the latter to be protonated and give the σ -1 ethyl complex **192** (Chapter 4.1.2). Another concern was the sensitivity of the resulting azarhodacyclobutanes to acidic media (Chapter 4.3). In the studies reported by Lebel *et al.* the acid formation is countered by the use of K_2CO_3 , which proved effective for neutralization in spite of the low solubility of the base in CH_2Cl_2 or acetone.³¹⁰⁻³¹²

Indeed, treating a CD_2Cl_2 solution of **152** with **198** under standard conditions, led to formation of the desired azarhodacyclobutane only in trace quantities. Formation of significant amounts of **192** along with a number of other side products was detected by mass spectrometry. We thus added 3-5 equivalents of the solid carbonate bases NaHCO_3 , Na_2CO_3 and K_2CO_3 to the mixture before addition of nitrene precursor **198**. In all cases, the product mixture still consisted of mostly undesired by-products and only small amounts of the Troc-protected azarhodacyclobutane. Therefore, pyridine (5 equivalents) was employed as soluble base which greatly improved the reaction outcome. In addition, it was found that lowering the reaction temperature to -78°C further decreased the by-product formation in the reaction. A sodium bicarbonate work-up was necessary to prevent acidic decomposition

of the products upon concentrating the reaction mixture on the rotary evaporator. Two isomeric azarhodacyclobutanes were formed as major products in a 1:1 mixture based on mass spectrometry and ^1H NMR spectral analysis of the crude reaction mixture (Scheme 4.5).



Scheme 4.5 Formation of two isomeric Troc-protected azarhodacyclobutanes.

Purification of the product mixture by HPLC proved difficult. The products were prone to decomposition during chromatography, and even after extensive method development, only mixtures of both isomers could be obtained. We assumed the two isomers to be compounds **202** and **203**, which have identical configurations as **190** and **191**, respectively.

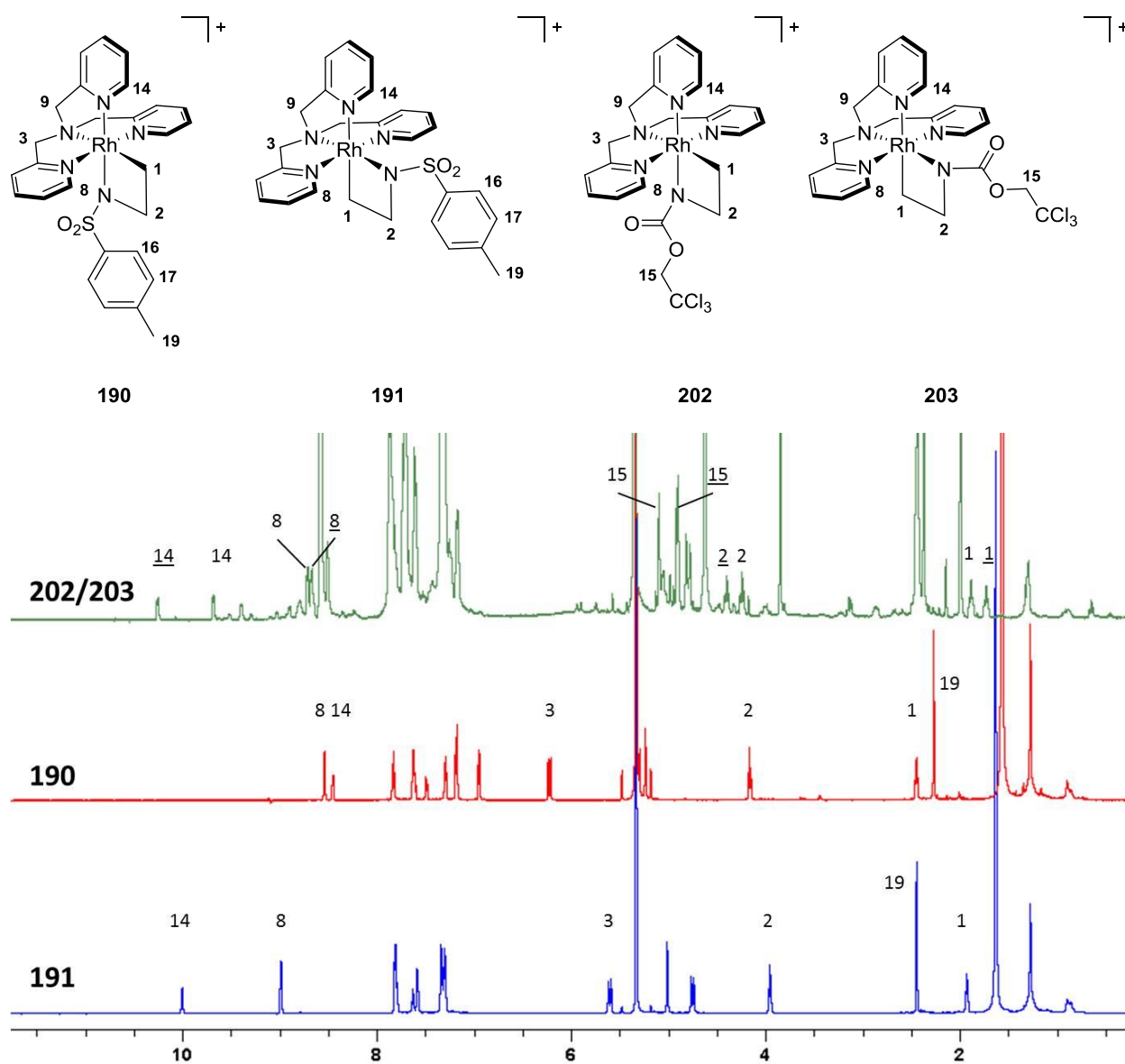
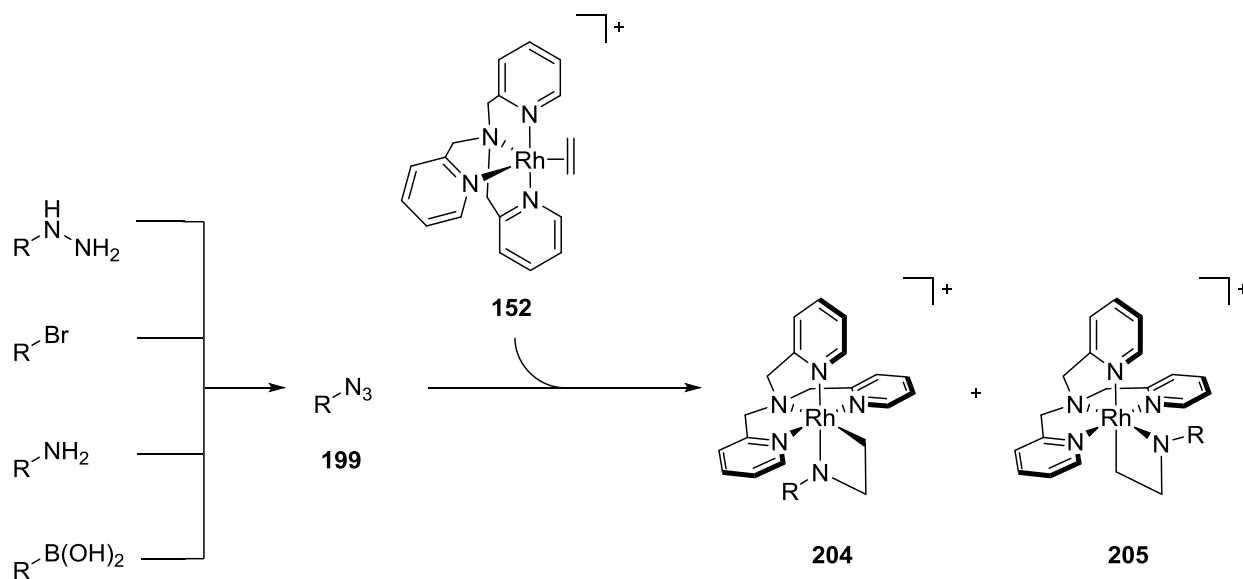


Figure 4.9 Comparison of ^1H NMR spectra of Ts-protected azarhodacyclobutanes **190**, **191** and a mixture of Troc-protected azarhodacyclobutanes **202/203** (600 MHz, CD_2Cl_2 , 298K).

However, detailed NMR spectroscopic studies did not support this assumption. With the aid of COSY and NOESY spectra it was possible to assign a contiguous set of characteristic ^1H NMR signals to each of the isomers present in the mixture. Figure 4.9 shows the ^1H NMR spectrum of a mixture of the isomers in which the signals of one isomer are labelled with underscored numbers and the signals corresponding to the other isomer are labelled with

The fact that we observe sharp ^1H NMR signals without line-broadening for both rotamers indicates that the rotational barrier is sufficiently high at room temperature. Studies have correlated an increase of electron density on the amine with an increased barrier for C–N bond rotation.³¹⁵ This suggests a high electron density on the rhodium center. Furthermore, steric constraints could have an impact on the rotational barrier in **203**.

We had previously shown that toluenesulfonyl azide (**196**) was a suitable oxidant for the selective preparation of tosyl protected azarhodacyclobutane **191** (Chapter 4.2.1). We were interested whether other organic azides would be similarly able to perform oxidation of **152** to azarhodacyclobutanes. Azides can be prepared in a simple manner from hydrazines,³¹⁶ halides,^{317,318} anilines^{318,319} or boronic acids.³²⁰ Thus they would provide a formidable entry into a wide variety of *N*-substituted azarhodacyclobutanes (Scheme 4.6).



R = alkyl, aryl, acyl

Scheme 4.6 Organic azides could act as versatile oxidants for *N*-substituted azarhodacyclobutanes.

We therefore prepared a selection of alkyl, aryl and acyl azides to test them in the oxidation of **152**. Under the standard conditions for the PhINTs based formation of **190** and

191, a solution of **152** in CD₂Cl₂ was treated with one equivalent of azide **206a-f** and the reaction progress was monitored by MS and ¹H NMR spectroscopy (Figure 4.10).

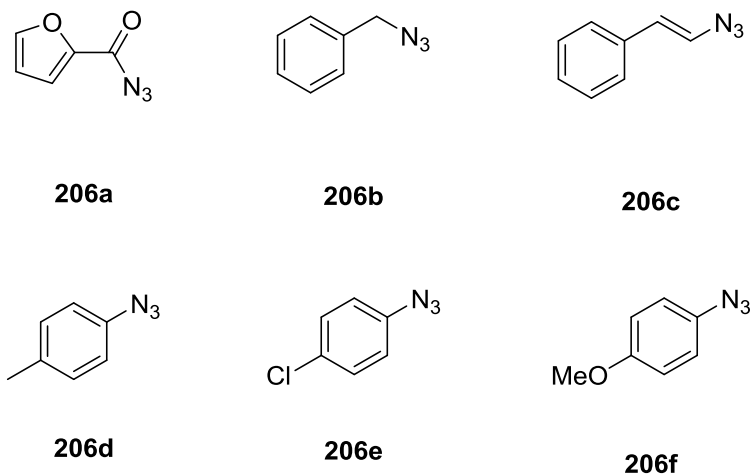
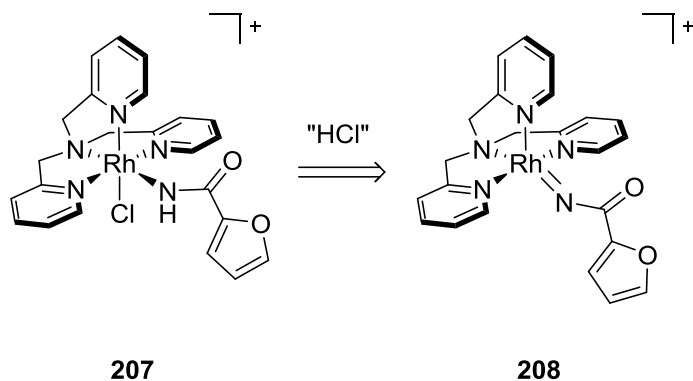


Figure 4.11 A selection of organic azides to test as nitrene precursors.

To our disappointment, in none of the cases the corresponding azarhodacyclobutanes **204** or **205** were detected. In general, a number of unidentified TPA-rhodium complexes were formed. Only when a solution of **152** and **206a** in CD₂Cl₂ was irradiated in a UV reactor at 350nm for 16 hours a major product was formed, which was tentatively assigned to be structure **207** by MS and NMR spectroscopy. Compound **207** is a by-product analogous to **193** which can potentially be derived by quenching of a transient metal imido species, **208** (Scheme 4.7).



In summary, of the alternative nitrene precursors tested, we found that toluenesulfonyl azide, **196** was complementary in its reactivity to PhINTs as nitrene precursor and allowed selective preparation of Ts-protected isomer **191**. The Ns-protected azarhodacyclobutanes **200** and **201** could be prepared in an analogous fashion as in the oxidation with PhINTs. Finally, the carbamate based nitrene precursor **198** furnished the Troc-protected azarhodacyclobutane **203** as the *syn*- and *anti*-rotamers, while the other organic azides employed all failed to produce the corresponding azarhodacyclobutanes. More extensive studies will have to be performed on the latter approach considering its versatility if successful.

4.3 Reactivity of Azarhodacyclobutanes

Having prepared a variety of different *N*-substituted azarhodacyclobutanes, we turned to investigate their reactivity. As mentioned earlier, the Ts-protected azarhodacyclobutanes **190** and **191** did not interconvert, even at elevated temperatures. They generally exhibited remarkable thermal stability. Reflux in acetonitrile or water over 30 minutes returned a mixture of **190** and **191** unchanged (Figure 4.12). Heating in DMSO for prolonged periods of time led to gradual decomposition. The octahedral 18 electron configuration of the complexes along with the rigidity of the TPA ancillary ligand are likely explanations for the observed stability.

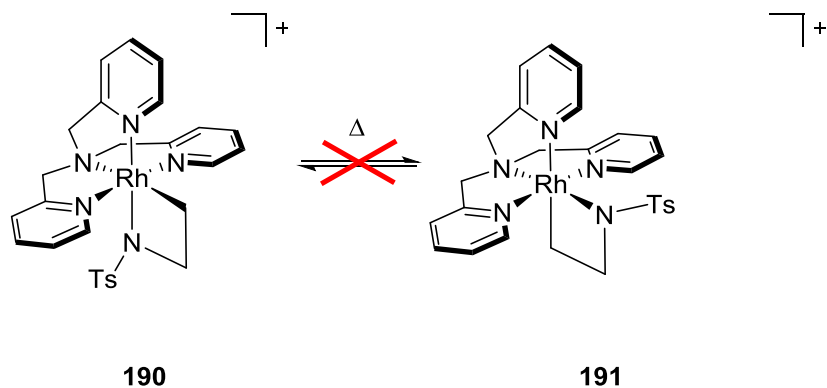
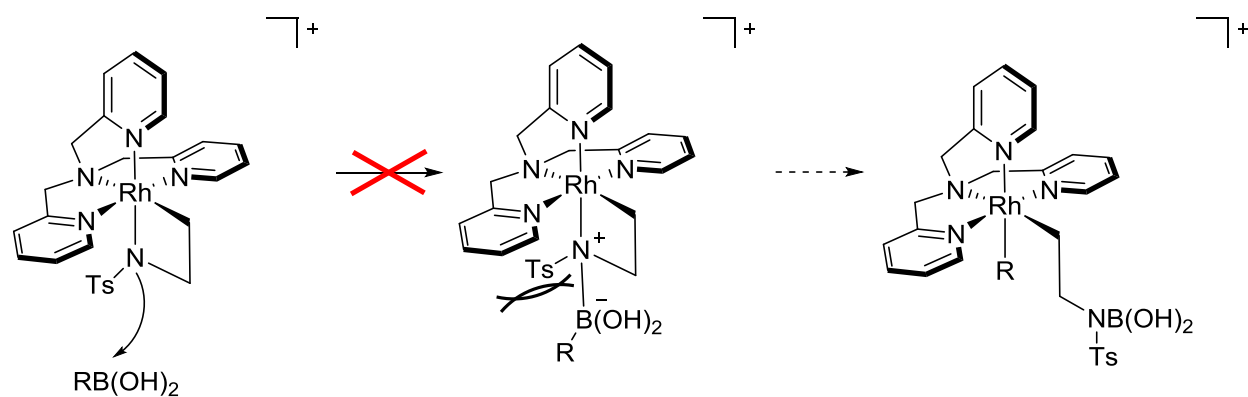


Figure 4.12 Thermal stability of **190** and **191**

We had previously shown that rhodaoxetane **153** could undergo transmetalation with boronic acids and esters (Chapter 2.1.1).²⁵² We anticipated that the azarhodacyclobutanes might exhibit similar reactivity. However, when **190** and **191** were exposed to organoboron reagents, no reaction was observed over the course of one week. This lack of reactivity can be best explained in light of the proposed transmetalation mechanism with oxarhodacyclobutanes. We surmised that the rhodaoxetane oxygen coordinates to the boron to form an “ate” complex prior to transmetalation (Chapter 2.1.2). In case of the azarhodacyclobutanes, coordination would be disfavoured by both the sterics and electronics of the tosyl substituent (Scheme 4.8).



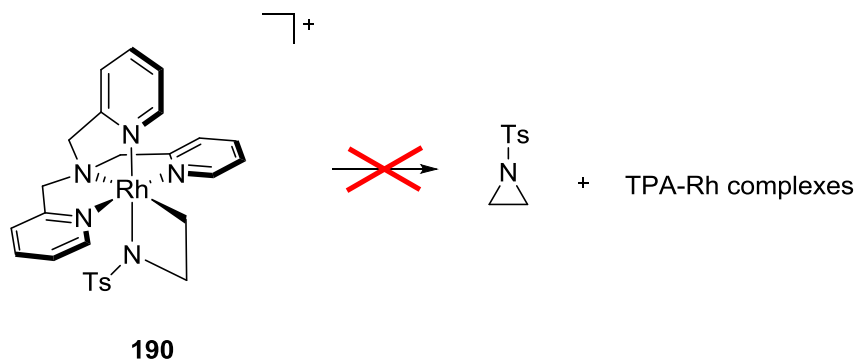
Scheme 4.8 Azarhodacyclobutane **190** is unreactive towards boronic acids.

Likewise, the ability of rhodaoxetane **153** to perform migratory insertion with electron deficient alkynes was demonstrated in Chapter 2.3. When azarhodacyclobutane **190** was exposed to diethylacetylene dicarboxylate under identical conditions, no conversion of the starting material was observed within 1 week. A similar rationale as above for the non-reactivity of **190** due to steric and electronic properties of the tosyl group can be invoked.

An attempt to de-protect **190** and **191** with sodium naphthalenide according to literature procedures³⁰⁶ led to complete decomposition of the azarhodacyclobutanes. We could, therefore, not test this hypothesis any further.

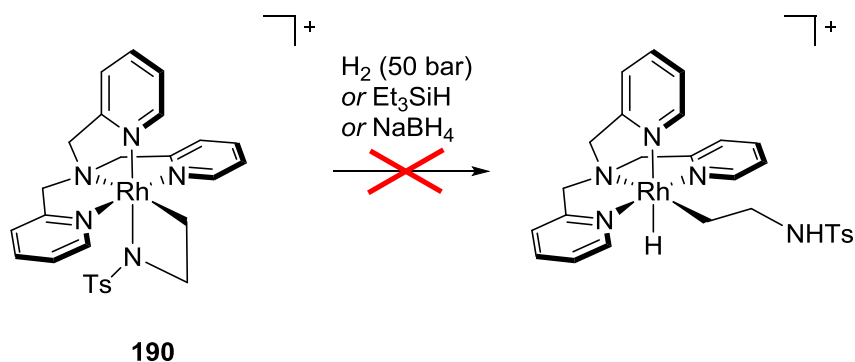
The reductive elimination of aziridines from an intermediate azaferrocyclobutane had been proposed by Halfen and co-workers.²³⁸ In our case, no formation of tosyl-aziridine by C-N reductive elimination from **190** or **191** could be detected (Scheme 4.9). The

formation of a azametallacyclobutanes by insertion of the metal into an aziridine had been reported by different groups.^{206,240,243-245} The extrusion of an aziridine from an azametallacyclobutane by C-N reductive elimination constitutes the microscopic reverse but has to date only been observed after oxidation of the metal center.²⁴⁰



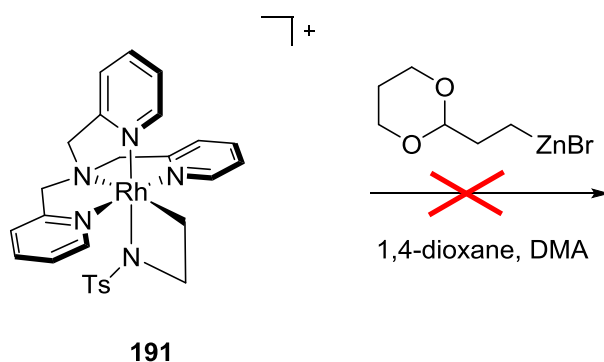
Scheme 4.9 No reductive elimination of aziridines from **190** was observed.

Azametallacyclobutanes had also been proposed as intermediates in the hydroamination of alkynes and alkenes catalyzed by early transition metal imido species (Chapter 1.3.1.2).^{215,220,222-231} We were thus interested to explore the possibility to reductively open azarhodacyclobutanes **190** and **191**. Various reducing agents were employed including dihydrogen (1, 4, 50 bar, MeOH, r.t.), triethylhydrosilane (1.5 equiv., CD₂Cl₂, r.t.) and sodium borohydride (4 equiv., MeOD, r.t.) but no reactivity was observed under the applied conditions and the azahodacyclobutane remained unchanged (Scheme 4.10).



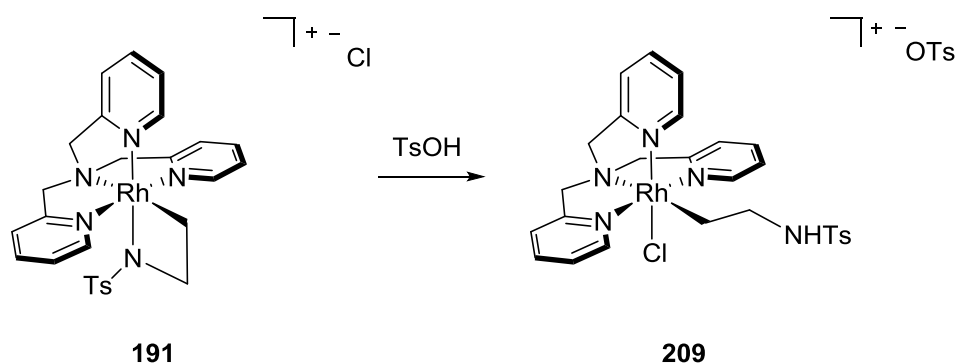
Scheme 4.10 Lack of reactivity of **190** towards reducing agents.

Recently, an azanickelacyclobutane was found to be an intermediate in the Ni catalyzed coupling of aziridines with organozinc halides.²⁴⁵ A direct transmetalation from the zinc reagent to the azanickelacyclobutane was demonstrated which prompted us to test organozinc halides as reaction partners for azarhodacyclobutanes. However, under otherwise identical conditions as reported in the literature, the starting material remained unchanged for 2 days after which decomposition to unidentified products occurred (Scheme 4.11).



Scheme 4.11 No transmetalation with organozinc halides.

De Bruin *et al.* had reported the protonation and subsequent ring opening of rhodaoxetane **153** when treated with acids.¹⁸⁷ We anticipated that **209** could be generated from **190** in the presence of acid (Scheme 4.12). Indeed, treatment of **190**.Cl with toluenesulfonic acid led to the quantitative formation of a new product. In analogy to the reported reactivity of oxarhodacyclobutanes, we propose that this ring opening occurs after protonation of the ring nitrogen and following displacement by a chloride ligand. The shift of H1 and H2 in the ¹H NMR spectrum was indicative of ring opening. In addition, the mass spectrum showed a dominant signal at 626 m/z with a characteristic chloride isotope pattern. Treatment of **190**.PF₆ with toluenesulfonic acid in the absence of a strongly coordinating counterion (such as Cl⁻) did not lead to ring opening, but allowed recovery of the azametallacyclobutane.



Scheme 4.12 Acidic ring opening of **191**.

This ring opening was also observed with the Troc-protected azarhodacyclobutane **203**. Indeed, in the formation of **203**, the ring-opened product was a commonly observed by-product which could not be entirely suppressed, even in the presence of pyridine as acid scavenger.

Deprotection and extensive reactivity studies of the Ns-protected azarhodacyclobutanes **201** and **202** as well as Troc-protected **203** will yet have to be undertaken and will hopefully show a more diverse reactivity than **190** and **191**.

4.4 Experimental

4.4.1 General Information

All experiments were carried out under standard Schlenk techniques under an atmosphere of dry nitrogen employing degassed solvents unless stated otherwise. All reagents were used as received without further purification. Room temperature corresponds to $\sim 20^\circ\text{C}$. NMR spectra were recorded on Bruker Avance 300, 400 and 600 MHz spectrometers. ^1H NMR spectra are reported in parts per million and were referenced to residual solvent (5.32 ppm for CD_2Cl_2 , 3.31 for MeOD). ^{13}C NMR spectra were performed as proton decoupled experiments with spin echo and are reported in parts per million, referenced to residual solvent (53.84 ppm for CD_2Cl_2 , 49.00 for MeOD). ^{15}N NMR spectra (long range ^1H - ^{15}N HMQC and ^1H - ^{15}N HSQC) were referenced to CH_3NO_2 at 0 ppm (IUPAC recommended standard) as well as pyridine at 0 ppm for better comparison with literature reports.³⁰⁵ The coupling constant for long range $^lJ_{(\text{H}-\text{N})}$ coupling was set to 10 Hz in the ^1H -

^{15}N HMQC and ^1H - ^{15}N HSQC experiments. For determination of the $^2J_{(\text{Rh-N})}$ coupling constant by ^1H - ^{15}N HSQC the FID resolution was increased to 1.2 Hz by reducing the width of the spectral window to 10 ppm and increasing the TD value in the F1 domain to 512. The multiplicities are abbreviated as follows: s = singlet, d = doublet, d[AB] = doublet in an AB system, dt = doublet of triplets, t = triplet, m = multiplet) MS-data was obtained on a Waters LC/MS for low resolution and Waters/Micromass LCT for high resolution spectra.

HPLC was performed on a Varian ProStar system with a Varian ProStar 325 UV detector and a Varian 1200L triple quadrupole mass spectrometer for parallel UV (254nm) and MS detection. A double end-capped Varian Intertsil ODS (C18) column (150x4.6mm) was employed for separation. The solvent gradient used for successful separation of **190** and **191** was H_2O /acetonitrile 98/2 – 70/30 over 10 minutes then isocratic at 10/90 over 2 minutes at a flow rate of 2mL/min. A 4/1 post-column splitter was installed and UV/MS parallel detection was performed. The UV detector was set to 254nm. The MS was filtered for $m/z = 590$ in Q1. Retention times given refer to the apex of the peak.

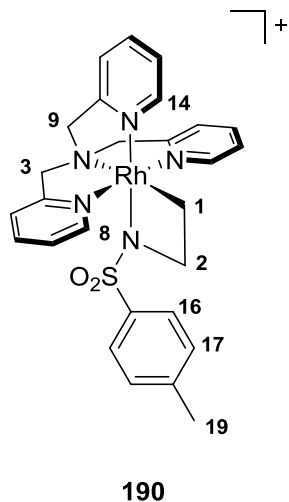
NMR yields were obtained by referencing 2 or 3 well isolated signals of the desired product to the aryl-proton signals of 1,3,5-trimethoxybenzene (TMB, 99+% purity, Sigma Aldrich) or tetramethylsilane (TMS, 99.9% purity, Alfa Aesar). TMB was added as 1/3 equivalent of starting material (standard solution: 48mg/mL; $\delta = 6.08$ ppm in CD_2Cl_2). TMS was added as 1/12 equivalent of starting material. Quantitative ^1H -NMR was performed with a calibrated 30 degree P1 pulse and delay + acquisition time being a minimum of $5 * T_1$ of the slowest relaxing product signal. Yields are averaged over a minimum of two experiments.

4.4.2 Experimental Procedures

TPA (*N,N,N* trispyridylmethyl amine) was prepared according to a literature procedure²⁸⁷ and purified by recrystallization from boiling hexanes to give bright yellow needles. The nitrene precursors [*N*-(4-toluenesulfonyl)imino]phenyliodinane (PhINTs),³⁰³ 4-toluenesulfonyl azide (TsN_3), **196**,³⁰⁷ [*N*-(4-nitrophenylsulfonyl)imino]phenyliodinane (PhINNs), **197**,³⁰⁹ and 2,2,2-trichloroethyl-*N*-tosyloxycarbamate (TrocNHOTs), **198**,³¹¹ were prepared according to literature procedures. Chloramine-T trihydrate was purchased from Sigma Aldrich and used as received. The azides **206a** and **206b** were prepared from the

corresponding halides according to a literature procedure.³¹⁷ The azides **206c-f** were prepared from the corresponding boronic acids according to a literature procedure.³²⁰

4.4.2.1 Preparation of TPA-Azarhodacyclobutane **190.PF₆** (Isolable Scale) in CH₃OH



[RhCl(C₂H₄)₂]₂ (50 mg, 0.13 mmol, Alfa Aesar) and TPA (75 mg, 0.26 mmol) were weighed into a flame-dried 8 mL reaction vial equipped with a stir bar and a screw cap with a PTFE septum. The vial was sealed with a septum and brought out of the drybox. Dry, degassed methanol (5 mL) was added via syringe and the resulting solution was stirred at -78 °C for one hour. The flask was taken out of the dry ice/acetone bath and let warm to room temperature. PhINTs (47 mg, 0.26 mmol) was added to the reaction mixture through a powder funnel. The reaction mixture darkened within minutes from a dark green to a deep rust-coloured, almost black, solution. After stirring for 2 h, the solution was filtered through glass-wool into a flask containing KPF₆ (51 mg, 0.26 mmol, 99.9% purity, Sigma Aldrich). Hexanes (40mL) was added and the solution cooled until a yellow-green precipitate formed which was filtered, washed twice with cold hexane and then dried. The isolated crude yield was 89 mg (47%).

HPLC separation allowed for isolation of **190.PF₆** in an overall yield of 9 mg (5%) after repeated injections as collected from the UV detector.

NOTE: the preparation could also be performed completely under “bench top conditions” with minimal effect on the yield and purity of the product.

^1H NMR (CD_2Cl_2 , 600 MHz, 298K): δ 8.55 (d, 2H, $^3J_{\text{H,H}} = 5.4$ Hz, H8), 8.47 (d, 1H, $^3J_{\text{H,H}} = 7.7$ Hz, H14), 7.84 (apparent t, 2H, $^3J_{\text{H,H}} = 7.7$ Hz, 6.3 Hz, H6), 7.62 (t, apparent t, 2H, $^3J_{\text{H,H}} = 8.0$ Hz, 6.7 Hz, H12), 7.54 (d, 2H, $^3J_{\text{H,H}} = 7.7$ Hz, H5), 7.32 (apparent t, 2H, $^3J_{\text{H,H}} = 6.3$ Hz, 5.7 Hz, H7), 7.26-7.14 (m, 4H, H11, H13, H16), 6.95 (d, 2H, $^3J_{\text{H,H}} = 7.7$ Hz, H17), 6.29 (d[AB], 2H, $^2J_{\text{H,H}} = 15.4$ Hz, H3ax), 4.94 (d[AB], 2H, $^2J_{\text{H,H}} = 15.4$ Hz, H3eq), 4.82 (s, 2H, H9), 4.13 (t, 2H, $^3J_{\text{H,H}} = 7.8$ Hz, H2), 2.48 (dt, 2H, $^3J_{\text{H,H}} = 7.8$ Hz, $^2J_{\text{Rh,H}} = 2.0$ Hz, H1), 2.26 (s, 3H, H19).

^{13}C NMR (CD_2Cl_2 , 150 MHz, 298 K): δ 166.3 (C4), 163.3 (C10), 150.5 (C8), 149.6 (C14), 140.9 (C15), 140.3 (C18), 139.3 (C6), 138.8 (C12), 129.2 (C17), 126.4 (C16), 125.5 (C7), 125.0 (C5, C13), 123.1 (C11), 66.5 (C3), 66.2 (C9), 58.2 (C2), 21.3 (C19), 8.1 (d, $^2J(\text{Rh-C}) = 18.4$ Hz, C1).

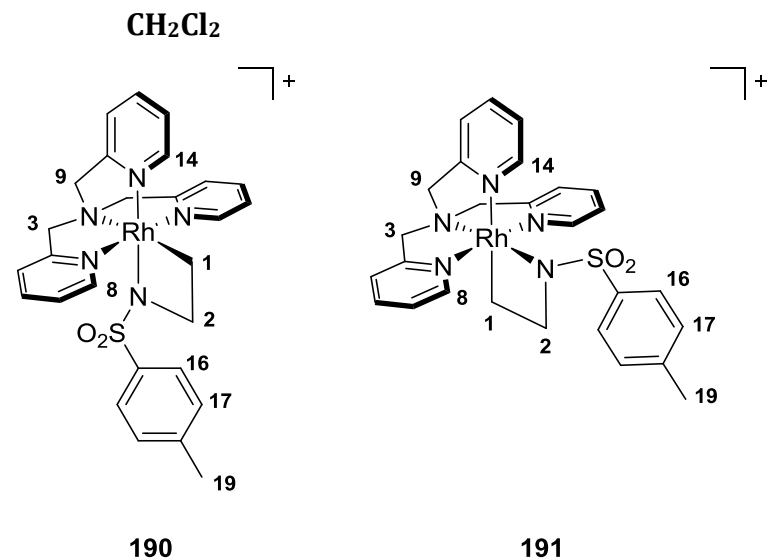
HRMS: Calcd: 590.1097 ($\text{C}_{27}\text{H}_{29}\text{N}_5\text{O}_2\text{SRh}^+$). Found: 590.1091

ESI-MS negative mode: 145 (PF_6^-)

Elem. anal. calc. for $\text{C}_{27}\text{H}_{29}\text{N}_5\text{O}_2\text{SRh}^+\text{PF}_6^-$: C 44.09%, H 3.97%, N 9.52%; found: C 43.36%, H 4.13%, N 9.47%

Note: The elemental analysis results reported above do not fully meet the criteria for a pass. The found value for carbon is slightly too low (tolerance $\pm 0.4\%$)

4.4.2.2 Preparation of TPA-Azarhodacyclobutane 190.Cl and 191.Cl (Isolable Scale) in



$[\text{RhCl}(\text{C}_2\text{H}_4)_2]_2$ (100 mg, 0.257 mmol, Alfa Aesar) was weighed into a flame-dried 25 mL Schlenk flask equipped with a stir bar. The flask was fitted with a Teflon septum and put

under an N₂ atmosphere. Dry, degassed methylene chloride (5 mL) was added via syringe and the resulting solution was stirred and cooled to -78 °C. While the solution was cooling, TPA (150 mg, 0.516 mmol) was weighed into a 20 mL scintillation vial in a N₂ filled drybox. The vial was sealed with a septum and brought out of the drybox. Dry, degassed methylene chloride (5 mL) was used to transfer the TPA solution into the cooled Rh-dimer solution by dropwise addition with a syringe. The resulting mixture was left stirring at -78 °C for one hour. The flask was taken out of the dry ice/acetone bath and let warm to room temperature. PhINTs (180 mg, 1.029 mmol) was added to the reaction mixture through a powder funnel against a counter-flow of N₂. The reaction mixture darkened within minutes from a light olive-green to a deep rust-coloured, almost black, solution. After stirring for 2 h the volatiles were removed *in vacuo* to give a dark grey-green powder. The isolated crude yield was 221mg (58%).

For purification the product was dissolved in 5mL CH₂Cl₂ and extracted twice with 2mL deionized H₂O. Both, the organic and the aqueous phase contained notable amounts of **190** and **191**. HPLC separation of the organic phase allowed for base-line separation of the two isomers. **190** (6:55 min) and **191** (8:40 min) could be isolated as pure compounds in small quantities after repeated injections as collected from the UV detector.

NOTE: the preparation could also be performed under “bench top conditions” with minimal effect on the yield and purity of the product.

190, ¹H NMR (CD₂Cl₂, 600 MHz, 298K): δ 8.54 (d, 2H, ³J_{H,H} = 5.4 Hz, H8), 8.45 (d, 1H, ³J_{H,H} = 7.7 Hz, H14), 7.83 (apparent t, 2H, ³J_{H,H} = 7.7 Hz, 6.3 Hz, H6), 7.65-7.58 (m, 3H, H5, H12), 7.49 (d, 1H, ³J_{H,H} = 7.7 Hz, H11), 7.29 (apparent t, 2H, ³J_{H,H} = 6.3 Hz, 5.7 Hz, H7), 7.20-7.15 (m, 3H, H13, H16), 6.95 (d, 2H, ³J_{H,H} = 7.7 Hz, H17), 6.22 (d[AB], 2H, ²J_{H,H} = 15.3 Hz, H3ax), 5.41 (d[AB], 2H, ²J_{H,H} = 15.3 Hz, H3eq), 5.30 (s, 2H, H9), 4.16 (t, 2H, ³J_{H,H} = 7.8 Hz, H2), 2.44 (dt, 2H, ³J_{H,H} = 7.8 Hz, ²J_{Rh,H} = 2.0 Hz, H1), 2.27 (s, 3H, H19).

¹³C NMR (CD₂Cl₂, 150 MHz, 298 K): δ 166.3 (C4), 163.3 (C10), 150.5 (C8), 149.6 (C14), 140.9 (C15), 140.3 (C18), 139.3 (C6), 138.8 (C12), 129.2 (C17), 126.4 (C16), 125.5 (C7), 125.0 (C5, C13), 123.1 (C11), 66.5 (C3), 66.2 (C9), 58.2 (C2), 21.3 (C19), 8.1 (d, ²J(Rh-C) = 18.4 Hz, C1).

^{15}N chemical shifts extracted from $^1\text{H}/^{15}\text{N}$ HMQC and $^1\text{H}-^{15}\text{N}$ HSQC (CD_2Cl_2 , 600 MHz, 298 K, referenced to CH_3NO_2 at 0 ppm): δ -155, -156, -338, -379 (d, $J_{(\text{Rh}-\text{N})} = 14$ Hz); referenced to pyridine at 0 ppm: δ 112, 111, -71, -113

HRMS: Calcd: 590.1097 ($\text{C}_{27}\text{H}_{29}\text{N}_5\text{O}_2\text{SRh}^+$). Found: 590.1092

191, ^1H NMR (CD_2Cl_2 , 600MHz, 298K): δ 10.01 (d, 1H, $^3J_{\text{H,H}} = 5.3$ Hz, H14), 8.99 (d, 2H, $^3J_{\text{H,H}} = 5.1$ Hz, H8), 7.85-7.76 (m, 4H, H5, H6), 7.63 (dd, 1H, $^3J_{\text{H,H}} = 7.6$ Hz, 5.5 Hz, H12), 7.58 (d, 2H, $^3J_{\text{H,H}} = 7.5$ Hz, H16), 7.37-7.26 (m, 6H, H7, H11, H13, H17), 5.60 (d[AB], 2H, $^2J_{\text{H,H}} = 15.5$ Hz, H3eq), 5.01 (s, 2H, H9), 4.75 (d[AB], 2H, $^2J_{\text{H,H}} = 15.5$ Hz, H3ax), 3.95 (t, 2H, $^3J_{\text{H,H}} = 6.9$ Hz, H2), 2.44 (s, 3H, H19), 1.92 (dt, 2H, $^3J_{\text{H,H}} = 6.9$ Hz, $^2J_{\text{Rh,H}} = 1.7$ Hz, H1).

^{13}C NMR (CD_2Cl_2 , 150 MHz, 298 K): δ 161.9 (C4), 157.2 (C10), 153.8 (C8), 152.6 (C14), 141.8 (C15), 140.9 (C18), 139.2 (C6), 138.8 (C12), 129.8 (C7), 126.8 (C5), 125.9 (C17), 125.5 (C13), 123.7 (C16), 121.4 (C11), 70.1 (C3), 69.3 (C9), 58.0 (C2), 21.4 (C19), 1.6 (d, $^2J_{(\text{Rh}-\text{C})} = 16$ Hz, C1).

^{15}N chemical shifts extracted from $^1\text{H}/^{15}\text{N}$ HMQC (CD_2Cl_2 , 600 MHz, 298 K, referenced to CH_3NO_2 at 0 ppm): δ -114, -145, -350, -370; referenced to pyridine at 0 ppm: δ 152, 121, -84, -104.

HRMS: Calcd: 590.1097 ($\text{C}_{27}\text{H}_{29}\text{N}_5\text{O}_2\text{SRh}^+$). Found: 590.1102.

4.4.2.3 General Procedure for preparation of TPA-azarhodacyclobutane 190.Cl and 191.Cl in different solvents (NMR scale)

$[\text{RhCl}(\text{C}_2\text{H}_4)_2]_2$ (100 mg, 0.257 mmol, Alfa Aesar) was weighed into a flame-dried 25 mL Schlenk flask equipped with a stir bar. The flask was fitted with a Teflon septum and put under an N_2 atmosphere. Dry, degassed methylene chloride (5.0 mL) was added via syringe and the resulting solution was stirred and cooled to -78°C . While the solution was cooling, TPA (150 mg, 0.516 mmol) was weighed into a 20 mL scintillation vial in a N_2 filled drybox. The vial was sealed with a septum and brought out of the drybox. Dry, degassed methylene chloride (5.0 mL) was used to transfer the TPA solution into the cooled Rh-dimer solution by dropwise addition with a syringe. The resulting mixture was left stirring at -78°C for one hour. The flask was taken out of the dry ice/acetone bath and let warm to room temperature.

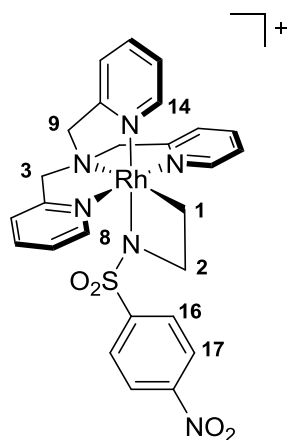
This solution was transferred in 1 mL portions into 6 different reaction vials each fitted with stir bars and fitted with a screwcap with a PTFE septum. The solvent was removed on high vacuum under stirring and the residue was taken up in the deuterated solvent of interest (CD_2Cl_2 , CDCl_3 , CD_3OD , CD_3CN , $(\text{CD}_3)_2\text{CO}$, D_2O).

PhINTs (9 mg, 0.0516 mmol) was added and the reaction mixture was stirred at room temperature for 8 hours. The mixture was filtered through glass wool and HPLC-MS analysis was performed to find the ratio of **190:191**.

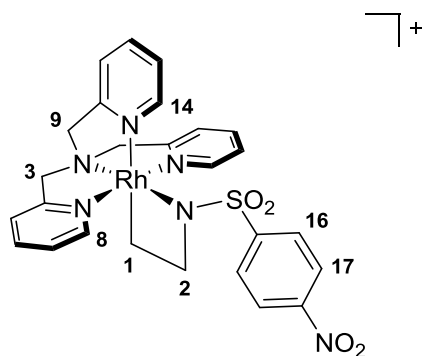
4.4.2.4 General NMR-Scale Procedure for Preparation of TPA-Azarhodacyclobutanes 190, 191, 200, 201 and 203

In a N_2 filled drybox, an NMR tube was charged with $[\text{RhCl}(\text{C}_2\text{H}_4)_2]_2$ (10 mg, 0.0257 mmol, Alfa Aesar). The tube was fitted with a screwcap with a PTFE septum and brought out of the drybox. Dry, degassed d_2 -methylene chloride (0.30 mL) was added via syringe and the resulting solution was stirred and cooled to $-78\text{ }^\circ\text{C}$. While the solution was cooling, TPA (15 mg, 0.0516 mmol) was weighed into a 5 mL vial in the drybox. The vial was sealed with a septum and brought out of the drybox. Dry, degassed d_2 -methylene chloride (0.30 mL) was used to transfer the TPA solution into the cooled Rh-dimer solution by dropwise addition with a syringe. With a microsyringe 2,4,6-trimethoxybenzene solution or tetramethylsilane as internal standard was added. After one hour the solution was allowed to warm to room temperature. One equivalent of the nitrene precursor (0.0516 mmol) was added, the tube was inverted several times and let stand at room temperature for 8 hours.

The following spectral data are in part extracted from crude mixtures and are partly incomplete or over-integrate due to overlapping signals.



200

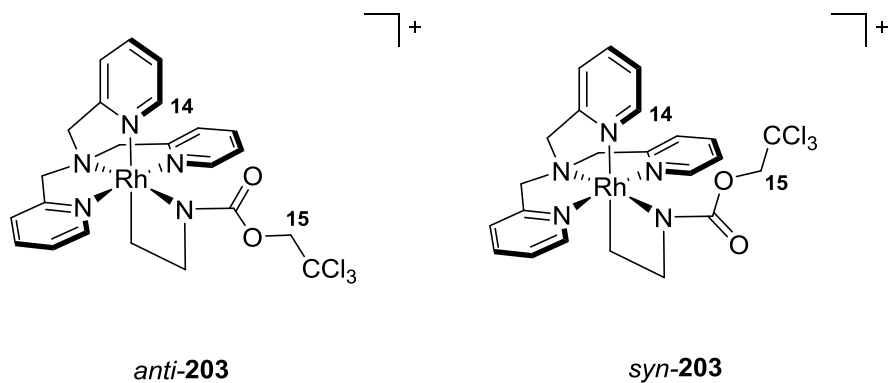


201

200, ^1H NMR (CD_2Cl_2 , 600 MHz, 298K): δ 8.52 (d, 2H, $^3J_{\text{H,H}} = 5.6$ Hz, H8), 8.43 (d, 1H, $^3J_{\text{H,H}} = 5.6$ Hz, H14), 8.21-8.15 (m, 1H), 7.95 (d, 2H, $^3J_{\text{H,H}} = 8.3$ Hz), 7.85 (d, 2H, $^3J_{\text{H,H}} = 7.6$ Hz), 7.66 (d, 2H, $^3J_{\text{H,H}} = 7.6$ Hz), 7.60 (t, 1H, $^3J_{\text{H,H}} = 6.9$ Hz), 7.43 (d, 2H, $^3J_{\text{H,H}} = 8.7$ Hz), 7.29 (t, 2H, $^3J_{\text{H,H}} = 6.6$ Hz), 7.18 (t, 1H, $^3J_{\text{H,H}} = 6.6$ Hz), 6.15 (d[AB], 2H, $^2J_{\text{H,H}} = 15.3$ Hz, H3ax), 4.21 (t, 2H, $^3J_{\text{H,H}} = 7.7$ Hz, H2), 2.48 (dt, 2H, $^3J_{\text{H,H}} = 7.9$ Hz, $^2J_{\text{Rh,H}} = 2.2$ Hz, H1).

^{13}C NMR (CD_2Cl_2 , 150 MHz, 298 K): δ 165.9, 150.4, 149.5, 139.4, 138.7, 127.2, 125.4, 125.0, 124.9, 123.7, 123.2, 122.8, 66.4 (C3), 66.0 (C9), 58.0 (d, $^3J_{\text{Rh,H}} = 4$ Hz, C2), 8.2 (d, $^2J_{\text{Rh,H}} = 18$ Hz, C1).

201, ^1H NMR (CD_2Cl_2 , 400MHz, 298K): δ 9.94 (d, 1H, $^3J_{\text{H,H}} = 6.0$ Hz, H14), 8.95 (d, 2H, $^3J_{\text{H,H}} = 5.4$ Hz, H8), 8.41-7.20 (m, H_{Aryl}), 5.16 (d[AB], 2H, $^2J_{\text{H,H}} = 15.3$ Hz, H3eq), 4.84-4.71 (m, 4H, H3ax + H9), 4.03 (t, 2H, $^3J_{\text{H,H}} = 7.8$ Hz, H2), 2.02-1.93 (m, 2H, H1).



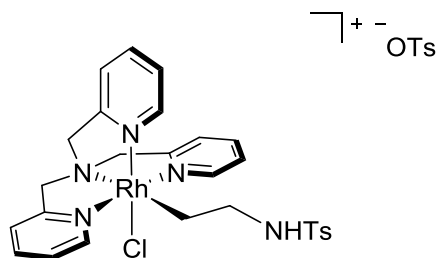
anti-203, ^1H NMR (CD_2Cl_2 , 400MHz, 298K): δ 10.27 (d, 1H, $^3J_{\text{H,H}} = 5.5$ Hz, H14), 8.68 (d, 2H, $^3J_{\text{H,H}} = 5.7$ Hz, H8), 4.88 (s, 2H, H15), 4.40 (t, 2H, $^3J_{\text{H,H}} = 7.8$ Hz, H2), 1.74 (dt, 2H, $^3J_{\text{H,H}} = 5.3$ Hz, $^2J_{\text{Rh,H}} = 2.5$ Hz, H1).

^{13}C NMR (CD_2Cl_2 , 100 MHz, 298 K): δ 153.1 (C14), 152.3 (C8), 74.7 (C15), 57.5 (d, $^3J_{\text{Rh,H}} = 4$ Hz, C2), 0.3 (d, $^2J_{\text{Rh,H}} = 16.5$ Hz, C1).

syn-203, ^1H NMR (CD_2Cl_2 , 400MHz, 298K): δ 9.69 (d, 1H, $^3J_{\text{H,H}} = 5.2$ Hz, H14), 8.72 (d, 2H, $^3J_{\text{H,H}} = 6.6$ Hz, H8), 5.06 (s, 2H, H15), 4.24 (t, 2H, $^3J_{\text{H,H}} = 7.7$ Hz, H2), 1.89 (dt, 2H, $^3J_{\text{H,H}} = 6.0$ Hz, $^2J_{\text{Rh,H}} = 2.1$ Hz, H1).

^{13}C NMR (CD_2Cl_2 , 100 MHz, 298 K): δ 151.6 (C14), 150.6 (C8), 75.3 (C15), 58.2 (d, $^3J_{\text{Rh,H}} = 4.2$ Hz, C2), 2.9 (d, $^2J_{\text{Rh,H}} = 16.5$ Hz, C1).

4.4.2.5 Reaction of 190.Cl with Toluenesulfonic Acid; Preparation of 209



209

190.Cl (4 mg, 0.006 mmol) was dissolved in 0.5 mL CD_2Cl_2 and placed in an NMR tube. Toluenesulfonic acid (2 mg, 0.012 mmol) was added and the tube was sealed and inverted multiple times. The reaction progress was monitored via ^1H NMR spectroscopy and it was

found that the reaction was complete after 2 hours at room temperature. The following data are from the crude reaction mixture of **209**:

^1H NMR (CD_2Cl_2 , 600MHz, 298K): δ 8.51 (d, 1H, $^3\text{J}(\text{H,H}) = 5.9$ Hz), 8.47 (d, 2H, $^3\text{J}(\text{H,H}) = 5.6$ Hz), 7.77-6.67 (m, 2H, partly overlapped by residual TsOH), 7.59 (t, 1H, $^3\text{J}(\text{H,H}) = 7.5$ Hz), 7.53 (d, 2H, $^3\text{J}(\text{H,H}) = 7.7$ Hz), 7.38 (d, 1H, $^3\text{J}(\text{H,H}) = 7.4$ Hz), 7.34-7.20 (m, 5H), 7.19-7.14 (m, 2H), 5.59 (d[AB], 2H, $^2\text{J}(\text{H,H}) = 15.3$ Hz), 5.35-5.27 (m, 4H, partly overlapped by CHDCl_2), 3.42 (t, 2H, $^3\text{J}(\text{H,H}) = 6.3$ Hz), 3.13 (dt, 2H, $^3\text{J}(\text{H,H}) = 6.2$ Hz, $^2\text{J}(\text{Rh,H}) = 1.9$ Hz), 2.38 (s, 3H).

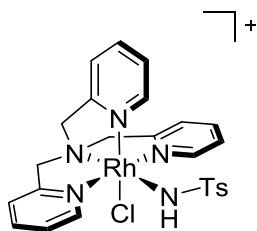
^{13}C NMR (CD_2Cl_2 , 150 MHz, 298 K): δ 165.7, 165.3, 150.9, 148.3, 139.6, 139.3, 129.9, 129.0, 125.5, 125.3, 124.9, 123.2, 66.9, 66.1, 47.7, 32.5 (d, $^2\text{J}(\text{Rh,C}) = 25.3$ Hz), 21.6.

ESI-MS: 626/628 (M^+ , 3/1 intensity \rightarrow $^{35}\text{Cl}/^{37}\text{Cl}$ isotope pattern).

4.4.3 Identification of By-Products

Formation and characterization of by-product **192** has been reported before by De Bruin.¹⁸⁷ Two further by-products of the reaction could be isolated and investigated by NMR spectroscopy and mass spectrometry.

4.4.3.1 [TPA-Rh(Cl)(NHTs)]PF₆, **193**



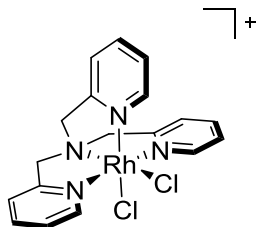
193

^1H NMR (CD_2Cl_2 , 600MHz, 298K): δ 9.40 (d, 1H, $^3\text{J}(\text{H,H}) = 5.9$ Hz), 8.58 (d, 2H, $^3\text{J}(\text{H,H}) = 5.4$ Hz), 7.89 (t, 2H, $^3\text{J}(\text{H,H}) = 7.9$ Hz), 7.74 (t, 1H, $^3\text{J}(\text{H,H}) = 7.6$ Hz), 7.58 (d, 2H, $^3\text{J}(\text{H,H}) = 7.9$ Hz), 7.39-7.30 (m, 2H), 7.27-7.19 (m, 4H), 7.05 (d, 2H, $^3\text{J}(\text{H,H}) = 7.9$ Hz), 6.25 (d[AB], 2H, $^2\text{J}(\text{H-H}) = 15.2$ Hz), 4.99 (s, 2H), 4.87 (d[AB], 2H, $^2\text{J}(\text{H-H}) = 15.2$ Hz), 3.12 (s, 1H), 2.37 (s, 3H).

^{13}C NMR (CD_2Cl_2 , 150 MHz, 298 K): δ 165.7, 163.8, 151.9, 150.7, 140.7, 140.5, 129.1, 126.6, 126.0, 125.9, 124.5, 122.2, 71.2, 69.6, 21.5.

ESI-MS: positive: 598/600 (M^+ , 3/1 intensity \rightarrow $^{35}\text{Cl}/^{37}\text{Cl}$ isotope pattern); negative: 145 (PF_6).

4.4.3.2 [TPA-Rh(Cl)₂]Cl, 194



194

^1H NMR (CD_2Cl_2 , 600MHz, 298K): δ 9.60 (d, 1H, $^3J(\text{H,H}) = 5.9$ Hz), 8.98 (d, 2H, $^3J(\text{H,H}) = 5.6$ Hz), 7.93 (dt, 2H, $^3J(\text{H,H}) = 7.7$ Hz, $^4J(\text{H,H}) = 0.9$ Hz), 7.79 (t, 1H, $^3J(\text{H,H}) = 7.8$ Hz), 7.69 (d, 2H, $^3J(\text{H,H}) = 7.8$ Hz), 7.48-7.40 (m, 4H).

^{13}C NMR (CD_2Cl_2 , 150 MHz, 298 K): δ 162.5, 161.8, 150.9, 149.2, 139.8, 139.6, 125.4, 125.1, 123.8, 121.4, 70.2, 69.4.

ESI-MS: 463/465/467 (M^+ , 9/6/1 intensity \rightarrow $^{35}\text{Cl}/^{37}\text{Cl}$ isotope pattern).

5 Formation of Substituted Azarhodacyclobutanes

After the successful formation of unsubstituted azarhodacyclobutanes through oxidation of Rh-ethylene complexes by various nitrogen-based oxidants, we set out to explore whether substituted azarhodacyclobutanes could be accessed in a similar fashion as we have demonstrated before in the formation of substituted rhodaoxetanes (Chapter 3). This chapter will describe our efforts towards this end. The preparation of the substituted TPA-Rh-olefin complexes **179** and **180** has already been described in chapter 3. However, as the steric properties of the ligand had a substantial effect on the selectivity in the formation of substituted azarhodacyclobutanes, this chapter will begin by presenting the preparation of the related MeTPA-Rh-olefin complexes. Next, the oxidation with PhINTs will be showcased followed by a brief discussion of the observed reactivity of the resulting substituted azarhodacyclobutanes.

As mentioned in the introduction to Chapter 3, Carla Rigling has contributed to this part of the project by investigating the oxidation of the substituted TPA-olefin complexes with PhINTs. In combination with results presented in Chapter 3 parts of the work in this chapter have been submitted as a full article. The results disclosed here are extended in scope and discussion compared to the submitted data.

5.1 Preparation of MeTPA-Rhodium Complexes with Substituted Olefins

In the preparation of TPA-Rh complexes with substituted olefins **179** and **180**, we had noted a preference for the formation of isomer **179** in which the olefin substituent was oriented away from the central pyridyl arm of the TPA ligand (Chapter 3.1). It seemed obvious to invoke steric factors for this preference. We anticipated that a more sterically demanding ligand, e.g. MeTPA, **160** (Chapter 2.2.3.2), would favour the orientation of the olefin substituent away from the bulky ligand to an even greater degree, thereby increasing the ratio of olefin isomers. To test this hypothesis, we prepared complex **210**, bearing MeTPA and added styrene derivatives **178g-l** in a method identical to that for formation of complexes **179** and **180** (Chapter 3.1). This resulted in the formation of **211** and **212**, in varying ratios depending on the olefin (Table 5.1).

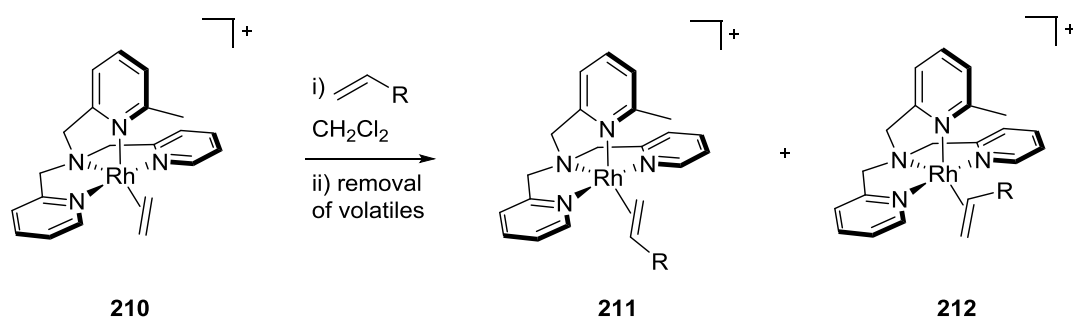
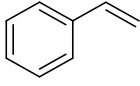
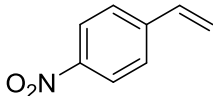
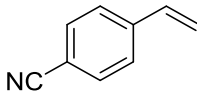
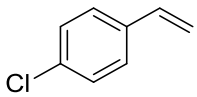
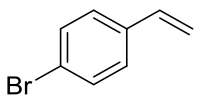
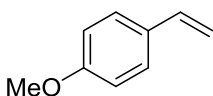


Table 5.1 Olefin exchange with MeTPA complex **210**.

Entry ^a	Olefin	Ratio	Selected ¹ H NMR shifts of major isomer ^b		
			δ H1	δ H2a	δ H2b
1	178g 	11:1 211g:212g	3.82	2.70	2.26
2	178h 	8:1 211h:212h	3.90	2.77	2.45
3	178i 	12:1 211i:212i	3.83	2.71	2.36
4	178j 	10:1 211j:212j	3.77	2.66	2.29
5	178k 	10:1 211k:212k	3.75	2.64	2.28
6	178l 	8:1 211l:212l	3.85-3.77	2.69-2.60	2.22

^a Conditions: 0.5 eq. [RhCl(C₂H₄)₂]₂, 1 eq. MeTPA, CH₂Cl₂, -78 °C, 1h; then 1.5 eq. olefin, warm to r.t., 30 min; removal of volatiles. ^b 300 MHz, 298K, CD₂Cl₂.

The ^1H NMR spectra of the MeTPA complexes **211** and **212** resemble the spectra of the corresponding TPA complexes **179** and **180** in most aspects. The crude spectrum of the styrene complex **211g** is shown in Figure 5.1. Expectedly, no signal can be found for H20, which was usually the most downfield signal with a chemical shift around 9.3 ppm. Instead, the newly introduced methyl group on the central pyridyl arm of the ligand gives rise to a singlet at 3.43 ppm. The shifts of the remaining ortho-pyridine protons, H8 and H14 appear at 8.07 ppm (d, $^3J = 5.5$ Hz, 1H, H8/14) and 7.65 ppm (d, $^3J = 5.5$ Hz, 1H, H8/14) which is similar to the chemical shifts in the corresponding TPA complex (8.11 ppm and 8.01 ppm). Likewise, the olefinic protons H1 (3.82 ppm, ddd, $^3J_{trans} = 10.7$ Hz, $^3J_{cis} = 8.2$ Hz, $^2J_{Rh,H} = 2.7$ Hz, 1H), H2a (2.70 ppm, ddd, $^3J_{trans} = 10.3$ Hz, $^2J = 3.1$ Hz, $^2J_{Rh,H} = 1.8$ Hz, 2H), and H2b (2.26 ppm, ddd, $^3J = 7.8$ Hz, $^2J = 3.1$ Hz, $^2J_{Rh,H} = 2.3$ Hz, 1H) have almost identical shifts and coupling constants as in **179g** (H1: 3.85 ppm, ddd, $^3J_{trans} = 10.5$ Hz, $^3J_{cis} = 8.0$ Hz, $^2J_{Rh,H} = 2.7$ Hz, 1H; H2a: 2.65 ppm, ddd, $^3J_{trans} = 10.5$ Hz, $^2J = 3.4$ Hz, $^2J_{Rh,H} = 2.1$ Hz, 2H; H2b: 2.25 ppm, ddd, $^3J = 7.9$ Hz, $^2J = 3.2$ Hz, $^2J_{Rh,H} = 2.5$ Hz, 1H). Accordingly, the signals for the minor isomer, **212** resembled those of the corresponding TPA complexes **180**.

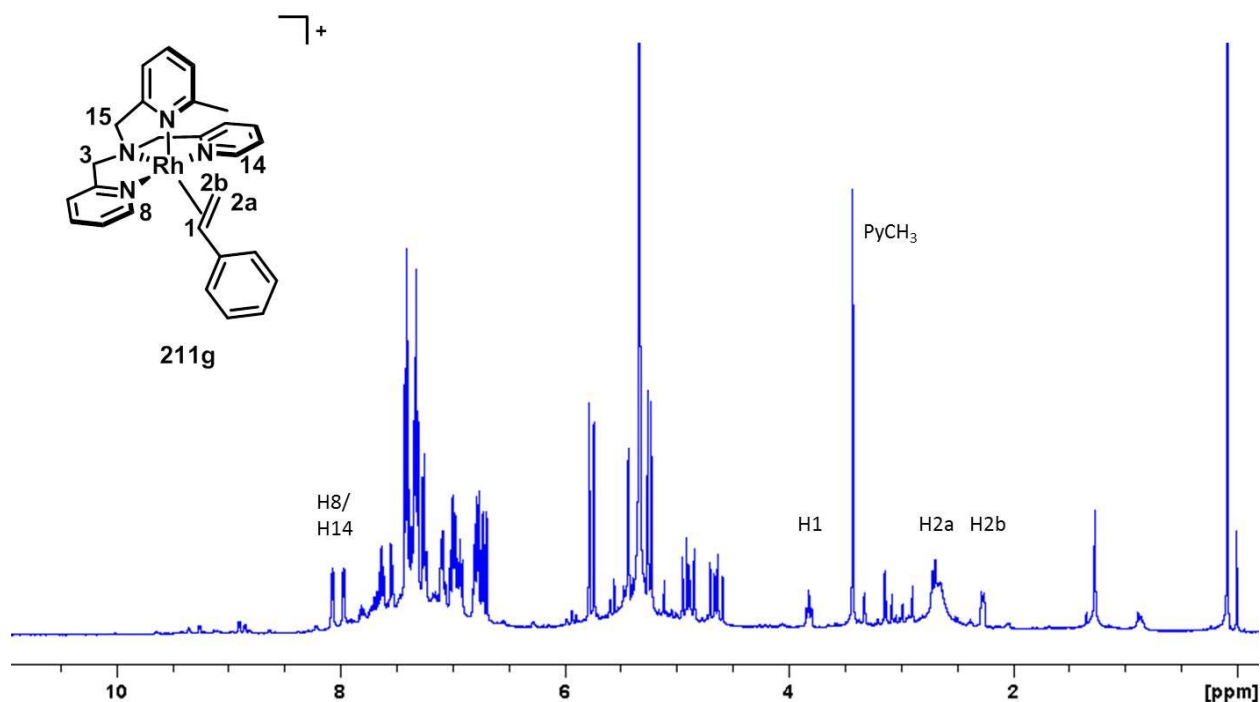


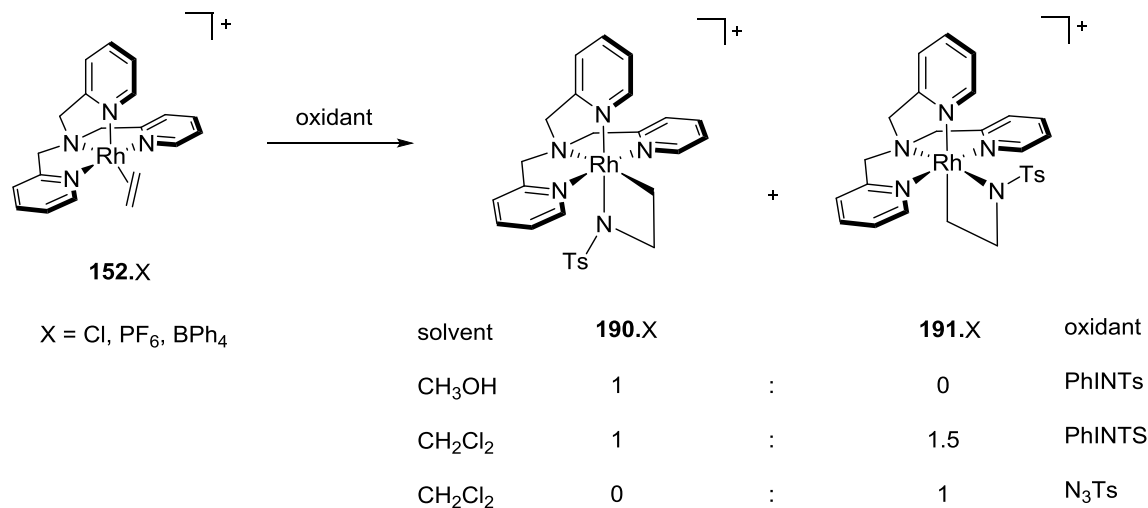
Figure 5.1 Crude ^1H NMR spectrum of **211g** (300 MHz, 298K, CD_2Cl_2).

For every olefin tested, the ratio of **211:212** increased relative to the ratio of **179:180**, consistent with our hypothesis. For example, the ratio of major to minor product for the complexes of styrene increased from 4:1 with the TPA ligand (**179g:180g**) to 11:1 employing MeTPA (**211g:212g**).

5.2 Oxidation with PhINTs

5.2.1 Oxidation of TPA-Rh-Olefin Complexes with PhINTs

Having established that the sterics of the ancillary ligand do have a marked effect on the selectivity of the formation of the Rh-olefin complexes, we next explored the oxidation of olefin complexes **179** and **180** as well as **211** and **212** with PhINTs. First, the transformation employing the TPA-Rh-olefin complexes **179** and **180** will be presented. With ethylene as the olefinic ligand, we had previously shown that two isomers, **190** and **191**, were formed in aprotic solvents, but that only **190** was formed in protic solvents (Scheme 5.1, Chapter 4). As such, we selected MeOD as the solvent, anticipating that the reaction would be more selective than using an aprotic solvent. To our surprise, the oxidation was not successful in MeOD, and instead led to a complex mixture of unidentified products. In comparison, CD₂Cl₂ was found to be a suitable solvent.



Scheme 5.1 Solvent dependent formation of unsubstituted azarhodacyclobutanes.

We expected the formation of up to four possible isomers **213**, **214**, **215** and **216** (Figure 5.2). Isomers **213** and **214** have a configuration analogous to **190** with the ring nitrogen cis to the central nitrogen atom of the TPA ligand but differ by the location of the substituent (R) on the azametallacycle. In contrast, isomers **215** and **216** are analogous to **191** and again are regioisomers of each other with respect to the location of the substituent.

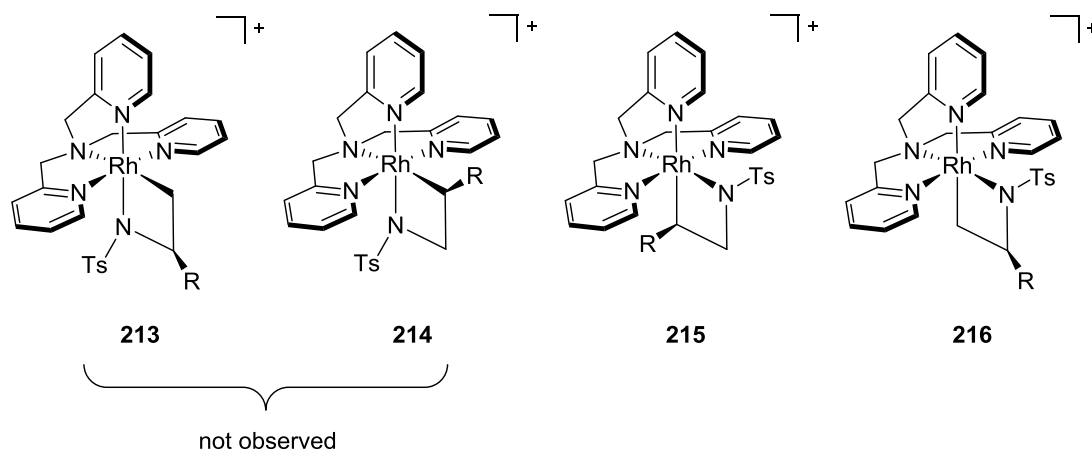


Figure 5.2 Four possible isomers in the formation of substituted azarhodacyclobutanes

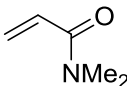
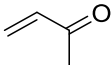
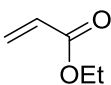
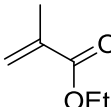
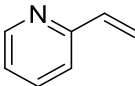
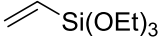
The Rh-olefin complexes were treated with PhINTs in a solution of CD₂Cl₂ at -10°C. In each case, the reaction mixture was allowed to slowly warm to room temperature and was stirred for another 12 hours before it was subjected to analysis by NMR spectroscopy and mass spectrometry. The low- and high-resolution ESI mass spectra confirmed formation of the substituted azarhodacyclobutanes.

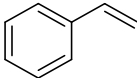
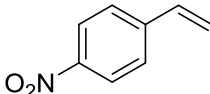
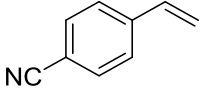
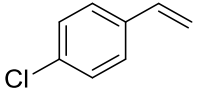
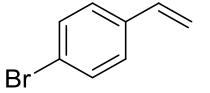
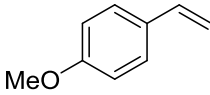
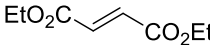
The reactions proceeded with good-to-excellent regioselectivity, generating isomer **215** as the major or sole product. Notably, electron deficient olefins, which were unreactive in H₂O₂ oxidation, underwent oxidation with excellent selectivity for **215**. With styrene derivatives, complex **216** was also obtained. It is noteworthy that only complexes **215** and **216** (which have comparable geometry to complex **190**) were generated. PhINTs oxidation of complex **152** under the same conditions generated a 1:1.5 mixture of isomers **190** and **191**. Whereas we were able to obtain complex **190** selectively using a protic solvent, under no circumstances were we ever able to obtain isomer **191** exclusively using PhINTs as the oxidant. Selective formation of **191** was only possible when tosyl azide (N₃Ts) was employed as the oxidant instead (Scheme 5.1, Chapter 4.2.2). To date, the basis for this selectivity with

substituted olefins is not fully understood. Possible mechanisms will be considered later in this chapter and in greater depth in Chapter 6. Another remarkable feature is that the regioselectivity for the incorporation of the heteroatom is for the less substituted olefin carbon. This selectivity is reversed from the formation of rhodaoxetanes, in which the heteroatom is attached to the more substituted carbon of the double bond (Chapter 3.2).

NMR yields of the major isomer (**215a-l**, **217**) are shown in Table 5.2. The highest yields were observed for complexes **215c** (32%) and **215f** (33%). These yields are comparable with the formation of unsubstituted azarhodacyclobutane **191** (39% in CD₂Cl₂ formed in a mixture with 22% of **191**). Several product complexes (**215c**, **e-f** as major isomer, **215/216g, i** as mixture of major and minor isomer, **216l** as minor isomer) could be isolated via semi-preparative HPLC in sufficient amounts for NMR analysis. As in the formation of **190** and **191**, a number of by-products were also formed, some of which could be identified as other TPA-Rh complexes (Chapter 4.4).

Table 5.2 Oxidation of TPA-Rh complexes with PhINTs

Entry ^a	Olefin	Ratio	NMR yield ^b	Selected ¹ H NMR shifts of major isomer ^c		
				δ H1	δ H2a	δ H2b
1	178a 	>95:5 215a:216a	10%	3.29	4.11	3.86
2	178b 	>95:5 215b:216b	8%	2.75	4.08	3.86
3	178c 	>95:5 215c:216c	32%	2.69	4.10	3.94
4	178d 	>95:5 215d:216d	9%			
5	178e 	>95:5 215e:216e	18%	3.52	4.18	4.25
6	178f 	>95:5	33%	1.23	3.84	4.14

Entry ^a	Olefin	Ratio	NMR yield ^b	Selected ¹ H NMR shifts of major isomer ^c		
				δ H1	δ H2a	δ H2b
		215f:216f				
7	178g 	5:1	12%	3.50	4.08	4.25
		215g:216g				
8	178h 	4:1	7%			
		215h:216h				
9	178i 	3:1	9%	3.51	4.07	4.27
		215i:216i				
10	178j 	5:1	9%			
		215j:216j				
11	178k 	6:1	19%			
		215k:216k				
12	178l 	3:1	5%			
		215l:216l				
13	178m 	217	21%			

^a Conditions: 0.5 eq. [RhCl(C₂H₄)₂]₂, 1 eq. TPA, CH₂Cl₂, -78 °C, 1h; then 1.5 eq. olefin, warm to r.t., 30 min; removal of volatiles; then CH₂Cl₂(or CD₂Cl₂ for NMR scale), 1 eq. PhINTs, -10 °C to r.t., 12h. ^b NMR yields based on tetramethylsilane as internal standard. ^c 300 MHz, 400 MHz or 600 MHz, 298K, CD₂Cl₂.

A representative ¹H NMR spectrum is shown for complex **215e** in Figure 5.3. In analogy to the ¹H NMR spectrum of unsubstituted azarhodacyclobutane **191**, a characteristic doublet for H20 at 10.02 ppm (d, ³J = 5.4 Hz) was observed. Most likely the de-shielding of the axial ortho pyridine proton is caused by a magnetic anisotropy effect of the ring current in the tosyl moiety. Further signals characteristic of the TPA ligand are H8 and H14 at 9.03

ppm (d, $^3J = 5.6$ Hz) and 8.78 ppm (d, $^3J = 5.6$ Hz), respectively. The methylene protons H3 (4.55 ppm, d[AB], $^2J = 16.5$ Hz, 1H; 4.49 ppm, d[AB], $^2J = 16.5$ Hz, 1H), H9 (5.51 ppm, d[AB], $^2J = 15.5$ Hz, 1H; 4.84 ppm, d[AB], $^2J = 15.5$ Hz, 1H) and H15 (4.71 ppm, d[AB], $^2J = 17.5$ Hz, 1H; 4.64 ppm, d[AB], $^2J = 17.5$ Hz, 1H) appeared as pairs of [AB] doublets with large geminal coupling constants of 15-18 Hz in a range between 5.51 ppm and 4.49 ppm. Of the ring protons, H1 was observed as a doublet of doublets of doublets with Rh coupling at 3.52 ppm (ddd, $^3J_{cis} = 8.0$ Hz, $^3J_{trans} = 3.6$ Hz, $^2J_{Rh,H} \sim 3.6$ Hz). Furthermore, H2a and H2b were observed as doublets of doublets at 4.18 ppm (dd, $^2J_{gem} = 10.4$ Hz, $^3J_{cis} = 8.0$ Hz) and 4.25 ppm (dd, $^2J_{gem} = 10.4$ Hz, $^3J_{trans} = 3.8$ Hz), respectively.

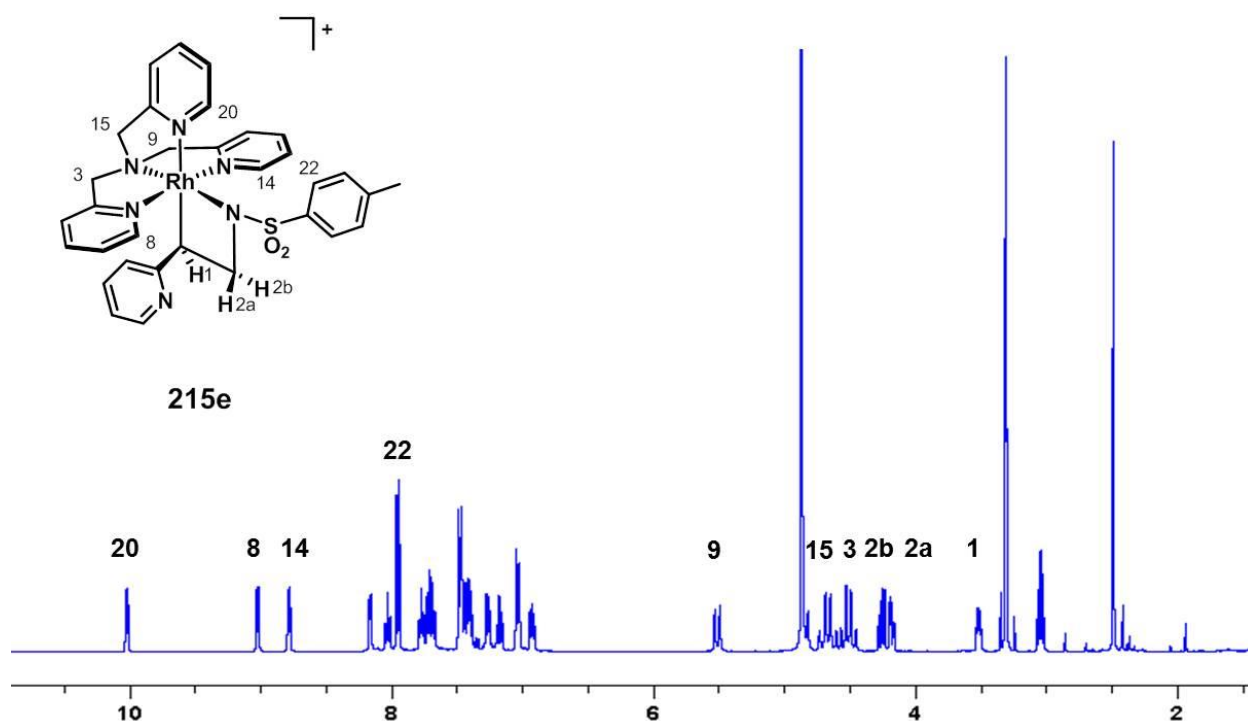


Figure 5.3 ^1H NMR spectrum of **215e** (400MHz, 298K, MeOD)

NOESY experiments allowed for unambiguous determination of the relative configuration. Cross peaks were observed between H1 and H14 (weak), H2b and H14, as well as H2a and H8 (weak). Final evidence for the formation of isomers **215** and **216** over formation of isomers **213** and **214** was provided by a NOE contact between the ring proton H1 and H9 (which is adjacent to the central N atom of the TPA ligand). This demonstrates that H1 must be *cis* to the central TPA amine. In addition, a cross peak between H22 on the

tosyl group and H20 on the central TPA pyridyl ring indicates that these moieties must be in a cis relationship (Figure 5.4).

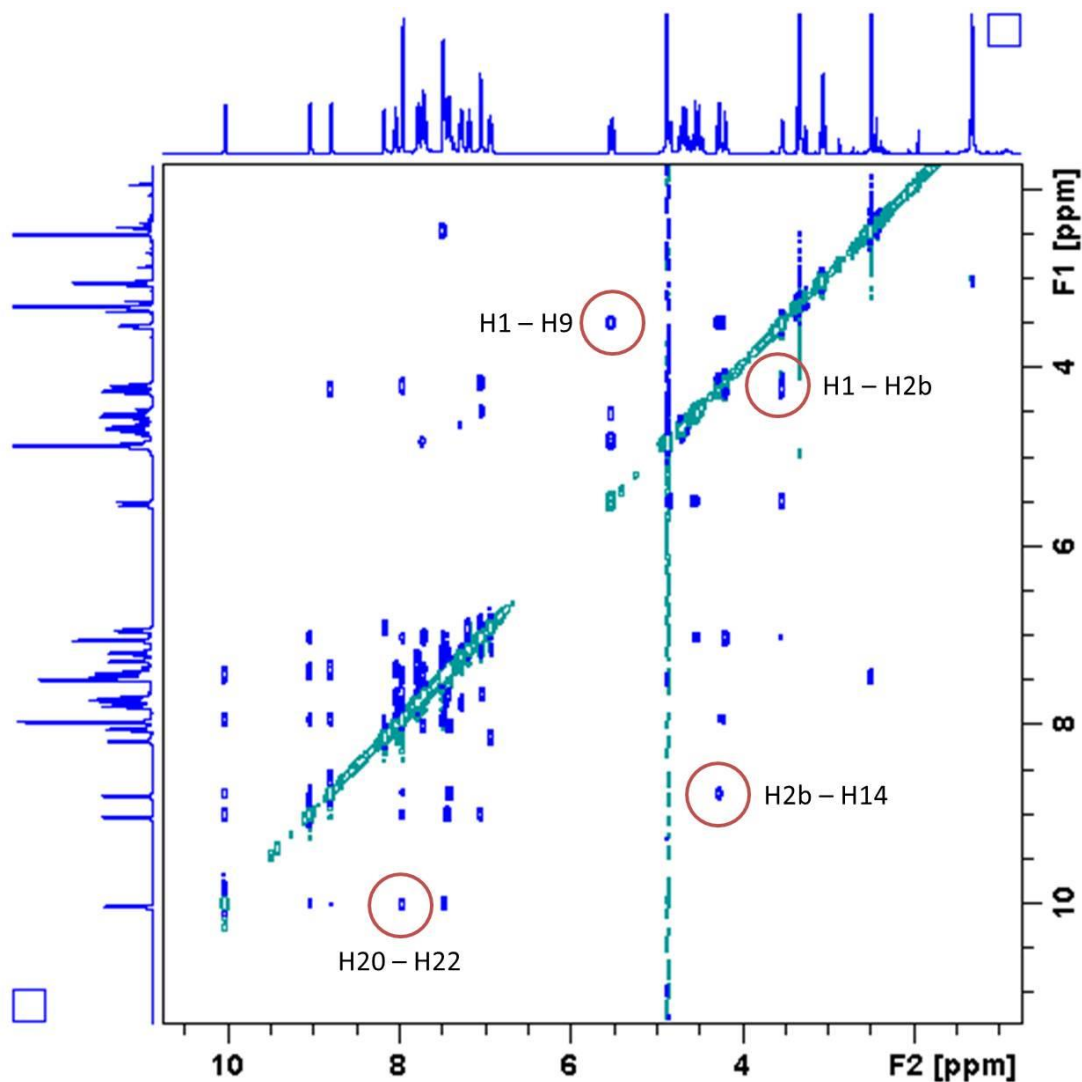


Figure 5.4 Indicative correlations in NOESY spectrum of **215e** (400MHz, 298K, MeOD)

Characterization of the complexes **215a-d**, **215f** and **215g-l** could be performed in an analogous fashion. The minor isomer **216l** resulting from oxidation of the TPA-Rh-*para*-methoxystyrene complex could be isolated in sufficient amount and purity from semi-preparative HPLC to allow for assignment of the ¹H NMR spectrum (Figure 5.5). A characteristic feature of the ¹H NMR spectrum of the minor isomers is the downfield shift of the H14 signal to 9.85 ppm (d, ³J = 5.4 Hz, 1H), compared to the major isomer at 9.00 ppm (d, ³J = 5.6 Hz, 1H). Due to the now adjacent nitrogen atom, the signal of H1 is likewise shifted

downfield to 5.27 ppm (apparent t, $^3J = 8.6$ Hz, 1H) from 3.46-3.34 (m, 1H) in the major isomer. For the remaining styrene complexes, the identification of characteristic signals was possible in the crude product mixture.

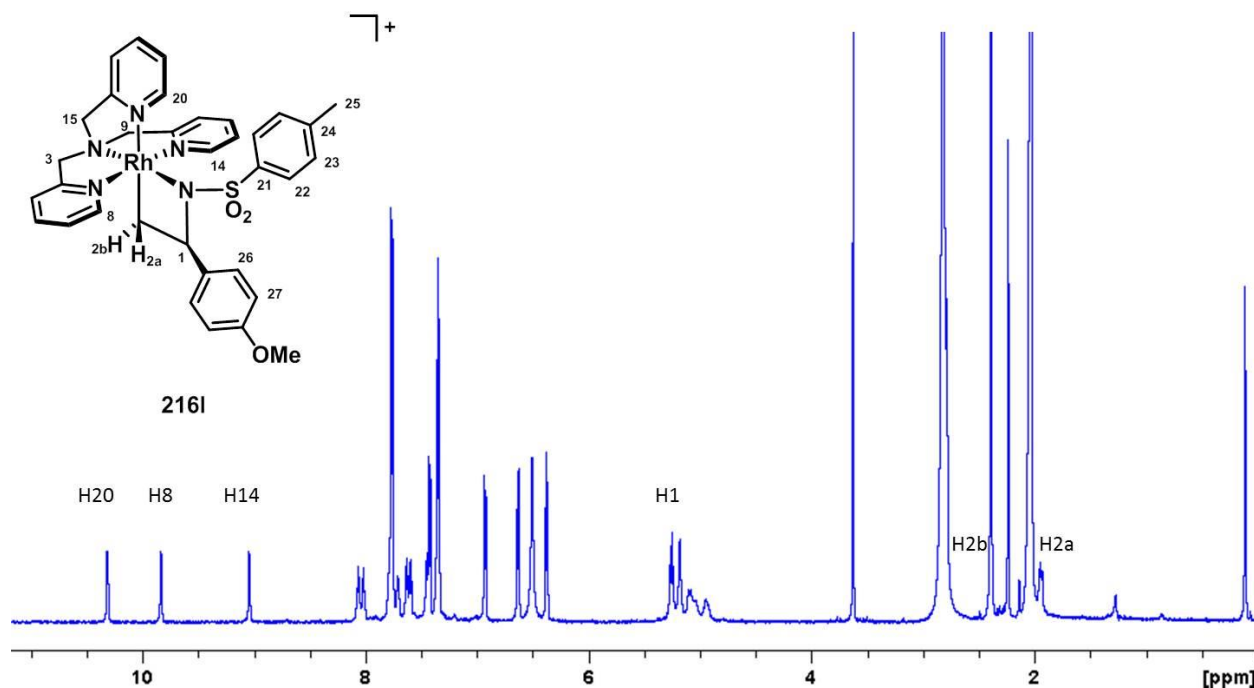


Figure 5.5 ^1H NMR spectrum of **216l** (400MHz, 298K, d_6 -acetone)

5.2.2 Oxidation of a TPA-Rh Complex with a Symmetrically Substituted Olefin

A special case was the oxidation of complex **179m** bearing the symmetrically disubstituted diethylfumarate as olefinic ligand. While no regioisomerism is expected after oxidation, there is a chance of the formation of trans and cis stereoisomers (**218** and **219** respectively, Figure 5.6), depending on the mechanism of the reaction.

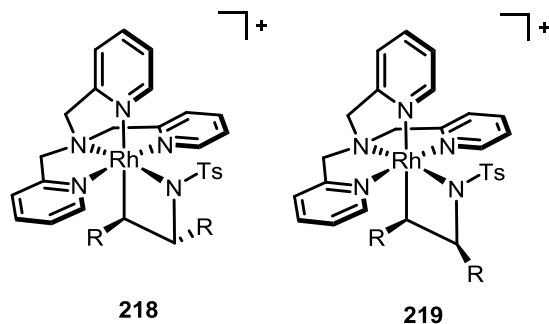


Figure 5.6 Possible stereoisomers with disubstituted olefins

HPLC-MS analysis of the crude product showed two signals in a 98:2 ratio. The major product was unambiguously identified as **218** by ^1H NMR spectroscopy and it was verified by NOESY experiments that the trans relationship of the ester substituents had been retained. Unfortunately, we were not able to isolate and characterize the minor product. Mechanistic considerations regarding azarhodacyclobutane formation and the observed selectivity are presented in Chapter 6.

5.2.3 Oxidation of MeTPA-Rh-Olefin Complexes with PhINTs

We had previously demonstrated the impact of sterics on controlling the ratio of formation of the Rh olefin complexes **211** and **212**. We, therefore, were interested whether the regioselectivity in the formation of the corresponding azarhodacyclobutanes would experience a similar influence. Thus, the MeTPA complexes **211g-l** and **212g-l** were subjected to PhINTs oxidation and the crude reaction mixtures were studied by NMR and HPLC-MS (Figure 5.7). The MeTPA-Rh-olefin complexes were not studied in H_2O_2 oxidation due to the already excellent selectivity with TPA as auxiliary ligand (Chapter 3).

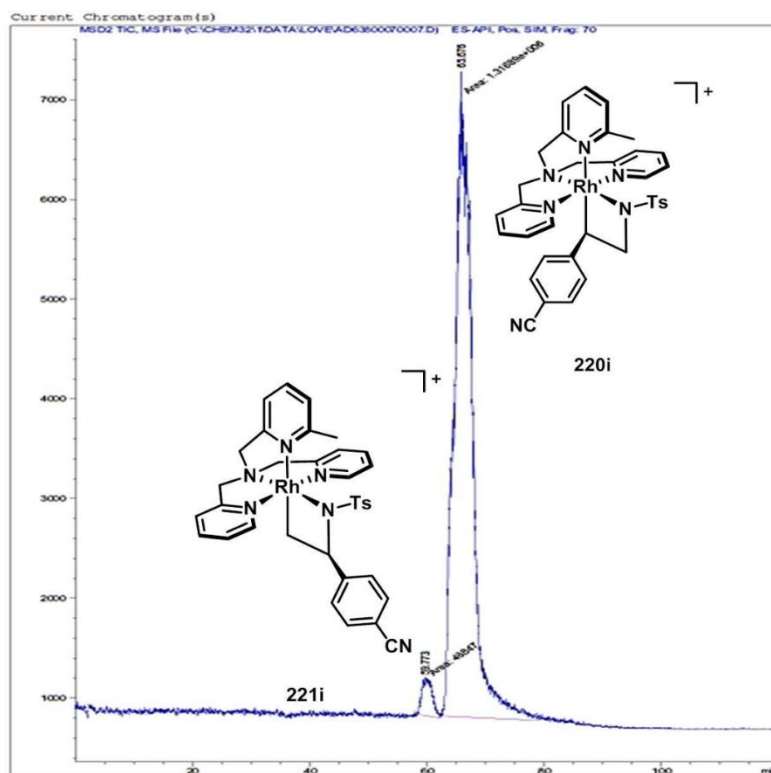


Figure 5.7 HPLC-MS of a crude reaction mixture of **220i** and **221i**.

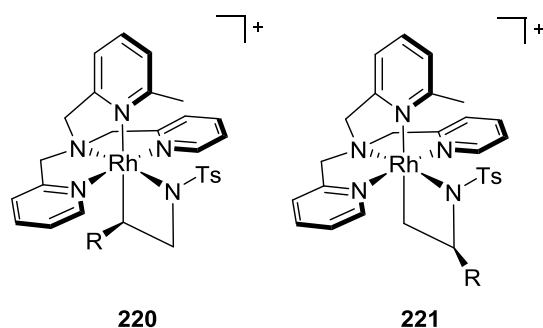
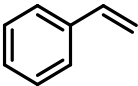
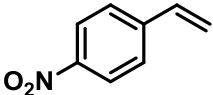
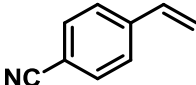
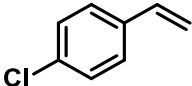
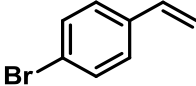
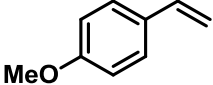


Table 5.3 Oxidation of MeTPA-Rh complexes with PhINTs

Entry ^a	Olefin	Ratio
1	178g 	28:1 220g:221g
2	178h 	20:1 220h:221h
3	178i 	11:1 220i:221i
4	178j 	19:1 220j:221j
5	178k 	18:1 220k:221k
6	178l 	14:1 220l:221l

^a Conditions: 0.5 eq. [RhCl(C₂H₄)₂]₂, 1 eq. TPA, CH₂Cl₂, -78 °C, 1h; then 1.5 eq. olefin, warm to r.t., 30 min; removal of volatiles; then CH₂Cl₂(or CD₂Cl₂ for NMR scale), 1 eq. PhINTs, -10 °C to r.t., 12h. ^b 400 MHz, 298K, CD₂Cl₂.

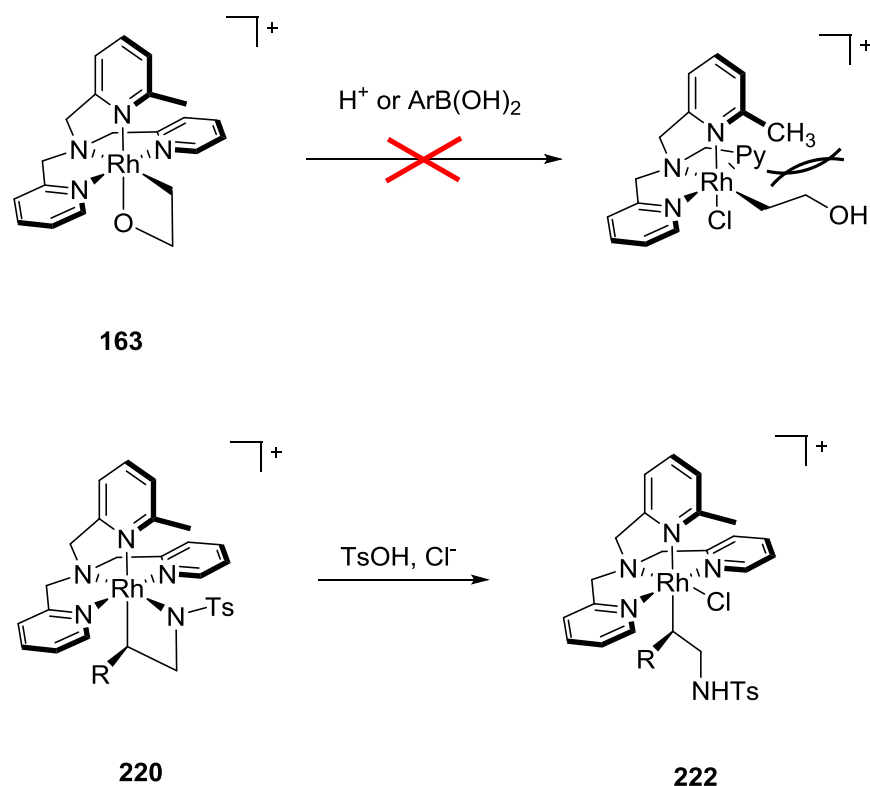
To our delight, we found that the ratios of the oxidized MeTPA complexes **220:221** were significantly higher than for the corresponding TPA complexes and ranged from 11:1 – 28:1. The major to minor ratio in the styrene complex for example was increased more than

six-fold from 5:1 in the TPA complex (Table 5.2, entry 7) to 28:1 in the MeTPA complex (Table 5.3, entry 1). This observation illustrates well the steric control exhibited by the ligand.

5.3 Preliminary Reactivity Studies

The remarkable stability of the unsubstituted azarhodacyclobutanes has already been demonstrated in Chapter 4. We have not yet undertaken extensive reactivity studies on the substituted azarhodacyclobutanes but were specifically interested to see whether any reactivity could be observed towards CO. As mentioned earlier, Alper had proposed an azarhodacyclobutane intermediate in the carbonylation of aziridines to give β -lactams as early as 1983.²⁰⁶ A key step in this proposed mechanism was the insertion of CO into a substituted azarhodacyclobutane (Scheme 1.44). However, pressurizing **215g** with up to 50 bar of CO in methanol at room temperature over 6 hours left the starting material unchanged with no sign of CO insertion. Potentially, longer reaction times and/or higher temperatures could lead to successful insertion.

In accordance with the ring-opening of the unsubstituted azarhodacyclobutanes **190** and **191** mediated by strong acid, the substituted MeTPA azarhodacyclobutanes **220g-l** and **221g-l** also underwent ring-opening when exposed to toluenesulfonic acid in methanol at room temperature. This experiment served as a further confirmation for a configuration in which the ring-nitrogen is trans to the central nitrogen atom on the ligand. In comparison, the MeTPA-rhodoxetane **163** (in which the ring-oxygen is cis to the central ligand nitrogen) could not be ring opened by acid¹⁸⁷ or in the presence of boronic acids (Chapter 2.2.3.2, Scheme 2.15). This was attributed to steric hindrance through the ortho-methyl group on the central pyridyl arm. In the case where the heteroatom is oriented trans to the central nitrogen atom on the ligand, this steric hindrance is considerably reduced. The cyclobutane thus opens with the alkyltosylamino group pointing away from the ortho-methyl group on the central ligand pyridyl arm as indicated in structure **222** (Scheme 5.2). We only obtained MS data for the ring-opened.



Scheme 5.2 Acid mediated ring opening of azarhodacyclobutanes bearing a MeTPA ligand.

5.4 Experimental

5.4.1 General Information

All experiments were carried out under air free conditions employing standard Schlenk techniques but with regular wet solvents which were freeze-pump-thawed during the reaction set-up. Note that all oxidation experiments could also be performed under bench top conditions open to air without significant impact on the reaction outcome. All reagents were used as received without further purification. Room temperature corresponds to ~ 20 °C.

NMR spectra were recorded on Bruker Avance 300, 400 and 600 MHz spectrometers. ^1H and ^{13}C NMR spectra are reported in parts per million and were referenced to residual solvent (CD_2Cl_2 : $\delta\text{H} = 5.32$ ppm $\delta\text{C} = 53.84$ ppm; acetone- d_6 : $\delta\text{H} = 2.05$ ppm, $\delta\text{C} = 206.26$ ppm, MeOD: $\delta\text{H} = 3.31$ ppm, $\delta\text{C} = 49.00$ ppm). ^{15}N NMR spectra (long range $^1\text{H}/^{15}\text{N}$ HMQC) were referenced to CH_3NO_2 as external standard at 0 ppm. The coupling constant for long range

$^1\text{H}/^{15}\text{N}$ HMQC was set to 10 Hz. The multiplicities are abbreviated as follows: s = singlet, d = doublet, t = triplet, q = quartet, m = multiplet, br = broad signal, ob = obscured signal, d[AB] = second order doublet. All spectra were obtained at 25 °C. TopSpin 3.0 was used for data processing. Unless otherwise denoted coupling constants correspond to $^1\text{H}/^1\text{H}$ couplings.

MS-data were obtained on a Waters LC/MS instrument for low resolution and Waters/Micromass LCT for high resolution spectra.

Semi preparative HPLC was performed on a Varian ProStar system with a Varian ProStar 325 UV detector operating at 254 nm and a Varian 1200L triple quadrupole mass spectrometer with Electrospray Ionization. For semi-preparative mode a TMS-end-capped Phenomenex Luma C18(2) column (250x10 mm, 5 μm , 100 Å) was employed and a 99/1 post column splitter was installed for UV/MS parallel detection. Gradients of H_2O /acetonitrile were used at 5mL flow. Repeated injection of 200 μL of the crude product in 70/30 H_2O /acetonitrile allowed purification as collected from the UV detector.

Analytical HPLC was performed on the above system and an Agilent 1260 system with a 6120 single quadrupole LC/MS system using a TMS-end-capped Phenomenex Luma C18(2) column (150x4.6 mm, 5 μm , 100 Å). The MS was set to SIM (single ion monitoring) mode for m/z = mass of the corresponding positively charged complex. 2 μL of a solution of approximately 0.5 mg of the crude reaction mixture in 10 mL 70/30 H_2O /acetonitrile was injected. For successful separation solvent gradients of H_2O /acetonitrile were used at a flow rate of 0.4 mL/min. All retention times given refer to the apex of the peak. Retention times and isomer ratios are averaged over two injections.

NMR yields were obtained by referencing 2 or 3 well-resolved signals in the starting material and product spectra to the tetramethylsilane protons (TMS, 99.9% purity, Alfa Aesar). ^1H NMR was performed with a calibrated 30 or 45 degree P1 pulse and delay + acquisition time being 5 x T1. Assignments of the signals in the ^1H and ^{13}C NMR spectra were made as far as possible with the aid of 2D spectroscopy (COSY, NOESY, HSQC, HMBC). ^1H NMR assignment of the signals in the crude reaction mixture are partly incomplete and over-integrate due to overlapping signals with the other isomer, excess starting material (olefin) and by-products.

5.4.2 Experimental Procedures

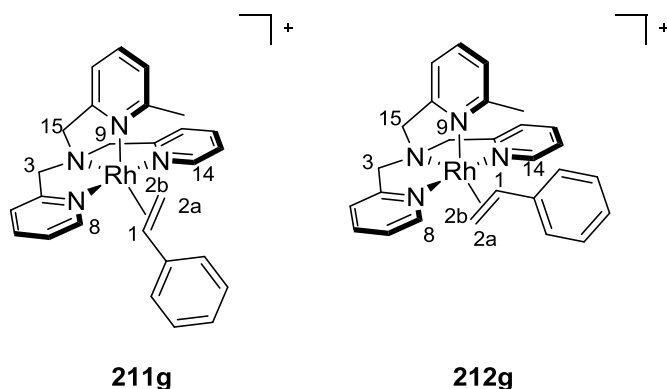
TPA (*N,N,N*-trispyridylmethyl amine) and MeTPA (*N*-[(6-methyl-2-pyridyl)methyl]-*N,N*-di(2-pyridylmethyl)amine)) were prepared according to literature procedures and purified by recrystallization from boiling petrol ether (40 – 60 °C).²⁸⁷ *N*-(*p*-toluenesulfonyl)iminophenyl iodine (PhINTs) was synthesized according to a literature procedure.³⁰³

5.4.2.1 Preparation of MeTPA-Rh-Olefin Complexes 211 and 212 (NMR scale) in Dichloromethane

5.4.2.1.1 General Procedure

[RhCl(C₂H₄)₂]₂ (50 mg, 0.13 mmol, 0.5 equiv., Alfa Aesar) was weighed into a 5 mL reaction vial. The vial was equipped with a magnetic stir bar and sealed with a screw cap fitted with a PTFE coated rubber septum. CH₂Cl₂ (1mL) was added, the resulting solution was frozen in a liquid nitrogen bath and the vial evacuated for 5 minutes on a Schlenk manifold. Dry N₂ was then used to back-fill the vial. MeTPA (80 mg, 0.26 mmol, 1 equiv.) was weighed into a small vial and dissolved in CH₂Cl₂ (1mL). The resulting solution was transferred with a syringe on top of the frozen Rh-dimer suspension and allowed to freeze. Two more freeze-pump-thaw cycles were performed and subsequently the vial was kept at -78 °C with stirring. After 1 h the solution was transferred in 0.4 mL portions into five NMR tubes sealed under N₂ with a screw cap fitted with a PTFE coated rubber septum. The alkene of interest (1.5 equiv.) was added to the solution, the NMR tube was inverted several times and the solution was allowed to warm to room temperature. After 30 minutes the volatiles were removed on high vacuum and CD₂Cl₂ was added for NMR analysis.

[MeTPA-Rh-Styrene]Cl, 211/212g



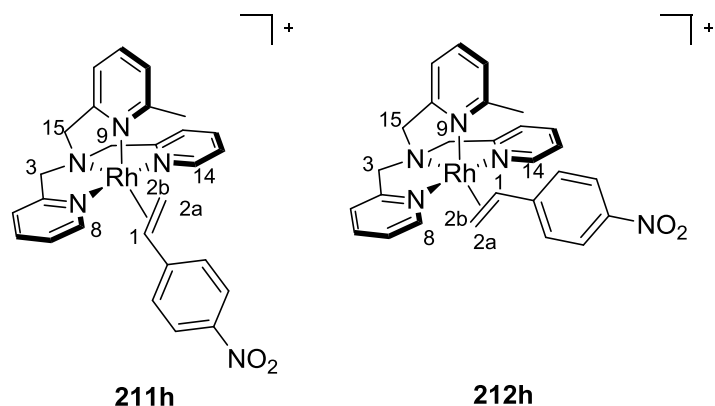
The title compound was synthesized from 4-styrene (8.3 μ L, 0.08 mmol, 1.5 equiv.) according to the general procedure. The reaction produced **211g:212g** in a 11:1 ratio.

211g (*major*) ^1H NMR (300 MHz; CD_2Cl_2): δ 8.07 (d, $^3J = 5.5$ Hz, 1H, H8/14), 7.97 (d, $^3J = 5.5$ Hz, 1H, H8/14), 7.65 (t, $^3J = 7.9$ Hz, 1H, H_{py}), 7.54 (d, $^3J = 7.9$ Hz, 1H, H_{py}), 7.45-7.21 (m, 14H, H_{py}), 7.12-6.89 (m, 6H, H_{py}), 6.79 (d, $^3J = 7.4$ Hz, 1H, H_{py}), 5.44 (d[AB], $^2J = 15.5$ Hz, 1H, H3/9/15), 5.42 (d[AB], $^2J = 15.5$ Hz, 1H, H3/9/15), 4.92 (d[AB], $^2J = 14.7$ Hz, 1H, H3/9/15), 4.86 (d[AB], $^2J = 17.8$ Hz, 1H, H3/9/15), 4.68 (d[AB], $^2J = 14.7$ Hz, 1H, H3/9/15), 4.61 (d[AB], $^2J = 17.8$ Hz, 1H, H3/9/15), 3.82 (ddd, $^3J_{\text{trans}} = 10.7$ Hz, $^3J_{\text{cis}} = 8.2$ Hz, $^2J_{\text{Rh}, \text{H}} = 2.7$ Hz, 1H, H1), 3.43 (s, 3H, PyCH_3), 2.70 (ddd, $^3J_{\text{trans}} = 10.3$ Hz, $^2J = 3.1$ Hz, $^2J_{\text{Rh}, \text{H}} = 1.8$ Hz, 2H, H2a), 2.26 (ddd, $^3J = 7.8$ Hz, $^2J = 3.1$ Hz, $^2J_{\text{Rh}, \text{H}} = 2.3$ Hz, 1H, H2b).

212g (*minor*) ^1H NMR (300 MHz; CD_2Cl_2): δ 4.10-4.01 (m, 1H, H1), 2.96-2.91 (m, 1H, H2a), 2.08-2.01 (m, 1H, H2b).

LRMS (ESI, product mixture): $[\text{C}_{27}\text{H}_{28}\text{N}_4\text{Rh}]^+$: m/z 511.2 (M^+).

[MeTPA-Rh-4-nitrosytrene]Cl, 211/212h

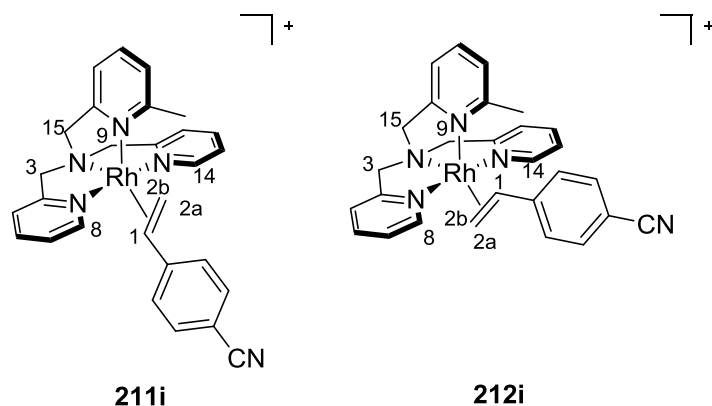


The title compound was synthesized from 4-nitrosytrene (10.2 μ L, 0.08 mmol, 1.5 equiv.) according to the general procedure. The reaction produced **211h**:**212h** in a 8:1 ratio.

211h (*major*) ^1H NMR (300 MHz; CD_2Cl_2): δ 8.11 (d, $^3J = 5.2$ Hz, 1H, H8/14), 7.99 (d, $^3J = 5.2$ Hz, 1H, H8/14), 7.72-7.51 (m, 6H, H_{py}), 7.46-7.34 (m, 2H, H_{py}), 7.21-6.94 (m, 7H, H_{py}), 5.62 (d[AB], $^2J = 15.6$ Hz, 1H, H3/9/15), 5.46 (d[AB], $^2J = 15.6$ Hz, 1H, H3/9/15), 5.11 (d[AB], $^2J = 15.1$ Hz, 1H, H3/9/15), 5.00 (d[AB], $^2J = 18.0$ Hz, 1H, H3/9/15), 4.69 (d[AB], $^2J = 18.0$ Hz, 1H, H3/9/15), 4.63 (d[AB], $^2J = 15.1$ Hz, 1H, H3/9/15), 3.90 (ddd, $^3J_{\text{trans}} = 10.6$ Hz, $^3J_{\text{cis}} = 8.0$ Hz, $^2J_{\text{Rh,H}} = 2.7$ Hz, 1H, H1), 3.42 (s, 3H, PyCH_3), 2.77 (ddd, $^3J_{\text{trans}} = 10.4$ Hz, $^2J = 3.8$ Hz, $^2J_{\text{Rh,H}} = 1.8$ Hz, 1H, H2a), 2.45 (ddd, $^3J_{\text{cis}} = 7.6$ Hz, $^2J = 3.9$ Hz, $^2J_{\text{Rh,H}} = 2.1$ Hz, 1H, H2b).

212h (*minor*) ^1H NMR (300 MHz; CD_2Cl_2): δ 8.49 (d, $^3J = 4.6$ Hz, 1H, H8/14), 8.25 (d, $^3J = 5.7$ Hz, 1H, H8/14), 4.25-4.15 (m, 1H, H1), 2.30-2.23 (m, 1H, H2b).

[MeTPA-Rh-4-cyanostyrene]Cl, 211/212i



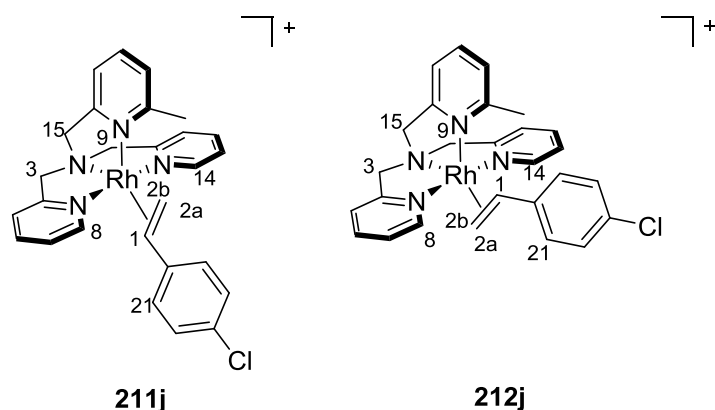
The title compound was synthesized from 4-cyanostyrene (10.3 μ L, 0.08 mmol, 1.5 equiv.), according to the general procedure. The reaction produced 211i:212i in a 12:1 ratio.

211i (*major*) ^1H NMR (300 MHz; CD_2Cl_2): δ 8.07 (d, $^3J = 5.1$ Hz, 1H, H8/14), 7.97 (d, $^3J = 5.4$ Hz, 1H, H8/14), 7.70-7.34 (m, 13H, H_{py}), 7.17-6.97 (m, 10H, H_{py}), 5.62 (d[AB], $^2J = 15.5$ Hz, 1H, H3/9/15), 5.43 (d[AB], $^2J = 15.5$ Hz, 1H, H3/9/15), 5.11 (d[AB], $^2J = 15.1$ Hz, 1H, H3/9/15), 5.00 (d[AB], $^2J = 18.1$ Hz, 1H, H3/9/15), 4.69 (d[AB], $^2J = 18.1$ Hz, 1H, H3/9/15), 4.62 (d[AB], $^2J = 15.1$ Hz, 1H, H3/9/15), 3.83 (ddd, $^3J_{\text{trans}} = 10.5$ Hz, $^3J_{\text{cis}} = 7.8$, $^2J_{\text{Rh}, \text{H}} = 2.8$ Hz, 1H, H1), 3.41 (s, 3H, PyCH_3), 2.71 (ddd, $^3J_{\text{trans}} = 10.3$ Hz, $^2J = 3.8$ Hz, $^2J_{\text{Rh}, \text{H}} = 1.8$ Hz, 1H, H2a), 2.36 (ddd, $^3J_{\text{cis}} = 7.7$ Hz, $^2J = 3.8$ Hz, $^2J_{\text{Rh}, \text{H}} = 2.2$ Hz, 1H, H2b).

212i (*minor*) ^1H NMR (300 MHz; CD_2Cl_2): δ 8.49 (d, $^3J = 4.6$ Hz, 1H, H8/14), 8.21 (d, $^3J = 5.5$ Hz, 1H, H8/14), 4.13-4.04 (m, 1H, H1), 2.98-2.91 (m, 1H, H2a).

LRMS (ESI, product mixture): $[\text{C}_{28}\text{H}_{27}\text{N}_5\text{Rh}]^+$: m/z 536.1 (M^+).

[MeTPA-Rh-4-chlorostyrene]Cl, 211/212j

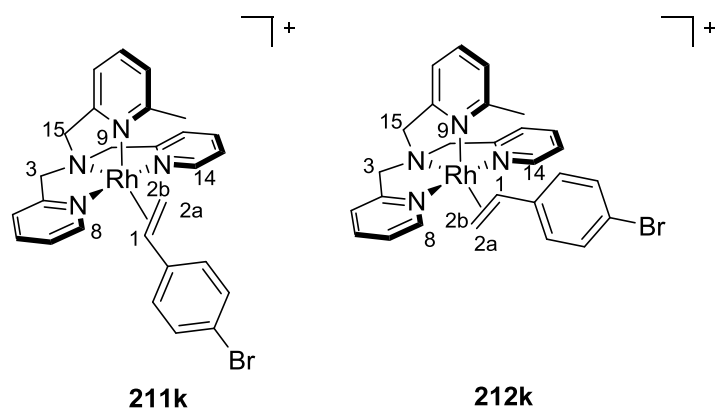


The title compound was synthesized from 4-chlorostyrene (9.6 μ L, 0.08 mmol, 1.5 equiv.) according to the general procedure. The reaction produced 211j:212j in a 10:1 ratio.

211j (*major*) ^1H NMR (300 MHz; CD_2Cl_2): δ 8.07 (d, $^3J = 5.3$ Hz, 1H, H8/14), 7.97 (d, $^3J = 5.3$ Hz, 1H, H8/14), 7.70-7.56 (m, 2H, H_{py}), 7.46-7.26 (m, 11H, H_{py}), 7.19-6.90 (m, 8H, H_{py}), 6.78 (d, $^3J = 6.8$ Hz, 1H, H21), 5.54 (d[AB], $^2J = 15.6$ Hz, 1H, H3/9/15), 5.44 (d[AB], $^2J = 15.6$ Hz, 1H, H3/9/15), 5.05 (d[AB], $^2J = 15.2$ Hz, 1H, H3/9/15), 4.94 (d[AB], $^2J = 17.8$ Hz, 1H, H3/9/15), 4.70 (d[AB], $^2J = 15.0$ Hz, 1H, H3/9/15), 4.66 (d[AB], $^2J = 17.8$ Hz, 1H, H3/9/15), 3.77 (ddd, $^3J_{\text{trans}} = 10.5$ Hz, $^3J_{\text{cis}} = 8.0$ Hz, $^2J_{\text{Rh,H}} = 2.7$ Hz, 1H, H1), 3.42 (s, 3H, PyCH_3), 2.66 (ddd, $^3J_{\text{trans}} = 10.1$ Hz, $^2J = 3.5$ Hz, $^2J_{\text{Rh,H}} = 1.9$ Hz, 1H, H2a), 2.29 (ddd, $^3J_{\text{cis}} = 7.8$ Hz, $^2J = 3.3$ Hz, $^2J_{\text{Rh,H}} = 2.3$ Hz, 1H, H2b).

212j (*minor*) ^1H NMR (300 MHz; CD_2Cl_2): δ 8.50 (d, $^3J = 5.0$ Hz, 1H, H8/14), 8.20 (d, $^3J = 5.4$ Hz, 1H, H8/14), 4.04-3.94 (m, 1H, H1), 2.90-2.83 (m, 1H, H2a), 2.12-2.05 (m, 1H, H2a).

[MeTPA-Rh-4-bromostyrene]Cl, 211/212k

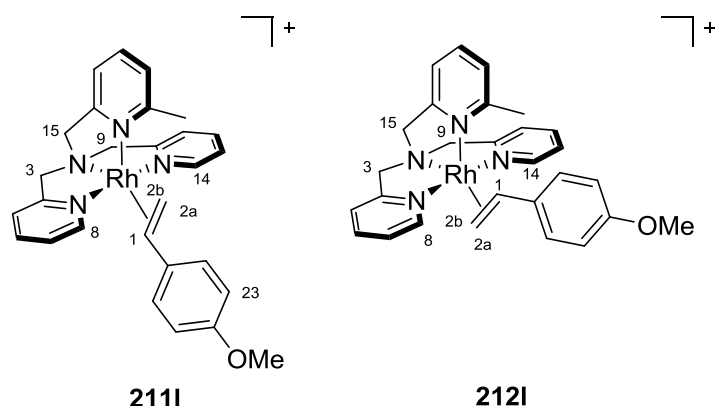


The title compound was synthesized from 4-bromostyrene (10.5 μ L, 0.08 mmol, 1.5 equiv.) according to the general procedure. The reaction produced 211k:212k in a 10:1 ratio.

211k (*major*) ^1H NMR (300 MHz; CD_2Cl_2): δ 8.06 (d, $^3J = 5.2$ Hz, 1H, H8/14), 7.95 (d, $^3J = 5.5$ Hz, 1H, H8/14), 7.69-7.54 (m, 2H, H_{py}), 7.51-7.25 (m, 13H, H_{py}), 7.19-6.83 (m, 10H, H_{py}), 5.54 (d[AB], $^2J = 15.3$ Hz, 1H, H3/9/15), 5.42 (d[AB], $^2J = 15.3$ Hz, 1H, H3/9/15), 5.05 (d[AB], $^2J = 14.8$ Hz, 1H, H3/9/15), 4.93 (d[AB], $^2J = 18.1$ Hz, 1H, H3/9/15), 4.69 (d[AB], $^2J = 14.7$ Hz, 1H, H3/9/15), 4.66 (d[AB], $^2J = 18.1$ Hz, 1H, H3/9/15), 3.75 (ddd, $^3J_{\text{trans}} = 10.6$ Hz, $^3J_{\text{cis}} = 8.0$ Hz, $^2J_{\text{Rh,H}} = 2.8$ Hz, 1H, H1), 3.41 (s, 3H, PyCH_3), 2.64 (ddd, $^3J_{\text{trans}} = 10.4$ Hz, $^2J = 3.3$ Hz, $^2J_{\text{Rh,H}} = 1.5$ Hz, 1H, H2a), 2.28 (ddd, $^3J_{\text{cis}} = 7.7$ Hz, $^2J = 3.3$ Hz, $^2J_{\text{Rh,H}} = 2.1$ Hz, 1H, H2b).

212k (*minor*) ^1H NMR (300 MHz; CD_2Cl_2): δ 8.50 (d, $^3J = 4.5$ Hz, 1H, H8/14), 8.19 (d, $^3J = 5.2$ Hz, 1H, H8/14), 4.02-3.92 (m, 1H, H1), 2.11-2.03 (m, 1H, H2a).

[MeTPA-Rh-4-Methoxystyrene]Cl, 211/212l



The title compound was synthesized from 4-methoxystyrene (10.4 μ L, 0.08 mmol, 1.5 equiv.) according to the general procedure. The reaction produced 211l:212l in a 8:1 ratio.

211l (*major*) ^1H NMR (300 MHz; CD_2Cl_2): δ 8.09 (d, $^3J = 5.1$ Hz, 1H, H8/14), 7.96 (d, $^3J = 5.2$ Hz, 1H, H8/14), 7.69-7.29 (m, 10H, H_{py}), 7.20-6.81 (m, 11H, H_{py}), 6.39 (d, $^3J = 9.0$ Hz, 1H, H22), 5.53-5.40 (m, 2H, H3/9/15), 4.98 (d[AB], $^2J = 14.6$ Hz, 1H, H3/9/15), 4.88 (d[AB], $^2J = 17.6$ Hz, 1H, H3/9/15), 4.73 (d[AB], $^2J = 14.6$ Hz, 1H, H3/9/15), 4.63 (d[AB], $^2J = 17.8$ Hz, 1H, H3/9/15), 3.85-3.77 (partly overlapped, H1), 3.58 (s, 3H, OCH_3), 3.43 (s, 3H, PyCH_3), 2.69-2.60 (m, 1H, H2a), 2.22 (ddd, $^3J_{\text{cis}} = 7.8$ Hz, $^2J = ^2J_{\text{Rh, H}} \sim 2.5$ Hz, 1H, H2b).

212l (*minor*) ^1H NMR (300 MHz; CD_2Cl_2): δ 8.50 (d, $^3J = 4.3$ Hz, 1H, H8/14), 2.07-1.96 (m, 1H, H2b).

LRMS (ESI, product mixture): $[\text{C}_{28}\text{H}_{31}\text{N}_4\text{ORh}]^+$: m/z 541.3 (M^+).

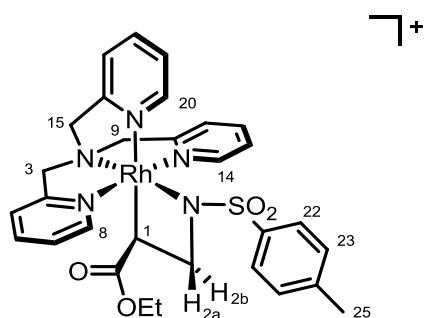
5.4.2.2 Preparation of Substituted TPA-Azarhodacyclobutane Complexes 215 and 216 in Dichloromethane

5.4.2.2.1 Isolable Scale - General Procedure

$[\text{RhCl}(\text{C}_2\text{H}_4)_2]_2$ (0.5 equiv., Alfa Aesar) was weighed into a 10 mL reaction vial. The vial was equipped with a magnetic stir bar and sealed with a screw cap fitted with a PTFE coated rubber septum. CH_2Cl_2 (10 mL/mmol) was added, the resulting solution was frozen in a liquid nitrogen bath and the vial evacuated for 5 minutes on a Schlenk manifold. Dry N_2 was then used to back-fill the vial. TPA (1 equiv.) was weighed into a small vial and dissolved

in CH₂Cl₂ (5 mL/mmol). The resulting solution was transferred with a syringe on top of the frozen Rh-dimer suspension and allowed to freeze. The olefin substrate (1.5 equiv.) was added by microsyringe. Two more freeze-pump-thaw cycles were performed and subsequently the vial was kept at -78 °C with stirring. After 2 h the volatiles were removed on high vacuum and the residue was dissolved in degassed CH₂Cl₂ (20 mL/mmol TPA). The solution was cooled to -10 °C and PhINTs (1 equiv.) were added. The reaction mixture was allowed to slowly warm to room temperature and was kept stirring over a period of 12h during which it darkened to a green/black solution. The volatiles were removed on a rotary evaporator and the crude was subject to purification on semi-preparative HPLC.

[TPA-ethylacrylate-azarhodacyclobutane]Cl, 215c



215c

The title compound was synthesized from [RhCl(C₂H₄)₂]₂ (49 mg, 0.13 mmol, 0.5 equiv.), TPA (73 mg, 0.25 mmol, 1 equiv.) ethylacrylate (140 µL, 0.38 mmol, 1.5 equiv.) and PhINTs (94 mg, 0.25 mmol, 1 equiv.), according to the general procedure. Semi-preparative HPLC separation was performed with a H₂O/acetonitrile gradient starting at 10% ACN and increasing to 90% over 26 minutes, then isocratic flow at 90% until 37 minutes, with a 5mL/min flow rate. The product was collected from 10.5 – 21 minutes along with some impurities of TPA and TsNH₂.

Yield after purification: 19 mg (11 %)

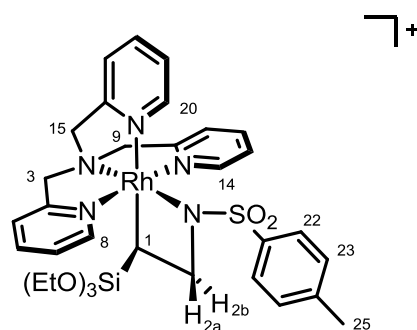
¹H-NMR (600 MHz; acetone-d₆): δ 10.12 (d, ³J = 5.4 Hz, 1H, H20), 9.08 (d, ³J = 5.5 Hz, 1H, H14), 8.90 (d, ³J = 5.5 Hz, 1H, H8), 8.10 (t, ³J = 7.5 Hz, 1H, H12), 7.99 (d, ³J = 7.3 Hz, 1H, H11), 7.95-7.89 (m, 3H, H6 + H22), 7.78-7.74 (m, 1H, H18), 7.71-7.66 (m, 1H, H5), 7.53 (t, ³J = 6.5 Hz, 1H, H13), 7.50 (t, ³J = 6.6 Hz, 1H, H7), 7.46 (d, ³J = 7.1 Hz, 1H, H17), 7.43 (t, ³J = 6.6 Hz, 1H,

H19), 7.40 (d, $^3J = 7.9$ Hz, 2H, H23), 5.60-5.48 (m, 3H, H3 + H9 + H15), 5.17 (d[AB], $^2J = 15.3$ Hz, 1H, H9), 5.02 (d[AB], $^2J = 16.4$ Hz, 1H, H3), 4.94 (d[AB], $^2J = 17.9$ Hz, 1H, H15), 4.10 (dd, $^2J = 9.8$ Hz, $^3J = 4.9$ Hz, 1H, H2a), 3.94 (dd, $^2J = 9.7$ Hz, $^3J = 7.9$ Hz, 1H, H2b), 3.57 (dq, $^2J = 10.8$, $^3J = 7.1$ Hz, 1H, -OCH₂CH₃), 3.18 (dq, $^2J = 10.8$, $^3J = 7.1$ Hz, 1H, -OCH₂CH₃), 2.69 (ddd, $^3J = 7.7$, $^3J = 4.6$, $^2J_{Rh,H} = 3.2$ Hz, 1H, H1), 2.43 (s, 3H, H25), 0.92 (t, $^3J = 7.1$ Hz, 3H, -OCH₂CH₃).

¹³C-NMR (151 MHz; acetone-d₆): δ 180.9 (C(O)OEt), 164.9, 164.0, 160.1, 154.3 (C14), 153.1 (C20), 152.7 (C8), 142.8, 142.0, 140.5 (C12), 139.9 (C6), 139.8 (C18), 130.2 (2C, C23), 127.6 (2C, C22), 126.6 (C13), 126.2 (C11), 125.8 (C7), 125.5 (C19), 124.4 (C5), 122.6 (C17), 70.87 (C15), 70.1 (C9), 68.4 (C3), 60.3 (-OCH₂CH₃), 58.0 (d, $^2J_{Rh,C} = 4.0$ Hz, C2), 21.4 (C25), 14.3 (-OCH₂CH₃), 12.7 (d, $^1J_{Rh,C} = 16.4$ Hz, C1).

¹⁵N chemical shifts extracted from ¹H/¹⁵N HMQC (600 MHz; acetone-d₆, referenced to CH₃NO₂ at 0 ppm): δ -127(N_{Py, central}), -148 (N_{Py}), -151(N_{Py}), -369(N_{cycle}).

[TPA-triethoxyvinylsilane-azarhodacyclobutane]Cl, 215e



215e

The title compound was synthesized from $[\text{RhCl}(\text{C}_2\text{H}_4)_2]_2$ (46 mg, 0.12 mmol, 0.5 equiv., Alfa Aesar) TPA (68 mg, 0.24 mmol, 1 equiv.), vinyltriethoxysilane (100 μL , 0.46 mmol, 2 equiv., Strem Chemicals) and PhINTs (88.0 mg, 0.24 mmol, 1 equiv.) according to a slightly modified procedure (2 equiv. of olefin instead of 1.5 equiv.). HPLC separation was performed with a H_2O /acetonitrile isocratic flow at 30% ACN for 17 minutes followed by a gradient increasing to 35% ACN until 22 minutes and finally increasing to 70% until 25.5 minutes. The product was collected from 13.5 – 16 minutes

Yield after purification: 23 mg (12%).

^1H -NMR (600 MHz; acetone- d_6): δ 10.05 (d, $^3J = 5.3$ Hz, 1H, H20), 9.21 (d, $^3J = 5.4$ Hz, 1H, H14), 8.84 (d, $^3J = 5.4$ Hz, 1H, H8), 8.08 (t, $^3J = 7.7$ Hz, 1H, H12), 7.92-7.84 (m, 4H, H6 + H11 + H22), 7.76 (t, $^3J = 7.6$ Hz, 1H, H18), 7.65 (d, $^3J = 7.7$ Hz, 1H, H5), 7.56 (t, $^3J = 6.5$ Hz, 1H, H13), 7.46 (d, $^3J = 7.7$ Hz, 1H, H17), 7.42 (t, $^3J = 6.5$ Hz, 1H, H19), 7.39 (d, $^3J = 8.0$ Hz, 2H, H23), 7.34 (t, $^3J = 6.5$ Hz, 1H, H7), 5.61 (d[AB], $^2J = 15.8$ Hz, 1H, H3), 5.49 (d[AB], $^2J = 15.9$ Hz, 1H, H3), 5.47 (d[AB], $^2J = 17.6$ Hz, 1H, H15). 5.30 (s, 2H, H9), 4.75 (d[AB], $^2J = 17.5$ Hz, 1H, H15), 4.14 (apparent t, $^3J = 9.6$ Hz, 1H, H2b), 3.84 (apparent t, $^3J = 9.6$ Hz, 1H, H2a), 3.58 (dq, $^2J = 10.1$ Hz, $^3J = 7.0$ Hz, 3H, $-\text{OCH}_2\text{CH}_3$), 3.55 (dq, $^2J = 10.1$ Hz, $^3J = 6.96$ Hz, 3H, $-\text{OCH}_2\text{CH}_3$), 2.43 (s, 3H, H25), 1.23 (apparent dt, $^3J = 9.6$, $^2J_{\text{Rh,H}} = 2.5$ Hz, 1H, H1), 0.98 (t, $J = 7.0$ Hz, 9H, $-\text{OCH}_2\text{CH}_3$).

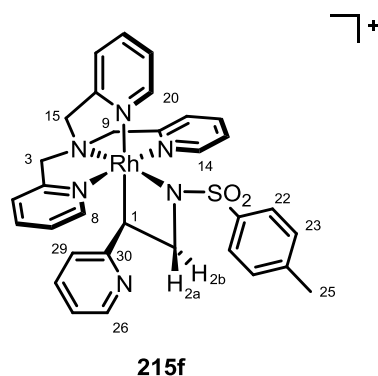
^{13}C NMR (151 MHz; acetone- d_6): δ 165.9 (C4), 164.2 (C10), 159.9 (C16), 154.5 (C14), 152.82 (C20), 152.77 (C8), 142.3 (C21), 141.5 (C24), 140.0 (C12), 139.35 (C18), 139.19 (C6), 130.1 (C23), 127.5 (C22), 126.2 (C13), 125.52 (C11), 125.32 (C19), 125.17 (C7), 124.0 (C5), 122.4

(C17), 70.5 (C15), 69.31 (C9), 69.25 (C3), 58.9 (-OCH₂CH₃), 58.1 (d, ²J_{Rh,C} = 4.2, C2), 21.4 (C25), 18.5 (-OCH₂CH₃), -9.1 (d, ¹J_{Rh,C} = 18.3, C1)

¹⁵N chemical shifts extracted from ¹H/¹⁵N HMQC (600 MHz; acetone-d₆, referenced to CH₃NO₂ at 0 ppm): δ 43 (N_{Py}, central), -12 (N_{Py}), -16 (N_{Py}), -417 (N_{amine}), -453 (N_{cycle}).

HRMS (ESI): calc. [C₃₃H₄₃N₅O₅RhSSi]⁺: 752.1809; found: 752.1804.

[TPA-vinylpyridine-azarhodacyclobutane]Cl, 215f



The title compound was synthesized from [RhCl(C₂H₄)₂]₂ (45 mg, 0.12 mmol, 0.5 equiv., Alfa Aesar) TPA (68 mg, 0.24 mmol, 1 equiv.), vinylpyridine (38.8 μL, 0.36 mmol, 1.5 equiv., Sigma Aldrich) and PhINTs (88.0 mg, 0.24 mmol, 1 equiv.) according the general procedure. HPLC separation was performed with a H₂O/acetonitrile gradient starting at 10% ACN and increasing to 50% over 26 minutes, then isocratic flow at 90% until 37 minutes, with a 5mL/min flow rate. The product was collected from 15-19 and 21-33 minutes (impurity at 19-21 minutes was avoided).

Yield after purification: 15 mg (8%).

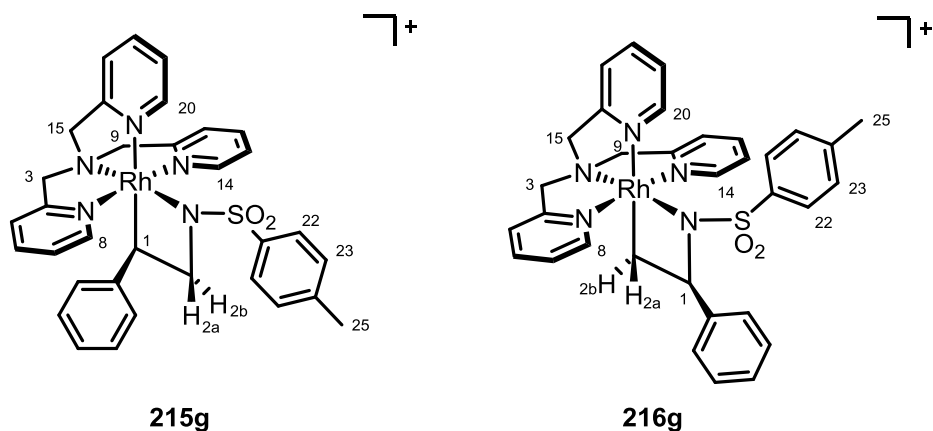
¹H-NMR (600 MHz; acetone-d₆): δ 10.03 (d, ³J = 5.5 Hz, 1H, H20), 9.03 (d, ³J = 5.5 Hz, 1H, H8), 8.78 (d, ³J = 5.5 Hz, 1H, H14), 8.16 (d, ³J = 5.0 Hz, 1H, H26), (8.03 (t, ³J = 7.7 Hz, 1H, H12), 7.95 (d, ³J = 8.0 Hz, 2H, H22), 7.77 (dt, ³J = 7.8 Hz, ⁴J = 1.6, 1H, H18), 7.72 (d, ³J = 7.7 Hz, 1H, H11), 7.67 (dt, ³J = 7.7 Hz, ⁴J = 1.1, 1H, H6), 7.50-7.39 (m, 5H, H7 + H13 + H19 + H23), 7.27 (d, ³J = 7.9 Hz, 1H, H17), 7.18 (t, ³J = 7.5 Hz, 1H, H28), 7.06-7.02 (m, 2H, H5 + H29), 6.93 (dd, ³J = 5.2 Hz, ³J = 5.0 Hz, 2H, H27) 5.51 (d[AB], ²J = 15.5 Hz, 1H, H9), 4.84 (d[AB], ²J = 15.5 Hz, 1H, H9), 4.71 (d[AB], ²J = 17.5 Hz, 1H, H15), 4.64 (d[AB], ²J = 17.5 Hz, 1H, H15), 4.55 (d[AB], ²J = 16.5

Hz, 1H, H3), 4.49 (d[AB], $^2J = 16.5$ Hz, 1H, H3), 4.14 (dd, $^2J = 10.7$, Hz, $^3J_{cis} = 8.1$ Hz, 1H, H2b), 4.14 (dd, $^2J = 10.7$, Hz, $^3J_{trans} = 3.9$ Hz, 1H, H2a), 3.54-3.50 (m, 1H, H1), 2.50 (s, 3H, H25).

^{13}C NMR (151 MHz; acetone- d_6): δ 170.4 (C4), 164.0 (C10), 163.7 (C30), 159.2 (C16), 154.1 (C14), 153.20 (C8/20), 153.16 (C8/20), 149.3 (C26), 143.6 (C21/24), 141.0 (C21/24), 140.9 (C12), 140.3 (C18), 140.0 (C6), 137.7 (C28), 130.8 (2C, C23), 127.7 (2C, C22), 127.0 (C18), 126.8 (C7/13), 126.2 (C7/13), 125.5 (C11), 124.0 (C5/29), 122.6 (C5/29), 122.3 (C17), 120.9 (C27), 71.5 (C15), 70.5 (C9), 69.4 (C3), 62.2 (d, $^2J_{Rh,C} = 4.2$, C2), 21.5 (C25), 21.3 (d, $^1J_{Rh,C} = 16.4$, C1)

^{15}N chemical shifts extracted from $^1\text{H}/^{15}\text{N}$ HMQC (600 MHz; acetone- d_6 , referenced to CH_3NO_2 at 0 ppm): δ 96 ($\text{N}_{\text{Py-subst}}$), 20 ($\text{N}_{\text{Py,TPA central}}$), -25 ($\text{N}_{\text{Py, TPA}}$), -34 ($\text{N}_{\text{Py, TPA}}$), -434 (N_{amine}), -464 (N_{cycle}).

[TPA-styrene-azarhodacyclobutane]Cl, **215/216g**



The title compound was synthesized from $[\text{RhCl}(\text{C}_2\text{H}_4)_2]_2$ (54 mg, 0.14 mmol, 0.5 equiv.), TPA (81 mg, 0.28 mmol, 1 equiv.), styrene (48 μL , 0.42 mmol, 1.5 equiv.) and PhINTs (104 mg, 0.28 mmol, 1 equiv.) according the general procedure. HPLC separation was performed with a H_2O /acetonitrile gradient starting at 10% ACN and increasing to 90% over 26 minutes, then isocratic flow at 90% until 37 minutes, with a 5mL/min flow rate. The purified material was subject to HPLC again with an isocratic flow at 30% ACN for 17 minutes. The major product **215g** was collected from 5.5-8 minutes (still containing ca. 10% **216g**) and a fraction with the minor product **216g** enriched from 8 – 10.5 minutes (ca 1:2 mix with **215g**).

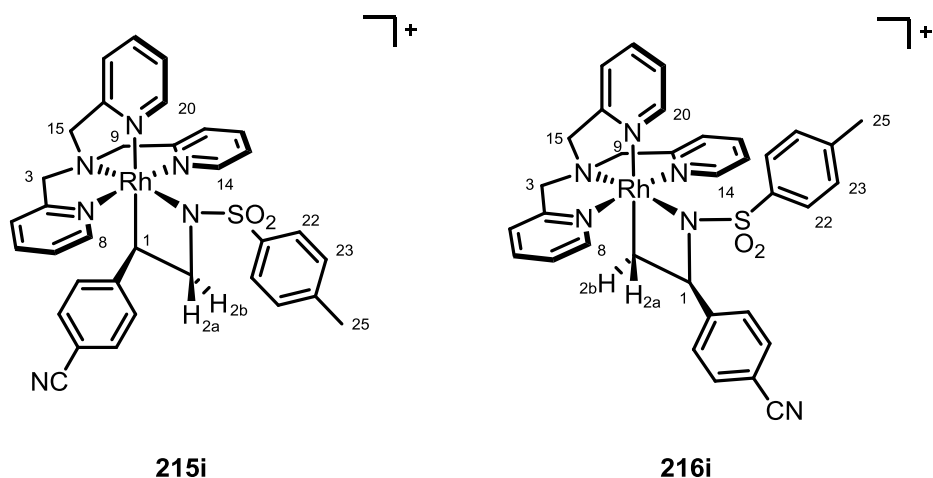
Combined yield after purification: 19 mg (9%)

215g (*major*) ^1H -NMR (600 MHz; acetone- d_6): δ 10.15 (d, $^3J = 5.3$ Hz, 1H, H20), 9.14 (d, $^3J = 5.5$ Hz, 1H, H8), 9.03 (d, $^3J = 5.5$ Hz, 1H, H14), 8.05 (t, $^3J = 8.0$ Hz, 1H, H12), 7.96 (d, $^3J = 8.1$ Hz, 2H, H22), 7.85 (d, $^3J = 7.4$ Hz, 1H), 7.82-7.71 (m, 2H), 7.50-7.44 (m, 4H), 7.43 (d, $^3J = 8.0$ Hz, 2H, H23), 7.33 (d, $^3J = 8.3$ Hz, 1H), 7.19 (d, $^3J = 8.4$ Hz, 1H), 6.96-6.71 (m, 4H), 5.42 (d[AB], $^2J = 16.2$ Hz, 1H, H3/9/15), 5.17 (d[AB], $^2J = 15.2$ Hz, 1H, H3/9/15), 5.09-5.01 (m, 3H, H3/9/15), 4.27 (dd, $^2J = 10.0$ Hz, $^3J = 8.3$ Hz, 1H, H2b), 4.08 (dd, $^2J = 10.1$ Hz, $^3J = 4.9$ Hz, 1H, H2a), 4.04 (d[AB], $^2J = 15.5$ Hz, 1H, H3/9/15), 3.50 (ddd, $^3J = 8.1$ Hz, $^3J = 4.8$ Hz, $^2J_{Rh,H} = 3.3$ Hz, 1H, H1), 2.45 (s, H25).

^{13}C -NMR (151 MHz; acetone- d_6): δ 164.0, 163.4, 159.1, 153.9, 153.0, 152.9, 140.0, 139.8, 139.4, 139.3, 139.2, 130.2 (2C), 129.1, 128.9, 128.3, 127.7 (2C), 127.1, 126.39, 126.37, 126.1, 125.6, 125.5, 125.2, 124.0, 122.0, 70.7, 70.0, 68.8, 63.7 (d $^1J_{Rh,C} = 4.6$ Hz, C2), 21.4, 19.5 (d, $^1J_{Rh,C} = 16.1$ Hz, C1).

216g (*minor*) ^1H -NMR (600 MHz; acetone- d_6): δ 10.31 (d, $^3J = 5.0$ Hz, 1H, H20), 9.82 (d, $^3J = 5.4$ Hz, 1H, H14), 9.07 (d, $^3J = 5.5$ Hz, 1H, H8), 8.08-6.74 (m, H_{Styr}, H_{Py}), 5.41 (d, $^2J = 15.6$ Hz, 1H, H3/9/15), 5.34 (apparent t, $J = 8.6$ Hz, 1H, H1), 5.30 (d[AB], $^2J = 15.7$ Hz, 1H, H3/9/15), 5.17 (m, 2H, H3/9/15), 5.09-5.01 (m, 1H, H3/9/15), 4.98 (d[AB], $^2J = 17.7$ Hz, 1H, H3/9/15), 2.42 (ddd, $^2J = 8.3$ Hz, $^3J_{cis} = 6.1$ Hz, $^2J_{Rh,H} = 2.3$ Hz, 1H, H2b), 2.23 (s, 3H, H25) 1.91 (ddd, $^2J = 8.4$ Hz, $^3J_{trans} = 6.2$ Hz, $^2J_{Rh,H} = 2.4$ Hz, 1H, H2a)

[TPA-4-cyanostyrene-azarhodacyclobutane]Cl, **215**/**216i**



The title compound was synthesized from $[\text{RhCl}(\text{C}_2\text{H}_4)_2]_2$ (49 mg, 0.13 mmol, 0.5 equiv.), TPA (73 mg, 0.25 mmol, 1 equiv.), 4-cyanostyrene (47 μL , 0.38 mmol, 1.5 equiv.) and PhINTs (93 mg, 0.25 mmol, 1 equiv.) according the general procedure. HPLC separation was performed with a H_2O /acetonitrile gradient starting at 10% ACN and increasing to 90% over 26 minutes, then isocratic flow at 90% until 37 minutes, with a 5mL/min flow rate. The purified material was subject to HPLC again with an isocratic flow at 30% ACN for 17 minutes. The major product **215i** was collected from 6.5-8 minutes (still containing ca. 10% **216i**) and the minor product **216i** from 8 – 10 minutes (still containing ca. 20% **215i**).

Combined yield after purification: 13 mg (7%)

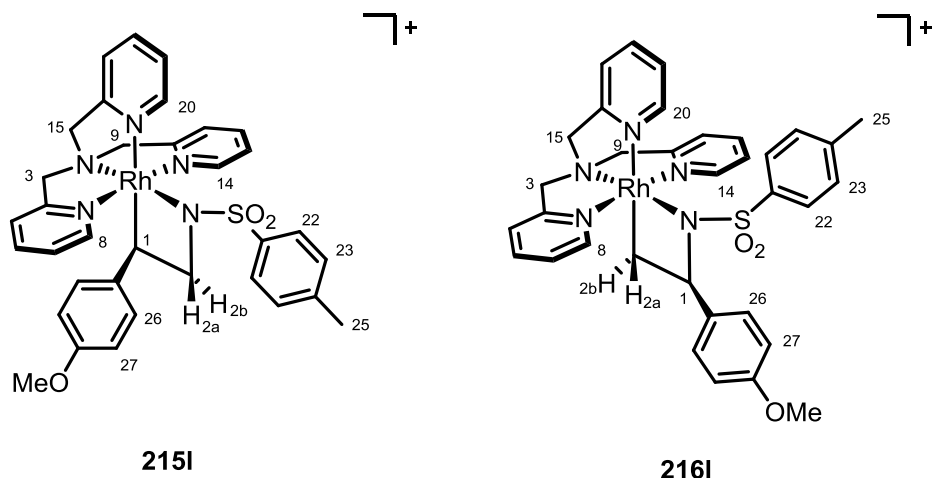
215i (*major*) ^1H -NMR (600 MHz; acetone- d_6): δ 10.16 (d, $^3J = 5.1$ Hz, 1H, H20), 9.20 (d, $^3J = 5.4$ Hz, 1H, H8), 8.96 (d, $^3J = 5.4$ Hz, 1H, H14), 8.36-6.86 (m, H_{Styr} , H_{Py}), 5.42-4.80 (m, 5H, H3/9/15), 4.34 (d[AB], $^2J = 16.3$ Hz, 1H, H3/9/15), 4.29 (d[AB], $^2J = 15.5$ Hz, 1H, H3/9/15), 4.25 (dd, $^2J = 10.3$ Hz, $^3J = 7.9$ Hz, 1H, H2b), 4.07 (dd, $^2J = 10.3$ Hz, $^3J = 3.4$ Hz, 1H, H2a), 3.51 (apparent dt, $^3J = 7.4$ Hz, $J = 3.5$ Hz, 1H, H1), 2.45 (s, 3H, H25).

216i (*minor*) ^1H -NMR (600 MHz; acetone- d_6): δ 10.32 (d, $^3J = 5.0$ Hz, 1H, H20), 9.81 (d, $^3J = 5.4$ Hz, 1H, H14), 9.13 (d, $^3J = 5.5$ Hz, 1H, H8), 8.08-6.74 (m, H_{Styr} , H_{Py}), 5.41 (d, $^2J = 15.6$ Hz, 1H, H3/9/15), 5.38 (apparent t, $J = 8.6$ Hz, 1H, H1), 5.2-4.87 (m, 6H, 1H, H3/9/15), 2.42 (ddd, $^2J = 8.3$ Hz, $^3J_{\text{cis}} = 6.1$ Hz, $^2J_{\text{Rh,H}} = 2.3$ Hz, 1H, H2b), 2.23 (s, 3H, H25) 1.87 (ddd, $^2J = 8.4$ Hz, $^3J_{\text{trans}} = 5.9$ Hz, $^2J_{\text{Rh,H}} = 1.9$ Hz, 1H, H2a)

^{13}C -NMR (151 MHz; acetone- d_6): δ 162.8, 162.7, 159.2, 158.0, 154.9 (C14), 152.3 (C20), 151.8 (C8), 138.8, 138.0, 135.9, 131.0 (2C), 128.1, 127.4, 124.9 (2C), 124.2, 123.6, 123.5, 122.3, 121.5, 121.0, 118.2, 108.4, 73.2 (d, $^2J_{\text{Rh,C}} = 4.2$ Hz, C2), 69.2, 68.8, 68.4, 20.3, 12.6 (d, $^1J_{\text{Rh,C}} = 16.7$ Hz, C1).

^{15}N chemical shifts extracted from $^1\text{H}/^{15}\text{N}$ HMQC (600 MHz; acetone- d_6 , referenced to CH_3NO_2 at 0 ppm): δ 37 ($\text{N}_{\text{Py,TPA}}$ central), -22 ($\text{N}_{\text{Py,TPA}}$), -34 ($\text{N}_{\text{Py,TPA}}$), -423 (N_{cycle}).

[TPA-4-methoxystyrene-azarhodacyclobutane]Cl, 215/216l



The title compound was synthesized from $[\text{RhCl}(\text{C}_2\text{H}_4)_2]_2$ (98mg, 0.25 mmol, 0.5 equiv.), TPA (146 mg, 0.50 mmol, 1 equiv.), 4-methoxystyrene (101 μL , 0.75 mmol, 1.5 equiv.) and PhINTs (187 mg, 0.50 mmol, 1 equiv.) according the general procedure. HPLC separation was performed with a H_2O /acetonitrile gradient starting at 10% ACN and increasing to 90% over 26 minutes, then isocratic flow at 90% until 37 minutes, with a 5mL/min flow rate. The purified material was subject to HPLC again with an isocratic flow at 30% ACN for 17 minutes. The crude reaction mixture of **215/216l** was purified by liquid/liquid extraction before isolating on the HPLC. The product was dissolved in 7 mL MeOH and extracted three times with 7 ml hexanes. MeOH was removed on a rotary evaporator and the product was redissolved in 7 mL DCM. The DCM phase was extracted twice with deionized water. Only trace amounts of product could be found in the aqueous phase. HPLC separation was performed with a H_2O /acetonitrile gradient starting at 10% ACN and increasing to 90% over 26 minutes, then isocratic flow at 90% until 37 minutes,

with a 5mL/min flow rate. The purified material was subject to HPLC again with an isocratic flow at 30% ACN for 17 minutes and allowed for isolation of the minor isomer **216l** eluting at 9-12 minutes. **215l** could not be obtained

Yield after purification: 10 mg (2%)

¹H-NMR (600 MHz; acetone-d₆): δ 10.33 (d, ³J = 4.9 Hz, 1H, H20), 9.85 (d, ³J = 5.4 Hz, 1H, H14), 9.06 (d, ³J = 5.2 Hz, 1H, H8), 8.08 (t, ³J = 7.1 Hz, 1H, H12), 8.03 (t, ³J = 7.0 Hz, 1H, H6), 7.81-7.77 (m, 3H, H18, H17, H11), 7.72 (d, ³J = 7.3 Hz, 1H, H5), 7.65 (t, ³J = 6.5 Hz, 1H, H7), 7.61 (t, ³J = 6.6 Hz, 1H, H13), 7.47 (dd, ³J = 7.4 Hz, ³J = 5.9 Hz, 1H, H19), 7.44 (d, ³J = 8.1 Hz, 2H, H22), 6.94 (d, ³J = 8.0 Hz, 2H, H23), 6.65 (d, ³J = 8.6 Hz, 2H, H26), 6.39 (d, ³J = 8.6 Hz, 2H, H27), 5.27 (apparent t, ³J = 8.6 Hz, 1H, H1), 5.30-4.94 (m, 6H, H3, H9, H15), 3.64 (s, 3H, -OMe), 2.43-2.37 (m, H2b) 2.25 (s, 3H, H25), 1.98-1.94 (m, 1H, H2a).

¹³C-NMR (151 MHz; acetone-d₆): δ 73.2 (d, ²J_{Rh,C} = 4.1 Hz, C1), 13.9 (d, ¹J_{Rh,C} = 16.4 Hz, C2).

¹⁵N chemical shifts extracted from ¹H/¹⁵N HMQC (600 MHz; acetone-d₆, referenced to CH₃NO₂ at 0 ppm): δ -16(N_{Py}), -17(N_{Py}), -30(N_{Py}), -420 (N_{cycle}).

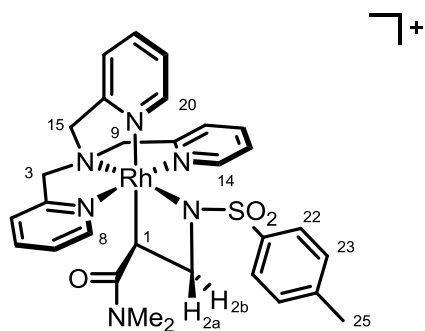
5.4.2.2.2 NMR scale - General Procedure

[RhCl(C₂H₄)₂]₂ (50 mg, 0.13 mmol, 0.5 equiv., Alfa Aesar) was weighed into a 5 mL reaction vial. The vial was equipped with a magnetic stir bar and sealed with a screw cap fitted with a PTFE coated rubber septum. CH₂Cl₂ (1mL) was added, the resulting solution was frozen in a liquid nitrogen bath and the vial evacuated for 5 minutes on a Schlenk manifold. Dry N₂ was then used to back-fill the vial. TPA (75 mg, 0.26 mmol, 1 equiv.) was weighed into a small vial and dissolved in CH₂Cl₂ (1mL). The resulting solution was transferred with a syringe on top of the frozen Rh-dimer suspension and allowed to freeze. Two more freeze-pump-thaw cycles were performed and subsequently the vial was kept at -78 °C with stirring. After 1 h the solution was transferred in 0.4 mL portions into five NMR tubes sealed under N₂ with a screw cap fitted with a PTFE coated rubber septum. The alkene of interest (1.5 equiv.) was added to the solution, the NMR tube was inverted several times and the solution was allowed to warm to room temperature. After 30 minutes the volatiles were removed on high vacuum and the residue was taken up in CD₂Cl₂ (0.4mL). TMS was added as internal standard, a reference spectrum was recorded and the tube was cooled to -

10 °C. Subsequently, PhINTs (18 mg, 0.05 mmol, 1 equiv.) was added via microsyringe, the tube was inverted several times and allowed to warm to room temperature. A product spectrum was recorded after 12 hours.

After removal of the volatiles 0.5 mg of the crude residue was dissolved in a H₂O/acetonitrile = 3/1 mixture (10 mL) and subject to HPLC-MS analysis on a Varian ProStar system with a Varian ProStar 325 UV detector operating at 254 nm and a Varian 1200L triple quadrupole mass spectrometer with Electrospray Ionization or on an Agilent 1260 system with a 6120 single quadrupole LC/MS system using a TMS-end-capped Phenomenex Luma C18(2) column (150x4.6 mm, 5 µm, 100 Å). The MS was set to SIM (single ion monitoring) mode for m/z = mass of the corresponding positively charged complex. 2 µL of the product solution were injected.

[TPA-ethylacrylate-azarhodacyclobutane]Cl, 215a



215a

The title compound was synthesized from *N,N*-dimethylacrylamide (8.3 μ L, 0.08 mmol, 1.5 equiv.) according to the general procedure.

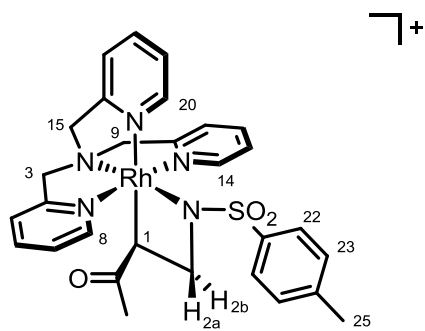
NMR yield: 10%

^1H NMR (300 MHz; CD_2Cl_2): δ 9.88 (d, $^3J = 4.5$ Hz, 1H, H20), 9.46 (d, $^3J = 5.5$ Hz, 1H, H8/14), 8.65 (d, $^3J = 5.6$ Hz, 1H, H8/14), 4.84 (d[AB], $^2J = 18.2$ Hz, 1H, H3/9/15), 4.72 (d[AB], $^2J = 15.9$ Hz, H3/9/15), 4.47 (d[AB], $^2J = 15.8$ Hz, 1H, H3/9/15), 4.11 (dd, $J = 9.5, 8.4$ Hz, 1H, H2b), 3.86 (dd, $J = 10.0, 8.4$ Hz, 1H, H2a), 3.29 (apparent dt, $^3J = 7.9$ Hz, $^2J_{\text{Rh,H}} = 3.0$ Hz, 1H, H1), 2.85 (s, 3H, -NMe), 2.63 (s, 3H, -NMe), 2.43 (s, 3H, H25).

No minor isomer detected.

LRMS (ESI): $[\text{C}_{30}\text{H}_{34}\text{N}_6\text{O}_3\text{RhS}]^+$: m/z 661.3 (M^+).

[TPA-methylvinylketone-azarhodacyclobutane]Cl, 215b



The title compound was synthesized from methylvinylketone (6.8 μ L, 0.08 mmol, 1.5 equiv.) according to the general procedure.

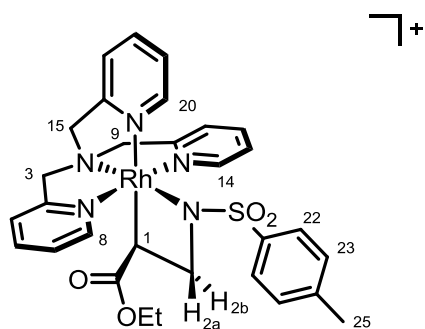
NMR yield: 8%

^1H NMR (300 MHz; CD_2Cl_2): δ 10.09 (d, $^3J = 5.3$ Hz, 1H, H20), 9.15 (d, $^3J = 5.4$ Hz, 1H, H8/14), 8.72 (d, $^3J = 5.7$ Hz, 1H, H8/14), 4.08 (dd, $^2J = 10.8$ Hz, $^3J = 2.9$ Hz, 1H, H2b), 3.86 (dd, $^2J = 10.9$ Hz, 7.5 Hz, 1H, H2a), 2.75 (apparent dt, $^3J = 6.9$ Hz, $J = 3.1$ Hz, 1H, H1).

No other isomer detected.

LRMS (ESI): $[\text{C}_{29}\text{H}_{31}\text{N}_5\text{O}_3\text{RhS}]^+$: m/z 632.2 (M^+).

[TPA-ethylacrylate-azarhodacyclobutane]Cl, 215c



The title compound was synthesized from ethylacrylate (8.5 μ L, 0.08 mmol, 1.5 equiv.) according to the general procedure.

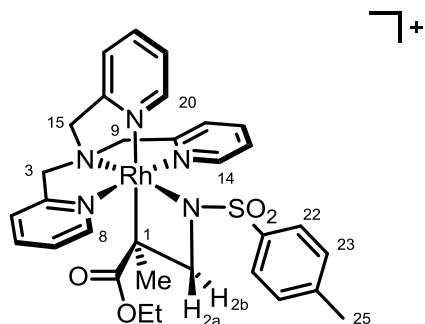
NMR yield: 32%

Characterization data reported above.

No other isomer detected.

LRMS (ESI): $[\text{C}_{30}\text{H}_{33}\text{N}_5\text{O}_4\text{RhS}]^+$: m/z 662.3 (M^+).

[TPA-ethylmethacrylate-azarhodacyclobutane]Cl, 215d



The title compound was synthesized from ethylmethacrylate (10.5 μL , 0.08 mmol, 1.5 equiv.) according to the general procedure.

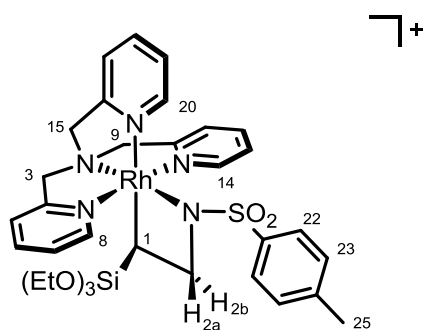
NMR yield: 9%

^1H NMR (300 MHz; CD_2Cl_2): δ 9.93 (d, $^3J = 5.3$ Hz, 1H, H20), 9.42 (d, $^3J = 5.3$ Hz, 1H, H8/14), 8.81 (d, $^3J = 4.7$ Hz, 1H, H8/14), 5.08 (d[AB], $^2J = 15.2$ Hz, 1H, H3/9/15), 4.87 (d[AB], $^2J = 16.1$ Hz, 1H, H3/9/15), 4.77 (d[AB], $^2J = 18.0$ Hz, 1H, H3/9/15), 3.66-3.56 (m, $-\text{OCH}_2\text{CH}_3$), 3.16-3.06 (m, $-\text{OCH}_2\text{CH}_3$), 0.86 (t, $^3J = 7.1$ Hz, 3H, $-\text{OCH}_2\text{CH}_3$).

No other isomer detected.

LRMS (ESI): $[\text{C}_{31}\text{H}_{35}\text{N}_5\text{O}_4\text{RhS}]^+$: m/z 676.3 (M^+).

[TPA-triethoxyvinylsilane-azarhodacyclobutane]Cl, 215e



The title compound was synthesized from triethoxyvinylsilane (18.8 μ L, 0.08 mmol, 1.5 equiv.) according to the general procedure.

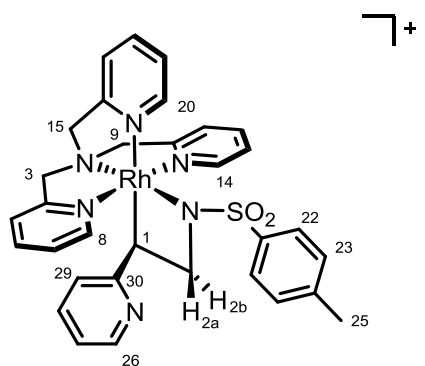
NMR yield: 33%

Characterization data reported above.

No other isomer detected.

LRMS (ESI): $[\text{C}_{33}\text{H}_{43}\text{N}_5\text{O}_5\text{RhSSi}]^+$: 752.4 (M^+).

[TPA-vinylpyridine-azarhodacyclobutane]Cl, 215f



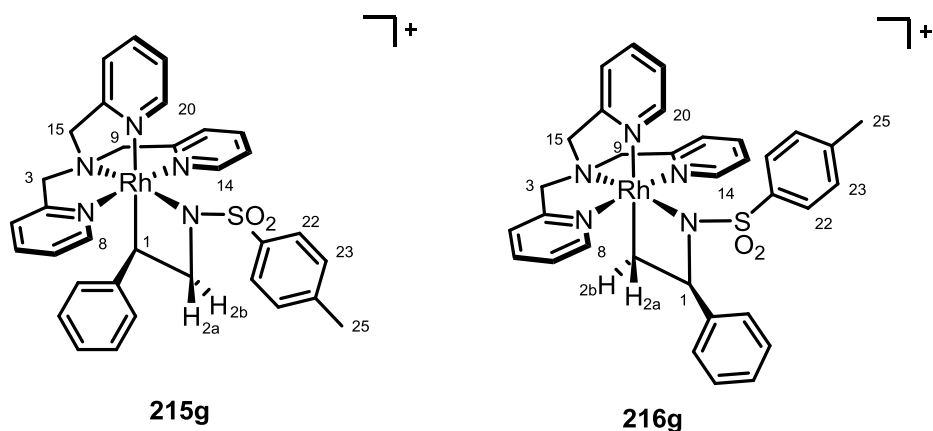
The title compound was synthesized from 2-vinylpyridine (8.6 μ L, 0.08 mmol, 1.5 equiv.) according to the general procedure.

NMR yield: 33%

Characterization data reported above.

No other isomer detected.

[TPA-styrene-azarhodacyclobutane]Cl, 215/216g



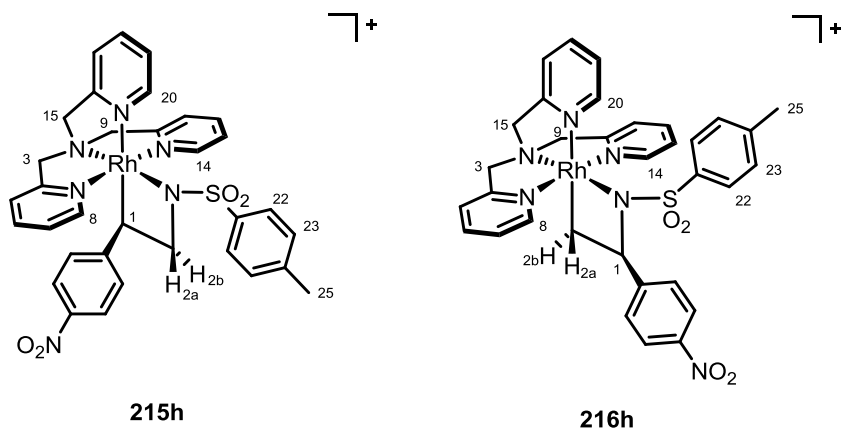
The title compound was synthesized from 4-styrene (8.3 μ L, 0.08 mmol, 1.5 equiv.) according to the general procedure. The reaction produced **215g:216g** in a 5:1 ratio.

NMR yield: 33%

Characterization data reported above.

LRMS (ESI, product mixture): $[\text{C}_{33}\text{H}_{33}\text{N}_5\text{O}_2\text{RhS}]^+$: m/z 666.3 (M^+).

[TPA-4-nitrostyrene-azarhodacyclobutane]Cl, 215/216h



The title compound was synthesized from 4-nitrostyrene (10.2 μ L, 0.08 mmol, 1.5 equiv.) according to the general procedure. The reaction produced **215h:216h** in a 4:1 ratio.

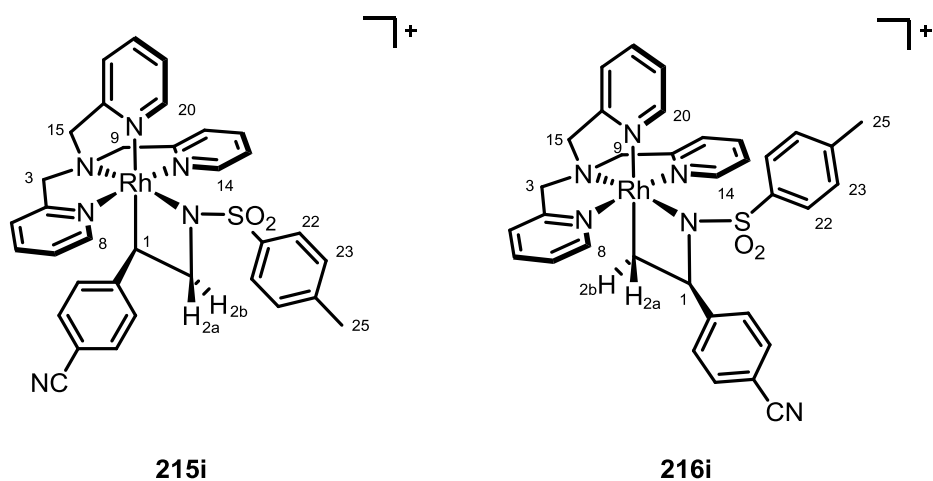
NMR yield: 7%

215h (*major*) ^1H NMR (300 MHz; CD_2Cl_2): δ 10.08 (d, $^3J = 5.5$ Hz, 1H, H20), 9.13 (d, $^3J = 5.5$ Hz, 1H, H8/14), 8.88 (d, $^3J = 5.5$ Hz, 1H, H8/14), 4.24 (dd, $^2J = 10.3$, $^3J_{\text{cis}} = 7.9$ Hz, 1H, H2b), 4.16 (d[AB], $^2J = 15.6$ Hz, 1H, H3/9/15), 4.06 (dd, $^2J = 10.3$, $^3J_{\text{trans}} = 3.4$ Hz, 1H, H2a), 3.35-3.28 (m, 1H, H1).

216h (*minor*) ^1H NMR (300 MHz; CD_2Cl_2): δ 10.24 (d, $^3J = 5.6$ Hz, 1H, H8/14/20), 9.75 (d, $^3J = 5.3$ Hz, 1H, H8/14/20), 9.50 (d, $^3J = 5.4$ Hz, 1H, H8/14/20).

LRMS (ESI, product mixture): $[\text{C}_{33}\text{H}_{32}\text{N}_6\text{O}_4\text{RhS}]^+$: m/z 711.2 (M^+).

[TPA-4-cyanostyrene-azarhodacyclobutane]Cl, **215/216i**



The title compound was synthesized from 4-cyanostyrene (10.3 μL , 0.08 mmol, 1.5 equiv.), according to the general procedure. The reaction produced **215i:216i** in a 3:1 ratio.

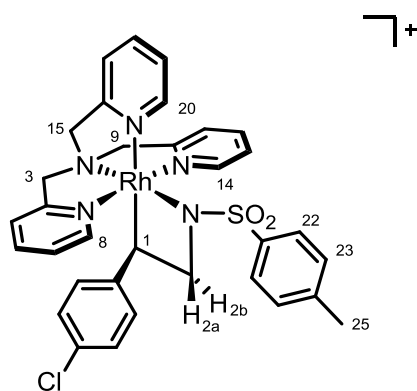
NMR yield: 9%

Characterization data reported above.

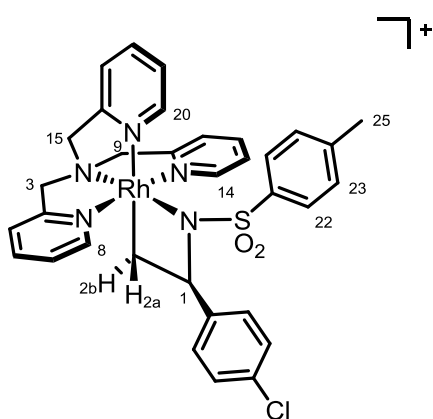
LRMS (ESI, product mixture): $[\text{C}_{34}\text{H}_{32}\text{N}_6\text{O}_2\text{RhS}]^+$: m/z 691.3(M^+).

HPLC-MS (Varian, ACN 10 – 50%, 15 min, 0.4mL flow rate): **215i** : **216i** = 77 : 23 \approx 3:1; retention time = 17.19 min (**215i**), retention time = 16.66 min (**216i**).

[TPA-4-chlorostyrene-azarhodacyclobutane]Cl, 215/216j



215j



216j

The title compound was synthesized from 4-chlorostyrene (9.6 μ L, 0.08 mmol, 1.5 equiv.) according to the general procedure. The reaction produced **215j**:**216j** in a 5:1 ratio.

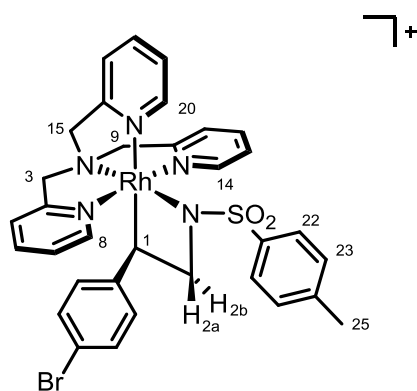
NMR yield: 9%

215j (*major*) ^1H -NMR (300 MHz; CD_2Cl_2): δ 10.06 (d, $^3J = 5.1$ Hz, 1H, H20), 9.08 (d, $^3J = 5.4$ Hz, 1H, H8/14), 8.93 (d, $^3J = 4.5$ Hz, H8/14), 4.23 (dd, $^2J = 10.1$ Hz, $^3J = 8.3$ Hz, 1H, H2b), 4.02 (dd, $^2J = 10.2$, $^3J = 4.9$ Hz, H2a), 3.26 (ddd, $^3J = 8.1$, $^3J = 4.7$, $^2J = 3.3$ Hz, 1H, H1).

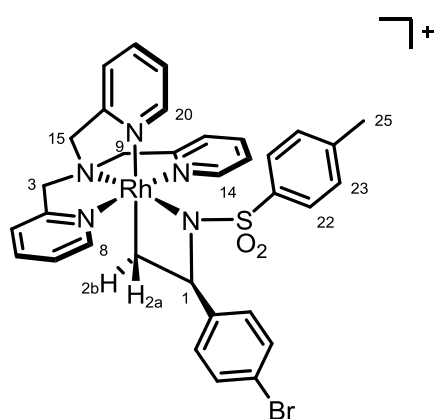
216j (*minor*) ^1H -NMR (300 MHz; CD_2Cl_2): δ 10.23 (d, $^3J = 5.4$ Hz, 1H, H8/14/20), 9.77 (d, $^3J = 5.2$ Hz, 1H, H8/14/20).

LRMS (ESI, product mixture): $[\text{C}_{33}\text{H}_{32}\text{ClN}_5\text{O}_2\text{RhS}]^+$: m/z 700.2 (M^+).

[TPA-4-bromostyrene-azarhodacyclobutane]Cl, 215/216k



215k



216k

The title compound was synthesized from 4-bromostyrene (10.5 μ L, 0.08 mmol, 1.5 equiv.) according to the general procedure. The reaction produced **215k**:**216k** in a 6:1 ratio.

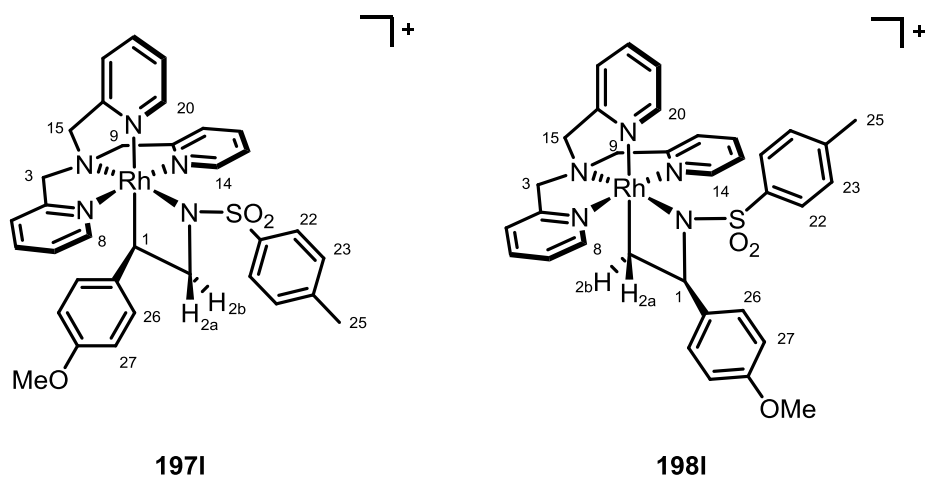
NMR yield: 19%

215k (*major*) ^1H -NMR (300 MHz; CD_2Cl_2): δ 10.06 (d, $^3J = 5.1$ Hz, 1H, H20), 9.08 (d, $^3J = 5.4$ Hz, 1H, H8/14), 8.94 (d, $^3J = 4.7$ Hz, 1H, H8/14), 4.34-4.26 (m, 1H, H2b), 4.14-4.08 (m, 1H, H2a), 3.25 (t, $J = 4.3$ Hz, 1H, H1).

216k (*minor*) ^1H -NMR (300 MHz; CD_2Cl_2): δ 10.24 (d, $^3J = 5.4$ Hz, H8/14/20), 9.78 (d, $^3J = 5.6$ Hz, H8/14/20).

LRMS (ESI, product mixture): $[\text{C}_{33}\text{H}_{32}\text{BrN}_5\text{O}_2\text{RhS}]^+$: m/z 744.2/746.1 (M^+).

[TPA-4-methoxystyrene-azarhodacyclobutane]Cl, 215/216l



The title compound was synthesized from 4-methoxystyrene (10.4 μ L, 0.08 mmol, 1.5 equiv.) according to the general procedure. The reaction produced **215l**:**216l** in a 3:1 ratio.

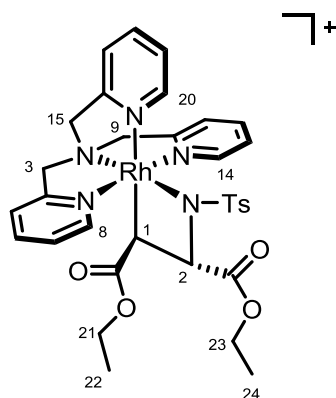
NMR yield: 5%

Characterization data reported above.

LRMS (ESI, product mixture): [C₃₄H₃₅N₅O₃RhS]⁺: m/z 696.3 (M⁺).

HPLC (Varian, ACN 10 – 50%, 15 min, 0.4mL flow rate) **215l** : **216l** = 66 : 34 \approx 2:1; retention time = 17.22 min (**216l**), retention time = 17.82 min (**215l**).

[TPA-diethylfumarate-azarhodacyclobutane]Cl, 218



202

The title compound was synthesized from diethylfumarate (13.1 μ L, 0.08 mmol, 1.5 equiv.) according to the general procedure.

NMR yield: 21%

^1H -NMR (400 MHz; CD_2Cl_2): δ 10.09 (d, $^3J = 5.5$ Hz, 1H, H20), 9.30 (d, $^3J = 5.5$ Hz, 1H, H8), 8.87 (d, $^3J = 5.3$ Hz, H14), 5.54 (d, $^3J_{\text{trans}} = 6.8$ Hz, 1H, H2), 2.71 (dd, $^3J_{\text{trans}} = 6.6$ Hz, $^2J_{\text{Rh,H}} = 3.3$ Hz, 1H, H1), 0.99 (t, $^3J = 7.2$ Hz, 3H, H22), 0.91 (t, $^3J = 7.2$ Hz, 3H, H24).

^{13}C -NMR (151 MHz; CD_2Cl_2): δ 71.5 (C2), 14.1 (d, $^1J_{\text{Rh,C}} = 18.5$ Hz)

HPLC (Agilent, ACN 10% \rightarrow 90%, 20 min, 0.4mL flow rate): major:minor = 98:2; retention time = 7.8 min (minor), 9.7 min (major)

5.4.2.3 Preparation of Substituted MeTPA-Azarhodacyclobutane Complexes 220 and 221 in Dichloromethane

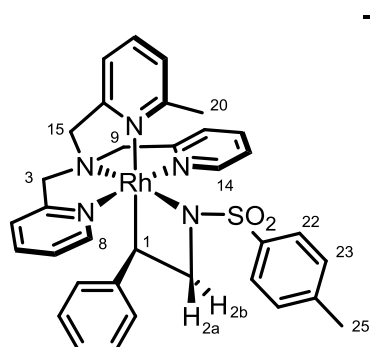
5.4.2.3.1 NMR Scale - General Procedure

$[\text{RhCl}(\text{C}_2\text{H}_4)_2]_2$ (50 mg, 0.13 mmol, 0.5 equiv., Alfa Aesar) was weighed into a 5 mL reaction vial. The vial was equipped with a magnetic stir bar and sealed with a screw cap fitted with a PTFE coated rubber septum. CH_2Cl_2 (1mL) was added, the resulting solution was frozen in a liquid nitrogen bath and the vial evacuated for 5 minutes on a Schlenk manifold. Dry N_2 was then used to back-fill the vial. MeTPA (80 mg, 0.26 mmol, 1 equiv.) was weighed into a small vial and dissolved in CH_2Cl_2 (1mL). The resulting solution was

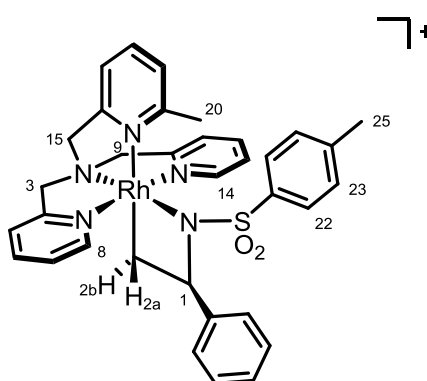
transferred with a syringe on top of the frozen Rh-dimer suspension and allowed to freeze. Two more freeze-pump-thaw cycles were performed and subsequently the vial was kept at -78 °C with stirring. After 1 h the solution was transferred in 0.4 mL portions into five NMR tubes sealed under N₂ with a screw cap fitted with a PTFE coated rubber septum. The alkene of interest (1.5 equiv.) was added to the solution, the NMR tube was inverted several times and the solution was allowed to warm to room temperature. After 30 minutes the volatiles were removed on high vacuum and the residue was taken up in CD₂Cl₂ (0.4mL). TMS was added as internal standard, a reference spectrum was recorded and the tube was cooled to -10 °C. Subsequently, PhINTs (18 mg, 0.05 mmol, 1 equiv.) was added via microsyringe, the tube was inverted several times and allowed to warm to room temperature. A product spectrum was recorded after 12 hours.

After removal of the volatiles 0.5 mg of the crude residue was dissolved in a H₂O/acetonitrile = 3/1 mixture (10 mL) and subject to HPLC-MS analysis on an Agilent 1260 system with a 6120 single quadrupole LC/MS system using a TMS-end-capped Phenomenex Luma C18(2) column (150x4.6 mm, 5 µm, 100 Å). The MS was set to SIM (single ion monitoring) mode for m/z = mass of the corresponding positively charged complex. 2 µL of the product solution were injected and a H₂O/acetonitrile gradient was applied starting at 10% ACN and increasing to 50% over 100 minutes, with a 0.4 mL/min flow rate.

[MeTPA-styrene-azarhodacyclobutane]Cl, 220/221g



220g



221g

The title compound was synthesized from 4-styrene (8.3 μ L, 0.08 mmol, 1.5 equiv.) according to the general procedure.

220g (*major*) $^1\text{H-NMR}$ (400 MHz; CD_2Cl_2): δ 9.87 (d, $^3J = 5.7$ Hz, 1H, H8), 9.06 (d, $^3J = 5.1$ Hz, 1H, H14), 7.97 (t, $^3J = 7.6$ Hz, 1H), 7.81 (d, $^3J = 7.9$ Hz, 2H, H22), 7.73-7.69 (m, 2H), 7.64 (d, $^3J = 7.6$ Hz, 1H), 7.57-7.52 (m, 2H), 7.43 (t, $^3J = 7.4$ Hz, 1H), 7.38 (t, $^3J = 6.3$ Hz, 1H), 7.33 (d, $^3J = 8.1$ Hz, 2H, H23), 7.25-7.12 (m, 4H), 7.05-6.99 (m, 2H), 4.93-4.75 (m, 4H, H3/9/15), 4.33-4.17 (m, 2H, H2b + H3/9/15), 3.98-3.90 (m, 2H, H2a + H3/9/15), 3.72-3.67 (m, 1H, H1), 3.19 (s, H20), 2.44 (s, H25).

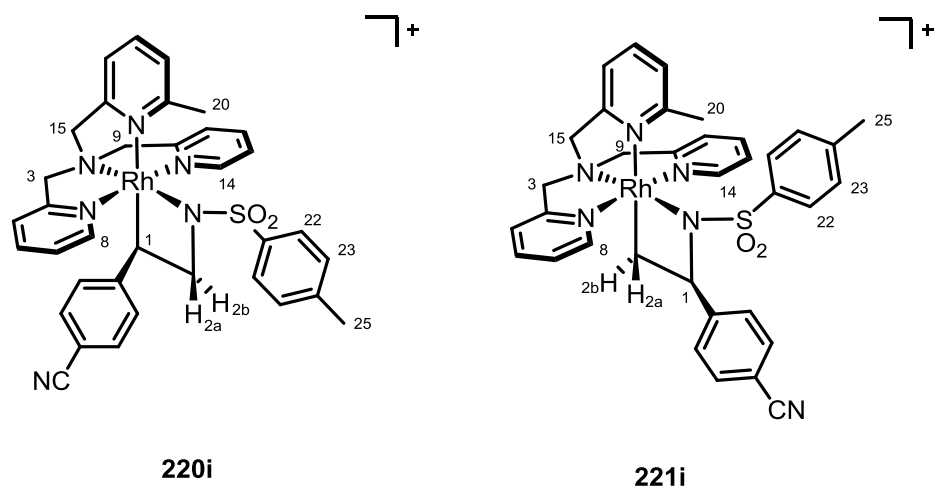
HPLC: **220g:221g** = 28:1; retention time = 65.2 min (220g), 68.9 min (221g)

HRMS (ESI): calc. $[\text{C}_{34}\text{H}_{35}\text{N}_5\text{O}_2\text{SRh}]^+$: 680.1570; found: 680.1567

220h (*major*) ¹H-NMR (400 MHz; CD₂Cl₂): δ 9.50 (d, ³J = 5.4 Hz, 1H, H8/14), 9.35 (d, ³J = 5.1 Hz, 1H, H8/14), 7.94-7.00 (m, H_{Py} + H_{Styr}), 4.99 (d[AB], ²J = 16.2 Hz, 1H, H3/9/15), 4.66-4.60 (m, 2H, H3/9/15), 4.33-4.25 (m, 2H, H2b + H3/9/15), 3.88-3.79 (m, 2H, H2a + H3/9/15), 3.18 (s, H20), 2.47 (s, H25).

HRMS (ESI): calc. $[\text{C}_{34}\text{H}_{34}\text{N}_6\text{O}_4\text{SRh}]^+$: 725.1411; found: 725.1417

[MeTPA-4-cyanostyrene-azarhodacyclobutane]Cl, 220/221i



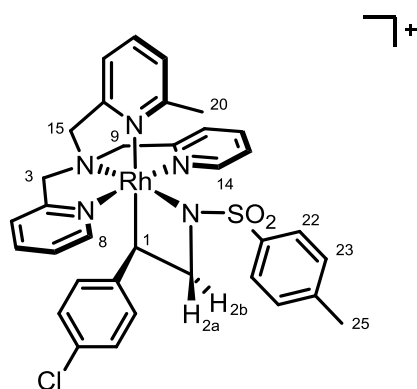
The title compound was synthesized from 4-cyanostyrene (10.3 μ L, 0.08 mmol, 1.5 equiv.), according to the general procedure.

220i (*major*) ^1H -NMR (400 MHz; CD_2Cl_2): δ 9.39 (d, $^3J = 6.0$ Hz, 1H, H8), 9.26 (d, $^3J = 5.7$ Hz, 1H, H14), 7.87 (t, $^3J = 7.6$ Hz, 1H), 7.70 (t, $^3J = 7.6$ Hz, 1H), 7.67 (d, $^3J = 8.1$ Hz, 2H), 7.62-7.56 (m, 2H), 7.45-7.34 (m, 4H) 7.20-7.08 (m, 3H), 7.04-6.92 (m, 3H), 5.01 (d[AB], $^2J = 16.0$ Hz, 1H, H3/9/15), 4.94 (d[AB], $^2J = 16.0$ Hz, 1H, H3/9/15), 4.69 (d[AB], $^2J = 16.0$ Hz, 1H, H3/9/15), 4.52 (d[AB], $^2J = 16.5$ Hz, 1H, H3/9/15), 4.48 (d[AB], $^2J = 16.5$ Hz, 1H, H3/9/15), 4.17-4.05 (m, 2H, H2), 3.74 (apparent dt, $^3J = 7.2$ Hz, $J = 3.1$ Hz, 1H, H1). 3.67 (d[AB], $^2J = 16.5$ Hz, 1H, H3/9/15), 3.03 (s, H20), 2.25 (s, H25).

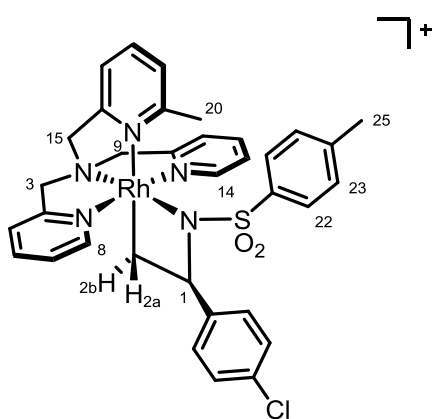
HPLC: **220i**:**221i** = 11:1; retention time = 50.4 min (220i), 51.8 min (221i)

HRMS (ESI): calc. $[\text{C}_{35}\text{H}_{35}\text{N}_6\text{O}_2\text{SRh}]^+$: 705.1522; found: 705.1519

[MeTPA-4-chlorostyrene-azarhodacyclobutane]Cl, 220/221j



220j



221j

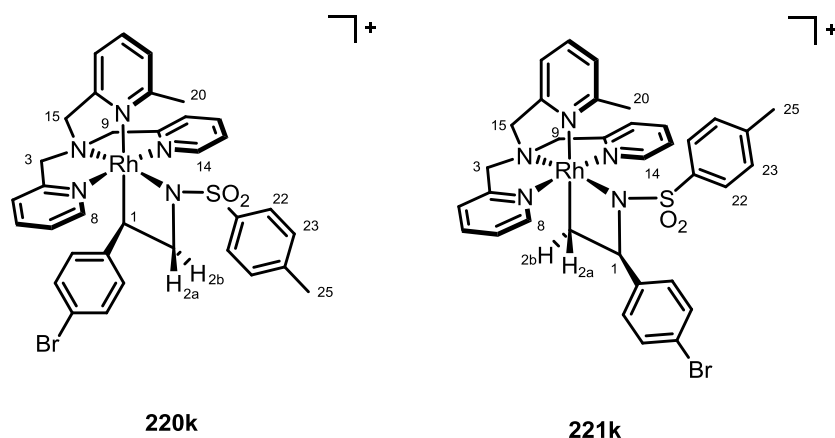
The title compound was synthesized from 4-chlorostyrene (9.6 μ L, 0.08 mmol, 1.5 equiv.) according to the general procedure.

220j (*major*) $^1\text{H-NMR}$ (400 MHz; CD_2Cl_2): δ 9.63 (d, $^3J = 5.5$ Hz, 1H, H8/14), 9.19 (d, $^3J = 5.5$ Hz, 1H, H8/14), 7.97-6.79 (m, $\text{H}_{\text{Py}} + \text{H}_{\text{Styr}}$), 5.19 (d[AB], $^2J = 14.5$ Hz, 1H, H3/9/15), 5.07 (d[AB], $^2J = 15.4$ Hz, 1H, H3/9/15), 4.92-4.67 (m, 3H, H3/9/15), 4.36 (d[AB], $^2J = 16.3$ Hz, 1H, H3/9/15), 4.26-4.14 (m, 1H, H2b), 3.99 (dd, $^2J = 11.7$, $^3J_{\text{trans}} = 9.0$, 1H, H2a) 4.17-4.05 (m, 2H, H2), 3.80 (apparent dt, $^3J = 8.1$ Hz, $J = 3.3$ Hz, 1H, H1), 3.16 (s, H20), 2.43 (s, H25).

HPLC: **220j**:**221j** = 11:1; retention time = 63.3 min (220j), 66.3 min (221j)

HRMS (ESI): calc. $[\text{C}_{34}\text{H}_{34}\text{N}_5\text{O}_2\text{SClRh}]^+$: 714.1176; found: 714.1177

[MeTPA-4-bromostyrene-azarhodacyclobutane]Cl, 220/221k



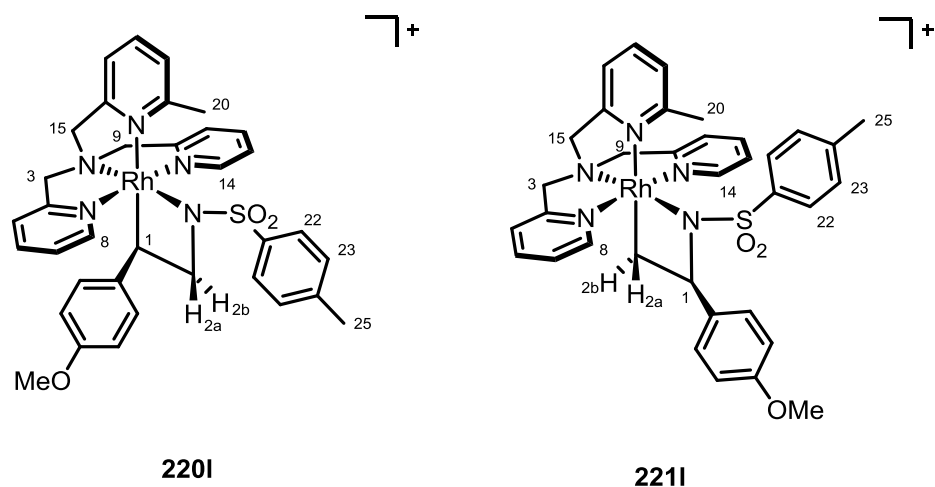
The title compound was synthesized from 4-bromostyrene (10.5 μ L, 0.08 mmol, 1.5 equiv.) according to the general procedure.

220k (*major*) $^1\text{H-NMR}$ (300 MHz; CD_2Cl_2): δ 9.64 (d, $^3J = 5.5$ Hz, 1H, H8/14), 9.18 (d, $^3J = 5.5$ Hz, 1H, H8/14), 8.05-6.90 (m, H_{Py} + H_{Styr}), 5.22 (d[AB], $^2J = 14.6$ Hz, 1H, H3/9/15), 5.06 (d[AB], $^2J = 16.3$ Hz, 1H, H3/9/15), 4.91 (d[AB], $^2J = 16.3$ Hz, 1H, H3/9/15), 4.77 (d[AB], $^2J = 15.7$ Hz, 1H, H3/9/15), 4.42 (d[AB], $^2J = 15.7$ Hz, 1H, H3/9/15), 4.26-4.16 (m, 1H, H2b), 4.17-4.05 (m, 2H, H2a), 3.98 (dd, $^2J = 11.2$, $^3J_{\text{trans}} = 8.4$ Hz, 1H, H2a), 3.78 (apparent dt, $^3J = 7.9$ Hz, $J = 3.4$ Hz, 1H, H1), 3.48 (d[AB], $^2J = 16.3$ Hz, 1H, H3/9/15), 3.16 (s, H20), 2.43 (s, H25).

HPLC: **220k:221k** = 18:1; retention time = 64.1 min (220k), 66.9 min (221k)

HRMS (ESI): calc. $[\text{C}_{34}\text{H}_{34}\text{N}_5\text{O}_2\text{SBrRh}]^+$: 758.0667; found: 758.0672

[MeTPA-4-methoxystyrene-azarhodacyclobutane]Cl, 220/221l



The title compound was synthesized from 4-methoxystyrene (10.4 μ L, 0.08 mmol, 1.5 equiv.) according to the general procedure.

220l (*major*) ^1H -NMR (600 MHz; CD_2Cl_2): δ 9.87 (d, $^3J = 5.2$ Hz, 1H, H8), 9.06 (d, $^3J = 5.2$ Hz, 1H, H14), 7.93 (t, $^3J = 7.4$ Hz, 1H), 7.79 (d, $^3J = 7.8$ Hz, 2H), 7.71-7.62 (m, 3H), 7.51 (t, $^3J = 6.5$ Hz, 1H) 7.41-7.27 (m, 5H), 7.21-7.10 (m, 3H), 7.02-6.86 (m, 2H), 5.09-4.94 (m, 4H, H3/9/15), 4.76 (d, $^2J = 15.7$ Hz, 1H, H3/9/15), 4.27-4.20 (m, 1H, H3/9/15), 4.17 (dd, $^2J = 10.4$, $^3J_{\text{cis}} = 6.6$, 1H, H2b), 3.93-3.83 (m, 2H, H2a + H1) 3.69 (s, 3H, -OMe) 3.16 (s, H20), 2.43 (s, H25).

HPLC: **220l:221l** = 14:1; retention time = 54.3 min (220l), 57.6 min (221l)

HRMS (ESI): calc. $[\text{C}_{35}\text{H}_{37}\text{N}_5\text{O}_3\text{SRh}]^+$: 694.1723; found: 694.1723

6 Preliminary Mechanistic Studies

In Chapters 4 and 5 the preparation and characterization of unsubstituted and substituted azarhodacyclobutanes has been discussed. In the formation of unsubstituted azarhodacyclobutanes **190**, **191**, **200**, **201** and **203**, it was shown that the selectivity for the formation of certain isomers could be influenced by the choice of solvent and oxidant. Furthermore, a different selectivity was observed, when the oxidation was performed on rhodium complexes bearing substituted olefins (**179**, **180**, **211**, **212**) instead of ethylene, under otherwise identical conditions.

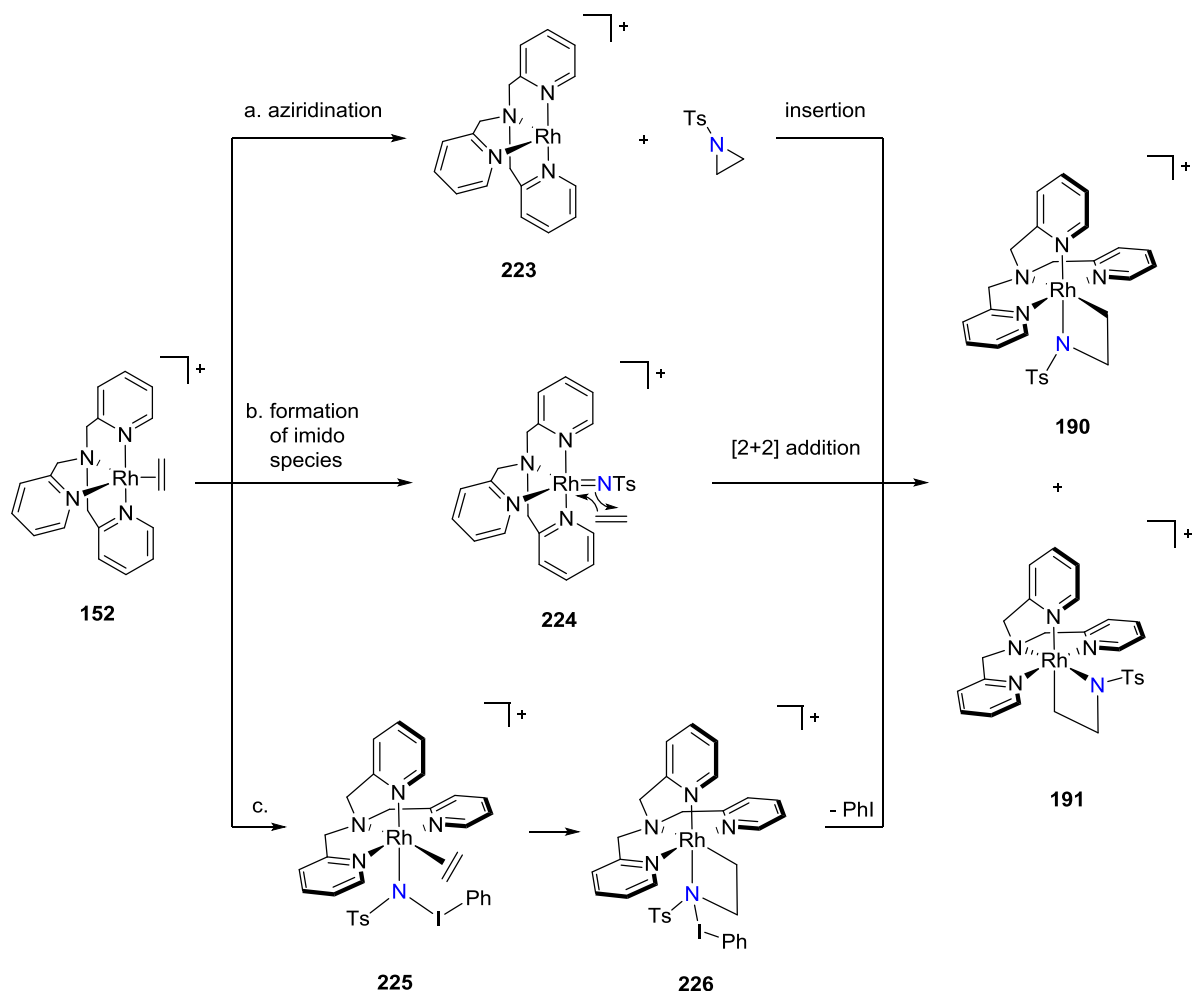
The mechanism of formation of unsubstituted rhodaoxetane **153** was studied in detail by Budzelaar *et al.*¹⁸⁶ However, at this time, we do not yet have a comprehensive mechanistic model for the formation of the corresponding azarhodacyclobutanes that is fully supported by experiment and calculations. In this chapter relevant experimental observations will be compiled and discussed in the light of three proposed mechanisms for the formation of these azametallacycles.

6.1 Three Possible Mechanisms

Among the most commonly postulated mechanisms of formation for azametallacyclobutanes are insertions of metals into aziridines and [2+2] cycloadditions of metal-imido species and olefins (Chapter 1.3).⁵

In the case of the oxidation of TPA-Rh-olefin complex **152** by PhINTs one can therefore envisage a direct aziridination of the olefin and a subsequent insertion of TPA-rhodium species **223** to form **190** and **191** (Scheme 6.1a). A similar insertion of rhodium into aziridines has been proposed by Alper²⁰⁶ and was later shown to be feasible for group 10 transition metals by Hillhouse (Ni),²⁴⁰ Wolfe (Pd)²⁴⁴ and Doyle (Ni, Chapter 1.3.2.1).²⁴⁵ At this point, the mechanism of formation of the aziridine from the bound olefin is not considered and the discussion will be focussed on whether the insertion can be observed and provide a possible pathway to the azarhodacyclobutane.

Alternatively, metal-imido species **224** can be formed from **152** and PhINTs which then undergoes a [2+2] cycloaddition with the free olefin (Scheme 6.1b).



Scheme 6.1 Proposed mechanisms for formation of azarhodacyclobutanes.

A similar mechanism was proposed by Halfen *et al.* for the Fe-catalyzed aziridination of olefins with PhINTs.²³⁸ They suggested initial formation of a Fe-tosylimido species (**126**) followed by [2+2] cyclization to form an azaferrocyclobutane (**127**) from which an aziridine was expelled after C-N reductive elimination (Scheme 1.42). Hillhouse *et al.* observed the formation of a transient azanickelacyclobutane by [2+2] addition of a Ni-imido compound and ethylene (Scheme 1.43).²³⁹ Through theoretical studies, Cundari furthermore validated the thermodynamic feasibility of cycloadditions between Ni-imido species and free olefins.²⁴¹

In addition, a mechanism akin to formation of rhodaoxetane **153** can be considered (Scheme 1.25).¹⁸⁶ In analogy to formation of Rh(III)-hydroxo-ethylene compound **72**, an

adduct of **152** and PhINTs can be formed, in which ethylene is still coordinated to rhodium (**225**). Ring-closure would then lead to compound **226**, which is transformed into the final azarhodacyclobutane through elimination of phenyliodide (PhI, Scheme 6.1c).

6.2 *Compilation of Relevant Experimental Data*

To date, we have not yet performed a systematic mechanistic study to fully elucidate the mechanism of azarhodacyclobutane formation. However, a number of experimental observations can help to gain first insights into the process of formation.

6.2.1 *Solvent Effect on Selectivity*

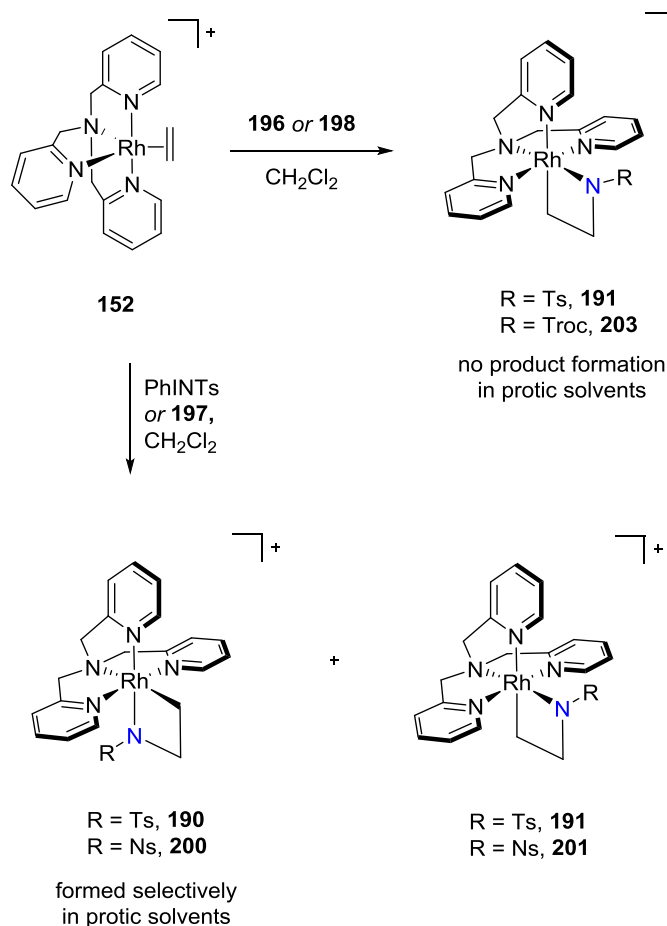
There is one obvious difference between the oxidation of ethylene by H₂O₂ versus PhINTs. In the former case, only one isomer is formed, compared with the formation of two isomers, **190** and **191**, in the latter case. Complexes **190** and **191** differ in the position of the ring nitrogen atom with respect to the central TPA amine. The isomers are afforded in varying ratios when the reaction is performed in non-protic solvents (Chapter 4.1.2). This effect seems to be independent of the polarity of the medium as e.g. reactions in acetonitrile ($\epsilon = 37.5$) and dichloromethane ($\epsilon = 8.9$) give identical results (**190**:**191** = 1:1.5). In contrast, selectivity for isomer **190** is achieved when protic solvents are present. A mixture of 15% methanol in dichloromethane significantly shifts the ratio towards **190** (**190**:**191** = 6.7:1) and carrying out the oxidation in a 1:1 mixture of these solvents yields exclusive formation of **190** as determined by HPLC-MS. The latter is also observed in pure methanol. However, the yield of **190** is reduced in comparison to the reaction in dichloromethane.

Thus, protic solvents either strongly favour the formation of **190** or inhibit the formation of **191**. The decrease in yield of **190** during reaction in protic solvents suggests inhibition of the formation of **191** rather than an acceleration of the formation of **190**. However, this is speculative.

6.2.2 *Effect of Oxidants on Selectivity*

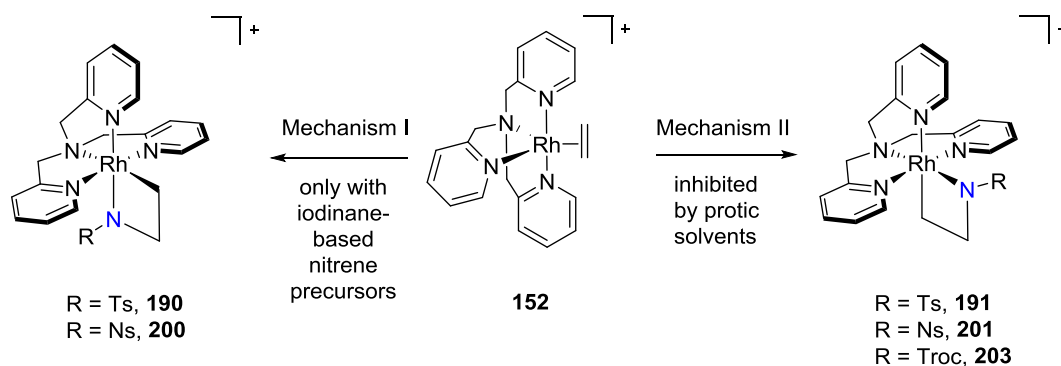
We have shown that oxidation with PhINTs and the nosyl-analogue, PhINNs (**197**), gave rise to a mixture of isomers when performed in aprotic solvents. In contrast, when tosyl

azide, **196**, or the carbamate-based nitrene precursor **198** were employed, only the isomer in which the ring nitrogen atom is trans to the central amine in TPA (**191** and **203** respectively) is formed (Chapter 4.2). When **196** or **198** were employed in methanol, no azarhodacyclobutane products were formed (Scheme 6.2).



Scheme 6.2 Different selectivity depending on oxidant.

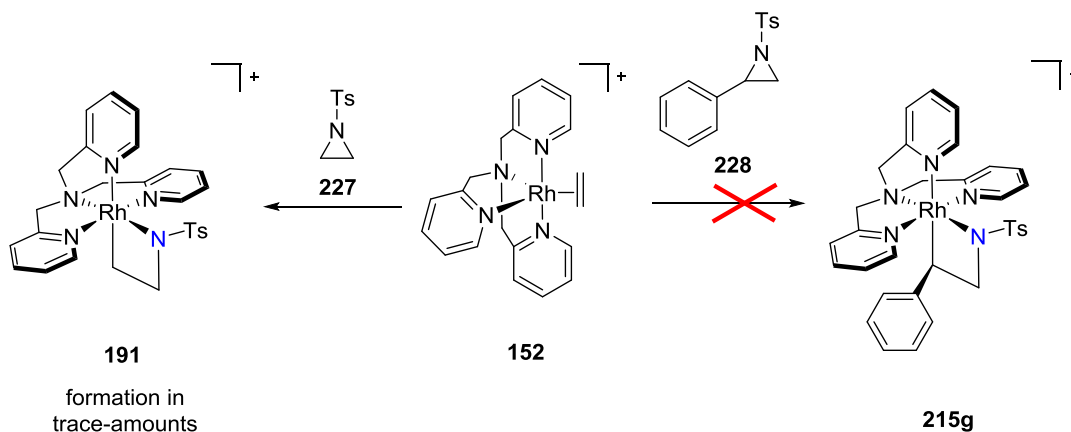
One possible explanation for the combined data so far involves two independent mechanisms for the formation of either isomer. Mechanism I leads to isomers **190** and **200** and is dependent on the employment of iodine-based nitrene precursors like PhINTs or PhINNs (**197**). Mechanism II, leading to **191**, **201** and **203**, is in effect with all nitrene precursors studied but is inhibited by protic solvents. When nitrene precursors based on hypervalent iodine like PhINTs or PhINNs (**197**) are used in aprotic solvents both mechanisms are effective at comparable rates (Scheme 6.3).



Scheme 6.3 Two different mechanisms are responsible for formation of the different isomers.

6.2.3 Attempts to Effect Insertion into Aziridines

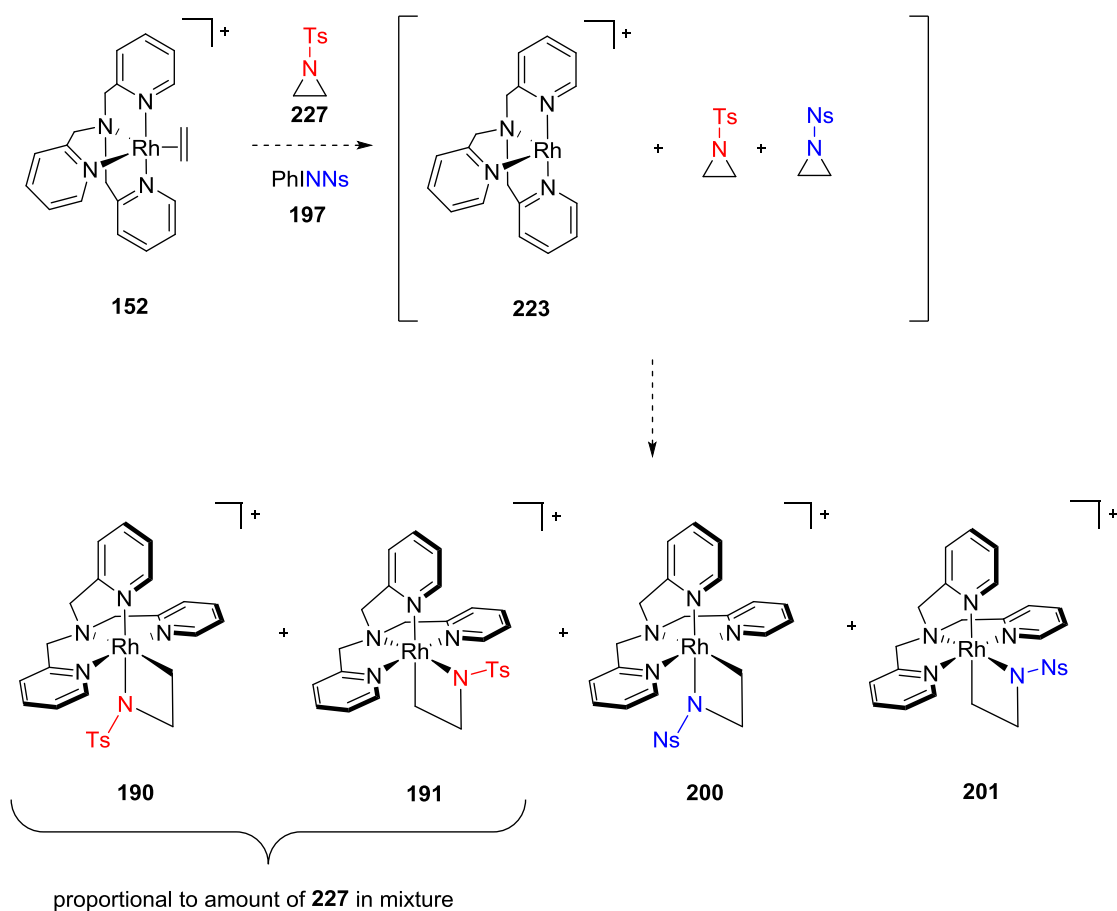
In order to test whether a mechanism was in operation involving formation of an aziridine and subsequent insertion of the Rh center (Scheme 6.1a), we exposed TPA-Rh-ethylene complex **152** to *N*-tosylaziridine, **227**, and *N*-tosylphenylaziridine, **228** (Scheme 6.4). A solution of **152** in CD_2Cl_2 remained unchanged for 12 hours when treated with **227**. After 24 hours, the ^1H NMR spectrum of the reaction mixture showed minor peaks that matched **191** in a mixture with otherwise decomposed products. At the same time, mass spectrometric analysis showed a small signal at 590 m/z corresponding to the azarhodacyclobutane. Conversely, a mixture of **152** and the substituted aziridine **228** showed only decomposition products after 24 hours without generation of the corresponding azarhodacyclobutane **215g**.



Scheme 6.4 Attempt to effect Rh insertion into aziridines

While insertion of TPA-rhodium complex **152** into unsubstituted tosylaziridine **227** seems to be feasible, the rate of the reaction compares poorly to the almost instantaneous formation of **190** and **191** under standard reaction conditions. Generation of the substituted azarhodacyclobutane **215g** is not observed at all through exposure to the corresponding aziridine which is otherwise complete after 12 hours under standard conditions. It has to be noted, that insertion of the “naked” TPA-Rh species **223** could occur at a significantly increased rate. However, the intermediate formation of an aziridine could at no time be observed by ^1H NMR during the course of the oxidation of **152** by PhINTs. It is thus questionable whether such a mechanism is in effect here but further studies have to be performed to conclusively rule out this possibility.

One potential experiment to further test this option involves the simultaneous exposure of **152** to tosylaziridine (**227**) and PhINNs (**197**). If indeed a fast aziridination event is occurring which produces an aziridine along with TPA-Rh species **223**, a mixture of tosyl and nosyl-substituted azarhodacyclobutanes should result (Scheme 6.5). The composition of this mixture would be directly related to the amount of tosylaziridine present in the starting mixture. If on the other hand, the product mixture consists predominantly of the nosyl-azarhodacyclobutanes **200** and **201**, evidence would further refute this pathway.

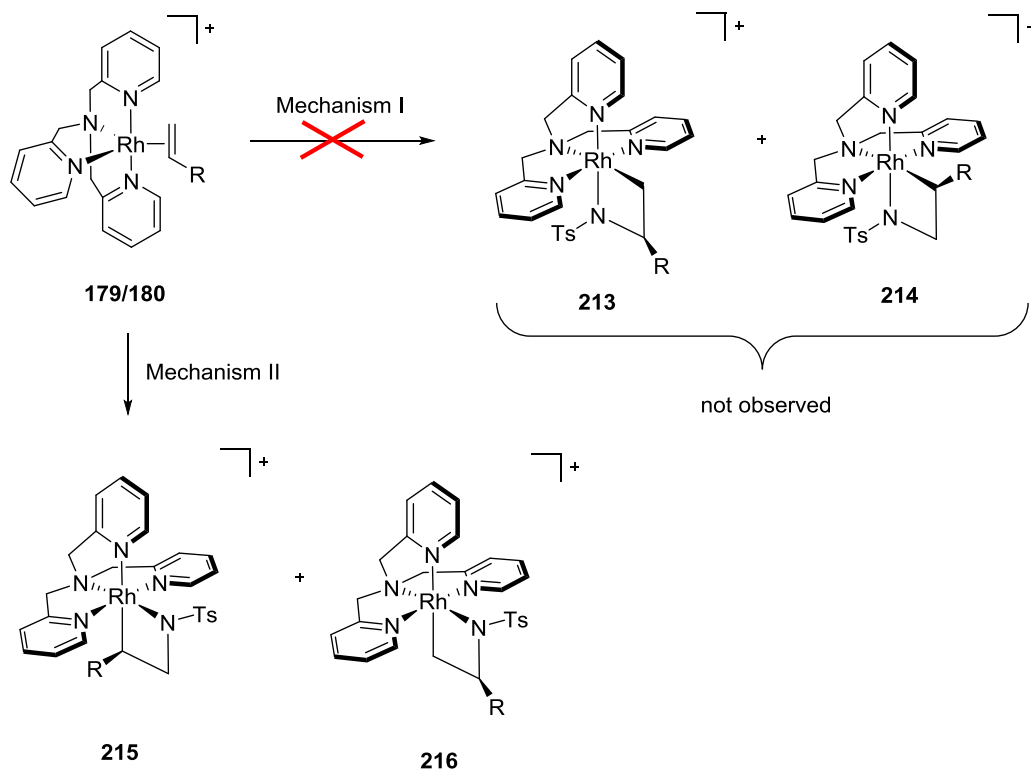


Scheme 6.5 Experiment to test whether aziridine insertion is occurring.

6.2.4 Observations in the Oxidation of Substituted Olefin Complexes

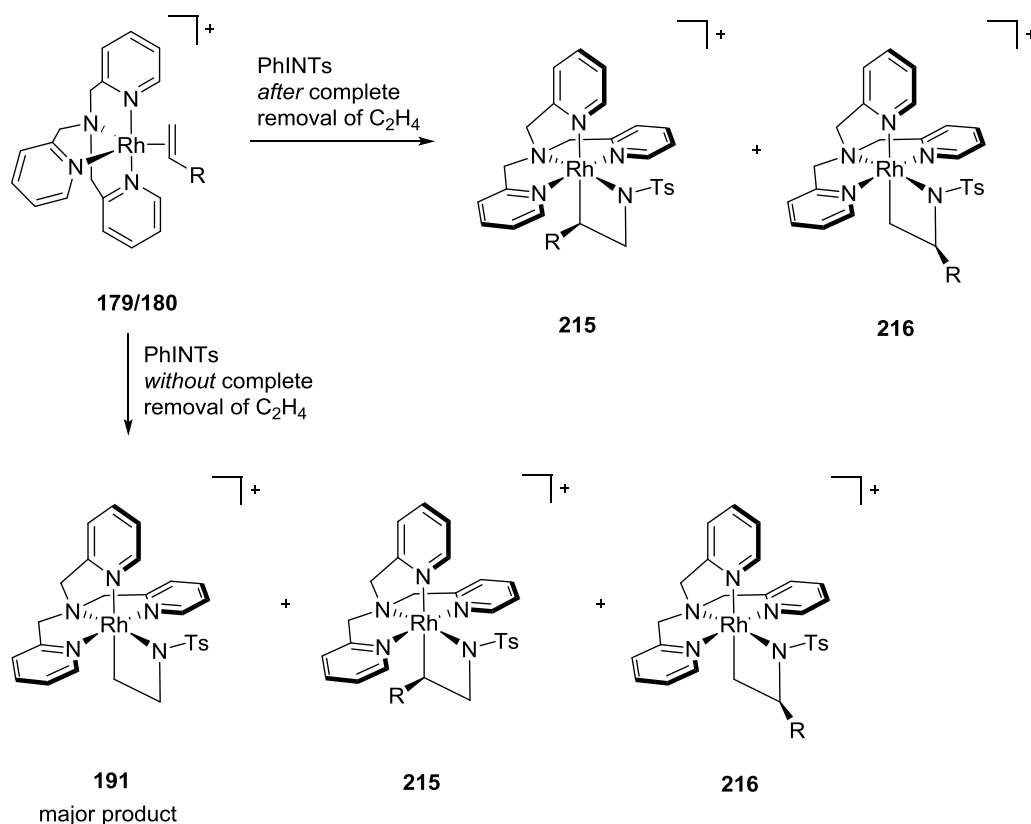
In the preparation of the substituted azametallacyclobutanes reported in Chapter 5, another important observation was made. When exposing the TPA-rhodium complexes bearing substituted olefins (**179**, **180**) in CH_2Cl_2 to the hypervalent iodine based oxidant PhINTs, only two isomers (**215**, **216**) are formed. Both have a configuration analogous to **191** but differ in the position of the olefin substituent (R). The isomers **213** and **214**, with configuration analogous to **190**, are not observed within the limits of detection (NMR spectroscopy and HPLC-MS). Although the criteria elaborated for mechanism I (iodinane based oxidant) above are met, only products following the pathway of mechanism II are generated (Scheme 6.6). When the oxidation was attempted in methanol, a complex mixture of unidentified products was produced indicating inhibition of both mechanisms. It therefore

seems that in the case of oxidation of substituted olefin complexes **179** and **180**, mechanism I is inhibited.



Scheme 6.6 Selectivity in the oxidation of substituted olefin complexes **179** and **180**.

In addition, the formation of an unsubstituted azarhodacyclobutane was observed when ethylene was not completely removed from the reaction mixture containing **179** and **180** (Scheme 6.7). Complete exchange of ethylene for the substituted olefin could be achieved even without the removal of ethylene as determined by ^1H NMR spectroscopy. However, as long as ethylene was still present in solution and the headspace of the reaction vessel, a significant amount of unsubstituted azarhodacyclobutane **191** was found in the product mixture. In case of styrene derivatives **179g-l**, the majority of the product formed was **191** even after prior full olefin exchange. Notably, the isomeric unsubstituted azarhodacyclobutane **190** was not found in the product mixture.



Scheme 6.7 Formation of unsubstituted azarhodacyclobutane **191**

if ethylene is not completely removed prior to oxidation.

NOESY spectra showed fast chemical exchange between the free and the coordinated substituted olefin in **179a** and **180a** (Figure 3.3). This exchange was not observed with the free ethylene still in solution. This data and the complete absence of any signals for bound ethylene in the mixture of **179/180** indicate that **191** (and all other isomers with the same general configuration) is, thus, formed from a reaction with the free olefin as e.g. a [2+2] cycloaddition described in Scheme 6.1b. This would require the formation of a Rh-imido species **224**. However, an oxidation of the coordinated olefin cannot be completely ruled out based on the existing data. Equilibrium between **152** and **179/180** could still exist even though it cannot be detected with the methods employed. Under Curtin Hammett conditions, a low energy barrier from **152** to **191** compared to a high activation energy for the transformation of **179/180** to **215/216** can produce the same results as observed here (Figure 6.1). To test this possibility, temperature studies will have to be performed. If Curtin

Hammett conditions apply, lowering the reaction temperature should increase the formation of **191** while raising the temperature should increase formation of the substituted azarhodacyclobutanes **215** and **216**.

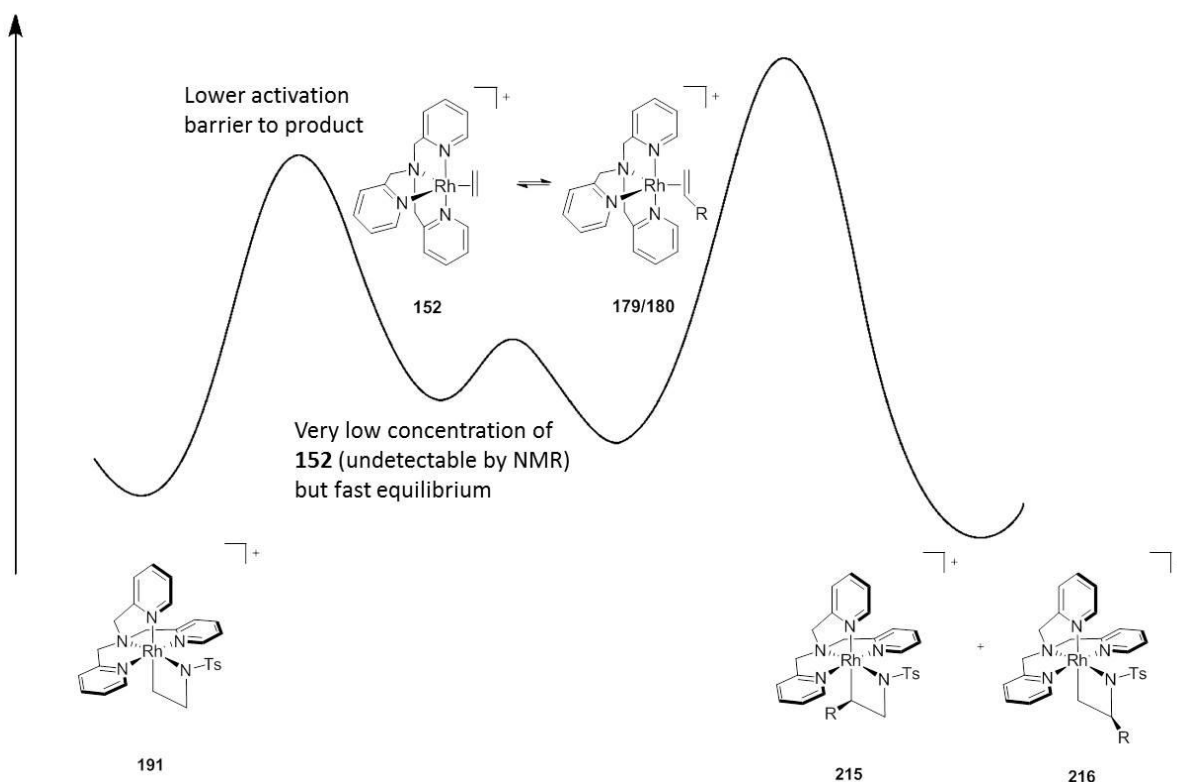
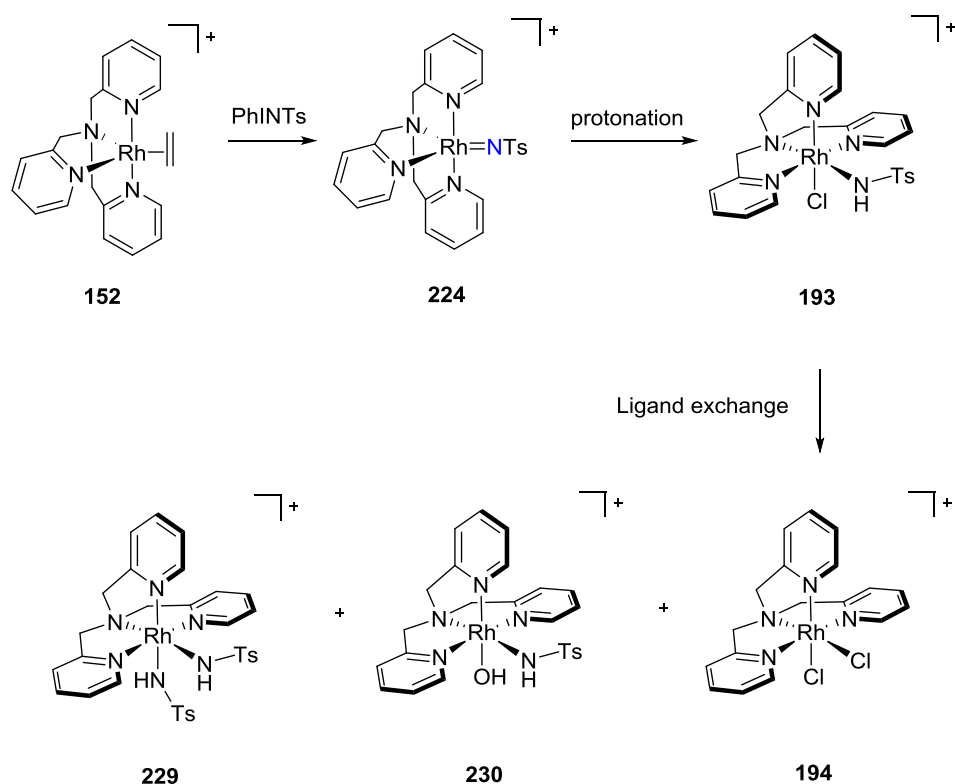


Figure 6.1 Curtin Hammett conditions could explain formation of **191**, even though **152** cannot be detected in the starting mixture.

6.2.5 Analysis of By-Products

A study of the by-products formed in the reaction can give additional insight into the mechanisms at work. Three by-products have been fully characterized (Figure 4.4.). The σ -ethyl complex **192** has already been reported by De Bruin as a result of protonation of the ethylene fragment in **152** in the presence of chloride.¹⁸⁷ Complex **193** on the other hand, is unique to the oxidations with nitrene precursors. It can be hypothesized that it is generated by protonation of TPA-Rh-imido species **224** which is formed from **152** and PhINTs (Scheme 6.8).



Scheme 6.8 Possible formation of different by-products.

Compound **194** could then arise from ligand exchange in **193**. Likewise, compounds **229** and **230** (for which corresponding signals can be found in MS) could be formed from **194**. A by-product similar to **193** was formed in the reaction of **152** with azide **206a** (Scheme 4.7).

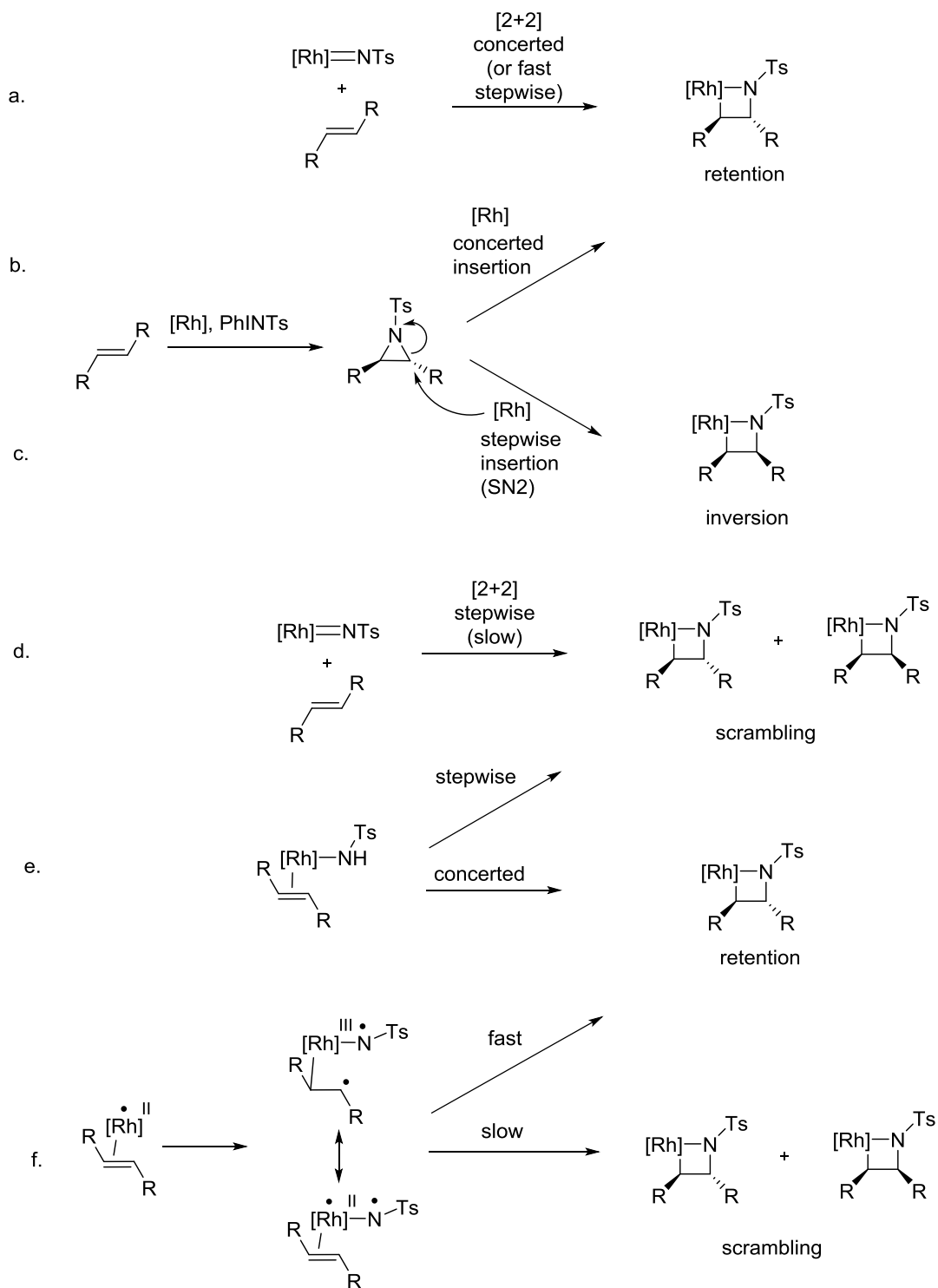
Early transition metal imido compounds are known to be very reactive and perform C-H activations and cycloadditions.^{213,214,233,234} As mentioned earlier, [2+2] cycloadditions have also been reported for late transition metal imido species.²³⁹ The number of by-products formed in the oxidation with PhINTs could be a further indication of the intermediacy of a highly reactive imido species.

6.2.6 Oxidation of a Symmetrically Substituted TPA-Rh Olefin Complex

The oxidation of complex **179m** bearing the symmetrically di-substituted diethylfumarate as olefinic ligand yielded a crude reaction mixture with two products with the appropriate m/z in a 98:2 ratio as determined by HPLC-MS analysis. The major product

was identified as compound **218** (Figure 5.6) in which the trans relationship of the ester substituents is retained. While the minor isomer could not be isolated and characterized, it is plausible to assume that it is compound **219** where the ester substituents are cis to each other. This observation can give additional mechanistic insight.

Retention of trans stereochemistry would be expected if the mechanism were to involve either a [2+2] cycloaddition of an imido species and an olefin or concerted one-atom insertion into an initially formed aziridine (Scheme 6.9a and b).⁵ Formation of a product with a cis configuration would be expected if olefin aziridination occurred, followed by oxidative addition of the aziridine via a S_N2-type mechanism (Scheme 6.9c).^{240,244} In addition, a mixture of cis and trans products could be formed if the reaction occurs in a stepwise fashion (e.g., breaking of the double bond and the formation of the two new σ bonds is sufficiently slow to allow bond rotation during the oxidation process, Scheme 6.9d). Additionally, a mechanism akin to the formation of oxarhodacyclobutanes **153** where the oxidation happens on the bound olefin could also be envisaged in a stepwise (scrambling) or concerted (retention) fashion (Chapter 1.2.2.3, Scheme 6.9e).



Scheme 6.9 Stereochemical implications of the reaction mechanism.

Finally, a radical mechanism can also be considered. Some hypervalent iodine(III) reagents can act as single electron oxidants.³²¹ If PhINTs is likewise able to perform a single electron oxidation, a transient Rh(II)-olefin species could be generated. Related work on open shell group 9 complexes was reported by de Bruin.³²²⁻³²⁹ The intermediate complexes thus generated could exhibit radical character on the metal or the olefin ligand. After coordination of the reduced tosyl-amino fragment radical recombination could yield the corresponding azarhodacyclobutanes. If this recombination was fast,³²⁸ retention of configuration would be observed, whereas a slow recombination would lead to scrambling (Scheme 6.9f). At this point, we have not yet undertaken any experiments considering the possibility of a radical pathway. To further test this option, radical inhibitors will have to be added to the reaction mixture to see if the reaction outcome is affected. Another possibility is the employment of vinylcyclopropane as olefin. An opening of the cyclopropane would indicate the involvement of a radical pathway. Monitoring the reaction by EPR can furthermore give information of the emergence of unpaired spins along the reaction coordinate.

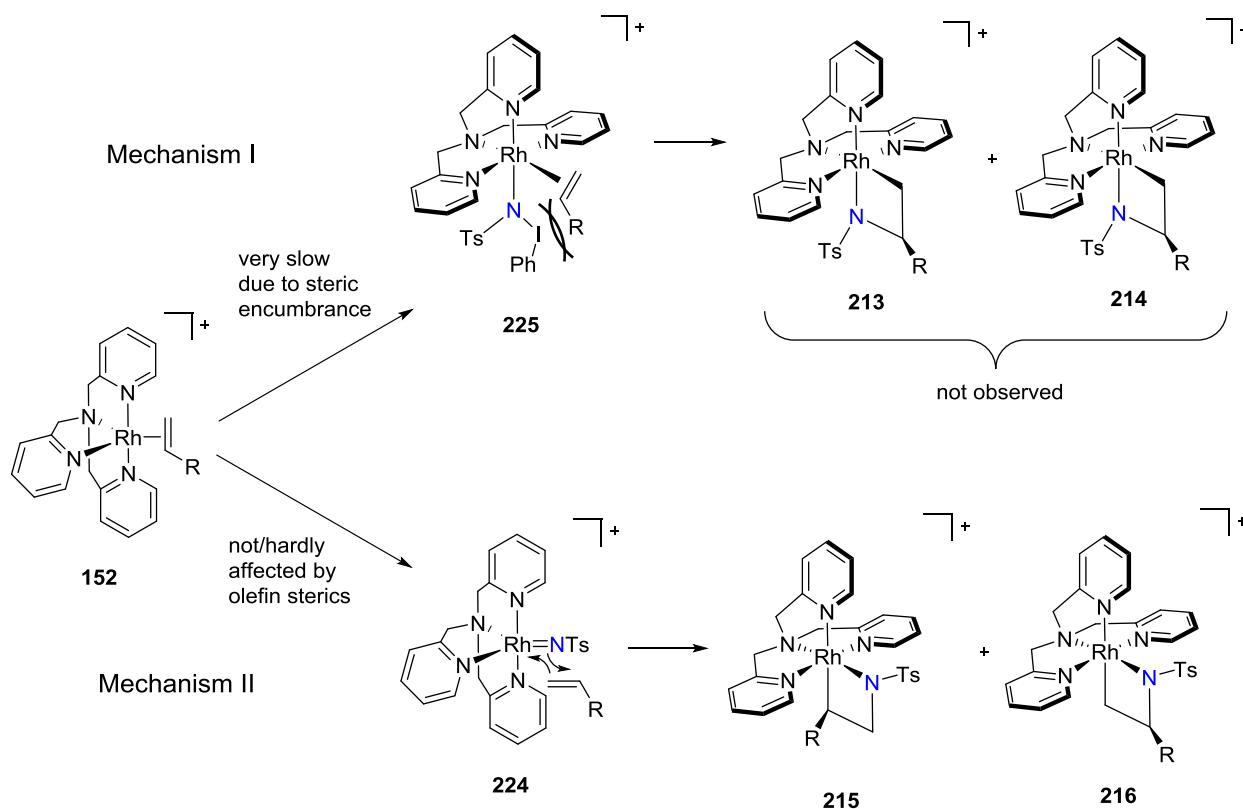
The major product formed shows a retention of the configuration. This retention of the stereochemistry excludes nucleophilic ring opening of an aziridine under which inversion of one stereocenter would have occurred (Scheme 6.9c.).

6.3 Reconciliation of Experimental Data and Proposed Mechanisms

Considering all data presented above, we propose that mechanism II, which leads to formation of isomer **191** and analogues, proceeds through rhodium imido compound **224** according to Scheme 6.1b. This intermediate can be formed from all nitrene precursors employed. Specifically, organic azides have been demonstrated to readily form Ni-imido species from a metal-arene complex.²³⁹ The selectivity for mechanism II when tosylazide (**196**) is employed as oxidant can be rationalized by this behaviour. The imido species **224** is quenched in protic solvents before it can undergo cycloaddition to the corresponding azametallacyclobutane. This explains the absence of isomers of type **191** and the formation of by-products like **193** when the reaction is performed in methanol.

In mechanism I, the oxidation appears to occur directly on the coordinated olefin as e.g. in the the formation of rhodaoxetane **153** (Scheme 6.1c). This assumption is based on the fact that isomers resulting from mechanism I – **190** and its analogues – have the same configuration as **153** with the heteroatom being cis to the central TPA amine. This pathway should be unaffected by protic solvents, which is also the case. Furthermore, only formation of **191** (next to **215** and **216**) is observed when substituted olefin complexes **179/180** are oxidized without prior removal of ethylene (Scheme 6.7). Isomer **190** could not be found. As discussed earlier, ethylene was only present free in solution but not bound in the form of complex **152** (according to NMR spectroscopy). Isomer **191** is expected to form through a [2+2] cycloaddition with the free olefin – a pathway which is still viable under these conditions. The lack of formation of isomer **190** in this process suggests that its formation needs to involve a bound ethylene species.

In the formation of substituted rhodaoxetanes described in Chapter 3 we had observed that the H₂O₂ based oxidation of the substituted olefin complexes **179** and **180** (1.5-2 h) was considerably slower than the oxidation of the unsubstituted complex **152** (minutes). The increased steric bulk of the bound olefin likely impedes the approach of the oxidant and the formation of the corresponding Rh(III)-hydroxo-olefin complex. If mechanism I is similar to the mechanism of rhodaoxetane formation, it would also likely be more sensitive to the steric properties of the olefins and oxidants than mechanism II. All oxidants employed are sterically more demanding than H₂O₂. The increased encumbrance of the olefins and oxidants combined could thus lead to a significant decrease in the reaction rate of mechanism I when substituted olefins are used as substrate. In comparison, formation of Rh-imido species **224** and the subsequent cycloaddition should be less (if at all) affected by the sterics of the olefins. This rationalization can be used to explain the absence of isomers **213** and **214** and exclusive formation of **215** and **216** in the oxidation of **179/180** in CD₂Cl₂ (Scheme 6.10).



Scheme 6.10 Possible effect of steric parameters on the reaction pathway with substituted olefins.

If mechanism II indeed follows a [2+2] pathway, the reaction rate should be first order in olefin concentration. In contrast, mechanism I would be independent of the olefin concentration. Thus, kinetic experiments which relate the concentration of the olefin to the reaction rate would be instructive for further elucidation. In addition, thorough theoretical investigations will provide insight into the energetic profiles of the various proposed reaction pathways.

7 Conclusions and Future Work

7.1 Summary and Conclusions

Oxa- and azarhodacyclobutanes have been proposed as reactive intermediates in a variety of transformations over the last few decades.⁴⁻⁶ Reactions where these structures are commonly invoked include olefin oxidation reactions, transformations of epoxides and aziridines, metathesis and coupling reactions among others. Oftentimes, the proposal of the intermediacy of oxa- and azarhodacyclobutanes is based on insufficient experimental and theoretical support and even had to be revoked in certain cases.^{107,113,116} In other cases however, oxa- and azarhodacyclobutanes could be prepared and isolated, allowing them to be subjected to further investigation. Nevertheless, systematic studies of such species remain scarce.

Our interest in these special compounds is two-fold. First, the ability to access a variety of oxa- and azarhodacyclobutanes in a controlled fashion allows deeper study of their formation and reactivity. This again enables more accurate assessments of the feasibility of their intermediacy in certain reactions. Equipped with these insights, the researcher is able to rationally design entirely new chemical transformations based on oxa- and azarhodacyclobutane intermediates. One can imagine for example, picking and choosing one way to form a heterometallacyclobutane selectively and another way to functionalize it, thus devising an unprecedented reaction pathway.

We have proposed such a new reaction based on a rhodaoxetane prepared before by De Bruin *et al.* In our envisaged carbohydroxylation protocol we propose the oxidation of a Rh-olefin complex to yield the corresponding oxarhodacyclobutane (rhodaoxetane) as a first step. The second step in the proposed catalytic cycle comprises of a transmetalation using an appropriate organometallic reagent. Finally, reductive elimination would liberate the carbohydroxylated product. With this protocol it would be possible to generate functionalized alcohols from simple olefin feedstock in a direct and modular fashion.

To this end, we have studied the reactivity of a previously reported rhodaoxetane towards organometallic reagents. We found that transmetalation was feasible with a wide

variety of alkenyl- and arylboronic acids and esters in good yields. The oxidation of the rhodium olefin complex and the subsequent transmetalation with organoboronic nucleophiles constitute two of three steps in the proposed catalytic cycle.²⁵²

The final step to close the cycle requires reductive elimination to form the carbohydroxylated products. A number of different approaches were tested to effect reductive elimination. Thermal treatment through conventional heating and microwave heating was inefficient as was the employment of electron-withdrawing additives. Similarly, when modifications were made to the ancillary ligand to increase reactivity by opening a coordination site or changing the steric and electronic properties of the ligand, reductive elimination did not occur. Lastly, combinations of the mentioned approaches were unsuccessful and ways to effect reductive elimination will thus remain under investigation.

The rhodaoxetanes were also found to react with electron poor alkynes by migratory insertion. The resulting six-membered oxametallacycle were fully characterized and it was found that insertion into the Rh-O bond had occurred.

Preparation of substituted rhodaoxetanes could be achieved by ligand exchange of ethylene for a variety of substituted olefins and subsequent oxidation by H₂O₂. The Rh-complexes bearing substituted olefins demonstrated selectivity for the configuration in which the olefin substituent was pointing away from the central pyridyl arm of the TPA ligand. After oxidation, only one out of four possible isomers was found to be formed within the limits of detection. The substituted rhodaoxetanes were fully characterized and it was shown that incorporation of the oxygen atom occurred exclusively on the more substituted carbon of the double bond.

The nitrogen analogues of rhodaoxetanes, azarhodacyclobutanes, were prepared from the same Rh-ethylene complex that served as starting material for formation of the rhodaoxetanes. Oxidation was performed with [*N*-(toluenesulfonyl)imino]phenyliodinane (PhINTs) and a mixture of two isomers was formed when the reaction was carried out in aprotic solvents. However, when protic solvents were employed, only one of the isomers was formed selectively.³⁰² Other nitrene precursors also successfully provided the corresponding azarhodacyclobutanes. Alternative iodine based oxidants produced results comparable to

PhINTs, while azide or carbamate-based nitrene precursors showed exclusive selectivity for one isomer. Thus, through the choice of protic reaction media paired with iodine based oxidants, one isomer could be selectively accessed while reaction in aprotic solvents with azide- or carbamate-based oxidants afforded the other isomer.

The azarhodacyclobutanes at hand showed remarkable chemical and thermal stability. They remained unchanged in boiling solutions of water or acetonitrile. Furthermore, no reactivity was observed with boronic acids, organozinc halides, alkynes, hydrogen gas, silanes, NaBH_4 and CO. Only in the presence of strong acid was the Rh-N bond cleaved, resulting in the formation of ring opened products.

Similar to the preparation of substituted rhodaoxetanes, azarhodacyclobutanes could be formed from rhodium complexes bearing substituted olefins. In all cases, one isomer was formed as the major or sole product. When styrene derivatives were used one regioisomer was also obtained as minor product in varying ratios. These ratios were found to be highly dependent on the steric properties of the ancillary ligand. When a more sterically demanding ancillary ligand was used, there was a significant increase in the ratio of major:minor product. In contrast to the substituted rhodaoxetanes, the heteroatom was preferentially incorporated on the less substituted carbon.

Preliminary mechanistic investigations on the formation of azarhodacyclobutanes allowed us to propose that the formation of two different isomers follows two independent mechanisms. One mechanism is only supported by iodine based nitrene precursors and the oxidation is suggested to happen on the coordinated olefin. The second mechanism appears to involve the formation of a Rh-imido species and subsequent $[2+2]$ cycloaddition with free olefin. The latter mechanism is inhibited by protic solvents.

In conclusion, this project, while being challenging in the experimental outworkings, has great potential to make significant contributions to the fundamental understanding of reactions in which oxa- and azametallacyclobutanes are proposed as intermediates. Some of the key insights are highlighted in the following. On several occasions we could testify to the remarkable stability of the compounds studied here. It is highly unusual e.g. that organometallic complexes are unaffected by refluxing in water or microwave heating to 180

°C. Furthermore, HPLC separation and purification of metal complexes is not a widely used technique due to the usual lability of such compounds. The array of advanced multidimensional and multinuclear NMR spectroscopy methods employed throughout the project will be instructive for further studies on related organometallic compounds. For example, the indirect elucidation of the Rh-N coupling constant in the azarhodacyclobutanes by $^1\text{H}/^{15}\text{N}$ HSQC is a powerful way to obtain structural information of nitrogen containing organometallic species without the need of ^{15}N labelling.

Probably the project's greatest appeal, however, is the opportunity to design entirely new reactions based on oxa- and azarhodacyclobutanes. The work presented herein constitutes a solid foundation for further studies towards catalytic functionalization of olefinic substrates. It can be conceived that such functionalizations could occur in a highly modular fashion. Depending on the oxidant, incorporation of the heteroatom of choice (O or N) can be directed followed by the introduction of hydrogen, an organic moiety (as shown in Chapter 2 with organoboronic acids) or potentially another heteroatom, depending on the choice of reagent the metallacycle is treated with. This could increase the complexity and value of the olefinic substrates substantially in just one transformation.

7.2 Future Work

The work presented here is in many aspects only the beginning of a long road which will hopefully lead to a deeper understanding of the intriguing chemistry of oxa- and azarhodacyclobutanes. Each chapter contains suggestions for future directions and research which will be briefly compiled in the following.

In the proposed carbohydroxylation protocol involving a rhodaoxetane intermediate, the final step is yet unsolved. More substantial modifications of the ancillary ligand might facilitate this transformation. A number of other ligands that are derived from the general TPA scaffold have been prepared but not yet been tested. Alternatively, different ligand motifs can be pursued which have been reported to support the formation of metallaoxetanes⁵⁴ or to facilitate $\text{C}(\text{sp}^2)\text{--}\text{C}(\text{sp}^3)$ reductive elimination from Rh(III) centers.²⁸⁴

The observed insertion of electron deficient alkynes should be studied further to expand the substrate scope and study the selectivity when terminal alkynes are employed. The reactivity of the resulting complexes could reveal interesting new pathways like formation of substituted furans after reductive elimination or generation of acyclic vinyl ethers.

The lack of reactivity of the *N*-tosyl azarhodacyclobutanes should inspire further research towards the deprotection of the ring nitrogen atom. The alternative nitrene precursors employed are a first step in this direction. After removal of the protecting group a much increased reactivity is anticipated, specifically, transmetalation, insertion reactions and reductive cleavage by hydrogen or hydride sources.

Further study of the feasibility to use organic azides as oxidants for the formation of azarhodacyclobutanes is advisable. If successful, a variety of azarhodacyclobutanes with modular *N*-substitution would become accessible.

Finally, to fully elucidate the mechanism of formation of azarhodacyclobutanes, systematic studies will have to be undertaken. Kinetic studies to determine the order of the reaction in olefin will allow differentiating between a mechanism encompassing oxidation on the coordinated olefin and a mechanism involving free olefin. The possibility of fast aziridination and subsequent insertion of the metal can be assessed by an experiment in which the Rh-olefin complex is simultaneously treated with a nitrene precursor and an external aziridine with different *N*-substitution. A potential radical pathway will have to be assessed. Using radical inhibitors and vinylcyclopropane as olefinic substrate ("radical clock") should give insight whether radical species are present during the transformation. These experimental investigations should be accompanied by computational studies to obtain insight into possible transition states and activation energies of the different reaction pathways.

References

1. Bartholomew, C.; Farrauto, R., Eds.; In *Industrial Catalytic Processes*; Wiley-Interscience: Hoboken, NJ, 2006.
2. Beller, M.; Bolm, C., Eds.; In *Transition Metals For Organic Synthesis*; Wiley-VCH: Weinheim, 2008.
3. Anastas, P. T.; Warner, J. C. *Green Chemistry: Theory and Practice*; Oxford University Press: New York: 1998.
4. Dauth, A.; Love, J. A. *Chem. Rev.* **2011**, *111*, 2010.
5. Dauth, A.; Love, J. A. *Dalton Trans.* **2012**, *41*, 7782.
6. Jørgensen, K. A.; Schiøtt, B. *Chem. Rev.* **1990**, *90*, 1483.
7. Deubel, D. V.; Loschen, C.; Frenking, G. *Top. Organomet. Chem.* **2005**, *12*, 109.
8. Biilmann, E. *Ber. Dtsch. Chem. Ges.* **1900**, *33*, 1641.
9. Biilmann, E. *Ber. Dtsch. Chem. Ges.* **1902**, *35*, 2571.
10. Biilmann, E. *Ber. Dtsch. Chem. Ges.* **1910**, *43*, 568.
11. Schrauth, W.; Schoeller, W.; Struensee, R. *Ber. Dtsch. Chem. Ges.* **1910**, *43*, 695.
12. Park, W. R. R.; Wright, G. F. *J. Org. Chem.* **1954**, *19*, 1325.
13. De Pasquale, R. J. *J. Chem. Soc., Chem. Commun.* **1973**, 157.
14. Sharpless, K. B.; Teranishi, A. Y.; Bäckvall, J. E. *J. Am. Chem. Soc.* **1977**, *99*, 3120.
15. Jørgensen, K. A. *Chem. Rev.* **1989**, *89*, 431.

16. Rappe, A. K.; Goddard, W. A. *Nature* **1980**, 285, 311.
17. Rappe, A. K.; Goddard, W. A. *J. Am. Chem. Soc.* **1980**, 102, 5114.
18. Rappe, A. K.; Goddard, W. A., III. *J. Am. Chem. Soc.* **1982**, 104, 448.
19. Rappe, A. K.; Goddard, W. A. *J. Am. Chem. Soc.* **1982**, 104, 3287.
20. Walba, D. M.; DePuy, C. H.; Grabowski, J. J.; Bierbaum, V. M. *Organometallics* **1984**, 3, 498.
21. Kang, H.; Beauchamp, J. L. *J. Am. Chem. Soc.* **1986**, 108, 5663.
22. Bäckvall, J. E.; Young, M. W.; Sharpless, K. B. *Tetrahedron Lett.* **1977**, 18, 3523.
23. Schlecht, M. F.; Kim, H. *Tetrahedron Lett.* **1986**, 27, 4889.
24. Schlecht, M. F.; Kim, H. J. *J. Org. Chem.* **1989**, 54, 583.
25. Barrett, A. G. M.; Barton, D. H. R.; Tsushima, T. *J. Chem. Soc., Perkin Trans. 1* **1980**, 639.
26. Torrent, M.; Deng, L.; Ziegler, T. *Inorg. Chem.* **1998**, 37, 1307.
27. Torrent, M.; Deng, L. Q.; Duran, M.; Sola, M.; Ziegler, T. *Can. J. Chem.* **1999**, 77, 1476.
28. Tia, R.; Adei, E. *Inorg. Chem.* **2009**, 48, 11434.
29. Harvey, J. N.; Poli, R.; Smith, K. M. *Coord. Chem. Rev.* **2003**, 238-239, 347.
30. Zhang, W.; Loebach, J. L.; Wilson, S. R.; Jacobsen, E. N. *J. Am. Chem. Soc.* **1990**, 112, 2801.
31. Irie, R.; Noda, K.; Ito, Y.; Matsumoto, N.; Katsuki, T. *Tetrahedron Lett.* **1990**, 31, 7345.

32. Siddall, T. L.; Miyaaura, N.; Huffman, J. C.; Kochi, J. K. *J. Chem. Soc., Chem. Commun.* **1983**, 1185.
33. Samsel, E. G.; Srinivasan, K.; Kochi, J. K. *J. Am. Chem. Soc.* **1985**, *107*, 7606.
34. Srinivasan, K.; Michaud, P.; Kochi, J. K. *J. Am. Chem. Soc.* **1986**, *108*, 2309.
35. Dalton, C. T.; Ryan, K. M.; Wall, V. M.; Bousquet, C.; Gilheany, D. G. *Top. Catal.* **1998**, *5*, 75.
36. McGarrigle, E. M.; Gilheany, D. G. *Chem. Rev.* **2005**, *105*, 1563.
37. Hamada, T.; Fukuda, T.; Imanishi, H.; Katsuki, T. *Tetrahedron* **1996**, *52*, 515.
38. Palucki, M.; Finney, N. S.; Pospisil, P. J.; Gueler, M. L.; Ishida, T.; Jacobsen, E. N. *J. Am. Chem. Soc.* **1998**, *120*, 948.
39. Finney, N. S.; Pospisil, P. J.; Chang, S.; Palucki, M.; Konsler, R. G.; Hansen, K. B.; Jacobsen, E. N. *Angew. Chem., Int. Ed. Engl.* **1997**, *36*, 1720.
40. Jacobsen, E. N.; Deng, L.; Furukawa, Y.; Martinez, L. E. *Tetrahedron* **1994**, *50*, 4323.
41. Bailey, N. A.; Fenton, D. E.; Kitchen, S. J.; Lilley, T. H.; Williams, M. G.; Tasker, P. A.; Leong, A. J.; Lindoy, L. F. *J. Chem. Soc., Dalton Trans.* **1991**, 2989.
42. Gou, S.; Zeng, Q.; Yu, Z.; Qian, M.; Zhu, J.; Duan, C.; You, X. *Inorg. Chim. Acta* **2000**, *303*, 175.
43. Imanishi, H.; Katsuki, T. *Tetrahedron Lett.* **1997**, *38*, 251.
44. Roithová, J.; Schröder, D. *J. Am. Chem. Soc.* **2007**, *129*, 15311.
45. Roithová, J.; Schröder, D. *Chem. Rev.* **2010**, *110*, 1170.
46. Groves, J. T.; Nemo, T. E. *J. Am. Chem. Soc.* **1983**, *105*, 5786.

47. Groves, J. T.; Myers, R. S. *J. Am. Chem. Soc.* **1983**, *105*, 5791.
48. Ostovic, D.; Bruice, T. C. *Acc. Chem. Res.* **1992**, *25*, 314.
49. Curet-Arana, M. C.; Emberger, G. A.; Broadbelt, L. J.; Snurr, R. Q. *J. Mol. Catal. A: Chem.* **2008**, *285*, 120.
50. Chatterjee, D.; Basak, S.; Mitra, A.; Sengupta, A.; Le Bras, J.; Muzart, J. *Catal. Commun.* **2005**, *6*, 459.
51. Chatterjee, D.; Basak, S.; Riahi, A.; Muzart, J. *J. Mol. Catal. A: Chem.* **2006**, *255*, 283.
52. Chatterjee, D.; Basak, S.; Mitra, A.; Sengupta, A.; Le Bras, J.; Muzart, J. *Inorg. Chim. Acta*, **2006**, *359*, 1325.
53. Cinellu, M. A.; Minghetti, G.; Cocco, F.; Stoccoro, S.; Zucca, A.; Manassero, M. *Angew. Chem., Int. Ed.* **2005**, *44*, 6892.
54. Khusnutdinova, J. R.; Newman, L. L.; Zavalij, P. Y.; Lam, Y.; Vedernikov, A. N. *J. Am. Chem. Soc.* **2008**, *130*, 2174.
55. Wu, J.; Sharp, P. R. *Organometallics* **2009**, *28*, 6935.
56. Alper, H.; Des Roches, D. *Tetrahedron Lett.* **1977**, *18*, 4155.
57. Pietsch, M. A.; Russo, T. V.; Murphy, R. B.; Martin, R. L.; Rappe, A. K. *Organometallics* **1998**, *17*, 2716.
58. Kuehn, F. E.; Santos, A. M.; Herrmann, W. A. *Dalton Trans.* **2005**, 2483.
59. Tan, H.; Espenson, J. H. *Inorg. Chem.* **1998**, *37*, 467.
60. Jonsson, S. Y.; Adolfsson, H.; Bäckvall, J. *Chem. --Eur. J.* **2003**, *9*, 2783.

61. Sica, D.; Musumeci, D.; Zollo, F.; De Marino, S. *Eur. J. Org. Chem.* **2001**, 3731.
62. Gable, K. P.; AbuBaker, A.; Zientara, K.; Wainwright, A. M. *Organometallics* **1999**, *18*, 173.
63. Zhu, Z.; Espenson, J. H. *J. Mol. Catal. A: Chem.* **1995**, *103*, 87.
64. Zhu, Z.; Al-Ajlouni, A.; Espenson, J. H. *Inorg. Chem.* **1996**, *35*, 1408.
65. Gable, K. P.; Zhuravlev, F. A.; Yokochi, A. F. T. *Chem. Commun.* **1998**, 799.
66. Gable, K. P.; Brown, E. C. *Organometallics* **2000**, *19*, 944.
67. Ziegler, J. E.; Zdilla, M. J.; Evans, A. J.; Abu-Omar, M. M. *Inorg. Chem.* **2009**, *48*, 9998.
68. Gable, K. P.; Juliette, J. J. *J. Am. Chem. Soc.* **1995**, *117*, 955.
69. Chen, X.; Zhang, X.; Chen, P. *Angew. Chem., Int. Ed.* **2003**, *42*, 3798.
70. Zhang, X.; Chen, X.; Chen, P. *Organometallics* **2004**, *23*, 3437.
71. Zhang, X.; Narancic, S.; Chen, P. *Organometallics* **2005**, *24*, 3040.
72. Narancic, S.; Chen, P. *Organometallics* **2005**, *24*, 10.
73. Böseken, J.; de Graaff, C. *Recl. Trav. Chim. Pays-Bas Belg.* **1922**, *41*, 199.
74. Criegee, R. *Liebigs Ann. Chem.* **1936**, 522, 75.
75. Criegee, R.; Marchand, B.; Wannowius, H. *Liebigs Ann. Chem.* **1942**, 550, 99.
76. Schröder, M. *Chem. Rev.* **1980**, *80*, 187.
77. Hentges, S. G.; Sharpless, K. B. *J. Am. Chem. Soc.* **1980**, *102*, 4263.

78. Jacobsen, E. N.; Marko, I.; Mungall, W. S.; Schroeder, G.; Sharpless, K. B. *J. Am. Chem. Soc.* **1988**, *110*, 1968.
79. Göbel, T.; Sharpless, K. B. *Angew. Chem., Int. Ed.* **1993**, *32*, 1329.
80. Kolb, H. C.; Andersson, P. G.; Bennani, Y. L.; Crispino, G. A.; Jeong, K. S.; Kwong, H. L.; Sharpless, K. B. *J. Am. Chem. Soc.* **1993**, *115*, 12226.
81. Kolb, H. C.; Andersson, P. G.; Sharpless, K. B. *J. Am. Chem. Soc.* **1994**, *116*, 1278.
82. Kolb, H. C.; VanNieuwenhze, M. S.; Sharpless, K. B. *Chem. Rev.* **1994**, *94*, 2483.
83. Norrby, P.; Kolb, H. C.; Sharpless, K. B. *J. Am. Chem. Soc.* **1994**, *116*, 8470.
84. Berrisford, D. J.; Bolm, C.; Sharpless, K. B. *Angew. Chem., Int. Ed.* **1995**, *34*, 1059.
85. Nelson, D. W.; Gypser, A.; Ho, P. T.; Kolb, H. C.; Kondo, T.; Kwong, H. L.; McGrath, D. V.; Rubin, A. E.; Norrby, P. O.; Gable, K. P.; Sharpless, K. B. *J. Am. Chem. Soc.* **1997**, *119*, 1840.
86. Deubel, D. V.; Frenking, G. *Acc. Chem. Res.* **2003**, *36*, 645.
87. Sundermeyer, J. *Angew. Chem., Int. Ed. Engl.* **1993**, *32*, 1144.
88. Nakajima, M.; Tomioka, K.; Iitaka, Y.; Koga, K. *Tetrahedron* **1993**, *49*, 10793.
89. Tomioka, K.; Nakajima, M.; Koga, K. *Tetrahedron Lett.* **1990**, *31*, 1741.
90. Tomioka, K.; Nakajima, M.; Iitaka, Y.; Koga, K. *Tetrahedron Lett.* **1988**, *29*, 573.
91. Hanson, J. R.; Hitchcock, P. B.; Reese, P. B.; Truneh, A. *J. Chem. Soc., Perkin Trans. 1* **1988**, 1465.
92. Lohray, B. B.; Bhushan, V.; Nandan, E. *Tetrahedron Lett.* **1994**, *35*, 4209.

93. Schröder, M.; Constable, E. C. *J. Chem. Soc., Chem. Commun.* **1982**, 734.
94. Norrby, P. O.; Kolb, H. C.; Sharpless, K. B. *Organometallics* **1994**, 13, 344.
95. Norrby, P.; Becker, H.; Sharpless, K. B. *J. Am. Chem. Soc.* **1996**, 118, 35.
96. Corey, E. J.; Jardine, P. D.; Virgil, S.; Yuen, P. W.; Connell, R. D. *J. Am. Chem. Soc.* **1989**, 111, 9243.
97. Corey, E. J.; Noe, M. C. *J. Am. Chem. Soc.* **1993**, 115, 12579.
98. Corey, E. J.; Noe, M. C.; Sarshar, S. *J. Am. Chem. Soc.* **1993**, 115, 3828.
99. Corey, E. J.; Noe, M. C.; Grogan, M. J. *Tetrahedron Lett.* **1994**, 35, 6427.
100. Corey, E. J.; Noe, M. C.; Sarshar, S. *Tetrahedron Lett.* **1994**, 35, 2861.
101. Corey, E. J.; Guzman-Perez, A.; Noe, M. C. *J. Am. Chem. Soc.* **1995**, 117, 10805.
102. Corey, E. J.; Guzman-Perez, A.; Noe, M. C. *Tetrahedron Lett.* **1995**, 36, 3481.
103. Corey, E. J.; Noe, M. C.; Guzman-Perez, A. *J. Am. Chem. Soc.* **1995**, 117, 10817.
104. Corey, E. J.; Noe, M. C.; Shouzhong, L. *Tetrahedron Lett.* **1995**, 36, 8741.
105. Corey, E. J.; Noe, M. C. *J. Am. Chem. Soc.* **1996**, 118, 11038.
106. Corey, E. J.; Noe, M. C. *J. Am. Chem. Soc.* **1996**, 118, 319.
107. Corey, E. J.; Noe, M. C.; Grogan, M. J. *Tetrahedron Lett.* **1996**, 37, 4899.
108. Corey, E. J.; Noe, M. C.; Ting, A. Y. *Tetrahedron Lett.* **1996**, 37, 1735.
109. Noe, M. C.; Corey, E. J. *Tetrahedron Lett.* **1996**, 37, 1739.

110. Corey, E. J.; Zhang, J. H. *Org. Lett.* **2001**, *3*, 3211.
111. Jørgensen, K. A.; Hoffmann, R. *J. Am. Chem. Soc.* **1986**, *108*, 1867.
112. Jørgensen, K. A. *Tetrahedron Lett.* **1990**, *31*, 6417.
113. Pidun, U.; Böhme, C.; Frenking, G. *Angew. Chem., Int. Ed. Engl.* **1996**, *35*, 2817.
114. Torrent, M.; Deng, L.; Duran, M.; Sola, M.; Ziegler, T. *Organometallics* **1997**, *16*, 13.
115. Dapprich, S.; Ujaque, G.; Maseras, F.; Lledos, A.; Musaev, D. G.; Morokuma, K. *J. Am. Chem. Soc.* **1996**, *118*, 11660.
116. DelMonte, A. J.; Haller, J.; Houk, K. N.; Sharpless, K. B.; Singleton, D. A.; Strassner, T.; Thomas, A. A. *J. Am. Chem. Soc.* **1997**, *119*, 9907.
117. Norrby, P. O.; Rasmussen, T.; Haller, J.; Strassner, T.; Houk, K. N. *J. Am. Chem. Soc.* **1999**, *121*, 10186.
118. Gisdakis, P.; Rösch, N. *J. Am. Chem. Soc.* **2001**, *123*, 697.
119. Ujaque, G.; Maseras, F.; Lledos, A. *J. Am. Chem. Soc.* **1999**, *121*, 1317.
120. Drudis-Sole, G.; Ujaque, G.; Maseras, F.; Lledos, A. *Top. Organomet. Chem.* **2005**, *12*, 79.
121. Tia, R.; Adei, E. *THEOCHEM* **2011**, 977, 140.
122. Cappel, D.; Tuellmann, S.; Loschen, C.; Holthausen, M. C.; Frenking, G. *J. Organomet. Chem.* **2006**, 691, 4467.
123. Hoelscher, M.; Leitner, W.; Holthausen, M. C.; Frenking, G. *Chem. --Eur. J.* **2005**, *11*, 4700.
124. Freeman, F.; Kappos, J. C. *J. Org. Chem.* **1986**, *51*, 1654.

125. Walba, D. M.; Wand, M. D.; Wilkes, M. C. *J. Am. Chem. Soc.* **1979**, *101*, 4396.
126. Lee, D. G.; Chen, T. *J. Am. Chem. Soc.* **1989**, *111*, 7534.
127. Dash, S.; Patel, S.; Mishra, B. K. *Tetrahedron* **2009**, *65*, 707.
128. Haunschild, R.; Frenking, G. *J. Organomet. Chem.* **2008**, *693*, 3627.
129. Wiberg, K. B.; Wang, Y.; Sklenak, S.; Deutsch, C.; Trucks, G. *J. Am. Chem. Soc.* **2006**, *128*, 11537.
130. Ogino, T.; Yaezawa, H.; Yoshida, O.; Ono, M. *Org. Biomol. Chem.* **2003**, *1*, 2771.
131. Drees, M.; Strassner, T. *J. Org. Chem.* **2006**, *71*, 1755.
132. Strassner, T.; Busold, M. *J. Phys. Chem. A* **2004**, *108*, 4455.
133. Strassner, T.; Busold, M. *J. Org. Chem.* **2001**, *66*, 672.
134. Frunzke, J.; Loschen, C.; Frenking, G. *J. Am. Chem. Soc.* **2004**, *126*, 3642.
135. Yip, W.; Yu, W.; Zhu, N.; Che, C. *J. Am. Chem. Soc.* **2005**, *127*, 14239.
136. Pearlstein, R. M.; Davison, A. *Polyhedron* **1988**, *7*, 1981.
137. Herrmann, W. A.; Marz, D.; Herdtweck, E.; Schäfer, A.; Wagner, W.; Kneuper, H. -. *Angew. Chem., Int. Ed. Engl.* **1987**, *26*, 462.
138. Herrmann, W. A.; Kühn, F. E. *Acc. Chem. Res.* **1997**, *30*, 169.
139. Romao, C. C.; Kuhn, F. E.; Herrmann, W. A. *Chem. Rev.* **1997**, *97*, 3197.
140. Gable, K. P.; Phan, T. N. *J. Am. Chem. Soc.* **1993**, *115*, 3036.
141. Gable, K. P.; Phan, T. N. *J. Am. Chem. Soc.* **1994**, *116*, 833.

142. Gable, K. P.; Juliette, J. J. J.; Gartman, M. A. *Organometallics* **1995**, *14*, 3138.
143. Gable, K. P.; Juliette, J. J. J. *J. Am. Chem. Soc.* **1996**, *118*, 2625.
144. Haunschild, R.; Frenking, G. *Z. Naturforsch., B: Chem. Sci.* **2007**, *62*, 367.
145. Haunschild, R.; Frenking, G. *Z. Anorg. Allg. Chem.* **2008**, *634*, 2145.
146. Haunschild, R.; Frenking, G. *J. Organomet. Chem.* **2009**, *694*, 4090.
147. Monteyne, K.; Ziegler, T. *Organometallics* **1998**, *17*, 5901.
148. Deubel, D. V.; Frenking, G. *J. Am. Chem. Soc.* **1999**, *121*, 2021.
149. Haunschild, R.; Loschen, C.; Tuellmann, S.; Cappel, D.; Hoelscher, M.; Holthausen, M. C.; Frenking, G. *J. Phys. Org. Chem.* **2007**, *20*, 11.
150. Deubel, D. V.; Schlecht, S.; Frenking, G. *J. Am. Chem. Soc.* **2001**, *123*, 10085.
151. Deubel, D. V. *J. Phys. Chem. A* **2002**, *106*, 431.
152. Jiang, J.; Gao, F.; Hua, R.; Qiu, X. *J. Org. Chem.* **2005**, *70*, 381.
153. Man, M. L.; Lam, K. C.; Sit, W. N.; Ng, S. M.; Zhou, Z.; Lin, Z.; Lau, C. P. *Chem. --Eur. J.* **2006**, *12*, 1004.
154. Guo, C.; Song, J.; Jia, J.; Zhang, X.; Wu, H. *Organometallics* **2010**, *29*, 2069.
155. Molinaro, C.; Jamison, T. F. *J. Am. Chem. Soc.* **2003**, *125*, 8076.
156. Aye, K. T.; Ferguson, G.; Lough, A. J.; Puddephatt, R. J. *Angew. Chem.* **1989**, *101*, 765.
157. Aye, K. T.; Gelmini, L.; Payne, N. C.; Vittal, J. J.; Puddephatt, R. J. *J. Am. Chem. Soc.* **1990**, *112*, 2464.

158. Schlodder, R.; Ibers, J. A.; Lenarda, M.; Graziani, M. *J. Am. Chem. Soc.* **1974**, *96*, 6893.
159. Lenarda, M.; Ros, R.; Traverso, O.; Pitts, W. D.; Baddley, W. H.; Graziani, M. *Inorg. Chem.* **1977**, *16*, 3178.
160. Dall'Antonia, P.; Graziani, M.; Lenarda, M. *J. Organomet. Chem.* **1980**, *186*, 131.
161. McCoy, J. R.; Farona, M. F. *J. Mol. Catal.* **1991**, *66*, 51.
162. Halle, L. F.; Armentrout, P. B.; Beauchamp, J. L. *Organometallics* **1983**, *2*, 1829.
163. Ivin, K. J.; Reddy, B. S. R.; Rooney, J. J. *J. Chem. Soc., Chem. Commun.* **1981**, 1062.
164. Hamilton, J. G.; Mackey, O. N. D.; Rooney, J. J.; Gilheany, D. G. *J. Chem. Soc., Chem. Commun.* **1990**, 1600.
165. Tebbe, F. N.; Parshall, G. W.; Reddy, G. S. *J. Am. Chem. Soc.* **1978**, *100*, 3611.
166. Schiøtt, B.; Jørgensen, K. A. *J. Chem. Soc., Dalton Trans.* **1993**, 337.
167. Pine, S. H.; Zahler, R.; Evans, D. A.; Grubbs, R. H. *J. Am. Chem. Soc.* **1980**, *102*, 3270.
168. Lee, J. B.; Ott, K. C.; Grubbs, R. H. *J. Am. Chem. Soc.* **1982**, *104*, 7491.
169. Anslyn, E. V.; Grubbs, R. H. *J. Am. Chem. Soc.* **1987**, *109*, 4880.
170. Ho, S. C.; Hentges, S.; Grubbs, R. H. *Organometallics* **1988**, *7*, 780.
171. Beckhaus, R.; Strauss, I.; Wagner, T.; Kiprof, P. *Angew. Chem., Int. Ed. Engl.*, **1993**, *32*, 264.
172. Beckhaus, R.; Oster, J.; Sang, J.; Strauss, I.; Wagner, M. *Synlett* **1997**, 241.
173. Böhme, U.; Beckhaus, R. *J. Organomet. Chem.* **1999**, *585*, 179.

174. Schwartz, D. J.; Smith, M. R.,III; Andersen, R. A. *Organometallics* **1996**, *15*, 1446.
175. Whinnery, L. L., Jr.; Henling, L. M.; Bercaw, J. E. *J. Am. Chem. Soc.* **1991**, *113*, 7575.
176. Bazan, G. C.; Schrock, R. R.; O'Regan, M. B. *Organometallics* **1991**, *10*, 1062.
177. Hartwig, J. F.; Andersen, R. A.; Bergman, R. G. *J. Am. Chem. Soc.* **1989**, *111*, 2717.
178. Hartwig, J. F.; Bergman, R. G.; Andersen, R. A. *J. Am. Chem. Soc.* **1990**, *112*, 3234.
179. Hartwig, J. F.; Bergman, R. G.; Andersen, R. A. *Organometallics* **1991**, *10*, 3326.
180. Hartwig, J. F.; Bergman, R. G.; Andersen, R. A. *Organometallics* **1991**, *10*, 3344.
181. Milstein, D.; Calabrese, J. C. *J. Am. Chem. Soc.* **1982**, *104*, 3773.
182. Milstein, D. *J. Am. Chem. Soc.* **1982**, *104*, 5227.
183. Calhorda, M. J.; Galvao, A. M.; Unaleroglu, C.; Zlota, A. A.; Frolow, F.; Milstein, D. *Organometallics* **1993**, *12*, 3316.
184. Zlota, A. A.; Frolow, F.; Milstein, D. *J. Am. Chem. Soc.* **1990**, *112*, 6411.
185. De Bruin, B.; Boerakker, M. J.; Donners, J. J. J. M.; Christiaans, B. E. C.; Schlebos, P. P. J.; De Gelder, R.; Smits, J. M. M.; Spek, A. L.; Gal, A. W. *Angew. Chem., Int. Ed. Engl.* **1997**, *36*, 2064.
186. Budzelaar, P. H. M.; Blok, A. N. J. *Eur. J. Inorg. Chem.* **2004**, *2004*, 2385.
187. De Bruin, B.; Boerakker, M. J.; Verhagen, J. A. W.; De Gelder, R.; Smits, J. M. M.; Gal, A. W. *Chem. --Eur. J.* **2000**, *6*, 298.
188. De Bruin, B.; Boerakker, M. J.; De Gelder, R.; Smits, J. M. M.; Gal, A. W. *Angew. Chem., Int. Ed.* **1999**, *38*, 219.

189. De Bruin, B.; Verhagen, J. A. W.; Schouten, C. H. J.; Gal, A. W.; Feichtinger, D.; Plattner, D. *A. Chem. --Eur. J.* **2001**, *7*, 416.
190. Bruin, B. d.; Boerakker, M. J.; Brands, J. A.; Donners, J. J. J. M.; Donners, M. P. J.; Gelder, R. d.; Smits, J. M. M.; Gal, A. W.; Spek, A. L. *Chem. --Eur. J.* **1999**, *5*, 2921.
191. Tejel, C.; Ciriano, M. A.; Sola, E.; del Río, M. P.; Ríos-Moreno, G.; Lahoz, F. J.; Oro, L. A. *Angew. Chem., Int. Ed.* **2005**, *44*, 3267.
192. del Río, M. P.; Ciriano, M. A.; Tejel, C. *Angew. Chem., Int. Ed.* **2008**, *47*, 2502.
193. Tejel, C.; Ciriano, M. In *Catalysis and Organometallic Chemistry of Rhodium and Iridium in the Oxidation of Organic Substrates*; Meyer, F., Limberg, C., Eds.; Springer Berlin Heidelberg: 2007; Vol. 22, pp 97-124.
194. Mindiola, D. J.; Hillhouse, G. L. *J. Am. Chem. Soc.* **2002**, *124*, 9976.
195. Szuromi, E.; Shan, H.; Sharp, P. R. *J. Am. Chem. Soc.* **2003**, *125*, 10522.
196. Weliange, N. M.; Szuromi, E.; Sharp, P. R. *J. Am. Chem. Soc.* **2009**, *131*, 8736.
197. Wu, J.; Sharp, P. R. *Organometallics* **2008**, *27*, 1234.
198. Szuromi, E.; Wu, J.; Sharp, P. R. *J. Am. Chem. Soc.* **2006**, *128*, 12088.
199. Wu, J.; Sharp, P. R. *Organometallics* **2008**, *27*, 4810.
200. Fehlhammer, W. P.; Hirschmann, P.; Stolzenberg, H. *J. Organomet. Chem.* **1982**, *224*, 165.
201. Fehlhammer, W. P.; Hirschmann, P.; Voelkl, A. *J. Organomet. Chem.* **1985**, *294*, 251.
202. Fehlhammer, W. P.; Hirschmann, P.; Voelkl, A. *J. Organomet. Chem.* **1986**, *302*, 379.

203. McGuire, M. A.; Hegedus, L. S. *J. Am. Chem. Soc.* **1982**, *104*, 5538.
204. Hegedus, L. S.; McGuire, M. A.; Schultze, L. M.; Chen, Y.; Anderson, O. P. *J. Am. Chem. Soc.* **1984**, *106*, 2680.
205. Ikariya, T.; Ishikawa, Y.; Hirai, K.; Yoshikawa, S. *J. Organomet. Chem.* **1985**, *288*, 311.
206. Alper, H.; Urso, F.; Smith, D. J. H. *J. Am. Chem. Soc.* **1983**, *105*, 6737.
207. Calet, S.; Urso, F.; Alper, H. *J. Am. Chem. Soc.* **1989**, *111*, 931.
208. Hegedus, L. S.; De Weck, G.; D'Andrea, S. *J. Am. Chem. Soc.* **1988**, *110*, 2122.
209. Hegedus, L. S.; Montgomery, J.; Narukawa, Y.; Snustad, D. C. *J. Am. Chem. Soc.* **1991**, *113*, 5784.
210. Dumas, S.; Hegedus, L. S. *J. Org. Chem.* **1994**, *59*, 4967.
211. Beckhaus, R.; Wagner, M.; Wang, R. *Eur. J. Inorg. Chem.* **1998**, 253.
212. De With, J.; Horton, A. D.; Orpen, A. G. *Organometallics* **1993**, *12*, 1493.
213. Walsh, P. J.; Hollander, F. J.; Bergman, R. G. *J. Am. Chem. Soc.* **1988**, *110*, 8729.
214. Walsh, P. J.; Hollander, F. J.; Bergman, R. G. *Organometallics* **1993**, *12*, 3705.
215. Walsh, P. J.; Baranger, A. M.; Bergman, R. G. *J. Am. Chem. Soc.* **1992**, *114*, 1708.
216. Baranger, A. M.; Walsh, P. J.; Bergman, R. G. *J. Am. Chem. Soc.* **1993**, *115*, 2753.
217. Müller, T. E.; Beller, M. *Chem. Rev.* **1998**, *98*, 675.
218. Nobis, M.; Drießen-Hölscher, B. *Angew. Chem. Int. Ed.* **2001**, *40*, 3983.
219. Müller, T. E.; Hultsch, K. C.; Yus, M.; Foubelo, F.; Tada, M. *Chem. Rev.* **2008**, *108*, 3795.

220. Tobisch, S. *Chem. --Eur. J.* **2007**, *13*, 4884.
221. Sweeney, Z. K.; Salsman, J. L.; Andersen, R. A.; Bergman, R. G. *Angew. Chem. Int. Ed.* **2000**, *39*, 2339.
222. McGrane, P. L.; Jensen, M.; Livinghouse, T. *J. Am. Chem. Soc.* **1992**, *114*, 5459.
223. Haak, E.; Bytschkov, I.; Doye, S. *Angew. Chem. Int. Ed.* **1999**, *38*, 3389.
224. Siebeneicher, H.; Doye, S. *J. Prakt. Chem.* **2000**, *342*, 102.
225. Bytschkov, I.; Doye, S. *Eur. J. Org. Chem.* **2001**, *2001*, 4411.
226. Janssen, T.; Severin, R.; Diekmann, M.; Friedemann, M.; Haase, D.; Saak, W.; Doye, S.; Beckhaus, R. *Organometallics* **2010**, *29*, 1806.
227. Shi, Y.; Ciszewski, J. T.; Odom, A. L. *Organometallics* **2001**, *20*, 3967.
228. Johnson, J. S.; Bergman, R. G. *J. Am. Chem. Soc.* **2001**, *123*, 2923.
229. Ackermann, L.; Bergman, R. G. *Org. Lett.* **2002**, *4*, 1475.
230. Ackermann, L.; Bergman, R. G.; Loy, R. N. *J. Am. Chem. Soc.* **2003**, *125*, 11956.
231. Bexrud, J. A.; Beard, J. D.; Leitch, D. C.; Schafer, L. L. *Org. Lett.* **2005**, *7*, 1959.
232. Straub, B. F.; Bergman, R. G. *Angew. Chem. Int. Ed.* **2001**, *40*, 4632.
233. Bennett, J. L.; Wolczanski, P. T. *J. Am. Chem. Soc.* **1994**, *116*, 2179.
234. Bennett, J. L.; Wolczanski, P. T. *J. Am. Chem. Soc.* **1997**, *119*, 10696.
235. Bashall, A.; McPartlin, M.; Collier, P. E.; Mountford, P.; Gade, L. H.; Trösch, D. J. M. *Chem. Commun.* **1998**, 2555.

236. Trösch, D. J. M.; Collier, P. E.; Bashall, A.; Gade, L. H.; McPartlin, M.; Mountford, P.; Radojevic, S. *Organometallics* **2001**, *20*, 3308.
237. Klotz, K. L.; Slominski, L. M.; Hull, A. V.; Gottsacker, V. M.; Mas-Balleste, R.; Que, J., Lawrence; Halfen, J. A. *Chem. Commun.* **2007**, 2063.
238. Klotz, K. L.; Slominski, L. M.; Riemer, M. E.; Phillips, J. A.; Halfen, J. A. *Inorg. Chem.* **2009**, *48*, 801.
239. Laskowski, C. A.; Miller, A. J. M.; Hillhouse, G. L.; Cundari, T. R. *J. Am. Chem. Soc.* **2011**, *133*, 771.
240. Lin, B. L.; Clough, C. R.; Hillhouse, G. L. *J. Am. Chem. Soc.* **2002**, *124*, 2890.
241. Cundari, T. R.; Vaddadi, S. *J. Mol. Struct.* **2006**, *801*, 47.
242. Celik, M. A.; Haunschild, R.; Frenking, G. *Organometallics* **2010**, *29*, 1560.
243. Wolfe, J. P.; Ney, J. E. *Org. Lett.* **2003**, *5*, 4607.
244. Ney, J. E.; Wolfe, J. P. *J. Am. Chem. Soc.* **2006**, *128*, 15415.
245. Huang, C.; Doyle, A. G. *J. Am. Chem. Soc.* **2012**, *134*, 9541.
246. Galakhov, M. V.; Gomez, M.; Jimenez, G.; Royo, P.; Pellinghelli, M. A.; Tiripicchio, A. *Organometallics* **1995**, *14*, 2843.
247. Fandos, R.; Hernandez, C.; Lopez-Solera, I.; Otero, A.; Rodriguez, A.; Ruiz, M. J.; Terreros, P. *Organometallics* **2000**, *19*, 5318.
248. Fandos, R.; Hernandez, C.; Otero, A.; Rodriguez, A.; Ruiz, M. J.; Terreros, P. *Eur. J. Inorg. Chem.* **2003**, 493.
249. Scott, M. J.; Lippard, S. J. *Organometallics* **1997**, *16*, 5857.

250. Bashall, A.; Collier, P. E.; Gade, L. H.; McPartlin, M.; Mountford, P.; Pugh, S. M.; Radojevic, S.; Schubart, M.; Scowen, I. J.; Trösch, D. J. M. *Organometallics* **2000**, *19*, 4784.
251. Klein, D. P.; Hayes, J. C.; Bergman, R. G. *J. Am. Chem. Soc.* **1988**, *110*, 3704.
252. Dauth, A.; Love, J. A. *Angew. Chem., Int. Ed.* **2010**, *49*, 9219.
253. Sawada, Y.; Matsumoto, K.; Katsuki, T. *Angew. Chem., Int. Ed.* **2007**, *46*, 4559.
254. Bode, J. W.; Carreira, E. M. *J. Am. Chem. Soc.* **2001**, *123*, 3611.
255. Brandi, A.; Cicchi, S.; Paschetta, V.; Gomez Pardo, D.; Cossy, J. *Tetrahedron Lett.* **2002**, *43*, 9357.
256. Suga, S.; Kageyama, Y.; Babu, G.; Itami, K.; Yoshida, J. *Org. Lett.* **2004**, *6*, 2709.
257. Miller, S. P.; Morgan, J. B.; Nepveux, F. J., V.; Morken, J. P. *Org. Lett.* **2004**, *6*, 131.
258. Jiang, D.; Peng, J.; Chen, Y. *Org. Lett.* **2008**, *10*, 1695.
259. Kirchberg, S.; Fröhlich, R.; Studer, A. *Angew. Chem., Int. Ed.* **2009**, *48*, 4235.
260. Melhado, A. D.; Brenzovich, W. E.; Lackner, A. D.; Toste, F. D. *J. Am. Chem. Soc.* **2010**, *132*, 8885.
261. Fagnou, K.; Lautens, M. *Chem. Rev.* **2003**, *103*, 169.
262. Sakai, M.; Ueda, M.; Miyaura, N. *Angew. Chem., Int. Ed.* **1998**, *37*, 3279.
263. Mori, A.; Danda, Y.; Fujii, T.; Hirabayashi, K.; Osakada, K. *J. Am. Chem. Soc.* **2001**, *123*, 10774.
264. Yoshida, K.; Ogasawara, M.; Hayashi, T. *J. Am. Chem. Soc.* **2002**, *124*, 10984.

265. Sakai, M.; Hayashi, H.; Miyaura, N. *Organometallics* **1997**, *16*, 4229.
266. Hay-Motherwell, R. S.; Koschmieder, S. U.; Wilkinson, G.; Hussain-Bates, B.; Hursthouse, M. B. *J. Chem. Soc., Dalton Trans.* **1991**, 2821.
267. Bruns, S.; Sinnwell, V.; Voss, J. *Magn. Reson. Chem.* **2003**, *41*, 269.
268. Hoogervorst, W. J.; Goubitz, K.; Fraanje, J.; Lutz, M.; Spek, A. L.; Ernsting, J. M.; Elsevier, C. J. *Organometallics* **2004**, *23*, 4550.
269. Douglas, T. M.; Chaplin, A. B.; Weller, A. S. *Organometallics* **2008**, *27*, 2918.
270. Yu, J.; Kuwano, R. *Angew. Chem., Int. Ed.* **2009**, *48*, 7217.
271. Miyaura, N.; Suzuki, A. *Chem. Rev.* **1995**, *95*, 2457.
272. Johnson, J. B.; Rovis, T. *Angew. Chem. Int. Ed.* **2008**, *47*, 840.
273. Pérez-Rodríguez, M.; Braga, A. A. C.; Garcia-Melchor, M.; Pérez-Temprano, M. H.; Casares, J. A.; Ujaque, G.; de Lera, A. R.; Álvarez, R.; Maseras, F.; Espinet, P. *J. Am. Chem. Soc.* **2009**, *131*, 3650.
274. Byers, P. K.; Canty, A. J.; Crespo, M.; Puddephatt, R. J.; Scott, J. D. *Organometallics* **1988**, *7*, 1363.
275. Procelewska, J.; Zahl, A.; Liehr, G.; vanEldik, R.; Smythe, N. A.; Williams, B. S.; Goldberg, K. I. *Inorg. Chem.* **2005**, *44*, 7732.
276. Luedtke, A. T.; Goldberg, K. I. *Inorg. Chem.* **2007**, *46*, 8496.
277. Mann, G.; Shelby, Q.; Roy, A. H.; Hartwig, J. F. *Organometallics* **2003**, *22*, 2775.
278. Yamashita, M.; Hartwig, J. F. *J. Am. Chem. Soc.* **2004**, *126*, 5344.

279. Hartwig, J. F. *Inorg. Chem.* **2007**, *46*, 1936.
280. Watkins, S. E.; Craig, D. C.; Colbran, S. B. *J. Chem. Soc., Dalton Trans.* **2002**, *0*, 2423.
281. Hicks, R. G.; Koivisto, B. D.; Lemaire, M. T. *Org. Lett.* **2004**, *6*, 1887.
282. Kittaka, A.; Sugano, Y.; Otsuka, M.; Ohno, M. *Tetrahedron* **1988**, *44*, 2821.
283. Britovsek, G. J. P.; England, J.; White, A. J. P. *Inorg. Chem.* **2005**, *44*, 8125.
284. Gatard, S.; Celenligil-Cetin, R.; Guo, C.; Foxman, B. M.; Ozerov, O. V. *J. Am. Chem. Soc.* **2006**, *128*, 2808.
285. Amgoune, A.; Bourissou, D. *Chem. Commun.* **2011**, *47*, 859.
286. Yamamoto, Y.; Han, X.; Ma, J. *Angew. Chem., Int. Ed.* **2000**, *39*, 1965.
287. Boldog, I.; Munoz-Lara, F. J.; Gaspar, A. B.; Munoz, M. C.; Seredyuk, M.; Real, J. A. *Inorg. Chem.* **2009**, *48*, 3710.
288. Astner, J.; Weitzer, M.; Foxon, S. P.; Schindler, S.; Heinemann, F. W.; Mukherjee, J.; Gupta, R.; Mahadevan, V.; Mukherjee, R. *Inorg. Chim. Acta* **2008**, *361*, 279.
289. Cramer, R. *J. Am. Chem. Soc.* **1967**, *89*, 4621.
290. Price, D. W.; Drew, M. G. B.; Hii, K. K.; Brown, J. M. *Chem. --Eur. J.* **2000**, *6*, 4587.
291. Błażejewska-Chadyniak, P.; Kubicki, M.; Maciejewski, H.; Marciniak, B. *Inorg. Chim. Acta* **2003**, *350*, 603.
292. Fitch, J. W.; Osterloh, W. T. *J. Organomet. Chem.* **1981**, *213*, 493.
293. Choi, J.; Sakakura, T. *Organometallics* **2004**, *23*, 3756.

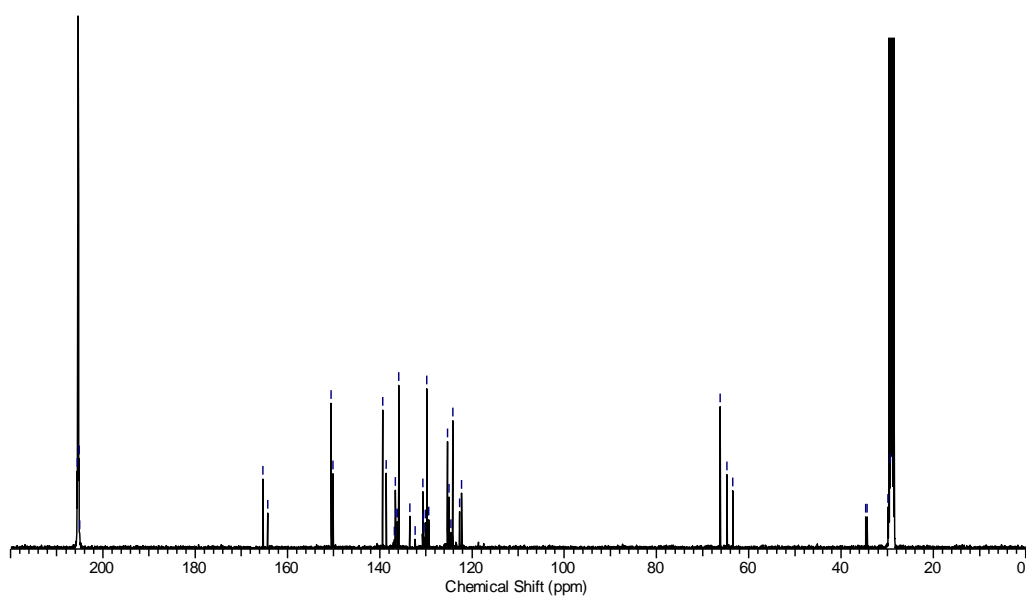
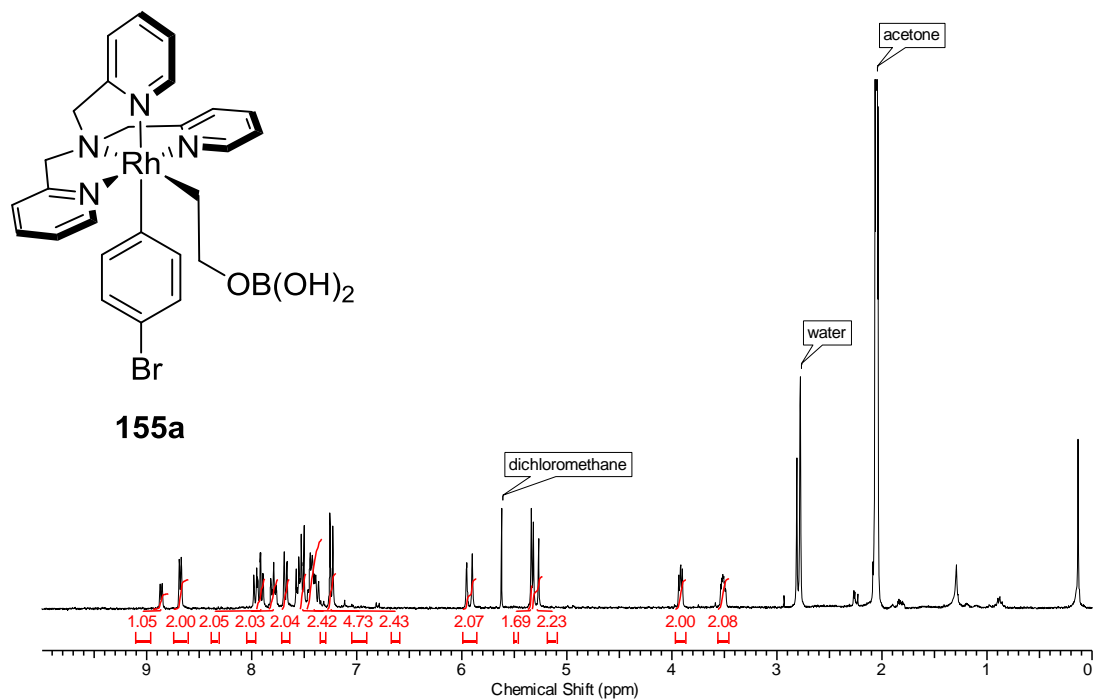
294. Büttner, T.; Breher, F.; Grützmacher, H. *Chem. Commun.* **2004**, 0, 2820.
295. Cramer, R. *J. Am. Chem. Soc.* **1964**, 86, 217.
296. Rossi, A. R.; Hoffmann, R. *Inorg. Chem.* **1975**, 14, 365.
297. Friedman, L. A.; Meiere, S. H.; Brooks, B. C.; Harman, W. D. *Organometallics* **2001**, 20, 1699.
298. Cramer, R. *J. Am. Chem. Soc.* **1972**, 94, 5681.
299. Aakermark, B.; Glaser, J.; Oehrstroem, L.; Zetterberg, K. *Organometallics* **1991**, 10, 733.
300. Xiong, Y.; Yao, S.; Driess, M. *J. Am. Chem. Soc.* **2009**, 131, 7562.
301. Muraoka, T.; Abe, K.; Haga, Y.; Nakamura, T.; Ueno, K. *J. Am. Chem. Soc.* **2011**, 133, 15365.
302. Dauth, A.; Love, J. A. *Angew. Chem. Int. Ed.* **2012**, 51, 3634.
303. Yamada, Y.; Yamamoto, T.; Okawara, M. *Chem. Lett.* **1975**, 361.
304. Evans, D. A.; Bilodeau, M. T.; Faul, M. M. *J. Am. Chem. Soc.* **1994**, 116, 2742.
305. Blacker, A. J.; Duckett, S. B.; Grace, J.; Perutz, R. N.; Whitwood, A. C. *Organometallics* **2009**, 28, 1435.
306. Bergmeier, S. C.; Seth, P. P. *Tetrahedron Lett.* **1999**, 40, 6181.
307. Jafarpour, M.; Rezaeifard, A.; Golshani, T. *Phosphorus, Sulfur Silicon Relat. Elem.* **2010**, 186, 140.
308. Fukuyama, T.; Jow, C.; Cheung, M. *Tetrahedron Lett.* **1995**, 36, 6373.

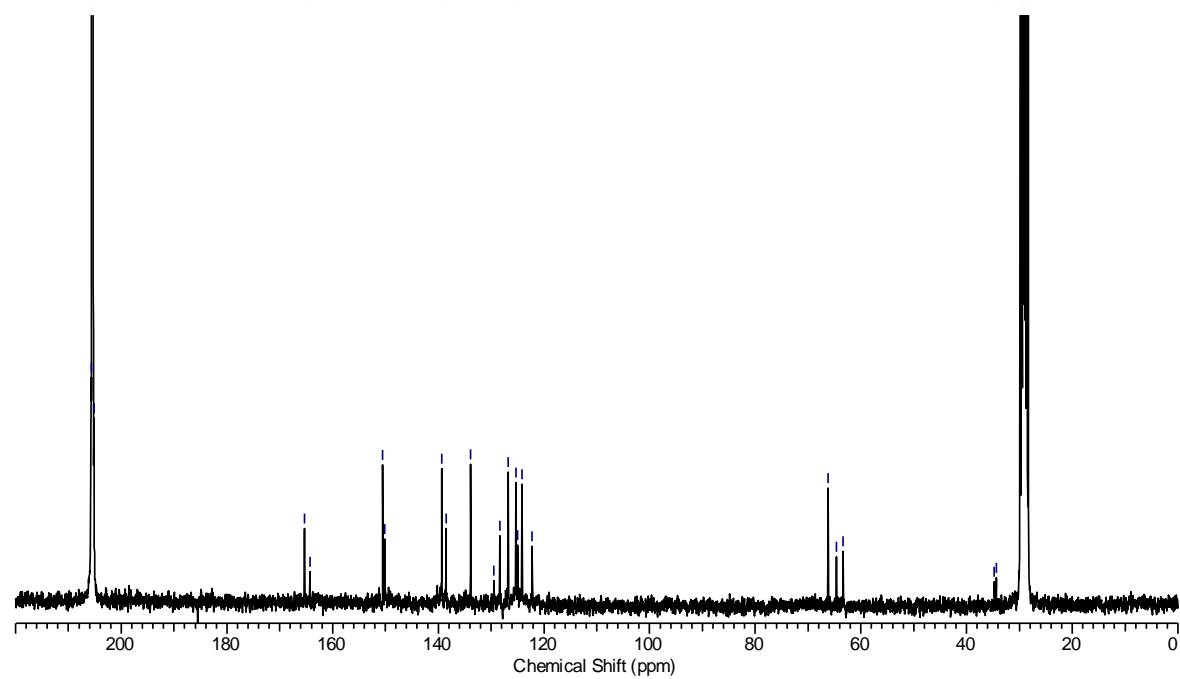
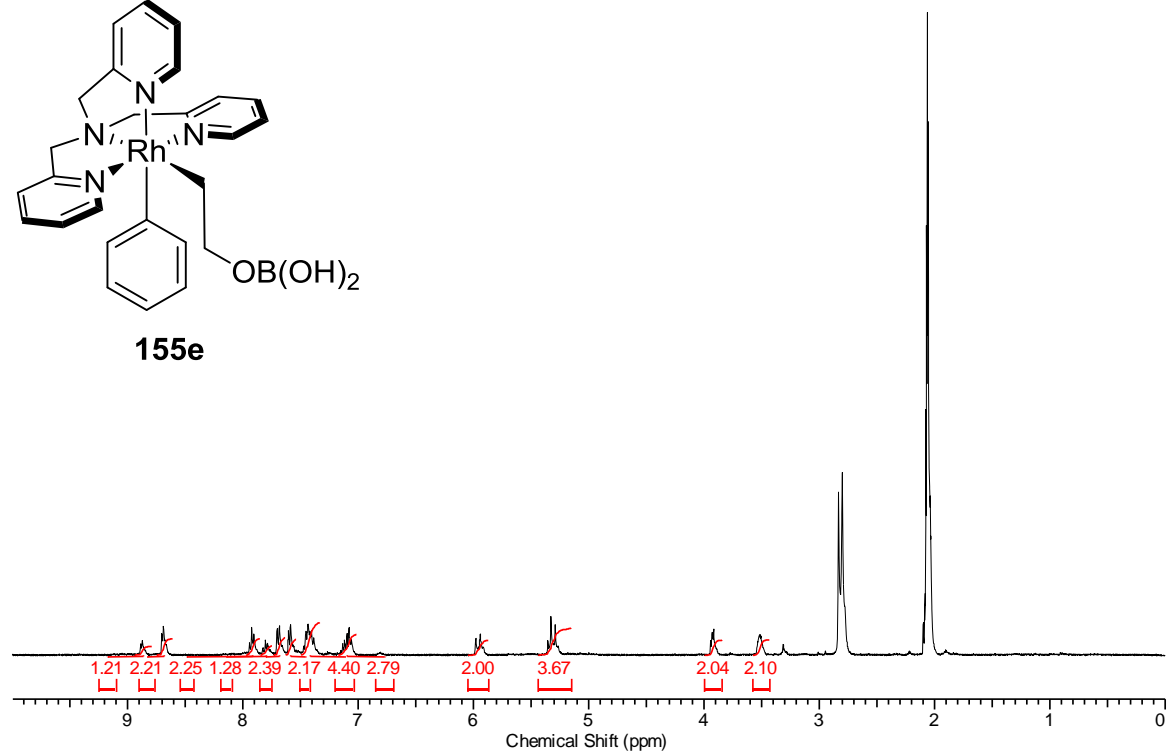
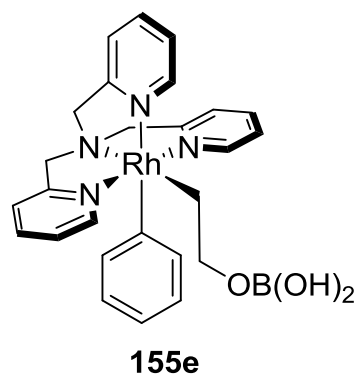
309. Södergren, M. J.; Alonso, D. A.; Bedekar, A. V.; Andersson, P. G. *Tetrahedron Lett.* **1997**, 38, 6897.
310. Lebel, H.; Huard, K.; Lectard, S. *J. Am. Chem. Soc.* **2005**, 127, 14198.
311. Lebel, H.; Huard, K. *Org. Lett.* **2007**, 9, 639.
312. Lebel, H.; Lectard, S.; Parmentier, M. *Org. Lett.* **2007**, 9, 4797.
313. Kost, D.; Kornberg, N. *Tetrahedron Lett.* **1978**, 19, 3275.
314. Marcovici-Mizrahi, D.; Gottlieb, H. E.; Marks, V.; Nudelman, A. *J. Org. Chem.* **1996**, 61, 8402.
315. Smith, B. D.; Goodenough-Lashua, D. M.; D'Souza, C. J. E.; Norton, K. J.; Schmidt, L. M.; Tung, J. C. *Tetrahedron Lett.* **2004**, 45, 2747.
316. Lindsay, R. O.; Allen, C. F. H. *Org. Synth* **1942**, 22, 96.
317. Swetha, M.; Ramana, P. V.; Shirodkar, S. G. *Org. Prep. Proc. Int.* **2011**, 43, 348.
318. Campbell-Verduyn, L.; Mirfeizi, L.; Dierckx, R. A.; Elsinga, P. H.; Feringa, B. L. *Chem. Commun.* **2009**, 0, 2139.
319. Baron, A.; Herrero, C.; Quaranta, A.; Charlot, M.; Leibl, W.; Vauzeilles, B.; Aukauloo, A. *Inorg. Chem.* **2012**, 51, 5985.
320. Tao, C.; Cui, X.; Li, J.; Liu, A.; Liu, L.; Guo, Q. *Tetrahedron Lett.* **2007**, 48, 3525.
321. Dohi, T.; Ito, M.; Yamaoka, N.; Morimoto, K.; Fujioka, H.; Kita, Y. *Tetrahedron* **2009**, 65, 10797.
322. de Bruin, B.; Peters, T. P. J.; Thewissen, S.; Blok, A. N. J.; Wilting, J. B. M.; de Gelder, R.; Smits, J. M. M.; Gal, A. W. *Angew. Chem. Int. Ed.* **2002**, 41, 2135

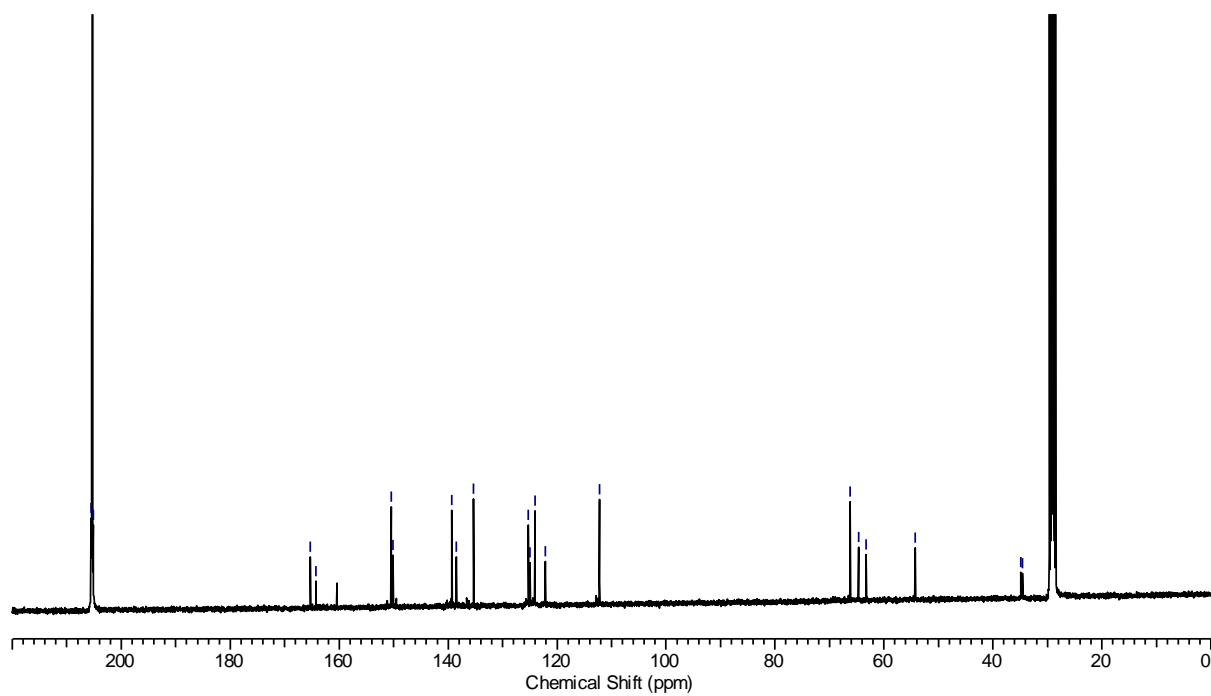
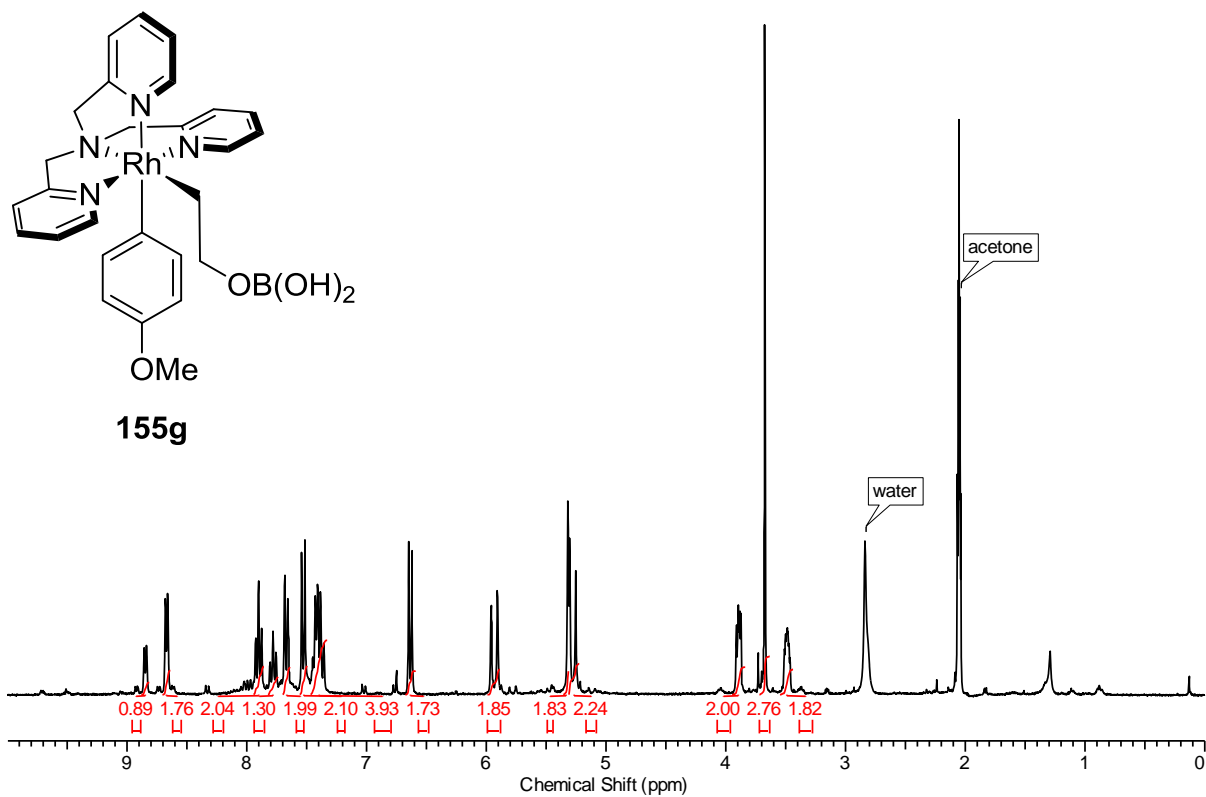
323. Hetterscheid, D. G. H.; Kaiser, J.; Reijerse, E.; Peters, T. P. J.; Thewissen, S.; Blok, A. N. J.; Smits, J. M. M.; de Gelder, R.; de Bruin, B. *J. Am. Chem. Soc.* **2005**, *127*, 1895.
324. de Bruin, B.; Thewissen, S.; Yuen, T. – W.; Peters, T. P. J.; Smits, J. M. M.; Gal, A. W. *Organometallics* **2002**, *21*, 4312.
325. Dzik, W. I.; Reek, J. N.; de Bruin, B. *Chem. --Eur. J.* **2008**, *14*, 7594.
326. de Bruin, B.; Hetterscheid, D. G. H. *Eur. J. Inorg. Chem.* **2007**, *2*, 211.
327. Lyaskovskyy, V.; Olivos Suárez, A. I.; Lu, H.; Jiang, H.; Zhang, X. P.; de Bruin, B. *J. Am. Chem. Soc.* **2011**, *133*, 12264;
328. Olivos Suarez, A. I.; Jiang, H.; Zhang, X. P.; de Bruin, B. *Dalton Trans.* **2011**, *40*, 5697.
329. Hetterscheid, D. G. H.; de Bruin, B. *J. Mol. Catal. A, Chemical* **2006**, *251*, 291.

Appendix

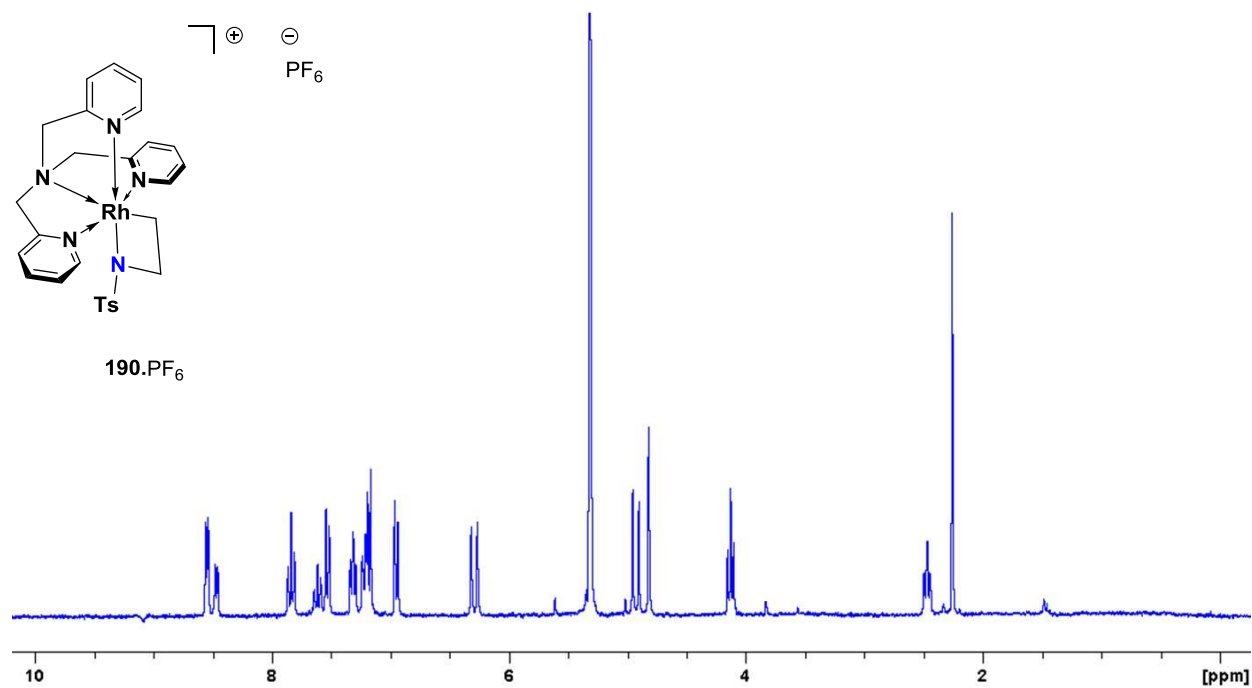
A.1 NMR Spectra



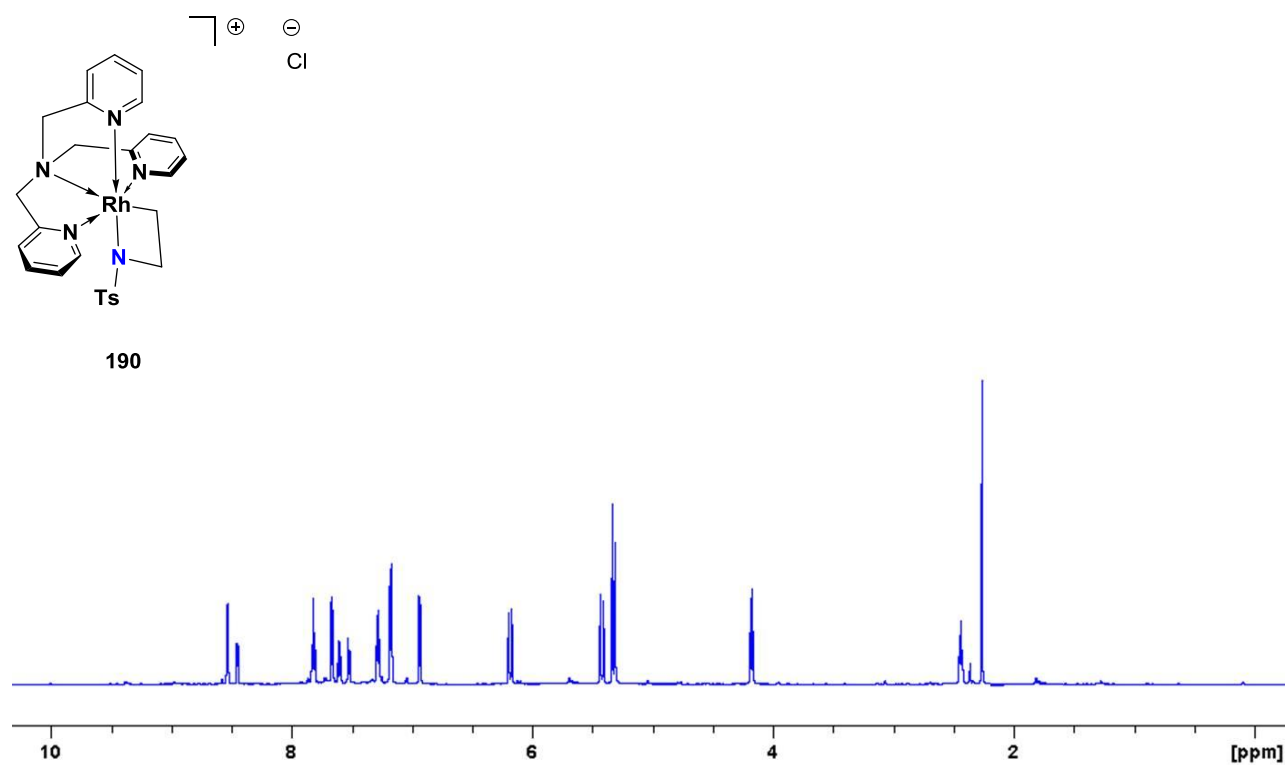




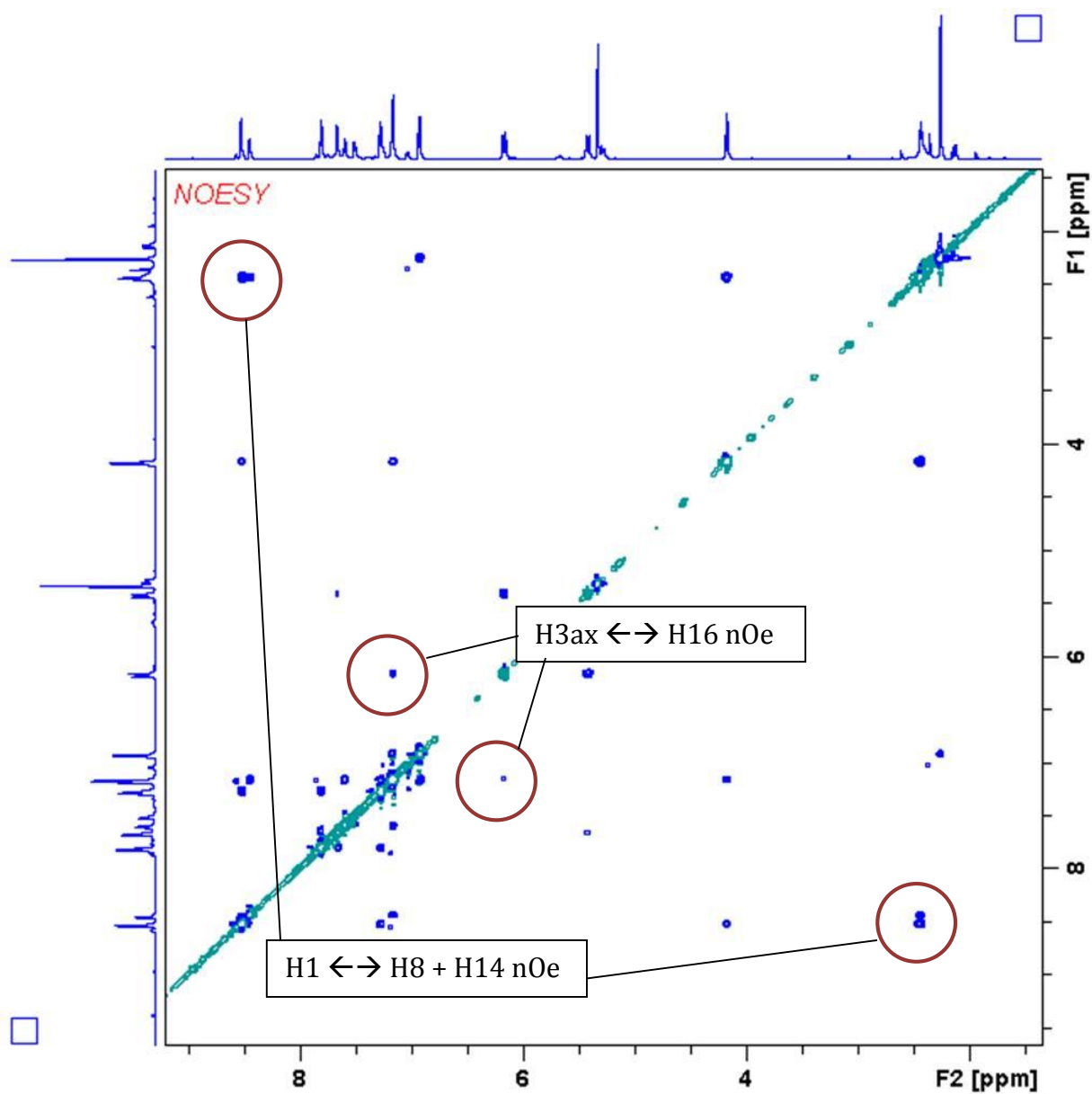
190.PF₆, ¹H NMR, CD₂Cl₂, 600 MHz, 298 K



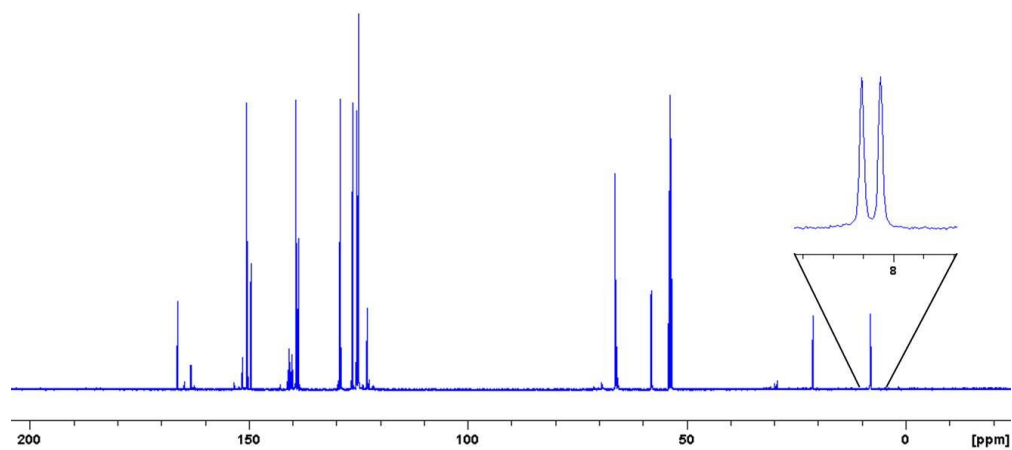
190.Cl, ¹H NMR, CD₂Cl₂, 600 MHz, 298 K



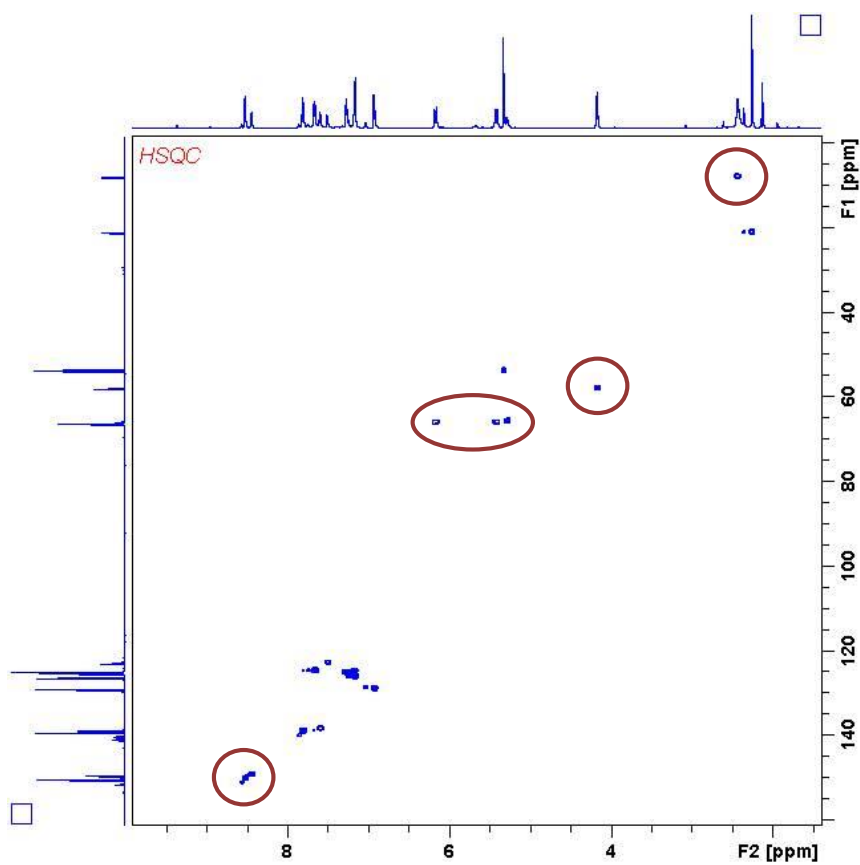
190, 2D-NOESY, CD₂Cl₂, 600 MHz, 298K, diagnostic nOe's highlighted



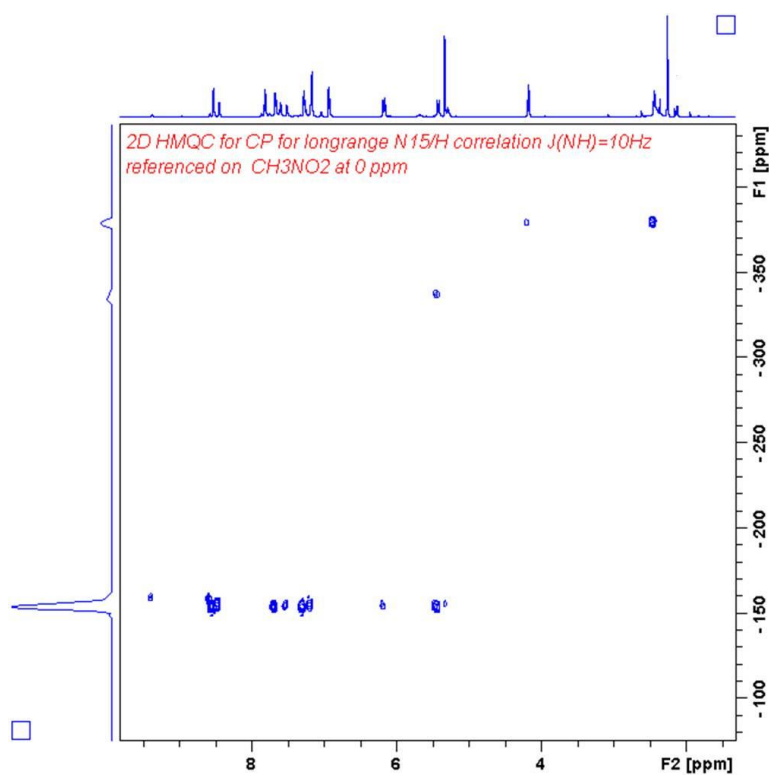
190 $^{13}\text{C}\{^1\text{H}\}$ NMR, CD_2Cl_2 , 150 MHz, 298 K, showing $^2J_{(\text{Rh}-\text{C})}$ coupling



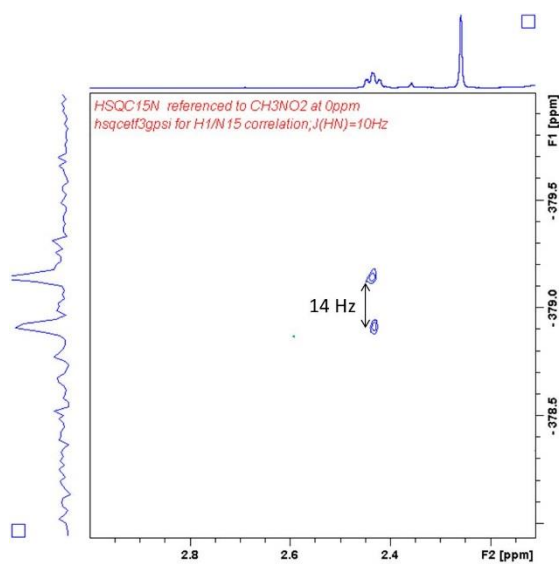
190, $^1\text{H}/^{13}\text{C}$ HSQC, CDCl_3 , 600 MHz, 298K, C1, C2, C3, C8, C14 highlighted



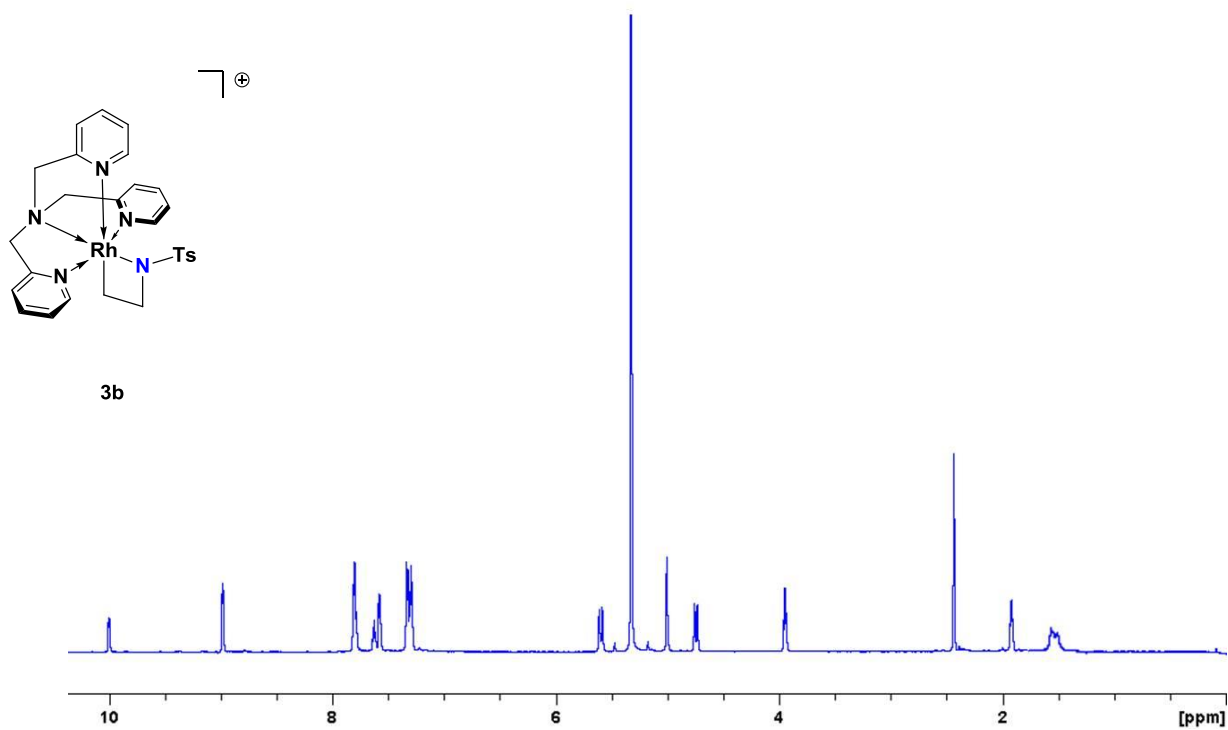
190, $^1\text{H}/^{15}\text{N}$ HMQC lr, CD_2Cl_2 , 600 MHz, detail, showing long range correlation with N_{pyr} ,
 Namine, $\text{N}_{\text{cyclobutane}}$



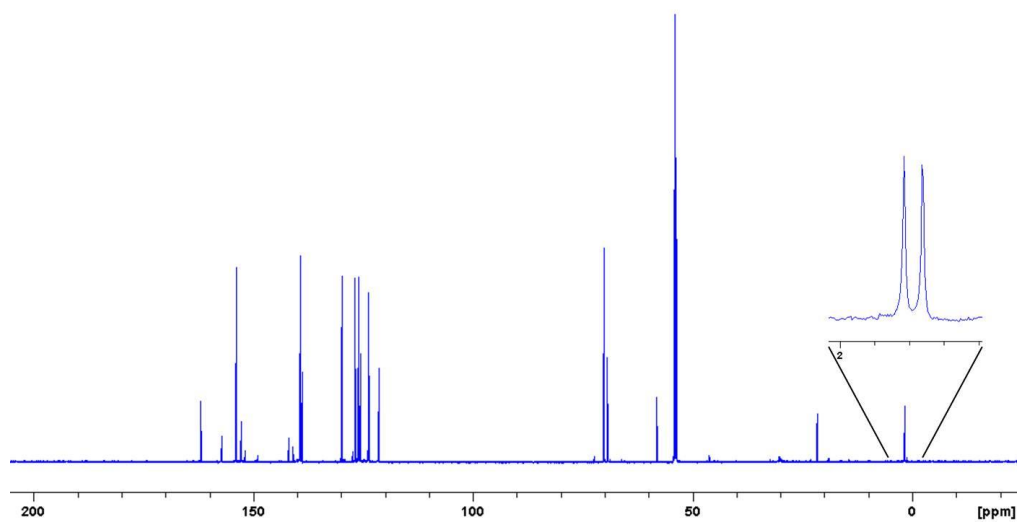
190, $^1\text{H}/^{15}\text{N}$ HSQC lr, CD_2Cl_2 , 600 MHz, detail, showing coupling $^2J_{(\text{Rh}-\text{N})}$



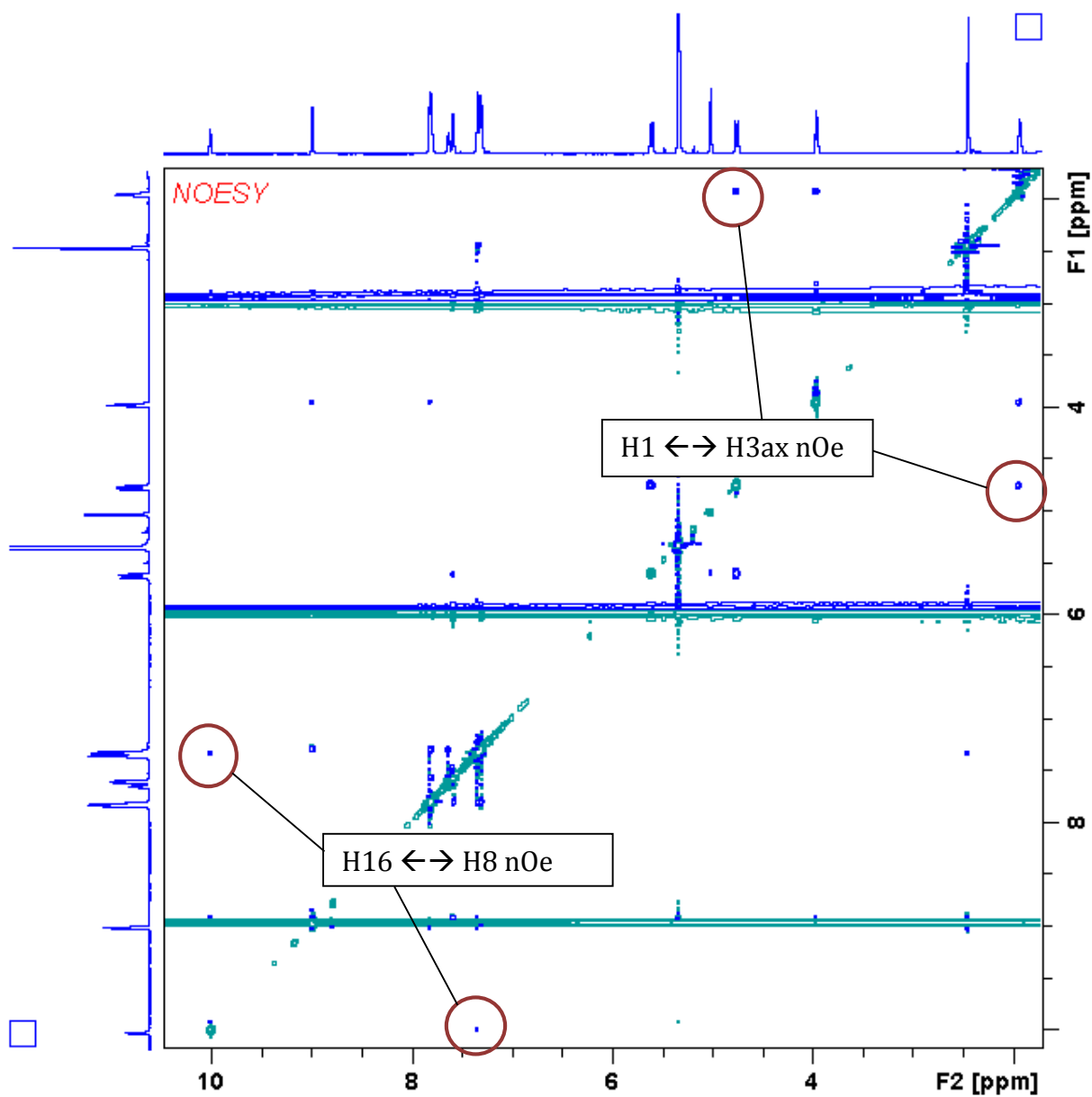
191, ^1H NMR, CD_2Cl_2 , 600 MHz, 298 K



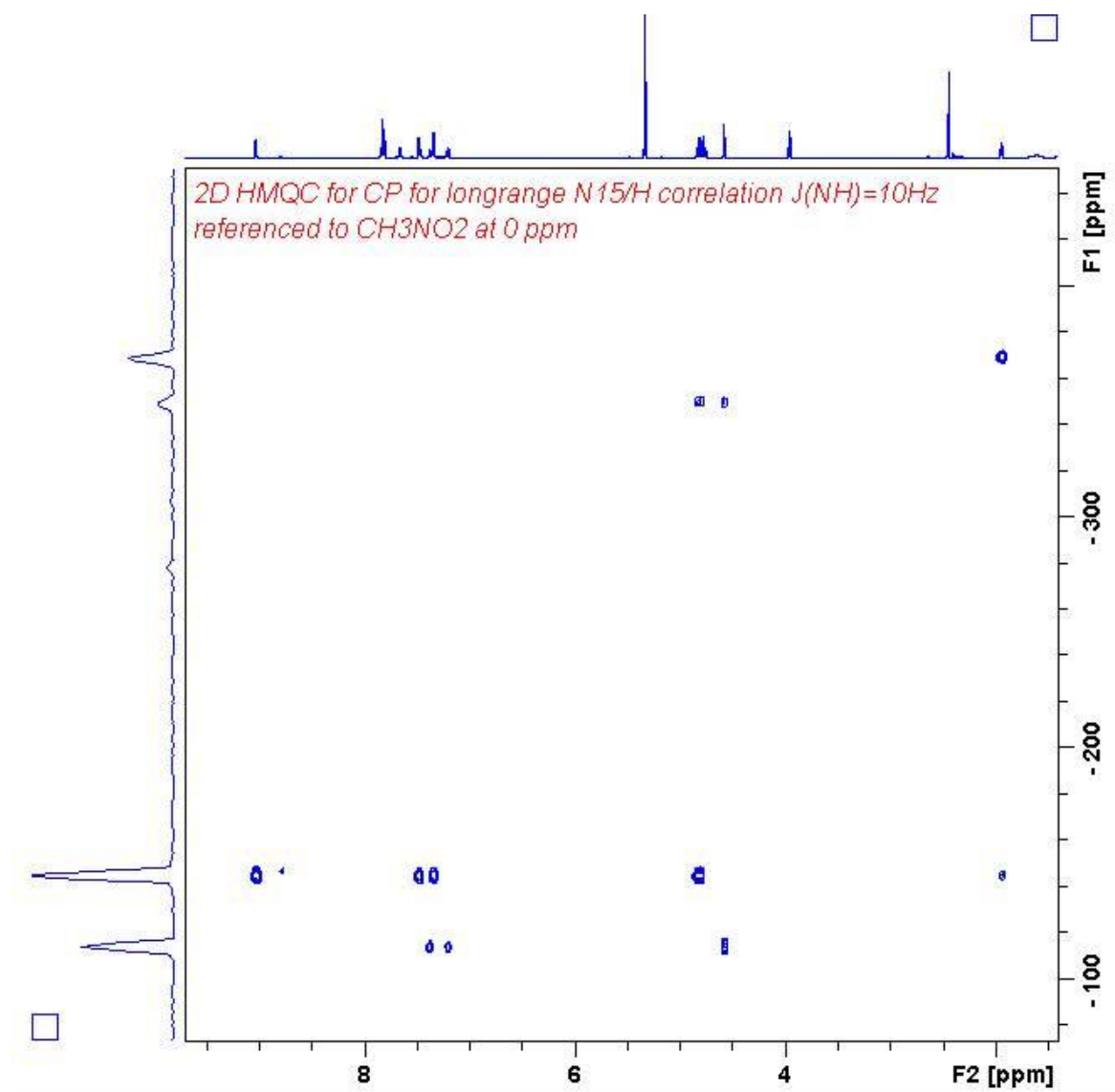
191, $^{13}\text{C}\{^1\text{H}\}$ NMR, CD_2Cl_2 , 150 MHz, 298 K, showing $^2J_{(\text{Rh}-\text{C})}$ coupling



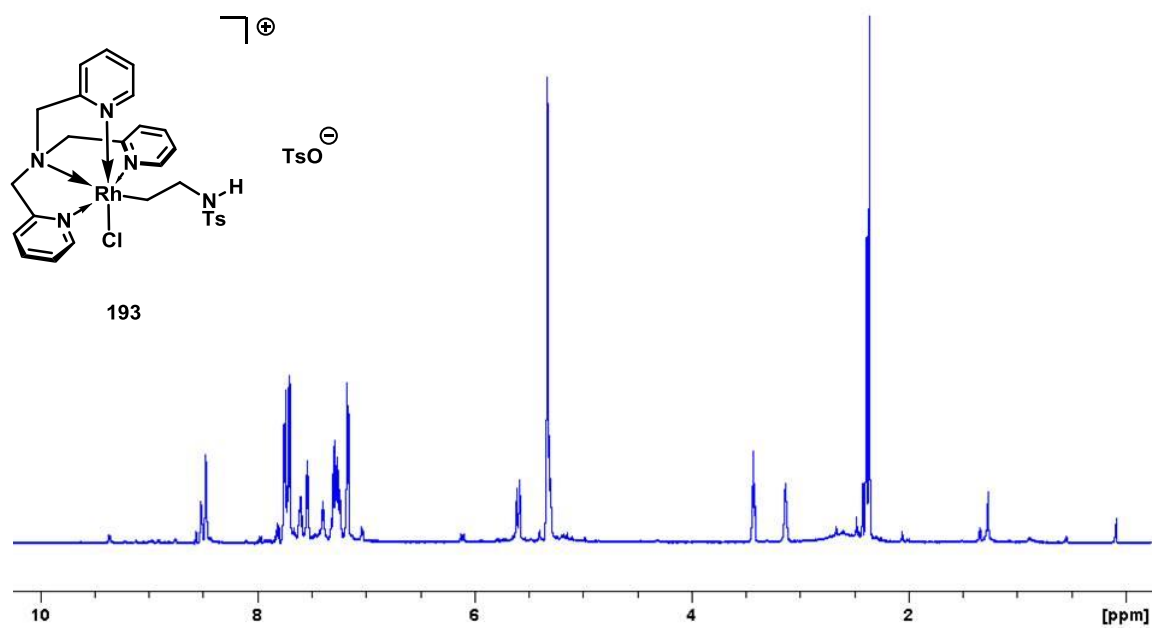
191, 2D-NOESY, CD₂Cl₂, 600 MHz, 298 K, diagnostic nOe's highlighted



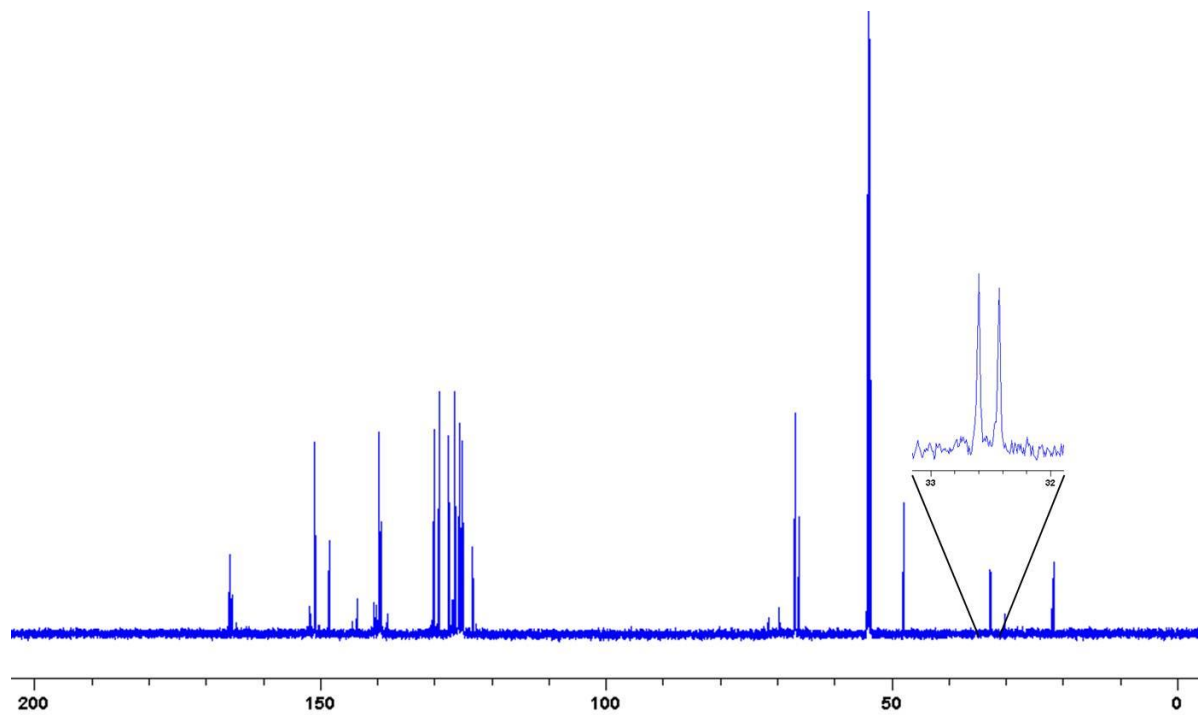
191, $^1\text{H}/^{15}\text{N}$ HMQC 1r, CD_2Cl_2 , 600 MHz, detail, showing long range correlation with N_{pyr} ,
Namine, $\text{N}_{\text{cyclobutane}}$



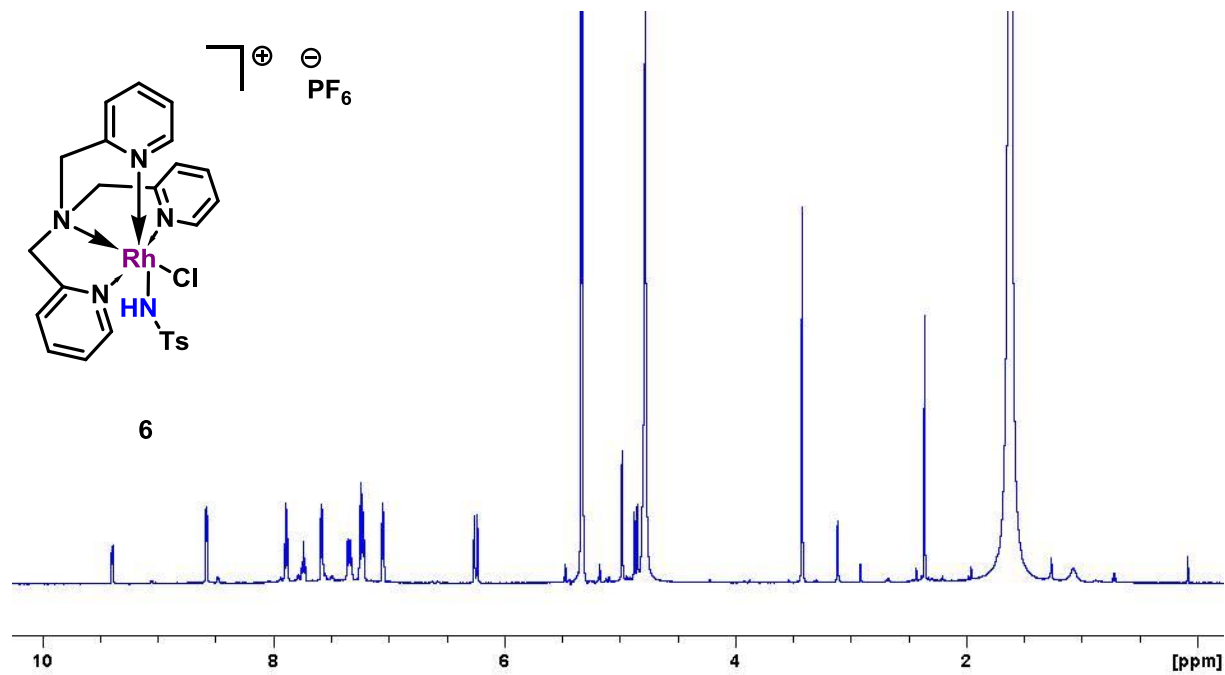
209.OTs, ^1H NMR, CD_2Cl_2 , 600 MHz, 298 K



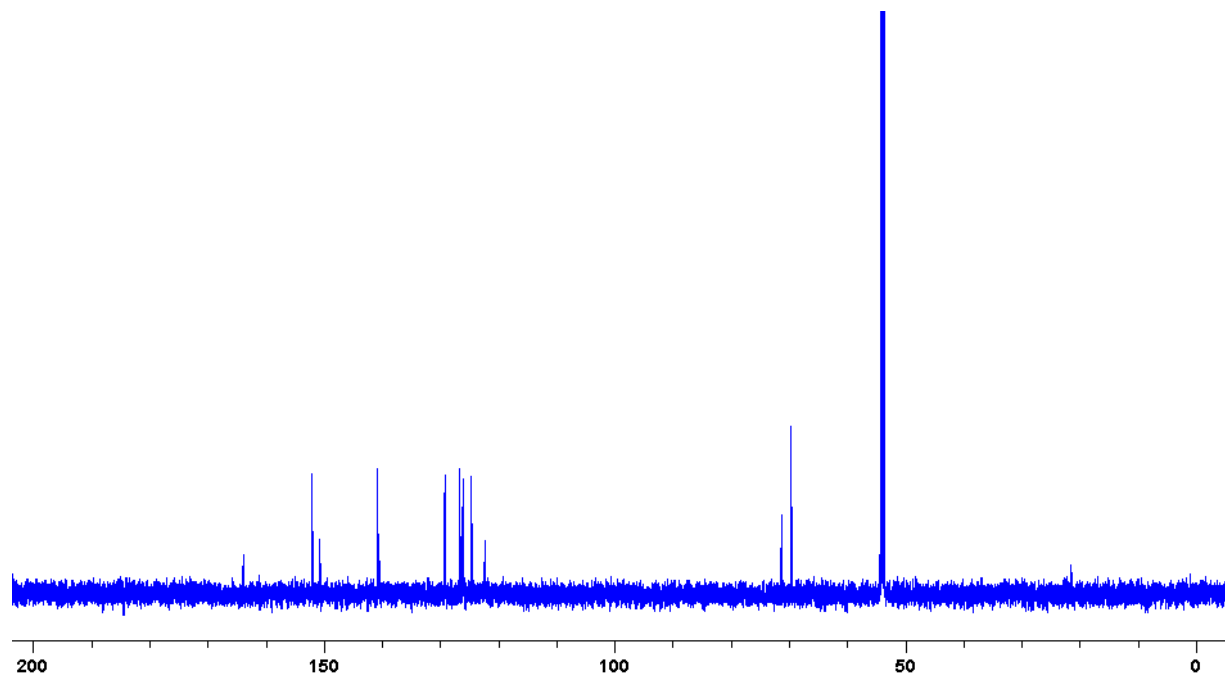
209.OTs, $^{13}\text{C}\{^1\text{H}\}$ NMR, CD_2Cl_2 , 150 MHz, 298 K



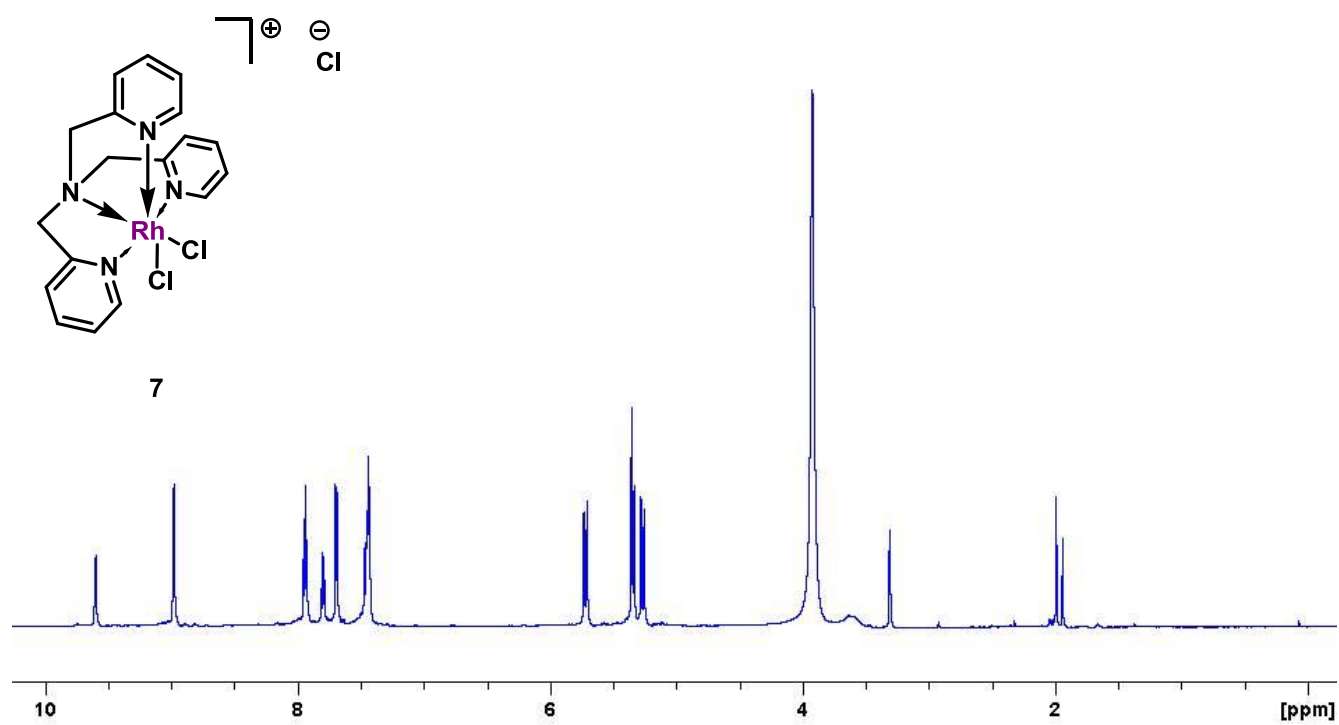
193.PF₆, ¹H NMR, CD₂Cl₂, 600 MHz, 298 K



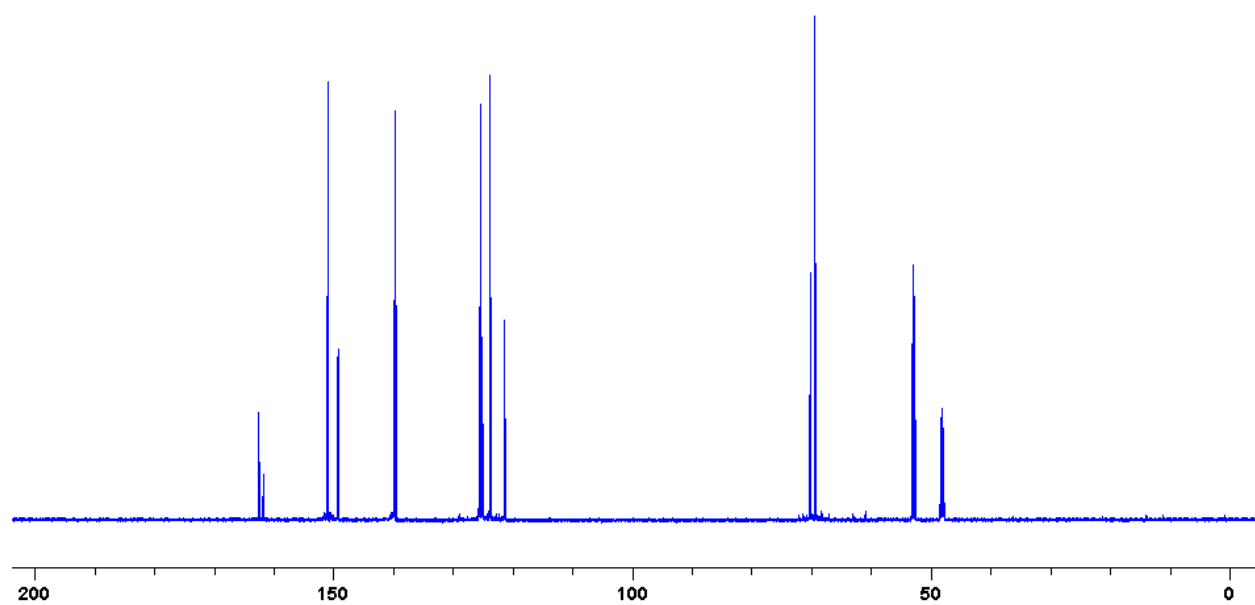
193.PF₆, ¹³C{¹H} NMR, CD₂Cl₂, 150 MHz, 298 K



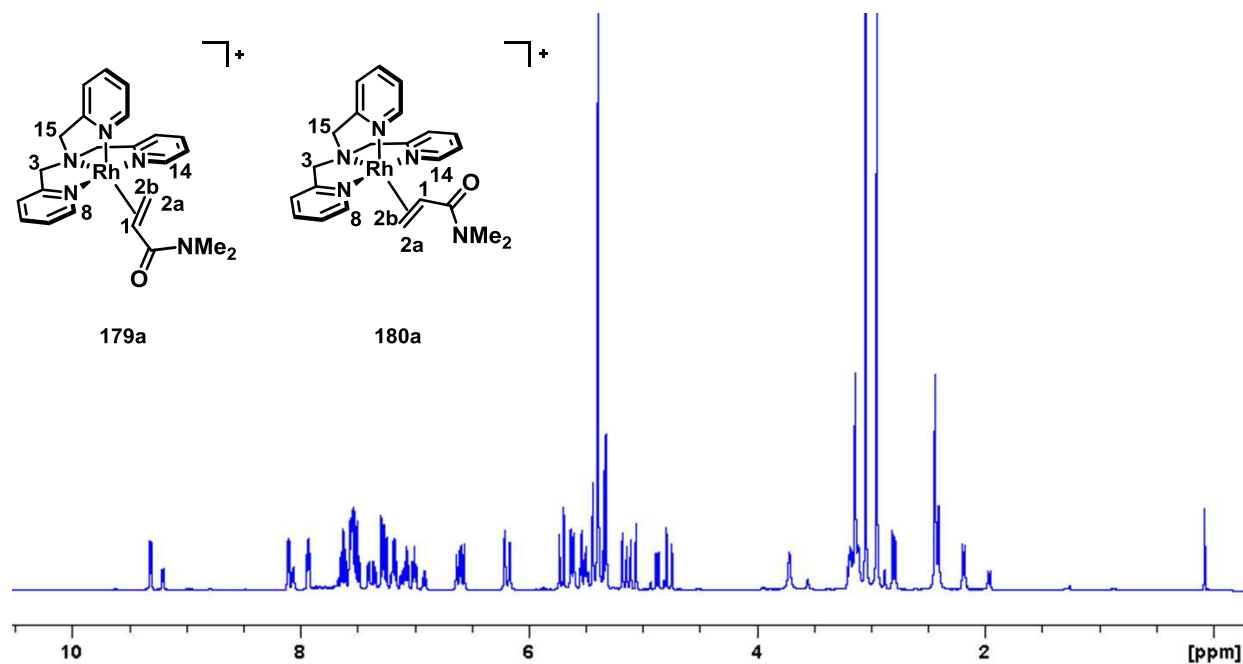
194.Cl, ^1H NMR, CD_2Cl_2 , 600 MHz, 298 K



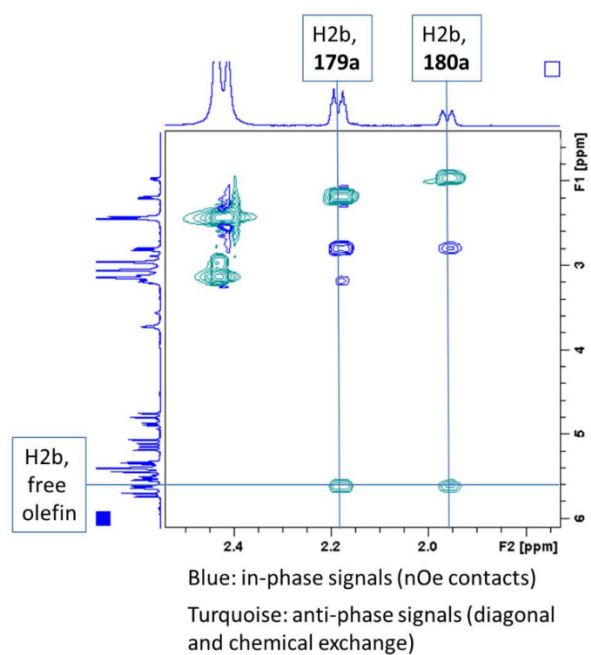
194.Cl, $^{13}\text{C}\{^1\text{H}\}$ NMR, CD_2Cl_2 , 150 MHz, 298 K



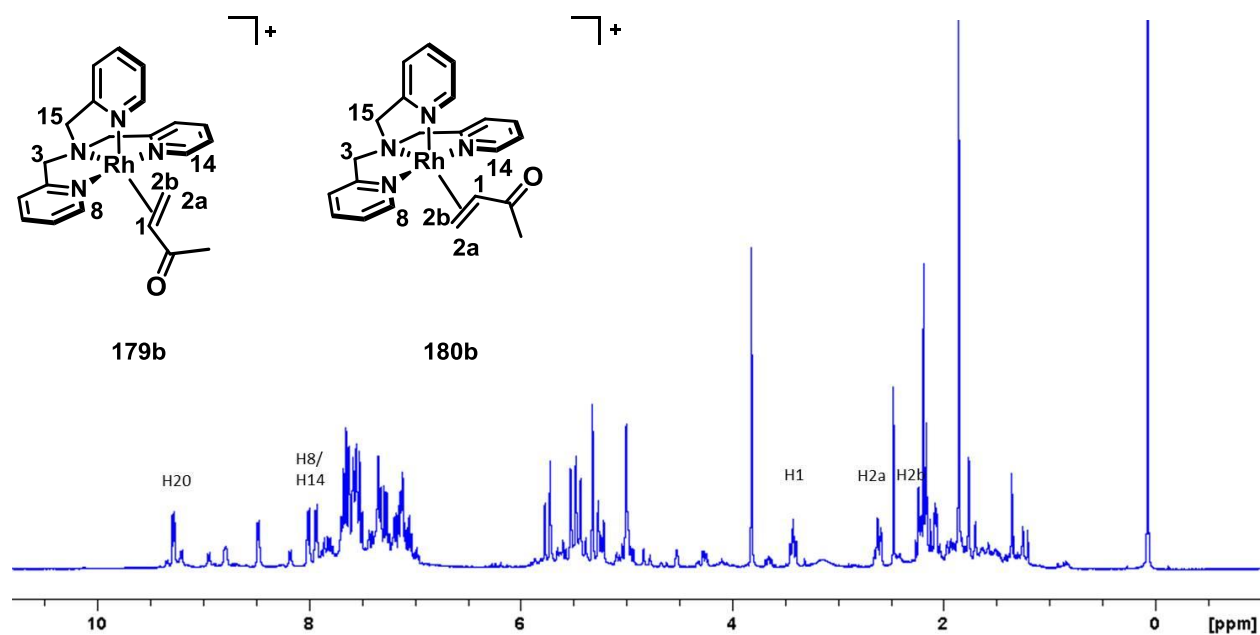
179a/180a, [TPA-Rh-N, N-Dimethylacrylamide]Cl, CD₂Cl₂



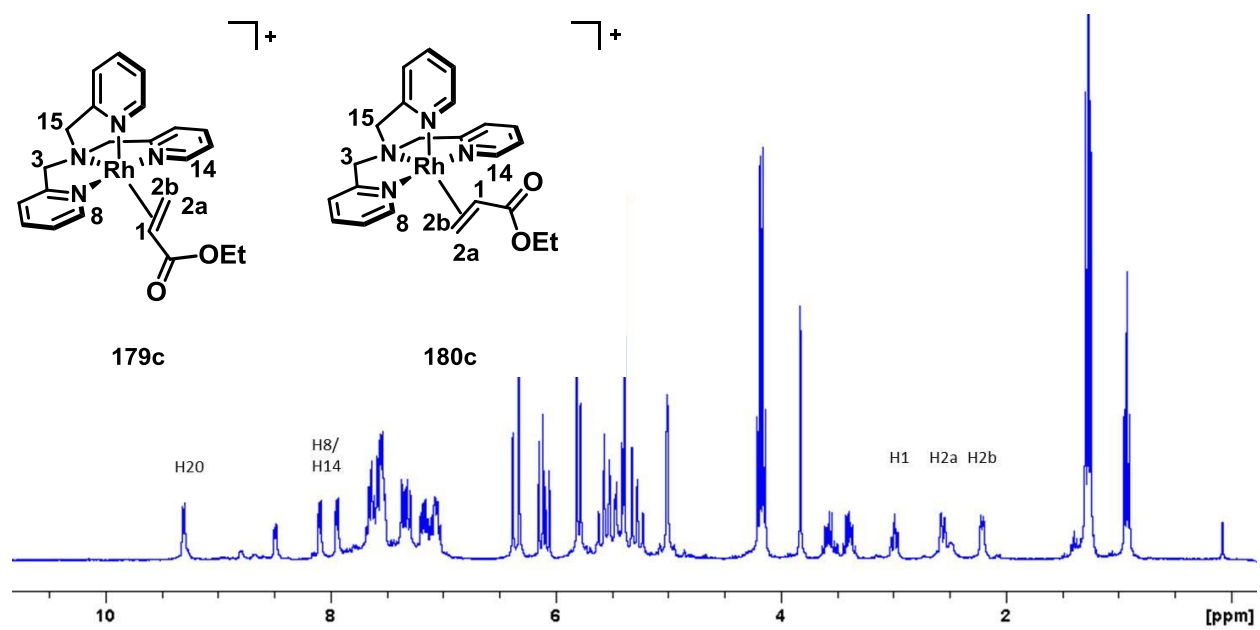
NOESY/chemical exchange:



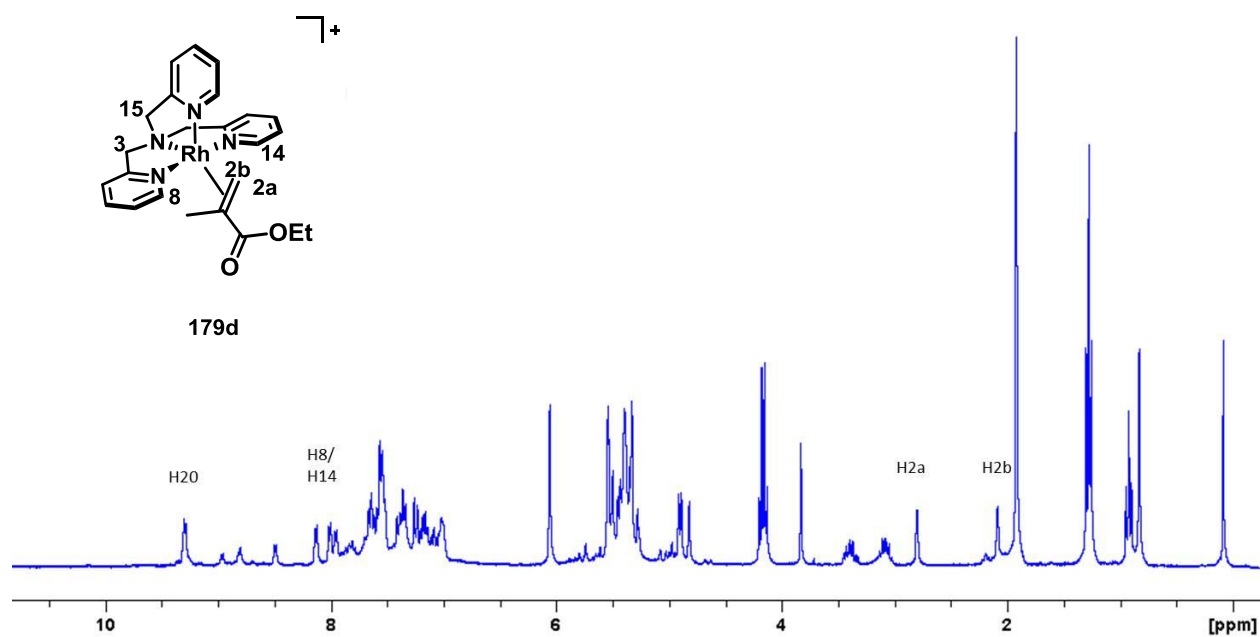
179b/180b [TPA-Rh-Methylvinylketone]Cl, CD₂Cl₂



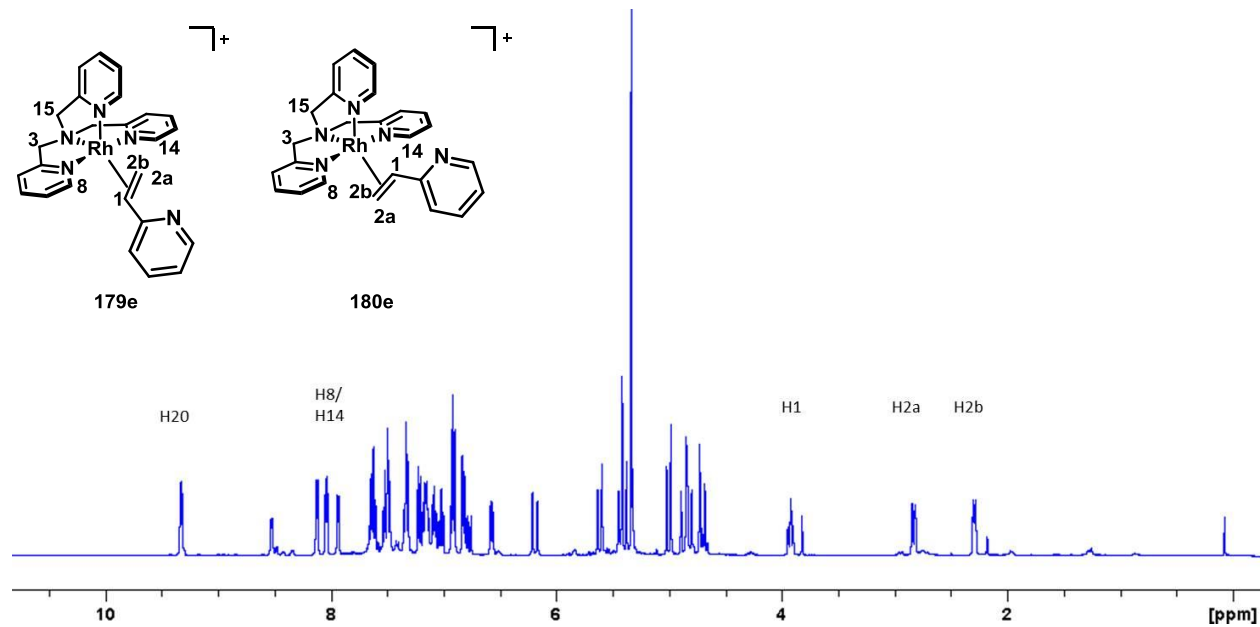
179c/180c, [TPA-Rh-Ethylacrylate]Cl, CD₂Cl₂



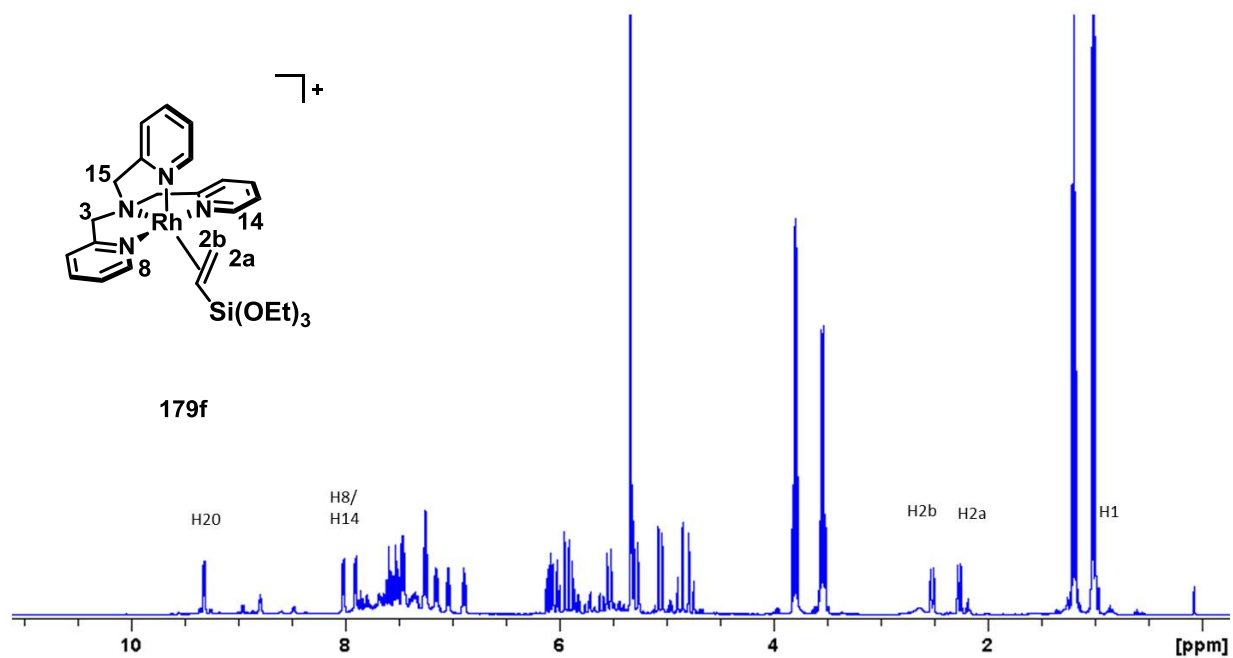
179d, [TPA-Rh-Methethylacrylate]Cl, CD₂Cl₂



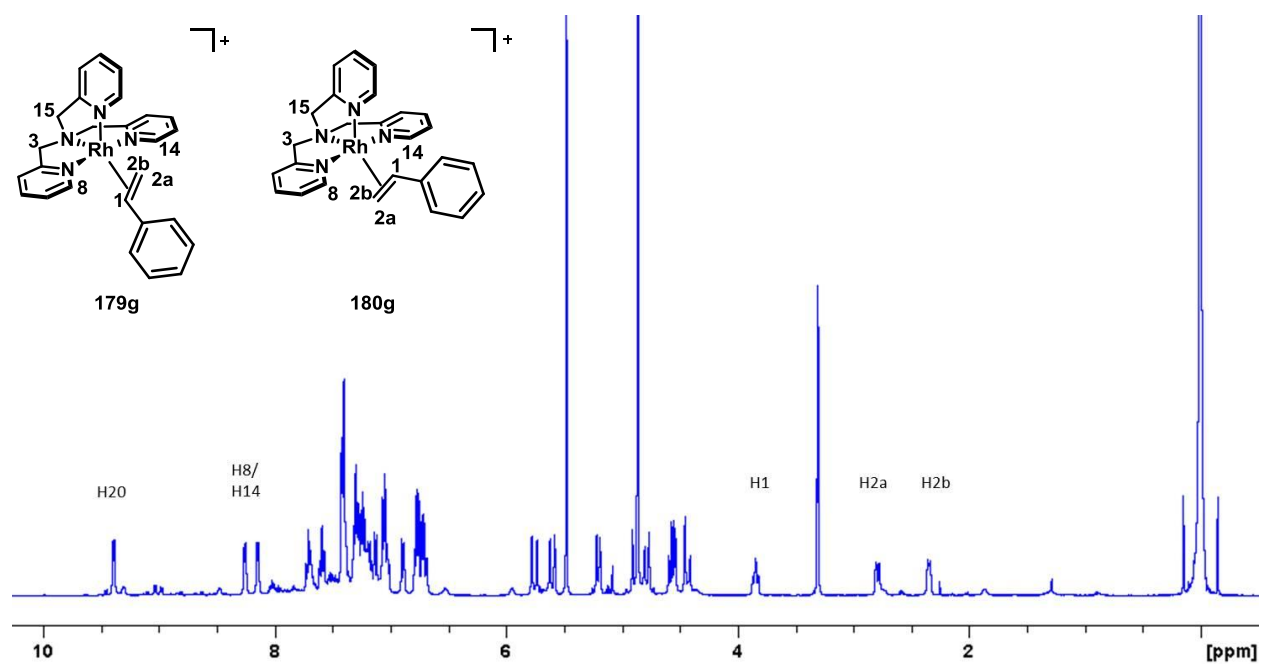
179e/180e, [TPA-Rh-vinylpyridine]Cl, CD₂Cl₂



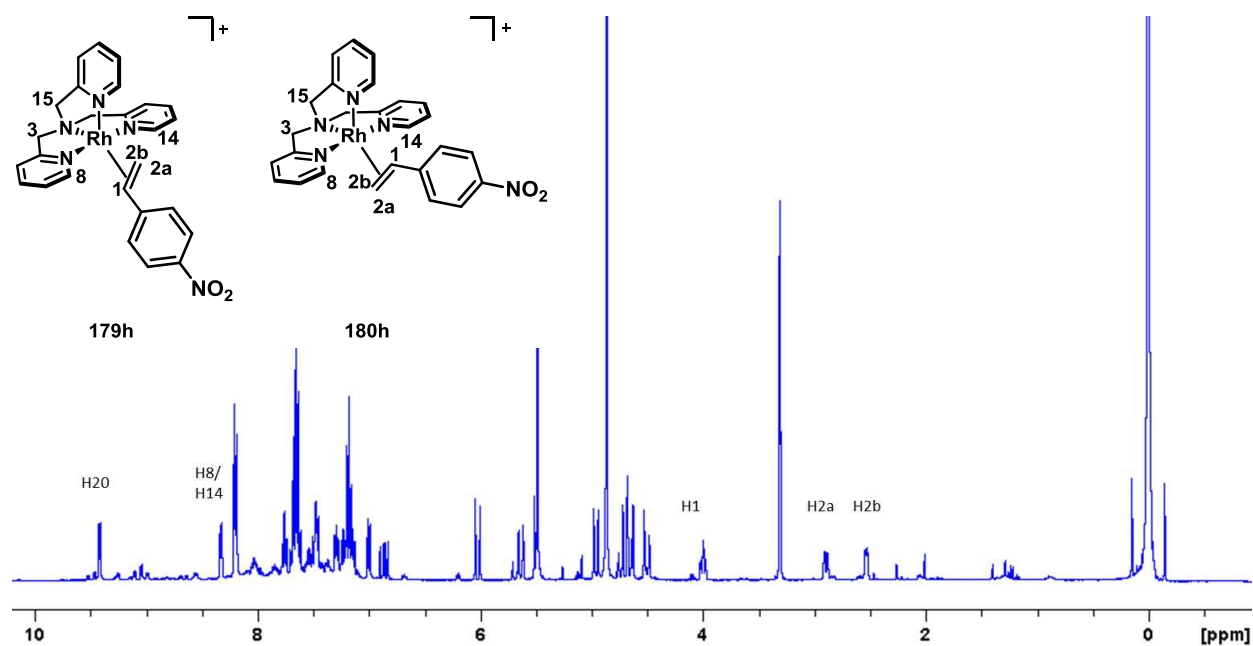
179 f, [TPA-Rh-triethoxyvinylsilane]Cl, CD₂Cl₂



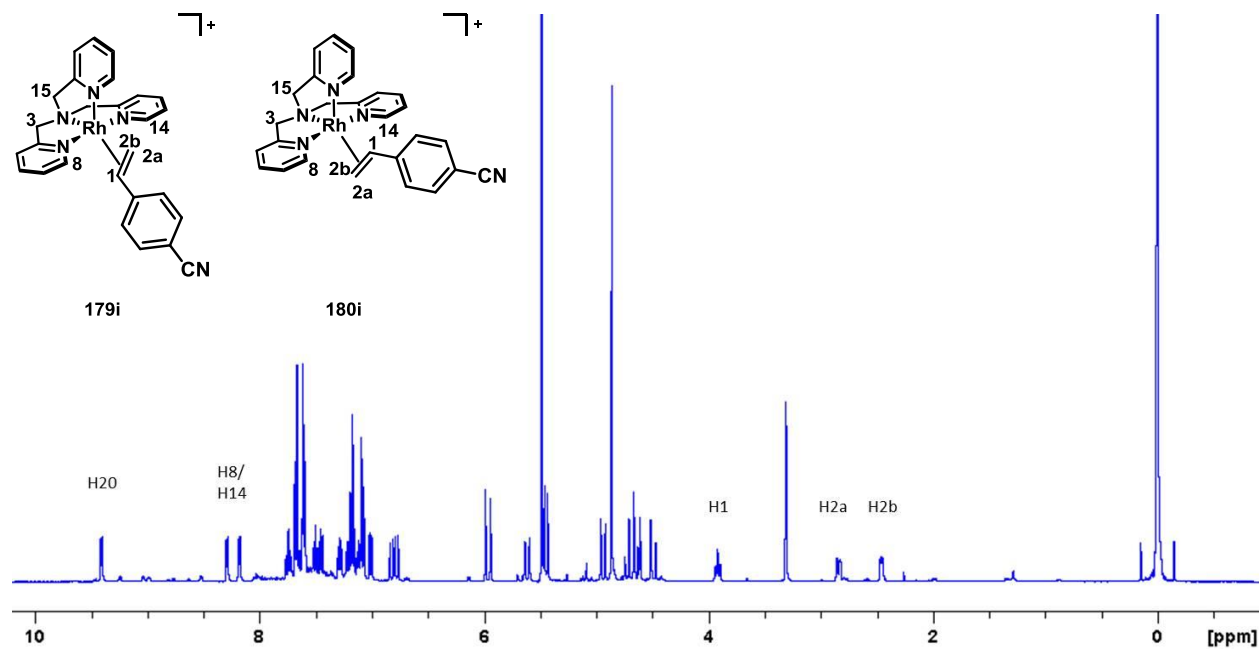
179g/180g, [TPA-Rh-Styrene]Cl, MeOD



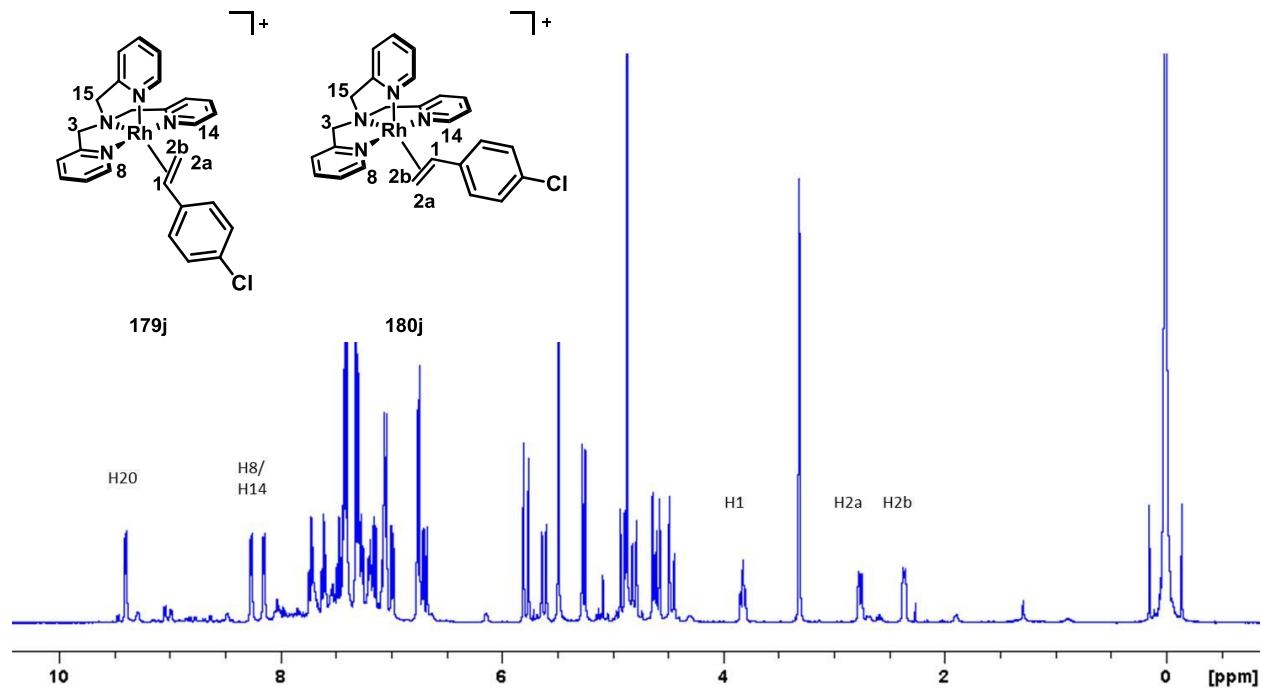
179h/180h, [TPA-Rh-4-nitrostyrene]Cl, MeOD



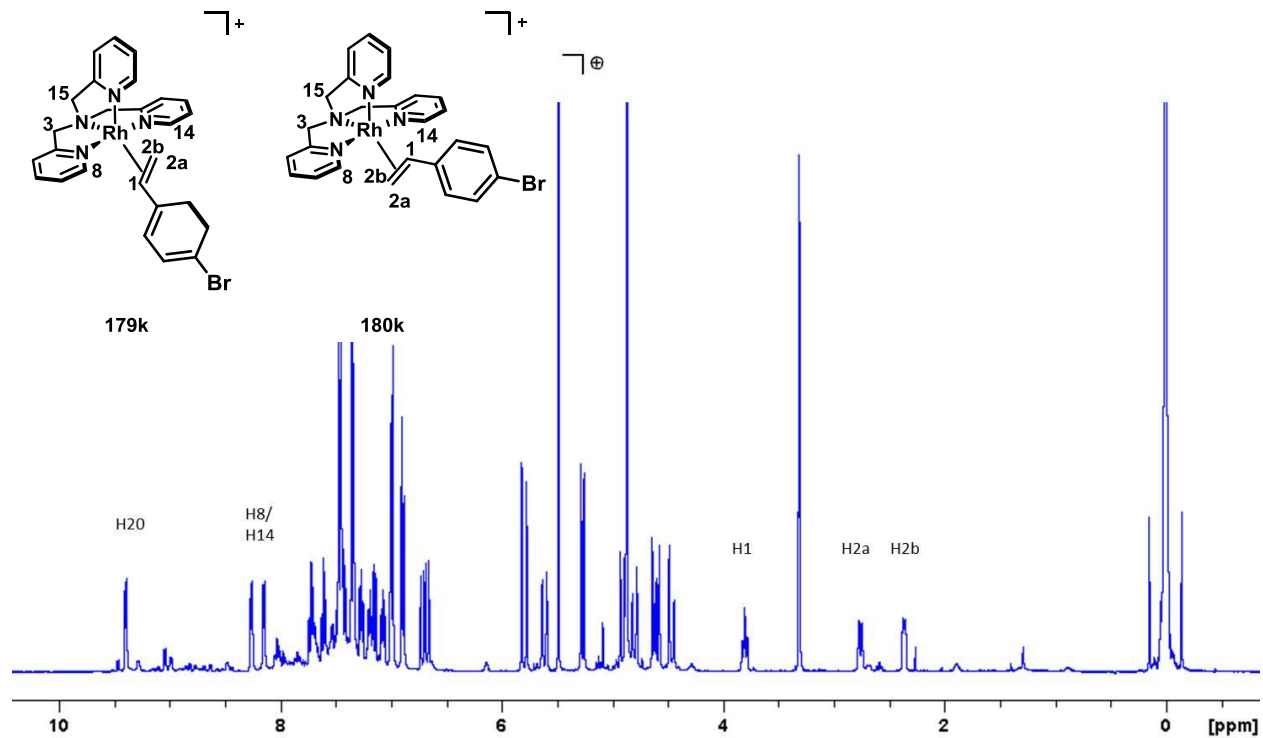
179i/180i, [TPA-Rh-4-cyanostyrene]Cl, MeOD



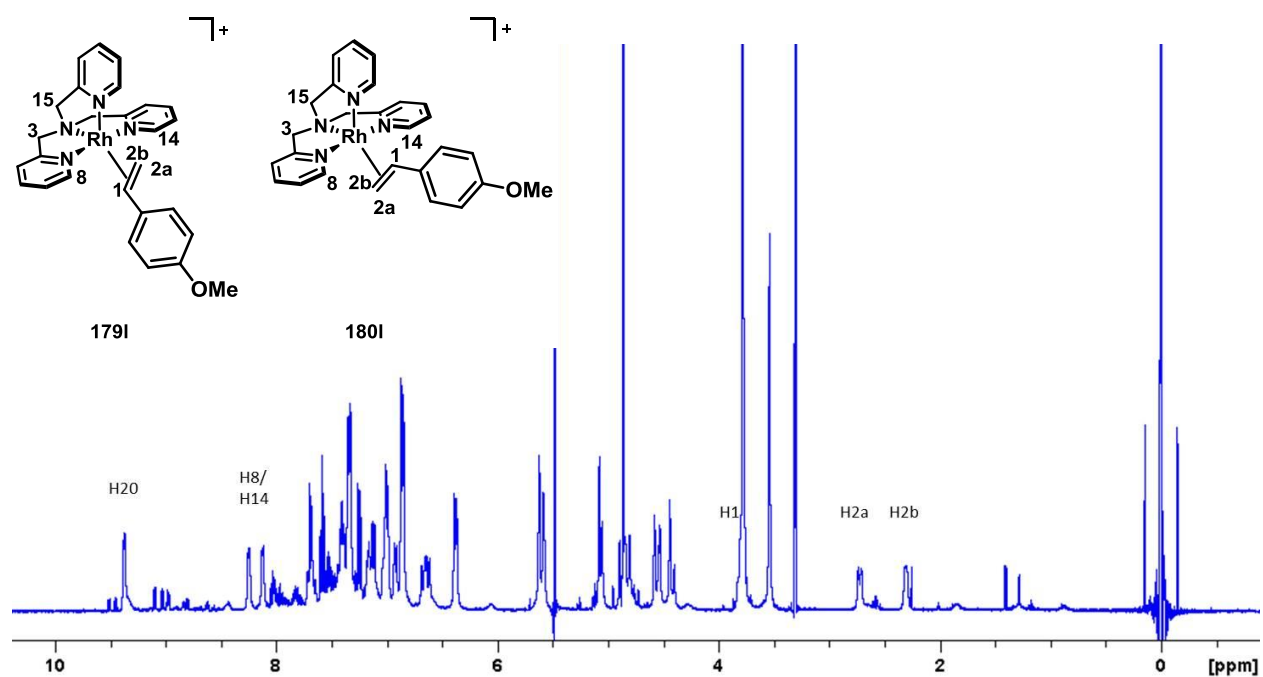
179j/180j, [TPA-Rh-4-chlorostyrene]Cl, MeOD



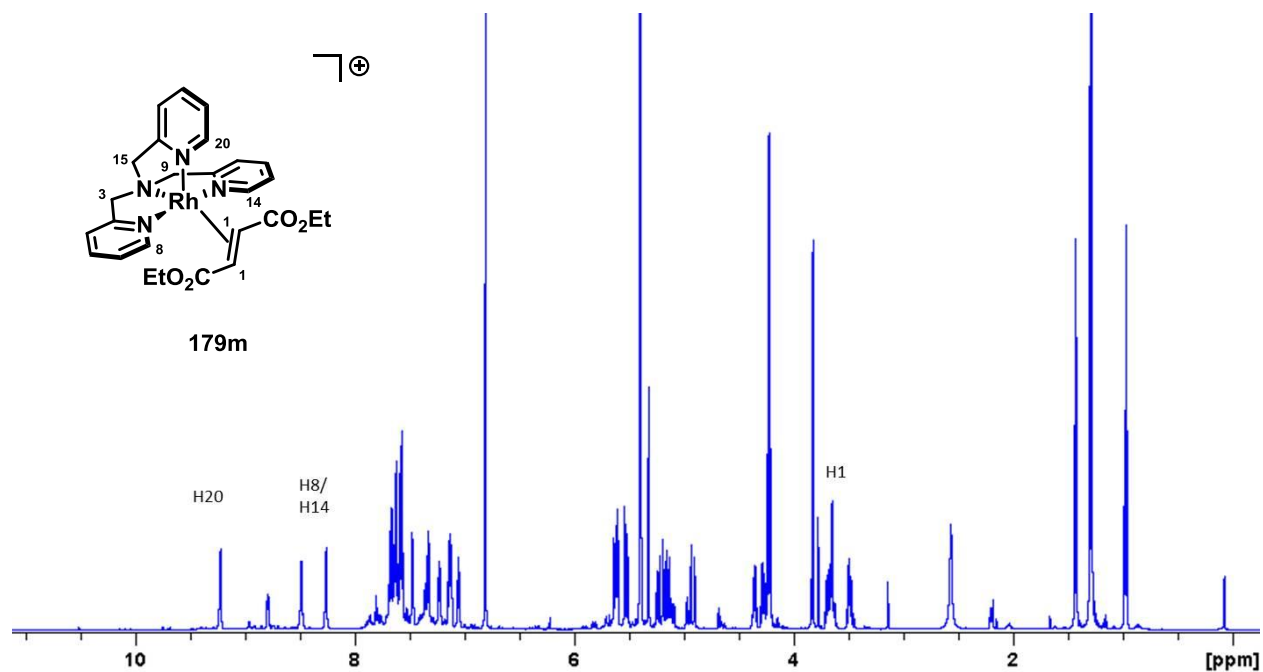
179k/180k, [TPA-Rh-4-bromostyrene]Cl, MeOD



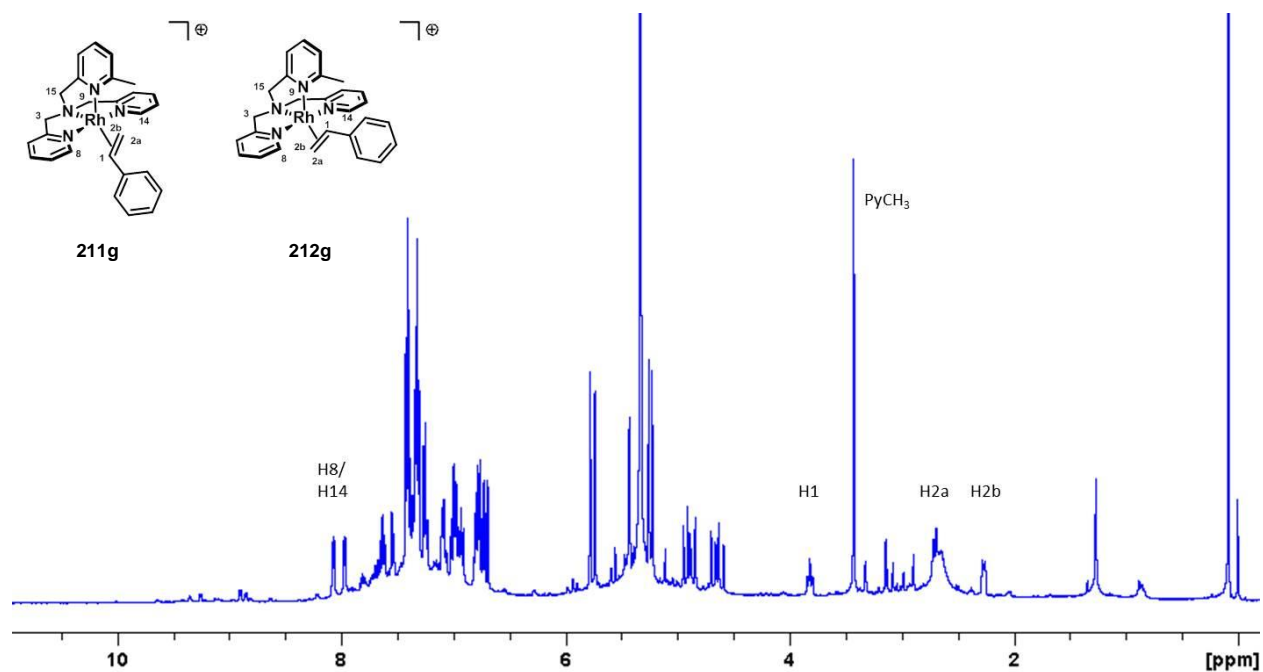
179l/180l, [TPA-Rh-4-Methoxystyrene]Cl, MeOD



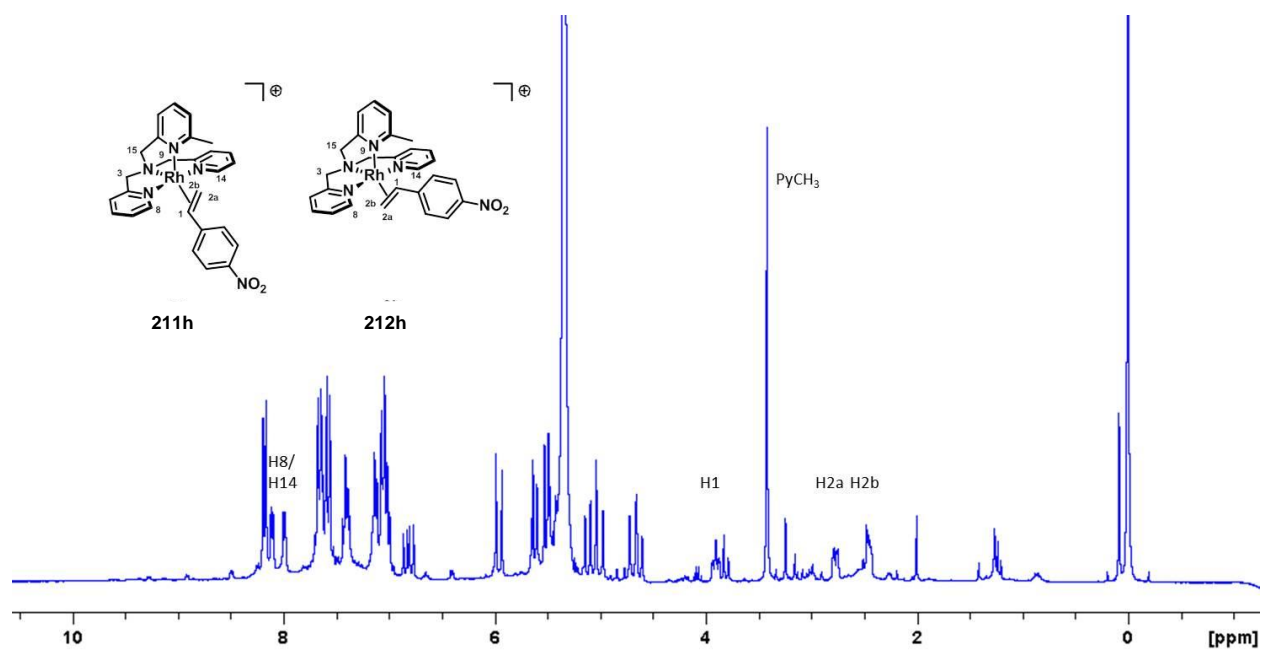
179m, [TPA-Rh-diethylfumurate]Cl, CD₂Cl₂



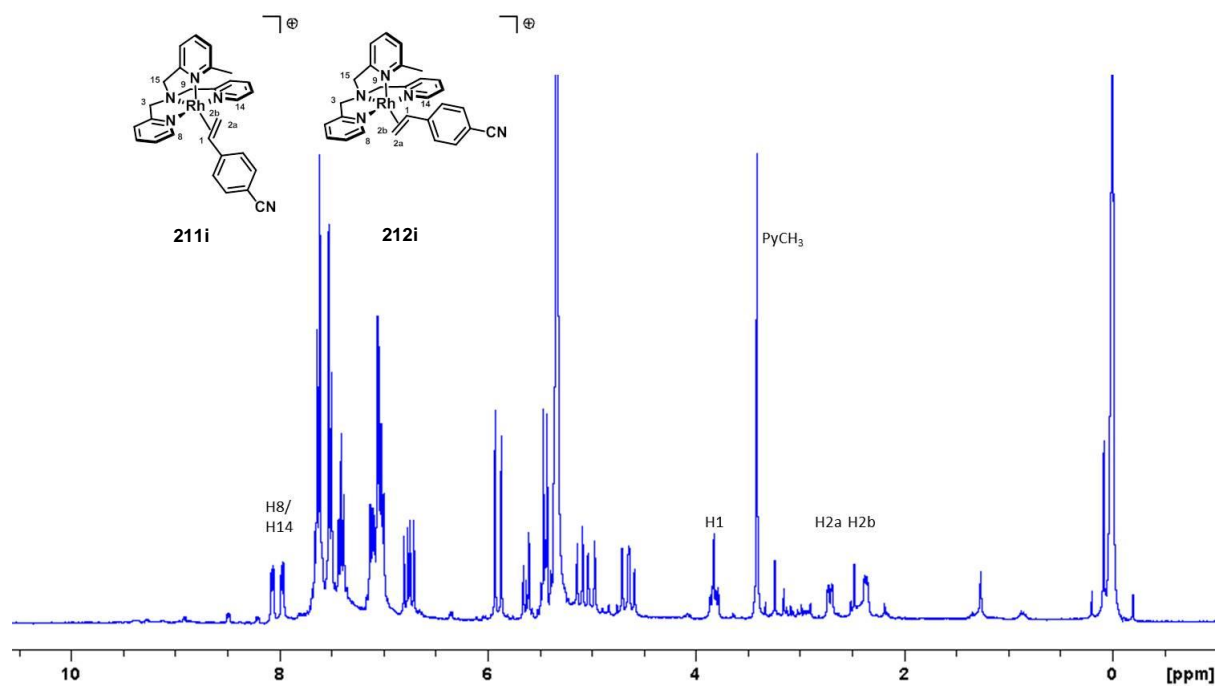
211g/212g, [MeTPA-Rh-Styrene]Cl, CD₂Cl₂



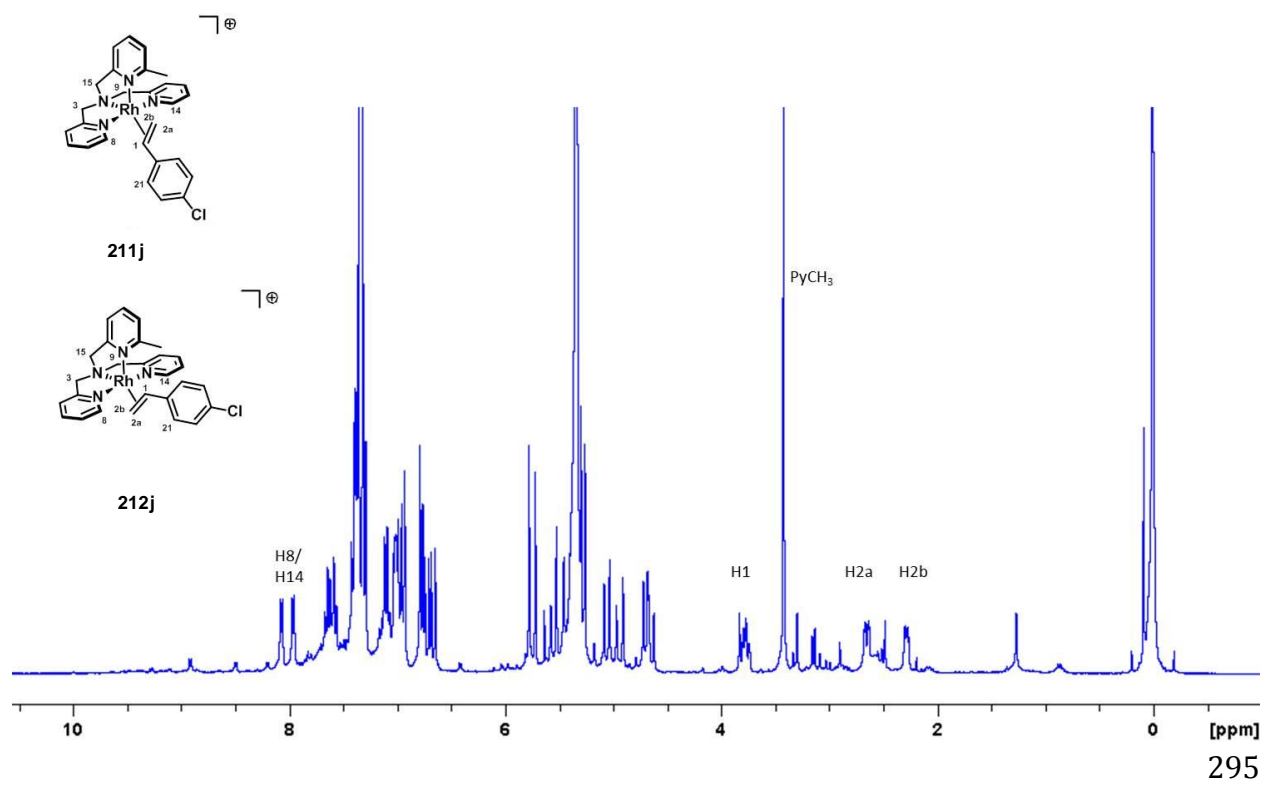
211h/212h, [MeTPA-Rh-4-nitrostyrene]Cl, CD₂Cl₂



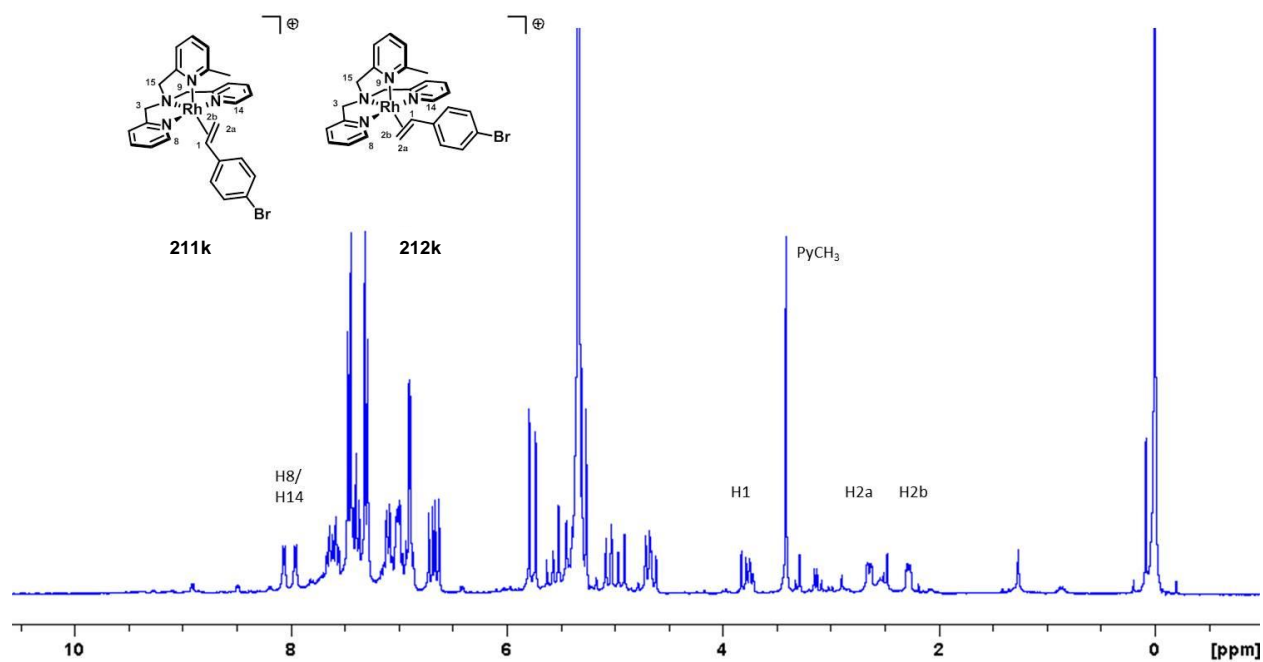
211i/212i, [MeTPA-Rh-4-cyanostyrene]Cl, CD₂Cl₂



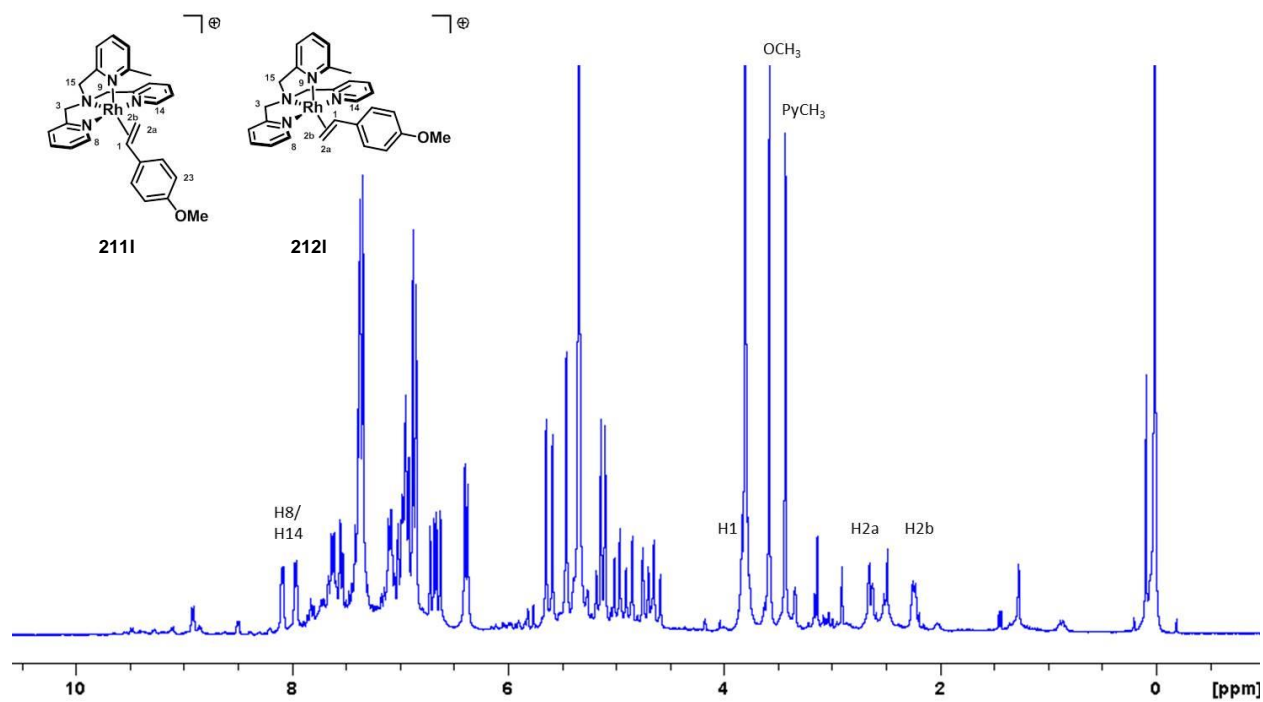
211j/212j, [MeTPA-Rh-4-chlorostyrene]Cl, CD₂Cl₂



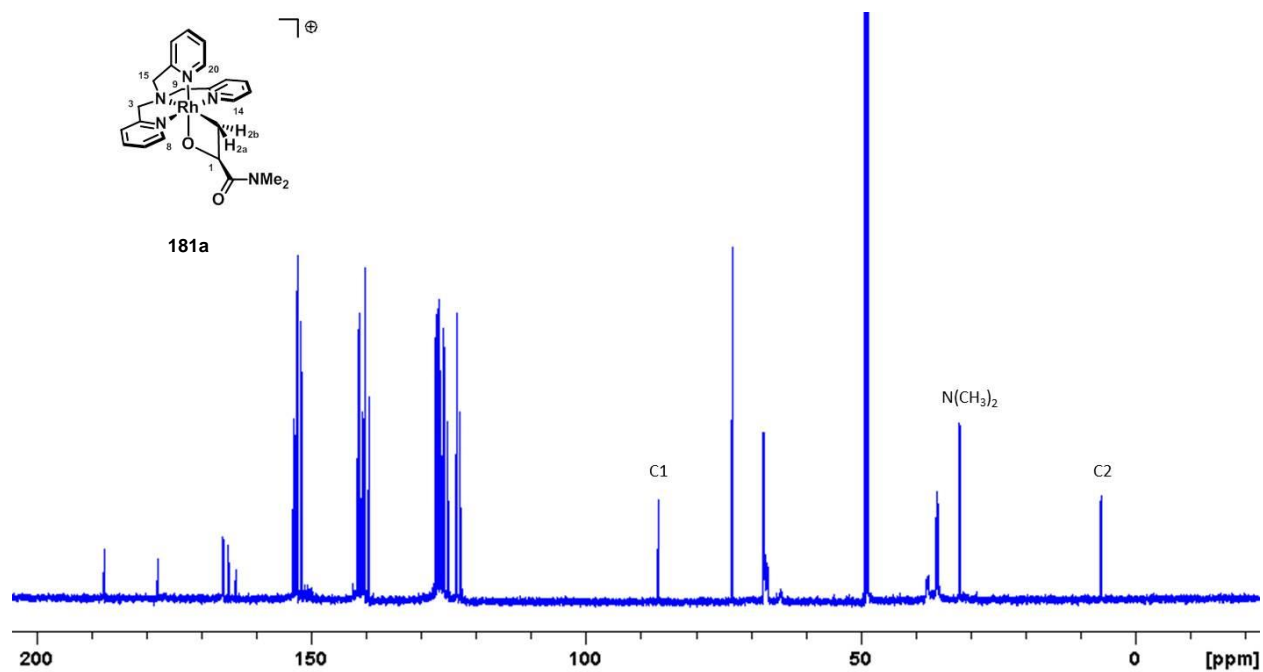
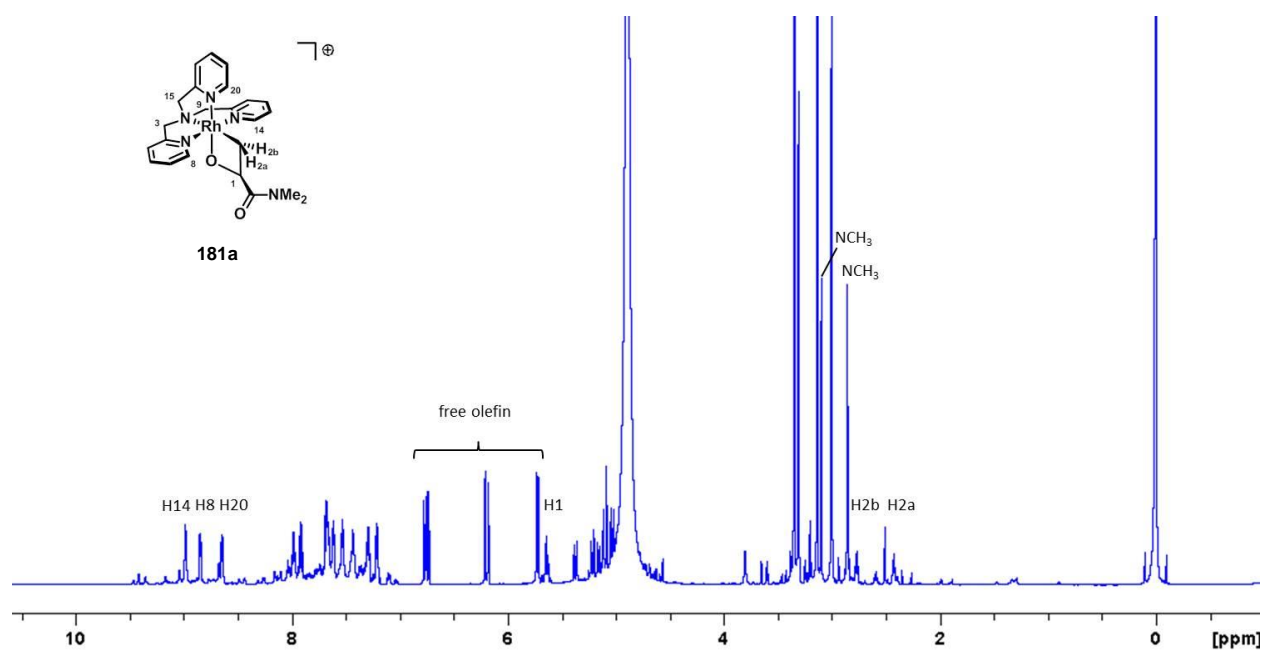
211k/212k, [MeTPA-Rh-4-bromostyrene]Cl, CD₂Cl₂



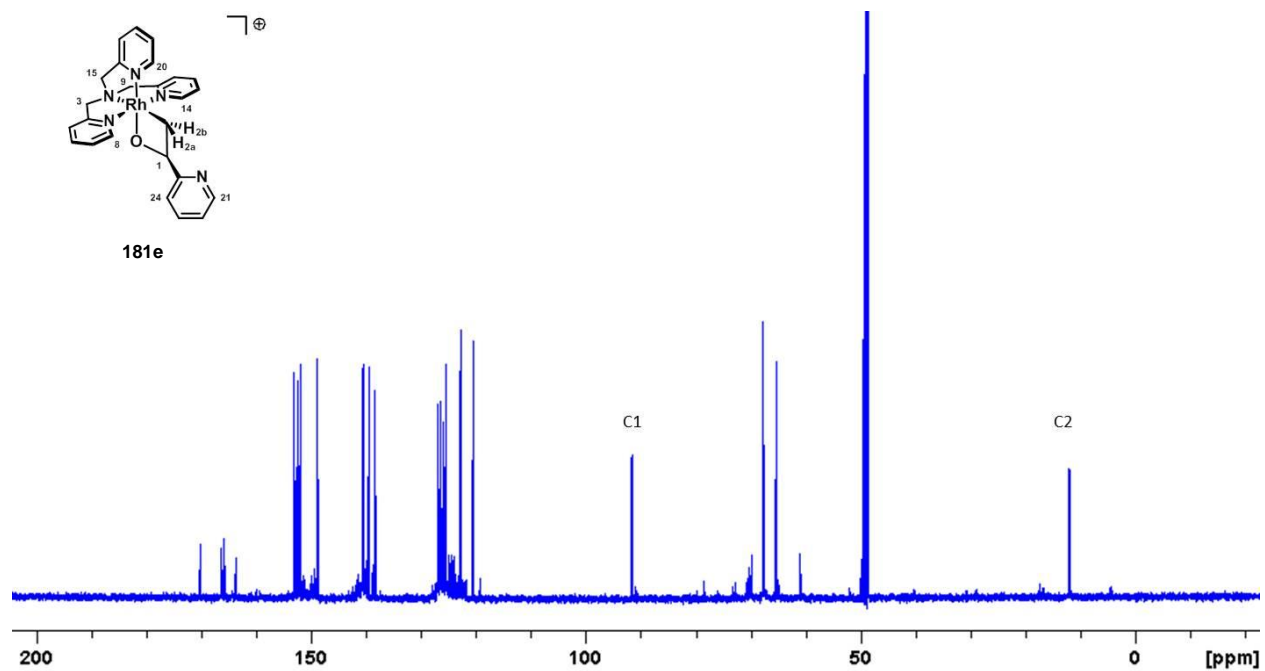
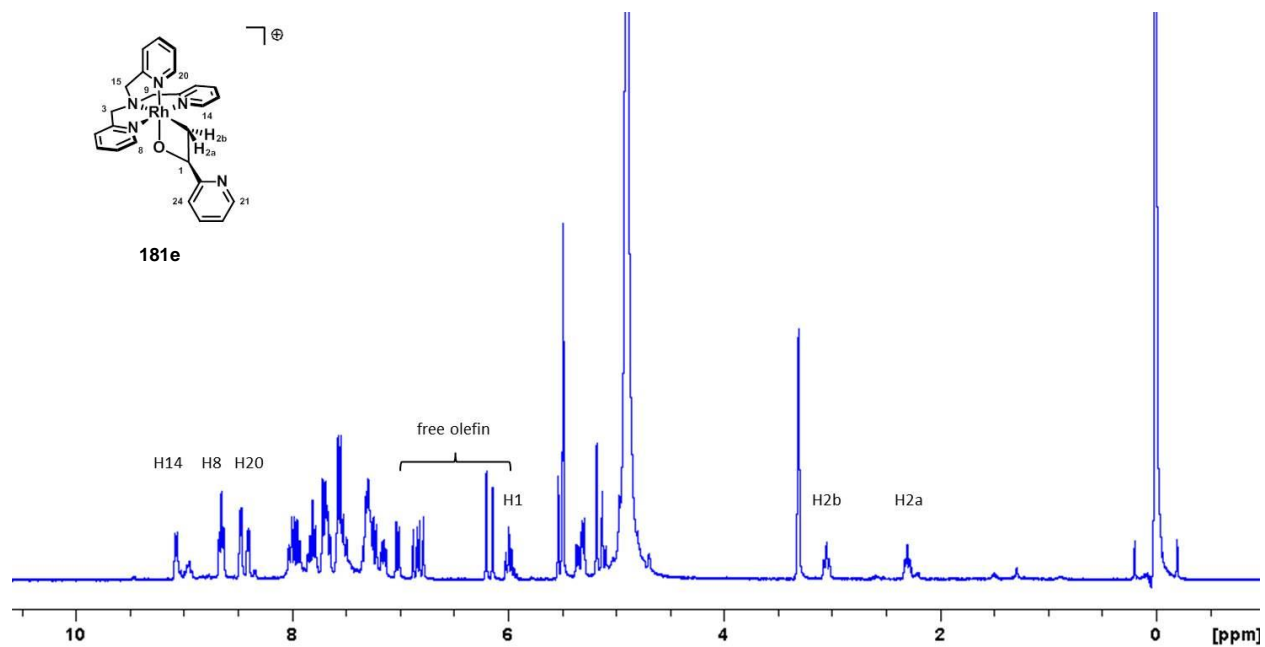
211l/212l, [MeTPA-Rh-4-Methoxystyrene]Cl, CD₂Cl₂



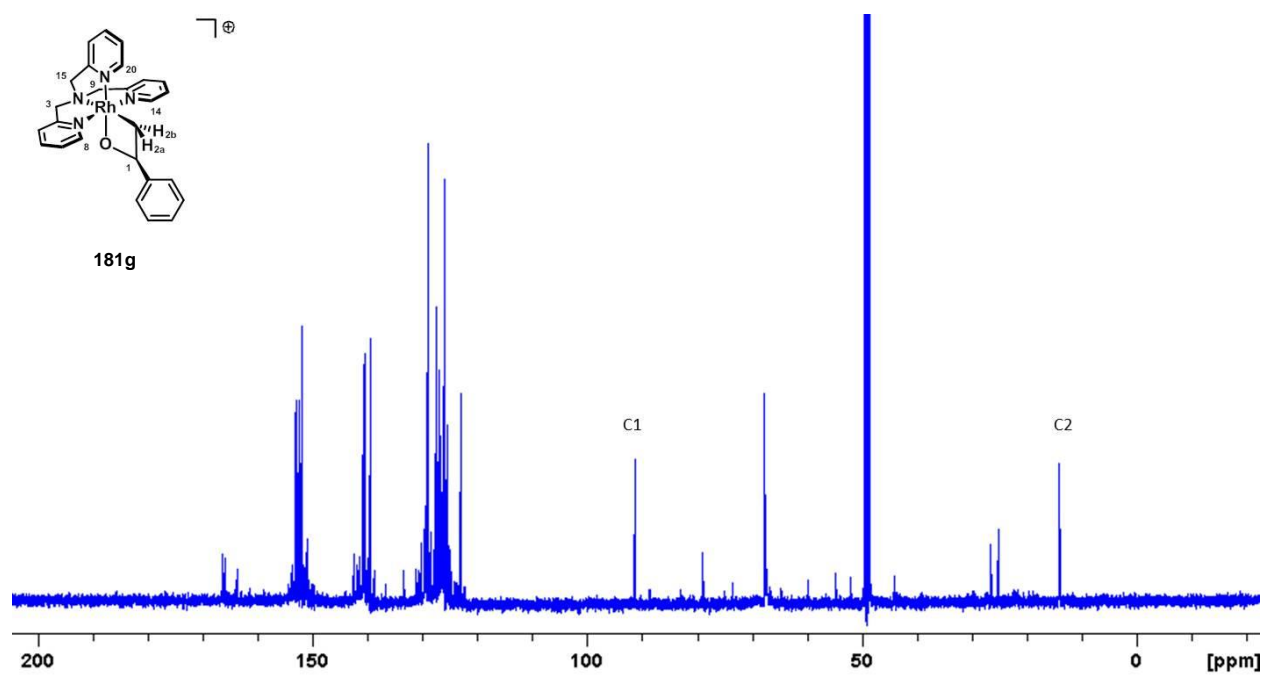
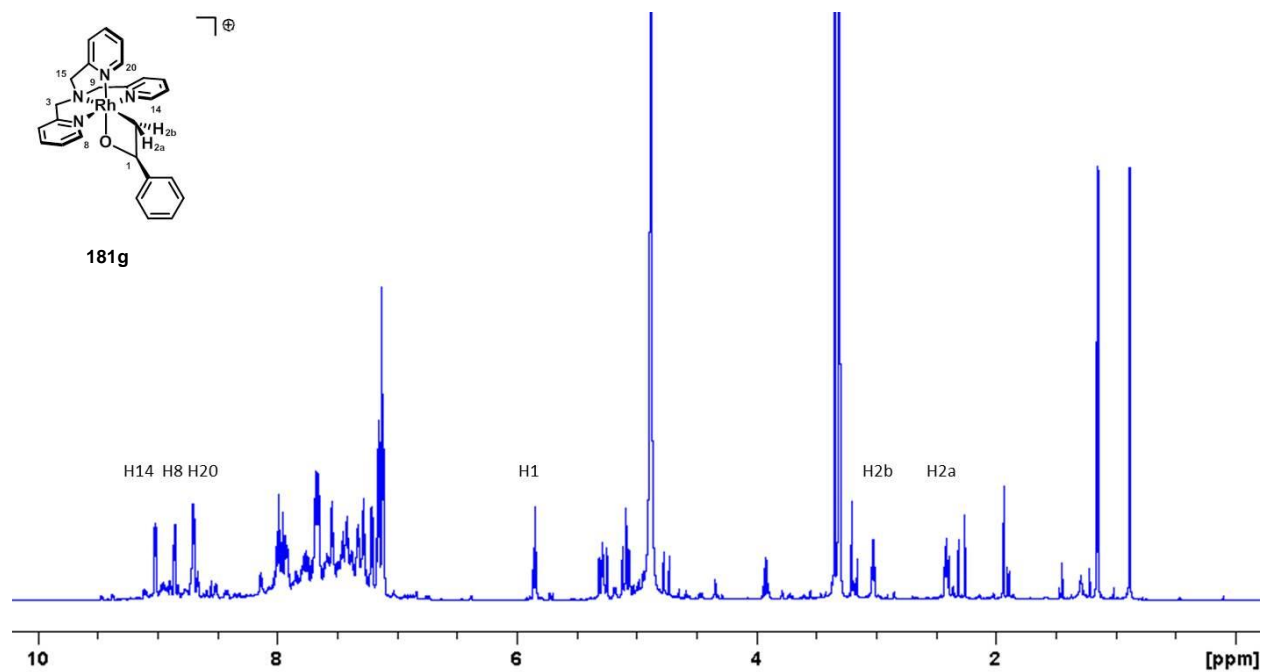
181a, [TPA-*N*, *N*-Dimethylacrylamide-oxarhodacyclobutane]Cl, MeOD



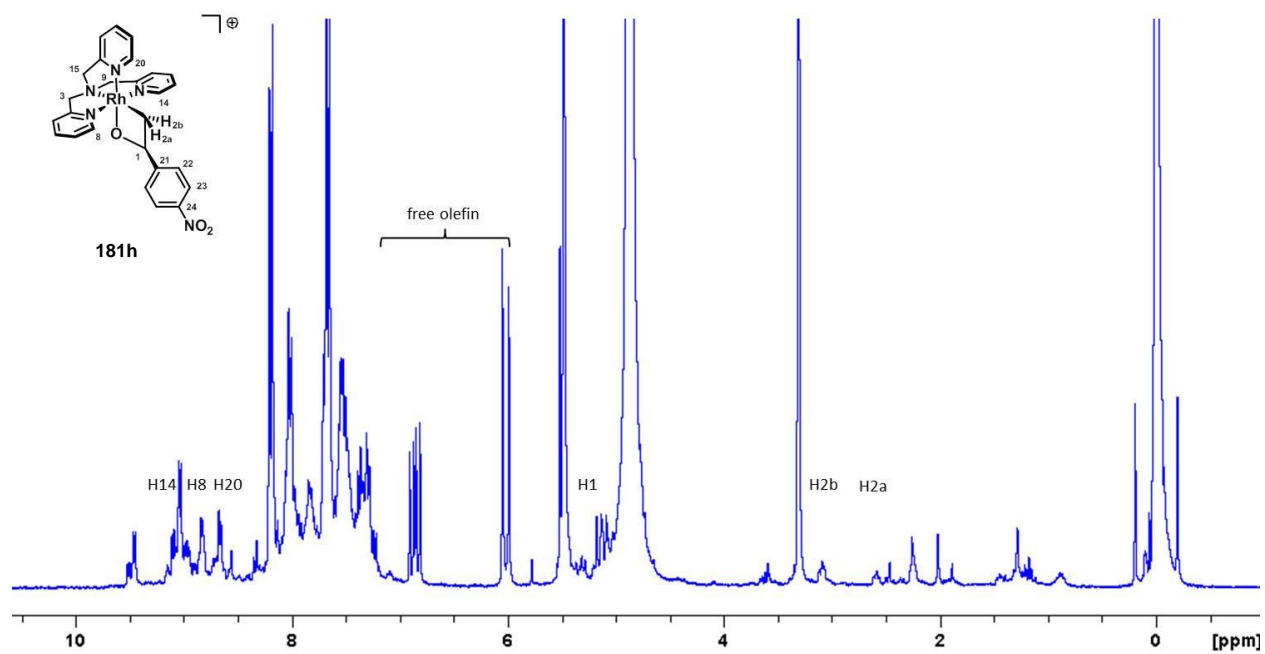
181e, [TPA-vinylpyridine-oxarhodacyclobutane]Cl, MeOD



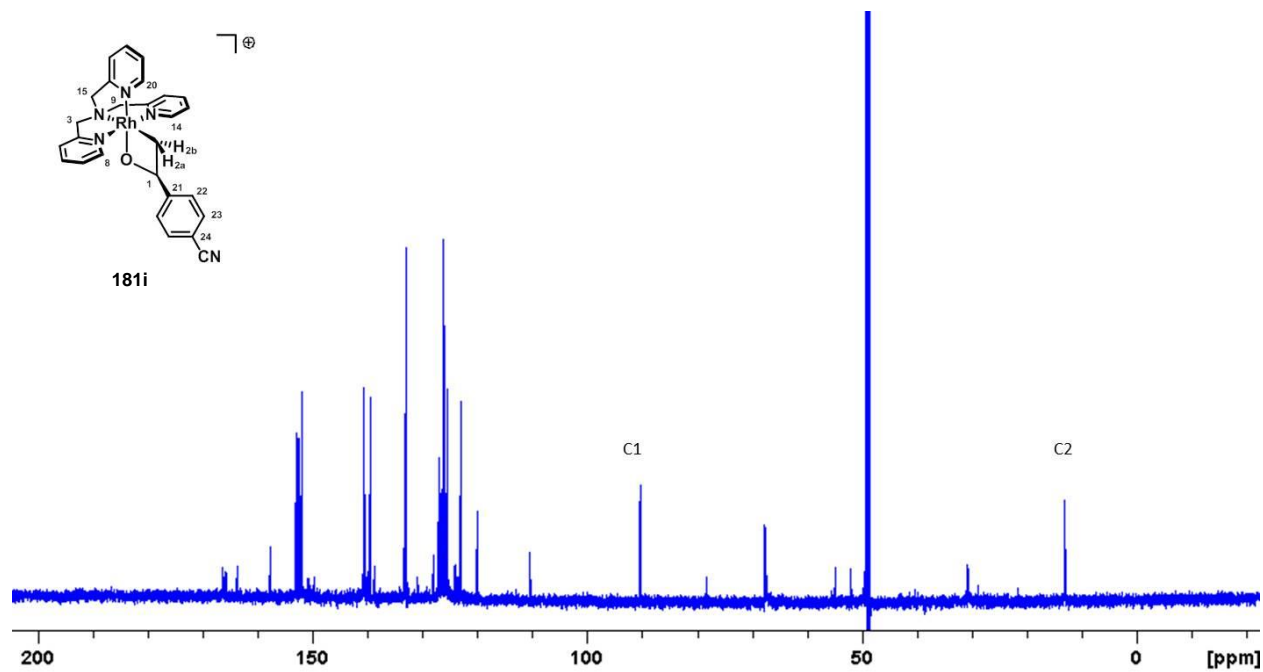
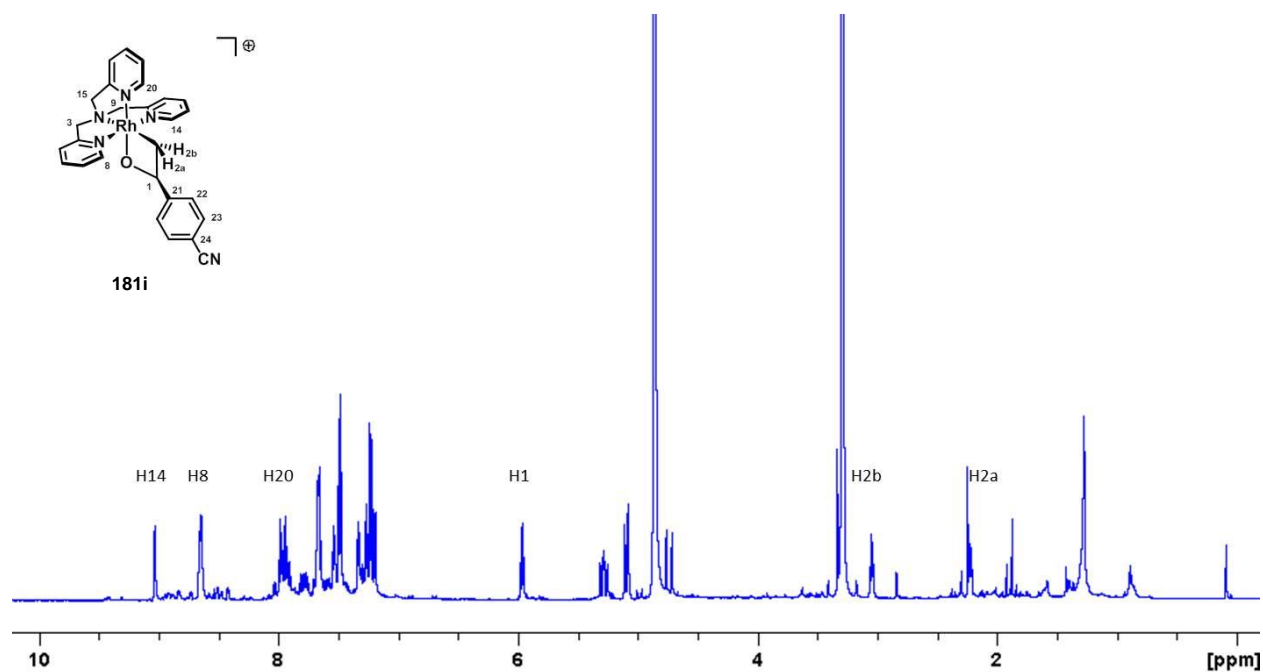
181g, [TPA-styrene-oxarhodacyclobutane]Cl, MeOD



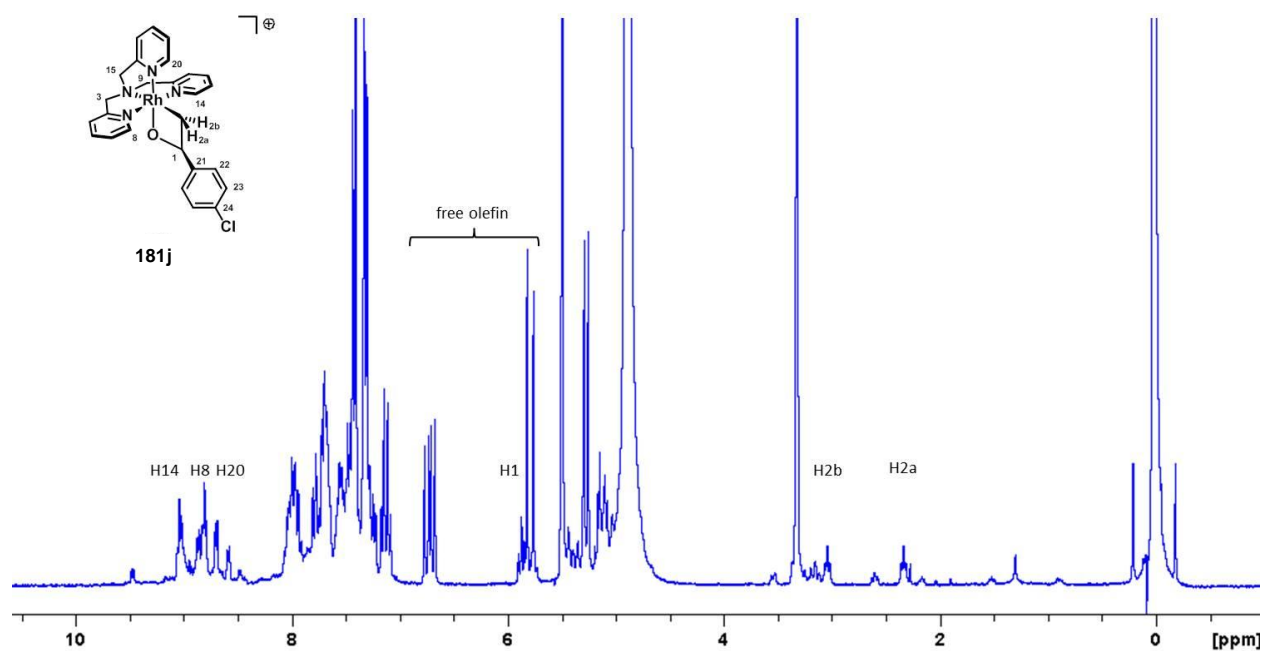
181h, [TPA-4-nitrostyrene-oxarhodacyclobutane]Cl, MeOD



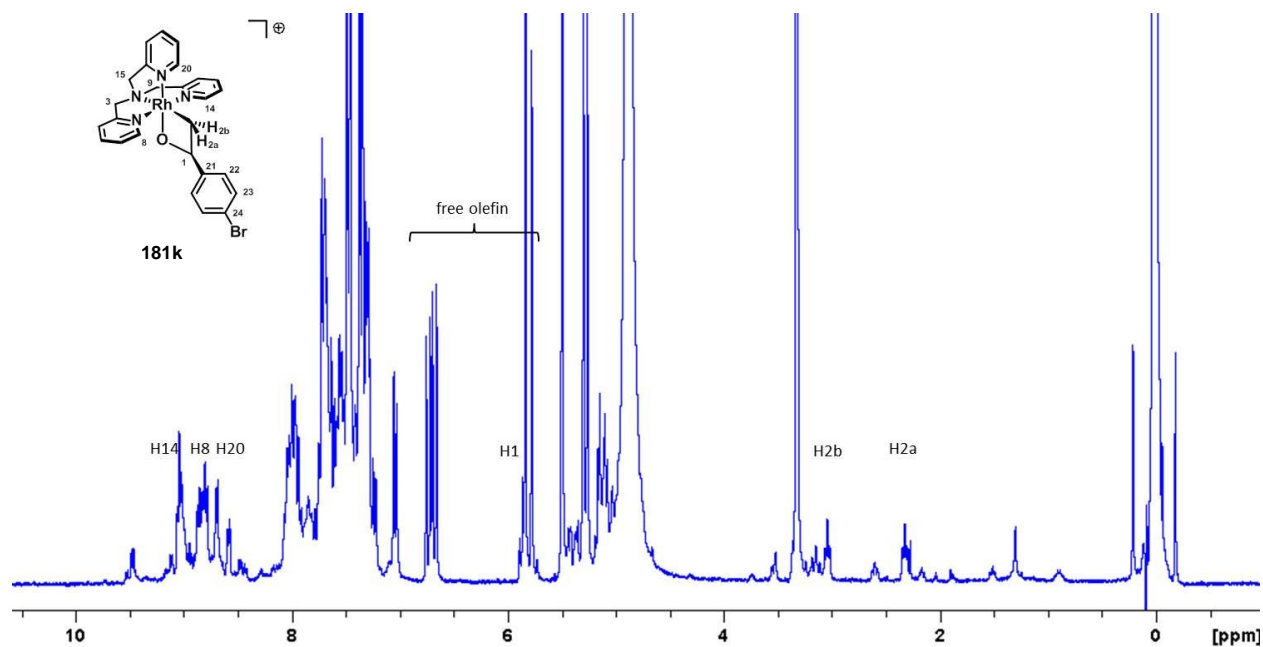
181i, [TPA-4-cyanostyrene-oxarhodacyclobutane]Cl, MeOD



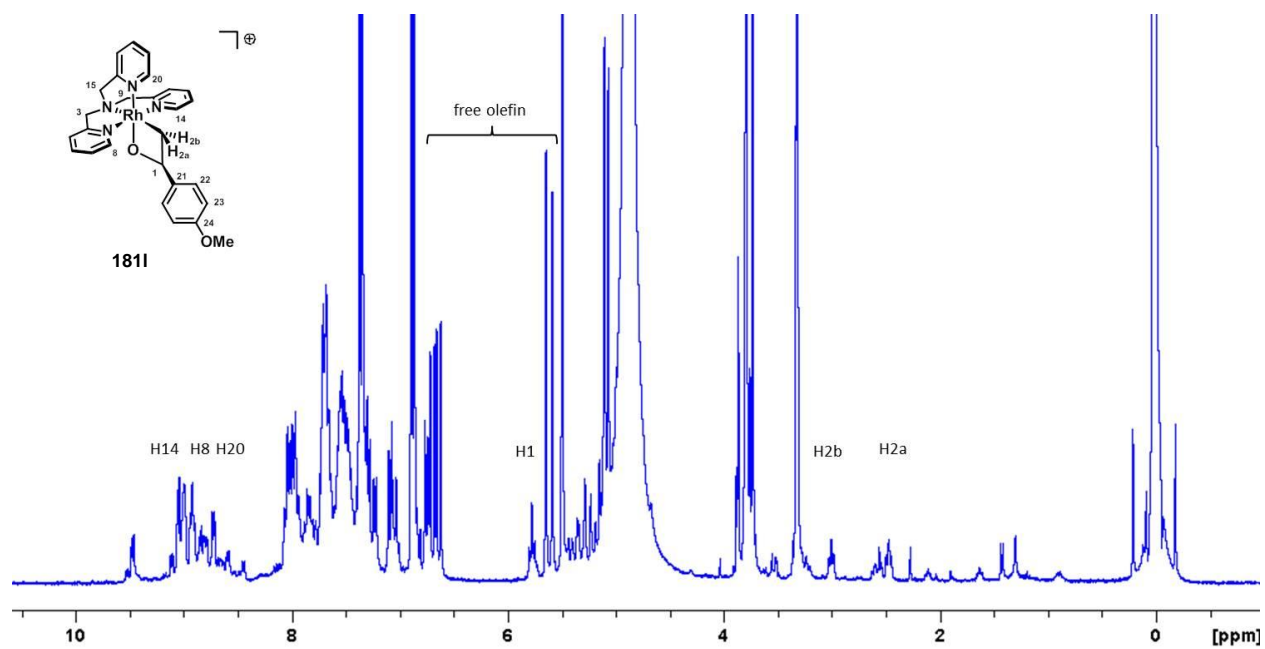
181j, [TPA-4-chlorostyrene-oxarhodacyclobutane]Cl, MeOD



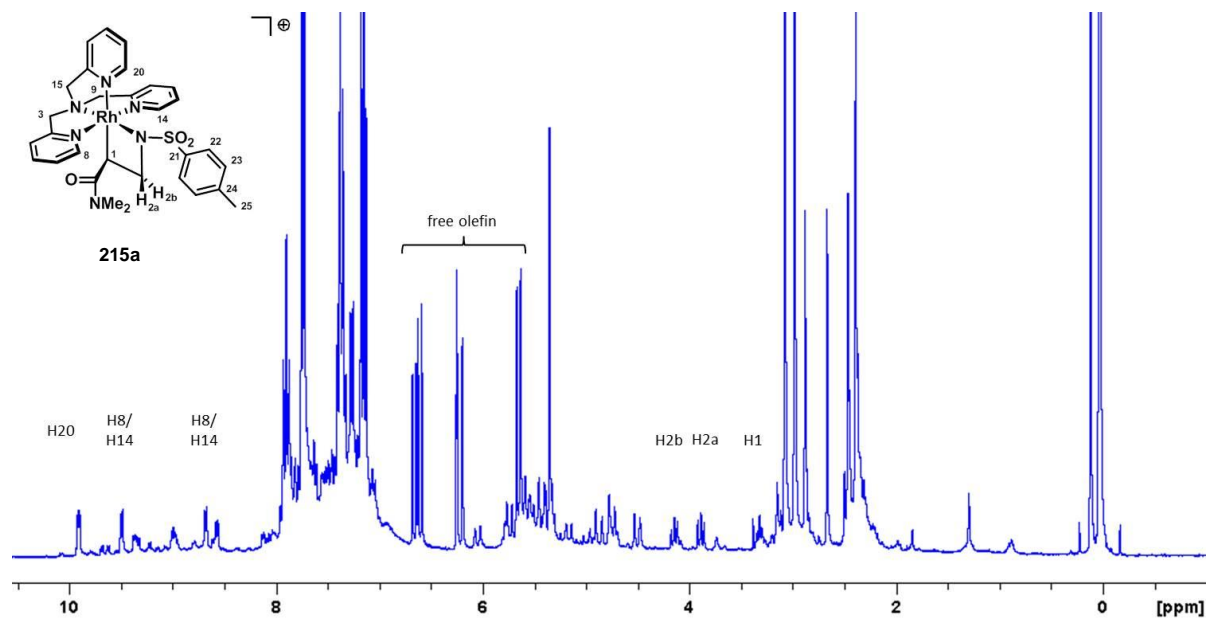
181k, [TPA-4-bromostyrene-oxarhodacyclobutane]Cl, MeOD



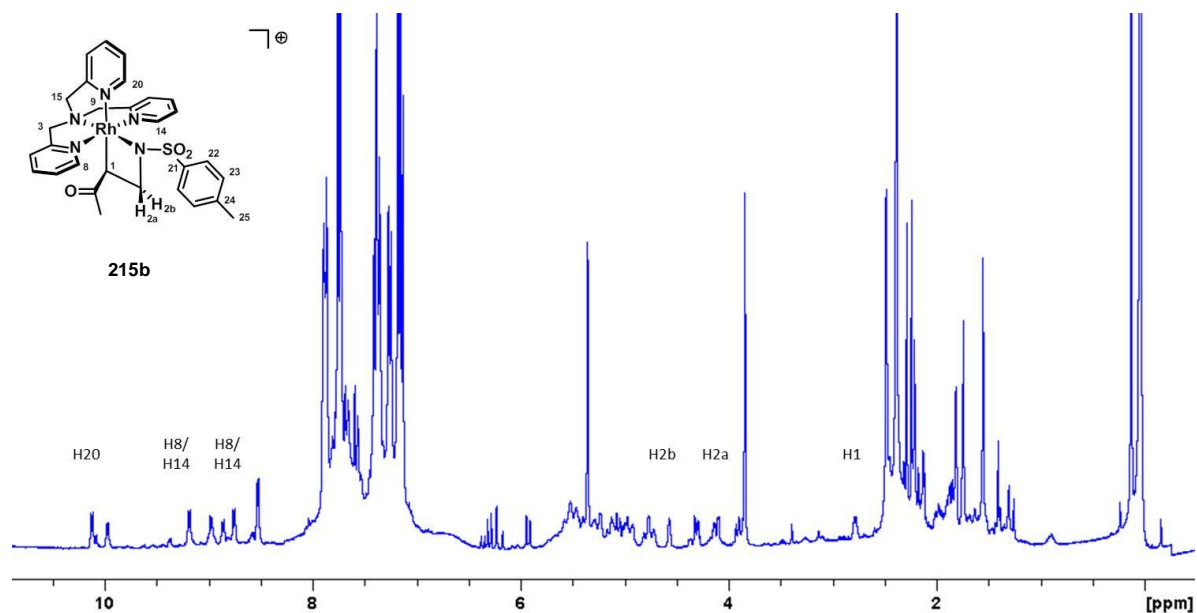
181I, [TPA-4-methoxystyrene-oxarhodacyclobutane]Cl, MeOD



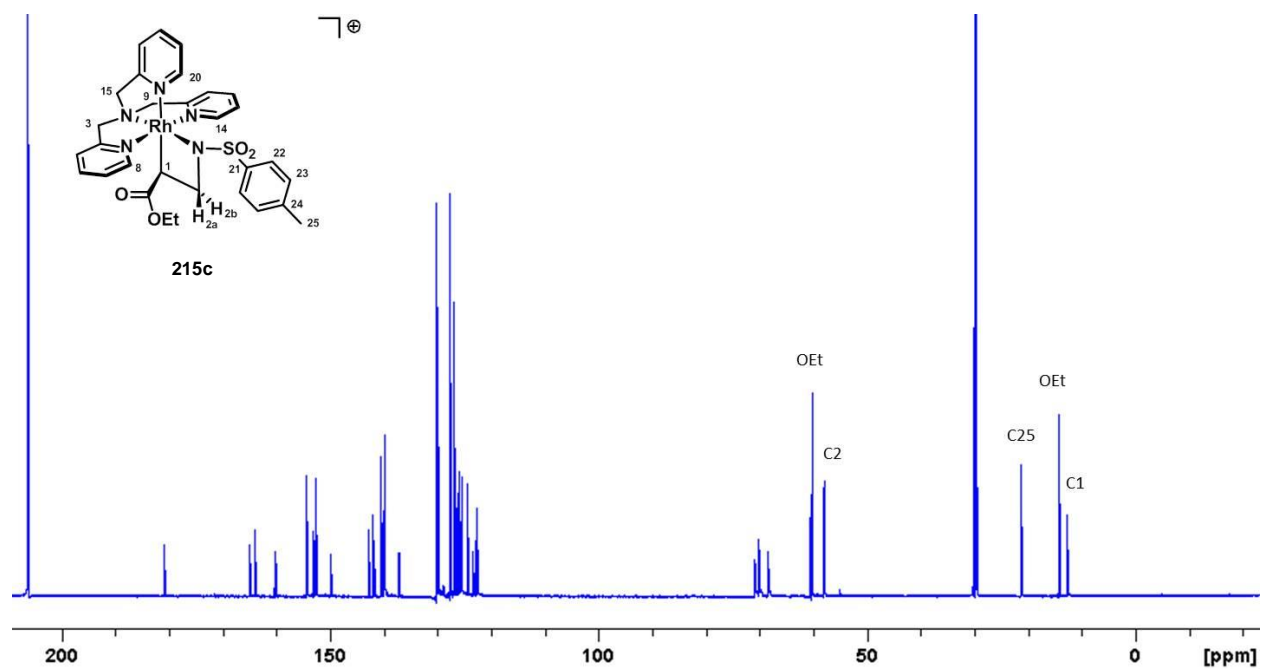
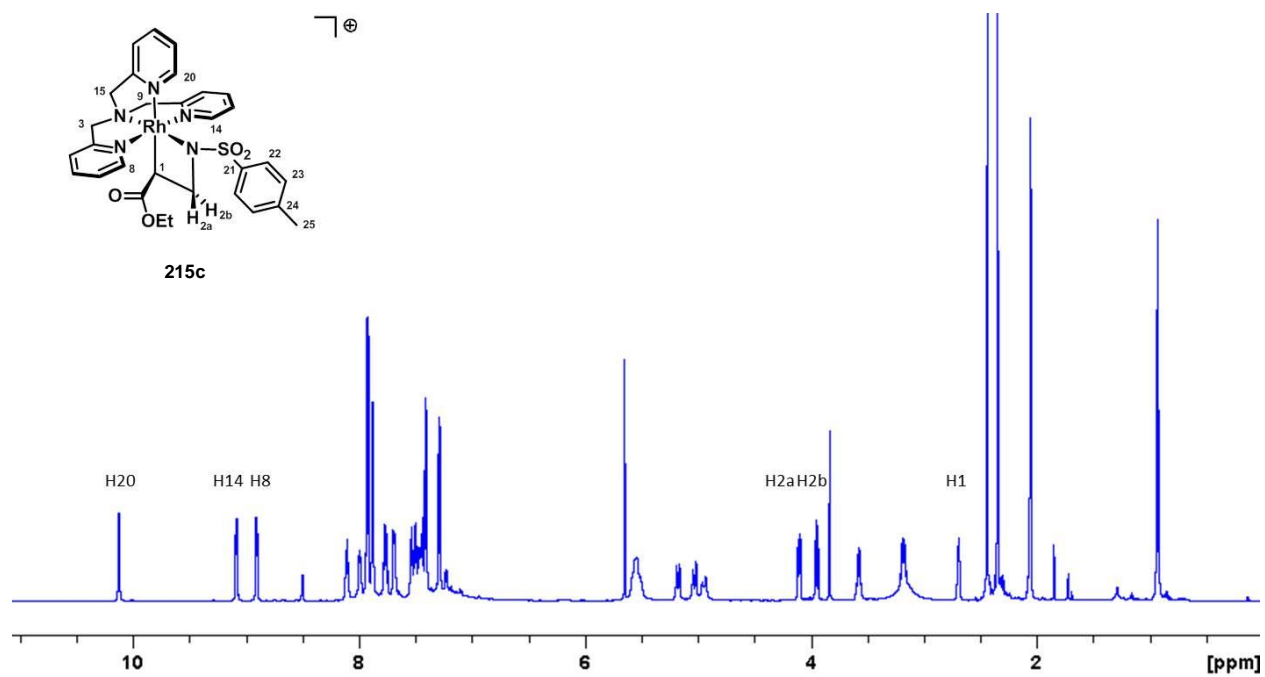
215a, [TPA-ethylacrylate-azarhodacyclobutane]Cl, CD₂Cl₂



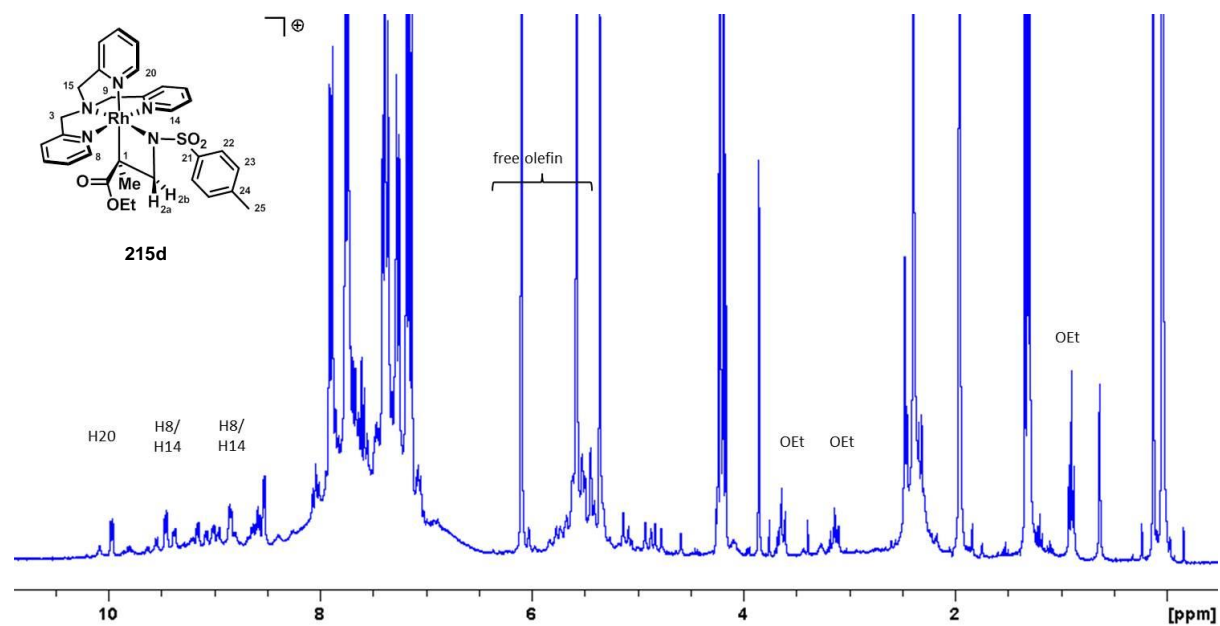
215b, [TPA-methylvinylketone-azarhodacyclobutane]Cl, CD₂Cl₂



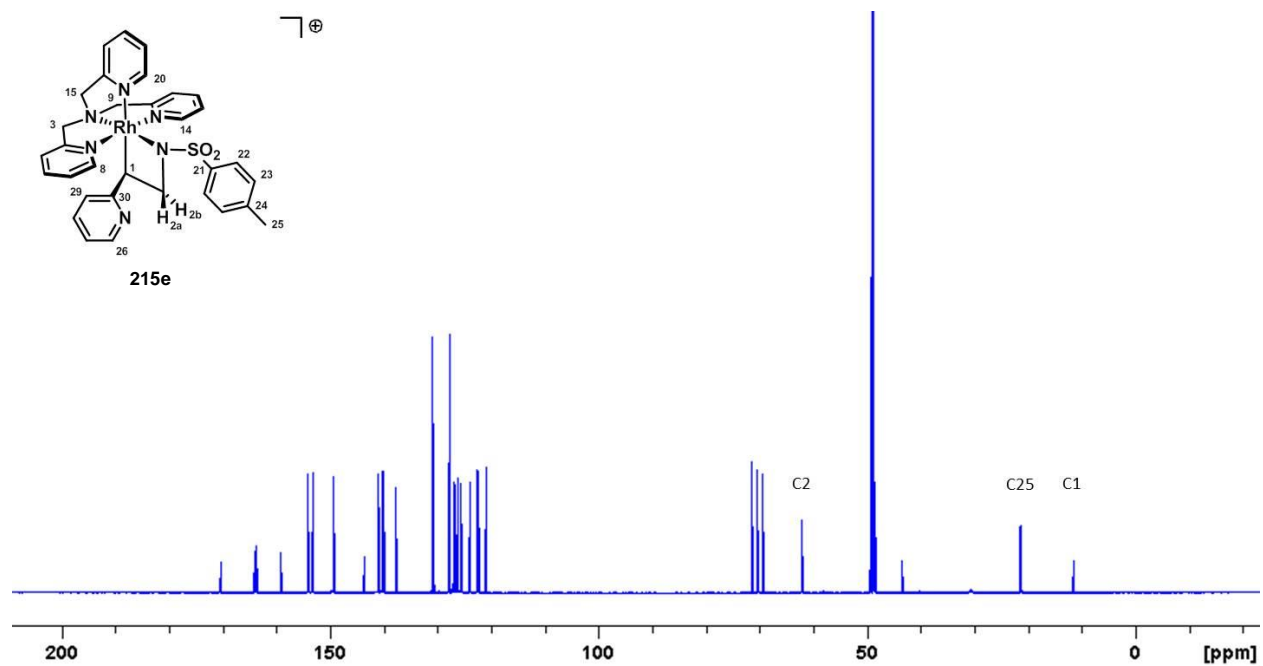
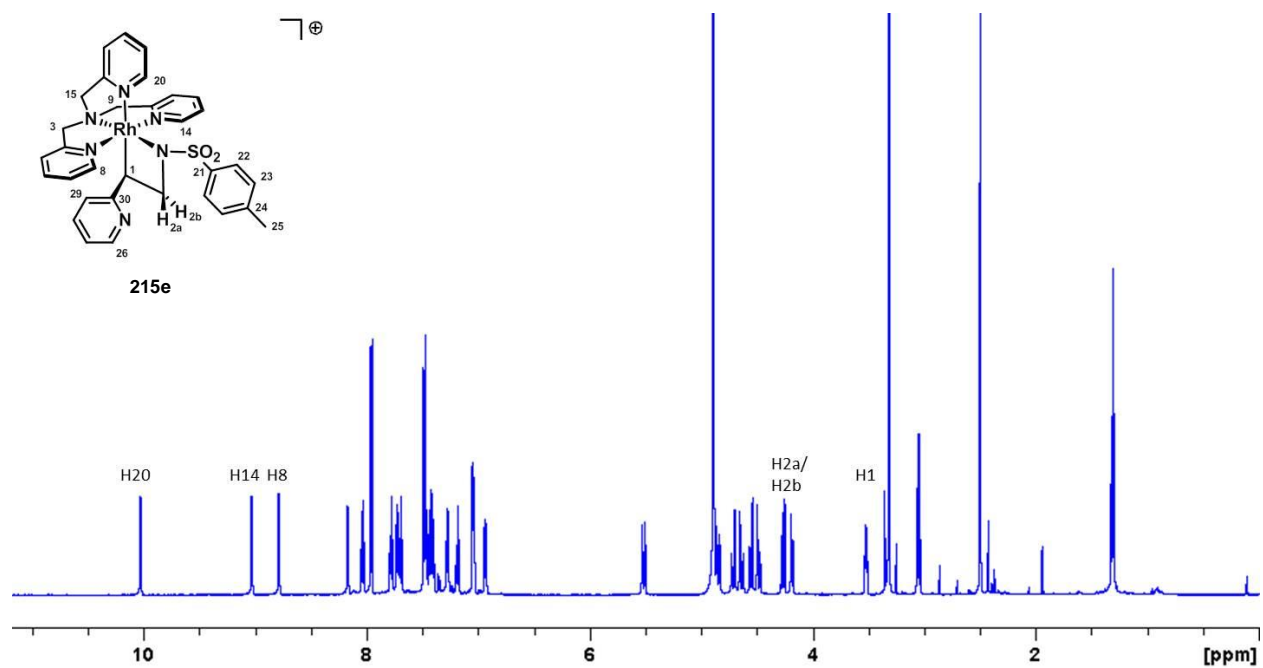
215c, [TPA-ethylacrylate-azarhodacyclobutane]Cl, *d*₆-acetone



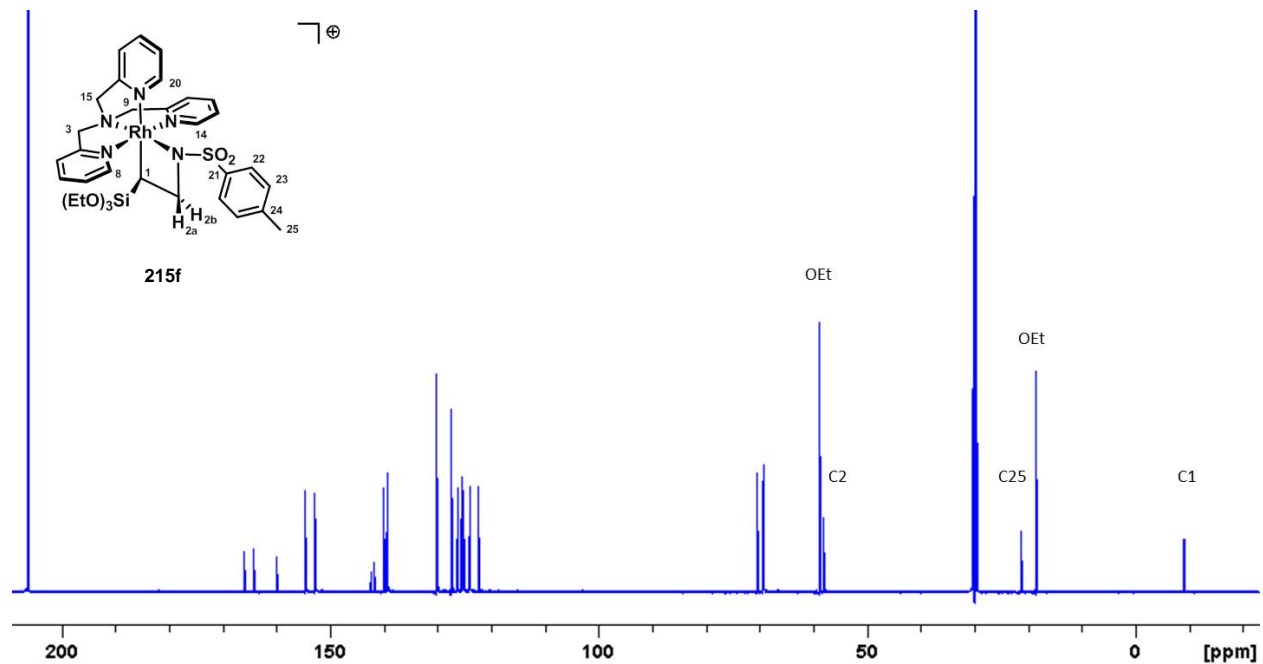
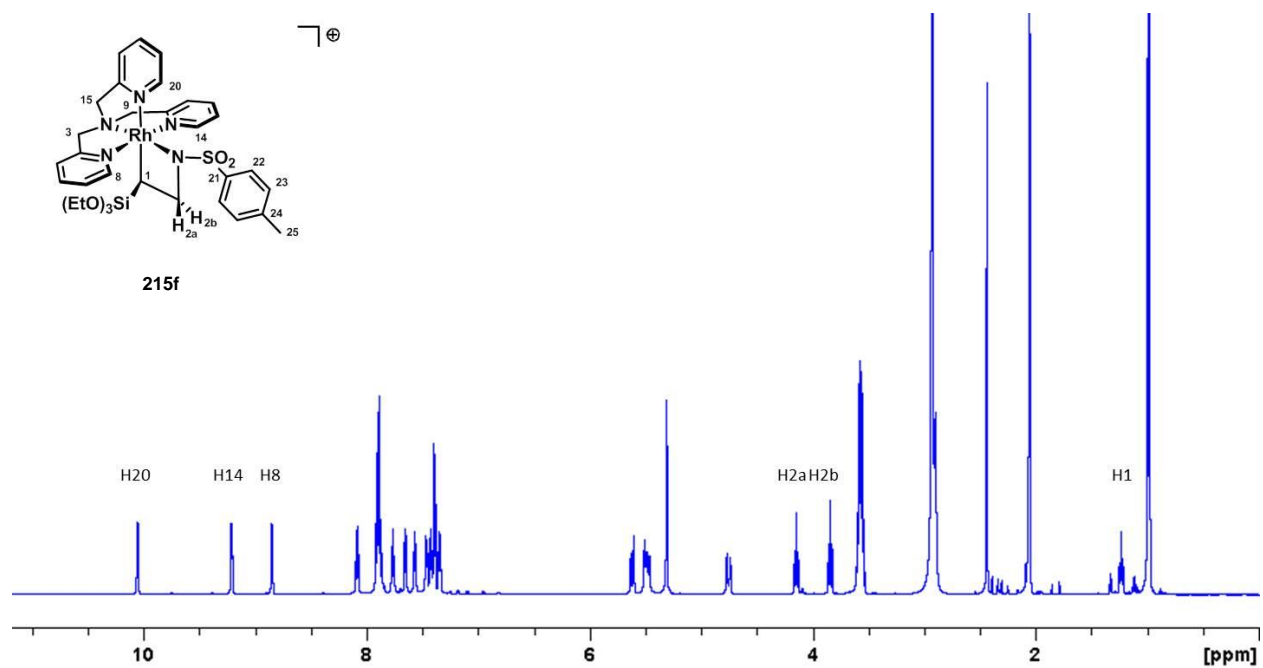
215d, [TPA-ethylmethacrylate-azarhodacyclobutane]Cl, CD₂Cl₂



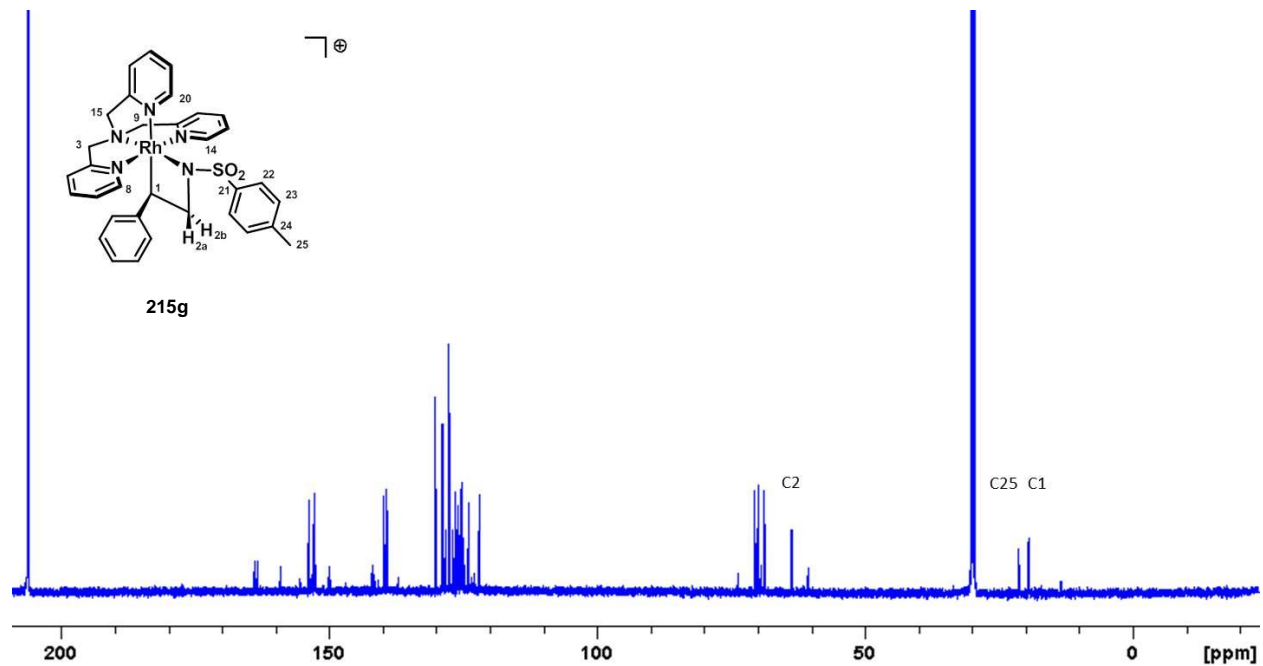
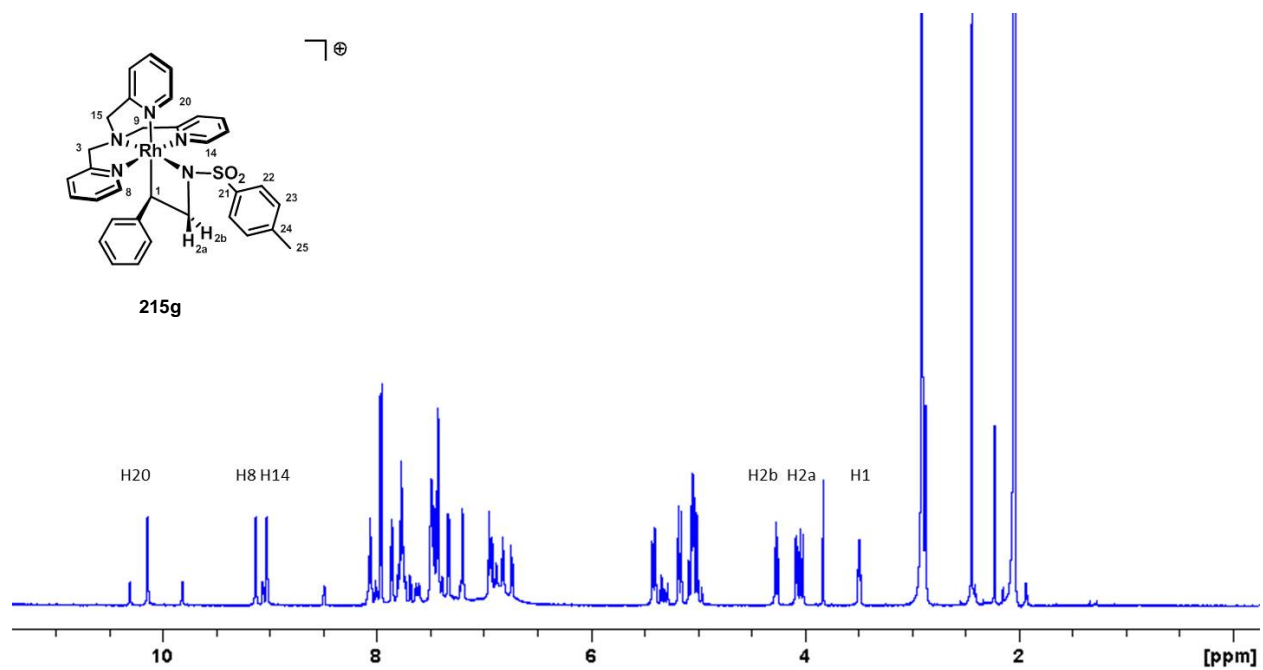
215e, [TPA-vinylpyridine-azarhodacyclobutane]Cl, CD₂Cl₂

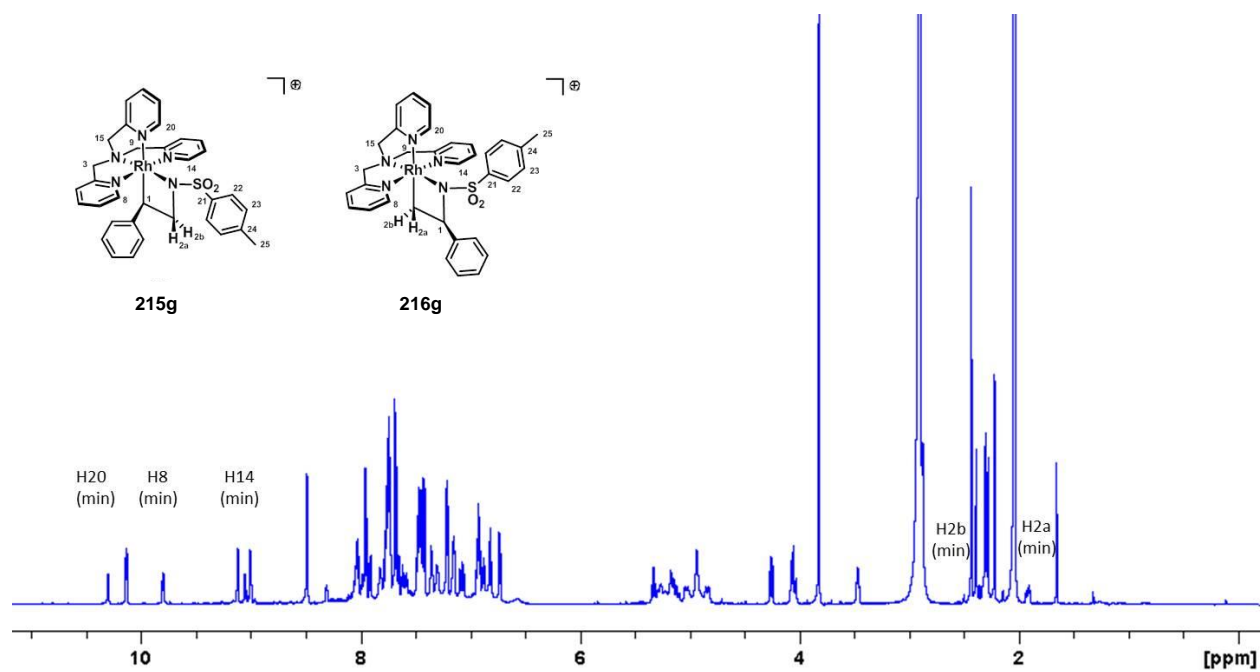


215f, [TPA-triethoxyvinylsilane-azarhodacyclobutane]Cl, *d*₆-acetone

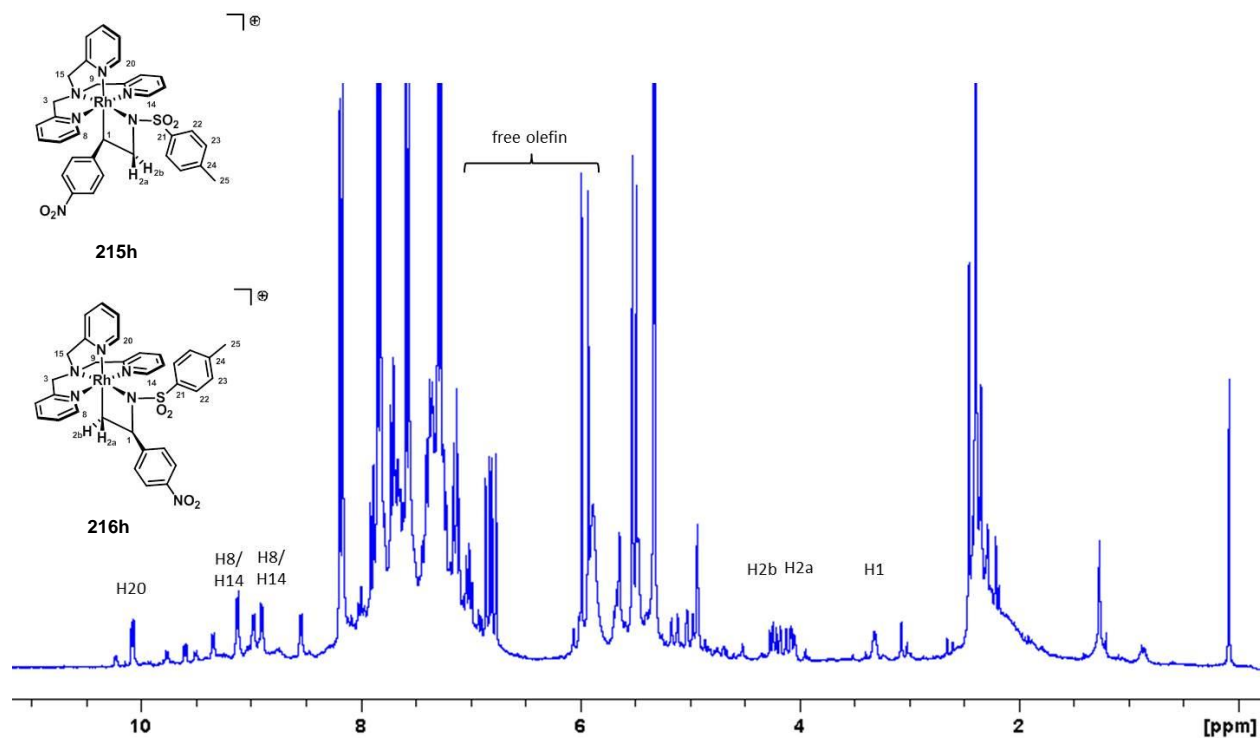


215g/216g [TPA-styrene-azarhodacyclobutane]Cl, *d*₆-acetone

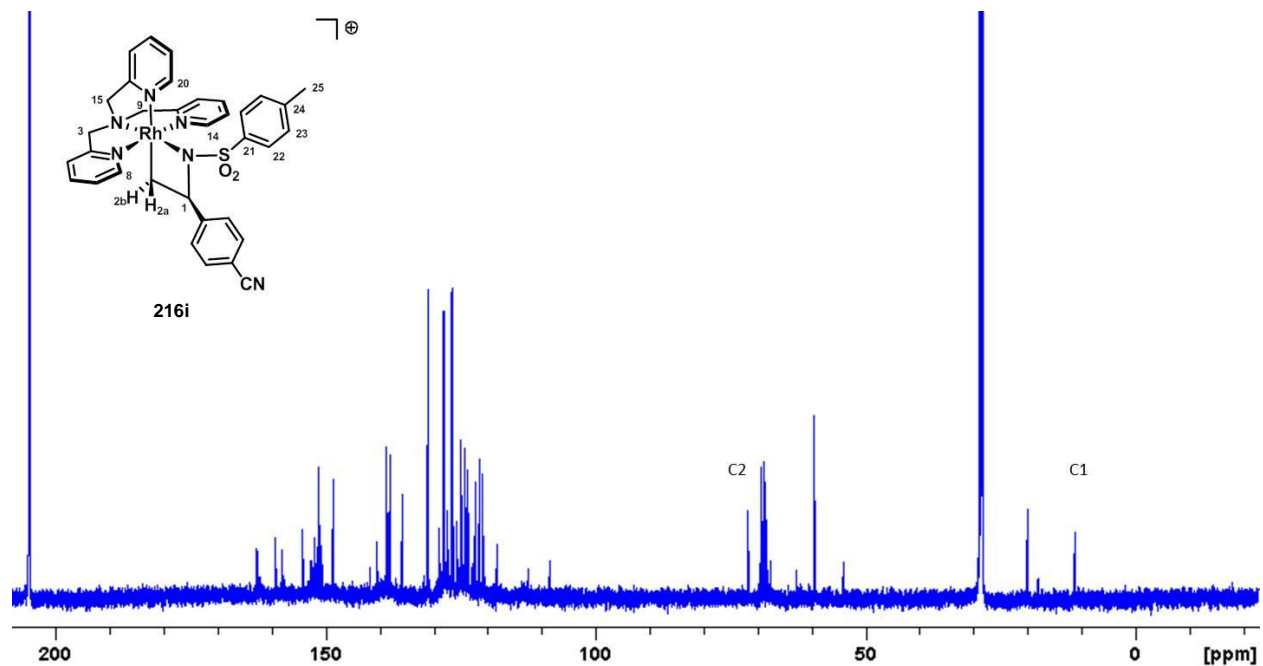
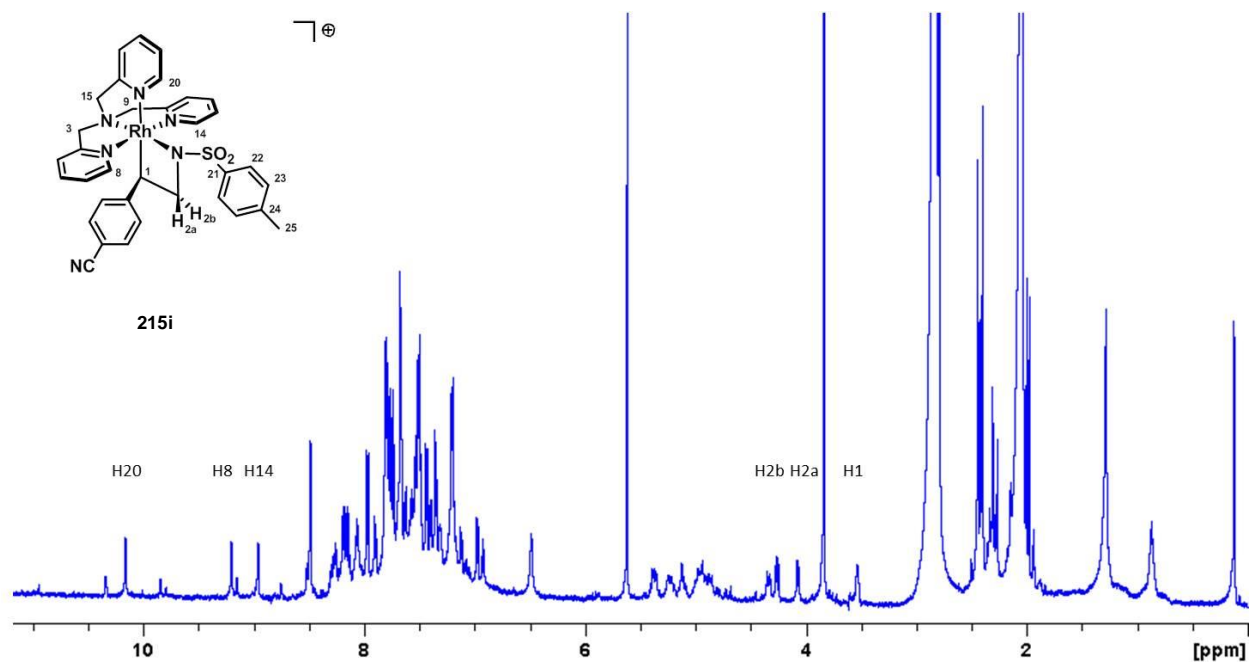




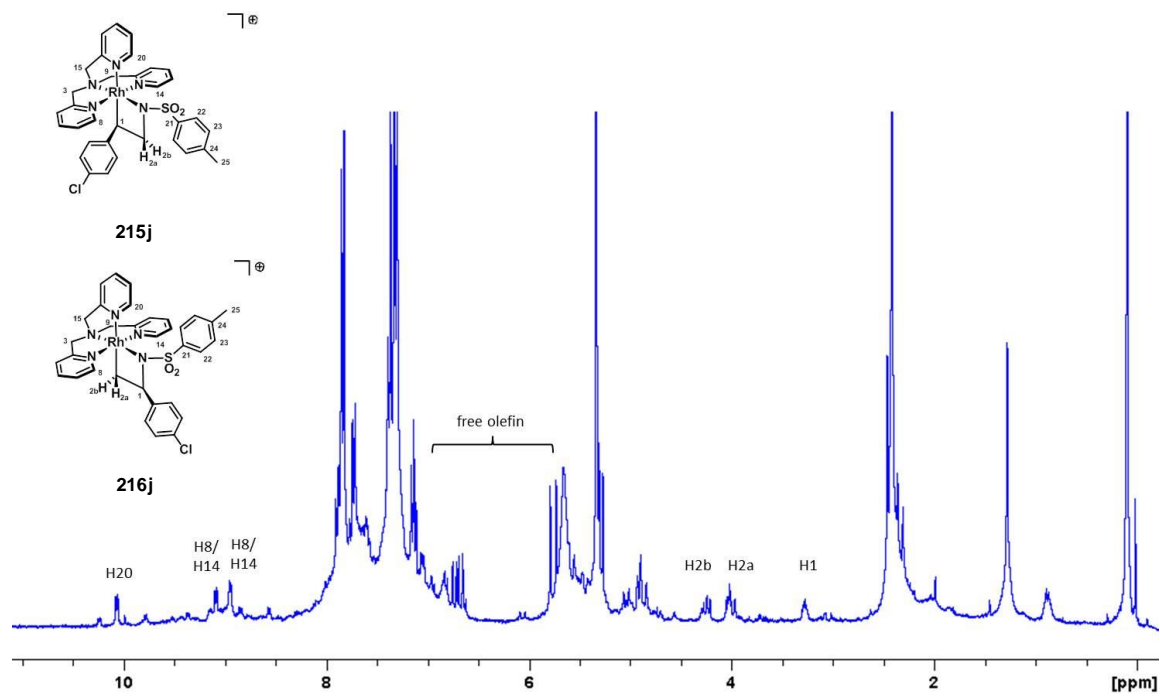
215h/216h, [TPA-4-nitrostyrene-azarhodacyclobutane]Cl, CD₂Cl₂



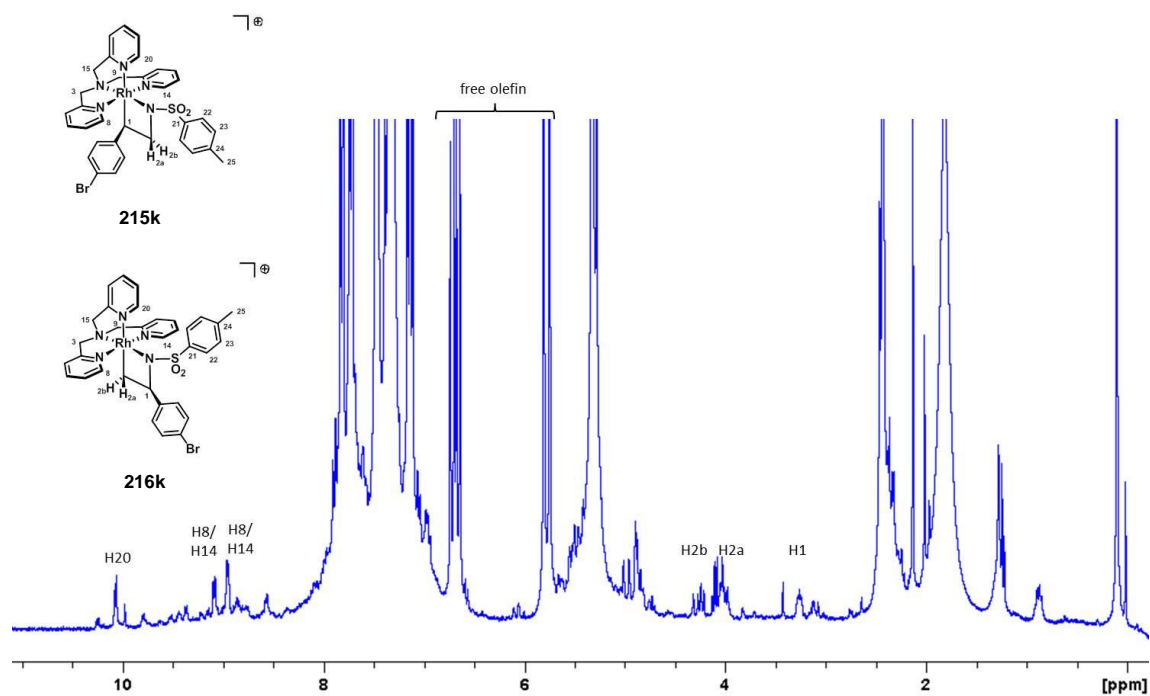
215i/216i, [TPA-4-cyanostyrene-azarhodacyclobutane]Cl, *d*₆-acetone



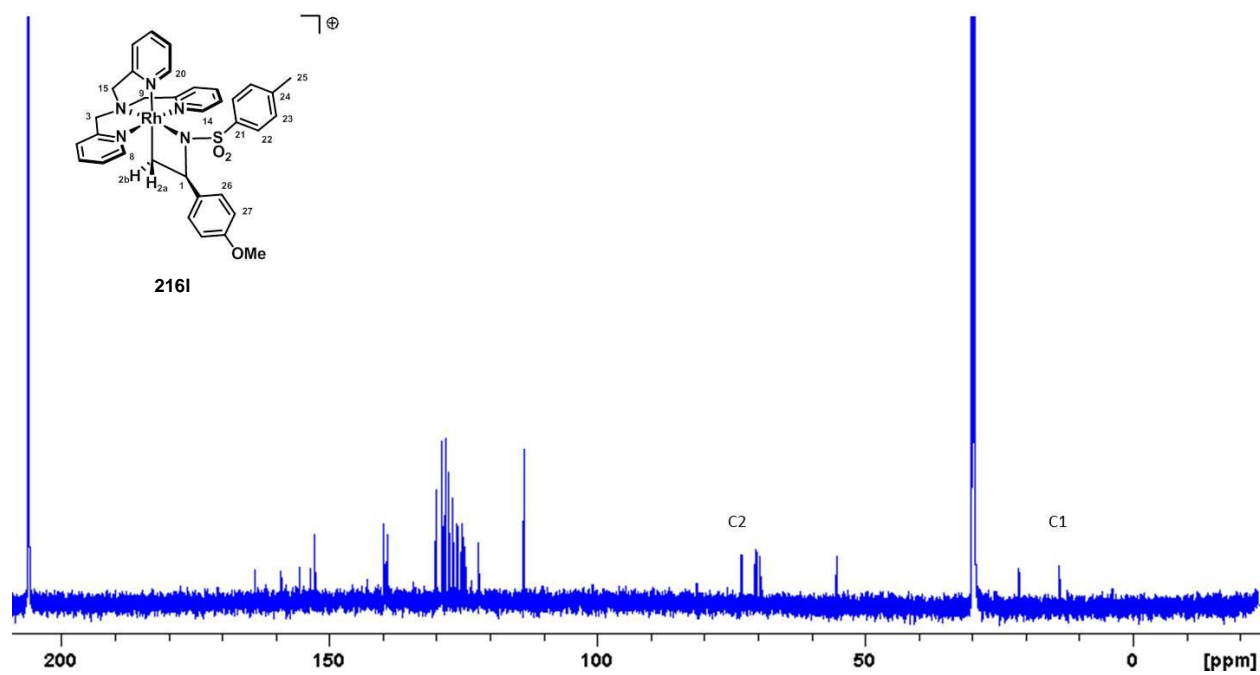
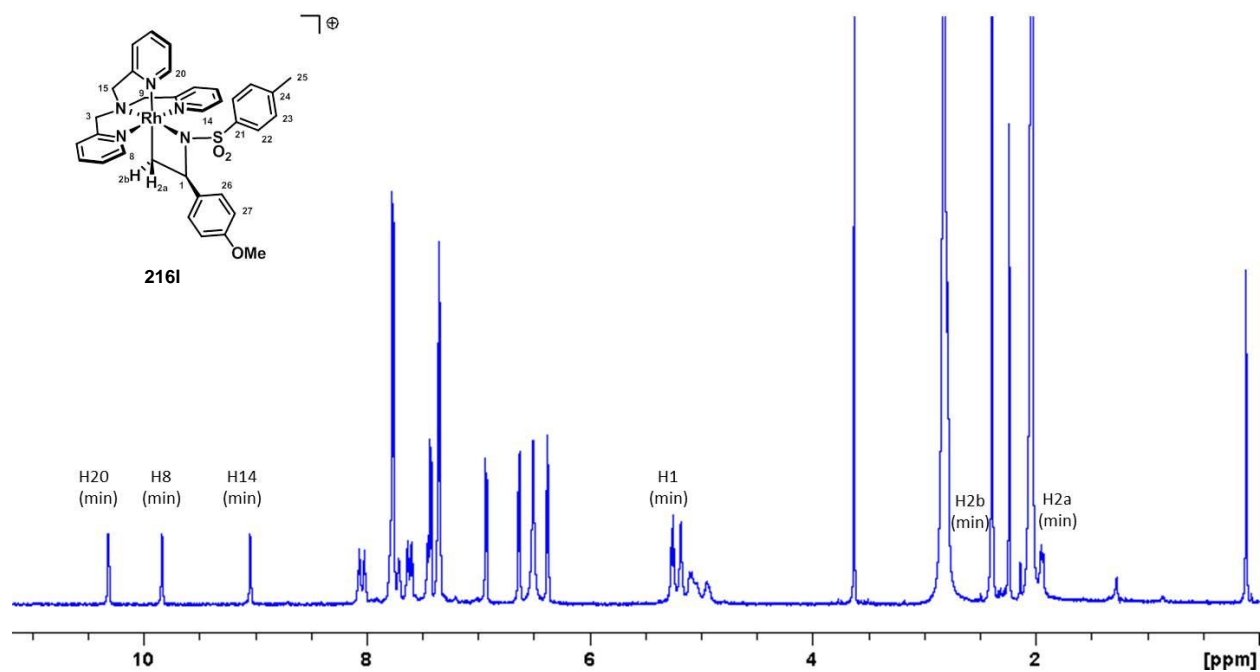
215j/216j, [TPA-4-chlorostyrene-azarhodacyclobutane]Cl, CD₂Cl₂



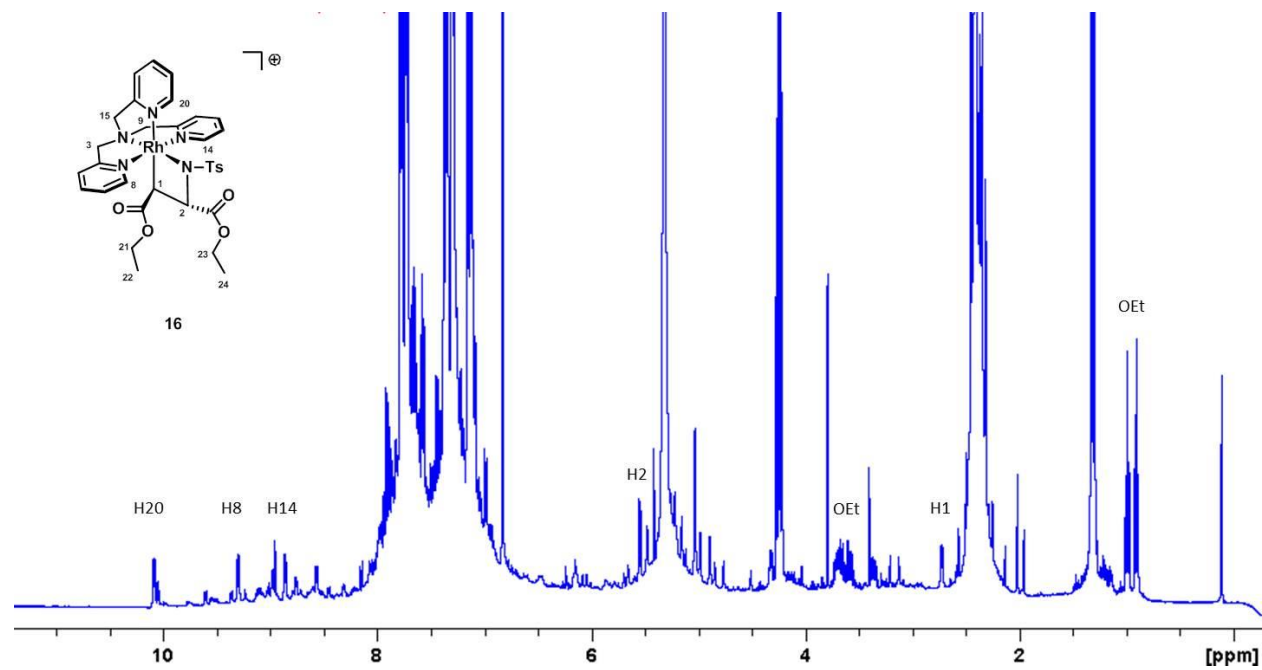
215k/216k, [TPA-4-bromostyrene-azarhodacyclobutane]Cl, CD₂Cl₂



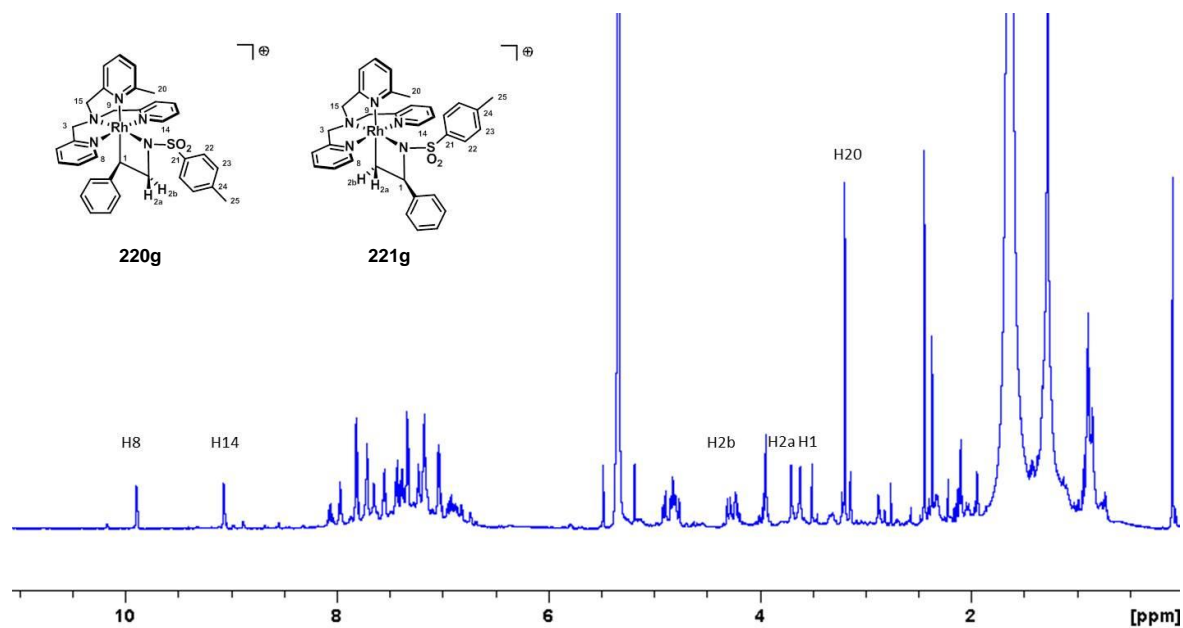
215l/216l, [TPA-4-methoxystyrene-azarhodacyclobutane]Cl, *d*₆-acetone



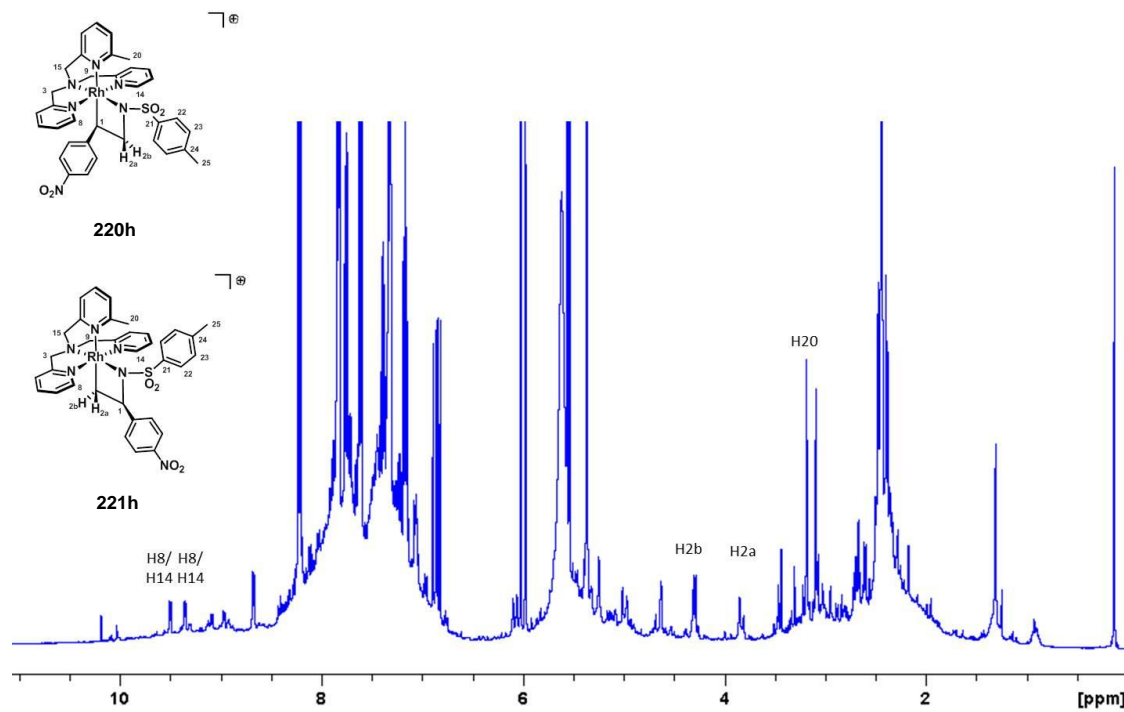
217, [TPA-diethylfumarate-azarhodacyclobutane]Cl, CD₂Cl₂



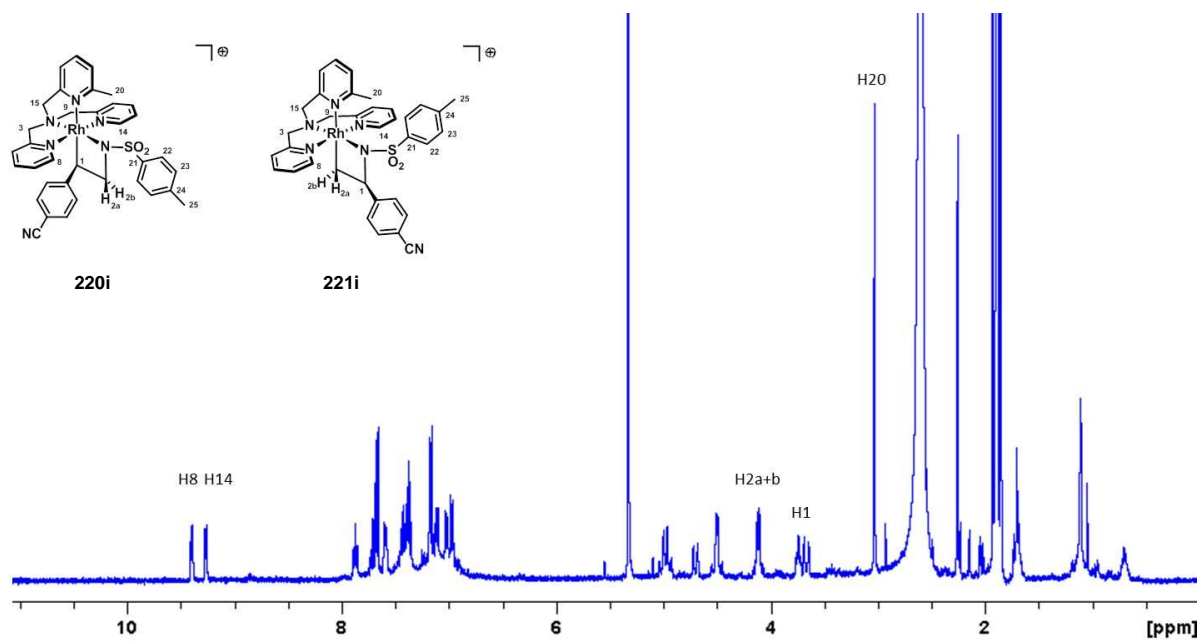
220g/221g, [MeTPA-styrene-azarhodacyclobutane]Cl, CD₂Cl₂



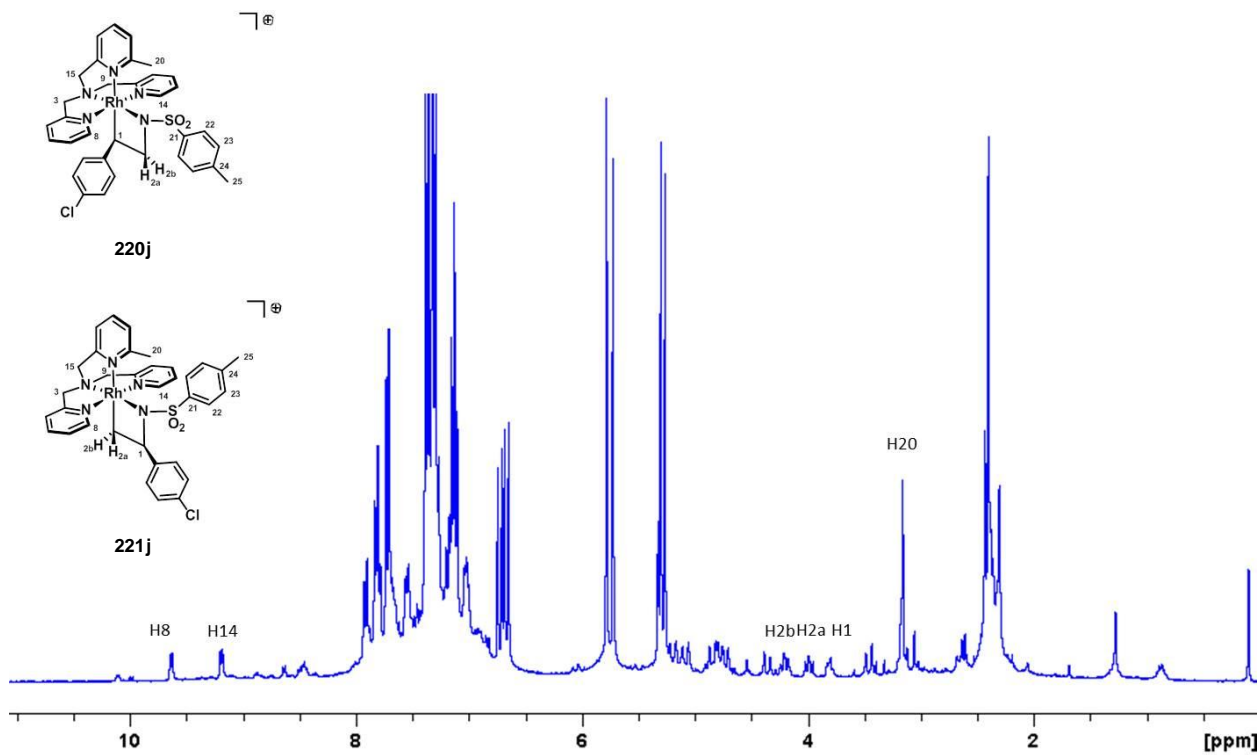
220h/221h, [MeTPA-4-nitrostyrene-azarhodacyclobutane]Cl, CD₂Cl₂



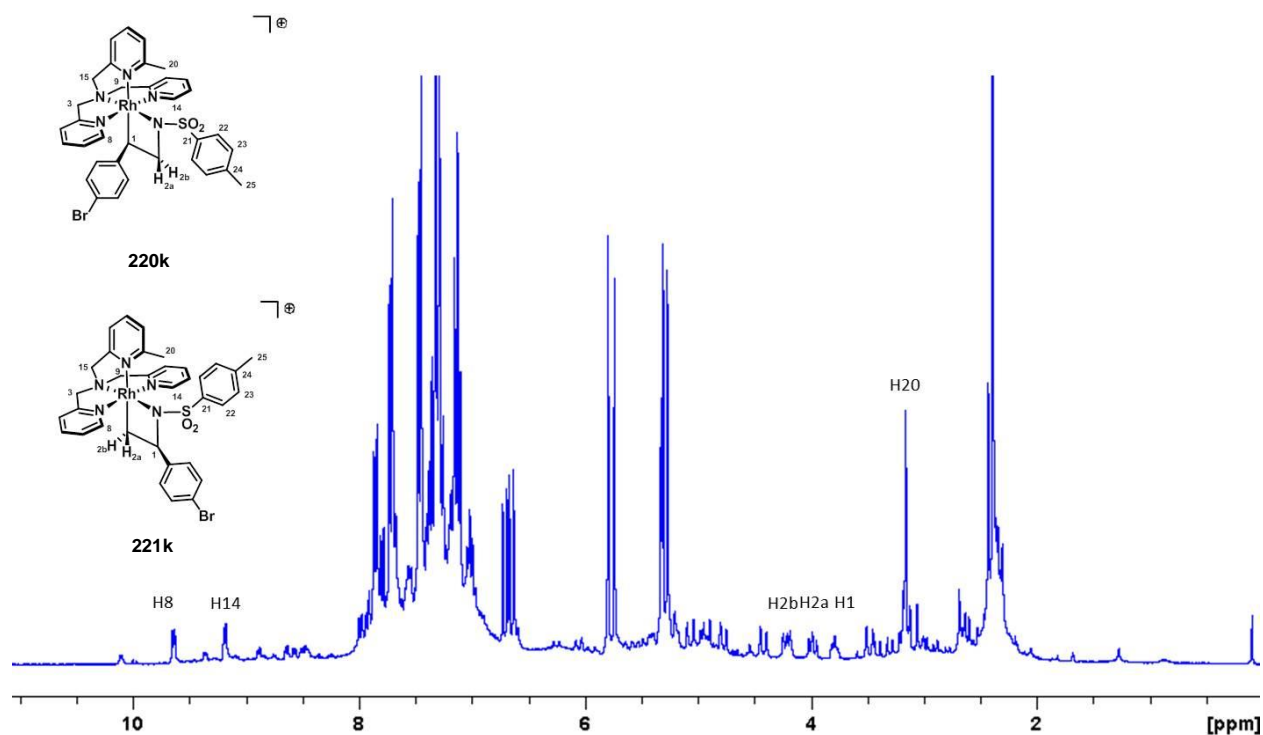
220i/221i, [MeTPA-4-cyanostyrene-azarhodacyclobutane]Cl, CD₂Cl₂



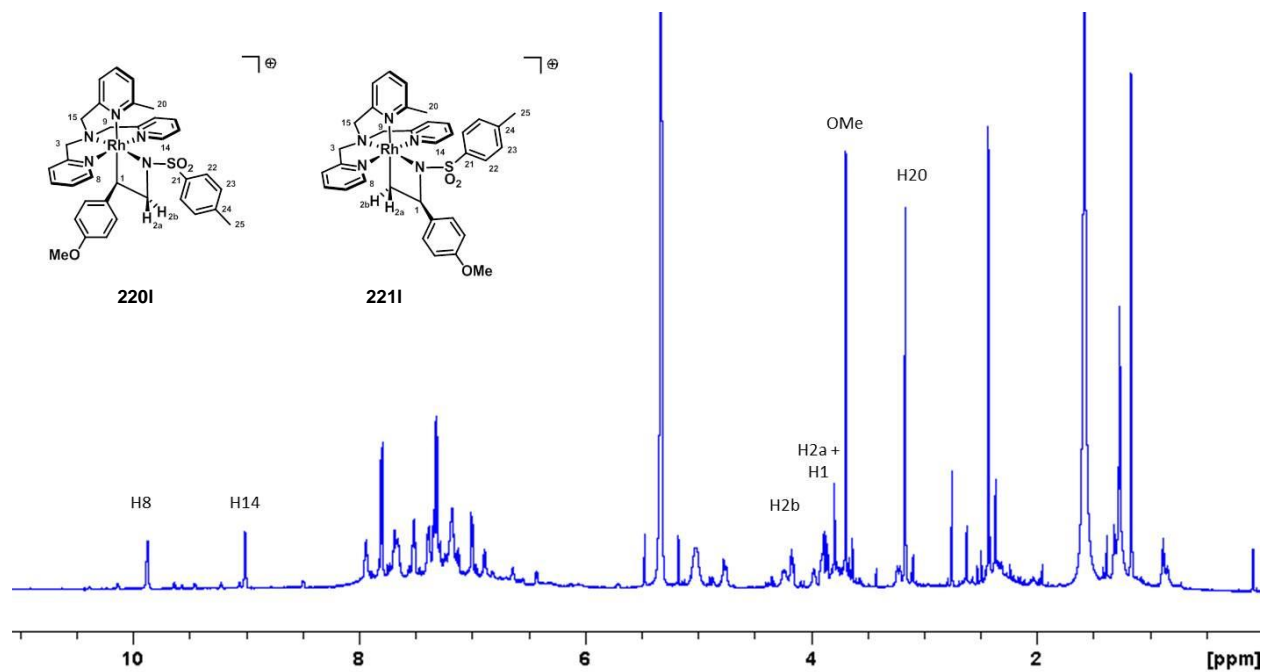
220j/221j, [MeTPA-4-chlorostyrene-azarhodacyclobutane]Cl, CD₂Cl₂



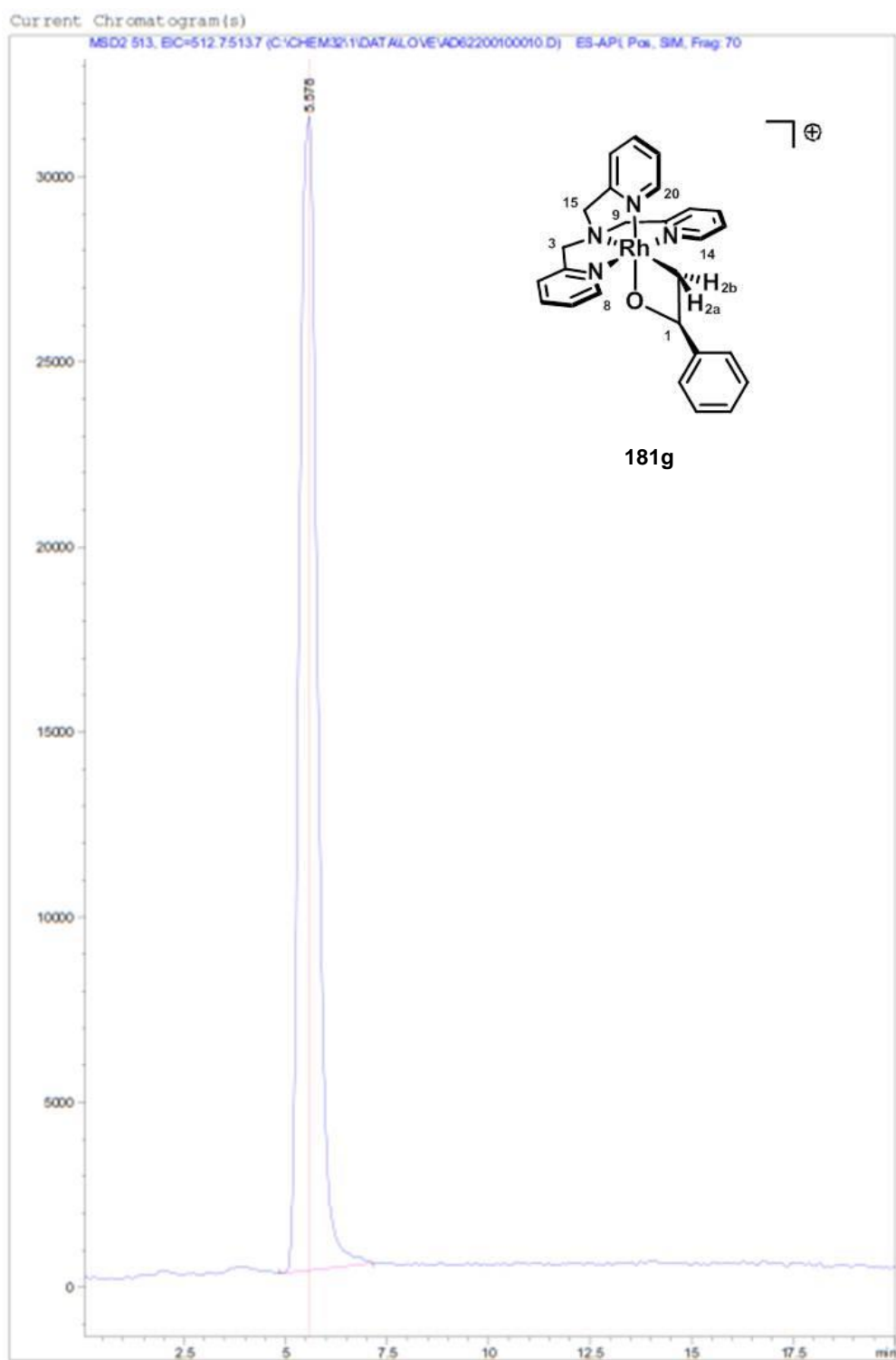
220k/221k, [MeTPA-4-bromostyrene-azarhodacyclobutane]Cl, CD₂Cl₂

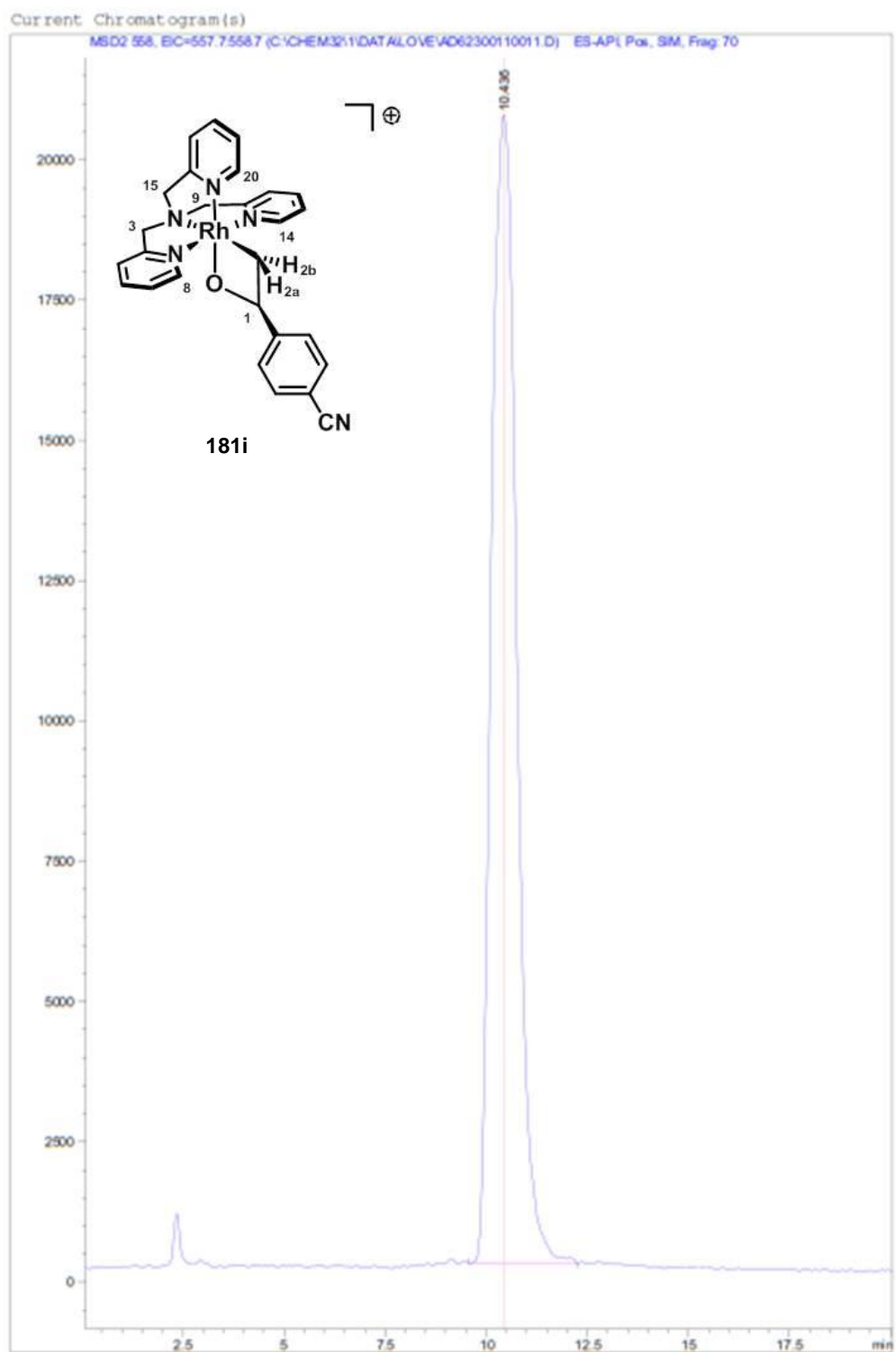


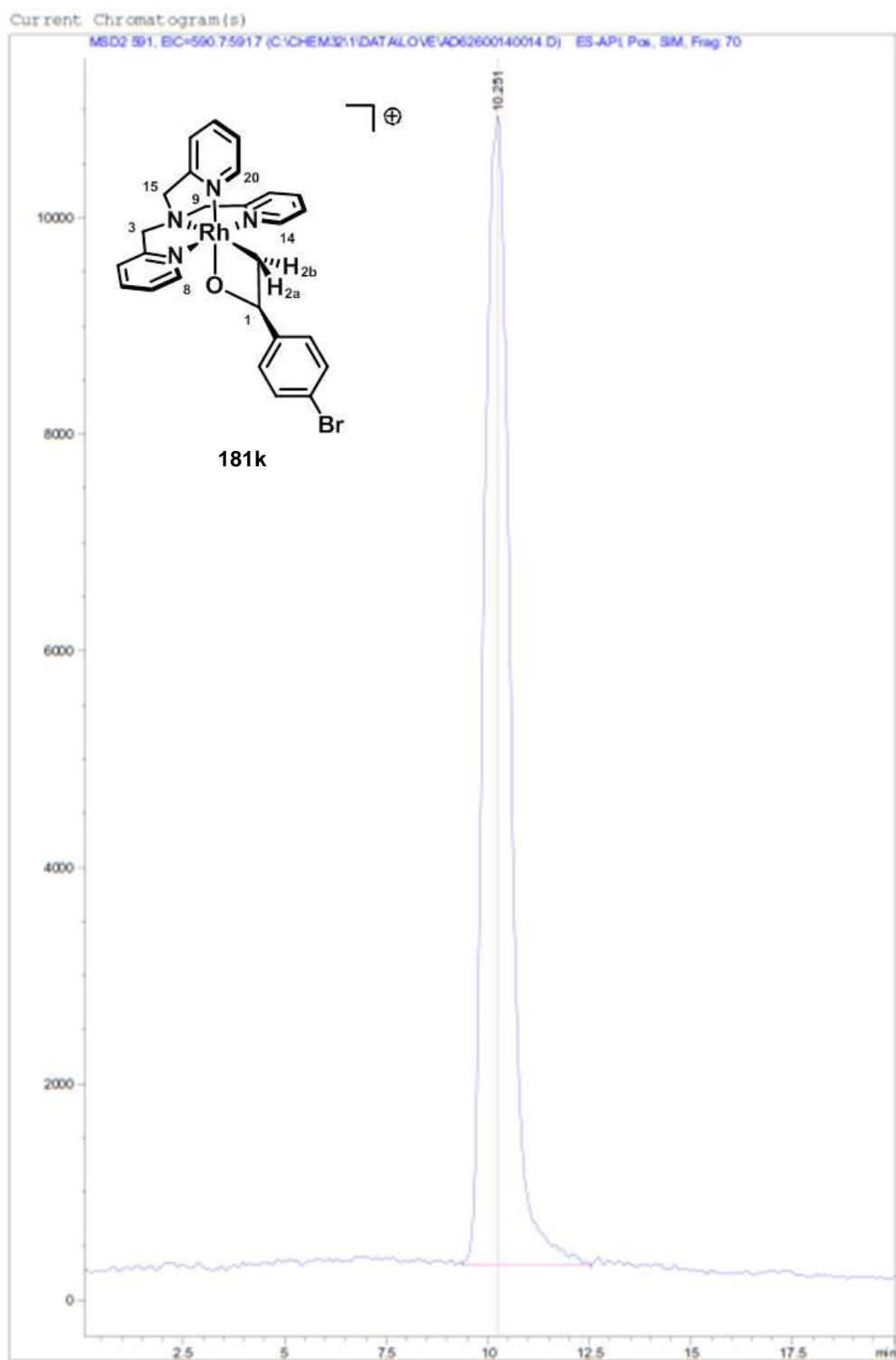
220l/221l, [MeTPA-4-methoxystyrene-azarhodacyclobutane]Cl, CD₂Cl₂

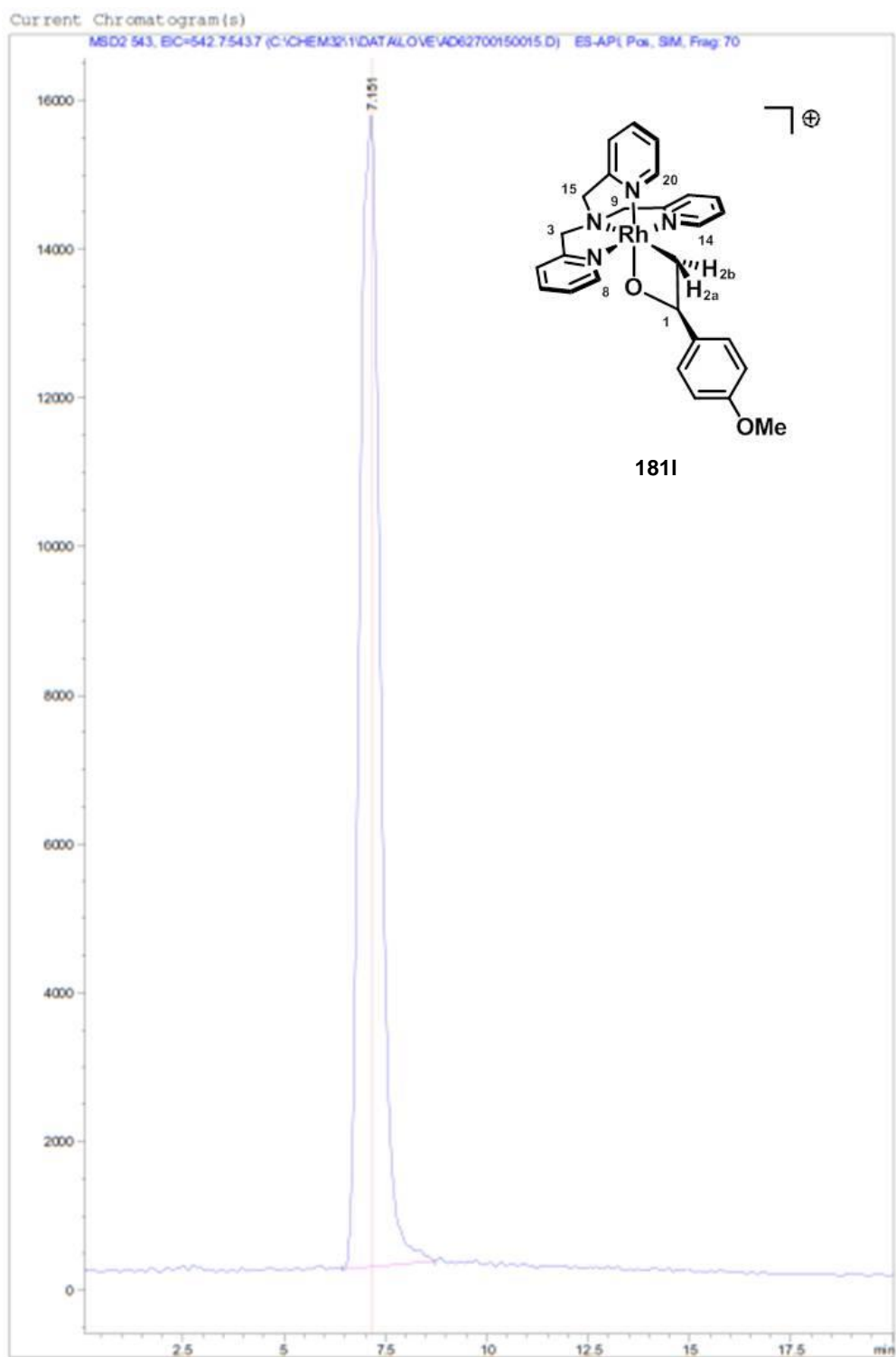


A.2 HPLC-MS chromatograms



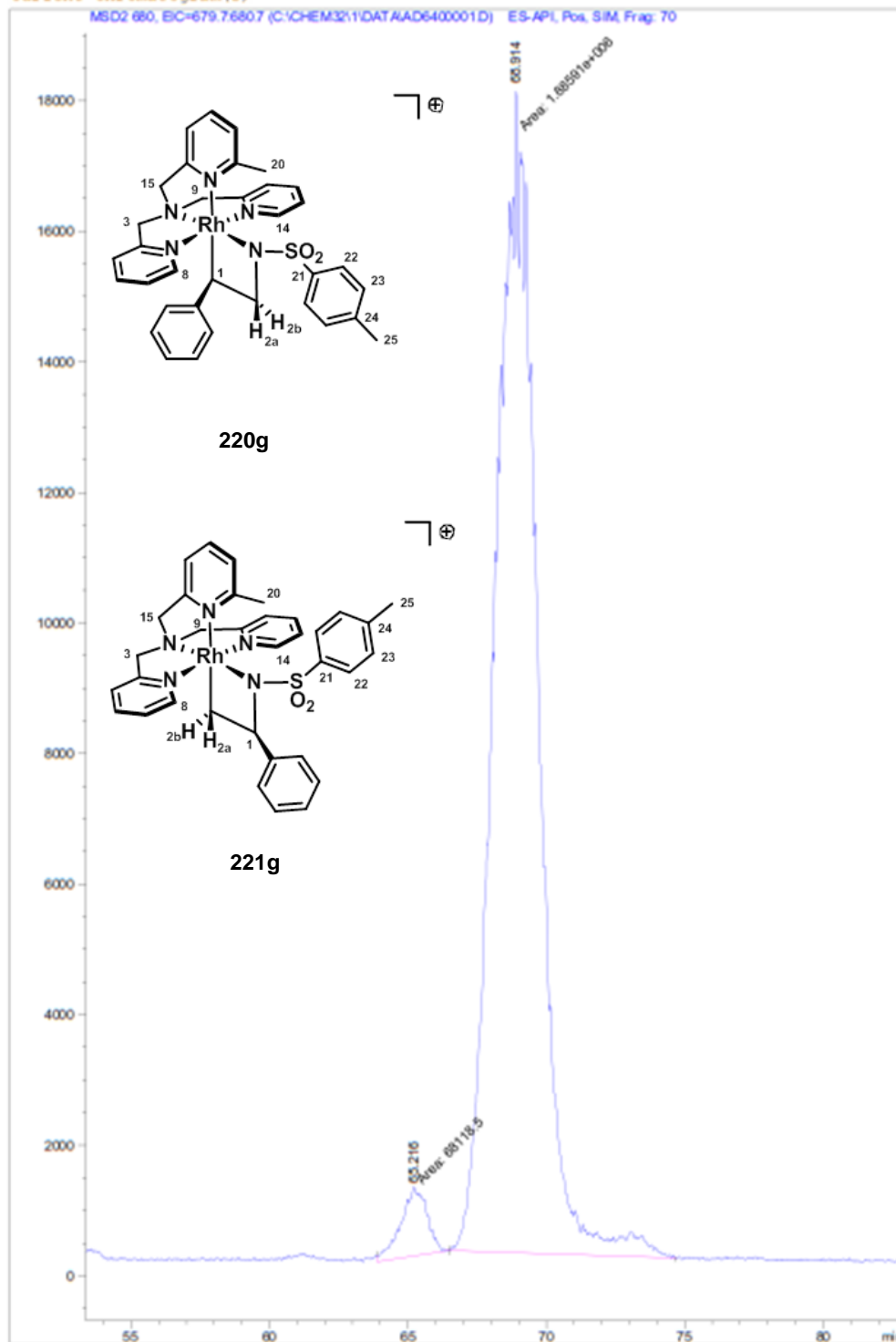


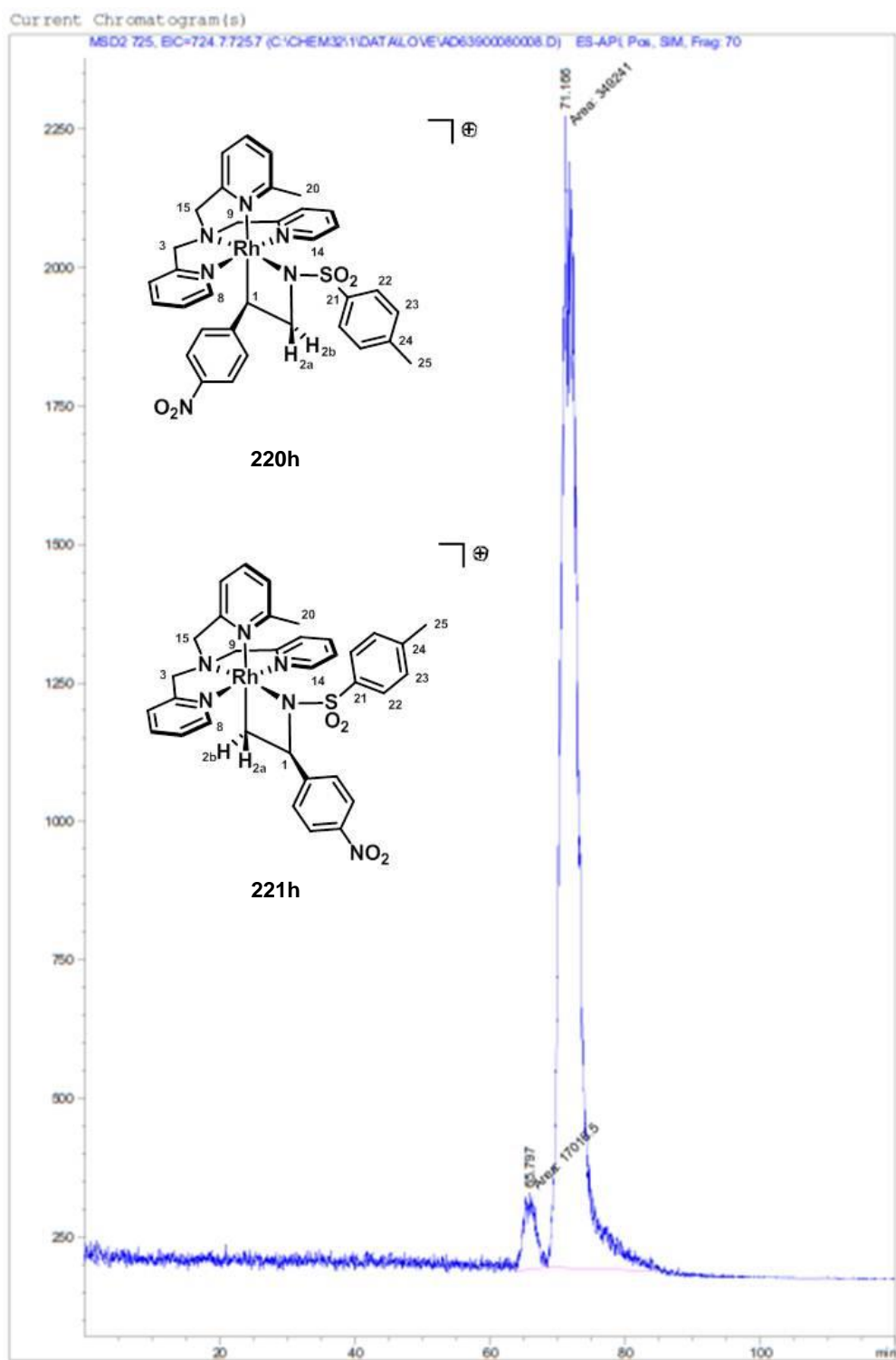


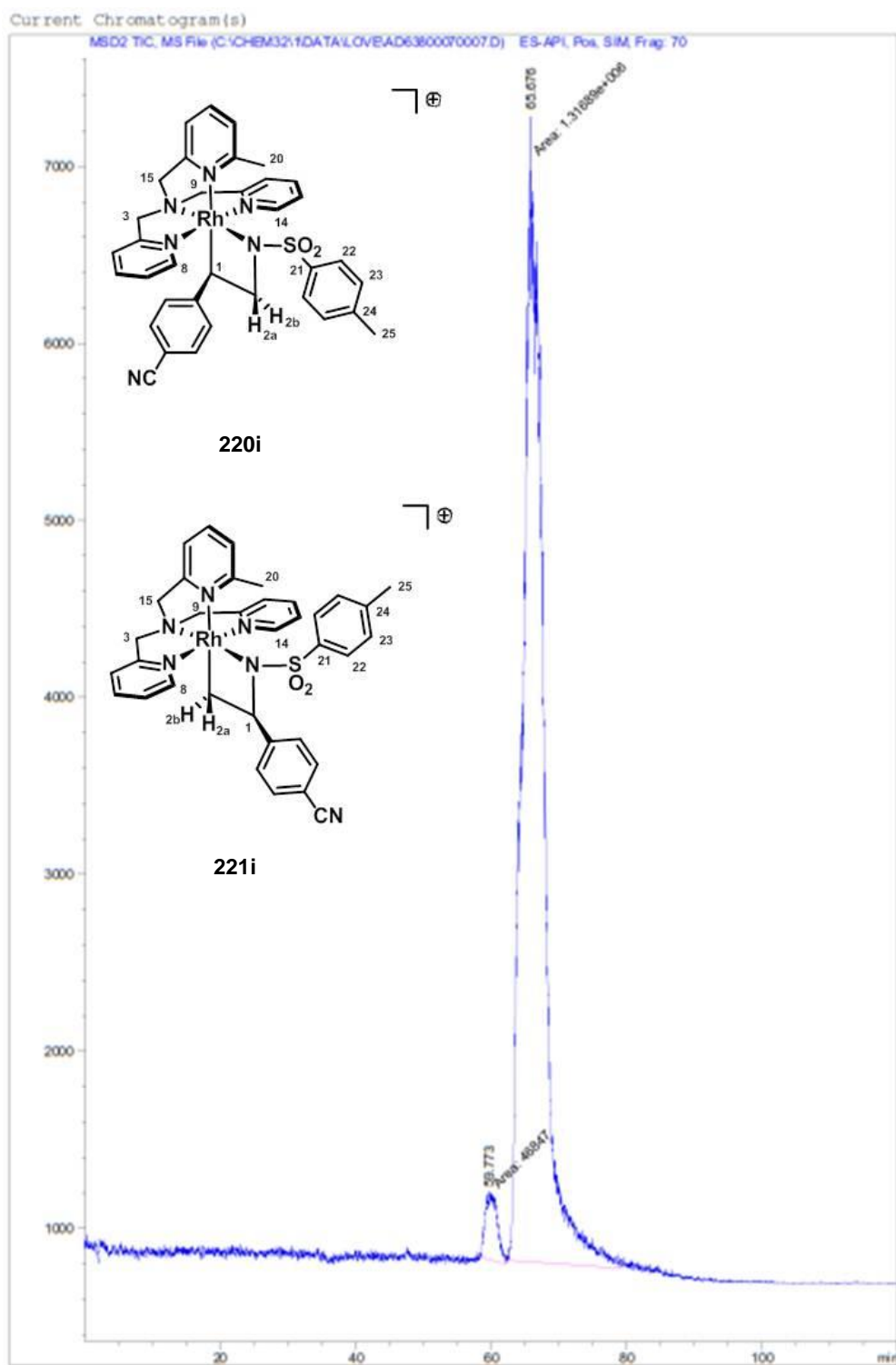


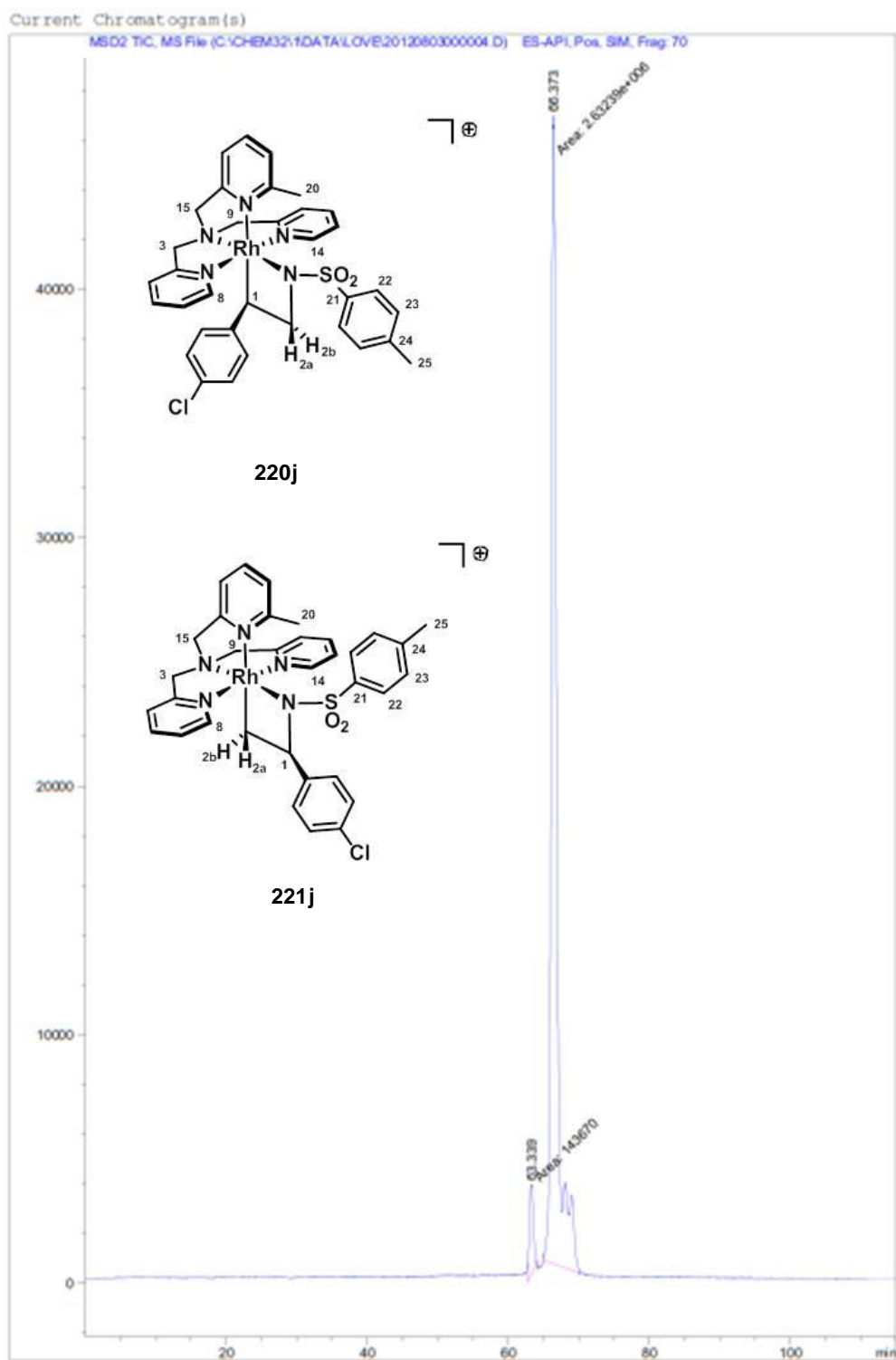
Current Chromatogram(s)

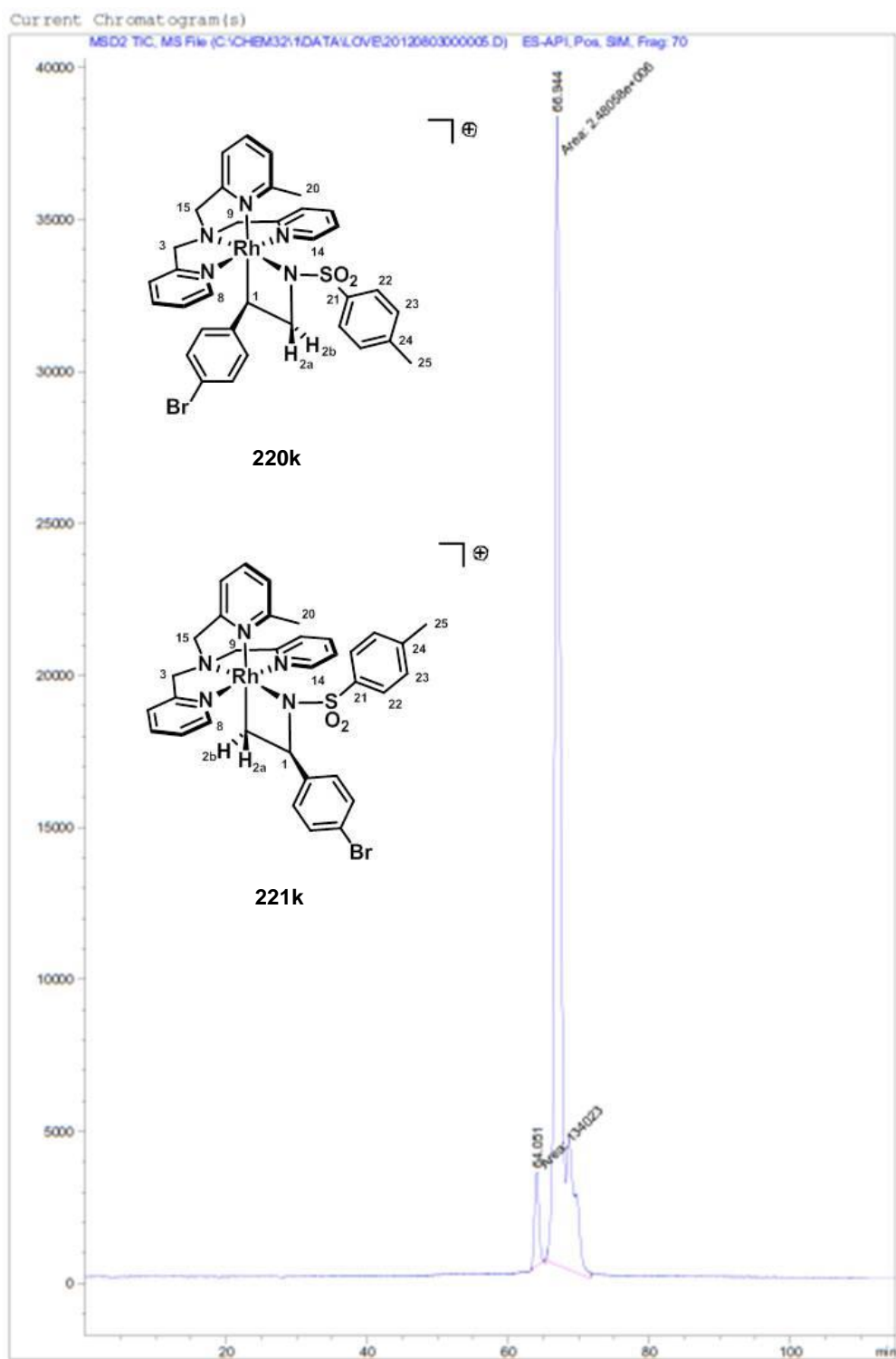
MSD2 680, EC=679.76807 (C:\CHEM32\1\DATA\AD6400001.D) ES-API, Pos, SIM, Frag: 70



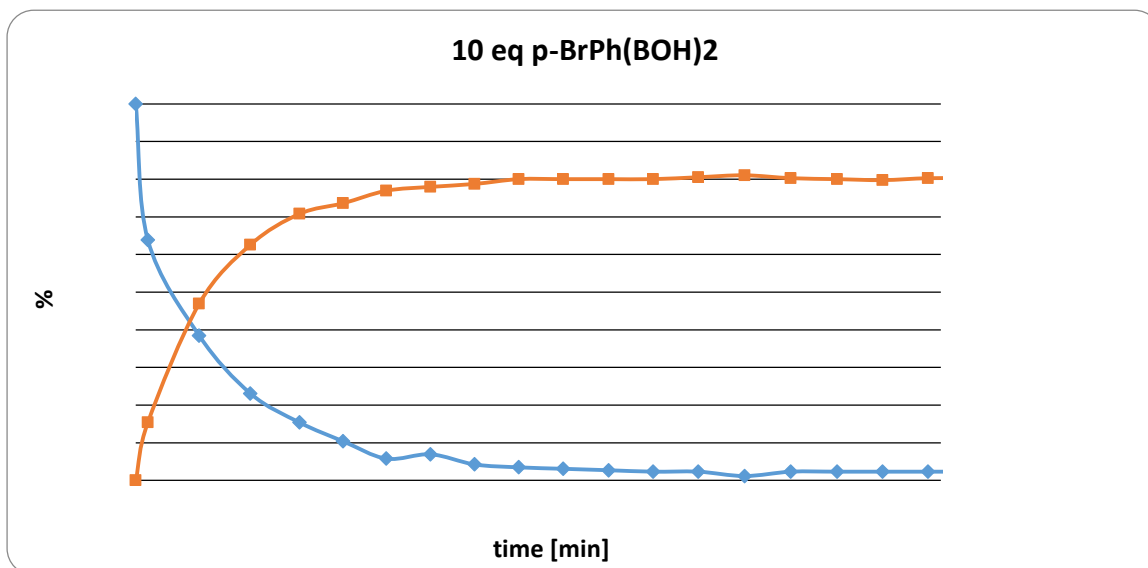
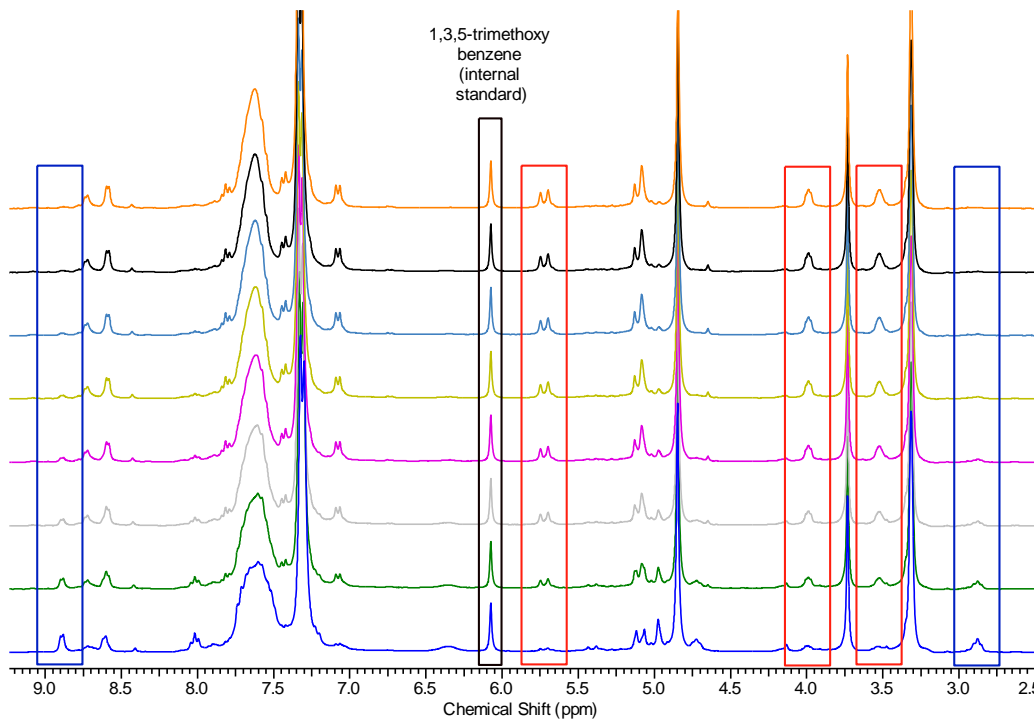








A.3 Sample plot for ^1H -NMR monitoring of transmetalation



Red line: transmetalation product **155a**,

integrated signals: $\delta = 5.91$ (d[AB²], 2H, $J = 15.1$ Hz), 3.94-3.88 (m, 2H), 3.54-3.46 (m, 2H)

Blue line: rhodaoxetane **153**

integrated signals: $\delta = 8.95$ (d, 1H, $J = 5.5$ Hz), 2.64 (dt, 2H, $^3J(\text{H,H}) = 7.3$ Hz, $^2J(\text{H,Rh}) = 2.5$ Hz)

Referenced to 1/3 equivalent of 1,3,5 trimethoxybenzene @ 6.10 ppm in d₄-methanol